frontiers | Research Topics

Oxidative metabolism in inflammation

Edited by
Pedro Gonzalez-Menendez, Rosa M. Sainz and
Pablo Andres Evelson

Published in
Frontiers in Immunology

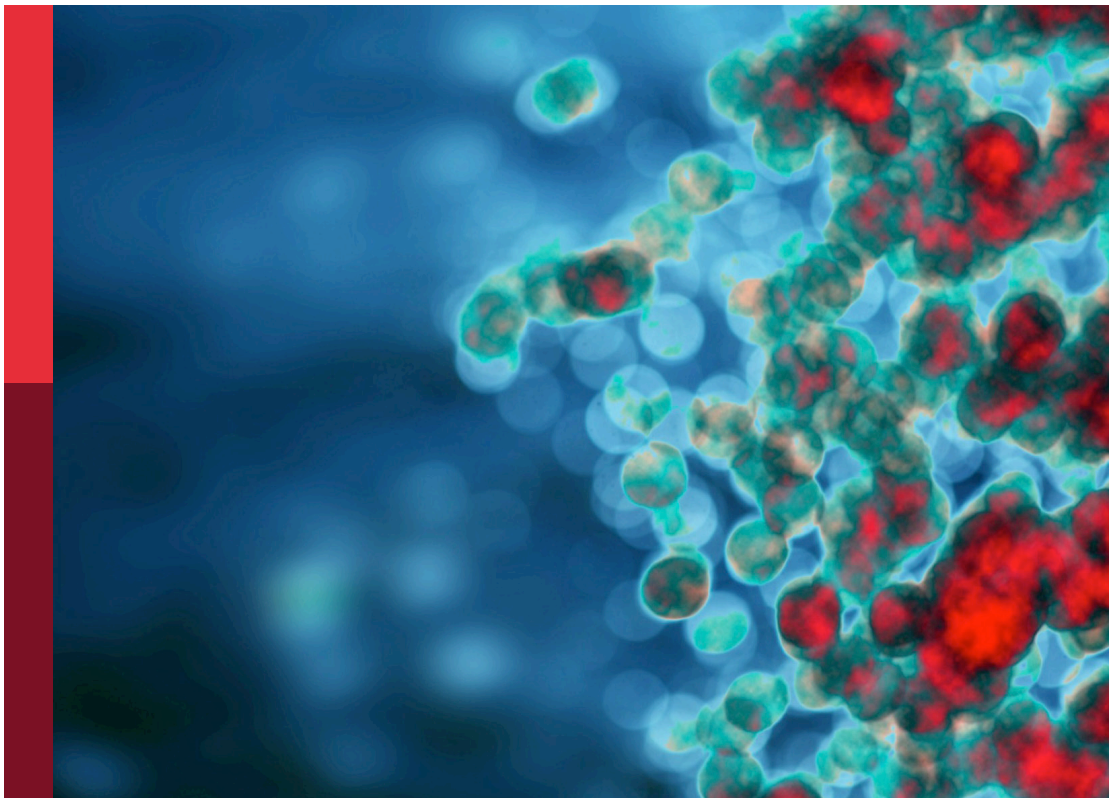

ISSN 1664-8714
ISBN 978-2-8325-5625-2
DOI 10.3389/978-2-8325-5625-2

About Frontiers

Frontiers is more than just an open access publisher of scholarly articles: it is a pioneering approach to the world of academia, radically improving the way scholarly research is managed. The grand vision of Frontiers is a world where all people have an equal opportunity to seek, share and generate knowledge. Frontiers provides immediate and permanent online open access to all its publications, but this alone is not enough to realize our grand goals.

Frontiers journal series

The Frontiers journal series is a multi-tier and interdisciplinary set of open-access, online journals, promising a paradigm shift from the current review, selection and dissemination processes in academic publishing. All Frontiers journals are driven by researchers for researchers; therefore, they constitute a service to the scholarly community. At the same time, the *Frontiers journal series* operates on a revolutionary invention, the tiered publishing system, initially addressing specific communities of scholars, and gradually climbing up to broader public understanding, thus serving the interests of the lay society, too.

Dedication to quality

Each Frontiers article is a landmark of the highest quality, thanks to genuinely collaborative interactions between authors and review editors, who include some of the world's best academicians. Research must be certified by peers before entering a stream of knowledge that may eventually reach the public - and shape society; therefore, Frontiers only applies the most rigorous and unbiased reviews. Frontiers revolutionizes research publishing by freely delivering the most outstanding research, evaluated with no bias from both the academic and social point of view. By applying the most advanced information technologies, Frontiers is catapulting scholarly publishing into a new generation.

What are Frontiers Research Topics?

Frontiers Research Topics are very popular trademarks of the *Frontiers journals series*: they are collections of at least ten articles, all centered on a particular subject. With their unique mix of varied contributions from Original Research to Review Articles, Frontiers Research Topics unify the most influential researchers, the latest key findings and historical advances in a hot research area.

Find out more on how to host your own Frontiers Research Topic or contribute to one as an author by contacting the Frontiers editorial office: frontiersin.org/about/contact

Oxidative metabolism in inflammation

Topic editors

Pedro Gonzalez-Menendez — University of Oviedo, Spain

Rosa M. Sainz — University of Oviedo, Spain

Pablo Andres Evelson — University of Buenos Aires, Argentina

Citation

Gonzalez-Menendez, P., Sainz, R. M., Evelson, P. A., eds. (2024). *Oxidative metabolism in inflammation*. Lausanne: Frontiers Media SA.

doi: 10.3389/978-2-8325-5625-2

Table of contents

frontiers | Frontiers in Immunology

TYPE Editorial
PUBLISHED 21 October 2024
DOI 10.3389/fimmu.2024.1507700

OPEN ACCESS

EDITED AND REVIEWED BY
Pietro Ghezzi,
University of Urbino Carlo Bo, Italy

*CORRESPONDENCE
Pedro Gonzalez-Menendez
gonzalezmpedro@uniovi.es
Rosa M. Sainz
sainzrosa@uniovi.es
Pablo Evelson
pevelson@ffyb.uba.ar

RECEIVED 08 October 2024
ACCEPTED 09 October 2024
PUBLISHED 21 October 2024

CITATION
Gonzalez-Menendez P, Sainz RM and Evelson P (2024) Editorial: Oxidative metabolism in inflammation.
Front. Immunol. 15:1507700.
doi: 10.3389/fimmu.2024.1507700

Editorial: Oxidative metabolism in inflammation

Pedro Gonzalez-Menendez[1,2,3]*, Rosa M. Sainz[1,2,3]* and Pablo Evelson[4,5]*

[1]Departamento de Morfología y Biología Celular, School of Medicine, Oviedo, Spain, [2]Instituto Universitario de Oncología del Principado de Asturias (IUOPA), University of Oviedo, Oviedo, Spain, [3]Instituto de Investigación Sanitaria del Principado de Asturias (ISPA), Hospital Universitario Central de Asturias (HUCA), Oviedo, Spain, [4]Facultad de Farmacia y Bioquímica, Departamento de Ciencias Químicas, Cátedra de Química General e Inorgánica, Universidad de Buenos Aires, Buenos Aires, Argentina, [5]CONICET, Instituto de Bioquímica y Medicina Molecular (IBIMOL), Universidad de Buenos Aires, Buenos Aires, Argentina

KEYWORDS

mitochondria, metabolism, oxidative stress, redox, inflammation, macrophages

Editorial on the Research Topic
Oxidative metabolism in inflammation

Mitochondria are integral to a multitude of cellular functions, including cell proliferation, metabolism, ATP production, and programmed cell death. They play an especially critical role in mediating inflammatory signaling pathways (1). When mitochondria become permeabilized, they can promote inflammation by releasing mitochondrial-derived damage-associated molecular patterns (DAMPs), which are potent triggers of the immune response (2). Furthermore, mitochondria are essential regulators of macrophage activation, differentiation, and survival (3). Alterations in mitochondrial oxidative metabolism significantly affect macrophage polarization: pro-inflammatory macrophages (M1) primarily rely on glycolysis for energy production, whereas anti-inflammatory macrophages (M2) depend on oxidative phosphorylation (OXPHOS) (4).

In addition to their role in energy metabolism, mitochondria are a major source of reactive oxygen species (ROS), contributing to oxidative stress through electron leakage in the electron transport chain (ETC) and the activity of certain mitochondrial enzymes (5). Oxidative stress is further heightened when macrophages are activated, although these cells possess self-defense mechanisms, such as metabolic reprogramming, to enhance their survival under these conditions (6). An increase in mitochondrial ROS production, or a decrease in antioxidant defenses, can result in significant cellular damage and inflammation. This link between elevated mitochondrial oxidative stress and chronic inflammation is associated with the pathogenesis of various diseases (7), highlighting the importance of mitochondrial function in maintaining cellular homeostasis and immune regulation (Figure 1).

Although the intricate relationship between mitochondrial metabolism and the innate immune response is well-established, the therapeutic use of antioxidants has not yielded the expected success/results (8). Moreover, the potential of metabolic reprogramming — whether through altering the metabolic environment or directly targeting mitochondrial function in macrophages for specific inflammatory diseases— remains largely underexplored. The Research Topic "*Oxidative metabolism in inflammation*" therefore aims to investigate whether shifts in oxidative metabolism, mitochondrial reactive oxygen

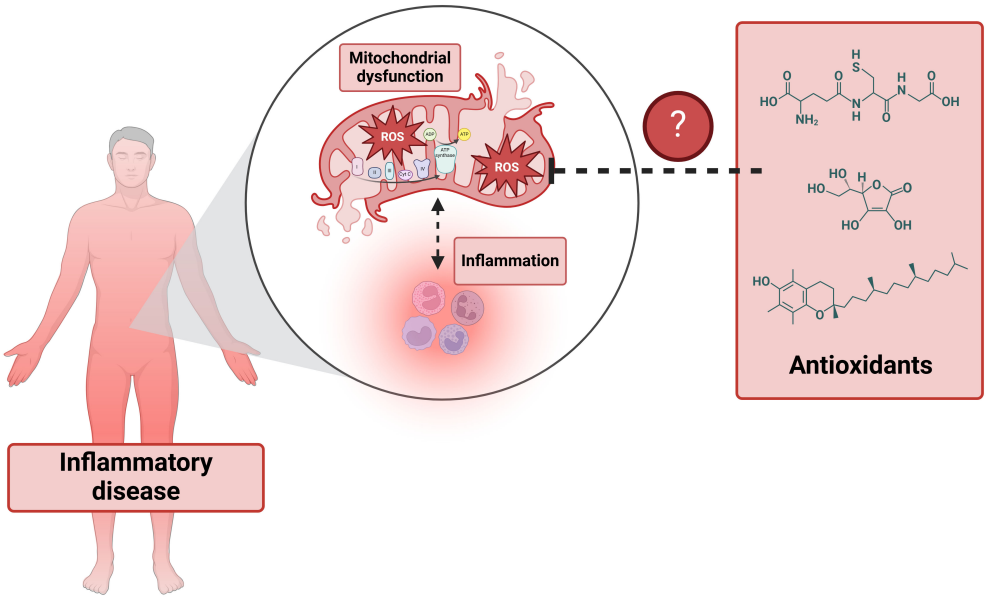

FIGURE 1
The interplay between inflammation and mitochondrial dysfunction in inflammatory diseases.

species (ROS) release, mitochondrial membrane potential, and changes in mitochondrial metabolites production/levels influence innate immunity and could serve as viable clinical targets.

This Research Topic comprises 12 articles that span a wide range of themes, from diseases directly linked to inflammation to responses and treatments associated with pathogenic infections, among other related topics. The Research Topic includes six original articles, two brief research reports, two bibliographic reviews, and two mini-reviews.

Sepsis is caused by the body's extreme response to an infection, leading to widespread inflammation. Thoppil et al. compile a bibliography on the role of the hormone and neurotransmitter norepinephrine in enhancing the anti-inflammatory response by influencing the oxidative metabolism of immune cells. On the other hand, Natalia Rodriguez-Rodriguez et al. summarize how HIV-1 infection inhibits OXPHOS while promoting glycolysis and fatty acid synthesis in immune cells. In original research, Golenkina et al. describe how suppressing leukotriene synthesis in neutrophils with mitochondria-targeted antioxidants, but not thiol-based ones, proves effective against *Salmonella typhimurium* infection. Additionally, Krasic et al. investigate the effects of the anti-inflammatory glucocorticoid methylprednisolone on multisystem inflammatory syndrome associated with COVID-19, noting that it boosts the antioxidant response in erythrocytes. However, patients with low catalase activity who do not respond well to treatment should avoid methylprednisolone, as it may be contraindicated.

Regarding specific inflammatory diseases, osteoarthritis is a degenerative condition characterized by cartilage breakdown, accompanied by increased oxidative stress and an altered inflammatory response (9). Xiong et al. review the effects of the neuroindole melatonin in osteoarthritis, highlighting its ability to reduce inflammation, oxidative stress, and chondrocyte death. Meanwhile, He et al. focus on the use of the diterpenoid alkaloid songorine, which they found to reduce inflammation in osteoarthritis by shifting macrophage polarization from the M1 to M2 phenotype, associated with a metabolic reprogramming towards OXPHOS. Additionally, Zhou et al. propose antioxidant therapy as a novel treatment for chronic rhinosinusitis with nasal polyps, finding that the carotenoid crocin inhibits both M1 and M2 macrophage polarization, reduces the expression of oxidative enzymes NOS2 and NOX1, and enhances the antioxidant capacity of anti-inflammatory M2 macrophages. Similarly, antioxidant therapy may be promising for acute inflammation. Liu et al. demonstrate that the drug troxerutin reduces oxidative stress and inflammation in jellyfish dermatitis by activating the antioxidant Nrf2/HO-1 pathway.

Several chronic diseases are associated with a pro-inflammatory phenotype, including diabetes, which is one of the most common chronic diseases worldwide and is linked to numerous complications due to inflammation (10). Nirenjen et al. have reviewed the role of pro-inflammatory cytokines involved in wound healing, a process that is generally impaired in individuals with diabetes. Furthermore, using single-cell RNA sequencing (RNA-seq), Qi et al. demonstrated that oxidative stress is elevated in peripheral blood mononuclear cells (PBMCs) from patients with ovulation disorders such as polycystic ovary syndrome, primary ovarian insufficiency, and menopause. In these patients, a decrease in naïve CD8 T cells and effector memory CD4 T cells was observed, while there was an increase in natural killer (NK) cells and regulatory NK cells. Non-alcoholic fatty liver disease (NAFLD) is also associated with oxidative stress, as demonstrated by Wang et al. using machine learning and weighted gene co-expression network analysis. They identified that *CDKN1B* and *TFAM* are closely related to oxidative stress in NAFLD.

The Research Topic has also been expanded to include technique articles describing new methods for studying oxidative metabolism in

innate immunity. In this regard, Flocke et al. have proposed a non-invasive method to monitor metabolism during inflammation. By using lipopolysaccharide (LPS)-doped Matrigen plugs in mice to induce inflammation, the authors performed $^{1}H/^{19}F$ magnetic resonance imaging (MRI) to track the recruitment of ^{19}F-labeled immune cells and ^{2}H magnetic resonance spectroscopy (MRS) to monitor the metabolic response.

In summary, this Research Topic deepens our understanding of mitochondria-dependent regulation in macrophage biology and explores the role of oxidative metabolism in inflammatory responses associated with chronic diseases and pathogenic organisms. These insights could lead to new clinical strategies for effectively treating acute and chronic inflammation.

Author contributions

PG-M: Writing – review & editing, Writing – original draft. RS: Writing – review & editing, Writing – original draft. PE: Writing – review & editing, Writing – original draft.

Funding

The author(s) declare financial support was received for the research, authorship, and/or publication of this article. PG-M is supported by the "Ramon y Cajal" program (RYC-2021-033856-I) from the Spanish Ministry of Science, Innovation and Universities, Agencia Estatal de Investigación (MICIU/AEI), and NextGenerationEU (EU/PRTR).

Acknowledgments

Figure 1 was created using BioRender (www.biorender.com).

Conflict of interest

The authors declare that the research was conducted in the absence of any commercial or financial relationships that could be construed as a potential conflict of interest.

The author(s) declared that they were an editorial board member of Frontiers, at the time of submission. This had no impact on the peer review process and the final decision.

Publisher's note

References

1. Marchi S, Guilbaud E, Tait SWG, Yamazaki T, Galluzzi L. Mitochondrial control of inflammation. *Nat Rev Immunol*. (2023) 23:159–73. doi: 10.1038/s41577-022-00760-x

2. Vringer E, Tait SWG. Mitochondria and cell death-associated inflammation. *Cell Death Differ*. (2023) 30:304–12. doi: 10.1038/s41418-022-01094-w

3. Wang Y, Li N, Zhang X, Horng T. Mitochondrial metabolism regulates macrophage biology. *J Biol Chem*. (2021) 297:100904. doi: 10.1016/j.jbc.2021.100904

4. Liu Y, Xu R, Gu H, Zhang E, Qu J, Cao W, et al. Metabolic reprogramming in macrophage responses. *biomark Res*. (2021) 9:1. doi: 10.1186/s40364-020-00251-y

5. Canton M, Sánchez-Rodríguez R, Spera I, Venegas FC, Favia M, Viola A, et al. Reactive oxygen species in macrophages: sources and targets. *Front Immunol*. (2021) 12:734229. doi: 10.3389/fimmu.2021.734229

6. Virág L, Jaén RI, Regdon Z, Boscá L, Prieto P. Self-defense of macrophages against oxidative injury: Fighting for their own survival. *Redox Biol*. (2019) 26:101261. doi: 10.1016/j.redox.2019.101261

7. Zuo L, Prather ER, Stetskiv M, Garrison DE, Meade JR, Peace TI, et al. Inflammaging and oxidative stress in human diseases: from molecular mechanisms to novel treatments. *Int J Mol Sci*. (2019) 20:4472. doi: 10.3390/ijms20184472

8. Biswas SK. Does the interdependence between oxidative stress and inflammation explain the antioxidant paradox? *Oxid Med Cell Longevity*. (2016) 2016:5698931. doi: 10.1155/2016/5698931

9. Ansari MY, Ahmad N, Haqqi TM. Oxidative stress and inflammation in osteoarthritis pathogenesis: Role of polyphenols. *BioMed Pharmacother*. (2020) 129:110452. doi: 10.1016/j.biopha.2020.110452

10. Rohm TV, Meier DT, Olefsky JM, Donath MY. Inflammation in obesity, diabetes, and related disorders. *Immunity*. (2022) 55:31–55. doi: 10.1016/j.immuni.2021.12.013

frontiers | Frontiers in Immunology

TYPE Review
PUBLISHED 27 July 2023
DOI 10.3389/fimmu.2023.1216321

OPEN ACCESS

EDITED BY
Rosa M. Sainz,
University of Oviedo, Spain

REVIEWED BY
Manjari Singh,
Assam University, India
Alin Laurentiu Tatu,
Dunarea de Jos University, Romania
Pedro Gonzalez-Menendez,
University of Oviedo, Spain

*CORRESPONDENCE
Vetriselvan Subramaniyan
subramaniyan.vetriselvan.monash.edu
Ling Shing Wong
lingshing.wong@newinti.edu.my
Gobinath Ramachawolran
r.gobinath@rcsiucd.edu.my

RECEIVED 03 May 2023
ACCEPTED 26 June 2023
PUBLISHED 27 July 2023

CITATION
Nirenjen S, Narayanan J, Tamilanban T, Subramaniyan V, Chitra V, Fuloria NK, Wong LS, Ramachawolran G, Sekar M, Gupta G, Fuloria S, Chinni SV and Selvaraj S (2023) Exploring the contribution of pro-inflammatory cytokines to impaired wound healing in diabetes.
Front. Immunol. 14:1216321.
doi: 10.3389/fimmu.2023.1216321

Exploring the contribution of pro-inflammatory cytokines to impaired wound healing in diabetes

S. Nirenjen[1], J. Narayanan[1], T. Tamilanban[1], Vetriselvan Subramaniyan[2,3]*, V. Chitra[1], Neeraj Kumar Fuloria[4], Ling Shing Wong[5]*, Gobinath Ramachawolran[6]*, Mahendran Sekar[7], Gaurav Gupta[8,9], Shivkanya Fuloria[4], Suresh V. Chinni[10,11] and Siddharthan Selvaraj[12]

[1]Department of Pharmacology, SRM College of Pharmacy, SRM Institute of Science and Technology, Kattankulathur, Tamil Nadu, India, [2]Jeffrey Cheah School of Medicine and Health Sciences, Monash University, Jalan Lagoon Selatan, Bandar Sunway, Petaling Jaya, Selangor, Malaysia, [3]Center for Transdisciplinary Research, Department of Pharmacology, Saveetha Dental College, Saveetha Institute of Medical and Technical Sciences, Saveetha University, Chennai, Tamil Nadu, India, [4]Faculty of Pharmacy, AIMST University, Bedong, Kedah, Malaysia, [5]Faculty of Health and Life Sciences, INTI International University, Nilai, Malaysia, [6]Department of Foundation, RCSI & UCD Malaysia Campus, Jalan Sepoy Lines, Georgetown, Pulau Pinang, Malaysia, [7]School of Pharmacy, Monash University Malaysia, Subang Jaya, Selangor, Malaysia, [8]School of Pharmacy, Suresh Gyan Vihar University, Jagatpura, Mahal Road, Jaipur, India, [9]Uttaranchal Institute of Pharmaceutical Sciences, Uttaranchal University, Dehradun, India, [10]Department of Biochemistry, Faculty of Medicine, Bioscience, and Nursing, MAHSA University, Jenjarom, Selangor, Malaysia, [11]Department of Periodontics, Saveetha Dental College and Hospitals, Saveetha Institute of Medical and Technical Sciences, Saveetha University, Chennai, India, [12]Faculty of Dentistry, AIMST University, Semeling, Kedah, Malaysia

Background: Impaired wound healing is the most common and significant complication of Diabetes. While most other complications of Diabetes have better treatment options, diabetic wounds remain a burden as they can cause pain and suffering in patients. Wound closure and repair are orchestrated by a sequence of events aided by the release of pro-inflammatory cytokines, which are dysregulated in cases of Diabetes, making the wound environment unfavorable for healing and delaying the wound healing processes. This concise review provides an overview of the dysregulation of pro-inflammatory cytokines and offers insights into better therapeutic outcomes.

Purpose of review: Although many therapeutic approaches have been lined up nowadays to treat Diabetes, there are no proper treatment modalities proposed yet in treating diabetic wounds due to the lack of understanding about the role of inflammatory mediators, especially Pro-inflammatory mediators- Cytokines, in the process of Wound healing which we mainly focus on this review.

Recent findings: Although complications of Diabetes mellitus are most reported after years of diagnosis, the most severe critical complication is impaired Wound Healing among Diabetes patients. Even though Trauma, Peripheral Artery Disease, and Peripheral Neuropathy are the leading triggering factors for the development of ulcerations, the most significant issue contributing to the development of complicated cutaneous wounds is wound healing impairment. It may even end up with amputation. Newer therapeutic approaches such as incorporating the additives in the present dressing materials, which include antimicrobial molecules and immunomodulatory cytokines is of better therapeutic value.

Summary: The adoption of these technologies and the establishment of novel therapeutic interventions is difficult since there is a gap in terms of a complete understanding of the pathophysiological mechanisms at the cellular and molecular level and the lack of data in terms of the assessment of safety and bioavailability differences in the individuals' patients. The target-specific pro-inflammatory cytokines-based therapies, either by upregulation or downregulation of them, will be helpful in the wound healing process and thereby enhances the Quality of life in patients, which is the goal of drug therapy.

KEYWORDS

wound healing, pro-inflammatory, diabetes mellitus, cytokines, therapeutic approach

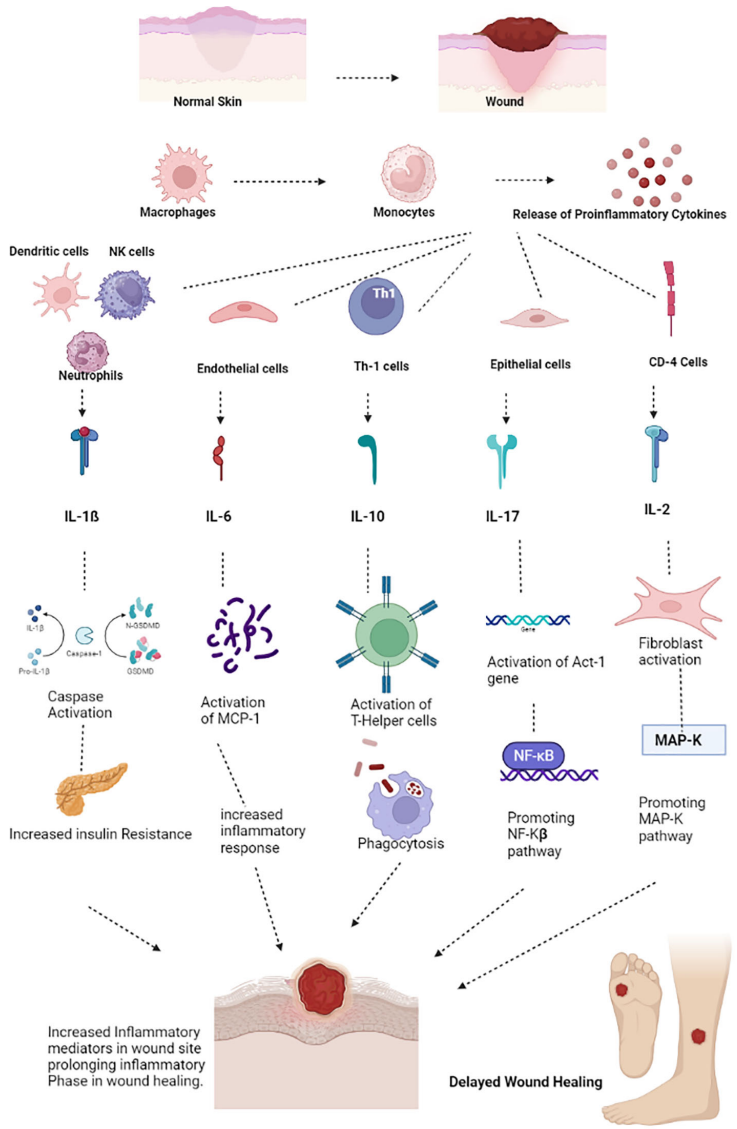

GRAPHICAL ABSTRACT

Highlights

- Impaired wound healing is a significant complication of Diabetes that remains a burden on patients as it can cause pain and suffering.
- Pro-inflammatory cytokines play a critical role in wound closure and repair, but their dysregulation in Diabetes creates an unfavorable environment for healing and delays the wound healing processes.
- This concise review offers insights into better therapeutic outcomes by providing an overview of the dysregulation of pro-inflammatory cytokines in diabetes mellitus.

Background

Diabetes is the most common metabolic disorder and is more prevalent than other metabolic disorders. It is a chronic condition characterized by marked elevations in blood glucose levels, known as hyperglycemia. Diabetes is a growing concern, with 2.6 million individuals diagnosed yearly; approximately 4% of the population struggles with this disorder. Type-2 Diabetes Mellitus affects an estimated 2.3 million people, while type-I DM affects around 0.3 million (1). Diabetes is one of the leading causes of death worldwide. A current statistical survey conducted by the National School of Economics stated that Diabetes is one of the ten leading causes of death, which estimates about 6.7 million deaths (2). The global economic burden of Diabetes Mellitus, along with its complications, is expected to reach 2.1 trillion in upcoming years, which equates to about 10% of the total National Health Budget. Diabetes and its complications have an impact on the financial status of the patient (3).

Although complications of Diabetes Mellitus are mostly reported after years of diagnosis, impaired wound healing among Diabetes patients is the most severe and critical complication. Even though trauma, peripheral artery disease, and peripheral neuropathy are the leading triggering factors for the development of ulcerations, the most significant issue contributing to the development of complicated cutaneous wounds is impaired wound healing, which may even result in amputation (4). Dysregulation or defects in the microcirculation, which are associated with peripheral artery disease and peripheral neuropathy, contribute to or result in impaired wound healing in Type-II Diabetes Mellitus. In individuals with type 1 diabetes, the high blood sugar levels can negatively affect each of these stages, leading to impaired wound healing. One of the main complications of type 1 diabetes is poor blood circulation. High blood sugar levels can damage blood vessels, reducing blood flow to the affected area. This diminished blood supply means that essential nutrients and oxygen required for proper wound healing may not reach the wound efficiently, slowing down the healing process. Moreover, individuals with type 1 diabetes often have weakened immune systems, making them more susceptible to infections. This is due to high blood sugar levels impairing the function of immune cells responsible for fighting off bacteria and other pathogens. As a result, wounds in people with type 1 diabetes are more prone to infections, which can further delay the healing process. Additionally, the long-term effects of high blood sugar levels can cause nerve damage, known as diabetic nephropathy. This condition can lead to a loss of sensation in the affected area, making it difficult for individuals to detect injuries or wounds. Delayed wound detection and lack of proper care can result in further complications and hinder the healing process (5). Both type 1 and type 2 diabetes can lead to poor blood circulation due to high blood sugar levels and blood vessel damage. Reduced blood flow to the wound site can hinder the delivery of oxygen and nutrients necessary for proper wound healing. Although there are several therapeutic approaches in treating Diabetes and its other complications, there are no proper treatment modalities proposed yet to treat non-healing diabetic wounds due to the lack of understanding about the underlying pathophysiological mechanisms of the role of inflammatory mediators, especially pro-inflammatory mediators such as cytokines, in the wound healing process. This review mainly focuses on this issue.

Mechanisms involved in the healing of wounds

The wound healing

When tissue integrity is compromised, an effective and intricate process called wound healing begins (6). The four stages of healing —hemostasis, inflammation, proliferation, and remodeling- are the most intricate processes and include several steps (7).

Hemostasis

Platelets are essential for hemostasis, the initial phase of tissue healing. As circulating platelets come into contact with the collagen of the wounded tissue, they become activated, gather, and stick to the damaged endothelium (8). When coagulation begins, fibrinogen is transformed into fibrin, forming the thrombus and the temporary extracellular matrix. When platelets are activated, they release proteins that cause neutrophils and monocytes to migrate and adhere to one another, as well as several growth factors, such as transforming growth factor-ß (TGF-ß) and platelet-derived growth factor (PDGF), that facilitate wound healing (9).

Abbreviations: DM, Diabetes Mellitus; PDGF, Platelet-Derived Growth Factor; T.G.F.- ß, Transforming Growth Factor- ß; VEGF, Vascular Endothelial Growth Factor; EPC, Endothelial Progenitor Cells; FGF-2, Fibroblast Growth Factor-2; IL, Interleukin; TNF- α, Tumor Necrosis Factor- α; M.M.P., Matrix Metallo Proteinases; MCP-1, Monocyte Chemoattractant Proteins; PAD-4, Protein Arginine Deiminase 4; HIF-1, Hypoxia Inducible Factor- 1; TIMP, Tissue Inhibitors of Metalloproteinases; S.T.Z., Streptozotocin; MAPK, Mitogen-Activated Protein Kinase; CTL, Cytotoxic T Lymphocytes; THC, Tetrahydro Curcumin; C.R.P., C- Reactive Protein; NF-K ß, Nuclear factor kappa B; TH, T-Helper Cells.

Inflammatory phase

As soon as an injury occurs, the inflammatory phase of wound healing begins as inflammatory cells infiltrate the wound site. The first cells to devour the injured tissue are neutrophils. When sticky molecules on the vascular endothelial surface near the wounded tissue are activated, neutrophils adhere to the endothelium. Then, neutrophils advance further into the tissue space through damaged capillaries or gaps between endothelial cells, a process known as diapedesis (10). Neutrophils are essential for tissue debridement and infection control. They also generate a variety of growth factors that encourage cell development and proteases that degrade the extracellular matrix, making them involved in the wound-healing process (11). When circulating monocytes enter the tissue area, they become mature macrophages (M2 Macrophages), creating an inflammatory response. Through phagocytosis, pro-inflammatory or activated macrophages (M1 macrophages) clear the wound of germs, foreign objects, apoptotic neutrophils, and injured tissue fragments (12). They also produce a range of cytokines and mediators that promote inflammation. Local mast cells also rapidly react to tissue damage and are crucial for wound healing (Figure 1). Mast cell degranulation produces proteinases that break down the extracellular matrix and several cytokines that stimulate neutrophil recruitment. T-lymphocytes arrive at the wound site in the late stages of inflammation and appear to coordinate tissue remodeling (13).

Proliferative phase

The wound enters the proliferative phase as inflammation subsides and macrophages change to an alternate activated or anti-inflammatory phenotype. The transition of macrophages from a pro-inflammatory phenotype to an alternative activated or anti-inflammatory phenotype plays a crucial role in the shift from

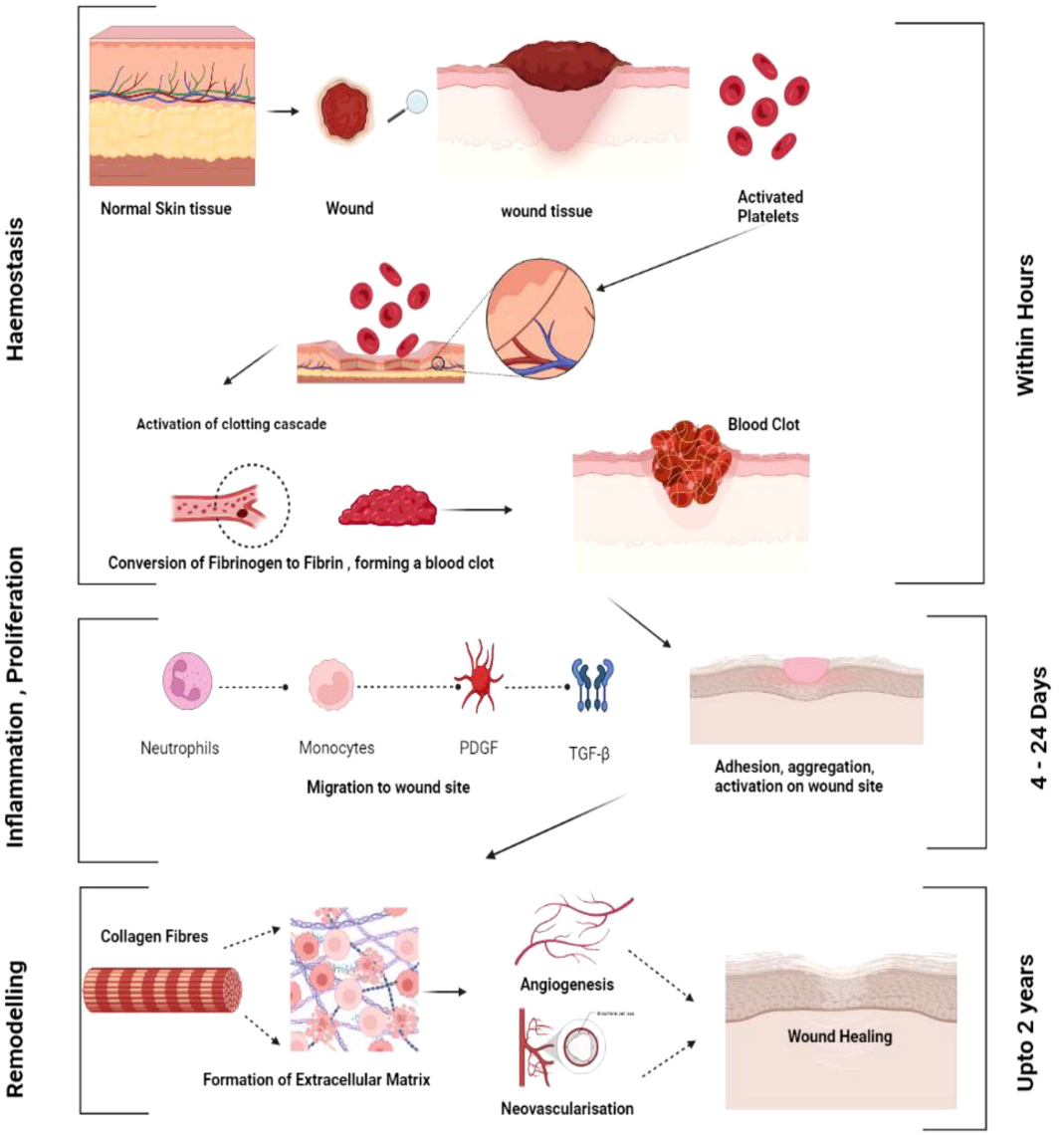

FIGURE 1
General mechanism of wound healing. Various phases of wound healing haemostasis, inflammation, proliferation and remodelling.

the inflammatory phase to the proliferative phase of wound healing. Complex molecular and cellular mechanisms govern this transition. During the inflammatory phase, macrophages are primarily of the pro-inflammatory M1 phenotype. These M1 macrophages produce and release pro-inflammatory cytokines such as interleukin-1 beta (IL-1β), tumor necrosis factor-alpha (TNF-α), interleukin-6 (IL-6), and interleukin-8 (IL-8). They are involved in phagocytosis, secretion of chemokines, and initiating the inflammatory response. However, as the inflammatory response subsides, the wound microenvironment undergoes changes that trigger the transition of macrophages to an anti-inflammatory or alternative-activated M2 phenotype. Several signaling molecules and cytokines contribute to the shift from M1 to M2 phenotype. Transforming growth factor-beta (TGF-β) and IL-10 are key cytokines promoting the M2 phenotype. These cytokines can be produced by other immune cells, such as regulatory T cells and Th2 lymphocytes, as well as by the macrophages themselves in an autocrine manner. Transcription factors play a critical role in regulating gene expression and macrophage polarization. Hypoxia-inducible factor-1 alpha (HIF-1α) and peroxisome proliferator-activated receptor-gamma (PPAR-γ) are two key transcription factors involved in promoting the shift to the M2 phenotype. Hypoxia, which is prevalent during the early stages of wound healing, can stabilize and activate HIF-1α, promoting the expression of M2-associated genes.

Macrophages have a crucial role in all stages of wound healing, especially proliferation and remodeling. Pro-inflammatory macrophages, also known as "M1" macrophages, primarily invade the site of damage to rid it of pathogens, foreign bodies, and dead cells. During the healing process of acute wounds, the local macrophage population changes from being mostly pro-inflammatory (M1) to anti-inflammatory (M2). Pro-inflammatory macrophages (M1) first invade the site of injury and eliminate pathogens, foreign debris, and dead cells. Cytokines that are anti-inflammatory M2 encourage cell migration and proliferation of keratinocytes, fibroblast, and endothelial cells to repair the dermis, epidermis, and vascular system. M2 macrophages have serious subsets such as M2a, M2b, and M2c that are pivotal in the proliferative phases of wound healing. IL-4/IL-13 stimulate M2a macrophages. Collagen precursors are produced by M2a macrophages and thereby stimulate the production of fibroblasts in wound healing. The proliferative phase of wound healing necessitates the production of the extracellular matrix (ECM), which is facilitated by M2a macrophages, and PDGF, which is crucial for the process of angiogenesis and is highly secreted by M2a macrophages. M2b macrophages release IL-6, IL-10, TNF, and express high levels of iNOS and produce MMPs, but they also dampen inflammation by upregulating IL-10 synthesis. M2c is stimulated by IL-10 and TGF-ß and produces high amounts of IL-1ß, MMP-9, IL-10, and TGF-β and significantly low amounts of IL-12. M2c engaged in the remodeling of the vascular structure and extracellular matrix (14).

Growth factors, such as vascular endothelial growth factor (VEGF) and TGF-β, which promote cell proliferation and protein synthesis, are also secreted by anti-inflammatory macrophages (M2 macrophages), along with a range of protease inhibitors, proteases, and anti-inflammatory mediators (15). Granulation tissue begins to replace the interim matrix. Using the intermediate matrix as a scaffold, growth factors released by macrophages promote fibroblast migration into the wound (16). The fibroblasts proliferate and begin producing extracellular matrix elements like collagen (fibroplasia). The development of new capillaries through angiogenesis enhances fibroblast growth. New blood vessels must form from an existing capillary network for the rapidly reproducing cells within the healing wound to receive oxygen and nutrients (17). On the other hand, vascularization is the process of generating new blood vessels from scratch by luring endothelial progenitor cells (also known as EPCs) from the bone marrow. A population of adult stem cells known as EPCs can differentiate into epithelial cells in response to tissue ischemia, promoting endothelial regeneration and neovascularization (18).

Angiogenesis is a dynamic, managed, and regulated process, and its major drivers include proangiogenic chemicals such as fibroblast growth factor-2 (FGF-2) and VEGF, as well as anti-angiogenic compounds that affect endothelial cells. FGF-2 appears to be released due to tissue disintegration during the first three days of wound healing, while VEGF release is mostly prompted by tissue hypoxia over the next three days (19). During the first proliferative phase, a microvascular network of fresh capillaries develops across the granulation tissue. Towards the conclusion of the healing process, blood vessel density declines (20). The proliferation of new capillaries gives the new connective tissue a characteristic granular look, earning it the name granulation tissue. When granulation tissue forms, keratinocytes migrate from the edges of the wound or around skin appendages to the new matrix and re-epithelialize. The incision is covered or epithelialized, and the granulation tissue is covered (21). Some growth factors released from the injured epidermis and encourage the proliferation of epithelial cells include endothelial growth factor (EGF), keratinocyte growth factor, and FGF-2 (22).

Remodeling phase

The remodeling phase of wound healing starts two to three weeks after the initial injury, and granulation tissue eventually develops into scar tissue. The density of blood vessels decreases, and collagen is organized and modified. During the remodeling phase, continuous collagen formation and breakdown occur and are principally kept in balance by the activity of matrix metalloproteinases (23). The tensile strength of the wound increases due to cross-linking, which is facilitated by the closer spacing of newly synthesized collagen fibers across tension lines. Wound contraction is an additional alternative in which myofibroblasts reduce the size of the wound by drawing the margins of the wound together (24).

Pathophysiology of diabetic wound healing

Open wounds that do not heal are referred to as non-healing wounds. Chronic ulcers are those that do not heal after a period of 12 weeks. Chronic diabetic wounds start off like acute wounds, but

the healing process is slowed down and interrupted at several points along the way. As a result, the usual acute ulcer repair is unsuccessful. The healing of wounds depends on several growth factors, including cytokines, proteases, cells, and extracellular elements (25). In diabetic patients, hyperglycemia, chronic inflammation, micro- and macro-circulatory dysfunction, hypoxia, autonomic and sensory neuropathy, and poor neuropeptide signaling all affect the healing of wounds (26). Advanced glycation end products and non-enzymatic glycation of proteins, such as collagen, can result in hyperglycemia (27). The solubility of the extracellular matrix is decreased by these end products, which also maintain the inflammatory changes seen in diabetes (28).

Non-healing wounds occur when there is a deviation from the normal physiological wound healing mechanism, making it a pathological condition. Diabetes and diabetic wounds bypass specific mechanisms in the wound-healing process and impact all three phases of wound-healing mechanisms (29). Firstly, in the inflammation phase, there is an increased infiltration of inflammatory cells in and around the dermis and vessel walls, elevating inflammatory cytokines such as IL-6, IL-1, and TNF-α, which eventually decreases the expression of various growth factors such as TGF-β following a negative feedback mechanism (30). On the other hand, in the proliferative phase, impaired angiogenesis and vasculogenesis eventually immobilize the migration of inflammatory cells that are involved in tissue repair (31). In the remodeling phase, there is an increase in the levels of MMP, which, in turn, degrades the extracellular matrix, which plays an inevitable role in the wound-healing process (20). The molecular mechanisms of wound healing mainly involve three important pathophysiological mechanisms: inflammation, tissue hypoxia, and the extracellular matrix.

Inflammation

Experimental and clinical evidence suggests that, unlike normal wound healing, diabetic wounds do not follow the usual sequence of wound healing mechanisms. There is a deviation from normal mechanisms, with overexpression of IL-1ß, TNF-α, and Monocyte Chemoattractant Proteins (MCP-1) in serum (30). Macrophages are the primary sources of pro-inflammatory cytokines, and macrophage dysfunction is a major pathophysiological mechanism in impaired wound healing in Diabetes. Macrophages play a critical role in the inflammatory phase, where the initiation of wound healing begins by helping in the formation of new tissues. Recent studies suggest the presence of myeloid cells in the wound site, which recruit more pro-inflammatory cytokines, resulting in delayed wound healing (32). Besides macrophages, increased expression of neutrophils also appears to have a harmful effect on wound healing mechanisms, as neutrophil infiltration is a primary process in prolonged inflammation. Other studies support the idea that neutrophil PAD-4 is highly expressed in patients with hyperglycemia and favors delayed wound healing. Treatment targets should focus on PAD-4 deficiency, which may improve wound healing in diabetic patients.

Tissue hypoxia

Hypoxia, or a deficiency in oxygen supply, can significantly affect various cellular processes, including the plasticity of circulating monocytes involved in wound healing. Monocytes are white blood cells that play a crucial role in immune responses and tissue repair. During wound healing, monocytes are recruited to the injured site and differentiate into macrophages, highly versatile cells capable of performing various functions, such as phagocytosis (engulfing and eliminating foreign substances), producing growth factors, and regulating inflammation. This process is known as monocyte/macrophage plasticity.

Hypoxia can affect the expression of various matrix metalloproteinases (MMPs) by monocytes/macrophages. MMPs are enzymes in remodeling the extracellular matrix (ECM), providing structural support to tissues. Hypoxia-induced MMPs can facilitate the breakdown and remodeling of the ECM during wound healing. Hypoxia stimulates the release of angiogenic factors, such as VEGF and platelet-derived growth factor (PDGF), by monocytes/macrophages. These factors promote the formation of new blood vessels (angiogenesis), essential for delivering oxygen and nutrients to the wound site. Hypoxia can modulate the cellular plasticity of circulating monocytes, promoting their recruitment, altering their phenotype, and enhancing their functional properties. These changes contribute to the wound-healing process by regulating inflammation, angiogenesis, ECM remodeling, and tissue repair (9).

The “angiogenic switch” refers to transitioning from limited angiogenesis (formation of new blood vessels) to a highly angiogenic state during certain physiological or pathological conditions. In the proliferative phase of wound healing, the angiogenic switch is crucial in supplying oxygen and nutrients to the healing tissue. During the early stages of wound healing, such as the inflammatory phase, there is initially limited angiogenesis due to vasoconstriction and the formation of blood clots to prevent excessive bleeding. However, as the wound progresses into the proliferative phase, which involves granulation tissue formation and re-epithelialization, the need for increased blood vessel formation arises. Hypoxia, or low oxygen levels, is a key trigger for the angiogenic switch during the proliferative phase of wound healing. When tissues are exposed to hypoxia, various molecular and cellular responses are activated to stimulate angiogenesis. The angiogenic switch, regulated by hypoxia-induced signaling pathways, plays a pivotal role in initiating and promoting angiogenesis during the proliferative phase of wound healing. The balance between proangiogenic and anti-angiogenic factors is dynamically regulated to ensure appropriate blood vessel formation and tissue revascularization.

Clinically, hypoxia refers to increased oxygen consumption by our body beyond its needs or decreased oxygen supply. Hypoxia tends to maintain the levels of Hypoxia Inducible Factor (HIF-1), which regulates numerous cellular processes, including angiogenesis and proliferation, and as a result, can cause delayed wound healing (33). However, the expression of HIF-I genes can lead to impaired angiogenesis and proliferation, resulting in delayed

wound healing. Conversely, the expression of HIF-α genes can improve the wound-healing process.

Extracellular matrix

The Extracellular matrix is a key environmental component in healing diabetic wounds, as it acts as a dynamic scaffold for cells and facilitates tissue development and regeneration (Figure 2). Fibroblasts aid in the rapid formation and deposition of the Extracellular matrix, which promotes not only cellular-level binding but also improves the process of regeneration and angiogenesis (34). The cohesion of the Extracellular matrix depends mainly on endopeptidases such as Matrix Metallo Proteases (MMP) and Tissue Inhibitors of Metalloproteinases (TIMP). In the case of inflammation in diabetic wounds, there is an over-expression of MMP and an under-expression of TIMP. MMP-9 plays a major role in cell migration and proliferation, aiding the wound-healing process by promoting the sequence of events of cell migration, proliferation, and collagen synthesis, thereby promoting wound healing (35).

Cytokines in wound healing

The most significant inflammatory chemicals, cytokines, are produced by tissue macrophages and blood monocytes. When there is an infection, leukocytes produce cytokines, and interleukins are produced toward the target cell. These cytokines cause an increase in IL levels by activating the signals within the target cells. This increase in IL levels can lead to Diabetes and result in a refractory repair and the onset of insulin resistance in patients with DM (Figure 3).

IL- 1β

Both blood monocytes and tissue macrophages produce IL-1β, a significant inflammatory cytokine. Following activation of the NALP3 inflammasome by caspase-1, IL-1ß cytokine is activated in the secretary lysosome by caspase-1 cleavage. In addition to inflammasome activation, IL-1β promotes inflammation by boosting bone marrow-derived leukocyte mobilization and liver-derived acute-phase protein production (36). Increased IL-1β has been associated with developing insulin resistance and slowed wound healing in Diabetes. IL-1β levels are elevated in human diabetic foot ulcers and decrease when the ulcers heal (37). Diabetic human and db/db mouse wound macrophages exhibit elevated IL-1β and NALP3 inflammasome components during the first ten days of healing, and inhibiting the inflammasome was associated with better wound healing in these models (38). Anakinra (Kineret), an IL-1β receptor antagonist, is frequently prescribed to treat rheumatoid arthritis (RA) (39). In normal mice, Anakinra has been shown to be effective at lowering the levels of TNF-α and IL-6 proteins in wound tissue during the first 48 hours following wound healing. Thus, inhibiting IL-1β function in diabetic wounds using neutralizing antibodies or a receptor antagonist may promote wound healing (40).

IL-6

T cells and macrophages secrete the cytokine IL-6, essential for host defense. In addition to promoting the growth of B lymphocytes, IL-6 stimulates the production of neutrophils in the bone marrow and the release of acute-phase proteins from the liver (41). Additionally, it affects leukocyte recruitment by causing endothelial cells to secrete IL-8 and MCP-1. Increased levels of IL-6 are related to insulin resistance and inflammation in β-cells in Diabetes. Rabbits fed the toxic glucose analog alloxan monohydrate have significantly higher levels of IL-6 wound expression than controls (42). They also had significantly delayed wound healing. In macrophages derived from normal mice, hyperglycemia tends to greatly increase IL-6 expression dose-dependently; this finding is likewise supported by mice treated with streptozotocin (STZ) and db/db mice's isolated macrophages (43). Compared to diabetic patients without foot ulcers, acute-phase proteins in the blood and IL-6 were considerably higher in diabetic individuals with foot ulcers. The increased IL-6 expression seen in diabetic wounds appears to correlate highly with glucose levels and wound chronicity. Models of corneal alkali burns have demonstrated that inhibiting the IL-6 receptor reduces inflammation, suggesting a possible usefulness in its application in chronic wounds (44). The anti-IL-6 receptor antibody tocilizumab (Actemra) is proven to effectively lower blood glucose levels in people with Type 2 diabetes (29). If IL-6 antibody therapy fails to reduce its expression in diabetic wound healing, natural therapies may be an alternative in mice given STZ. Injections over a period of seven weeks, curcumin, one of the primary components of turmeric, has been demonstrated to drastically lower circulating plasma levels of IL-6 (45). In contrast, employing curcumin-loaded nanofibers improved wound healing in an STZ-induced diabetes model and decreased the quantity of IL-6 produced *in vitro* from lipopolysaccharide-activated macrophages (46). These findings imply that decreasing levels of circulating IL-6, whether through antibody-mediated or natural means, may be an essential tool in treating diabetic wounds (Figure 4).

IL -10

IL-10 is an inflammatory cytokine that is synthesized by macrophages, dendritic cells, T-helper cells, and activated T-helper cells (47). IL-10R is expressed most in immune cells, especially macrophages, where it inhibits antigen presentation and promotes phagocytosis. IL-10R signaling is necessary for the expansion of anti-inflammatory macrophages that regulate mucosal defense in both mice and humans (48).

Type 2 diabetes, obesity, and decreased blood IL-10 levels are all linked (49). Wound-derived macrophages isolated from db/db mice express less IL-10 protein than those from db/+ mice over a period of seven days. Moreover, STZ-injected animals exhibited a significant decrease in tissue IL-10 protein levels than did control rats seven days after injury (50). IL-10 expression is reduced in

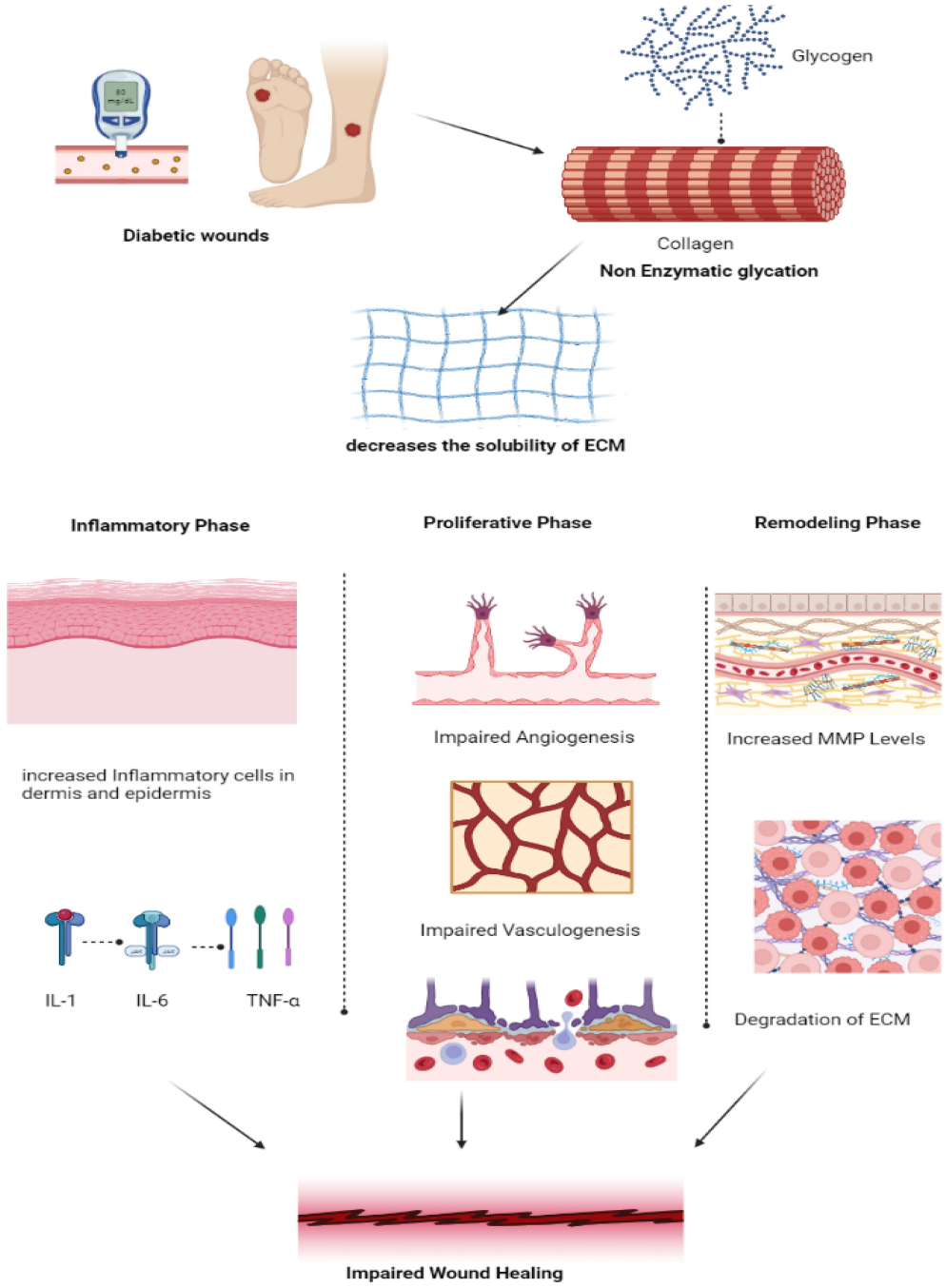

FIGURE 2
Pathogenesis of impaired wound healing in diabetes. In diabetic wounds, there is an impairment in the collagen synthesis thereby decreasing the solubility of the Extracellular matrix promoting increased inflammatory response by the release of pro-inflammatory cytokines IL-1, IL-6 and TNF-α in inflammatory phase. Whereas in proliferative phase, impairment in angiogenesis and vasculogenesis and in remodeling phase increased MMP leads to degradation of ECM thereby resulting in impaired wound healing. (IL – Interleukin, TNF- Tumor Necrosis Factor, MMP- Matrix Metalloproteinase, ECM- Extracellular Matrix).

human diabetic foot ulcers, particularly in endothelial cells and keratinocytes along wound borders (51). Recently, the topical application of curcumin to wounds of STZ-treated rats resulted in elevated IL-10 mRNA and protein levels, improved granulation tissue formation, and enhanced wound contraction (52, 53). As there is an increase in IL-10 in diabetic wounds, inhibiting IL-10 may present an intriguing possibility for enhancing healing.

IL – 17

IL-17 has a potential role in the pathophysiological manifestations of wound healing and could be used as a potential novel target for wound healing therapy (54). The IL-17 cytokine family consists of 5 subtypes: IL-17A, IL-17C, IL-17F, IL-17B, and IL-17E (55). Among these, IL-17B and IL-17E have not been well

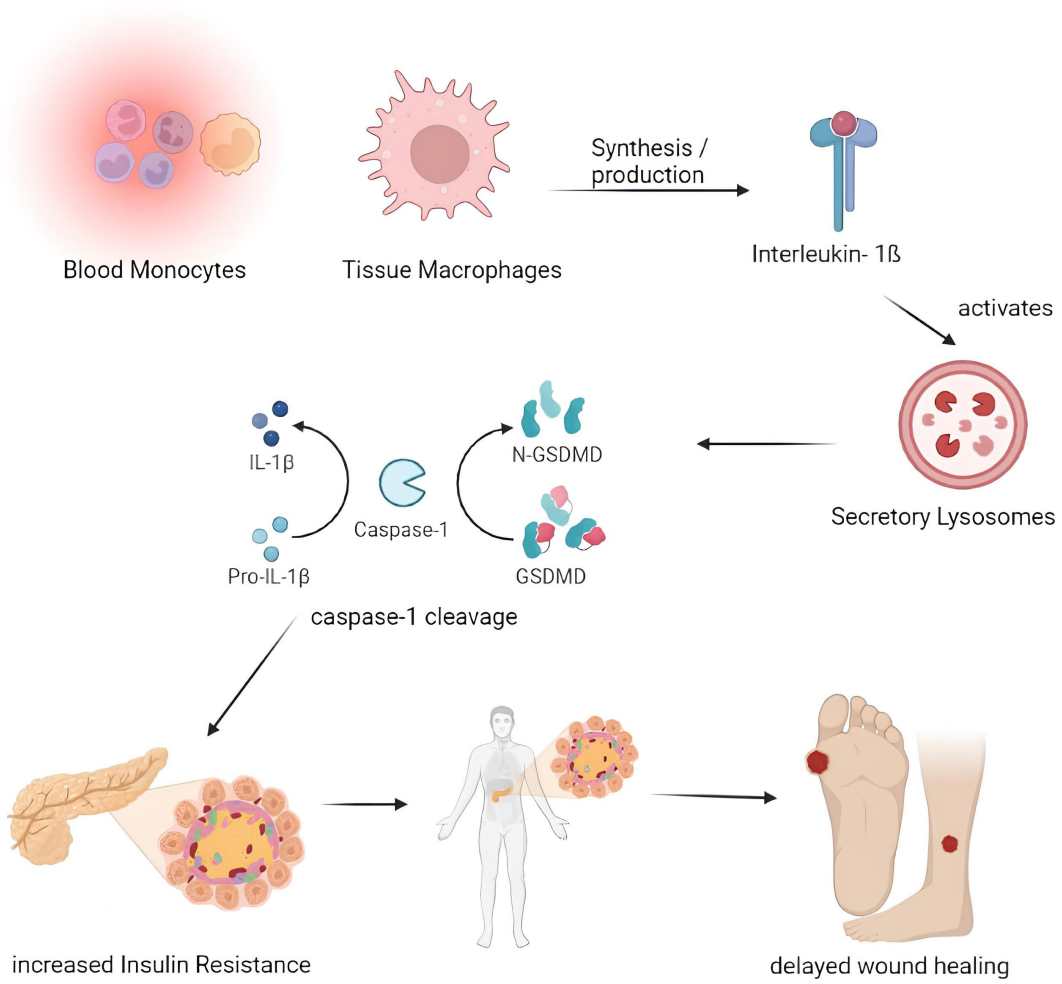

FIGURE 3
Pathogenesis of impaired wound healing involving IL-1β. Blood Monocytes and Tissue Macrophages synthesize the IL-1β which activates the secretory lysosomes and resulting in the Caspase- 1 cleavage through IL-1β and GSDMD which in turn results with increased insulin resistance thereby delays the process of wound healing. (IL – Interleukin, GSDMD - protein gasdermin D).

recognized, as their pathways have not been studied yet. These subfamilies of cytokines readily act upon the keratinocytes and promote the expression of chemokines, which eventually start recruiting more neutrophils to the wound site for the process of neutrophil infiltration, diapedesis, and thereby initiating wound healing (56).

The pathophysiological mechanism involved in IL-17 involves the following sequence of events. Firstly, cells of both innate and adaptive immunity, as well as a wide range of non-hematopoietic cells, activate the release of Transforming Growth Factor-β and several pro-inflammatory cytokines such as IL-1β, IL-6, and IL-23 (57). IL-1β promotes the release of IL-17C from the epithelial cells, while IL-23 stimulates the production of IL-17A and IL-17F from the T-Helper cells, which are the natural killer cells (58). Upon release of the IL-17 family (IL-17A, IL-17C, IL-17F), IL-17A and IL-17F bind with the IL-17RA/RC receptor, and IL-17 binds with the IL-17RA/RE receptor, forming a receptor complex. Upon binding, IL-17A, IL-17C, and IL-17F prompt conformational changes and activate the Act-1 gene, which, in turn, activates Mitogen-Activated Protein Kinase (MAPK) and Nuclear Factor-kβ signaling cascades (59). These signaling pathways lead to the expression of several peptides, chemokines, and cytokines, forming an inflammatory environment preferable for wound healing. Thus, in brief, upregulation of the IL-17-based signaling pathway may result in prolonged inflammation and delayed wound healing (Figure 5). IL-17 has some favorable roles in wound healing through the proliferation of keratinocytes and the release of antimicrobial peptides that could be used as a potential target in wound healing (60). IL-17-based therapeutics are now used in the healing of psoriatic wounds where there seems to be upregulation of IL-17A. The IL-17A receptor antagonist drug Secukinumab, an active monoclonal antibody drug, shows significant therapeutic outcomes in healing psoriatic wounds (61).

IL-2

IL-2 plays a significant role in wound healing as it is involved in the T-cell-mediated immune response and promotes wound healing by improving the strength of healed skin, thereby promoting wound

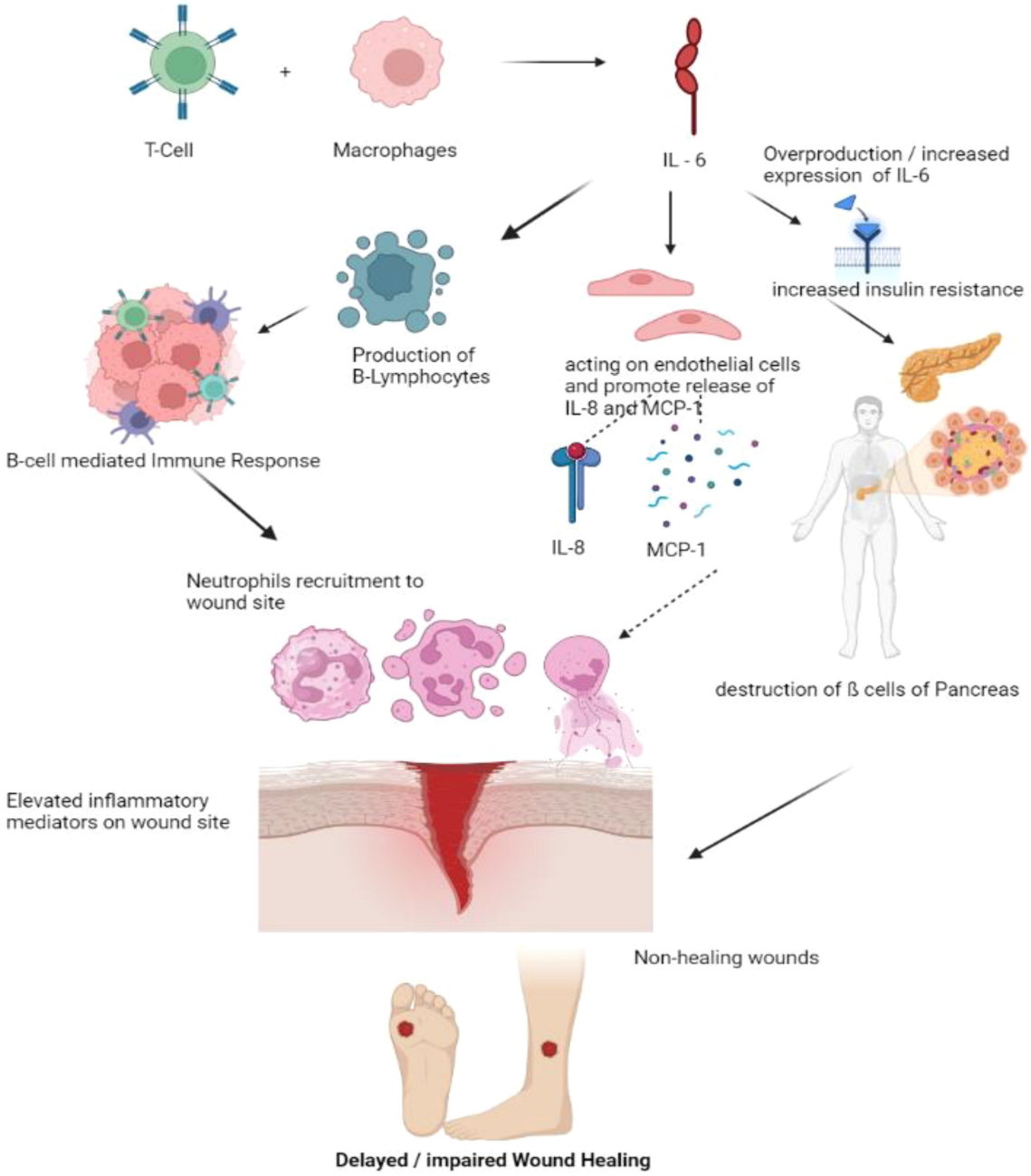

FIGURE 4
Pathogenesis of impaired wound healing involving IL-6. T- Cells and Macrophages secretes the IL-6. Over production or elevated IL-6 levels increases the insulin resistance, Synthesized IL-6 may also generate the B-cell mediated immune response, recruiting more neutrophils to the wound site and also promote the release of IL-8 and MCP thereby recruiting more inflammatory cells to wound site delaying the process of wound healing. (IL – Interleukin, MCP – Monocyte Chemoattractant Protein).

closure (62). Interestingly, most cell types, including skin cells and fibroblasts, express the IL-2 receptors, making them a suitable potential target for site-specific therapies in wound healing (63). IL-2 signaling is a complex cascade of events where IL-2 is produced by various cell types, such as Tetrahydro curcumin (THC), Cytotoxic T Lymphocytes (CTLs), Macrophages, Fibroblasts, and Keratinocytes. IL-2 receptors consist of three sub-units: IL-2Rα, IL-2Rβ, and IL-2Rγ. These subunits may have different affinities toward the specific receptors for IL-2 binding (64). IL-2 cell signaling involves the JAK-STAT pathway, where IL-2 readily binds to the receptors IL-2Rα, IL-2Rβ, and IL-2Rγ. IL-2Rβ recruits JAK-1, while JAK-2 is recruited by IL-2Rγ, and further phosphorylation of these proteins recruits several subtypes of STAT molecules, mainly STAT-1, STAT-3, STAT-5a, and STAT-B. Furthermore, activation of Pi3K and MAP-k results in the activation of the SHC proteins, which end up with mTOR signaling, promoting the process of inflammation and cell proliferation (65). At the wound site, IL-2 activates macrophages and NK cells and promotes the proliferation of B-lymphocytes and T-

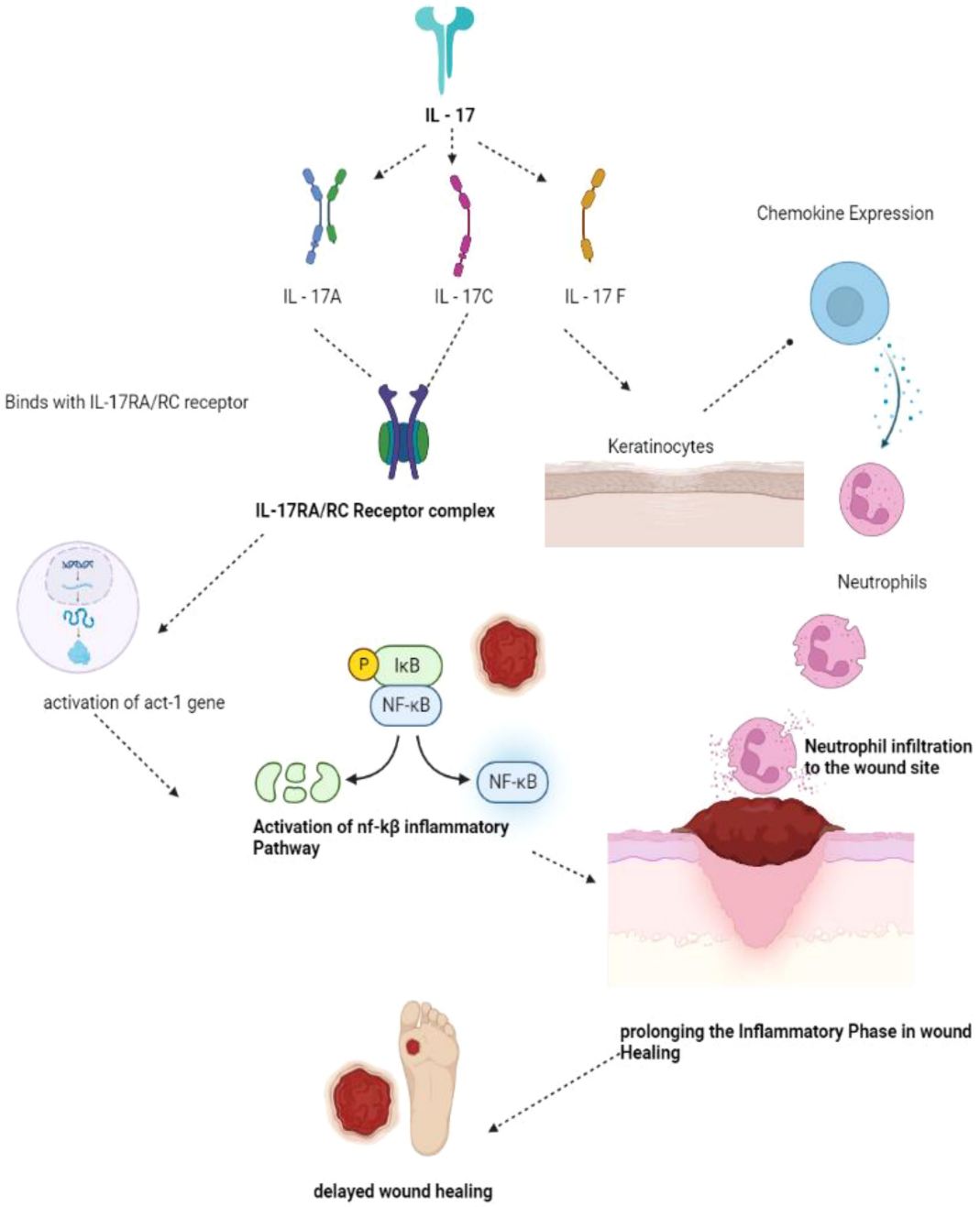

FIGURE 5
IL-17 mechanism of wound healing. IL- 17 has been sub classified as IL-17A, 17C and 17F. IL-17A and 17C binds with IL-17RA/RC forming the receptor complex in turn activates the act-1 gene activates NF-kB pathway of inflammation thereby prolonging the inflammatory phase delaying the wound healing phase. IL-17F acting on the keratinocytes produces neutrophils prolonging inflammatory phase and delaying the process of wound healing. (IL – Interleukins, NF-kB - Nuclear factor kappa B).

lymphocytes. IL-2 plays a crucial role in THC activation and is involved in the development and activation of TH-1 and TH-2, which are necessary for cutaneous wound healing (66).

The current treatment modalities involving IL-2 as a target are used to treat several carcinomas, such as melanoma and renal cell carcinoma (67). The route of administration of IL-2-based targeted therapies also has an impact on treatment. It is evident that systemic therapies of IL-2 have a narrow therapeutic index, and the ideal route of administration of IL-2-based drug therapies is usually intralesional as it is more effective (68). Decreased IL-2 signaling has been reported in patients with Diabetes mellitus due to poor phosphorylation of STAT-5 in the IL-2 signaling cascade as well as single nucleotide polymorphisms (SNP), which can eventually result in aberrant wound healing. IL-2 receptor-mediated targeted therapy will be helpful as it has been observed to be a potential target for wound healing in Diabetes (68).

Role of non- interleukin cytokines

TNF-α, TGF-β, and CRP are non-interleukin cytokines that also play a role in wound healing. TNF-α is a pro-inflammatory cytokine that, when present in lower concentrations, can initiate the process of inflammation in the inflammatory phase of wound healing (69). On the other hand, if present in higher concentrations, it can inhibit the process of wound healing by degrading the extracellular matrix formation in the remodeling phase of wound healing. TNF-α is synthesized mainly by macrophages, other than lymphocytes and adipose tissues. TNF-α, in turn, binds with TNFR-2 and activates the MAP-K and NF-Kβ signaling cascade, promoting the process of wound healing (70).

TGF-β is responsible for the recruitment of neutrophils and monocytes early in the process of wound healing (71). Besides this, it also plays a crucial role in the differentiation of monocytes into macrophages. Consequently, the formation of fibroblasts begins with the process of proliferation, resulting in the formation of an extracellular matrix that promotes wound healing (72). Patients with Diabetes mellitus show a reduction in TGF-β expression, and impaired TGF signaling delays the process of wound healing (32). CRP is one of the most common non-interleukin cytokines that serves as a pattern recognition receptor and increases the production of pro-inflammatory cytokines such as IL6, TNF-α, and IL-1ß, which are necessary for wound healing, mainly in the inflammatory phase of wound healing (73). Patients with Diabetes mellitus have elevated CRP levels in their blood, which can be used as a diagnostic marker in non-healing diabetic wounds (Table 1).

Conventional approaches in wound healing

Diabetes mellitus complications like diabetic foot ulcers are exceedingly costly and challenging to cure. There are numerous topical agents indicated to treat this condition. Magistral preparations are frequently blended to tailor a therapy for a particular patient's problem. This enables the patient to receive treatment that has been customized just for them. This Magistral Preparation of topical antimicrobial agents such as silver nitrate blended with a Peru balsam obtained from Myroxylon pereirae resin has a promising wound healing activity against non-healing diabetic wounds. Since ancient times, silver has been utilized for treating ailments. Silver-impregnated dressings appear to prevent or minimize the risk of amputations in a patient, as silver possesses excellent Antimicrobial Properties. Peru balsam proved to be an excellent antiseptic and antibacterial effect. For the rapid wound healing activity, Glycosaminoglycan derivatives, notably sulodexide, can be added to the Magistral preparations (74).

Despite the availability of several systemic antibiotics, topical antimicrobial treatment is widely used as it has several advantages; it may prevent the use of systemic antibiotics and thereby prevent antimicrobial resistance and improves patient compliance/adherence to the therapy and, most importantly, compared to systemic therapy, the risk of medication toxicity is significantly lower. In the normal course of wound healing, collagen develops, and the precise function of antiseptics is unveiled. Conventionally used Antiseptics are sodium hypochlorite and hexachlorophene, which are not widely used nowadays. The optimal topical agents should be formulated such that they possess antimicrobial capabilities, notably antibacterial activity against numerous gram-positive and gram-negative bacteria, as the wound region is susceptible to infectious pathogens (75). The commonly used topical formulations for treating chronic wounds are described in Table 2.

There are more non-healing wound forms that mirror non-healing diabetic wounds in several ways, mainly Peri -ulcers and vascular ulcers. The tissue surrounding an injury is known as the peri ulcers (also peri-wound). The typical peri-wound area limit is 4 cm, although it may go beyond that if there is skin injury on the exterior of the wound. Before a wound treatment plan is

TABLE 1 Role of pro-inflammatory and anti-inflammatory cytokines in wound healing.

S.No	Phases in Wound Healing	Pro-inflammatory Cytokines	Physiological role	Anti-inflammatory Cytokines	Physiological Role
1.	**Haemostasis Phase**	IL-1ß TNF-α IL-6 IL-8	• Initiate inflammatory response. • Promote vasodilation and increased vascular Permeability.	IL- 10 TGF-ß	• Suppress pro-inflammatory response. • Modulate extracellular matrix production.
2.	**Inflammatory Phase**	IL-1ß TNF-α IL-6 IL-8 IL-12	• Recruit immune cells to the wound site. • Enhance phagocytosis and clearance of debris. • Activate fibroblasts for tissue repair.	IL- 10 TGF-ß	• Limit excessive inflammation. • Promote angiogenesis. • Stimulate collagen synthesis.
3.	**Proliferative Phase**	IL-1ß TNF-α IL-6 IL-8	• Promote angiogenesis. • Induce proliferation and migration of Fibroblasts and Keratinocytes.	IL- 10 TGF-ß	• Stimulate fibroblast proliferation and matrix remodeling. • Support tissue remodeling.
4.	**Remodeling Phase**	IL- 10 TGF-ß	• Control inflammatory response • Modulate extracellular matrix remodeling	IL-1ß TNF-α IL-6 IL-8	• Resolve persistent inflammation. • Promote tissue maturation and stability.

recommended, the peri-wound evaluation is a crucial stage in the wound assessment process. Burning, itching, discomfort, and pain are common in peri-wound patients. Moisture barriers (ointments, salves, and films), topical corticosteroids, antiseptics, and antifungal agents, as well as moisture-regulating dressings like self-adaptive wound dressing, may be used as part of local treatment to protect the peri-wound and maintain its healthy functionality (80).

When the leg veins fail to properly push blood back up to your heart, venous ulcers (open sores) can develop. Pressure rises in the veins as a consequence of blood clotting. The untreated increased pressure and surplus fluid in the damaged region might result in an open sore; this entire process is collectively known as chronic venous insufficiency. The majority of venous ulcers develop on the leg, just above the ankle. This type of wound could take an extended period to heal completely (81).

Novel approaches in chronic wound healing

Wounds are considered chronic if there is a disruption of the normal wound-healing process, resulting in impaired wound healing for at least three months. Diabetic foot ulcers and non-healing pressure ulcers are among the most common types of chronic wounds. Diabetic wounds are particularly detrimental due to changes in the capillary system, such as thickening of the basement membrane, reduction in the size of the capillary vessel, and alterations in glucose levels, which may lead to vasoconstriction and ischemia, making the wound worse. Non-healing ulcers are a significant global burden, affecting over 40 million people per year. The most typical symptoms of chronic wounds are a prolonged inflammatory phase, phenotypic anomalies, including the expression of wound-healing proteins, and impaired formation of the extracellular matrix (82).

The application of different biomaterials and additive manufacturing technology in wound healing has gained significant attention in recent years. These approaches offer innovative solutions to enhance wound healing processes, improve treatment outcomes, and address the challenges associated with traditional wound management. Biomaterials for Wound Dressings, including hydrogels, films, foams, and nanofibers, are used to develop advanced wound dressings. These dressings can provide a moist wound environment, facilitate gas exchange, absorb exudate, and protect the wound from external contaminants. Incorporation of bioactive molecules, such as growth factors, antimicrobial agents, and extracellular matrix components, into the dressings can promote wound healing processes. Scaffold-based Tissue Engineering methods like Biomaterial scaffolds offer a three-dimensional (3D) framework to support cell adhesion, migration, and tissue regeneration. Biomaterial-based skin substitutes and dermal matrices have been developed to promote wound healing and tissue regeneration. These constructs provide a temporary or permanent replacement for damaged or lost skin tissue. They can support cell attachment, proliferation, and differentiation and may include bioactive factors to stimulate angiogenesis and collagen synthesis. Biomaterials can be engineered with bioactive coatings or nanoparticles to provide localized drug delivery systems. These coatings or nanoparticles can release therapeutic agents, growth factors, or antimicrobial agents in a controlled and sustained manner, promoting wound healing and preventing infections. Biomaterials and additive manufacturing techniques can be utilized to develop wearable devices or sensors for real-time monitoring of wound healing parameters. These devices can measure parameters like temperature, pH, moisture, oxygen levels, and biomarker

TABLE 2 Miscellaneous interleukins in wound healing.

S.No	Interleukins	Source	Physiological Function
1.	**Interleukin – 23**	Macrophages and dendritic cells	• IL-23 prompts T cells to continue generating IL-17 by acting on them. Similar signaling pathways can be activated by IL-23 and IL-12; however, IL-23 only slightly activates the STAT4 proteins involved in inflammation. • Additionally, pro-inflammatory cytokines, including IL-1, -6, and TNF- are stimulated by the autocrine/paracrine actions of IL-23 on macrophages underlining IL-23's role in the inflammatory process (76).
2.	**Interleukin - 4**	CD4+T cells (Th2)	• IL-4 influences both B and T cells. It is a B-cell proliferation factor that influences the selection of IgE and IgG1 isotypes. • It promotes Th2 differentiation and proliferation and prevents macrophage activation induced by IFN gamma. By lowering the production of fibronectin, IL-4 hindered the keratinocyte's response to wound healing (77).
3.	**Interleukins – 13**	CD4+T cells (Th2), N.K.T. cells and mast cells	• It influences B cells, epithelial cells, fibroblasts, monocytes, and fibroblasts. Significant effects of IL-13 include stimulation of IgE isotype flipping and B-cell proliferation and differentiation. • Increased collagen synthesis by fibroblasts, increased mucus production by epithelial cells, and inhibition of pro-inflammatory cytokine production are all results of IL-13 activation. Additionally, IL-13 and IL-4 work alongside the biological effects on inflammation & wound healing (78).
4.	**Interleukin - 31**	Th2 cells and dendritic cells.	• IL-31 stimulates the production of chemokines and the synthesis of IL-6, IL-16, and IL-32. • IL-31 aids in generating cell-mediated defenses against infections. It has also been noted to play a significant role in some chronic inflammatory conditions where there is delayed wound healing (69).
5.	**Interleukin - 33**	Mast cells and Th2 lymphocytes	• IL-33, influences a wide range of innate and immunological cells, including dendritic cells, T lymphocytes, and B lymphocytes. The cells seen in barrier areas have high levels of interleukin (IL)-33, which uses the ST2 receptor to transmit signals. • After acute inflammation, IL-33 signaling *via* ST2 is crucial for tissue homeostasis, supporting fibrinogenesis and wound repair at damage sites (79).

concentrations, providing valuable insights into wound healing progression and enabling timely interventions. The application of biomaterials and additive manufacturing technology in wound healing holds great potential to revolutionize wound care by providing tailored and advanced solutions. These approaches aim to accelerate healing, reduce complications, enhance patient comfort, and improve overall outcomes in the management of acute and chronic wounds. Continued research and development in this field are vital to further advance these technologies and bring them into clinical practice.

Macrophage polarization profiling refers to the characterization and classification of macrophages based on their functional properties and behavior. Macrophages are immune cells that play a crucial role in tissue healing and regeneration. They can exhibit different phenotypes or polarization states, broadly classified as pro-inflammatory (M1) or anti-inflammatory (M2). Native and regenerated silk biomaterials are biocompatible materials that have been used in various biomedical applications, including tissue engineering and drug delivery. Understanding how macrophages interact with these biomaterials and how they influence macrophage polarization is important for optimizing their performance and therapeutic outcomes. In a study focusing on macrophage polarization profiling on native and regenerated silk biomaterials, researchers aimed to investigate how these biomaterials modulate macrophage behavior and polarization. The study involved evaluating the response of macrophages to silk biomaterials and characterizing their polarization states. To perform the profiling, macrophages were cultured on the native and regenerated silk biomaterials. Various assays and techniques were employed to assess macrophage polarization, such as gene expression analysis, cytokine secretion profiling, and surface marker analysis. These methods provided insights into the specific polarization states and functional characteristics of macrophages on silk biomaterials. The results of the study shed light on how native and regenerated silk biomaterials influence macrophage polarization. Understanding the macrophage polarization profile on native and regenerated silk biomaterials has implications on the design and development of silk-based biomaterials for tissue engineering and other biomedical applications (83).

The regulation of decellularized matrix-mediated immune response refers to the control and modulation of the immune system's reaction when exposed to decellularized matrices. Decellularized matrices are natural or synthetic materials that have had their cellular components removed, leaving behind the extracellular matrix (ECM) structure. In the context of tissue engineering and regenerative medicine, decellularized matrices are used as scaffolds to support tissue regeneration and repair. However, when these matrices are implanted in the body, they can trigger an immune response. The immune response to decellularized matrices can vary, and it is desirable to regulate this response to promote tissue integration and prevent adverse reactions. Several strategies are employed to achieve immune regulation in decellularized matrix-mediated responses. One approach involves modifying the decellularized matrices to reduce the presence of immunogenic components and increase their biocompatibility. This can be achieved through various methods, such as optimizing the decellularization process, treating the matrices with enzymes or chemicals, or incorporating immunomodulatory factors into the matrices. Another strategy focuses on modulating the immune cells behavior and response to the decellularized matrices. This can be done by incorporating specific molecules or factors into the matrices that promote an anti-inflammatory or immune-tolerant environment. These factors can include growth factors, cytokines, or immunomodulatory agents. Overall, the regulation of decellularized matrix-mediated immune response involves modifying the matrices themselves to reduce immunogenicity, incorporating immunomodulatory factors, and controlling the release of bioactive molecules. These approaches aim to promote tissue integration, minimize inflammation, and improve the overall success of tissue engineering and regenerative medicine therapies using decellularized matrices (84).

Functional hydrogels have emerged as promising materials for diabetic wound management. Diabetic wounds are a significant complication of diabetes and often exhibit impaired healing due to factors such as reduced blood flow, chronic inflammation, and high glucose levels. Functional hydrogels offer unique properties that can address these challenges and promote wound healing. In recent advancements, functional hydrogels have been developed with specific characteristics tailored for diabetic wound management. These hydrogels possess attributes such as high-water content, biocompatibility, flexibility, and controlled release capabilities (Table 3). One key feature of functional hydrogels is their ability to maintain a moist environment at the wound site, which is crucial for optimal healing (85). They can absorb excess wound exudate while providing moisture to the wound bed, promoting cell migration, and facilitating the formation of new tissue. Functional hydrogels also exhibit bioactive properties by incorporating growth factors, antimicrobial agents, and extracellular matrix components. These bioactive components can enhance cell proliferation, angiogenesis, and collagen synthesis, thereby accelerating wound closure and tissue regeneration. Functional hydrogels can modulate the inflammatory response in diabetic wounds. By incorporating anti-inflammatory agents or immune-regulatory molecules, these hydrogels can help mitigate chronic inflammation commonly observed in diabetic wounds and create an environment conducive to healing. Additionally, functional hydrogels can be engineered to provide controlled drug release. They can deliver therapeutic agents such as growth factors, antibiotics, or wound healing-promoting compounds directly to the wound site, ensuring sustained and localized treatment. These hydrogels hold great potential in improving the healing outcomes of diabetic wounds by addressing the specific challenges associated with diabetes-induced impaired wound healing (86).

The current treatment of wounds focuses more on treating their etiology rather than conventional wound care, which involves wound debridement and the use of pre-existing dressings like gauze-woven cotton composite dressings due to their ease of use and cost-effectiveness. However, these conventional dressings have limitations, such as adherence to the wound bed and the presence of moisture, which can be addressed with newer synthetic dressings that provide comfort and promote wound healing. The most

TABLE 3 Different topical agents used in the treatment of non-healing diabetic ulcers.

S.No	Topical Agents	Formulation	Antimicrobial Spectrum	Advantages/Benefits
1.	**Acetic Acid**	Solution (0.5%, 0.25%, 0.1%)	Bactericidal against more gram-positive and gram-negative bacteria – Pseudomonas aeruginosa	Inexpensive and most widely used in wound healing.
2.	**Cetrimide**	Solution (40%)	Active against many bacteria and fungi	Exhibit excellent antiseptic action along with antimicrobial properties.
3.	**Chlorhexidine gluconate**	• Solution (2%, 4%) • Sponges • Wipes	Active against gram-positive bacteria (Staphylococcus aureus) and gram-negative (Pseudomonas aureus)	It exhibits a half-life of 6 hours and acts as a potential antiseptic agent.
4.	**Hexachlorophene**	• Liquid (3%) • Foam (0.23%)	Bacteriostatic against staphylococcus species and other gram-positive bacteria.	It has more retention capacity in the wound site and potentiates the wound-healing process.
5.	**Povidone Iodine**	• Ointment (1%) • Solution (10%)	Broad Spectrum against Staphylococcus aureus and Enterococci.	Potent wound healing activity and anti-allergic.
6.	**Silver Nitrate**	• Solution (0.5%, 10%, 25%) • Ointment (10%)	Silver ions are bactericidal against a broad spectrum of gram-positive and gram-negative bacteria.	Economical and widely used
7.	**Hydrogen Peroxide**	• Solution (1%, 3%) • Cream (1%)	The oxidizing agent, active against many gram-positive and gram-negative bacteria	Easily applicable and economical, widely used in cleansing the wound area.

advanced wound healing formulations available include film, foam, hydrogel, and hydrocolloids, which can be incorporated into conventional dressing materials. Hydrogels have promising wound healing potential in terms of exudate absorption, gas exchange from the wound site, and adherence to the wound bed (87). Newer therapeutic approaches aim to incorporate additives into present dressing materials, including antimicrobial molecules and immunomodulatory cytokines. While biological dressings can interact with the matrix in the wound bed to speed up the healing process, their use is limited due to decreased interaction with the wound tissue. Nanoparticles have a promising role in wound healing, both in terms of drug delivery and intrinsic activity (88).

Nanofibers are fine filaments produced by the process of electrospinning, which is economical and simple. Nanofiber meshes have a significant role in the treatment of wounds, as they partially replicate the extracellular matrix and support wound healing by maintaining moisture in the wound site, preventing wound dehydration and microbial contamination. Nanofibers can be natural polymers, polysaccharides, or proteins (89). The adoption of these technologies and the establishment of novel therapeutic interventions are difficult due to a gap in our complete understanding of the pathophysiological mechanisms at the cellular and molecular level, as well as a lack of data assessing safety and bioavailability differences among individual patients.

Conclusion

Diabetes and its complications remain a global burden, causing a significant increase in mortality and morbidity each year, as reported by WHO's health statistics. Even with the utmost care and disease-specific rational drug therapy, patients may still end up with permanent disabilities such as blindness, amputation, and renal failure. Treating diabetic wounds remains challenging due to the distortion in the tissue repair mechanism and the continuous cutaneous wounds that attract infectious pathogens to invade the wound tissue and form a colony. While surgical intervention by wound debridement is the gold standard and a better therapeutic option for treating diabetic wounds, non-invasive approaches are needed.

The concept of studying the underlying molecular and cellular level mechanisms of wound healing to formulate better therapeutic outcomes has emerged. The complicated process of wound healing is hampered by Diabetes, as shown in Figure 2, which also illustrates how the normal wound healing processes are affected. The initial stage of wound healing involves recruiting many inflammatory cells, such as cytokines, neutrophils, and chemokines. However, this process of recruitment is delayed in diseases like Diabetes. Pro-inflammatory cytokines play a crucial role in initiating wound healing, where there is an upregulation of IL-1ß, TNF-α, IL-6, TGF-ß, and CRP and a downregulation of IL-10. This leads to an unfavorable wound environment for the healing process. Rather than superficially treating diabetic wounds conventionally, which paves the way for re-infections, target-specific pro-inflammatory cytokines-based therapies, either by upregulation or downregulation of them, can be helpful in the wound healing process. This can enhance the quality of life in patients, which is the goal of drug therapy.

Author contributions

Conceptualization, SN, JN, TT, and VS; Resources, VC, GG, NF, MS, SF, GR, SS, LW, and SN; writing—original draft preparation, SN, JN, TT, VS, and VC; writing—review and editing, SN, JN, TT,

and VS. All authors contributed to the article and approved the submitted version.

Conflict of interest

The authors declare that the research was conducted in the absence of any commercial or financial relationships that could be construed as a potential conflict of interest.

Publisher's note

References

1. Khan MAB, Hashim MJ, King JK, Govender RD, Mustafa H, Al Kaabi J. Epidemiology of type 2 diabetes – global burden of disease and forecasted trends. *J Epidemiol Glob Health* (2019) 10(1):107. doi: 10.2991/jegh.k.191028.001

2. Bommer C, Sagalova V, Heesemann E, Manne-Goehler J, Atun R, Bärnighausen T, et al. Global economic burden of diabetes in adults: projections from 2015 to 2030. *Diabetes Care* (2018) 41(5):963–70. doi: 10.2337/dc17-1962

3. Yesudian CA, Grepstad M, Visintin E, Ferrario A. The economic burden of diabetes in India: a review of the literature. *Global Health* (2014) 10(1):80. doi: 10.1186/s12992-014-0080-x

4. Amin N, Doupis J. Diabetic foot disease: from the evaluation of the "foot at risk" to the novel diabetic ulcer treatment modalities. *World J Diabetes* (2016) 7(7):153. doi: 10.4239/wjd.v7.i7.153

5. Verhulst MJL, Loos BG, Gerdes VEA, Teeuw WJ. Evaluating all potential oral complications of diabetes mellitus. *Front Endocrinol (Lausanne)* (2019) 10:1–49. doi: 10.3389/fendo.2019.00056

6. American Diabetes Association. Diagnosis and classification of diabetes mellitus. *Diabetes Care* (2009) 32Suppl 1(Supplement_1):S62–7. doi: 10.2337/dc09-S062

7. Salazar JJ, Ennis WJ, Koh TJ. Diabetes medications: impact on inflammation and wound healing. *J Diabetes Complications* (2016) 30(4):746–52. doi: 10.1016/j.jdiacomp.2015.12.017

8. Periayah MH, Halim AS, Mat Saad AZ. Mechanism action of platelets and crucial blood coagulation pathways in hemostasis. *Int J Hematol Oncol Stem Cell Res* (2017) 11(4):319–27.

9. Rodrigues M, Kosaric N, Bonham CA, Gurtner GC. Wound healing: a cellular perspective. *Physiol Rev* (2019) 99(1):665–706. doi: 10.1152/physrev.00067.2017

10. Singh Y, Fuloria NK, Fuloria S, Subramaniyan V, Almalki WH, Al-Abbasi FA, et al. A European pharmacotherapeutic agent roflumilast exploring integrated preclinical and clinical evidence for SARS CoV-2 mediated inflammation to organ damage. *Br J Clin Pharmacol* (2022) 88(8):3562–5. doi: 10.1111/bcp.15328

11. Wilgus TA, Roy S, McDaniel JC. Neutrophils and wound repair: positive actions and negative reactions. *Adv Wound Care (New Rochelle)* (2013) 2(7):379–88. doi: 10.1089/wound.2012.0383

12. Hirayama D, Iida T, Nakase H. The phagocytic function of macrophage-enforcing innate immunity and tissue homeostasis. *Int J Mol Sci* (2017) 19(1):92. doi: 10.3390/ijms19010092

13. Subramanian S, Duraipandian C, Alsayari A, Ramachawolran G, Wong LS, Sekar M, et al. Wound healing properties of a new formulated flavonoid-rich fraction from dodonaea viscosa jacq. *Leaves Extract Front Pharmacol* (2023) 14:1096905. doi: 10.3389/fphar.2023.1096905

14. Krzyszczyk P, Schloss R, Palmer A, Berthiaume F. The role of macrophages in acute and chronic wound healing and interventions to promote pro-wound healing phenotypes. *Front Physiol* (2018) 9:1–7. doi: 10.3389/fphys.2018.00419

15. Serra MB, Barroso WA, da Silva NN, Silva S do N, Borges ACR, Abreu IC, et al. From inflammation to current and alternative therapies involved in wound healing. *Int J Inflam* (2017) 2017:1–17. doi: 10.1155/2017/3406215

16. Olczyk P, Mencner Ł, Komosinska-Vassev K. The role of the extracellular matrix components in cutaneous wound healing. *BioMed Res Int* (2014) 2014:1–8. doi: 10.1155/2014/747584

17. DiPietro LA. Angiogenesis and wound repair: when enough is enough. *J Leukoc Biol* (2016) 100(5):979–84. doi: 10.1189/jlb.4MR0316-102R

18. Wang D, Li LK, Dai T, Wang A, Li S. Adult stem cells in vascular remodeling. *Theranostics.* (2018) 8(3):815–29. doi: 10.7150/thno.19577

19. Niu G, Chen X. Vascular endothelial growth factor as an anti-angiogenic target for cancer therapy. *Curr Drug Targets* (2010) 11(8):1000–17. doi: 10.2174/138945010791591395

20. Xue M, Jackson CJ. Extracellular matrix reorganization during wound healing and its impact on abnormal scarring. *Adv Wound Care (New Rochelle)* (2015) 4(3):119–36. doi: 10.1089/wound.2013.0485

21. Pastar I, Stojadinovic O, Yin NC, Ramirez H, Nusbaum AG, Sawaya A, et al. Epithelialization in wound healing: a comprehensive review. *Adv Wound Care (New Rochelle)* (2014) 3(7):445–64. doi: 10.1089/wound.2013.0473

22. Demidova-Rice TN, Hamblin MR, Herman IM. Acute and impaired wound healing. *Adv Skin Wound Care* (2012) 25(8):349–70. doi: 10.1097/01.ASW.0000418541.31366.a3

23. Lu P, Takai K, Weaver VM, Werb Z. Extracellular matrix degradation and remodeling in development and disease. *Cold Spring Harb Perspect Biol* (2011) 3(12). doi: 10.1101/cshperspect.a005058

24. Chitturi RT, Balasubramaniam AM, Parameswar RA, Kesavan G, Haris KTM, Mohideen K. The role of myofibroblasts in wound healing, contraction and its clinical implications in cleft palate repair. *J Int Oral Health* (2015) 7(3):75–80.

25. Guo S, DiPietro LA. Factors affecting wound healing. *J Dent Res* (2010) 89(3):219–29. doi: 10.1177/0022034509359125

26. Baltzis D, Eleftheriadou I, Veves A. Pathogenesis and treatment of impaired wound healing in diabetes mellitus: new insights. *Adv Ther* (2014) 31(8):817–36. doi: 10.1007/s12325-014-0140-x

27. Singh VP, Bali A, Singh N, Jaggi AS. Advanced glycation end products and diabetic complications. *Korean J Physiol Pharmacol* (2014) 18(1):1. doi: 10.4196/kjpp.2014.18.1.1

28. Zahoor I, Singh S, Behl T, Sharma N, Naved T, Subramaniyan V, et al. Emergence of microneedles as a potential therapeutics in diabetes mellitus. *Environ Sci pollut Res Int* (2022) 29(3):3302–22. doi: 10.1007/s11356-021-17346-0

29. Pradhan L, Nabzdyk C, Andersen ND, LoGerfo FW, Veves A. Inflammation and neuropeptides: the connection in diabetic wound healing. *Expert Rev Mol Med* (2009) 11:e2. doi: 10.1017/S1462399409000945

30. Brem H, Tomic-Canic M. Cellular and molecular basis of wound healing in diabetes. *J Clin Invest* (2007) 117(5):1219–22. doi: 10.1172/JCI32169

31. Landén NX, Li D, Ståhle M. Transition from inflammation to proliferation: a critical step during wound healing. *Cell Mol Life Sci* (2016) 73(20):3861–85. doi: 10.1007/s00018-016-2268-0

32. Krzyszczyk P, Schloss R, Palmer A, Berthiaume F. The role of macrophages in acute and chronic wound healing and interventions to promote pro-wound healing phenotypes. *Front Physiol* (2018) 9:419. doi: 10.3389/fphys.2018.00419

33. Hong WX, Hu MS, Esquivel M, Liang GY, Rennert RC, McArdle A, et al. The role of hypoxia-inducible factor in wound healing. *Adv Wound Care (New Rochelle)* (2014) 3(5):390–9. doi: 10.1089/wound.2013.0520

34. Tracy LE, Minasian RA, Caterson EJ. Extracellular matrix and dermal fibroblast function in the healing wound. *Adv Wound Care (New Rochelle)* (2016) 5(3):119–36. doi: 10.1089/wound.2014.0561

35. Cabral-Pacheco GA, Garza-Veloz I, Castruita-De la Rosa C, Ramirez-Acuña JM, Perez-Romero BA, Guerrero-Rodriguez JF, et al. The roles of matrix metalloproteinases and their inhibitors in human diseases. *Int J Mol Sci* (2020) 21(24). doi: 10.3390/ijms21249739

36. Fuloria S, Subramaniyan V, Karupiah S, Kumari U, Sathasivam K, Meenakshi DU, et al. A comprehensive review on source, types, effects, nanotechnology, detection, and therapeutic management of reactive carbonyl species associated with various chronic diseases. *Antioxidants (Basel)* (2020) 9(11):1075. doi: 10.3390/antiox9111075

37. Dai J, Shen J, Chai Y, Chen H. IL-1β impaired diabetic wound healing by regulating MMP-2 and MMP-9 through the p38 pathway. *Mediators Inflamm* (2021) 2021:1–10. doi: 10.1155/2021/6645766

38. Mirza RE, Fang MM, Weinheimer-Haus EM, Ennis WJ, Koh TJ. Sustained inflammasome activity in macrophages impairs wound healing in type 2 diabetic humans and mice. *Diabetes* (2014) 63(3):1103–14. doi: 10.2337/db13-0927

39. Goldbach-Mansky R. Blocking interleukin-1 in rheumatic diseases. *Ann N Y Acad Sci* (2009) 1182(1):111–23. doi: 10.1111/j.1749-6632.2009.05159.x

40. Thomay AA, Daley JM, Sabo E, Worth PJ, Shelton LJ, Harty MW, et al. Disruption of interleukin-1 signaling improves the quality of wound healing. *Am J Pathol* (2009) 174(6):2129–36. doi: 10.2353/ajpath.2009.080765

41. Tanaka T, Narazaki M, Kishimoto T. IL-6 in inflammation, immunity, and disease. *Cold Spring Harb Perspect Biol* (2014) 6(10):a016295–a016295. doi: 10.1101/cshperspect.a016295

42. Muller WA. Getting leukocytes to the site of inflammation. *Vet Pathol* (2013) 50 (1):7–22. doi: 10.1177/0300985812469883

43. Qu D, Liu J, Lau CW, Huang Y. IL-6 in diabetes and cardiovascular complications. *Br J Pharmacol* (2014) 171(15):3595–603. doi: 10.1111/bph.12713

44. King AJ. The use of animal models in diabetes research. *Br J Pharmacol* (2012) 166(3):877–94. doi: 10.1111/j.1476-5381.2012.01911.x

45. Genovese MC, Burmester GR, Hagino O, Thangavelu K, Iglesias-Rodriguez M, John GS, et al. Interleukin-6 receptor blockade or TNFα inhibition for reducing glycemia in patients with RA and diabetes: *post hoc* analyses of three randomized, controlled trials. *Arthritis Res Ther* (2020) 22(1):206.

46. Badr AM, Sharkawy H, Farid AA, El-Deeb S. Curcumin induces regeneration of β cells and suppression of phosphorylated-NF-κB in streptozotocin-induced diabetic mice. *J Basic Appl Zoology* (2020) 81(1):22.

47. Tamilarasi GP, Krishnan M, Sabarees G, Gouthaman S, Alagarsamy V, Solomon VR. Emerging trends in curcumin embedded electrospun nanofibers for impaired diabetic wound healing. *Appl Nano* (2022) 3(4):202–32. doi: 10.3390/applnano3040015

48. Trinchieri G. Interleukin-10 production by effector T cells: Th1 cells show self-control. *J Exp Med* (2007) 204(2):239–43. doi: 10.1084/jem.20070104

49. Iyer SS, Cheng G. Role of interleukin 10 transcriptional regulation in inflammation and autoimmune disease. *Crit Rev Immunol* (2012) 32(1):23–63. doi: 10.1615/CritRevImmunol.v32.i1.30

50. Canecki-Varžić S. Association between interleukin-10 gene (-1082g/A) polymorphism and type 2 diabetes, diabetes-related traits, and microvascular complications in the Croatian population. *Acta Clin Croat* (2018) 57(1):71–81.

51. Eming SA, Werner S, Bugnon P, Wickenhauser C, Siewe L, Utermöhlen O, et al. Accelerated wound closure in mice deficient for interleukin-10. *Am J Pathol* (2007) 170 (1):188–202. doi: 10.2353/ajpath.2007.060370

52. Xu F, Zhang C, Graves DT. Abnormal cell responses and role of TNF-α in impaired diabetic wound healing. *BioMed Res Int* (2013) 2013:1–9. doi: 10.1155/2013/754802

53. Yen YH, Pu CM, Liu CW, Chen YC, Chen YC, Liang CJ, et al. Curcumin accelerates cutaneous wound healing *via* multiple biological actions: the involvement of TNF-α, MMP-9, α-SMA, and collagen. *Int Wound J* (2018) 15(4):605–17. doi: 10.1111/iwj.12904

54. Hadian Y, Bagood MD, Dahle SE, Sood A, Isseroff RR. Interleukin-17: potential target for chronic wounds. *Mediators Inflamm* (2019) 2019:1–10. doi: 10.1155/2019/1297675

55. Brevi A, Cogrossi LL, Grazia G, Masciovecchio D, Impellizzieri D, Lacanfora L, et al. Much more than IL-17A: cytokines of the IL-17 family between microbiota and cancer. *Front Immunol* (2020) 11:1–19. doi: 10.3389/fimmu.2020.565470

56. Su Y, Richmond A. Chemokine regulation of neutrophil infiltration of skin wounds. *Adv Wound Care (New Rochelle)* (2015) 4(11):631–40. doi: 10.1089/wound.2014.0559

57. Yu H, Lin L, Zhang Z, Zhang H, Hu H. Targeting NF-κB pathway for the therapy of diseases: mechanism and clinical study. *Signal Transduct Target Ther* (2020) 5(1):209.

58. Zenobia C, Hajishengallis G. Basic biology and role of interleukin-17 in immunity and inflammation. *Periodontol 2000.* (2015) 69(1):142–59. doi: 10.1111/prd.12083

59. Ge Y, Huang M, Yao Ym. Biology of interleukin-17 and its pathophysiological significance in sepsis. *Front Immunol* (2020) 11:1–13. doi: 10.3389/fimmu.2020.01558

60. Majumder S, McGeachy MJ. IL-17 in the pathogenesis of disease: good intentions gone awry. *Annu Rev Immunol* (2021) 39:537–56. doi: 10.1146/annurev-immunol-101819-092536

61. Subramaniyan V, Chakravarthi S, Jegasothy R, Seng WY, Fuloria NK, Fuloria S, et al. Alcohol-associated liver disease: a review on its pathophysiology, diagnosis and drug therapy. *Toxicol Rep* (2021) 8:376–85. doi: 10.1016/j.toxrep.2021.02.010

62. Doersch KM, DelloStritto DJ, Newell-Rogers MK. The contribution of interleukin-2 to effective wound healing. *Exp Biol Med (Maywood)* (2017) 242 (4):384–96. doi: 10.1177/1535370216675773

63. Liao W, Lin JX, Leonard WJ. IL-2 family cytokines: new insights into the complex roles of IL-2 as a broad regulator of T helper cell differentiation. *Curr Opin Immunol* (2011) 23(5):598–604. doi: 10.1016/j.coi.2011.08.003

64. Liao W, Lin JX, Leonard WJ. Interleukin-2 at the crossroads of effector responses, tolerance, and immunotherapy. *Immunity* (2013) 38(1):13–25. doi: 10.1016/j.immuni.2013.01.004

65. Shevach EM. Application of IL-2 therapy to target T regulatory cell function. *Trends Immunol* (2012) 33(12):626–32. doi: 10.1016/j.it.2012.07.007

66. Jiang T, Zhou C, Ren S. Role of IL-2 in cancer immunotherapy. *Oncoimmunology.* (2016) 5(6):e1163462. doi: 10.1080/2162402X.2016.1163462

67. den Otter W, Jacobs JJL, Battermann JJ, Hordijk GJ, Krastev Z, Moiseeva E v, et al. Local therapy of cancer with free IL-2. *Cancer Immunol Immunother* (2008) 57 (7):931–50. doi: 10.1007/s00262-008-0455-z

68. Long SA, Cerosaletti K, Bollyky PL, Tatum M, Shilling H, Zhang S, et al. Defects in IL-2R signaling contribute to diminished maintenance of FOXP3 expression in CD4 (+)CD25(+) regulatory T-cells of type 1 diabetic subjects. *Diabetes* (2010) 59(2):407–15. doi: 10.2337/db09-0694

69. Xu J, Zanvit P, Hu L, Tseng P-Y, Liu N, Wang F, et al. The cytokine TGF-β induces interleukin-31 expression from dermal dendritic cells to activate sensory neurons and stimulate wound itching. *Immunity* (2020) 53:371–83. doi: 10.1016/j.immuni.2020.06.023

70. Zhang JM, An J. Cytokines, inflammation, and pain. *Int Anesthesiol Clin* (2007) 45(2):27–37. doi: 10.1097/AIA.0b013e318034194e

71. Xu F, Zhang C, Graves DT. Abnormal cell responses and role of TNF-α in impaired diabetic wound healing. *BioMed Res Int* (2013) 2013:754802:1–9. doi: 10.1155/2013/754802

72. Pakyari M, Farrokhi A, Maharlooei MK, Ghahary A. Critical role of transforming growth factor beta in different phases of wound healing. *Adv Wound Care (New Rochelle)* (2013) 2(5):215–24. doi: 10.1089/wound.2012.0406

73. el Gazaerly H, Elbardisey DM, Eltokhy HM, Teaama D. Effect of transforming growth factor beta 1 on wound healing in induced diabetic rats. *Int J Health Sci (Qassim)* (2013) 7(2):160–72. doi: 10.12816/0006040

74. Sproston NR, Ashworth JJ. Role of c-reactive protein at sites of inflammation and infection. *Front Immunol* (2018) 9:754. doi: 10.3389/fimmu.2018.00754

75. Nwabudike LC, Tatu AL. Magistral prescription with silver nitrate and Peru balsam in difficult-to-Heal diabetic foot ulcers. *Am J Ther* (2018) 25:e679–80. doi: 10.1097/MJT.0000000000000622

76. Savvatis K, Pappritz K, Becher PM, Lindner D, Zietsch C, Volk H-D, et al. Interleukin-23 deficiency leads to impaired wound healing and adverse prognosis after myocardial infarction. *Circ Heart Fail* (2014) 7:161–71. doi: 10.1161/CIRCHEARTFAILURE.113.000604

77. Serezani APM, Bozdogan G, Sehra S, Walsh D, Krishnamurthy P, Sierra Potchanant EA, et al. IL-4 impairs wound healing potential in the skin by repressing fibronectin expression. *J Allergy Clin Immunol* (2017) 139:142–51. doi: 10.1016/j.jaci.2016.07.012

78. Nguyen JK, Austin E, Huang A, Mamalis A, Jagdeo J. The IL-4/IL-13 axis in skin fibrosis and scarring: mechanistic concepts and therapeutic targets. *Arch Dermatol Res* (2020) 312:81–92. doi: 10.1007/s00403-019-01972-3

79. Di Carmine S, Scott MM, McLean MH, McSorley HJ. The role of interleukin-33 in organ fibrosis. *Discovery Immunol* (2022) 123:1–9. doi: 10.1093/discim/kyac006

80. Dumville JC, Lipsky BA, Hoey C, Cruciani M, Fiscon M, Xia J. Topical antimicrobial agents for treating foot ulcers in people with diabetes. *Cochrane Database Syst Rev* (2017) 6:CD011038. doi: 10.1002/14651858.CD011038.pub2

81. Rowledge A, Miller C, Perry E, McGuiness W, Frescos N. The diabetic foot ulcer periwound: a comparison of visual assessment and a skin diagnostic device. *Wound Pract Res* (2016) 24:1–9.

82. Raffetto JD, Ligi D, Maniscalco R, Khalil RA, Mannello F. Why venous leg ulcers have difficulty healing: overview on pathophysiology, clinical consequences, and treatment. *J Clin Med* (2020) 10:1–7. doi: 10.3390/jcm10010029

83. Roy S, Sharma A, Ghosh S. Macrophage polarization profiling on native and regenerated silk biomaterials. *ACS Biomater Sci Eng* (2022) 8(2):659–71. doi: 10.1021/acsbiomaterials.1c01432

84. Chakraborty J, Roy S, Ghosh S. Regulation of decellularized matrix mediated immune response. *Biomaterials Sci* (2020) 8(5):1194–215. doi: 10.1039/C9BM01780A

85. Ghosal K, Chakraborty D, Roychowdhury V, Ghosh S, Dutta S. Recent advancement of functional hydrogels toward diabetic wound management. *ACS Omega* (2022) 7(48):43364–80. doi: 10.1021/acsomega.2c05538

86. Gao D, Zhang Y, Bowers DT, Liu W, Ma M. Functional hydrogels for diabetic wound management. *APL Bioengineering* (2021) 5(3):89–95. doi: 10.1063/5.0046682

87. Frykberg RG, Banks J. Challenges in the treatment of chronic wounds. *Adv Wound Care (New Rochelle)* (2015) 4(9):560–82. doi: 10.1089/wound.2015.0635

88. Dhivya S, Padma VV, Santhini E. Wound dressings - a review. *Biomed (Taipei)* (2015) 5(4):22. doi: 10.7603/s40681-015-0022-9

89. Azimi B, Maleki H, Zavagna L, de la Ossa JG, Linari S, Lazzeri A, et al. Bio-based electrospun fibers for wound healing. *J Funct Biomater* (2020) 11(3):67. doi: 10.3390/jfb11030067

frontiers | Frontiers in Immunology

TYPE Original Research
PUBLISHED 14 August 2023
DOI 10.3389/fimmu.2023.1249582

OPEN ACCESS

EDITED BY
Pedro Gonzalez-Menendez,
University of Oviedo, Spain

REVIEWED BY
Matthew D. Taylor,
Feinstein Institute for Medical Research, United States
Mahendran Sekar,
Monash University Malaysia, Malaysia

*CORRESPONDENCE
Milica Bajcetic
mbajcetic@doctor.com

RECEIVED 28 June 2023
ACCEPTED 31 July 2023
PUBLISHED 14 August 2023

CITATION
Krasic S, Vukomanovic V, Ninic S, Pasic S, Samardzija G, Mitrovic N, Cehic M, Nesic D and Bajcetic M (2023) Mechanisms of redox balance and inflammatory response after the use of methylprednisolone in children with multisystem inflammatory syndrome associated with COVID-19. *Front. Immunol.* 14:1249582. doi: 10.3389/fimmu.2023.1249582

Mechanisms of redox balance and inflammatory response after the use of methylprednisolone in children with multisystem inflammatory syndrome associated with COVID-19

Stasa Krasic[1], Vladislav Vukomanovic[1,2], Sanja Ninic[1], Srdjan Pasic[2,3], Gordana Samardzija[4], Nemanja Mitrovic[4], Maja Cehic[1], Dejan Nesic[5] and Milica Bajcetic[2,6]*

[1]Cardiology Department, Mother and Child Health Institute of Serbia, Belgrade, Serbia, [2]Faculty of Medicine, University of Belgrade, Belgrade, Serbia, [3]Immunology Department, Mother and Child Health Institute of Serbia, Belgrade, Serbia, [4]Pathology Department, Mother and Child Health Institute of Serbia, Belgrade, Serbia, [5]Faculty of Medicine, Institute of Medical Physiology, University of Belgrade, Belgrade, Serbia, [6]Institute of Pharmacology, Clinical Pharmacology and Toxicology, School of Medicine, University of Belgrade, Belgrade, Serbia

Background: Multisystem inflammatory syndrome in children (MIS-C) associated with being infected with coronavirus-19 (COVID-19) is a life-threatening condition resulting from cytokine storm, increased synthesis of reactive oxygen species (ROSs), and hyperinflammation occurring in genetically predisposed children following an infection with SARS-CoV-2.

Aim: The primary aims of our study were to identify changes in the activity of antioxidant enzymes in erythrocytes and total oxidative status in plasma after being treated with methylprednisolone (MP).

Methods: A prospective cohort study of 67 children (56.7% male) under 18 with MIS-C being treated with MP was conducted at the Mother and Child Health Institute from January 2021 to April 2022. The impact of the therapy was assessed on the basis of the clinical condition, haematological and biochemical blood parameters, and echocardiographic findings.

Results: 59.7% of patients presented cardiovascular (CV) manifestations, while myocardial dysfunction was observed in half of all patients (50.7%). A severe clinical course was observed in 22/67 patients. Children with CV involvement had a significantly higher relative concentration of B lymphocytes and lower relative concentration of NK cells than patients without CV issues ($p < 0.001$ and $p = 0.004$, respectively). Patients with severe MIS-C had a lower relative count of NK cells than those with moderate MIS-C ($p = 0.015$). Patients with myocardial dysfunction had a higher total oxidative plasma status (TOPS) than children without ($p = 0.05$), which implicates pronounced oxidative stress in the former cohort. In patients with shock, lower erythrocytes superoxide dismutase (SOD) activity was observed on admission compared to patients without shock ($p =$

0.04). After MP was administered, TOPS was significantly reduced, while catalase (CAT) and SOD activity increased significantly. Treatment failure (TF) was observed in 6 patients, only females (p=0.005). These patients were younger (p=0.05) and had lower CAT activity on admission (p=0.04) than patients with favorable treatment responses. In the group of patients with TF, TOPS increased after treatment (before 176.2 ± 10.3 mV, after 199.0 ± 36.7 mV).

Conclusion: MP leads to rapid modulation of TOPS and increases the activity of antioxidant enzymes in erythrocytes resulting in clinical and echocardiographic improvement. Based on the observed changes in the activity of the antioxidant enzymes, we can conclude that s hydrogen peroxide is the dominant ROS in patients with MIS-C. Patients with TF showed reduced CAT activity, whereas the treatment with MP led to pronounced oxidation. This implies that low CAT activity may be a contraindication for using MP.

KEYWORDS

MIS-C, oxidation-reduction potential, superoxide dismutase, catalase, lymphocytes immunophenotype, methylprednisolone

Introduction

Multisystem inflammatory syndrome in children (MIS-C) associated with coronavirus-19 (COVID-19) is a life-threatening condition resulting from cytokine storm and hyperinflammation in genetically predisposed children following a symptomatic or asymptomatic infection with SARS-CoV-2. MIS-C manifests 2-6 weeks after the acute COVID-19 condition, and serum SARS-CoV-2 antibodies are detected in most patients (1–8).

Although MIS-C shares some characteristics with toxic shock syndrome (TSS), macrophage activation syndrome (MAS), and Kawasaki disease (KD), the pathophysiological mechanisms of MIS-C are still unknown. The primary pathophysiological mechanism is the uncontrolled activation of the inflammatory cascade that occurs in response to SARS-CoV-2, i.e. as a consequence of the virus-induced autoimmune reaction in genetically susceptible individuals (1, 9).

The virus-induced autoimmune response leads to endothelial dysfunction, increased vascular permeability, capillary leakage, hypoalbuminemia, hyponatremia, hypovolemia, and shock. Hyperinflammation and significant micro-and macrovascular damage lead to an increased synthesis of reactive oxygen species (ROSs) and reactive nitrogen species (RNSs) and to reduced availability and/or increased consumption of antioxidants, disrupting redox homeostasis. The excess of ROSs creates oxidative stress (OS), damaging cellular lipids, proteins, and nucleic acids (10–12).

Previous studies have shown the importance of OS in the acute phase of KD. In patients with KD, administering intravenous immunoglobulins (IVIGs) in the early phase reduces the ROS level and inflammatory response by an independent mechanism; therefore, ROS levels might be a valuable biomarker for evaluating the response to therapy (13–15). Although no prospective studies have investigated OS in MIS-C, and the OS was modulated after the therapy, we believe that OS has a significant pathophysiological role due to its similarity with KD.

The primary study aims were to (1) identify changes in the activity of antioxidant enzymes in erythrocytes following treatment with methylprednisolone (MP) and indirectly assess the activity of dominant reactive species in children with MIS-C associated with COVID-19 (2); identify changes in total oxidative plasma status (TOPS) following treatment with MP (3); evaluate the inflammatory response by determining the peripheral blood immunophenotype. The secondary aim was to determine the correlation between OS parameters and the peripheral blood immunophenotype using biochemical and haematological blood parameters and echocardiographic findings.

Methods

A prospective cohort study of children under 18 with MIS-C associated with COVID-19 was conducted at the Mother and Child Health Institute from January 2021 to April 2022. The MIS-C diagnosis was made according to the WHO's recommendations (4). Patient evaluation on admission involved a detailed medical history, complete physical examination, and standard haematological and biochemical blood analyses. Blood samples were also taken to determine OS parameters, the SARS-CoV-2 antibody level, and the peripheral blood immunophenotype (Figure 1). On admission, an ECG was taken, and an echocardiographic examination was performed. Patients were treated with corticosteroids (CSs) in the form of pulses of MP or MP in standard doses. The treatment protocol is shown in Figure 1.

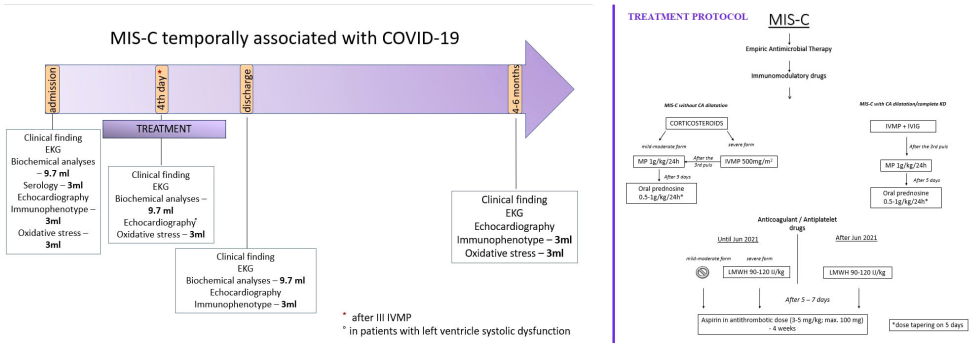

FIGURE 1
The manuscript methodology graphical presentation with our Institutional treatment protocol.

The impact of the therapy was assessed based on the clinical condition, haematological and biochemical blood parameters, and echocardiographic findings. On the third day in the hospital, the following was evaluated: standard haematological and biochemical blood analyses, oxidation-reduction potential, and activity of antioxidant enzymes in erythrocytes. An echocardiographic examination was also performed if the patients had signs of myocardial dysfunction on admission.

Before discharge, standard haematological and biochemical blood analyses, the immunophenotype of peripheral blood lymphocytes, and the echocardiographic examination were re-examined.

The clinical condition, laboratory analyses, redox status, immunophenotype of peripheral blood lymphocytes, and echocardiographic findings were evaluated 4-6 months after the acute illness.

Treatment failure (TF) was defined as the persistence of fever (> 38°C or > 100.4°F) for 48 hours after therapy initiation or the occurrence of acute left ventricular (LV) systolic dysfunction (ejection fraction (EF) < 55%) and a need for vasoactive drugs.

Inclusion criteria

Patients with MIS-C associated with COVID-19 being treated at the Mother and Child Health Institute between January 2021 and April 2022 were included in the study. The diagnosis was made based on the WHO's recommendations (4):

1) Fever and elevated inflammatory markers for 3 days or more,
2) 2 of the following: (A) rash or bilateral non-purulent conjunctivitis or mucocutaneous inflammation signs (oral, hands, or feet); (B) hypotension or shock; (C) features of myocardial dysfunction, pericarditis, valvulitis, or coronary abnormalities (including echocardiogram findings or elevated troponin or N-terminal pro-B-type natriuretic peptide); (D) evidence of coagulopathy (elevated prothrombin time, partial thromboplastin time, and elevated D-dimers); and (E) acute gastrointestinal problems (diarrhoea, vomiting, or abdominal pain),
3) Positive RT-PCR, antigen test, or serology; or any contact with patients with COVID-19,
4) Exclusion: other microbial cause of inflammation.

Exclusion criteria

All children who (1) used antioxidants (2), had elevated oxidative stress: smoking, congenital metabolic diseases, or (3) had chronic kidney disease, systemic or pulmonary hypertension, or endocrinological disorders were excluded from the study.

Ethics statement

Informed written consent was signed by the parents of all children, along with assent where appropriate. Informed consent was given after the nature, and possible consequences of the studies were explained. The Institutional Ethics Committee approved the study (No 8/62).

Determination of oxidative stress parameters

Sample preparation and analysis of antioxidant enzyme activity and oxidation-reduction potential (ORP) were performed at the Institute of Pharmacology, Clinical Pharmacology and Toxicology, Faculty of Medicine in Belgrade.

Activities of erythrocytes antioxidant enzymes

From all subjects, 3 ml of peripheral venous blood was collected with a heparinized syringe (0.2 ml of heparin). Erythrocytes and plasma are separated by centrifugation

(10minutes at 5000 rpm, 4°C). Separated erythrocytes are washed three times with physiological solution by centrifugation (10 minutes at 5000 rpm, 4°C), and thus prepared are stored at -80° C. Before the start of the work, the samples are thawed, and the activity of the enzymes superoxide dismutase (SOD), catalase (CAT), glutathione peroxidase (GSH-Px), glutathione reductase (GR) is determined in them by the spectrophotometry method on the HEλIOS device (Thermo Spectronic, UK).

Aliquots of three times washed erythrocytes were lysed by ice-cold distilled water. Hemoglobin (Hb) concentration was measured by the method of Drabkin and Austin (16). To determine the activity of Cu/Zn SOD, it was necessary to remove hemoglobin by Tsuchihashi (17). The activity of erythrocyte Cu/Zn SOD was measured according to the Misra and Fridovich method, catalase (CAT) according to the Beutler, glutathione reductase (GR) according to the Glatzle, and glutathione peroxidase (GSH-Px) according to Paglia and Valentine method (18–21).

Oxidation-reduction potential (ORP)

TOPS was the static measure of ORP which was determined at room temperature on a RedoxSYS System (AytuBioScience, Inc., Englewood, CO). The plasma (40 μL) sample is dripped onto the previously placed sensor, after which the automatic reading process begins. After 5 seconds, when the ORP values become stable, the millivolts (mV) value is read. Higher TOPS, i.e. static ORP values, stand for pronounced oxidation (22).

Flow cytometry

3 ml of whole blood samples in a tube with EDTA were submitted to the Immunological Laboratory of the Mothers and Children Health Institute of Serbia for lymphocyte immunophenotyping.

100 μl of whole blood was mixed with 20 μl of Multitest™ 6-Color in 1 TBNK tube and the second HU TH1/2/17 Phenotyping Kit. The test tubes were incubated at room temperature, in the dark, for 15 minutes and lysed with FACS lysis buffer (Becton Dickinson) for 15 minutes. Before staining with the HU TH1/2/17 Phenotyping Kit, the sample was incubated with an activation cocktail (Leukocyte Activation Cocktail, with BD GolgiPlug) according to the manufacturer's recommendations. After centrifugation and subsequent washing, the cells were suspended in 400 μl of cell-wash solution (Becton Dickinson) and analyzed using the FACS CANTOII cytometer (Becton Dickinson) in the DIVA software.

Statistics

The descriptive statistics used included mean, median, standard deviation (SD), interquartile range (IQR), and the total number and percentage (%) of monitored parameters. The difference in the distribution of specific parameters among the studied groups was determined using $\chi 2$ or Fisher's test. Shapiro–Wilk and Kolmogorov–Smirnov tests were used to test the normality of the distribution of numerical variables. Groups were compared using Student's t-test and the Mann–Whitney test. Paired t-tests and the Wilcoxon test were used to compare 2 related samples. Pearson or Spearman tests were tested for correlation between parameters in different groups. The data were processed using the statistical software SPSS 25.0 for Windows 10. All statistical methods were considered statistically significant, $p \leq 0.05$

Using a sample size calculator for a significance level (CI) of 95% and a margin of error of 5%, the estimated sample size is 23 patients.

Results

The study included 67 patients, 38 male (56.7%) and 29 female (43.3%); the mean age was 9.2 (IQR 6.3–12.9) years. There was no difference in age between genders (p = 0.2). Serological blood tests for SARS-CoV-2 were positive in 64 patients (95.5%), while 3 (4.5%) had positive PCR or Ag tests from a nasopharyngeal swab.

All patients had a fever lasting a median of 5 (IQR 4-6) days. Most children (75%) had gastrointestinal manifestations. Three patients underwent appendectomies. Hepatitis and pancreatitis were present in 18/67 and 7/67 patients respectively. Cardiovascular manifestation was present in 40/67 patients (59.7%), while myocardial dysfunction was observed in half of all patients (50.7%). Children with myocardial dysfunction were older than patients with normal myocardial function (10.2 (IQR 7.7 – 13.9) vs 7.5 (4.2 – 11.6) years; p = 0.04). A severe clinical course and ICU admission were observed in 22/67 patients. These patients more often had hepatitis (p = 0.003) and pancreatitis (p = 0.004). A 3-year-old boy with moderate MIS-C had intracardiac thrombosis. A 7-year-old patient, who had previously undergone cardiac surgery to correct transposition of the great arteries in the neonatal period, died, on the third day in hospital.

Initial laboratory findings revealed elevated proinflammatory markers (CRP, fibrinogen, D-dimers) and low serum sodium, phosphate, albumin, and platelet counts (Table 1). Elevated cardiac troponin I (cTnI) and proBNP were observed in 44.9% and 83.9% of patients. The average proBNP was 2455.5 pg/mL (IQR 1352.7–>5000). In patients with elevated cTnI, the median cTnI value was 0.27 ng/mL (IQR 0.17–0.59).

Patients' age correlated positively with CRP and fibrinogen on admission (rr = 0.38, p = 0.002; rr = 0.34, p = 0.007, respectively). CRP correlated positively with fibrinogen (rr = 0.35, p = 0.01). The cTnI level on admission correlated positively with proBNP (rr = 0.4, p = 0.009). A moderate positive correlation was found between proBNP and the relative count of B lymphocytes (rr = 0.54, p = 0.007), whereas proBNP correlated negatively with NK cells (rr = -0.58, p = 0.003). A mild to moderate negative correlation was found between proBNP and albumin (rr = -0.3, p = 0.03) and between proBNP and sodium level (rr = -0.27, p = 0.04). CRP and proBNP correlated mildly to moderately positively (rr = 0.31, p = 0.02). A moderate negative correlation was found between platelet count and D-dimers (rr = -0.4, p < 0.001).

In patients with CV manifestations, higher serum concentrations of CRP and proBNP were observed in comparison

TABLE 1 Difference between laboratory analysis at admission, 3rd in hospital day, and at discharge.

Laboratory analysis	Admission	3rd day	discharge	P-value Admission-3rd day Admission-discharge
C-reactive protein (mg/L)	127.8 (92.7-206.8)	50.2 (27.5 – 96)	3.1 (1.4 – 7.3)	<0.001 <0.001
Platelet count (* 10^9)	152 (111.7 – 206.2)	215 (146 – 326)	505 (417 – 640)	<0.001 <0.001
Sodium (mmol/L)	133 (130 – 135)	137 (136 – 139)	137 (136 – 139)	<0.001 <0.001
Albumin (g/L)	35 (31 – 38)	33 (30 – 36)	39 (37 – 41)	0.08 <0.001
Phosphate (mmol/L)	1 (0.85 – 1.17)	1.04 (0.84 – 1.23)	1.29 (1.15 – 1.46)	0.388 <0.001
LDH (IU/L)	546 (473 – 643)	421 (386.2 – 544.5)	434 (363 – 486)	<0.001 <0.001
SGOT (IU/L)	31 (21 – 52)	19.5 (14.2 – 30.5)	21.0 (17.0 – 34.5)	<0.001 <0.001
SGPT (IU/L)	24 (17 – 48)	24 (15 – 48.5)	36 (21 – 61.2)	0.19 0.03
Fibrinogen (g/L)	5.4 (4.1 – 6.6)	3.1 (2.45 – 23.75)	2.4 (2 – 2.8)	0.002 <0.001
D – dimers (ng/mL)	739 (397 – 1445)	549 (327 – 725)	207 (127 – 416)	0.08 <0.001
proBNP (pg/mL)	1907.5 (977.7 – >5000)	2252 (553.9 – 3858.7)	153.0 (86.2 – 292.5)	0.12 <0.001
cTnI (ng/mL)	0.1 (0.05 – 0.25)	0.17 (0.1 – 0.4)	0.1 (0.08 – 0.13)	0.183 0.168
LV EF (%)	58 (52 – 68)	59 (56 – 65)	69 (65 – 73)	0.007 <0.001
LV EDD Z score	0.25 (-0.6 – 0.9)	0.5 (-0.2 – 1.22)	-0.1 (-0.8 – 0.5)	0.4 0.003

LDH, lactate dehydrogenase; SGOT, serum glutamic-oxaloacetic transaminase; SGPT, serum glutamic-pyruvic transaminase; cTnI, cardiac troponin I; proBNP, pro B type natriuretic peptide.

to patients without CV manifestations (CRP 186.5, IQR 117.3–253.7, vs 101.8, IQR 54.2–134.1 mg/L, $p < 0.001$; proBNP 3418, IQR 1576.0–5750.0 vs 938, IQR 406.5–1821, $p < 0.001$). Children with CV involvement had a significantly higher relative concentration of B lymphocytes and lower relative concentration of NK cells than patients without CV manifestations (B cells 35.5, IQR 25.5–46.2 vs 20.5, IQR 12.7–23.2%, $p < 0.001$; NK cells 9.0, IQR 5.75–14.0 vs 15.5, IQR 13.7–19.0%, $p = 0.004$). Patients with severe MIS-C had a lower relative count of NK cells than those with moderate MIS-C (9, IQR 4.5–13.5% vs 14.0, IQR 12.0–17.0%; $p = 0.015$).

The TOPS and the values of individual antioxidant enzymes on admission are shown in Table 2. The CAT level was higher in male patients than in female patients (129668.7 ± 20641.4 vs 96203.8 ± 36893.9µmol H_2O_2/min/g Hb; P=0.006), while girls had a higher GSH-Px level than boys (22.1 ± 4.7 vs 17.1 ± 3.1 µmol NADPH/min/mg Hb; P=0.004). Patients with myocardial dysfunction had a higher TOPS than children without myocardial involvement (191.7, IQR 184.1 – 219.0 vs 171.2, IQR 165.4 – 188.0 mV; P=0.05). A moderate positive correlation was found between TOPS and proBNP (rr = 0.49, $p = 0.01$), TOPS and CRP (rr = 0.4, $p = 0.04$), and TOPS and relative concentration of B lymphocytes (rr = 0.59, $p = 0.004$), while a negative correlation was observed between TOPS and relative concentration of T lymphocytes (rr = -0.52, $p = 0.01$) (Figure 2). In patients with shock, lower erythrocyte SOD activity was observed on admission in comparison to patients without shock (2002.8 ± 255.6 vs 2269.8 ± 341.5 U/g of Hb; P=0.04), and to patients admitted to the ICU (2020.7 ± 231.5 vs 2292.1 ± 355.9 U/g of Hb; P=0.04).

The average LV EF was 50.7 ± 13.2% in patients with myocardial dysfunction. A moderate negative correlation was found between LV EF and the relative count of B lymphocytes (rr = -0.48, $p = 0.017$) and a positive correlation between LV EF and relative NK cells (rr = 0.45, $p = 0.02$). The left ventricle end-diastolic diameter (EDD) Z score correlated positively with TOPS (rr = 0.54, $p = 0.005$) and negatively with SOD activity (rr = -0.45, P=0.02) (Figure 3). A moderate negative correlation was observed between LV EF and proBNP (rr = -0.58, $p < 0.001$), and LV EF and CRP (rr = -0.41, $p = 0.001$).

10.3389/fimmu.2023.1249582

TABLE 2 Total oxidation-reduction potential, activities of antioxidant enzymes from erythrocytes, and lymphocyte immunophenotype before and after methylprednisolone therapy.

	Before treatment	After treatment	P-value	Follow-up
Static ORP(mV)	188 (IQR 169.9 – 211.9)	176.3 (IQR 161.3 – 187.6)	**0.04**	176.7 (IQR160.2 – 200.6)
CAT (µmol H_2O_2/min/gHb)	121715 (IQR 99409.5 – 138218.8)	137833.6 (IQR 122799.1 – 148845.9)	**0.028**	150627 (IQR 138129.1 – 157628.7)
GSH –Px (µmol NADPH/min/mg Hb)	17.9 (IQR 15.2 – 22.1)	17.6 (IQR 15.3 – 20.4)	0.92	12.7 (IQR 10.5 – 15.2)
GR (µmol NADPH/min/mg Hb)	4.8 (IQR 4.4 – 5.6)	4.7 (IQR 4.3 – 5.5)	0.96	4.8 (IQR 4.14 – 5.6)
SOD (U/g of Hb)	2160.1 (IQR 1868.1 – 2507.9)	2665.5 (IQR 2369.5 – 3035.5)	**0.002**	2709.6 (IQR2528.1 – 3135.4)
B-lym(%)	25 (IQR 20.2 – 37.7)	31.5 (IQR 22.2 – 39.7)	0.97	13.5 (IQR 10.2 – 17.5)
T-lym(%)	59.5 (IQR 50.5 – 64.0)	61 (IQR 50.7 – 71.0)	0.12	71 (IQR 68 – 74.5)
CD4/CD3+ (%)	32.5 (IQR 23.7 – 38.0)	30.5 (IQR 26.5 – 34.5)	0.39	35.5 (IQR 31.7 – 37.0)
CD8/CD3+	21.0 (IQR 14.7 – 24.0)	25.0 (IQR 18.2 – 28.5)	0.10	26 (IQR 23.2 – 33.0)
NK cells	13.5 (IQR 7.25 – 15.0)	6.5 (IQR 4.0 – 12.7)	0.08	13 (IQR 11 – 19.25)

ORP, oxidation-reduction potential; Gp-x, glutathione peroxidase; GR, glutathione reductase; SOD, superoxide dismutase.
The bold values have statistically significance.

Treatment

All patients were treated with MP; 79.1% received pulses of MP. Blood samples were taken from all patients after the MP treatment. TOPS decreased significantly, while CAT and SOD increased after MP administration (Table 2). On the other hand, CRP, fibrinogen, D-dimers, and proBNP decreased, while sodium, phosphate, and albumin increased significantly (Table 1). After the therapy, significant improvement in LV EF was observed as soon as the third day in the hospital (p = 0.007), and a significant reduction in LV EDD was observed on discharge (p = 0.003).

TF was observed in 6 patients; all were treated with MP pulses. Only females had TF (P=0.005). These patients were younger than patients with favorable treatment responses (5.8 (IQR 3.3 – 8) vs 9.5 (IQR 6.6 – 13.1) years; P=0.05). These patients had lower CAT activity on admission than those without TF (98942, IQR 79337 - 102569 vs 123378, IQR 109669 – 141778.9 µmol H_2O_2/min/g Hb; P=0.04). Additionally, patients with CAT and SOD activity lower than 117000µmol H_2O_2/min/g Hb and 1800U/g of Hb, respectively, had more frequent TF (p=0.03 and p=0.027, respectively). In the group of patients with TF, no TOPS reduction or CRP were noted (p = 0.42, p = 0.16, respectively). In those patients, TOPS increased

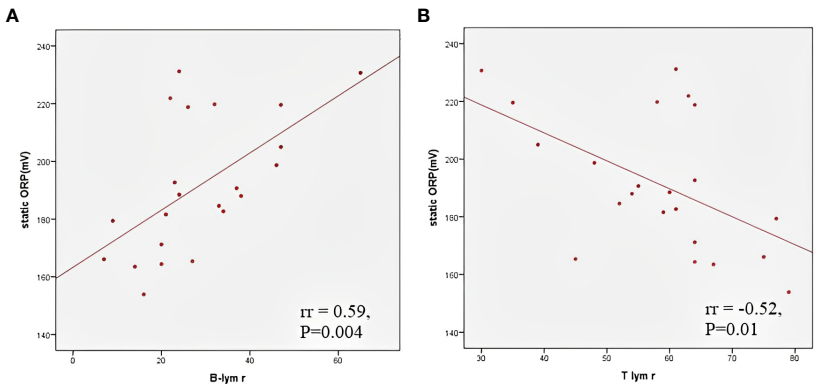

FIGURE 2
Correlation between total oxidation-reduction stress potential and relative B **(A)** and T **(B)** lymphocyte count.

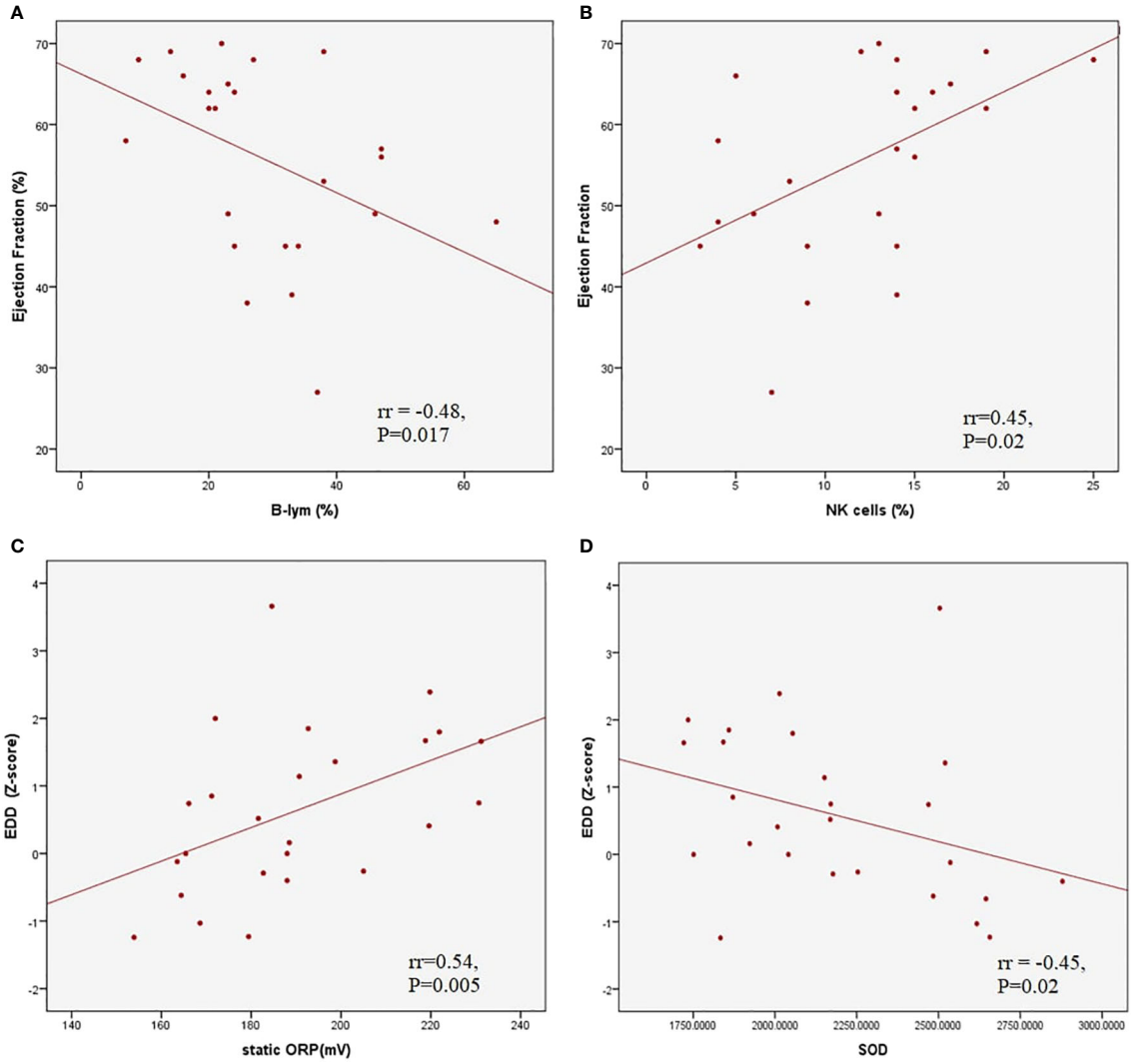

FIGURE 3
Correlations between left ventricle ejection fraction and relative B **(A)** and Natural Killer **(B)** lymphocyte count; correlations between left ventricle end diastolic dimater Z score and total oxidation-reduction potential **(C)** and superoxide dysmutase activity **(D)**.

after treatment (before 176.2 ± 10.3 mV, after 199.0 ± 36.7 mV) (Figure 4). The severity of the clinical presentation did not affect the outcome of the disease and TF.

14 patients received inotropic drug support–dopamine with/without dobutamine for 3 days (IQR 2.5–4.5). In patients treated with dopamine, SOD activity was significantly lower on admission (2020.66 ± 231.5 vs 2292.0 ± 355.9 U/g of Hb; p = 0.04).

Follow-up

Control laboratory analysis was refused by 5.9% of patients' parents (4 patients loss to follow-up), while echocardiography was performed in all children. Control laboratory analysis six months after acute illness yielded entirely normalized results (Table 2). Echocardiography examination identified normal systolic function of the LV (EF 66.4 ± 4.1%) and EDD (Z score 0.12, IQR -0.57–0.59). A significant decrease in the relative count of B lymphocytes was found compared to the relative count of B lymphocytes during acute illness (P = 0.004), while T lymphocytes increased significantly (p = 0.003). In patients with CV manifestations, significant elevation in the relative count of NKs cells was observed in the follow-up period compared to on admission (13, IQR 11–22% vs 9, IQR 5.8–14%; p = 0.04). Reduction of TOPS was observed in comparison to the TOPS on admission (p = 0.04), while SOD and CAT increased significantly (p = 0.001) (Figure 5).

Discussion

The primary pathophysiological mechanism of MIS-C is the uncontrolled activation of the inflammatory cascade in response to SARS-CoV-2 (10).

Clinical presentation in MIS-C patients varies and involves a systemic cytokine storm (IL6, CCL2, CXCL8, CXCL9, CXCL10, CXCL11) with gastrointestinal, cardiac, vascular, hematologic,

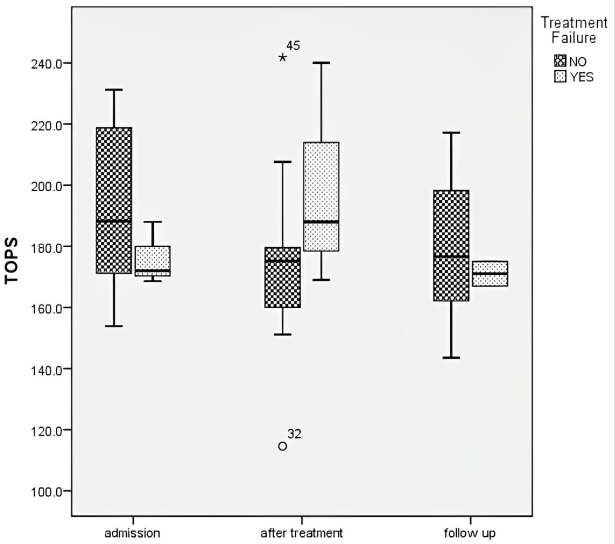

FIGURE 4
Total oxidation-reduction potential dynamics in different groups regarding treatment failure.

mucocutaneous, neurologic, and/or respiratory pathology and fever (23). Half of our patients had myocardial dysfunction, while almost 20% had shock. Myocardial dysfunction was commonly observed in older children. The mortality rate is around 2% (23), but in our study, only 1 patient, who had undergone surgery to correct transposition of the great arteries, died.

Endothelial dysfunction and hyperinflammation increased vascular permeability and decreased sodium, albumin, and phosphate levels, while elevating CRP, fibrinogen, D-dimers, and proBNP. We found a negative correlation between proBNP and sodium and albumin level. In contrast, proBNP correlated positively with CRP. These laboratory findings can be explained by highly intensive inflammation resulting in third-space loss of fluid, sodium, and albumin or renal sodium loss and myocardial dysfunction.

Oxidative has also been suggested as a major mechanism that causes endothelial dysfunction and primary pathophysiological processes in autoimmune diseases, KD, and TSS (10, 11). Additionally, we found that TOPS on admission correlated positively with CRP and proBNP, which means patients with much more intense inflammation had higher TOPS and more pronounced myocardial dysfunction. ROSs can directly impair contractile function by modifying proteins central to excitation-contraction coupling (24), negatively affect the disposition of myocardial calcium (Ca^{2+}), cause arrhythmia, and contribute to cardiac remodeling by inducing hypertrophic signaling, fibrosis, apoptosis, and necrosis (25). Consequently, myocardial stunning in MIS-C might progress to myocardial necrosis. Authors have previously found a relationship between the severity of OS and the New York Heart Association (NYHA) functional class, hs-CRP levels and proBNP in patients with heart failure (26).

Significant endothelial damage and increased cytokine concentration results in an increase in NADPH oxidase and myeloperoxidase (MPO) activity, leading to further "leakage" of superoxide anions (O_2^-) into the extracellular space and increased consumption of antioxidants, resulting in OS. O_2^-, the most abundant radical species, is also the first stage of the bacterial-killing reaction, which is followed by the production of other free radicals, such as hydrogen peroxide (H_2O_2) by SOD (27). We showed that our patients had low SOD levels before MP

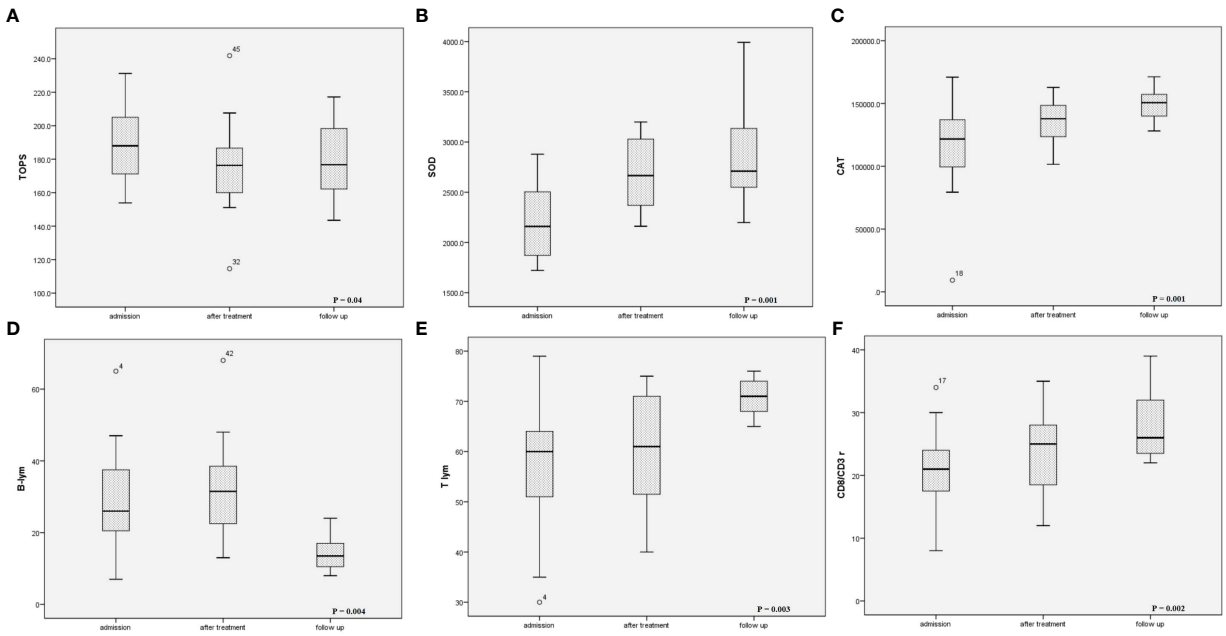

FIGURE 5
Changes of **(A)** oxidation-reduction potential, **(B)** superoxide dismutase activity, **(C)** catalase activity, **(D)** B-lymphocytes relative count, **(E)** T-lymphocytes relative count, and **(F)** CD8/CD3+ during follow up period.

treatment, especially those admitted to the ICU. This is in line with evidence that in patients with a diagnosis of hyperinflammatory syndrome, including MIS-C, there are increases in lipoperoxidation as well as reduced antioxidant capacity (10, 28). Additionally, SOD activity correlated negatively with LV EDD Z score, which can be explained by the fact that O_2^- shows a concentration-dependent negative inotropic effect (29). Abnormal RyR2 function caused by OS leads to diastolic Ca^{2+} leaking and depletes sarcoplasmic reticulum Ca^{2+} stores. It reduces cytoplasmic Ca^{2+} transients, impairing contractile force generation (30).

Coronary artery involvement is more frequent in KD than in MIS-C, with MIS-C patients instead having myocardial stunning, which can be explained by the different cytokine profiles. In KD, elevated IL17A suggests more pronounced arterial damage in KD than in MIS-C, while chemokines lead to myocardial dysfunction (31, 32).

Our patients had elevated B cells and decreased T cells. Additionally, as the total OS increased, the B lymphocyte level increased, and the T cells decreased. Previous studies have shown an increase in absolute numbers of naïve B cells (short-lived plasmablasts), immature B cells, and atypical memory B cells, all of which fit with a potential humoral response in patients with MIS-C, often weeks after clearance of SARS-CoV-2, raising the possibility that these are autoreactive expansions of antibody-secreting cells (25, 33). Patients with CV involvement had higher levels of B cells, which can be explained by the fact that patients with a severe form of MIS-C formed autoantibodies that bind to endothelial cells, contributing to endothelial dysfunction and multisystemic inflammation, which is characteristic of these patients (10, 20, 34, 35). In our MIS C patients before MP therapy, a decrease in LV EF was noted with an increase in the relative concentration of B cells and raised proBNP.

We showed that NK cells were lower in patients with CV involvement. A positive correlation was found between LV EF and NK cells on admission. Patients with myocarditis, dilatative cardiomyopathy (DCM), and coronary artery disease have severely low NK cells and NK cytotoxicity levels, leading to defects in their frequency and functionality. Although myocardial dysfunction in MIS-C has not been shown to be the consequence of direct myocardial injury but rather immune system-mediated myocardial stunning, it has been concluded that NK cells may be able to directly control autoimmune inflammation of the heart, such as in myocarditis or DCM (36, 37).

We have previously shown that CSs are the best choice of drug in patients with MIS-C associated with COVID-19 because they lead to prompt normalization of body temperature, biochemical and haematological blood parameters, and echocardiographic parameters (37, 38).

Through their genomic effects, CSs reduce promoter activities on pro-inflammatory genes and increase the expression of anti-inflammatory mediators. Another mechanism of action of CSs is transrepression, which leads to suppressed expression of immunoregulatory and proinflammatory proteins such as cytokines (IL1, IL2, IL6, TNF-α, IFN-γ) and prostaglandins. The rapid non-genomic effects of CSs also play an essential role, as clinical effects can be observed quickly after administration of high doses, because they promptly reduce the hyperinflammatory response, suppressing vasodilation and increasing vascular permeability by inhibiting the expression of cytokines (TNF-α, IL-6, IL -1α, IL-1β and chemokines: CXCL9 and CXCL10) within a few minutes (Figure 6). IVIGs decrease IL6 concentration on the third and fourth day of the disease, and the level of CXCL9 and CXCL10 decreases after only 5 days (37–39), which could explain the better response to CSs in MIS-C patients (29).

In patients with KD, IVIGs in the early phase reduce the ROS level and the inflammatory response by an independent mechanism (13–15). In our study, in MP-responding patients, the ROS concentration significantly decreased immediately after the end of

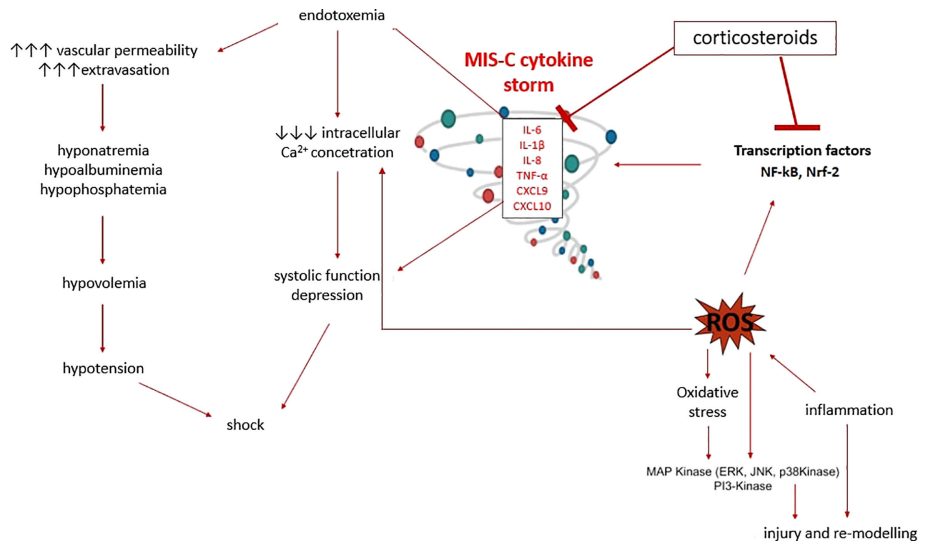

FIGURE 6
MIS-C pathogenesis and corticosteroids effects.

the treatment. TOPS may therefore be a useful biomarker when assessing response to therapy. Additionally, we showed that CAT and SOD activity increased after therapy.

Treatment failure was observed only in the female population and in younger patients. On admission, patients with TF had CAT and SOD activity lower than 117000 μmol H_2O_2/min/g of Hb and 1800U/g of Hb, respectively. Therefore, the combined effect of $O_2^-$and H_2O_2plays a significant role in the TF. In these patients, besides the treatment, TOPS increased.

During the follow-up period, we showed that the relative count of T cells increased, with B cells decreasing in observed patients. Rajamanickam A et al. concluded that 6–9 months post-recovery, the numbers of naïve, immature, and atypical memory B cells were reduced. In contrast, the numbers of classical memory, activated memory, and plasma cells were increased compared to pre-treatment numbers (33). Additionally, the NK cell level increased in patients with CV manifestation during the follow-up period of our investigation. In patients with coronary artery disease, a 12-month follow-up showed that a continued deficiency of NK cells was correlated with low-grade cardiac inflammation. In contrast, patients that had restored circulating NK cells had little to no cardiac inflammation (36). The activity of both enzymes, SOD and CAT, were suppressed at the admission, in the acute phase of illness, before MP therapy. The reduction of hyperinflammation in our study was accompanied by restoring the activity of the SOD and CAT, the enzymes of antioxidant defense, during the 4 to 6 months follow-up period.

Limitations

The most significant limitation of the study is the limited number of patients, which makes it difficult to derive definitive statements about pathogenesis and redox balance modulation after the therapy was applied. Randomized multicentre studies need to be conducted in order to establish treatment protocols with a significant level of recommendation.

Conclusion

The etiopathogenesis of and best treatment for MIS-C associated with COVID-19 are still unknown, but it is a life-threatening condition which other viruses can probably provoke. Our study showed that humoral immune cells play a significant role in the pathogenesis of MIS-C, while patients with a low concentration of NK cells develop myocardial dysfunction. In the acute phase, ROS are elevated, and the dominant ROS is hydrogen peroxide. Erythrocytes serve as a sink for hydrogen peroxide in the circulation and, in this way, protect blood vessels. Patients with significantly greater inflammation had higher TOPS and proBNP with myocardial dysfunction. We have previously suggested MP as the best-choice therapy for MIS-C. The use of MP leads to a rapid modulation of TOPS, which correlates with an improvement in the clinical condition and a decrease in the concentration of positive reactants (CRP, fibrinogen) of the acute phase and an increase in negative reactants (albumin). MP treatment led to a rapid increase in antioxidant defence enzymes. TF was noted in younger children and girls only. These patients had significantly lower CAT values on admission, meaning that hydrogen peroxide significantly influenced the severity of the clinical presentation and the response to the therapy applied.

Data availability statement

The original contributions presented in the study are included in the article/supplementary materials, further inquiries can be directed to the corresponding author/s.

Ethics statement

The studies involving humans were approved by Mother and Child Health Institute of Serbia. The studies were conducted in accordance with the local legislation and institutional requirements. Written informed consent for participation in this study was provided by the participants' legal guardians/next of kin.

Author contributions

All authors have been active participants in the research (including participation in the conception, execution, and writing of the manuscript). Authors confirm: that the work described has not been published before; that it is not under consideration for publication anywhere else; that its publication has been approved by all co-authors, as well as by the responsible authorities.

Funding

The work was supported by the Ministry of Education, Science and Technological Development of the Republic of Serbia, Grant No. OI173014.

Acknowledgments

We thank Miss Verica Bogdanovic for her technical assistance in the laboratory.

Conflict of interest

The authors declare that the research was conducted in the absence of any commercial or financial relationships that could be construed as a potential conflict of interest.

Publisher's note

References

1. McMurray JC, May JW, Cunningham MW, Jones OY. Multisystem inflammatory syndrome in children (MIS-C), a post-viral myocarditis and systemic vasculitis—A critical review of its pathogenesis and treatment. *Front Pediatr* (2020) 8:1123. doi: 10.3389/fped.2020.626182

2. Radia T, Williams N, Agrawal P, Harman K, Weale J, Cook J, et al. Multi-system inflammatory syndrome in children & adolescents (MIS-C): A systematic review of clinical features and presentation. *Paediatr Respir Rev* (2021) 38:51–7. doi: 10.1016/j.prrv.2020.08.001

3. Pouletty M, Borocco C, Ouldali N, Caseris M, Basmaci R, Lachaume N, et al. Paediatric multisystem inflammatory syndrome temporally associated with SARS-CoV-2 mimicking Kawasaki disease (Kawa-COVID-19): A multicentre cohort. *Ann Rheumatic Dis* (2020) 79(8):999–1006. doi: 10.1136/annrheumdis-2020-217960

4. Jiang L, Tang K, Levin M, Irfan O, Morris SK, Wilson K, et al. COVID-19 and multisystem inflammatory syndrome in children and adolescents. *Lancet Infect Dis [Internet]* (2020) 20(11):e276–88. doi: 10.1016/S1473-3099(20)30651-4

5. Brodsky NN, Ramaswamy A, Lucas CL. The mystery of MIS-C post-SARS-CoV-2 infection. *Trends Microbiol* (2020) 28(12):956–8. doi: 10.1016/j.tim.2020.10.004

6. Lai CC, Shih TP, Ko WC, Tang HJ, Hsueh PR. Severe acute respiratory syndrome coronavirus 2 (SARS-CoV-2) and coronavirus disease-2019 (COVID-19): The epidemic and the challenges. *Int J Antimicrob Agents* (2020) 55(3):105924. doi: 10.1016/j.ijantimicag.2020.105924

7. Yousef MS, Idris NS, Yap C, Alsubaie AA, Kakodkar P. Systematic review on the clinical presentation and management of the COVID-19 associated multisystem inflammatory syndrome in children (MIS-C). *AIMS Allergy Immunol* (2021) 5 (1):38–55. doi: 10.3934/Allergy.2021004

8. Ahmed M, Advani S, Moreira A, Zoretic S, Martinez J, Chorath K, et al. Multisystem inflammatory syndrome in children: A systematic review. *EClinicalMedicine* (2020) 26:100527. doi: 10.1016/j.eclinm.2020.100527

9. Bohn MK, Yousef P, Steele S, Sepiashvili L, Adeli K. MultiInflammatory syndrome in children: A view into immune pathogenesis from a laboratory perspective. *J Appl Lab Med* (2021) 7(1):1–11. doi: 10.1093/jalm/jfab114

10. Graciano-Machuca O, Villegas-Rivera G, López-Pérez I, Macías-Barragán J, Sifuentes-Franco S. Multisystem inflammatory syndrome in children (MIS-C) following SARS-CoV-2 infection: role of oxidative stress. *Front Immunol* (2021) 12:110. doi: 10.3389/fimmu.2021.723654

11. Perrone S, Cannavò L, Manti S, Rullo I, Buonocore G, Esposito SMR, et al. Pediatric multisystem syndrome associated with SARS-CoV-2 (MIS-C): the interplay of oxidative stress and inflammation. *Int J Mol Sci* (2022) 23(21):12836. doi: 10.3390/ijms232112836

12. Rahal A, Kumar A, Singh V, Yadav B, Tiwari R, Chakraborty S, et al. Oxidative stress, prooxidants, and antioxidants: the interplay. *BioMed Res Int* (2014) 2014:761264. doi: 10.1155/2014/761264

13. Yahata T, Hamaoka K. Oxidative stress and Kawasaki disease: how is oxidative stress involved from the acute stage to the chronic stage? *Rheumatol (Oxford)* (2017) 56 (1):6–13. doi: 10.1093/rheumatology/kew044

14. Ishikawa T, Seki K. The association between oxidative stress and endothelial dysfunction in early childhood patients with Kawasaki disease. *BMC Cardiovasc Disord* (2018) 18(1):30. doi: 10.1186/s12872-018-0765-9

15. Kaneko K, Takahashi M, Yoshimura K, Kitao T, Yamanouchi S, Kimata T, et al. Intravenous immunoglobulin counteracts oxidative stress in Kawasaki disease. *PediatrCardiol* (2012) 33(7):1086–8. doi: 10.1007/s00246-012-0229-4

16. Drabkin D, Austin H. Spectrophotometric studies: Preparations from washed blood cells. *J Biol Chem* (1935) 112:51–5. doi: 10.1016/S0021-9258(18)74965-X

17. Tsuchihashi M. Zur kenntnis der blutkatalase. *Biochem Z* (1923) 140:65–72.

18. Misra HP, Fridovich I. The role of superoxide anion in the autoxidation of epinephrine and a simple assay for superoxide dismutase. *J Biol Chem* (1972) 247:3170–5. doi: 10.1016/S0021-9258(19)45228-9

19. Beutler E. Catalase. A manual of biochemical methods. In: Beutler E, editor. *Red cell metabolism*. New York, NY: Grune and Stratton (1982). p. 105–6.

20. Paglia DE, Valentine WN. Studies on the quantitative and qualitative characterization of erythrocyte glutathione peroxidase. *J Lab Clin Med* (1967) 70:158–69.

21. Glatzle D, Vuilleumier JP, Weber F, Decker K. Glutathione reductase test with whole blood, a convenient procedure for the assessment of the riboflavin status in humans. *Experientia.* (1974) 30:665–7. doi: 10.1007/BF01921531

22. Opačić M, Stević Z, Baščarević V, Živić M, Spasić M, Spasojević I. Can oxidation-reduction potential of cerebrospinal fluid be a monitoring biomarker in amyotrophic lateral sclerosis? *Antioxid Redox Signal* (2018) 28(17):1570–5. doi: 10.1089/ars.2017.7433

23. Ramaswamy A, Brodsky NN, Sumida TS, Comi M, Asashima H, Hoehn KB, et al. Immune dysregulation and autoreactivity correlate with disease severity in SARS-CoV-2-associated multisystem inflammatory syndrome in children. *Immunity* (2021) 54(5):1083–1095.e7. doi: 10.1016/j.immuni.2021.04.003

24. Tsutsui H, Kinugawa S, Matsushima S. Oxidative stress and heart failure. *Am J Physiol Heart Circ Physiol* (2011) 301(6):H2181–90. doi: 10.1152/ajpheart.00554.2011

25. Münzel T, Camici GG, Maack C, Bonetti NR, Fuster V, Kovacic JC. Impact of oxidative stress on the heart and vasculature: part 2 of a 3-part series. *J Am Coll Cardiol* (2017) 70(2):212–29. doi: 10.1016/j.jacc.2017.05.035

26. Szczurek W, Szyguła-Jurkiewicz B. Oxidative stress and inflammatory markers - the future of heart failure diagnostics? *Kardiochir Torakochirurgia Pol* (2015) 12 (2):145–9. doi: 10.5114/kitp.2015.52856

27. Bajčetić M, Spasić S, Spasojević I. Redox therapy in neonatal sepsis: reasons, targets, strategy, and agents. *Shock* (2014) 42(3):179–84. doi: 10.1097/SHK.0000000000000198

28. Alonso de Vega JM, Díaz J, Serrano E, Carbonell LF. Oxidative stress in critically ill patients with systemic inflammatory response syndrome. *Crit Care Med* (2002) 30 (8):1782–6. doi: 10.1097/00003246-200208000-00018

29. Schrier GM, Hess ML. Quantitative identification of superoxide anion as a negative inotropic species. *Am J Physiol* (1988) 255(1 Pt 2):H138–43. doi: 10.1152/ajpheart.1988.255.1.H138

30. Aimo A, Castiglione V, Borrelli C, Saccaro LF, Franzini M, Masi S, et al. Oxidative stress and inflammation in the evolution of heart failure: From pathophysiology to therapeutic strategies. *Eur J Prev Cardiol* (2020) 27(5):494–510. doi: 10.1177/2047487319870344

31. Consiglio CR, Cotugno N, Sardh F, Pou C, Amodio D, Rodriguez L, et al. The immunology of multisystem inflammatory syndrome in children with COVID-19. *Cell* (2020) 183(4):968–81. doi: 10.1016/j.cell.2020.09.016

32. Altara R, Mallat Z, Booz GW, Zouein FA. The CXCL10/CXCR3 axis and cardiac inflammation: implications for immunotherapy to treat infectious and noninfectious diseases of the heart. *J Immunol Res* (2016) 2016:4396368. doi: 10.1155/2016/4396368

33. Rajamanickam A, Nathella PK, Venkataraman A, Varadarjan P, Kannan S, Pandiarajan AN, et al. Unique cellular immune signatures of multisystem inflammatory syndrome in children. *PloS Pathog* (2022) 18(11):e1010915. doi: 10.1371/journal.ppat.1010915

34. Gruber CN, Patel RS, Trachtman R, Lepow L, Amanat F, Krammer F, et al. Mapping systemic inflammation and antibody responses in multisystem inflammatory syndrome in children (MIS-C). *Cell* (2020) 183(4):982–995.e14. doi: 10.1016/j.cell.2020.09.034

35. Carter MJ, Fish M, Jennings A, Doores KJ, Wellman P, Seow J, et al. Peripheral immunophenotypes in children with multisystem inflammatory syndrome associated with SARS-CoV-2 infection. *Nat Med* (2020) 26(11):1701–7. doi: 10.1038/s41591-020-1054-6

36. Ong S, Rose NR, Čiháková D. Natural killer cells in inflammatory heart disease. *Clin Immunol* (2017) 175:26–33. doi: 10.1016/j.clim.2016.11.010

37. VukOmanovic VA, Krasic S, Prijic S, Ninic S, Minic P, Petrovic G, et al. Differences between pediatric acute myocarditis related and unrelated to SARS-CoV-2. *Pediatr Infect Dis J* (2021) 40(5):E173–8. doi: 10.1097/INF.0000000000003094

38. VukOmanovic V, Krasic S, Prijic S, Ninic S, Popovic S, Petrovic G, et al. Recent experience: corticosteroids as a first-line therapy in children with multisystem inflammatory syndrome and COVID-19-related myocardial damage. *Pediatr Infect Dis J* (2021) 40(11):e390–4. doi: 10.1097/INF.0000000000003260

39. Caldarale F, Giacomelli M, Garrafa E, Tamassia N, Morreale A, Poli P, et al. Plasmacytoid dendritic cells depletion and elevation of IFN-γ Dependent chemokines CXCL9 and CXCL10 in children with multisystem inflammatory syndrome. *Front Immunol* (2021) 12:113. doi: 10.3389/fimmu.2021.654587

frontiers | Frontiers in Immunology

TYPE Brief Research Report
PUBLISHED 28 September 2023
DOI 10.3389/fimmu.2023.1258027

OPEN ACCESS

EDITED BY
Pablo Andres Evelson,
University of Buenos Aires, Argentina

REVIEWED BY
Mahendran Sekar,
Monash University Malaysia, Malaysia
Martin F. Desimone,
University of Buenos Aires, Argentina

*CORRESPONDENCE
Ulrich Flögel
floegel@uni-duesseldorf.de

RECEIVED 13 July 2023
ACCEPTED 11 September 2023
PUBLISHED 28 September 2023

CITATION
Flocke V, Temme S, Bouvain P, Grandoch M and Flögel U (2023) Noninvasive assessment of metabolic turnover during inflammation by *in vivo* deuterium magnetic resonance spectroscopy. *Front. Immunol.* 14:1258027. doi: 10.3389/fimmu.2023.1258027

Noninvasive assessment of metabolic turnover during inflammation by *in vivo* deuterium magnetic resonance spectroscopy

Vera Flocke[1], Sebastian Temme[2,3], Pascal Bouvain[1], Maria Grandoch[3,4] and Ulrich Flögel[1,3]*

[1]Experimental Cardiovascular Imaging, Institute for Molecular Cardiology, Heinrich Heine University Düsseldorf, Düsseldorf, Germany, [2]Department of Anaesthesiology, University Hospital Düsseldorf, Düsseldorf, Germany, [3]University Hospital Düsseldorf, Cardiovascular Research Institute Düsseldorf (CARID), Düsseldorf, Germany, [4]Institute for Translational Pharmacology, Heinrich Heine University Düsseldorf, Düsseldorf, Germany

Background: Inflammation and metabolism exhibit a complex interplay, where inflammation influences metabolic pathways, and in turn, metabolism shapes the quality of immune responses. Here, glucose turnover is of special interest, as proinflammatory immune cells mainly utilize glycolysis to meet their energy needs. Noninvasive approaches to monitor both processes would help elucidate this interwoven relationship to identify new therapeutic targets and diagnostic opportunities.

Methods: For induction of defined inflammatory hotspots, LPS-doped Matrigel plugs were implanted into the neck of C57BL/6J mice. Subsequently, $^{1}H/^{19}F$ magnetic resonance imaging (MRI) was used to track the recruitment of ^{19}F-loaded immune cells to the inflammatory focus and deuterium (^{2}H) magnetic resonance spectroscopy (MRS) was used to monitor the metabolic fate of [6,6-$^{2}H_2$]glucose within the affected tissue. Histology and flow cytometry were used to validate the *in vivo* data.

Results: After plug implantation and intravenous administration of the ^{19}F-containing contrast agent, $^{1}H/^{19}F$ MRI confirmed the infiltration of ^{19}F-labeled immune cells into LPS-doped plugs while no ^{19}F signal was observed in PBS-containing control plugs. Identification of the inflammatory focus was followed by i.p. bolus injection of deuterated glucose and continuous ^{2}H MRS. Inflammation-induced alterations in metabolic fluxes could be tracked with an excellent temporal resolution of 2 min up to approximately 60 min after injection and demonstrated a more anaerobic glucose utilization in the initial phase of immune cell recruitment.

Conclusion: $^{1}H/^{2}H/^{19}F$ MRI/MRS was successfully employed for noninvasive monitoring of metabolic alterations in an inflammatory environment, paving the way for simultaneous *in vivo* registration of immunometabolic data in basic research and patients.

KEYWORDS

inflammation, metabolism, neutrophils, glycolysis, deuterium, magnetic resonance spectroscopy and imaging

Introduction

Inflammation and metabolism are closely intertwined processes that influence each other in multiple ways (1, 2). During an inflammatory response, the body requires additional energy to support the activation and proliferation of immune cells involved in the immune response and successful healing. Metabolic pathways are redirected to generate the necessary energy and substrates for these processes (3), while immune cells, especially macrophages and T cells, undergo metabolic reprogramming during inflammation (4). On the other hand, inflammatory cytokines, such as interleukin-6 (IL-6) and tumor necrosis factor-alpha (TNF-α), can affect insulin sensitivity, glucose, and lipid metabolism (5), potentially leading to insulin resistance. In line with this, chronic low-grade inflammation is linked to various metabolic disorders, including obesity, type 2 diabetes, and cardiovascular diseases (6, 7).

In order to harness this interplay for clinical decision-making, as well as to further delineate the mechanisms on how inflammation and metabolism interact, noninvasive approaches that monitor both processes *in vivo* would be highly desirable. In this context, the metabolism of glucose is especially of major interest, since, in particular, in the initial inflammatory phase, infiltrating immune cells mainly rely on glycolysis to cover their energy demand (8, 9). Positron emission tomography (PET) using [2-^{18}F]fluorodeoxyglucose (FDG) is an established and sensitive tool for glucose imaging (10), which has also been applied for visualization of inflammation via the enhanced glucose uptake of the affected tissue (11). However, it has several limitations since it requires radioactive tracers and is restricted to monitor glucose uptake, whereas further metabolic turnover of the ingested glucose remains unclear (12). Furthermore, an increased glucose uptake is not specific for inflamed tissue and occurs also, e.g., in cancer [known as the Warburg effect (13)] and thus is a rather indirect readout for inflammation.

In the present study, the power of multinuclear magnetic resonance (MR) techniques was used to specifically resolve inflammatory and metabolic processes in parallel but at different levels: The ^{19}F nucleus was employed to track immune cell trafficking, ^{2}H (deuterium) for monitoring metabolic turnover, and conventional ^{1}H MR imaging (MRI) for anatomical assessment of the inflamed tissue. ^{19}F MRI emerged over the last decade as a background-free approach for inflammation imaging (14, 15), while ^{2}H MR spectroscopy (MRS) is a novel, noninvasive method for tracking the pathway of deuterated substrates, which has yet be mainly used for analysis of cerebral or cancer metabolism (16–18). Here, these approaches were combined for the first time to monitor metabolic changes via ^{2}H MRS in inflamed tissue identified by $^{1}H/^{19}F$ MRI. To this end, an easy and reproducible murine inflammation model was applied, making use of an implanted Matrigel plug doped with LPS (19) for an efficient recruitment of circulating immune cells into this experimental inflammatory focus.

Methods

Animal experiments

Eight- to 12-week-old male C57BL/6J mice (Janvier) were housed at the central animal facility of the Heinrich Heine University (Düsseldorf, Germany). All animal studies were approved by the "Landesamt für Natur, Umwelt und Verbraucherschutz Nordrhein-Westfalen" and were performed in accordance with the national guidelines on animal care (file references 81-02.04.2018.A007 and 81-02.04.2023.A050). The mice were fed with a standard chow diet and received tap water *ad libitum*.

Inflammation model (Matrigel/LPS)

To implant the Matrigel plug, mice were anesthetized with isoflurane and placed on a 37°C warming plate. Fifty microliters of a fluid Matrigel solution mixed with LPS (1 μg/μL; BD Biosciences) or PBS as control were injected s.c. into the neck, which turned into a solid gel at body temperature forming a jellylike plug stable over a period of several weeks (19).

Magnetic resonance imaging and spectroscopy

General

Data were recorded at vertical Bruker AVANCE^{III} and AVANCE NEO 9.4T wide bore NMR spectrometers driven by ParaVision 5.1 and 360v3.2, respectively, and operating at a frequency of 400.21 MHz for ^{1}H, 376.54 MHz for ^{19}F, and 61.43 MHz for ^{2}H measurements. Images

were acquired using Bruker microimaging units Micro 2.5 with actively shielded gradient sets (1.5 T/m) and resonators/coils depending on the application (all Bruker, see below). Mice were anesthetized with 1.5% isoflurane and kept at 37°C.

$^{1}H/^{19}F$ MRI

Data were acquired using a 25-mm resonator tuneable to both ^{1}H and ^{19}F. For visualization of inflammatory processes, mice received an intravenous bolus injection of a 10% perfluoro-15-crown-5 ether emulsion (PFC, 3 mM/kg BW) 24 h prior to MRI to ensure appropriate PFC-loading of circulating immune cells (15). After acquisition of ^{1}H datasets, the resonator was tuned to ^{19}F, and morphologically matching ^{19}F images were recorded. For superimposing the images of both nuclei, the "hot iron" color look-up table provided by ParaVision was applied to ^{19}F images. ^{1}H MR reference images were recorded by a multislice rapid acquisition with relaxation enhancement (RARE) sequence: RARE factor 16, field of view (FOV) 2.56 × 2.56 mm^2, matrix 256×256, slice thickness (ST) 0.5–1 mm, 1–4 averages, and acquisition time (TAcq) 0.5–6 min. Corresponding ^{19}F images were recorded from the same FOV using a RARE sequence with the following parameters: RARE factor 32, matrix 64 × 64, ST 2 mm, 256 averages, and TAcq 21 min. For a more detailed description of the ^{19}F MRI approach, acquisition parameters, and quantification procedures, please refer to Refs (15, 20).

^{1}H MRI combined with ^{2}H MRS

In separate experiments, a 12 × 8 mm^2 transmit/receive ^{2}H surface coil inserted into a 30-mm ^{1}H saw resonator was utilized for metabolic measurements. The mice were placed with their neck (containing the Matrigel plug) on the surface coil, and for application of deuterated glucose during the MR session, a Vasofix Safety IV Catheter (Braun Melsungen AG) was inserted into the peritoneal cavity. After insertion in the magnet, the correct positioning was verified by ^{1}H MRI. Subsequently, fieldmap-based shimming (MAPSHIM) followed by manual adjustment was carried out to optimize the field homogeneity in the region of interest. Thereafter, ^{2}H MR spectra were recorded over the entire Matrigel region for determination of glucose metabolism [rectangular pulse, 60° flip angle; repetition time (TR), 350 ms; spectral width, 15 ppm; data size, 300 points; averages, 300; TAcq, 2 min]. After acquisition of baseline spectra, mice received an i.p. bolus injection of 2 mg/g [6,6-$^{2}H_2$]glucose per body weight followed by continuous monitoring of deuterated metabolites over 60 min. Spectra were processed and deconvoluted with TopSpin (Bruker). Exponential weighting resulting in a 10-Hz line broadening was applied and chemical shifts were referenced to the resonance frequency of water at 4.7 ppm. Signal intensities were obtained by integration and normalized to their background values under baseline conditions, or for calculation of metabolic fluxes, absolute intensities were used.

Flow cytometry

After termination of all MRI/MRS measurements, mice were sacrificed without disrupting the Matrigel plug located in the neck. Matrigel plugs were carefully excised, digested with Collagenase D (0.075 U/mL) and DNase I (200 U/mL; both Roche Applied Sciences), and prepared for flow cytometry as previously described (19, 21, 22). In brief, cells were resuspended in ice-cold MACS buffer (phosphate-buffered saline, 2 mM EDTA, and 0.5% bovine serum albumin) and stained with antibodies against the following molecules to identify T cells, B cells, monocytes, or macrophages: anti-CD45(PE), anti-CD3(FITC), anti-B220(APC), anti-CD11b(APC), anti-Gr1(PE.Cy7), anti-Ly6c(APC.Cy7), anti-CD11c(FITC), anti-MHCII(PE), and anti-F4/80(PerCP5.5). All antibodies were purchased from Miltenyi Biotec (Bergisch Gladbach, Germany) or BioLegend (Amsterdam, Netherlands) and diluted (1:200–400) in ice-cold MACS buffer. Cells were stained for 30 min at 4°C, washed three times with cold MACS buffer, and finally resuspended in 250 µL of MACS buffer. Dead cells were labeled with DAPI (4′,6-diamidino-2-phenylindole; 1 µg/mL) and excluded from the analysis. FACS datasets were acquired on a CantoII (BD Biosciences) and analyzed using FACSDiva (BD Biosciences) or FlowJo™ (v10.8; Ashland, OR, USA). The following expression patterns were used for identification of the immune cell subtypes: T cells: $CD45^+$ and $CD3^+$; B cells: $CD45^+$ and $B220^+$; neutrophil granulocytes: $CD11b^+$, $Gr1^{hi}$, and $Ly6c^+$; inflammatory monocytes: $CD11b^+$, $Gr1^+$, and $Ly6c^{hi}$; macrophages: $CD11b^+$, $Gr1^{low/neg}$, $Ly6c^{low/neg}$, $CD11c^+$, $MHCII^+$, and $F4/80^+$.

Immunofluorescence microscopy

Excised Matrigel plugs were embedded in Tissue-Tek (Weckert Labortechnik, Kitzingen, Germany) and frozen at −20°C. Sections of 8–10 µm were cut and fixed as previously described (15, 19). Matrigel samples were fixed for 10 min in Zamboni's fixative, washed with PBS, and blocked (10% goat serum in PBS containing 0.1% saponin) for 10 min. Subsequently, Matrigel sections were stained with anti-CD11b mAb (1:100; Serotec; Düsseldorf, Germany) overnight at 4°C. After washing with PBS, samples were incubated with anti-rat-IgG-phycoerythrin (PE)-coupled secondary mAb (1:1,000 in blocking buffer; ThermoFisher) for 30 min at 4°C and washed again three times with PBS. Finally, sections were embedded in ProLong Gold antifade reagent (with DAPI; Invitrogen). Slices were analyzed using an Olympus BX61 fluorescence microscope equipped with a 12-bit CCD monochrome (F-View II) driven by CellSense Dimension software. Images were analyzed and processed with Fiji (23).

Statistics

Statistical analysis was performed using GraphPad 9.5. Normal distribution was tested using Shapiro–Wilk test. For comparison of treatment groups, a two-way ANOVA or an unpaired-samples Students *t*-test was used. A p-value < 0.05 was considered statistically significant.

10.3389/fimmu.2023.1258027

Results

For induction of defined inflammatory conditions, we made use of a previously described murine model with neck implantation of an LPS-doped Matrigel plug, while using PBS-doped plugs as respective negative control (19). The successful formation of an inflammatory hotspot within the neck of mice was verified by $^{1}H/^{19}F$ MR inflammation imaging (14) 1 day after implantation of the doped Matrigel plugs. To this end, PFCs that are preferentially phagocytosed by circulating neutrophils/monocytes were injected intravenously for visualization of the infiltrating immune cells. Figure 1A shows the anatomical location of the Matrigel plug that clearly emerged as a bright oval structure in T2-weighted ^{1}H MRI of the neck region. Merging of subsequently

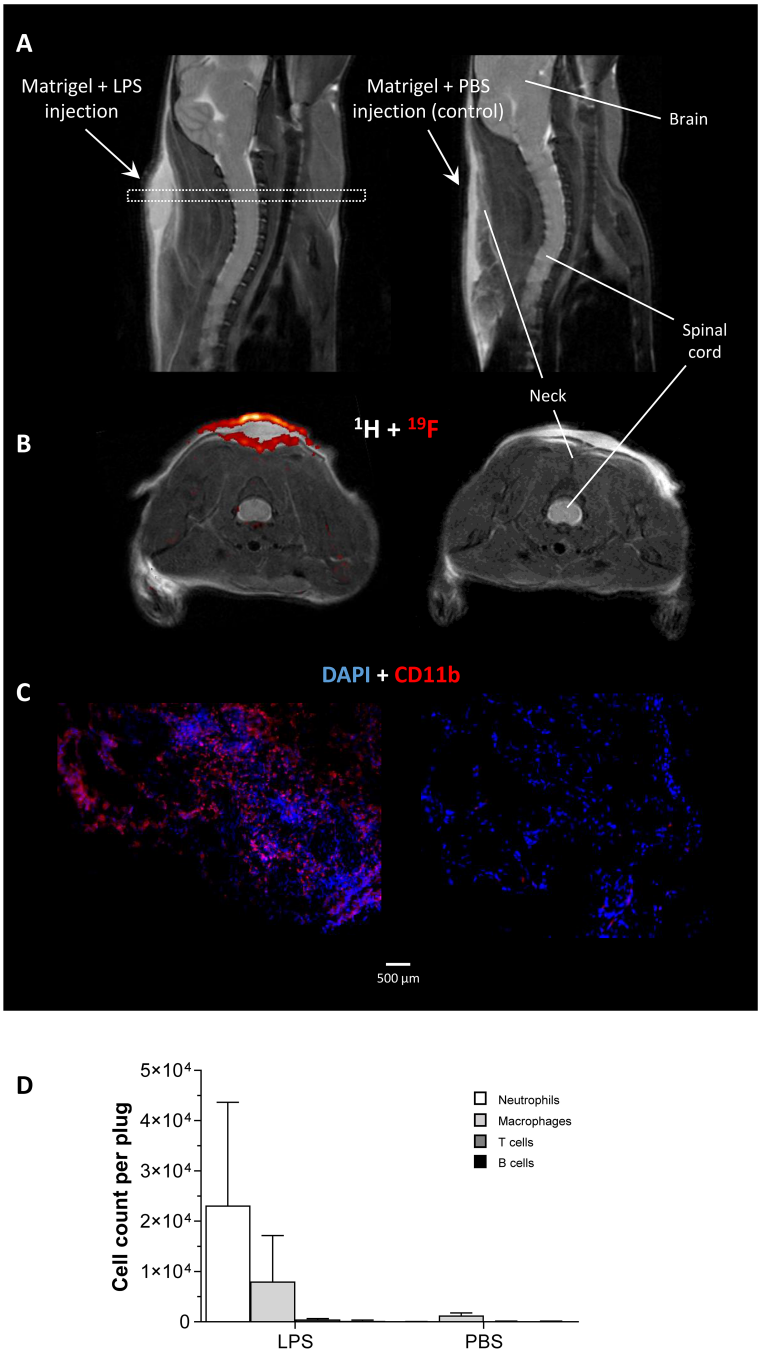

FIGURE 1
In vivo and *ex vivo* validation of the experimental inflammatory focus. **(A)** Sagittal T2-weighted ^{1}H MR images visualizing the injected Matrigel doped with 1 µg/µL LPS/PBS in the neck of healthy C57BL/6J mice as bright structure. The dotted rectangle indicates the slice localization in **(B)**. **(B)** Axial $^{1}H/^{19}F$ MRI on day 1 after Matrigel implantation revealed only in LPS-doped plugs an infiltration of ^{19}F-loaded immune cells. **(C)** Immunohistochemistry of excised plugs confirmed the *in vivo* findings in **(B)**. **(D)** Flow cytometric analysis of immune cells isolated from LPS/PBS-doped Matrigel plugs indicating neutrophils as the predominant cell population recruited to the inflammatory focus at that time point.

10.3389/fimmu.2023.1258027

acquired ^{1}H and ^{19}F images (Figure 1B) demonstrated the presence of ^{19}F-loaded immune cells predominantly in the border region of the LPS-doped Matrigel plug, while no ^{19}F signal was found in PBS-doped control plugs. These *in vivo* findings were underpinned by both histology and flow cytometry corroborating the marginal location of immune cells in the plug (Figure 1C) and revealing neutrophils as the predominant cell population infiltrating the plug at this early time point after implantation (Figure 1D).

After confirming the presence of inflammatory foci (Figure 2A), mice were placed with their neck on a 12 × 8 mm^2 transmit/receive ^{2}H surface coil inserted into a 30-mm ^{1}H saw resonator (Figure 2B). This setup allowed the unambiguous localization of the Matrigel plug by ^{1}H MRI (Figure 2C left) and the sensitive acquisition of ^{2}H MR spectra with the surface coil, whose penetration depth and excitation profile essentially encompassed the Matrigel plug and surrounding scapular muscles (Figure 2C right). After acquisition of baseline spectra, mice received an i.p. bolus injection of 2 mg/g [6,6-$^{2}H_2$]glucose per body weight followed by continuous monitoring of ^{2}H MR spectra over 60 min (Figure 2D). Figure 3A illustrates the route of the injected ^{2}H label (blue) through glycolysis and TCA cycle with the ^{2}H MRS-detectable metabolites (in the millimolar range) highlighted in red, i.e., glucose, lactate, and

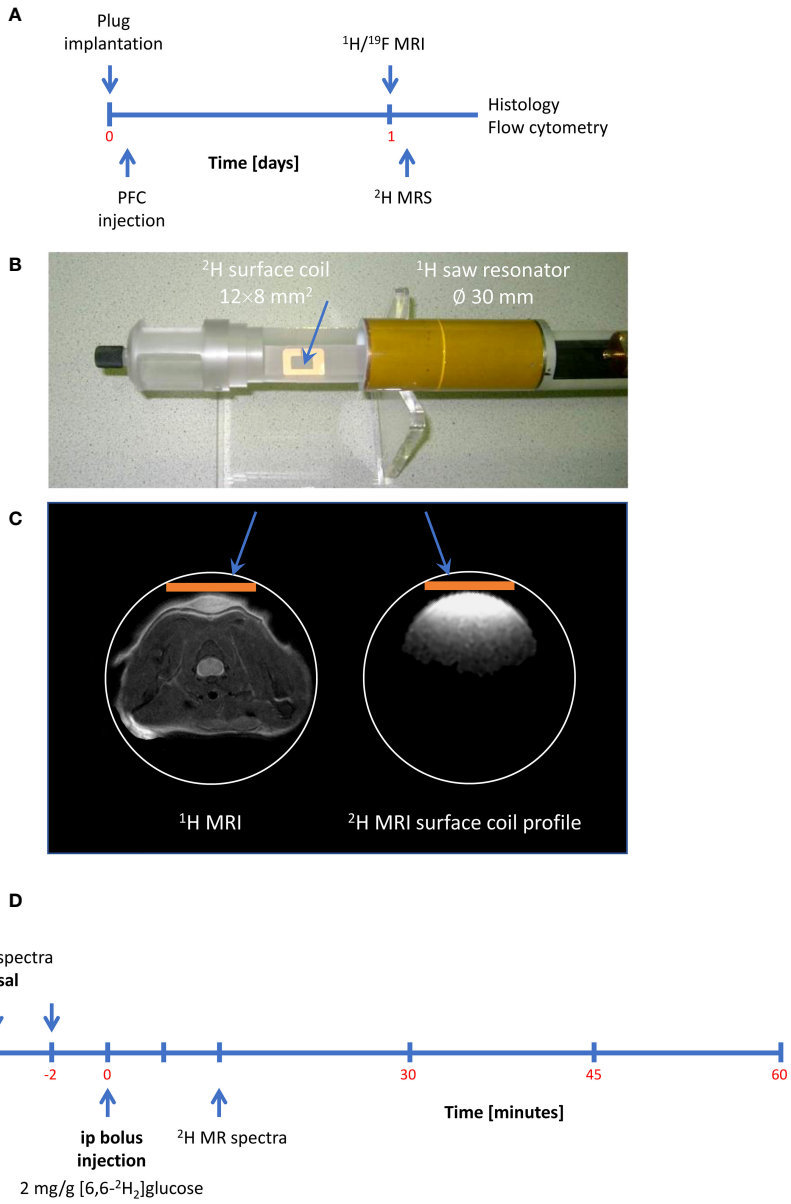

FIGURE 2
Setup and workflow for ^{2}H MRS. **(A)** Timeline with plug implantation, inflammation imaging, metabolic measurements, and histology/flow cytometry. **(B)** ^{2}H MRS was carried out with a ^{2}H surface coil inserted into a ^{1}H volume resonator. **(C)** Anatomic localization of the plug with the volume resonator (left) and excitation profile of the ^{2}H surface coil (orange bar) acquired from a D_2O phantom (right) demonstrating that the penetration depth of the surface coil is restricted to the dimensions of the Matrigel plug and the surrounding scapular muscles. **(D)** Workflow for ^{2}H MRS: After acquisition of baseline spectra, mice received an intraperitoneal bolus of 2 mg/g [6,6-$^{2}H_2$]glucose per body weight followed by continuous acquisition of ^{2}H MR spectra.

10.3389/fimmu.2023.1258027

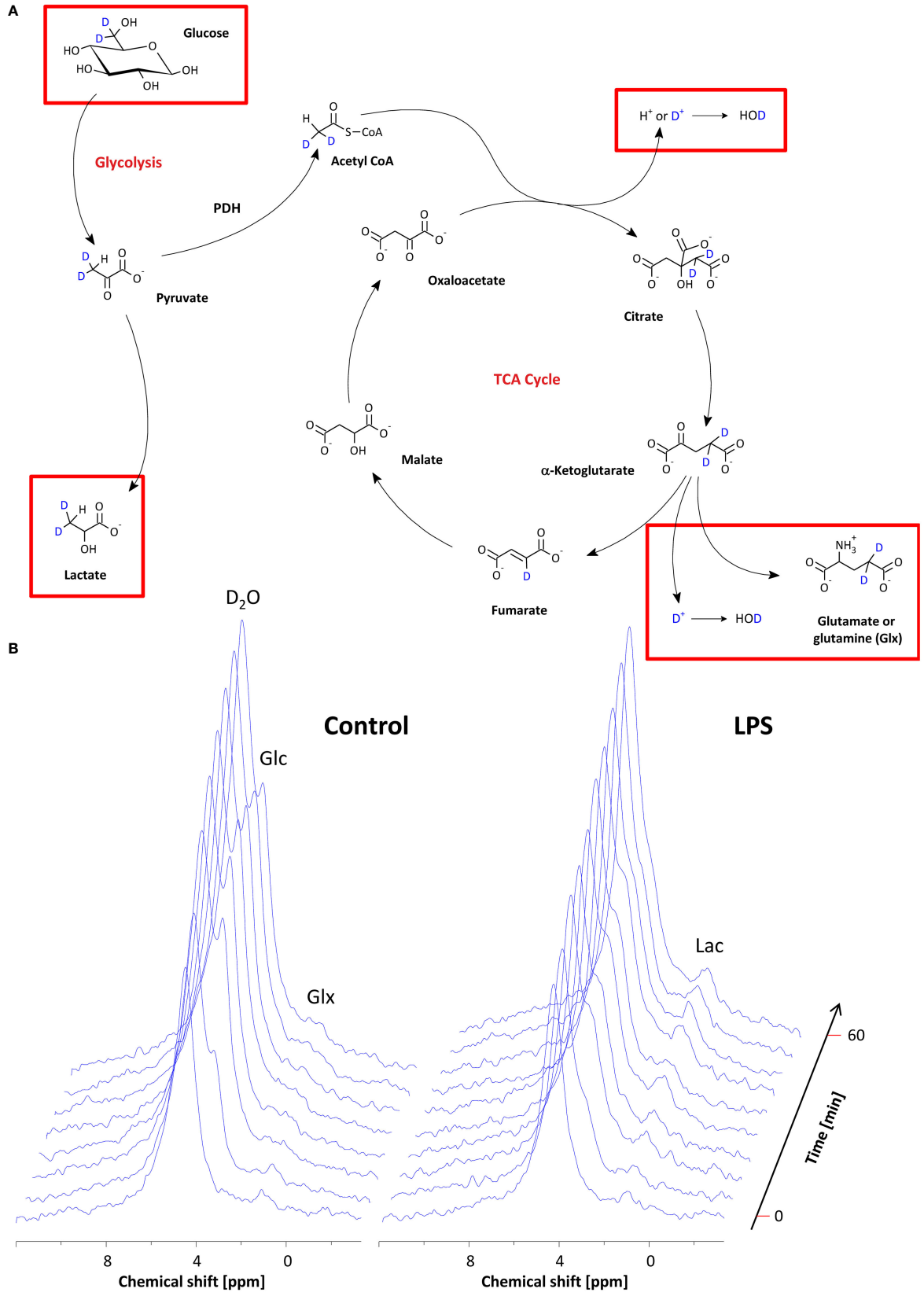

FIGURE 3
Monitoring of the metabolic fate of [6,6-$^{2}H_2$]glucose by ^{2}H MRS. **(A)** Scheme of the metabolic pathway for [6,6-$^{2}H_2$]glucose through glycolysis and the TCA cycle. The red rectangles indicate the metabolites that are within the detection range of ^{2}H MRS. **(B)** Stack plot of ^{2}H MR spectra over the entire observation period for mice with PBS-doped (left) and LPS-doped (right) Matrigels, respectively. See the text for detailed explanations.

10.3389/fimmu.2023.1258027

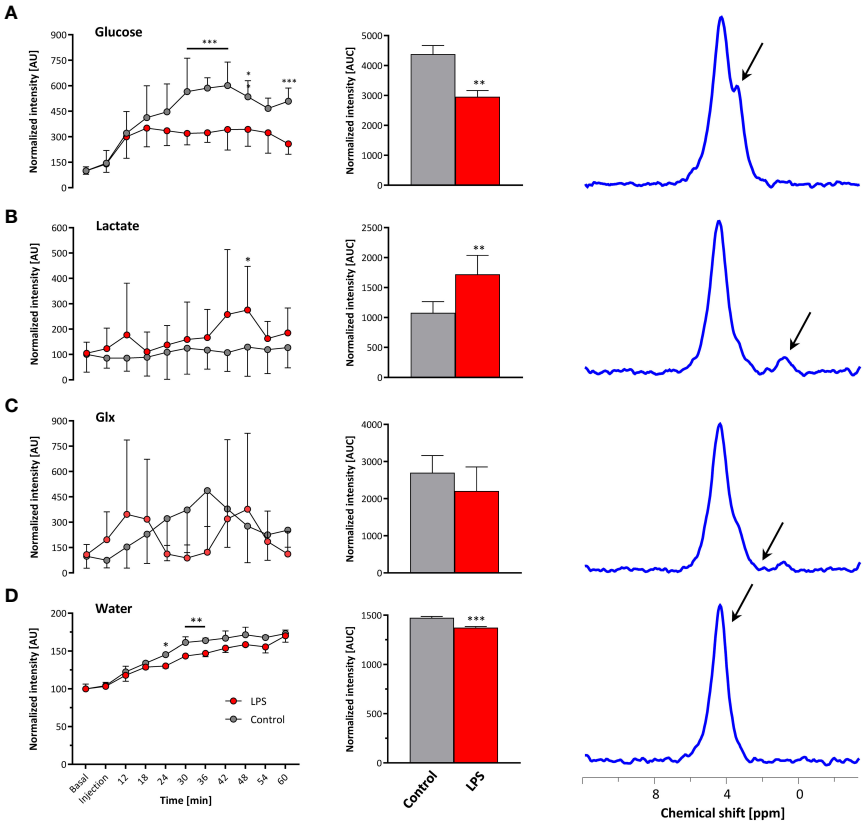

FIGURE 4
Quantification of ^{2}H MR spectra over time. All measurements were normalized to spectra acquired under baseline conditions accounting for the natural background of ^{2}H (0.01%). Gray, control mice with Matrigel/PBS; red, mice with Matrigel/LPS; left, time course over 60 min; middle, area under the curve (AUC); right, representative ^{2}H MR spectrum with the respective metabolite for **(A)** glucose, **(B)** lactate, **(C)** Glx, and **(D)** water. Data are presented as means ± SD; *p < 0.05, **p < 0.01, ***p < 0.001; *n* = 9–12; two-way ANOVA for the time courses and unpaired Student's *t*-test for the respective AUC.

glutamate/glutamine (Glx)—the latter cannot be spectrally resolved *in vivo* because of the broad linewidth of ^{2}H MR spectra. Importantly, during formation of the enol form of acetyl-CoA prior to entry into the TCA cycle, one of the two deuteria can be split off (with a probability of 2/3)—this is eventually found in water and yields only a monolabeled citrate and Glx (not shown in the schematic).

Baseline spectra showed a prominent signal at 4.7 ppm (Figure 3B bottom lanes) caused by the natural abundant ^{2}H in water. Injection of [6,6-$^{2}H_2$] glucose gave rise to a fast increase of the corresponding ^{2}H signal at 3.8 ppm and the subsequent appearance of the downstream metabolites Glx (i.e., glutamine + glutamate) and lactate at 2.4 and 1.3 ppm, respectively, accompanied by a continuously increasing water signal. The temporal development of ^{2}H MR spectra over the entire observation period of 60 min is illustrated in Figure 3B with typical examples for mice with Matrigel plugs doped with LPS (right) and PBS as control (left). As can be recognized, the glucose (Glc) signal declined much quicker in the presence of LPS while concomitantly lactate levels were clearly elevated as compared to control conditions. Quantification of spectra for *n* = 9–12 independent experiments (Figures 4A–D) confirmed these findings and calculation of Lac/Glc ratios over the entire observation period after application of the labeled glucose (LPS 1.18 ± 0.08 vs. PBS 0.90 ± 0.12; $p < 0.05$) further supported the notion of an enhanced lactate formation at the expense of increased glucose consumption under inflammatory conditions. Of note, this was also accompanied by a significantly lower incorporation of ^{2}H label into water (Figure 4D).

Taking the naturally occurring ^{2}H signal from water (Figure 3B bottom lanes) as an internal reference, absolute turnover rates can also be calculated: Assuming a content of 110 M hydrogen in H_2O, an approximately 75% tissue water content (24), and a ^{2}H natural abundance of 0.0115% in water (25, 26), the detected baseline signal reflects an amount of ~9.5 mM deuterons (27). Considering now the total increase of the water signal (Figure 4D, middle) over the observation period of 60 min, the deuterium turnover from [6,6-$^{2}H_2$]glucose to water is calculated to be 0.81 ± 0.07 mM/min under control conditions, while it was significantly diminished to 0.64 ± 0.04 mM/min under LPS exposure ($p < 0.05$, *n* = 9–12).

Discussion

In the present work, ^{2}H MRS was applied in combination with ^{19}F MR inflammation imaging *in vivo* to monitor the metabolic fate of deuterated glucose within neutrophil-infiltrated inflammatory hotspots noninvasively and in real time. The findings of this study

demonstrate that ^{2}H MRS can indeed be successfully used to reveal metabolic signatures in inflammatory environments, specifically identified by hot spot ^{19}F MRI together with anatomical ^{1}H MRI.

The obtained results clearly point to an enhanced utilization of glycolysis for energy production in the region of the inflammatory hotspot. Increased lactate levels and enhanced glucose turnover are classical indicators for a predominant anaerobic metabolism, which is further supported by the lower flux of the ^{2}H label to water. In the long term, all deuterons of [6,6-$^{2}H_2$]glucose will end up in the body water pool, but in the initial phase after bolus injection, the highest probability for the ^{2}H label being transferred to water is given when it enters the aerobic pathway: if the label runs through the TCA cycle, it can be cleaved off either during formation of citrate or when it does not leave the cycle via α-ketoglutarate, but instead passes into fumarate (Figure 3A). Thus, the diminished ^{2}H incorporation into water is overtly indicative for a lower utilization of glucose via the TCA cycle. In contrast, under control conditions, glucose turnover within the field of view covered by the surface coil (Figure 2C) is mainly determined by aerobic metabolism of the surrounding scapular muscles.

While this finding is not surprising *per se*, it nonetheless highlights the potential of multinuclear MR approaches to discriminate complex immunometabolic processes at separate levels in parallel (here, ^{1}H, ^{2}H, and ^{19}F for anatomy, metabolism, and immune cells, respectively). Of course, compared to FDG-PET (10), the present approach is restricted to metabolites that are present in the millimolar range, but it lacks any harmful radiation and also allows monitoring of downstream metabolites as well as absolute turnover rates. Alternative MR approaches relying on the ^{13}C nucleus offer better spectral resolution than ^{2}H, but either require substantial longer acquisition times even without volume selection (normal ^{13}C) or are limited to non-ideal substrates (e.g., pyruvate) as well as very short temporal windows of observation (hyperpolarized ^{13}C; approximately 1 min). Nevertheless, owing to the dramatically enhanced sensitivity of the latter method, it provides superior spatial resolution within this time frame (28). On the other hand, a variety of deuterated substrates are readily available commercially for ^{2}H MRS and applications for deuterated acetate, choline, fumarate, and β-hydroxybutyrate have already been described (29, 30), but the field is definitely still in its infancy here. Of note, ongoing advances in technology, such as denoising, undersampling, or indirect readout [as used in (28, 30, 31)] will further improve the sensitivity for detection of deuterated metabolites.

In the present study, a ^{2}H surface coil was utilized together with a ^{1}H volume resonator—while this setup provided excellent coverage and superior sensitivity for the near-surface inflammation model used, it is not suitable for metabolic analysis of deeper organs or tissue. However, this approach can be further developed by designing triple-tuned volume resonators to allow simultaneous acquisition (32) of ^{1}H/^{2}H/^{19}F MR images for true temporal co-registration of inflammatory/metabolic processes without penetration limits—not only for basic research to analyze their interwoven relationships *in vivo*, but also in the long run also for clinical decision-making in immunologic and metabolic disease states, as the feasibility of both ^{19}F inflammation and deuterium metabolic imaging in the clinical setting has already been demonstrated (16, 33–36).

Conclusions and perspectives

In summary, the results of this study demonstrate that ^{2}H MRS can be successfully used to reveal real-time metabolic signatures in inflammatory environments—specifically identified by ^{1}H/^{19}F MRI. In contrast to the current gold standard FDG-PET that detects glucose uptake only, the present approach discriminates inflammation and metabolism at different levels in parallel and enables the much more meaningful assessment of metabolic turnover through glycolysis and TCA cycle with analysis of downstream metabolites.

In the future, this approach can be employed to noninvasively and longitudinally characterize in depth the immunometabolic interplay in diseases, such as diabetes or obesity, but also its impact on autoimmunity, (innate) immune memory, tumor microenvironment, and hematopoiesis for identification of new therapeutic targets. As the MR techniques used in this study could be readily transferred to human scanners, they could also serve to assess the degree of immunometabolic responses in patients to tailor individual treatment regimens.

Data availability statement

The original contributions presented in the study are included in the article/supplementary material. Further inquiries can be directed to the corresponding author.

Ethics statement

The animal study was approved by Landesamt für Natur, Umwelt und Verbraucherschutz Nordrhein-Westfalen. The study was conducted in accordance with the local legislation and institutional requirements.

Author contributions

VF: Data curation, Formal Analysis, Investigation, Validation, Visualization, Writing – original draft. ST: Data curation, Formal Analysis, Investigation, Validation, Visualization, Writing – review & editing. PB: Methodology, Resources, Writing – review & editing. MG: Conceptualization, Project administration, Supervision, Writing – review & editing. UF: Conceptualization, Funding acquisition, Project administration, Supervision, Validation, Visualization, Writing – review & editing.

Funding

The authors declare financial support was received for the research, authorship, and/or publication of this article. This work was supported by the Deutsche Forschungsgemeinschaft (INST 208/764-1 FUGG to UF).

Acknowledgments

Parts of this work have been published as abstract at the ISMRM & SMRT Virtual Conference & Exhibition 2020 (37).

Conflict of interest

The authors declare that the research was conducted in the absence of any commercial or financial relationships that could be construed as a potential conflict of interest.

Publisher's note

References

1. Chavakis T. Immunometabolism: Where immunology and metabolism meet. *J Innate Immun* (2022) 14:1–3. doi: 10.1159/000521305

2. Gaber T, Strehl C, Buttgereit F. Metabolic regulation of inflammation. *Nat Rev Rheumatol* (2017) 13:267–79. doi: 10.1038/nrrheum.2017.37

3. Pearce EL, Pearce EJ. Metabolic pathways in immune cell activation and quiescence. *Immunity* (2013) 38:633–43. doi: 10.1016/j.immuni.2013.04.005

4. Sun L, Yang X, Yuan Z, Wang H. Metabolic reprogramming in immune response and tissue inflammation. *Arterioscler Thromb Vasc Biol* (2020) 40:1990–2001. doi: 10.1161/ATVBAHA.120.314037

5. Shi J, Fan J, Su Q, Yang Z. Cytokines and abnormal glucose and lipid metabolism. *Front Endocrinol (Lausanne)* (2019) 10:703. doi: 10.3389/fendo.2019.00703

6. Van Gaal LF, Mertens IL, De Block CE. Mechanisms linking obesity with cardiovascular disease. *Nature* (2006) 444:875–80. doi: 10.1038/nature05487

7. Saltiel AR, Olefsky JM. Inflammatory mechanisms linking obesity and metabolic disease. *J Clin Invest* (2017) 127:1–4. doi: 10.1172/JCI92035

8. O'Neill LAJ, Kishton RJ, Rathmell J. A guide to immunometabolism for immunologists. *Nat Rev Immunol* (2016) 16:553–65. doi: 10.1038/nri.2016.70

9. Viola A, Munari F, Sánchez-Rodríguez R, Scolaro T, Castegna A. The metabolic signature of macrophage responses. *Front Immunol* (2019) 10:1462. doi: 10.3389/fimmu.2019.01462

10. Iking J, Staniszewska M, Kessler L, Klose JM, Lückerath K, Fendler WP, et al. Imaging inflammation with positron emission tomography. *Biomedicines* (2021) 9:212. doi: 10.3390/biomedicines9020212

11. Love C, Tomas MB, Tronco GG, Palestro CJ. FDG PET of infection and inflammation. *Radiographics* (2005) 25:1357–68. doi: 10.1148/rg.255045122

12. Phelps ME, Huang SC, Hoffman EJ, Selin C, Sokoloff L, Kuhl DE. Tomographic measurement of local cerebral glucose metabolic rate in humans with (F-18)2-fluoro-2-deoxy-D-glucose: validation of method. *Ann Neurol* (1979) 6:371–88. doi: 10.1002/ana.410060502

13. Warburg O, Wind F, Negelein E. The metabolism of tumors in the body. *J Gen Physiol* (1927) 8:519–30. doi: 10.1085/jgp.8.6.519

14. Bouvain P, Temme S, Flögel U. Hot spot 19F magnetic resonance imaging of inflammation. *Wiley Interdiscip Rev Nanomed Nanobiotechnol* (2020) 12:e1639. doi: 10.1002/wnan.1639

15. Flögel U, Ding Z, Hardung H, Jander S, Reichmann G, Jacoby C, et al. *In vivo* monitoring of inflammation after cardiac and cerebral ischemia by fluorine magnetic resonance imaging. *Circulation* (2008) 118:140–8. doi: 10.1161/CIRCULATIONAHA.107.737890

16. De Feyter HM, Behar KL, Corbin ZA, Fulbright RK, Brown PB, McIntyre S, et al. Deuterium metabolic imaging (DMI) for MRI-based 3D mapping of metabolism in vivo. *Sci Adv* (2018) 4:eaat7314. doi: 10.1126/sciadv.aat7314

17. Lu M, Zhu X-H, Zhang Y, Mateescu G, Chen W. Quantitative assessment of brain glucose metabolic rates using in *vivo* deuterium magnetic resonance spectroscopy. *J Cereb Blood Flow Metab* (2017) 37:3518–30. doi: 10.1177/0271678X17706444

18. Hesse F, Somai V, Kreis F, Bulat F, Wright AJ, Brindle KM. Monitoring tumor cell death in murine tumor models using deuterium magnetic resonance spectroscopy and spectroscopic imaging. *Proc Natl Acad Sci USA* (2021) 118:e2014631118. doi: 10.1073/pnas.2014631118

19. Temme S, Jacoby C, Ding Z, Bönner F, Borg N, Schrader J, et al. Technical advance: Monitoring the trafficking of neutrophil granulocytes and monocytes during the course of tissue inflammation by noninvasive 19F MRI. *J Leukoc Biol* (2014) 95:689–97. doi: 10.1189/jlb.0113032

20. Ebner B, Behm P, Jacoby C, Burghoff S, French BA, Schrader J, et al. Early assessment of pulmonary inflammation by 19F MRI. *vivo. Circ Cardiovasc Imaging* (2010) 3:202–10. doi: 10.1161/CIRCIMAGING.109.902312

21. Flögel U, Burghoff S, van Lent PLEM, Temme S, Galbarz L, Ding Z, et al. Selective activation of adenosine A2A receptors on immune cells by a CD73-dependent prodrug suppresses joint inflammation in experimental rheumatoid arthritis. *Sci Transl Med* (2012) 4:146ra108. doi: 10.1126/scitranslmed.3003717

22. Borg N, Alter C, Görldt N, Jacoby C, Ding Z, Steckel B, et al. CD73 on T-cells orchestrates cardiac wound healing after myocardial infarction by purinergic metabolic reprogramming. *Circulation* (2017) 136:297–313. doi: 10.1161/CIRCULATIONAHA.116.023365

23. Schindelin J, Arganda-Carreras I, Frise E, Kaynig V, Longair M, Pietzsch T, et al. Fiji: an open-source platform for biological-image analysis. *Nat Methods* (2012) 9:676–82. doi: 10.1038/nmeth.2019

24. Lorenzo I, Serra-Prat M, Yébenes JC. The role of water homeostasis in muscle function and frailty: A review. *Nutrients* (2019) 11:1857. doi: 10.3390/nu11081857

25. Harris RK, Becker ED, Cabral de Menezes SM, Goodfellow R, Granger P. NMR nomenclature. Nuclear spin properties and conventions for chemical shifts (IUPAC Recommendations 2001). *Pure Appl Chem* (2001) 73:1795–818. doi: 10.1351/pac200173111795

26. Rosman KJR, Taylor PDP. Isotopic compositions of the elements 1997. *Pure Appl Chem* (1998) 70:217–35. doi: 10.1351/pac199870010217

27. De Feyter HM, de Graaf RA. Deuterium metabolic imaging - Back to the future. *J Magn Reson* (2021) 326:106932. doi: 10.1016/j.jmr.2021.106932

28. von Morze C, Engelbach JA, Blazey T, Quirk JD, Reed GD, Ippolito JE, et al. Comparison of hyperpolarized 13C and non-hyperpolarized deuterium MRI approaches for imaging cerebral glucose metabolism at 4.7 T. *Magn Reson Med* (2021) 85:1795–804. doi: 10.1002/mrm.28612

29. Chen Ming Low J, Wright AJ, Hesse F, Cao J, Brindle KM. Metabolic imaging with deuterium labeled substrates. *Prog Nucl Magn Reson Spectrosc* (2023) 134–135:39–51. doi: 10.1016/j.pnmrs.2023.02.002

30. Soni ND, Swain A, Jacobs P, Juul H, Armbruster R, Nanga RPR, et al. *In vivo* assessment of β-hydroxybutyrate metabolism in mouse brain using deuterium (2H) MRS. *Magn Reson Med* (2023) 90:259–69. doi: 10.1002/mrm.29648

31. Niess F, Hingerl L, Strasser B, Bednarik P, Goranovic D, Niess E, et al. Noninvasive 3-dimensional 1H-magnetic resonance spectroscopic imaging of human brain glucose and neurotransmitter metabolism using deuterium labeling at 3T. *Invest Radiol* (2023) 58:431–7. doi: 10.1097/RLI.0000000000000953

32. Lopez Kolkovsky AL, Carlier PG, Marty B, Meyerspeer M. Interleaved and simultaneous multi-nuclear magnetic resonance in *vivo*. Review of principles, applications and potential. *NMR BioMed* (2022) 35:e4735. doi: 10.1002/nbm.4735

33. Bönner F, Gastl M, Nienhaus F, Rothe M, Jahn A, Pfeiler S, et al. Regional analysis of inflammation and contractile function in reperfused acute myocardial infarction by in *vivo* 19F cardiovascular magnetic resonance in pigs. *Basic Res Cardiol* (2022) 117:21. doi: 10.1007/s00395-022-00928-5

34. Ahrens ET, Helfer BM, O'Hanlon CF, Schirda C. Clinical cell therapy imaging using a perfluorocarbon tracer and fluorine-19 MRI. *Magn Reson Med* (2014) 72:1696–701. doi: 10.1002/mrm.25454

35. Ahrens ET, Helfer BM, O'Hanlon CF, Lister DR, Bykowski JL, Messer K, et al. Method for estimation of apoptotic cell fraction of cytotherapy using in *vivo* fluorine-19 magnetic resonance: pilot study in a patient with head and neck carcinoma receiving tumor-infiltrating lymphocytes labeled with perfluorocarbon nanoemulsion. *J Immunother Cancer* (2023) 11:e007015. doi: 10.1136/jitc-2023-007015

36. Serés Roig E, De Feyter HM, Nixon TW, Ruhm L, Nikulin AV, Scheffler K, et al. Deuterium metabolic imaging of the human brain in *vivo* at 7 T. *Magn Reson Med* (2023) 89:29–39. doi: 10.1002/mrm.29439

37. Flocke V, Bouvain P, Temme S, Flögel U. Monitoring inflammation-associated metabolic alterations by deuterium MRS. *Proc Intl Soc Mag Reson Med* (2020) 28:3082. Available at: cds.ismrm.org/protected/20MProceedings/PDFfiles/3082.html.

frontiers | Frontiers in Immunology

TYPE Mini Review
PUBLISHED 07 November 2023
DOI 10.3389/fimmu.2023.1271098

OPEN ACCESS

EDITED BY
Pedro Gonzalez-Menendez,
University of Oviedo, Spain

REVIEWED BY
Ana Gutierrez Del Arroyo,
Queen Mary University of London,
United Kingdom
Martin Helán,
St. Anne's University Hospital, Czechia
Trim Lajqi,
Heidelberg University Hospital, Germany

*CORRESPONDENCE
Joby Thoppil
Joby.thoppil@utsouthwestern.edu

RECEIVED 01 August 2023
ACCEPTED 24 October 2023
PUBLISHED 07 November 2023

CITATION
Thoppil J, Mehta P, Bartels B, Sharma D and Farrar JD (2023) Impact of norepinephrine on immunity and oxidative metabolism in sepsis.
Front. Immunol. 14:1271098.
doi: 10.3389/fimmu.2023.1271098

Impact of norepinephrine on immunity and oxidative metabolism in sepsis

Joby Thoppil[1]*, Prayag Mehta[1], Brett Bartels[1], Drashya Sharma[2] and J. David Farrar[2]

[1]Department of Emergency Medicine, University of Texas, Southwestern Medical Center, Dallas, TX, United States, [2]Department of Immunology, University of Texas (UT) Southwestern Medical Center, Dallas, TX, United States

Sepsis is a major health problem in the United States (US), constituting a leading contributor to mortality among critically ill patients. Despite advances in treatment the underlying pathophysiology of sepsis remains elusive. Reactive oxygen species (ROS) have a significant role in antimicrobial host defense and inflammation and its dysregulation leads to maladaptive responses because of excessive inflammation. There is growing evidence for crosstalk between the central nervous system and the immune system in response to infection. The hypothalamic-pituitary and adrenal axis and the sympathetic nervous system are the two major pathways that mediate this interaction. Epinephrine (Epi) and norepinephrine (NE), respectively are the effectors of these interactions. Upon stimulation, NE is released from sympathetic nerve terminals locally within lymphoid organs and activate adrenoreceptors expressed on immune cells. Similarly, epinephrine secreted from the adrenal gland which is released systemically also exerts influence on immune cells. However, understanding the specific impact of neuroimmunity is still in its infancy. In this review, we focus on the sympathetic nervous system, specifically the role the neurotransmitter norepinephrine has on immune cells. Norepinephrine has been shown to modulate immune cell responses leading to increased anti-inflammatory and blunting of pro-inflammatory effects. Furthermore, there is evidence to suggest that norepinephrine is involved in regulating oxidative metabolism in immune cells. This review attempts to summarize the known effects of norepinephrine on immune cell response and oxidative metabolism in response to infection.

KEYWORDS

norepinephrine, oxidative metabolism, sepsis, sympathetic nervous system, immune cells

Introduction

Sepsis ranks as the tenth leading contributor of mortality in the United States and stands as the second most prevalent cause of death among patients in the Intensive Care Unit (ICU) (1). Sepsis frequently leads to mortality, with rates ranging from 20 to 50 percent worldwide due to refractory multiple organ dysfunction (1–4). Although sepsis is

fundamentally thought to be an inflammatory disease, anti-inflammatory therapies have been unsuccessful at reducing mortality. Consequently, current treatment guidelines focus on early identification and intervention. The nervous and immune systems are intrinsically related (5). Immune system molecules and cells cross the blood–brain barrier and send signals which allow for central input. The binding of soluble immune signaling molecules to receptors expressed on the surface of various types of central nervous system (CNS) cells produce cellular responses that direct the sympathetic nervous system (SNS) to secrete norepinephrine (NE) (5). The CNS via the SNS can also induce the adrenal gland to secrete epinephrine systemically. Accumulated evidence over the past two decades suggests that NE acts as a neurotransmitter/neuromodulator within primary and secondary lymphoid organs (6). Therefore, once activated sympathetic nerve terminals release NE which directly act on adrenoreceptors expressed on immune cells within these organs. Similarly, circulating epinephrine released by the adrenal gland can also act on adrenoreceptors (6). Neurons also possess receptors for cytokines and chemokines secreted by the immune system allowing for fine tuning of the local immune response (7).

It has long been established that endotoxin released from bacterial cell walls induces SNS activity (7, 8). Early investigations identified alterations in the level of sympathetic nerve activity by assessing circulating levels of NE and Epi in times of infection and shock. These studies identified consistently that endotoxin exposure led to increased levels of circulating NE, suggesting enhanced sympathetic nerve activity (8). Therefore, immune cell activation following peripheral infectious challenges likely increases the level of CNS mediated regulatory mechanisms (8). NE acts by interacting with adrenergic receptors (ADRs) which are expressed on the surfaces of the cells of the immune system. In human leukocytes, β-ADRs are expressed on natural killer (NK) cells, monocytes, B cells, $CD8^+$ T cells, and $CD4^+$ T cells (9–12). Studies have also confirmed that β-ADR signaling can regulate various functions in the immune system (9–12). For example, in response to NE B-cell costimulatory molecules and IgE secretion is increased; in monocytes and macrophages NE signaling results in decreased proinflammatory cytokine production; in T cells, Th1 cytokine production by $CD4^+$ T cells is decreased, and regulatory T-cell function is enhanced as a result of NE (9–12). Moreover, there is indication that the SNS can regulate the migration of stem cells from the bone marrow to their designated niche (13). This review will focus on direct noradrenergic (NE) innervation on immune tissue via the SNS.

The effect of NE on immune cells

NE has been demonstrated to have an overall anti-inflammatory effect, mediated primarily through β-ADRs. Post-ganglionic sympathetic nerve fibers, which release NE as their primary neurotransmitter, intricately innervate primary and secondary lymphoid tissues (6, 14). Immune cells establish direct contact with the dendrites of these neurons. Most notably, both innate and adaptive immune cells express adrenergic receptors, predominantly the β2-adrenergic receptor (β2-ADR) allowing them to directly engage with the SNS (6, 14). *In-vitro* studies have shown many anti-inflammatory immunologic effects, including decreased pro-inflammatory tumor necrosis factor alpha (TNF-alpha), Interleukin (IL)-6, and IL-8, and stimulation of anti-inflammatory cytokine IL-10. Many of norepinephrine's effects have been shown to be dose dependent (15). In macrophages, beta-adrenergic stimulation increases cAMP and inhibits nuclear factor kappa-light-chain-enhancer of activated B cells (NF-κB) from entering the nucleus, reducing pro-inflammatory cytokine transcription, as well as increased production of anti-inflammatory IL-10 (16). IL-10 was shown to markedly inhibit endotoxin-induced TNF-alpha production by mouse and rat macrophages *in vitro* (17). The norepinephrine-induced stimulation of IL-10, in addition to attenuation of TNF-alpha and IL-6, have been shown to be diminished by beta-blockade with medications such as metoprolol and propranolol (15). In other *in vitro* studies, NE diminishes NK cell cytotoxicity in a dose-dependent manner and downregulates IL-2 production through β2-ADR modulation. These effects were mitigated by administration of propranolol but not by atenolol, indicating an effect mediated by the β2-ADR.

Deletion of β2-ADRs in macrophages and dendritic cells have led to significant attenuation of IL-10 and increased TNF-alpha in response to lipopolysaccharide (LPS) administration (9, 18). *In-vivo* sepsis models showed increased mortality with β2-ADR deletion (9, 18). As part of the neuroinflammatory reflex, vagal nerve stimulation induces NE release from the spleen, resulting in acetylcholine secretion by CD4+ T-cells. Modulation of alpha-7 cholinergic receptors on macrophages by acetylcholine leads to suppression of pro-inflammatory cytokines (19). In animal models, stimulation of the vagal nerve attenuates systemic inflammation, whereas interruption of this cascade by vagotomy increased susceptibility to septic shock secondary to endotoxin effects (19). In patients with traumatic brain injury, SNS activation induces IL-10 release, which is associated with an immunosuppressive monocyte phenotype and increased infection rate. Norepinephrine, as well as epinephrine, was found to exert immunosuppressive effects in LPS-stimulated human whole blood, as well as isolated monocytes *in vitro* (15). A study of monocytes from congestive heart failure patients again demonstrated norepinephrine's immunomodulatory effects through β-ADRs, with notable attenuation of IL-10 production in CHF patients (20).

Studies are limited regarding norepinephrine's effects on granulocytes. While limited clinical data exists regarding specific immunologic effects of norepinephrine in humans, observational studies have shown increased mortality with elevated arterial norepinephrine levels (15, 21). NE has also been shown to directly promote both gram-positive and gram-negative bacterial growth *in-vitro* (15). Other studies have shown that NE reduced polymorphonuclear (PMN) cell migration, CD11b/CD18 expression, and production in response to stress (22). Beis et. al., found that NE signaling resulted in increased neutrophil and monocyte numbers during psychosocial stressors which could be reduced by blockade of β-ADRs (23).

NE also generates diverse regulatory patterns in T-lymphocytes (24). Many studies have demonstrated that catecholamines prompt heightened lymphocyte activation coupled with intense Th1 and Th2 cytokine production. A significant portion of these effects are orchestrated by β-ADRs (25). Gene expression analysis of *in-vivo* memory CD8 T cells, which express higher levels of beta-adrenergic receptors compared to naïve cells, has shown to have increased expression of inflammatory cytokines (26). Adrenergic signaling has increased expansion and function of natural killer cells *in vivo*, in response to viral infection (27). Administration of norepinephrine causes an early transient elevation in overall number and function of $CD8^+$ T cells and NK cells, though did not show significant changes in $CD4^+$ T cells or B cells (28). Figure 1 summarizes the theorized effects of NE on immune cells.

Oxidative metabolism and sepsis

Reactive oxygenated species (ROS) are small short-lived oxygen-containing molecules that are highly reactive due to the negative charge accumulated by an excess oxygen molecule. Examples of ROS include superoxide anions, hydrogen peroxide (H_2O_2), and hydroxyl radicals. ROS are byproducts of reactions occurring in various cellular compartments i.e., the cytoplasm, cell membrane, endoplasmic reticulum (ER), mitochondria and peroxisome, as integral processes of fundamental metabolic function. ROS participates in normal physiological processes of the immune system. ROS signaling plays a significant role in immune cell activation, differentiation and signaling (9, 29–31). It has been reported that ROS participates extensively in T cell activation (9, 29–32). In macrophages and other phagocytic immune cell lines ROS play a significant role in activation and in their microbicidal activity (9, 29–31). The major source and generation of intracellular ROS is the mitochondrial electron transport chain. Under basal conditions there is a balance between oxidative and anti-oxidative metabolism which maintains mitochondrial homeostasis (29, 30).

ROS assume a crucial role in both antimicrobial host defense and inflammation. In humans, their deficiency leads to recurrent and severe bacterial infections, whereas uncontrolled release results in excessive inflammation (33). Upon activation of surface receptors, host immune cells release substantial amounts of ROS at infection sites (33). Simultaneously, activation by Fc and integrin directly induces heightened ROS production (33). Moreover, G-protein coupled receptors (GPCRs) binding to bacterial peptides can both prime cells and trigger low levels of ROS production (33). The engagement of these receptors initiates intracellular signaling pathways, that culminate in the activation of downstream effector proteins. This process includes the assembly of the NADPH oxidase complex, ultimately leading to ROS production by this complex (33). Furthermore, ROS can permeate the membranes of bacterial pathogens and inflict damage intracellularly (33). Sustained infectious insults as seen in sepsis pathophysiology results in accelerated production and release of ROS. This accelerated production leads to inefficiencies within the mitochondria due to alterations in oxygen consumption, impaired glucose and lipid metabolism, resulting in mitochondrial dysfunction (34). Likewise, increased release of ROS leads to cellular damage, DNA damage and apoptosis in adjacent tissues and cells (35). Furthermore, persistent infection results in overwhelming and depleting the natural antioxidant defense mechanisms the body has evolved to combat excess ROS production.

There is an abundance of evidence that points to excess ROS contributing to the maladaptive responses in inflammatory states leading to metabolic and global dysfunction (35). In response to inflammatory triggers and ROS signaling, leukocytes initiate the

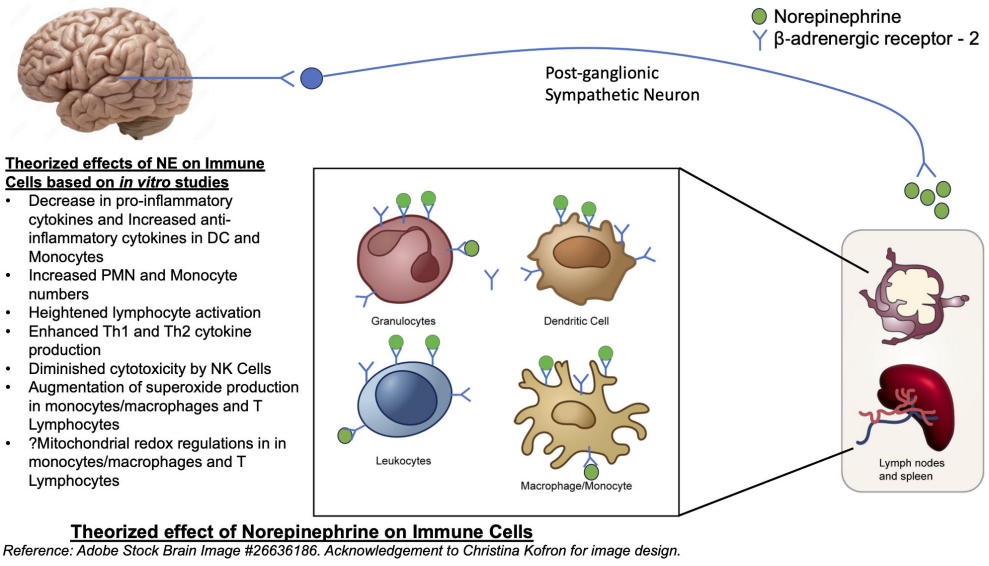

FIGURE 1
Theorized effect of Norepinephrine on Immune cells. Reference: Adobe Stock Brain Image #26636186.

synthesis and release of proinflammatory cytokines. Specifically, there is evidence to suggest that ROS plays a role in the release of cytokines induced by LPS, NF-κB activation by thrombin and downstream endothelial cell activation (35). Similarly, research demonstrates that mitochondrial production of H_2O_2 contributes to NF-κB activation in endothelial cells of aged rat arteries, and that curtailing of ROS activity can reduce hypoxia-triggered endothelial NF-κB activation and IL-6 secretion (35). Much research has also highlighted that cardiac myocyte dysfunction in sepsis is a result of continued oxidative stress (30, 36–39). Sepsis induced oxidative stress is a complex interplay of inflammatory responses, mitochondrial dysfunction and depletion of antioxidant resources. Research is still ongoing but, efforts to promote anti-inflammation and antioxidant treatments in the management of sepsis have largely been unsuccessful.

Oxidative stress, NE and sepsis

Sepsis is characterized by widespread alterations in metabolism, both at the systemic and organ-specific level in response to an infection. These changes can escalate and lead to dysregulation which results in circulatory changes and septic shock (34, 40, 41). The most common consequences of sepsis are impaired vascular permeability, cardiac malfunction, and mitochondrial dysfunction leading to impaired metabolism and, if left unchecked, shock. It has been reported that patients treated with a non-lethal dose of endotoxin and without demonstrable organ dysfunction have enhanced metabolic rates and oxygen consumption by approximately 37-55% as to basal metabolism (42). However, patients with sepsis or septic shock do not seem to have the same enhancement of metabolism and consumption and that the level of attenuation of this response correlates with disease severity (42). Precise mechanisms responsible for this attenuation is unknown (30).

NE has been identified as being superior to other vasopressors in a systematic review of randomized controlled trials evaluating in-hospital and 28-day mortality in septic shock patients (43). A meta-analysis showed that early administration of NE, which varied per study evaluated but was defined <6 hours after identification of septic shock, resulted in statistically significant reduction in short-term morality (44). The mechanisms for this remain unclear, but NE plays a role in regulating the immune response to infection and combating shock.

There is also evidence to suggest that NE is intimately involved in regulating oxidative metabolism. Research has shown that NE augments the generation of superoxide in freshly isolated primary human PBMCs by means of NADPH oxidase, mediated by α-adrenergic receptors. This effect promotes adherence of monocytes to the endothelium (24, 45). Case et. al., demonstrated that mitochondrial metabolism and superoxide-mediated redox signaling play a regulatory role in the T-lymphocyte response to NE (24). They hypothesized that the T-lymphocyte phenotype could be influenced by NE and superoxide production which could result in specific changes in cytokine expression (24). Mechanisms elucidating the role of NE in lymphocyte activation and regulation remain unclear but, oxidative metabolism may be involved. In ovarian surface epithelial cells, NE is protective against bleomycin induced oxidative damage (46). Additionally, Case et al. posited that NE appears to have a multifaceted regulatory effect on various cellular processes including metabolism and mitochondrial redox regulation (24). Systemic diseases associated with elevated inflammatory signaling and metabolic dysfunction such as atherosclerosis, diabetes, COPD, vitiligo, heart failure, Parkinson's disease and stroke have all demonstrated altered redox balances as a potential mechanism for disease progression (47–51). Dysregulation of PBMC redox balance has been implicated in many of the disease processes listed above (47–51).

Immune cell specific dysregulation in sepsis

Immune cell specific dysregulation in sepsis is a relatively new avenue of research that has been highlighted due to pandemic research and the advent of single cell RNA sequencing technology. Three notable studies utilized scRNAseq to identify specific PBMC populations contributing to disease progression in sepsis (52–54). Wen et. al., found a distinct monocyte population, CD14+ monocytes, that were important in the early recovery phase of Sars-CoV-2 infected patients whereas clonal expansion of T and B cells were important in later recovery stages (52). Zhang et. al., found that intensive expansion of highly cytotoxic effector T cell subsets, was associated with convalescence in moderate Sars-CoV-2 patients. In severe SARS-CoV-2 patients, there was profound immune exhaustion and broad T cell expansion. This study illustrates the dynamic nature of the immune system in response to Sars-CoV-2 (53). Similar to Wen et. al, Reyes et. al, found that in emergency department patients presenting with sepsis due to urinary tract infections the same CD14+ monocytes were present in the blood of these patients (54). They noted that this monocyte population was also present in ICU patients with sterile inflammation. They hypothesized that particular gene signatures may be able to distinguish sterile *vs* non-sterile inflammatory populations (54). In this review, we have highlighted the ubiquitous effects of NE and its impact on immunity in sepsis. Therefore, it is possible that NE may mediate some of the dysfunction in specific cell populations in sepsis which may underlie sepsis pathogenesis. This research is still in its nascent stages and is ongoing.

NE and trained immunity in sepsis

Trained immunity refers to the long-lasting memory traits of innate immunity. Specifically, studies have shown that sustained changes in epigenetic marks and metabolic pathways can leads to an altered transcriptional response to a subsequent challenge (55, 56). The implications of trained immunity are that reprogrammed immunocytes can respond more rapidly and effectively, in particularly to distinct pathogens and markers of infection allowing for improved immune function. In sepsis, however, these trained immunity programs may lead to antagonistic inflammatory cues and ultimately tolerance of an infectious burden. In contrast, tolerance may also allow for repair and protective mechanisms (57). The exact

relationship is not clearly understood and there is little to date on trained immunity in sepsis (55), but its implications could lead to the development of novel treatment strategies. Zhang et. al., has identified 3 subpopulations of monocytes with distinct cellular transcriptional programs in response to induction by 4 different inducers of trained immunity (56). These findings are consistent with the studies regarding distinct monocyte populations identified in response to COVID-19 infection (52–54). There is also some literature linking catecholamines with trained immunity. Netea et. al., found that exposure to high levels of catecholamines can result in long lasting pro-inflammatory changes in myeloid cells in cardiovascular disease (55). Similarly, Slusher et. al., found that catecholamine release in acute maximal exercise can exert a pro-inflammatory response in isolated monocytes exposed to LPS (58). There is a role here for the sympathetic nervous system in trained immunity in sepsis but, it remains unclear at this time. It is clear, however, that this is a highly complex, multi-faceted event that is regulated by diverse alterations of signaling pathways, chromatin modulation and metabolic re-wiring. Further research is needed to elucidate the intricacies of nervous system input in response to infection and training of immunocytes.

Impact of NE and β-blockers in septic shock

There is a growing body of evidence to suggest that early norepinephrine administration during sepsis resuscitation may be beneficial in mitigating shock (44, 59–61). In 2019, the phase II CENSER trial identified that early low dose norepinephrine in adults with sepsis and hypotension results in significantly increased shock control by 6 hours (60). In 2020, a prospective ICU based propensity-score based analysis also demonstrated that an early start of norepinephrine might be safe and limit fluid resuscitation and lead to better outcomes (62). However, these studies have only focused on the vascular effects and have not evaluated the impact of NE on the immune system. Stolk et. al., performed a bench to bedside study in mice and humans that found that NE has anti-inflammatory effects in sepsis and that could lead to deleterious effects and immunoparalysis which could contribute to sepsis progression (21). This study contradicts much of the clinically relevant data that demonstrates a beneficial effect of NE in sepsis treatment. Limiting Stolk et. al.'s findings are that their study did not directly assess immunoparalysis and limited their analysis on the cytokines TNF-a and IL-10 to assess host response (63).

The value of NE in the management of septic shock has always been understood to be a result of its effect on the vascular endothelium and promotion of cardiac output preventing circulatory collapse. Traditionally, this has translated to shortened hospital length of stays and reduced mortality in septic shock (64). However, some recent trials have highlighted that allowing for some permissive hypotension in patients ≥65 years with septic shock showed no differences in 90-day mortality, and higher blood pressure values (≥65 mmHg) did not add further benefits (65, 66). The Surviving Sepsis Campaign (SSC) has suggested adding vasopressin as an adjunctive therapy to NE in the management of septic shock with the intent of rising MAP to target with the thoughts that this would prevent the deleterious consequences of an excessive adrenergic load (67). However, these recommendations were weak and based on low quality of evidence. Furthermore, there haven't been any large scale trials evaluating the efficacy of vasopressin compared to NE (68).

There is also growing evidence to suggest β-blockers may have a positive impact on mortality in sepsis. The BEAST study found that β-blockers exposure prior to the onset of sepsis, maybe associated with better outcomes (69). A systematic review and meta-analysis found that patients with persistent tachycardia despite fluid resuscitation treated with β-blockers had lower 28-d mortality (70). The potential benefits of β-blocker therapy in sepsis include improved heart rate control thereby decreasing myocardial oxygen demand in septic patients (71). In addition, β-blockers are also thought to block the adrenergic up-regulation thought to contribute to sepsis mortality (72). Similar to Stolk et. al.'s findings, if true, this would argue against NE treatment as NE's effects are mediated by the β2 adrenergic receptor. No large scale clinical trial has evaluated the effect of β-blockers in the treatment of sepsis and the risk of hypotension has somewhat also limited their evaluation (72).

As this review as highlighted, the role of NE is quite complex. It is clear that NE has ubiquitous effects on a variety of immune cells and vascular endothelium which can impact sepsis pathogenesis. Further research is necessary to realize NE's impact on immunity in sepsis. There must be a reason that for the past 50 years, NE remains the first-line vasopressor of choice and has the best safety and tolerance profile in patients with septic shock (63).

Discussion

It is clear that NE has a multi-faceted role in sepsis and this review only begins to shed light on the intricate interaction between the nervous system, immune system and immunocyte oxidative metabolism. This review highlights that there are intertwined relationships between the nervous and immune systems where communications occur in a bi-directional manner. Sepsis is ranked as a top contributor to mortality in the United States and treatment paradigms have yielded little results in mitigating mortality. The scope of sepsis research has predominantly concentrated on reducing pathogen load and providing supportive care with measures like anti-pyretics, fluids, antibiotics/anti-virals and anti-inflammatory agents (73). There has been a notable shortage of emphasis on uncovering strategies for immune system augmentation. Instead of exclusively focusing on diminishing pathogen burden, perhaps treatment can also focus on immune enhancing strategies harnessing inherent responses to infection. Furthermore, elucidating the trained immune response, or identifying specific immune cell populations involved in sepsis mediated immune dysfunction will be key to the development of novel treatment strategies. NE has been associated with improved outcomes in septic shock. This has been traditionally ascribed to its role as vasopressor and its effects on peripheral

vascular resistance (43) However, with this knowledge that NE interacts with immune cells directly and alters their signaling patterns and metabolic pathways, particularly those that regulate ROS production, it begs the questions of whether NE has larger role in sepsis than just promoting peripheral vascular resistance. This would have implications for earlier norepinephrine use.

This review has underscored the role of NE in governing the bodys response to infection (8–11, 13, 14, 25, 28, 74), alongside its involvement in regulating oxidative metabolism within immune cells (24, 45). The potential for NE dysregulation to contribute to sepsis pathology is worth considering with implications for early introduction of NE in septic patients as therapy. Systemic and organ-specific changes in bioenergetics and metabolism characterize the dysregulated response to infection is sepsis and septic shock. Understanding the pathophysiological mechanisms underlying SNS regulation and mitochondrial dysfunction in sepsis may pave the way for new diagnostic strategies and therapeutic approaches. These findings may help physicians to identify distinct subgroups of sepsis patients or even sub-populations of cells for more directed treatment strategies.

Author contributions

JT: Conceptualization, Writing – original draft. PM: Writing – original draft. BB: Writing – review & editing. DS: Writing – review & editing. JF: Writing – review & editing.

Funding

The author(s) declare that no financial support was received for the research, authorship, and/or publication of this article.

Acknowledgments

Acknowledgement to Christina Kofron for Figure image design.

Conflict of interest

The authors declare that the research was conducted in the absence of any commercial or financial relationships that could be construed as a potential conflict of interest.

Publisher's note

References

1. Martin GS, Mannino DM, Eaton S, Moss M. The epidemiology of sepsis in the United States from 1979 through 2000. *N Engl J Med* (2003) 348(16):1546–54. doi: 10.1056/NEJMoa022139

2. Rhee C, Dantes R, Epstein L, Murphy DJ, Seymour CW, Iwashyna TJ, et al. Incidence and trends of sepsis in US hospitals using clinical vs claims data, 2009-2014. *JAMA* (2017) 318(13):1241–9. doi: 10.1001/jama.2017.13836

3. Rudd KE, Johnson SC, Agesa KM, Shackelford KA, Tsoi D, Kievlan DR, et al. Global, regional, and national sepsis incidence and mortality, 1990-2017: analysis for the Global Burden of Disease Study. *Lancet* (2020) 395(10219):200–11. doi: 10.1016/S0140-6736(19)32989-7

4. Mayr VD, Dunser MW, Greil V, Jochberger S, Luckner G, Ulmer H, et al. Causes of death and determinants of outcome in critically ill patients. *Crit Care* (2006) 10(6): R154. doi: 10.1186/cc5086

5. Andersson U, Tracey KJ. Neural reflexes in inflammation and immunity. *J Exp Med* (2012) 209(6):1057–68. doi: 10.1084/jem.20120571

6. Elenkov IJ, Wilder RL, Chrousos GP, Vizi ES. The sympathetic nerve–an integrative interface between two supersystems: the brain and the immune system. *Pharmacol Rev* (2000) 52(4):595–638.

7. Gaskill PJ, Khoshbouei H. Dopamine and norepinephrine are embracing their immune side and so should we. *Curr Opin Neurobiol* (2022) 77:102626. doi: 10.1016/j.conb.2022.102626

8. Kohm AP, Sanders VM. Norepinephrine and beta 2-adrenergic receptor stimulation regulate CD4+ T and B lymphocyte function *in vitro* and *in vivo*. *Pharmacol Rev* (2001) 53(4):487–525.

9. Agac D, Estrada LD, Maples R, Hooper LV, Farrar JD. The beta2-adrenergic receptor controls inflammation by driving rapid IL-10 secretion. *Brain Behav Immun* (2018) 74:176–85. doi: 10.1016/j.bbi.2018.09.004

10. Maestroni GJ. Sympathetic nervous system influence on the innate immune response. *Ann N Y Acad Sci* (2006) 1069:195–207. doi: 10.1196/annals.1351.017

11. Qiao G, Bucsek MJ, Winder NM, Chen M, Giridharan T, Olejniczak SH, et al. beta-Adrenergic signaling blocks murine CD8(+) T-cell metabolic reprogramming during activation: a mechanism for immunosuppression by adrenergic stress. *Cancer Immunol Immunother.* (2019) 68(1):11–22. doi: 10.1007/s00262-018-2243-8

12. Lorton D, Bellinger DL. Molecular mechanisms underlying beta-adrenergic receptor-mediated cross-talk between sympathetic neurons and immune cells. *Int J Mol Sci* (2015) 16(3):5635–65. doi: 10.3390/ijms16035635

13. Katayama Y, Battista M, Kao WM, Hidalgo A, Peired AJ, Thomas SA, et al. Signals from the sympathetic nervous system regulate hematopoietic stem cell egress from bone marrow. *Cell* (2006) 124(2):407–21. doi: 10.1016/j.cell.2005.10.041

14. Sharma D, Farrar JD. Adrenergic regulation of immune cell function and inflammation. *Semin Immunopathol* (2020) 42(6):709–17. doi: 10.1007/s00281-020-00829-6

15. Stolk RF, van der Poll T, Angus DC, van der Hoeven JG, Pickkers P, Kox M. Potentially inadvertent immunomodulation: norepinephrine use in sepsis. *Am J Respir Crit Care Med* (2016) 194(5):550–8. doi: 10.1164/rccm.201604-0862CP

16. Takenaka MC, Guereschi MG, Basso AS. Neuroimmune interactions: dendritic cell modulation by the sympathetic nervous system. *Semin Immunopathol* (2017) 39 (2):165–76. doi: 10.1007/s00281-016-0590-0

17. Xing Z, Ohkawara Y, Jordana M, Graham FL, Gauldie J. Adenoviral vector-mediated interleukin-10 expression *in vivo*: intramuscular gene transfer inhibits cytokine responses in endotoxemia. *Gene Ther* (1997) 4(2):140–9. doi: 10.1038/sj.gt.3300371

18. Grailer JJ, Haggadone MD, Sarma JV, Zetoune FS, Ward PA. Induction of M2 regulatory macrophages through the beta2-adrenergic receptor with protection during endotoxemia and acute lung injury. *J Innate Immun* (2014) 6(5):607–18. doi: 10.1159/000358524

19. Angus DC, van der Poll T. Severe sepsis and septic shock. *N Engl J Med* (2013) 369(9):840–51. doi: 10.1056/NEJMra1208623

20. Ng TM, Toews ML. Impaired norepinephrine regulation of monocyte inflammatory cytokine balance in heart failure. *World J Cardiol* (2016) 8(10):584–9. doi: 10.4330/wjc.v8.i10.584

21. Stolk RF, van der Pasch E, Naumann F, Schouwstra J, Bressers S, van Herwaarden AE, et al. Norepinephrine dysregulates the immune response and compromises host defense during sepsis. *Am J Respir Crit Care Med* (2020) 202 (6):830–42. doi: 10.1164/rccm.202002-0339OC

22. Scanzano A, Schembri L, Rasini E, Luini A, Dallatorre J, Legnaro M, et al. Adrenergic modulation of migration, CD11b and CD18 expression, ROS and

interleukin-8 production by human polymorphonuclear leukocytes. *Inflammation Res* (2015) 64(2):127–35. doi: 10.1007/s00011-014-0791-8

23. Beis D, von Kanel R, Heimgartner N, Zuccarella-Hackl C, Burkle A, Ehlert U, et al. The role of norepinephrine and alpha-adrenergic receptors in acute stress-induced changes in granulocytes and monocytes. *Psychosom Med* (2018) 80(7):649–58. doi: 10.1097/PSY.0000000000000620

24. Case AJ, Roessner CT, Tian J, Zimmerman MC. Mitochondrial superoxide signaling contributes to norepinephrine-mediated T-lymphocyte cytokine profiles. *PloS One* (2016) 11(10):e0164609. doi: 10.1371/journal.pone.0164609

25. Torres KC, Antonelli LR, Souza AL, Teixeira MM, Dutra WO, Gollob KJ. Norepinephrine, dopamine and dexamethasone modulate discrete leukocyte subpopulations and cytokine profiles from human PBMC. *J Neuroimmunol* (2005) 166(1-2):144–57. doi: 10.1016/j.jneuroim.2005.06.006

26. Slota C, Shi A, Chen G, Bevans M, Weng NP. Norepinephrine preferentially modulates memory CD8 T cell function inducing inflammatory cytokine production and reducing proliferation in response to activation. *Brain Behav Immun* (2015) 46:168–79. doi: 10.1016/j.bbi.2015.01.015

27. Diaz-Salazar C, Bou-Puerto R, Mujal AM, Lau CM, von Hoesslin M, Zehn D, et al. Cell-intrinsic adrenergic signaling controls the adaptive NK cell response to viral infection. *J Exp Med* (2020) 217(4). doi: 10.1084/jem.20190549

28. Sanders VM, Baker RA, Ramer-Quinn DS, Kasprowicz DJ, Fuchs BA, Street NE. Differential expression of the beta2-adrenergic receptor by Th1 and Th2 clones: implications for cytokine production and B cell help. *J Immunol* (1997) 158(9):4200–10. doi: 10.4049/jimmunol.158.9.4200

29. Biswal S, Remick DG. Sepsis: redox mechanisms and therapeutic opportunities. *Antioxid Redox Signal* (2007) 9(11):1959–61. doi: 10.1089/ars.2007.1808

30. Nagar H, Piao S, Kim CS. Role of mitochondrial oxidative stress in sepsis. *Acute Crit Care* (2018) 33(2):65–72. doi: 10.4266/acc.2018.00157

31. Viola A, Munari F, Sanchez-Rodriguez R, Scolaro T, Castegna A. The metabolic signature of macrophage responses. *Front Immunol* (2019) 10:1462. doi: 10.3389/fimmu.2019.01462

32. Chen X, Song M, Zhang B, Zhang Y. Reactive oxygen species regulate T cell immune response in the tumor microenvironment. *Oxid Med Cell Longev* (2016) 2016:1580967. doi: 10.1155/2016/1580967

33. Nguyen GT, Green ER, Mecsas J. Neutrophils to the ROScue: mechanisms of NADPH oxidase activation and bacterial resistance. *Front Cell Infect Microbiol* (2017) 7:373. doi: 10.3389/fcimb.2017.00373

34. Preau S, Vodovar D, Jung B, Lancel S, Zafrani L, Flatres A, et al. Energetic dysfunction in sepsis: a narrative review. *Ann Intensive Care* (2021) 11(1):104. doi: 10.1186/s13613-021-00893-7

35. Forrester SJ, Kikuchi DS, Hernandes MS, Xu Q, Griendling KK. Reactive oxygen species in metabolic and inflammatory signaling. *Circ Res* (2018) 122(6):877–902. doi: 10.1161/CIRCRESAHA.117.311401

36. van Gastel J, Hendrickx JO, Leysen H, Santos-Otte P, Luttrell LM, Martin B, et al. beta-arrestin based receptor signaling paradigms: potential therapeutic targets for complex age-related disorders. *Front Pharmacol* (2018) 9:1369. doi: 10.3389/fphar.2018.01369

37. Corbi G, Conti V, Russomanno G, Longobardi G, Furgi G, Filippelli A, et al. Adrenergic signaling and oxidative stress: a role for sirtuins? *Front Physiol* (2013) 4:324. doi: 10.3389/fphys.2013.00324

38. Drosatos K, Lymperopoulos A, Kennel PJ, Pollak N, Schulze PC, Goldberg IJ. Pathophysiology of sepsis-related cardiac dysfunction: driven by inflammation, energy mismanagement, or both? *Curr Heart Fail Rep* (2015) 12(2):130–40. doi: 10.1007/s11897-014-0247-z

39. Yao X, Carlson D, Sun Y, Ma L, Wolf SE, Minei JP, et al. Mitochondrial ROS Induces Cardiac Inflammation via a Pathway through mtDNA Damage in a Pneumonia-Related Sepsis Model. *PloS One* (2015) 10(10):e0139416. doi: 10.1371/journal.pone.0139416

40. Singer M, Deutschman CS, Seymour CW, Shankar-Hari M, Annane D, Bauer M, et al. The third international consensus definitions for sepsis and septic shock (Sepsis-3). *JAMA* (2016) 315(8):801–10. doi: 10.1001/jama.2016.0287

41. Hotchkiss RS, Moldawer LL, Opal SM, Reinhart K, Turnbull IR, Vincent JL. Sepsis and septic shock. *Nat Rev Dis Primers.* (2016) 2:16045. doi: 10.1038/nrdp.2016.45

42. Kreymann G, Grosser S, Buggisch P, Gottschall C, Matthaei S, Greten H. Oxygen consumption and resting metabolic rate in sepsis, sepsis syndrome, and septic shock. *Crit Care Med* (1993) 21(7):1012–9. doi: 10.1097/00003246-199307000-00015

43. Vasu TS, Cavallazzi R, Hirani A, Kaplan G, Leiby B, Marik PE. Norepinephrine or dopamine for septic shock: systematic review of randomized clinical trials. *J Intensive Care Med* (2012) 27(3):172–8. doi: 10.1177/0885066610396312

44. Li Y, Li H, Zhang D. Timing of norepinephrine initiation in patients with septic shock: a systematic review and meta-analysis. *Crit Care* (2020) 24(1):488. doi: 10.1186/s13054-020-03204-x

45. Deo SH, Jenkins NT, Padilla J, Parrish AR, Fadel PJ. Norepinephrine increases NADPH oxidase-derived superoxide in human peripheral blood mononuclear cells via alpha-adrenergic receptors. *Am J Physiol Regul Integr Comp Physiol* (2013) 305(10):R1124–32. doi: 10.1152/ajpregu.00347.2013

46. Patel PR, Hegde ML, Theruvathu J, Mitra SA, Boldogh I, Sowers L. Norepinephrine reduces reactive oxygen species (ROS) and DNA damage in ovarian surface epithelial cells. *J Bioanal Biomed* (2015) 7(3):75–80. doi: 10.4172/1948-593X.1000127

47. Shirakawa R, Yokota T, Nakajima T, Takada S, Yamane M, Furihata T, et al. Mitochondrial reactive oxygen species generation in blood cells is associated with disease severity and exercise intolerance in heart failure patients. *Sci Rep* (2019) 9(1):14709. doi: 10.1038/s41598-019-51298-3

48. Prigione A, Begni B, Galbussera A, Beretta S, Brighina L, Garofalo R, et al. Oxidative stress in peripheral blood mononuclear cells from patients with Parkinson's disease: negative correlation with levodopa dosage. *Neurobiol Dis* (2006) 23(1):36–43. doi: 10.1016/j.nbd.2006.01.013

49. Fratta Pasini AM, Stranieri C, Ferrari M, Garbin U, Cazzoletti L, Mozzini C, et al. Oxidative stress and Nrf2 expression in peripheral blood mononuclear cells derived from COPD patients: an observational longitudinal study. *Respir Res* (2020) 21(1):37. doi: 10.1186/s12931-020-1292-7

50. Dell'Anna ML, Maresca V, Briganti S, Camera E, Falchi M, Picardo M. Mitochondrial impairment in peripheral blood mononuclear cells during the active phase of vitiligo. *J Invest Dermatol* (2001) 117(4):908–13. doi: 10.1046/j.0022-202x.2001.01459.x

51. Rodriguez-Iturbe B, Pons H, Johnson RJ. Role of the immune system in hypertension. *Physiol Rev* (2017) 97(3):1127–64. doi: 10.1152/physrev.00031.2016

52. Wen W, Su W, Tang H, Le W, Zhang X, Zheng Y, et al. Immune cell profiling of COVID-19 patients in the recovery stage by single-cell sequencing. *Cell Discovery* (2020) 6:31. doi: 10.1038/s41421-020-0168-9

53. Zhang JY, Wang XM, Xing X, Xu Z, Zhang C, Song JW, et al. Single-cell landscape of immunological responses in patients with COVID-19. *Nat Immunol* (2020) 21(9):1107–18. doi: 10.1038/s41590-020-0762-x

54. Reyes M, Filbin MR, Bhattacharyya RP, Billman K, Eisenhaure T, Hung DT, et al. An immune-cell signature of bacterial sepsis. *Nat Med* (2020) 26(3):333–40. doi: 10.1038/s41591-020-0752-4

55. Netea MG, Dominguez-Andres J, Barreiro LB, Chavakis T, Divangahi M, Fuchs E, et al. Defining trained immunity and its role in health and disease. *Nat Rev Immunol* (2020) 20(6):375–88. doi: 10.1038/s41577-020-0285-6

56. Zhang B, Moorlag SJ, Dominguez-Andres J, Bulut O, Kilic G, Liu Z, et al. Single-cell RNA sequencing reveals induction of distinct trained-immunity programs in human monocytes. *J Clin Invest.* (2022) 132(7). doi: 10.1172/JCI147719

57. Lajqi T, Kostlin-Gille N, Bauer R, Zarogiannis SG, Lajqi E, Ajeti V, et al. Training vs. Tolerance: the yin/yang of the innate immune system. *Biomedicines* (2023) 11(3). doi: 10.3390/biomedicines11030766

58. Slusher AL, Zuniga TM, Acevedo EO. Maximal exercise alters the inflammatory phenotype and response of mononuclear cells. *Med Sci Sports Exerc.* (2018) 50(4):675–83. doi: 10.1249/MSS.0000000000001480

59. Elbouhy MA, Soliman M, Gaber A, Taema KM, Abdel-Aziz A. Early use of norepinephrine improves survival in septic shock: earlier than early. *Arch Med Res* (2019) 50(6):325–32. doi: 10.1016/j.arcmed.2019.10.003

60. Permpikul C, Tongyoo S, Viarasilpa T, Trainarongsakul T, Chakorn T, Udompanturak S. Early use of norepinephrine in septic shock resuscitation (CENSER). A randomized trial. *Am J Respir Crit Care Med* (2019) 199(9):1097–105. doi: 10.1164/rccm.201806-1034OC

61. Ospina-Tascon GA, Hernandez G, Alvarez I, Calderon-Tapia LE, Manzano-Nunez R, Sanchez-Ortiz AI, et al. Effects of very early start of norepinephrine in patients with septic shock: a propensity score-based analysis. *Crit Care* (2020) 24(1):52. doi: 10.1186/s13054-020-2756-3

62. Hamzaoui O, Shi R. Early norepinephrine use in septic shock. *J Thorac Dis* (2020) 12(Suppl 1):S72–S7. doi: 10.21037/jtd.2019.12.50

63. Uhel F, van der Poll T. Norepinephrine in septic shock: A mixed blessing. *Am J Respir Crit Care Med* (2020) 202(6):788–9. doi: 10.1164/rccm.202006-2301ED

64. Guarino M, Perna B, Cesaro AE, Maritati M, Spampinato MD, Contini C, et al. Update on sepsis and septic shock in adult patients: management in the emergency department. *J Clin Med* (2023) 2023:12(9). doi: 10.3390/jcm12093188

65. Lamontagne F, Meade MO, Hebert PC, Asfar P, Lauzier F, Seely AJE, et al. Higher versus lower blood pressure targets for vasopressor therapy in shock: a multicentre pilot randomized controlled trial. *Intensive Care Med* (2016) 42(4):542–50. doi: 10.1007/s00134-016-4237-3

66. Lamontagne F, Richards-Belle A, Thomas K, Harrison DA, Sadique MZ, Grieve RD, et al. Effect of reduced exposure to vasopressors on 90-day mortality in older critically ill patients with vasodilatory hypotension: A randomized clinical trial. *JAMA* (2020) 323(10):938–49. doi: 10.1001/jama.2020.0930

67. Rhodes A, Evans LE, Alhazzani W, Levy MM, Antonelli M, Ferrer R, et al. Surviving sepsis campaign: international guidelines for management of sepsis and septic shock: 2016. *Intensive Care Med* (2017) 43(3):304–77. doi: 10.1007/s00134-017-4683-6

68. Shi R, Hamzaoui O, De Vita N, Monnet X, Teboul JL. Vasopressors in septic shock: which, when, and how much? *Ann Transl Med* (2020) 8(12):794. doi: 10.21037/atm.2020.04.24

69. Tan K, Harazim M, Simpson A, Tan YC, Gunawan G, Robledo KP, et al. Association between premorbid beta-blocker exposure and sepsis outcomes-the beta-

blockers in European and Australian/American septic patients (BEAST) study. *Crit Care Med* (2021) 49(9):1493–503. doi: 10.1097/CCM.0000000000005034

70. Hasegawa D, Sato R, Prasitlumkum N, Nishida K, Takahashi K, Yatabe T, et al. Effect of ultrashort-acting beta-blockers on mortality in patients with sepsis with persistent tachycardia despite initial resuscitation: A systematic review and meta-analysis of randomized controlled trials. *Chest* (2021) 159(6):2289–300. doi: 10.1016/j.chest.2021.01.009

71. Hamzaoui O, Teboul JL. The role of beta-blockers in septic patients. *Minerva Anestesiol.* (2015) 81(3):312–9.

72. Novotny NM, Lahm T, Markel TA, Crisostomo PR, Wang M, Wang Y, et al. beta-Blockers in sepsis: reexamining the evidence. *Shock* (2009) 31(2):113–9. doi: 10.1097/SHK.0b013e318180ffb6

73. Bauer M, Wetzker R. The cellular basis of organ failure in sepsis-signaling during damage and repair processes. *Med Klin Intensivmed Notfmed* (2020) 115(Suppl 1):4–9. doi: 10.1007/s00063-020-00673-4

74. Takamoto T, Hori Y, Koga Y, Toshima H, Hara A, Yokoyama MM. Norepinephrine inhibits human natural killer cell activity *in vitro*. *Int J Neurosci* (1991) 58(1-2):127–31. doi: 10.3109/00207459108987189

frontiers | Frontiers in Immunology

TYPE Original Research
PUBLISHED 04 December 2023
DOI 10.3389/fimmu.2023.1297484

OPEN ACCESS

EDITED BY
Pablo Andres Evelson,
University of Buenos Aires, Argentina

REVIEWED BY
Hong Zhang,
Second Affiliated Hospital of Soochow University, China
Sandra Cristina Zárate,
National Scientific and Technical Research Council (CONICET), Argentina

*CORRESPONDENCE
Bo Lv
lvbo@tongji.edu.cn
Zhigang Xue
xuezg@tongji.edu.cn
Yazhong Ji
jiyazhong@tongji.edu.cn

†These authors have contributed equally to the work

RECEIVED 20 September 2023
ACCEPTED 13 November 2023
PUBLISHED 04 December 2023

CITATION
Qi L, Li Y, Zhang L, Li S, Zhang X, Li W, Qin J, Chen X, Ji Y, Xue Z and Lv B (2023) Immune and oxidative stress disorder in ovulation-dysfunction women revealed by single-cell transcriptome.
Front. Immunol. 14:1297484.
doi: 10.3389/fimmu.2023.1297484

Immune and oxidative stress disorder in ovulation-dysfunction women revealed by single-cell transcriptome

Lingbin Qi[1†], Yumei Li[2†], Lina Zhang[1], Shuyue Li[1], Xunyi Zhang[1], Wanqiong Li[1], Jiaying Qin[1], Xian Chen[3], Yazhong Ji[1*], Zhigang Xue[1*] and Bo Lv[1*]

[1]Reproductive Medical Center, Department of Gynecology and Obstetrics, Tongji Hospital, Tongji University School of Medicine, Shanghai, China, [2]Department of Assisted Reproduction, Xiangya Hospital, Central South University, Changsha, China, [3]Shenzhen Key Laboratory of Reproductive Immunology for Peri-implantation, Shenzhen Zhongshan Institute for Reproductive Medicine and Genetics, Shenzhen Zhongshan Obstetrics and Gynecology Hospital (formerly Shenzhen Zhongshan Urology Hospital), Shenzhen, China

Introduction: Ovulation dysfunction is now a widespread cause of infertility around the world. Although the impact of immune cells in human reproduction has been widely investigated, systematic understanding of the changes of the immune atlas under female ovulation remain less understood.

Methods: Here, we generated single cell transcriptomic profiles of 80,689 PBMCs in three representative statuses of ovulation dysfunction, i.e., polycystic ovary syndrome (PCOS), primary ovarian insufficiency (POI) and menopause (MENO), and identified totally 7 major cell types and 25 subsets of cells.

Results: Our study revealed distinct cluster distributions of immune cells among individuals of ovulation disorders and health. In patients with ovulation dysfunction, we observed a significant reduction in populations of naïve CD8 T cells and effector memory CD4 T cells, whereas circulating NK cells and regulatory NK cells increased.

Discussion: Our results highlight the significant contribution of cDC-mediated signaling pathways to the overall inflammatory response within ovulation disorders. Furthermore, our data demonstrated a significant upregulation of oxidative stress in patients with ovulation disorder. Overall, our study gave a deeper insight into the mechanism of PCOS, POI, and menopause, which may contribute to the better diagnosis and treatments of these ovulatory disorder.

KEYWORDS

single-cell RNA sequencing, ovulation dysfunction, immune cell disorder, conventional dendritic cell, oxidative stress

Introduction

In recent decades, female infertility has become an increasing global concern. Knowledge of human reproduction has revealed that immune disorders can affect female fertility at multiple levels (1). Immune disorders affect hormonal glandular functions, such as thyroiditis, resulting in hyperprolactinemia that promotes ovulation dysfunction (2). Meanwhile, it has been reported that antibodies produced by immune cells are associated with high risk of infertility (3). Clinical evidence has confirmed that autoimmune diseases play a critical role in fertility decreasing (4). Ovulation disorder is the most frequent cause of female infertility and is present in approximately 40% of infertile women (5). The most common reasons for the decrease in ovulation function are polycystic ovary syndrome (PCOS), primary ovarian insufficiency (POI), and aging-induced ovarian reserve loss such as menopause (MENO). Although the immune cell types involved in these ovarian disorders are partially known, the essential immune subclusters, their transcriptomic characteristics, and changes in signaling pathways remain unclear (6–8). Sorting immune cells from peripheral blood using flow cytometry in bulk is unable to capture natural transcriptome characteristics. In addition, there still has no specific drugs for the treatment of either PCOS or POI (9, 10). Menopause, as a result of women losing their reproductive capacity and suffering from endocrine disorders with aging, also lacks immune cell data. Therefore, further studies are needed to understand specific anovulation-associated pathogenic factors.

Understanding immune alterations in peripheral blood is of paramount importance for unraveling the pathogenesis of ovulatory disorders. Comparative analysis of scRNA-seq datasets among individuals with varying health conditions, including PCOS, POI, and menopause, revealed notable changes in subsets of well-known cell types. It is widely acknowledged that naive T cells serve as precursors for effector and memory T cell subsets. Previous studies on mouse ovaries have indicated that a reduction in the proportion of naive CD4 T cells is associated with a diminished ability to mount an immune response, potentially contributing to age-related reproductive decline (11). Furthermore, a wealth of evidence suggests that effector memory CD4 T cells play a vital role in maintaining fetal-maternal immune tolerance and preventing pregnancy loss (12). Circulating and regulatory NK cells represent two major subtypes of NK cells distinguished by their expression of CD56. $CD56^{bright}$ NK cells, known as regulatory NK cells, generally constitute a small population and are recognized for their regulatory and immunomodulatory functions. Conversely, $CD56^{dim}$ NK cells, referred to as circulating NK cells, are the predominant subset of NK cells and possess potent cytotoxic and effector functions. Although NK cells contribute to the innate immune system and aid in preserving the integrity of ovarian tissue by eliminating cells with abnormal growth or function, an excessive number of NK cells may lead to chronic inflammation and tissue damage (13). Previous evidence has identified that elevated levels of NK cells in the ovary can disrupt proper follicular development by exerting cytotoxic effects on granulosa cells, which are essential for follicular growth and maturation (14). These findings highlight the disruption of T cell reserves and NK cell activation during anovulation, potentially causing a homeostatic imbalance within the immune system. Therefore, it is crucial to investigate these immune alterations in ovulatory disorders to gain a deeper understanding of their underlying mechanisms.

In this study, we utilized single-cell RNA sequencing (scRNA-seq) to explore the immune landscape at high resolution in peripheral blood mononuclear cells (PBMCs) from patients with ovulation failure and compared them to healthy individuals. We identified a total of 25 distinct cell clusters and investigated the major changes that occurred in each cell type. Our findings revealed a significant disturbance in the NK and T cell populations in individuals with ovulation disorders. Our data also highlighted the crucial role of cDC-mediated cell-cell interactions, especially contributing to the amplification of global inflammatory responses in individuals with immune dysfunction. Furthermore, we observed a significant upregulation of oxidative stress in patients with ovulation disorders. In addition to enhancing our understanding of the immune mechanisms underlying ovulation dysfunction, the present study suggests potential therapeutic strategies for mitigating ovarian dysfunction in female reproductive health.

Materials and methods

Ethics statement and clinical sample collection

This study was approved by the Ethics Committee of the Department of Medical and Life Science, Tongji University, and written informed consent was obtained from each participant (2020tjdx067). All sample collections were strictly performed according to the ethical and biosafety protocols approved by the institutional guidelines.

Blood samples were collected from the Shanghai Tongji Hospital (China) between November 2020 and January 2021. The cohort included individuals with MENO (n = 2), PCOS (n = 3), and POI (n = 3) for subsequent 10× genomic scRNA-seq. To eliminate the influence of medication, all volunteers were sampled without drug administration. The diagnosis of menopause, PCOS, and POI was based on detailed clinical symptoms according to a previous guide (15–17). The menopausal ages of the two individuals in the menopausal control group were 51 and 52 years, respectively. They joined the study control group at 1 and 3 years after the onset of menopause. Both women experienced natural menopause and were excluded from any immune disorders. The detailed clinical information and demographic characteristics of the patient cohort are shown in Table S1. PBMCs sequencing data of healthy females (n = 3) were downloaded from the 10× genomics dataset (https://www.10xgenomics.com/resources/datasets).

Single cell RNA library preparation and sequencing

PBMCs were isolated from whole blood samples according to the 10× Genomics Demonstrated Protocol (CG00039). Cell viability was assessed by trypan blue staining, and samples (cell viability >90%) were prepared using a 10× Genomics Single Cell 5' v2 Reagent Kit according to the manufacturer's instructions (10× Genomics). Each sequencing library was generated by using a unique sample index. The libraries were sequenced using an Illumina Nova6000.

Single-cell RNA data pre-processing and analysis

The raw 5′ scRNA-seq data were processed using CellRanger software (version 6.1.1). The transcripts were aligned to the human reference genome h38 using the function of "cellranger count" with the default parameter. All processed data were input into the respective folder, and downstream analysis was performed.

Main analyses in downstream were performed on Seurat R package (version 4.0.10) (18). Cells with less than 300 detected genes were filtered. After data filtering, raw counts were normalized to 10,000 reads by "NormalizeData" function with the default parameters. By using "FindVariableFeatures" function with the method of "vst" and 2000 highly variable genes were identified to perform principal component analysis (PCA). By using function of "FindIntegrationAnchors" and "IntegrateData", we reduced batch effect to reasonable degree and integrated the data from different batches to one Seurat object. The data were then scaled again using "ScaleData" and run a principal component analysis (PCA) and uniform manifold approximation and projection (UMAP) dimensionality reduction by using function of "RunPCA" and "RunUMAP." A nearest-neighbor graph using 30 dimensions of the PCA reduction was calculated using 'FindNeighbors,' followed by clustering using 'FindClusters' with a resolution of 0.6. Gene ontology enrichment analysis was performed by the clusterProfiler R package (version 3.9.0) (19). Lineage scores were calculated according to a published article (20) by calculating the sum of the logarithm of cpms among selected genes (see Table S2). Venn diagrams were constructed using the Venn R package (version 1.10). Statistical analyses were performed by ggsignif R packages (version 0.6.0).

Gene regulatory network analyses

To infer gene regulatory networks (GRNs) between fertile and infertile group, we used pySCENIC (version 0.12.0) (21) to perform regulatory networks analysis. The analysis steps consisted of three parts: creating a co-expression module *via* GRNBoost2, refining modules with cisTarget, and estimating the regulon activity by AUCell. The specific regulons among different groups (Health, MENO, PCOS and POI) were identified using the Regulon Specificity Score (RSS) according to standard tutorials. Gene regulatory networks were visualized with customization by cytoscape (version 3.16.1).

Receptor and ligand interactions analysis

To assess the cell–cell interactions and significant pathways, we performed all cell matrix from different group on CellChat R packages (version 1.1.3) (22). For put data into CellChat, we extracted large dgCMatrix from Seurat objects by using function of "GetAssayData." Briefly, we followed official supported workflow and loaded normalized data into CellChat by function of "createCellChat." We used CellChatDB in human secreted signaling as a ligand–receptor interaction database for subsequent analysis. Then, by using 'computeNetSimilarityPairwise' function, we identified signaling between healthy and POI. Differential expression of signaling pathway between healthy and POI was identified by function of 'identifyOverExpressedGenes.' To explore selected signaling pathway among different cell types, we ranked similarity of the shared signaling pathways by applying function of 'rankSimilarity.'

Statistical analysis

The bioinformatics data were statistically analyzed using ordinary one-way ANOVA or wilcox test with Graphpad Prism (version 9.4.1) and $P < 0.05$ was considered statistically significant. In this paper, one, two and three asterisks indicate $p < 0.05$, $p < 0.01$ and $p < 0.001$ respectively.

Results

Study design and single immune cell profiling among individuals with ovulation dysfunction

To characterize the immune properties of females who have experienced ovulation dysfunction, we generated an scRNA-seq dataset consisting of eight infertile females, including two females with menopause (MENO), three patients with polycystic ovary syndrome (PCOS), three patients with primary ovarian insufficiency (POI), and a control group of three healthy females (Figure 1A). Using the uniform manifold approximation and projection (UMAP) technique, we analyzed the distribution of various cell lineages in peripheral blood mononuclear cells (PBMCs) based on the expression of canonical cell markers. We observed that major cell types were present in all groups (Figures 1B, C). Specifically, we identified seven major cell clusters: CD4 T cells (CD3D, CD4), CD8 T cells (CD3D, CD8), natural killer (NK) cells (GNLY, CD16), B cells (CD79A, CD19), myeloid cells (CD14, LYZ), platelets (PPBP), and red blood cells (RBC) (Figure 1D). The distribution patterns of these major cell populations were comparable across patient groups (PCOS/POI/MENO) (Figure 1E).

10.3389/fimmu.2023.1297484

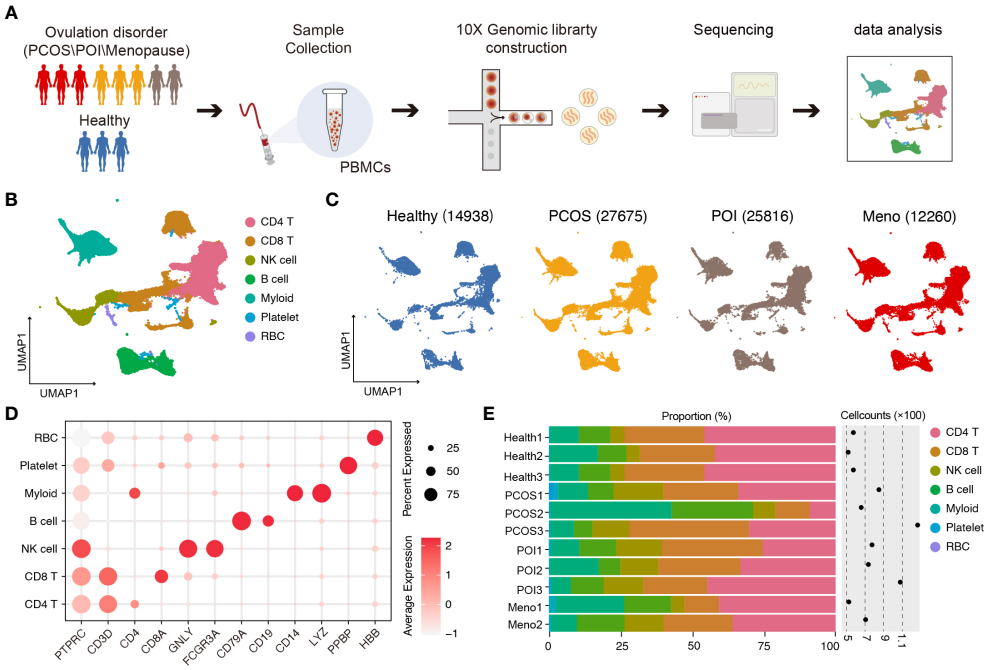

FIGURE 1
Single-cell transcriptomic profiles of PBMCs in ovulation-dysfunctional and healthy females. **(A)** Overview of sample collection, sequencing, and downstream analyses. **(B)** UMAP plot of the scRNA-seq profiled dataset for seven major cell types. **(C)** UMAP plot of the distribution of single cells among the different groups. **(D)**. Violin plots showing marker genes for diverse immune cell subsets. **(E)** Bar plot showing the percentage of major cell types in PBMCs of each individual. The cell counts for each sample are listed on the right-hand side.

Cellular characterization of individuals with ovulation disorder

Based on graph-based clustering of uniform manifold approximation and projection (UMAP) and specific gene markers, our data identified 25 cell subtypes, including CD4 naive T cells, CD4 central memory T cells, CD4 T helper cells, CD4 effector memory T cells, Treg, CD8 naive T cells, CD8 effector memory T cells, CD8 effector T cells, CD8 central memory T cells, mucosal associated invariant T cells, interferon-activated T cells, gamma-delta T cells, circulating NK cells, adaptive NK cells, regulatory NK cells, naive B cells, memory B cells, switch memory B cells, plasmblasts, CD14 monocytes, CD16 monocytes, conventional dendritic cells (cDCs), plasmacytoid dendritic cells (pDCs), platelets, and red blood cells (RBCs) (Figures 2A, B).

Specifically, within the CD4-positive T cell population, we distinguished CD4 naive T cells (marked by CCR7, LEF1, and TCF7), CD4 central memory T cells (characterized by high CCR7 expression and increased AQP3 and CD69 compared to CD4 naive T cells), CD4 effector memory T cells (identified by PRDM1 and low CCR7 expression), Tregs (expressing IL2RA and FOXP3), and CD4 Th1 cells (marked by CXCR3). In the CD8-positive T cell population, we identified CD8 naive T cells (marked by CCR7, LEF1, and TCF7), CD8 central memory T cells (showing high CCR7 expression and increased AQP3 and CD69 compared to CD8 naive T cells), CD8 effector memory T cells (characterized by GZMK expression), CD8 effector T cells (exhibiting high levels of GZMB, GNLY, and PRF1 but lacking CCR7 and IL7R expression), and mucosal-associated invariant T cells (MAIT) (marked by GZMK and high IL7R expression). Additionally, we identified CD4 and CD8 negative T cell subtypes, including gamma-delta T cells (expressing TRGC1, TRGC2, and TRDC) and interferon-activated cells (TIFN) (identified by ISG15 expression) (Figure 2B). We observed three distinct sub-clusters within the NK cell population: circulating NK cells (expressing FCGR3A and exhibiting dim NCAM1 expression), adaptive NK cells (marked by KLRC2 and dim NCAM1 expression), and regulatory NK cells (expressing FCGR3A, bright NCAM1, and KLRC1) (Figure 2B). We identified four different subtypes of B cells based on their gene expression profiles. Switched memory B cells expressed CD19 and CD27 but lacked IGHD expression, naive B cells expressed IGHD but lacked CD27 expression, memory B cells expressed both CD27 and IGHD, mature B cells expressed CD19 and MS4A1 but lacked CD27 expression, and plasmablasts expressed high levels of TNFRSF17 and CD27. Additionally, we identified CD14 monocytes (expressing CD14), CD16 monocytes (expressing FCGR3A), cDCs (marked by CD1C and ITGAX expression), and pDCs (expressing IL3RA, CLEC4C, and NRP1) (Figure 2B).

Comparing these cell subtypes across the anovulation groups with healthy females, we observed decreased proportions of CD4 naive T cells, CD8 naive T cells, and CD4 effector memory T cells, whereas all NK cell subtypes showed an increase (Figures 2C, S1) in the ovulation-dysfunction group. Specifically, the number of CD8 naive T cells significantly decreased in the MENO group, whereas CD4 effector memory T cells significantly decreased in the PCOS group (Figure 2D). The percentages of circulating and regulatory

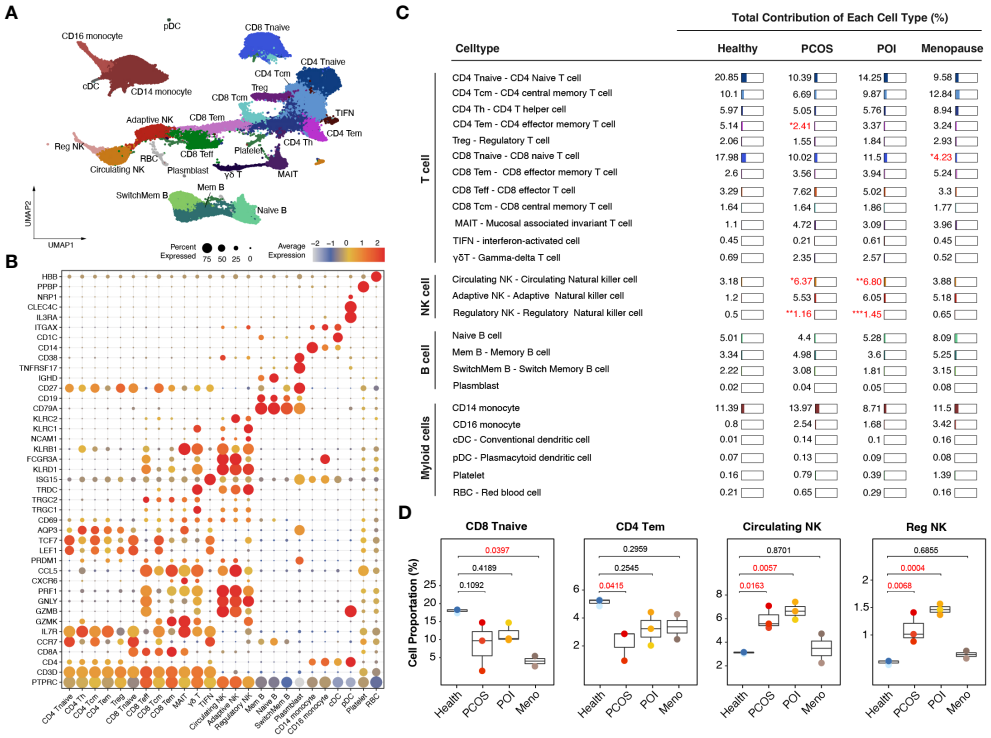

FIGURE 2
Immunological alterations in patients with ovulation disorders. **(A)** UMAP plot showing all the identified cells from ovulated and healthy females. **(B)** Violin plots showing special markers for all sub-cell types. **(C)** Table showing the percentages of each cell type among different groups (health/menopause/PCOS/POI). Ovulation-dysfunctional and healthy groups were expressed as percentages of the total immune cell types. **(D)** Boxplot showing the proportions of cells with significant differences in each sample colored by individual. The x-axis corresponds to each patient group. Significant differences compared to control samples were calculated by ordinary one-way ANOVA.

NK cells exhibited dramatic increases in the PCOS and POI groups (Figure 2D).

cDC-mediated cell–cell communication tends to disorder in ovulation-dysfunction groups

To investigate specific gene expression alterations for ovulation dysfunction, we conducted a detailed comparison of gene expression in five major cell types, CD4 T cells, CD8 T cells, NK cells, dendritic cells (DCs), and monocytes, between the ovulation-dysfunction group and the healthy group (Figure 3A). Interestingly, we observed that DCs exhibited the highest number of differentially expressed genes (both upregulated and downregulated) among the three ovulation-dysfunction groups, suggesting a potential key role for DCs in immune alterations associated with ovulation dysfunction (Figure 3A). Through interaction plots, we discovered that most of the differentially expressed genes were shared among the ovulation groups, with 264 common genes being upregulated and 329 common genes being downregulated (Figure 3B). Gene ontology (GO) analysis revealed that the upregulated genes were enriched for MHC-II antigen processing and presentation and regulation of immune cell activation, while the downregulated genes were enriched for oxidative phosphorylation and cellular respiration (Figure 3C).

To examine whether changes in DC function were related to the dynamics of NK cell subpopulations, we explored the strength of the interaction among different cell populations between the healthy and ovulation-dysfunction groups using the CellChat R package (Figure S2). The results demonstrated that the interaction strength sourcing from cDCs was significantly increased in all ovulation-dysfunction groups compared to that in the healthy group (Figures 3D, S2). Furthermore, to elucidate the specific signaling pathways involved in cDC-mediated cell–cell communication, we compared the communication probabilities mediated by ligand–receptor pairs from cDCs to almost other cell populations. Our findings revealed a predominant presence of signaling pathways involving MHC-I, MHC-II, and BAFF, which are known to play a significant role in promoting inflammatory responses in cDC-mediated cell–cell communication (Figure 3E). We found that the ligand–receptor pair of HLA-DRB5-CD4, HLA-DRB1-CD4, HLA-DRA-CD4, HLA-DQB1-CD4, HLA-DQA1-CD4, HLA-DPB1-CD4, HLA-DPA1-CD4, and HLA-DMA-CD4 significantly contributed to communication from cDCs to CD4 T cells and monocytes. HLA-A-CD8A/B, HLA-B-CD8 A/B, HLA-C-CD8 A/B significantly influenced communication from cDCs to CD8 T cells and TNFSF13B-TNFRSF13B/C significantly affected communication between cDCs and B cells (Figure 3E). These results collectively indicate that cDC may play an essential role in the progression of inflammation during ovulation dysfunction.

10.3389/fimmu.2023.1297484

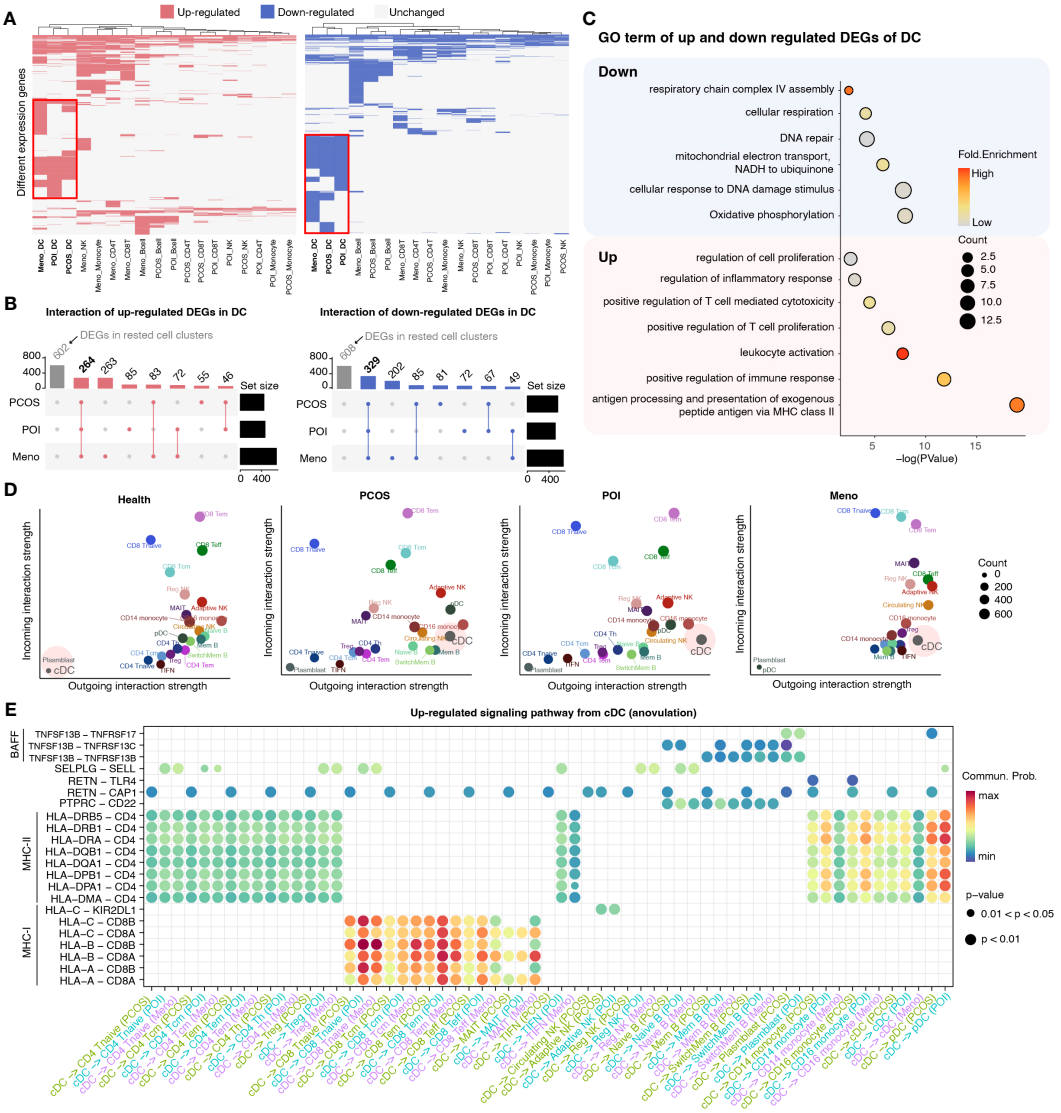

FIGURE 3
Detailed characterization of DCs in each ovulation-dysfunction group. **(A)** Heatmaps showing the distribution of DEGs between PCOS, POI, Meno, and Health groups in major cell subtypes. The red box shows the differential genes of DC cells by comparing PCOS, POI, and Meno to Health. **(B)** Upset plot showing upregulated (left) and downregulated (right) DEGs in DC. **(C)** The representative GO terms of upregulated and downregulated DEGs overlapped among PCOS, POI, and Meno in DCs. **(D)** A scatter plot of the outgoing and incoming interaction strengths identified significant changes in sending or receiving signals among diverse cell types in each group. **(E)** Overview of communication probabilities mediated by ligand–receptor pairs from cDCs to rested cell types significantly increased in the anovulatory groups.

Expression dynamics show abnormal immune activation in ovulation disorder

Given the substantial upregulation of pro-inflammatory pathways mediated by cDCs, we investigated alterations in pro-inflammatory factors among major inflammation-related cell types, such as CD8 T cells, monocytes, and B cells. To better estimate functional dynamics comprehensively, we calculated the lineage score according to published articles (20). Compared with the healthy group, all ovulation-dysfunction groups showed a significant increase in pro-inflammatory factors in CD8 T cells (Figure 4A). Furthermore, we observed a significant increase in cytotoxic factors in CD14 and CD16 monocytes in the ovulation-dysfunction groups (Figure 4B). These findings indicated the presence of aggravated inflammatory responses and immune disorders during the progression of ovulation dysfunction. To investigate which genes contributed to these immune changes, we examined the expression of all genes used to calculate the lineage score in Figures 5C, D across different cell types. Our analysis revealed substantial upregulation of numerous pro-inflammatory factors, including KLRB1, KLRD1, GZMA, GZMB, GZMK, PRF1, CCL5, and TNFRSF1A, in CD8 T cells in all ovulation-dysfunctional groups (Figure 4C). Compared to healthy individuals, pro-inflammatory cytokines such as ANPEP, TNF, and CCL5 were significantly elevated in both CD14 and CD16 monocytes of ovulation-dysfunction individuals (Figure 4D). It is well established that immunoglobulin class switching plays a crucial role in effective immune responses by allowing the immune system to adapt antibody production to different types of pathogens and immune

10.3389/fimmu.2023.1297484

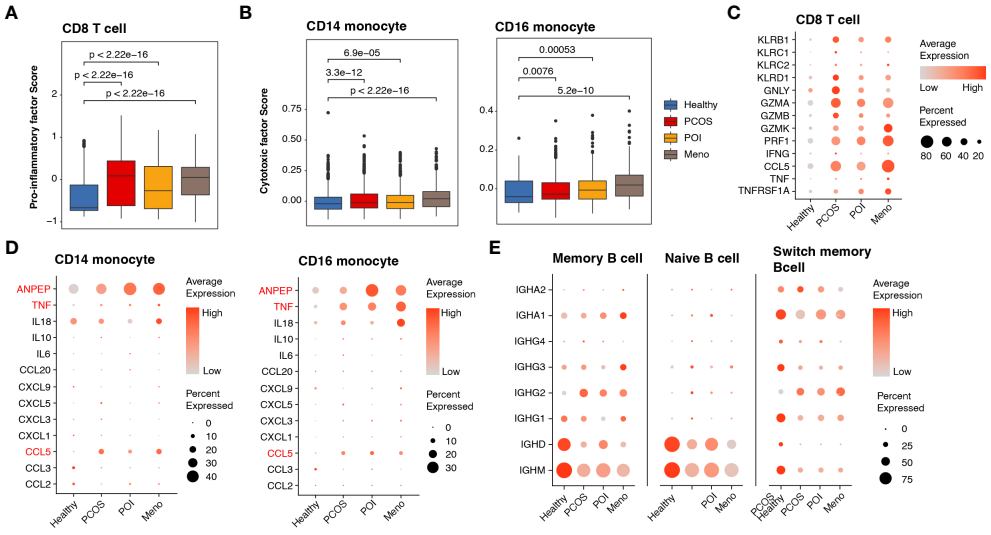

FIGURE 4
Abnormally activated cell cytotoxins and inflammatory response in ovulation dysfunction. **(A, B)** Box plot showing the lineage score of **(A)** pro-inflammatory factors in CD8 T cells and **(B)** cytotoxic mediators in both CD14 and CD16 monocytes and the different groups. **(C, D)** Dotplot depicting the expression of detailed genes for calculating the **(C)** pro-inflammatory factor score in CD8 T cells and **(D)** cytotoxic mediator score in CD14/CD16 monocytes among different groups. **(D)** Dotplot showing the expression of genes involved in immunoglobulin in the B cells of each group.

challenges (23). Our data indicated that B cells in the healthy group predominantly expressed IGHD/IGHM, whereas B cells in the ovulation-dysfunction groups mainly exhibited IGHA and IGHG. Together, our data revealed that CCL5 largely contributes to ovulation-related inflammation and indicates that the immunoglobulin class switch from IGHD/IGHM to IGHA/IGHG contributes to chronic inflammation during ovulation dysfunction.

Gene regulatory network analyses revealed key regulators involving in immune changes of cDC among ovulation-dysfunction patients

In view of the significant alterations in gene cluster expression in cDCs, we considered that some transcription factors may be the

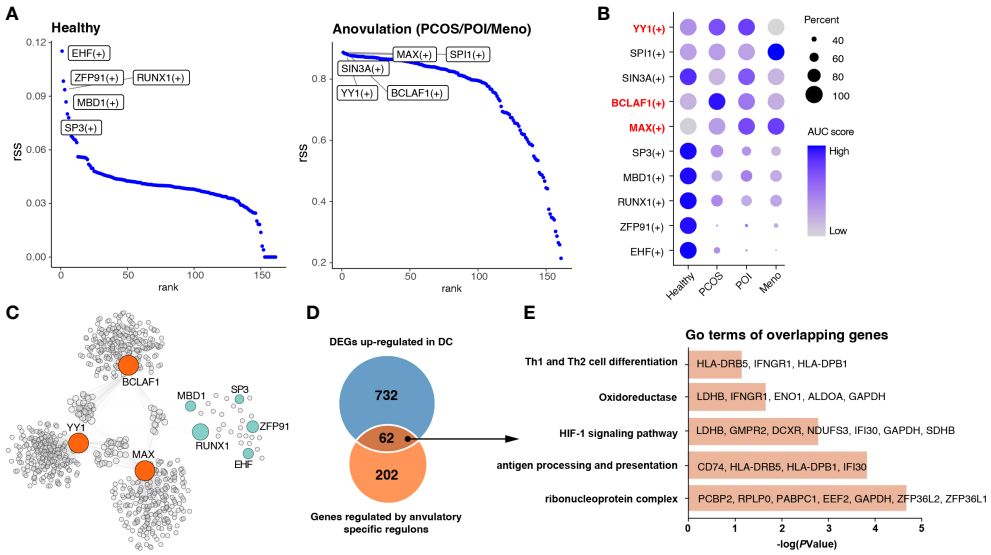

FIGURE 5
Identification of key regulons of DCs in ovulation disorders. **(A)** Rank of regulons in cDCs between healthy subjects and others (PCOS, POI, and MENO) based on the Regulon Specificity Score (RSS). The top-ranked regulon activities are shown in the picture. **(B)** Dotplot showing the AUC score for each regulon in each group. **(C)** Network of selected regulons and their target genes in group of ovulation-dysfunction and healthy group. **(D)** Venn diagram showing the overlapping genes that were upregulated in DCs and regulated by ovulation-specific regulons in **(C)**. **(E)** Bar plots of the representative GO terms of the overlapping genes.

main regulators resulting in immunological changes. All cDC were subjected to SCENIC analysis to construct the gene regulatory networks. Our results identified essential regulons among the four groups, and the top five most-active regulons in the healthy and each ovulation-dysfunction group are shown in Figure 5A. When considering the rank score, we observed that *EHF*, *ZFP91*, *RUNX1*, *MBD1*, and *SP3* were specifically upregulated in the healthy group, whereas *YY1*, *BCLAF1*, and *MAX* were specifically upregulated in the ovulation-dysfunction groups (Figures 5A, B). Using the eight regulons mentioned above, we constructed predicted regulatory networks (Figure 5C, Table S3). By mapping these networks with 794 unique upregulated DEGs in DCs (Figure 3A), an overlap of 62 genes, representing nearly 30% of the DEGs, was identified (Figure 5D). To gain further insight, we performed gene ontology (GO) analysis of these overlapping genes. The DEGs were enriched in functions such as antigen processing and presentation, Th1 and Th2 cell differentiation, and the HIF-1 signaling pathway (Figure 5E). These findings suggest that *YY1*, *BCLAF1*, and *MAX* play pivotal roles in immune changes in cDCs and cDC-mediated inflammatory response pathways. Overall, these results shed light on the transcriptional regulatory landscape of cDCs in the context of blood ovulation-dysfunction, highlighting the activation of specific transcription factors during immunological changes.

Global oxidative stress enhances in ovulation disorder

Analysis of DEGs revealed that in most PBMC cell types, genes involved in reducing oxidative stress, such as *JUN* and *JUND*, were significantly downregulated, whereas some genes associated with mitochondrial respiration, such as *MT-ATP8* and *MT-ND4L*, exhibited high expression levels (Figure S3). To assess whether increased oxidative stress is widely present during ovulation, we obtained data from monkeys and mice and investigated gene expression changes in oocytes and granulosa cells in high-fat mice and aged monkeys (24, 25) (Figures 6A, B). A comparison between oocytes and granulosa cells revealed a higher number of upregulated DEGs in the latter, including genes shared between mice and monkeys (Figures 6C, D). Gene ontology (GO) analysis demonstrated that the commonly upregulated DEGs in granulosa cells of both mice and monkeys were primarily associated with cellular responses to oxidative stress and DNA damage stimulus, mitochondrial translation, apoptotic process, and cell chemotaxis (Figure 6E). We further presented the expression profiles of DEGs involved in these pathways as a dot plot (Figure 6F) and observed that many of the genes involved in oxidative stress and mitochondrial energy metabolism (such as *NDUFV3*, *NDUFB6*,

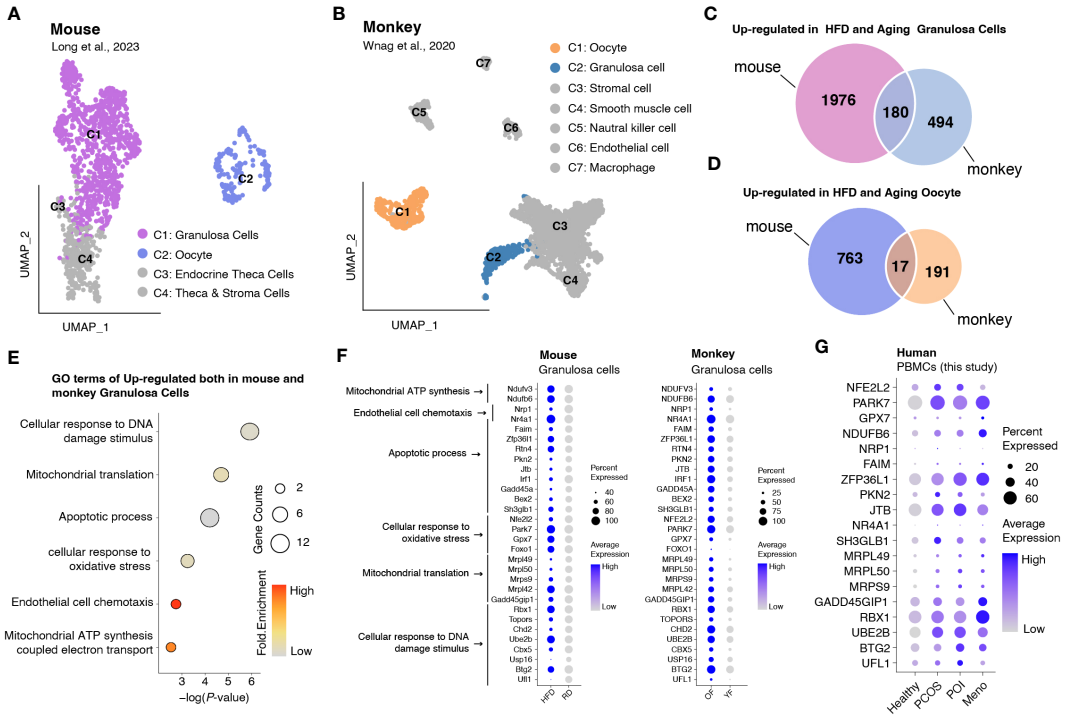

FIGURE 6
Integrated data analysis revealed that aberrant oxidative stress occurs in both granulosa cells and PBMCs during ovulation disorders. **(A)** UMAP plot of all identified cells from the HFD and RD mice. **(B)** UMAP plot of all the identified cells from young and aged monkeys. **(C)** Venn diagram showing the upregulation in HFD and aging granulosa cells. **(D)** Venn diagram showing the upregulation in HFD and aging oocytes. **(E)** Dotplot depicting representative GO terms of genes upregulated in both mouse and monkey granulosa cells. **(F,G)** Dotplot showing the expression of genes involved in representative GO terms in **(F)** granulosa cells of mice and monkeys separately and **(G)** PBMCs of humans in each group.

NFE2L2, *PARK7*, and *GPX7*), mitochondrial translation (such as *MRPL49*, *MRPL50*, and*MRPS9*), DNA damage stimulus response (*GADD45GIP1*, *RBX1*, *UBE2B*, *BTG2*, and *UFL1*), and apoptosis (*ZFP36L1*, *PKN2*, and *JTB*) that were highly expressed in granulosa cells were also highly expressed in human PBMCs (Figure 6G).

Discussion

This study investigated the immunological changes in patients with anovulation, including PCOS, POI, and menopause. Our findings suggest that aberrant changes in T and NK cell populations, augmented inflammatory responses mediated by cDCs, and global oxidative stress in PBMCs are common characteristics of ovarian dysfunction. Importantly, these aberrations may pose a high risk for long-term chronic inflammation and have detrimental effects on ovarian function. In summary, this study provides valuable insights into the immunological changes associated with anovulation, shedding light on the potential mechanisms and implications of therapeutic interventions.

Although long-term inflammatory reactions have been reported to potentially damage tissues and cells, affecting their function and structure (26), our study provides essential insights into the inflammatory response in various types of anovulation. CD8 T cells, CD14 monocytes, and CD16 monocytes are known to play critical roles in both cytotoxic and pro-inflammatory responses, contributing to immune defense against infections and regulation of inflammatory processes in different disease contexts (27, 28). Our findings demonstrated that a hyperinflammatory phenotype is significantly enhanced during anovulation, characterized by the upregulation of pro-inflammatory factors such as CCL5 in CD8 T cells and CD14/CD16 monocytes. Furthermore, we observed a shift in immunoglobulin production from IgD/IgM to IgA/IgG during anovulation. Previous research has suggested that IgA and IgG are two proinflammatory immunoglobulins (29), and immunoglobulin isotypes such as IgG can interact with Fc gamma receptors on immune cells to regulate their effector functions, including inflammation (30). These insights significantly advance our understanding of chronic inflammation in ovulatory disorders, emphasizing the crucial role of increased cytokine production from CD8+ T cells and monocytes, global oxidative stress, and immunoglobulin switching in inflammatory mediation. Targeting of these processes has the potential to alleviate chronic inflammation and restore normal ovulatory function.

Conventional dendritic cells (cDCs) play a crucial role in inflammation by interacting with various immune cells including CD4 T cells, CD8 T cells, B cells, and monocytes (31). They influence immune responses through cell–cell signaling and cytokine production, particularly *via* MHC-I, MHC-II, and BAFF pathways (31). CD8 T cells, also known as cytotoxic T cells, recognize antigens presented by MHC-I molecules and release cytotoxic molecules and proinflammatory cytokines upon activation (32). Monocytes, through MHC-II expression, scan for foreign antigens and initiate proinflammatory responses to modulate inflammation (33). Additionally, BAFF pathway activation can induce class switching in B cells, leading to the production of specific immunoglobulin isotypes, such as IgG and IgA, which are important for immune responses and inflammation (34). Our data showed that abnormal upregulation of the MHC-I, MHC-II, and BAFF pathways by cDCs was activated during anovulation, which is likely to intensify the inflammation response. Additionally, transcription factors such as YY1, BCLAF1, and MAX, are enriched in cDCs from women with ovulation disorders and are involved in antigen presentation. Abnormal activation of these factors impairs cDC immune activity. Targeting YY1, BCLAF1, and MAX could be a potential therapeutic strategy to restore cDC functionality and reduce inflammation during anovulation. Overall, the increased inflammatory response in women with ovulation disorders is directly linked to cDC-mediated immune signaling.

Previous studies have established that oxidative stress can provoke immune dysfunction by affecting immune cell function, cytokine and chemokine production, and the promotion of inflammation (35). In our study, we observed a consistent reduction in the expression of oxidative stress-related genes, including *JUN* and *FOS*, in almost all cellular clusters of peripheral blood mononuclear cells (PBMCs). Given that granulosa cells serve as the energy source for oocytes, abnormal levels of oxidative stress can affect oocyte development, potentially leading to ovulation disorders (36, 37). Supplementing our findings with transcriptome data derived from the ovaries of high-fat diet-induced mice and aging monkeys, we identified a concurrent upregulation of oxidative stress-related genes, specifically *NDUFV3*, *NDUFB6*, *NFE2L2*, *PARK7*, and *GPX7* (24), in both granulosa cells and PBMCs of women suffering from ovulatory disorders. Additionally, genes associated with DNA damage stimulus response (*GADD45GIP1*, *RBX1*, *UBE2B*, *BTG2*, and *UFL1*) and apoptosis progress (*ZFP36L1*, *PKN2*, and *JTB*) concurrently increase in response to oxidative stress were observed in our data. These findings imply that the irregular variations in oxidative stress levels in peripheral blood parallel those observed in granulosa cells across mammals, and aberrant oxidative stress may exacerbate DNA damage and cellular apoptosis. Together, our study revealed heightened oxidative stress, characterized by an imbalance between the production of reactive oxygen species (ROS) and antioxidant defense mechanisms, among patients with anovulation. This phenomenon could potentially serve as a valuable biological marker for ovulation disorders.

In conclusion, our study provides a comprehensive comparative analysis of the common types of ovulation disorders, revealing significant immune alterations in affected women. These alterations include an elevated inflammatory response and oxidative stress. Importantly, our findings highlight the central role of the cDC-centered signaling pathway in driving the excessive inflammatory response observed during anovulation. Consequently, targeting this pathway, as well as reducing oxidative stress and modulating CD8+ T cell and NK cell activity, presents a promising approach for enhancing immune function and restoring normal ovarian function in patients with ovulation disorders. However, it is crucial to acknowledge the limitations of our study, particularly its small

sample size. Therefore, further independent validation using techniques such as flow cytometry and additional functional experiments are necessary to confirm and strengthen these findings. Addressing these limitations will improve the reliability and significance of future research in this field.

Data availability statement

The datasets presented in this study can be found in online repositories. The names of the repository/repositories and accession number(s) can be found below: https://ngdc.cncb.ac.cn/, HRA003535.

Ethics statement

The studies involving humans were approved by the Ethics Committees of Department of Medical and Life Science, Tongji University. The studies were conducted in accordance with the local legislation and institutional requirements. The participants provided their written informed consent to participate in this study.

Author contributions

BL: Project administration, Supervision, Writing – original draft, Writing – review & editing. LQ: Conceptualization, Data curation, Investigation, Methodology, Software, Writing – original draft, Writing – review & editing. YL: Data curation, Formal Analysis, Resources, Writing – review & editing. LZ: Resources, Writing – review & editing. SL: Resources, Writing – review & editing. XZ: Resources, Writing – review & editing. WL: Formal analysis, Writing – review & editing. JQ: Formal Analysis, Writing – review & editing. XC: Investigation, Writing – review & editing. YJ: Funding acquisition, Project administration, Supervision, Writing – review & editing. ZX: Funding acquisition, Project administration, Supervision, Writing – review & editing.

Funding

The author(s) declare financial support was received for the research, authorship, and/or publication of this article. This study was supported by grants from the National Natural Science Foundation of China (81873832, 82071645) and Key-Area Research and Research Projects of Shanghai Science and Technology Commission (18411964300).

Acknowledgments

We thank Tongji Hospital and the School of Medicine for providing the valuable human sample resources. We thank many of our colleagues for their helpful discussion.

Conflict of interest

The authors declare that the research was conducted in the absence of any commercial or financial relationships that could be construed as a potential conflict of interest.

Publisher's note

Supplementary material

The Supplementary Material for this article can be found online at: https://www.frontiersin.org/articles/10.3389/fimmu.2023.1297484/full#supplementary-material

SUPPLEMENTARY FIGURE 1
Statistics of identified cell percentage in each group. Boxplot showing the percentages of all cell populations among different groups (Health/MENO/PCOS/POI).

SUPPLEMENTARY FIGURE 2
Overview of cell-cell communications.Heatmap displaying details of the differential interaction strength of health vs MENO(left), health vs PCOS (middle) and health vs POI (right). The right bar plot showing the sum of outgoing signaling. For color bar, red means increased signaling and blue means decreasing signaling in the second dataset comparing with the first one.

SUPPLEMENTARY FIGURE 3
Intersection of up-regulated and down-regulated DEGs of each group in major cell types. **(A, B)** Upset plot showing up-regulated **(A)** and down-regulated **(B)** DEGs among B cells, monocytes and dendritic cells between health and MENO, health and PCOS and health and POI separately. **(C, D)** Upset plot showing up-regulated **(A)** and down-regulated **(B)** DEGs among CD4 T cells, CD8 T cells and NK cells between health and MENO, health and PCOS and health and POI separately.

SUPPLEMENTARY TABLE 1
The clinical data statistics of patients with ovulation disorder.

SUPPLEMENTARY TABLE 2
Gene list showing interaction of DEGs of DCs in each group.

SUPPLEMENTARY TABLE 3
Tables of DC-special TFs and their targeted genes.

References

1. Brazdova A, Senechal H, Peltre G, Poncet P. Immune aspects of female infertility. *Int J Fertil Steril* (2016) 10(1):1–10. doi: 10.22074/ijfs.2016.4762

2. Sen A, Kushnir VA, Barad DH, Gleicher N. Endocrine autoimmune diseases and female infertility. *Nat Rev Endocrinol* (2014) 10(1):37–50. doi: 10.1038/nrendo.2013.212

3. Carp HJ, Selmi C, Shoenfeld Y. The autoimmune bases of infertility and pregnancy loss. *J Autoimmun* (2012) 38(2-3):J266–74. doi: 10.1016/j.jaut.2011.11.016

4. Piccinni MP, Lombardelli L, Logiodice F, Kullolli O, Parronchi P, Romagnani S. How pregnancy can affect autoimmune diseases progression? *Clin Mol Allergy* (2016) 14:11. doi: 10.1186/s12948-016-0048-x

5. Jose-Miller AB, Boyden JW, Frey KA. Infertility. *Am Fam Physician* (2007) 75 (6):849–56.

6. Petrikova J, Lazurova I, Yehuda S. Polycystic ovary syndrome and autoimmunity. *Eur J Intern Med* (2010) 21(5):369–71. doi: 10.1016/j.ejim.2010.06.008

7. Szeliga A, Calik-Ksepka A, Maciejewska-Jeske M, Grymowicz M, Smolarczyk K, Kostrzak A, et al. Autoimmune diseases in patients with premature ovarian insufficiency-our current state of knowledge. *Int J Mol Sci* (2021) 22(5):2594. doi: 10.3390/ijms22052594

8. Desai MK, Brinton RD. Autoimmune disease in women: endocrine transition and risk across the lifespan. *Front Endocrinol (Lausanne)* (2019) 10:265. doi: 10.3389/fendo.2019.00265

9. Corrie L, Gulati M, Vishwas S, Kapoor B, Singh SK, Awasthi A, et al. Combination therapy of curcumin and fecal microbiota transplant: Potential treatment of polycystic ovarian syndrome. *Med Hypotheses* (2021) 154:110644. doi: 10.1016/j.mehy.2021.110644

10. Huang QY, Chen SR, Chen JM, Shi QY, Lin S. Therapeutic options for premature ovarian insufficiency: an updated review. *Reprod Biol Endocrinol* (2022) 20(1):28. doi: 10.1186/s12958-022-00892-8

11. Ma L, Lu H, Chen R, Wu M, Jin Y, Zhang J, et al. Identification of key genes and potential new biomarkers for ovarian aging: A study based on RNA-sequencing data. *Front Genet* (2020) 11:590660. doi: 10.3389/fgene.2020.590660

12. Franasiak JM, Scott RT. Contribution of immunology to implantation failure of euploid embryos. *Fertil Steril* (2017) 107(6):1279–83. doi: 10.1016/j.fertnstert.2017.04.019

13. Zitti B, Bryceson YT. Natural killer cells in inflammation and autoimmunity. *Cytokine Growth Factor Rev* (2018) 42:37–46. doi: 10.1016/j.cytogfr.2018.08.001

14. Seshadri S, Sunkara SK. Natural killer cells in female infertility and recurrent miscarriage: a systematic review and meta-analysis. *Hum Reprod Update* (2014) 20 (3):429–38. doi: 10.1093/humupd/dmt056

15. Lumsden MA, Davies M, Sarri G. Guideline development group for menopause D, management. Diagnosis and management of menopause: the national institute of health and care excellence (NICE) guideline. *JAMA Intern Med* (2016) 176(8):1205–6. doi: 10.1001/jamainternmed.2016.2761

16. Rao P, Bhide P. Controversies in the diagnosis of polycystic ovary syndrome. *Ther Adv Reprod Health* (2020) 14. doi: 10.1177/2633494120913032

17. Fraison E, Crawford G, Casper G, Harris V, Ledger W. Pregnancy following diagnosis of premature ovarian insufficiency: a systematic review. *Reprod BioMed Online* (2019) 39(3):467–76. doi: 10.1016/j.rbmo.2019.04.019

18. Stuart T, Butler A, Hoffman P, Hafemeister C, Papalexi E, Mauck WM3rd, et al. Comprehensive integration of single-cell data. *Cell* (2019) 177(7):1888–902.e21. doi: 10.1016/j.cell.2019.05.031

19. Yu G, Wang LG, Han Y, He QY. clusterProfiler: an R package for comparing biological themes among gene clusters. *Omics* (2012) 16(5):284–7. doi: 10.1089/omi.2011.0118

20. Schwalie PC, Dong H, Zachara M, Russeil J, Alpern D, Akchiche N, et al. A stromal cell population that inhibits adipogenesis in mammalian fat depots. *Nature* (2018) 559(7712):103. doi: 10.1038/s41586-018-0226-8

21. Van de Sande B, Flerin C, Davie K, De Waegeneer M, Hulselmans G, Aibar S, et al. A scalable SCENIC workflow for single-cell gene regulatory network analysis. *Nat Protoc* (2020) 15(7):2247–76. doi: 10.1038/s41596-020-0336-2

22. Jin S, Guerrero-Juarez CF, Zhang L, Chang I, Ramos R, Kuan CH, et al. Inference and analysis of cell-cell communication using CellChat. *Nat Commun* (2021) 12 (1):1088. doi: 10.1038/s41467-021-21246-9

23. Yu K, Lieber MR. Current insights into the mechanism of mammalian immunoglobulin class switch recombination. *Crit Rev Biochem Mol Biol* (2019) 54 (4):333–51. doi: 10.1080/10409238.2019.1659227

24. Wang S, Zheng Y, Li J, Yu Y, Zhang W, Song M, et al. Single-cell transcriptomic atlas of primate ovarian aging. *Cell* (2020) 180(3):585–600.e19. doi: 10.1016/j.cell.2020.01.009

25. Long X, Yang Q, Qian J, Yao H, Yan R, Cheng X, et al. Obesity modulates cell-cell interactions during ovarian folliculogenesis. *iScience* (2022) 25(1):103627. doi: 10.1016/j.isci.2021.103627

26. Medzhitov R. Origin and physiological roles of inflammation. *Nature* (2008) 454 (7203):428–35. doi: 10.1038/nature07201

27. Kaech SM, Wherry EJ, Ahmed R. Effector and memory T-cell differentiation: implications for vaccine development. *Nat Rev Immunol* (2002) 2(4):251–62. doi: 10.1038/nri778

28. Ma WT, Gao F, Gu K, Chen DK. The role of monocytes and macrophages in autoimmune diseases: A comprehensive review. *Front Immunol* (2019) 10:1140. doi: 10.3389/fimmu.2019.01140

29. Fleming A, Castro-Dopico T, Clatworthy MR. B cell class switching in intestinal immunity in health and disease. *Scand J Immunol* (2022) 95(2):e13139. doi: 10.1111/sji.13139

30. Castro-Dopico T, Clatworthy MR. IgG and fcgamma receptors in intestinal immunity and inflammation. *Front Immunol* (2019) 10:805. doi: 10.3389/fimmu.2019.00805

31. Martin-Gayo E, Yu XG. Role of dendritic cells in natural immune control of HIV-1 infection. *Front Immunol* (2019) 10:1306. doi: 10.3389/fimmu.2019.01306

32. Pishesha N, Harmand TJ, Ploegh HL. A guide to antigen processing and presentation. *Nat Rev Immunol* (2022) 22(12):751–64. doi: 10.1038/s41577-022-00707-2

33. Yang J, Zhang L, Yu C, Yang XF, Wang H. Monocyte and macrophage differentiation: circulation inflammatory monocyte as biomarker for inflammatory diseases. *biomark Res* (2014) 2(1):1. doi: 10.1186/2050-7771-2-1

34. Schneider P. The role of APRIL and BAFF in lymphocyte activation. *Curr Opin Immunol* (2005) 17(3):282–9. doi: 10.1016/j.coi.2005.04.005

35. Morris G, Gevezova M, Sarafian V, Maes M. Redox regulation of the immune response. *Cell Mol Immunol* (2022) 19(10):1079–101. doi: 10.1038/s41423-022-00902-0

36. Fan W, Yuan Z, Li M, Zhang Y, Nan F. Decreased oocyte quality in patients with endometriosis is closely related to abnormal granulosa cells. *Front Endocrinol (Lausanne)* (2023) 14:1226687. doi: 10.3389/fendo.2023.1226687

37. Alam MH, Miyano T. Interaction between growing oocytes and granulosa cells in vitro. *Reprod Med Biol* (2020) 19(1):13–23. doi: 10.1002/rmb2.12292

frontiers | Frontiers in Immunology

TYPE Review
PUBLISHED 24 January 2024
DOI 10.3389/fimmu.2024.1331934

OPEN ACCESS

EDITED BY
Rosa M. Sainz,
University of Oviedo, Spain

REVIEWED BY
Josefa Leon,
Fundación para la Investigación Biosanitaria de Andalucía Oriental (FIBAO), Spain
Jehan J. El-Jawhari,
Nottingham Trent University, United Kingdom

*CORRESPONDENCE
Hong Sun
sunhong002@gmc.edu.cn
Hua Yang
yanghua0203@gmc.edu.cn
Yong Zhuang
76574569@qq.com

RECEIVED 02 November 2023
ACCEPTED 04 January 2024
PUBLISHED 24 January 2024

CITATION
Xiong Z, Peng G, Deng J, Liu M, Ning X, Zhuang Y, Yang H and Sun H (2024) Therapeutic targets and potential delivery systems of melatonin in osteoarthritis. *Front. Immunol.* 15:1331934. doi: 10.3389/fimmu.2024.1331934

Therapeutic targets and potential delivery systems of melatonin in osteoarthritis

Zhilin Xiong[1], Guoxuan Peng[1], Jin Deng[2], Miao Liu[1], Xu Ning[1], Yong Zhuang[1]*, Hua Yang[1]* and Hong Sun[1,2]*

[1]Department of Orthopaedics, The Affiliated Hospital of Guizhou Medical University, Guiyang, China, [2]Department of Emergence Surgery, The Affiliated Hospital of Guizhou Medical University, Guiyang, China

Osteoarthritis (OA) is a highly prevalent age-related musculoskeletal disorder that typically results in chronic pain and disability. OA is a multifactorial disease, with increased oxidative stress, dysregulated inflammatory response, and impaired matrix metabolism contributing to its onset and progression. The neurohormone melatonin, primarily synthesized by the pineal gland, has emerged as a promising therapeutic agent for OA due to its potential to alleviate inflammation, oxidative stress, and chondrocyte death with minimal adverse effects. The present review provides a comprehensive summary of the current understanding regarding melatonin as a promising pharmaceutical agent for the treatment of OA, along with an exploration of various delivery systems that can be utilized for melatonin administration. These findings may provide novel therapeutic strategies and targets for inhibiting the advancement of OA.

KEYWORDS

osteoarthritis, melatonin, inflammation, oxidative stress, chondrocyte death, delivery systems

1 Introduction

Osteoarthritis (OA) is a prevalent age-related irreversible musculoskeletal disorder, recognized as a primary cause of chronic pain and disability. It is characterized by persistent synovitis, progressive degradation of articular cartilage, secondary formation of osteophytes, and remodeling of subchondral bone (1–3). The pathogenesis of OA is influenced by a myriad of risk factors, encompassing age, obesity, gender, genetic predisposition, and joint injuries (4). As a refractory condition, OA can not only give rise to localized symptoms such as pain, joint deformity, and joint dysfunction but also coexist with comorbidities including diabetes, cardiac ailments, and mental health disorders, which significantly augments the likelihood of serious adverse events (5). The global prevalence of OA stands at approximately 7% of the world's population, equating to around 500 million individuals, and the number continues to rise due to the worldwide obesity epidemic and the aging demographic (6, 7). The high incidence of adverse effects

and the rapid increase in the prevalence of OA impose a substantial financial burden on society, families, and individuals, while also posing a significant threat to public health (8, 9).

The main pathological characteristics of OA include the loss of chondrocytes, degradation of the cartilage matrix, and synovitis, ultimately leading to terminal OA (10). The treatment for OA involves halting the loss of chondrocytes, promoting the production of cartilage matrix, and reducing synovitis. A wide range of therapeutic approaches have been employed for the treatment of OA, including minimally invasive surgery, conventional surgical procedures, muscle strengthening exercises, physiotherapy interventions, sodium hyaluronate injections, corticosteroids administration, and nonsteroidal anti-inflammatory drugs (NSAIDs) (11, 12). Furthermore, several emerging therapeutic strategies have demonstrated promising initial outcomes, including the transplantation of autologous chondrocytes, and the intra-articular administration of platelet-rich plasma and mesenchymal stem cells (MSCs) (13–15). Unfortunately, current therapies for individuals with OA yield unsatisfactory outcomes due to the lack of effective interventions to impede chondrocyte loss and articular cartilage deterioration (16). The investigation of novel therapeutic targets for this intricate disease is thus imperative.

The endogenous indole hormone melatonin is primarily secreted in the pineal gland, synthesized from tryptophan through a series of derivative reactions (17). The release of melatonin into the circulation of cerebrospinal fluid and bloodstream facilitates its subsequent delivery to distant organs and tissues to regulate inflammation, provide antioxidant protection, inhibit tumor growth, and promote anti-aging effects (18–21). The findings of multiple studies have demonstrated that melatonin exerts a protective effect against the development of OA through mechanisms such as inflammation reduction, elimination of excess free radicals, and promotion of matrix synthesis (22). Consequently, the potential clinical application of melatonin characterized by minimal adverse effects, holds great promise as a viable strategy for the treatment of OA. The intra-articular injection of melatonin is an optimal choice due to the absence of lymphatic and circulatory networks in hyaline cartilage. However, due to the short half-life of melatonin, it is necessary to administer injections as frequently as twice a week (23). To minimize the frequency of intra-articular injection, several delivery systems have been employed for the sustained release of melatonin. The present review provides an overview of the therapeutic advantages and delivery systems of melatonin in the progression of OA. These findings may offer a comprehensive understanding of forthcoming studies on melatonin-based treatment for OA.

2 The role of oxidative stress, inflammation, and chondrocyte death in OA

2.1 Oxidative stress in OA

The imbalance between oxidation and antioxidants leads to oxidative stress (24). Reactive oxygen species (ROS), which are byproducts generated during aerobic metabolism, are unstable and reactive molecules such as superoxide anion (O_2^-), hydroxyl radical (OH-), hydrogen peroxide and (H_2O_2). The catalysis of ROS occurs in peroxisomes and mitochondria through the action of Nitric Oxide Synthase (NOS), Xanthine Oxidase (XO), NADPH oxidases (NOXs) (25). Under physiological conditions, O_2^- is the most abundant type of ROS, with the majority being generated by mitochondria. Mitochondria, known as the "powerhouse" of eukaryotic cells, convert nutrient molecules into adenosine triphosphate (ATP) through oxidative phosphorylation (26). Although the conventional consensus posits that chondrocytes derive their energy through anaerobic glycolysis in an oxygen-deprived environment, the ample oxygen supply on the surface area of articular cartilage fosters conducive conditions for aerobic respiration (27, 28). The respiratory chain, located in the inner membrane of mitochondria, is widely recognized as the primary source of ROS and generates approximately 2%–3% of O_2^- as a byproduct during oxidative phosphorylation (29). Additionally, mitochondria play a crucial role in regulating the synthesis of antioxidant systems such as NADH/NAD+, NADPH/NADP+, and GSH/GSSG. In pathological conditions, however, mitochondrial homeostasis is disrupted, leading to an excessive generation of O_2^-. Excessive production of O_2^- leads to mitochondrial dysfunction by reducing the membrane potential of mitochondria and causing damage to mitochondrial DNA (mtDNA), thereby amplifying the generation of O_2^-. Not only does H_2O_2 originate from XO during the conversion of hypoxanthine to xanthine, but it can also be generated from O_2^- upon activation of superoxide dismutase (SOD). Reactive nitrogen species (RNS) encompass a group of reactive molecules derived from O_2^- and NO, which are accountable for inducing nitrosative stress that contributes to cellular damage. Endothelial NOS (eNOS), neuronal NOS (nNOS), and inducible NOS (iNOS) represent three distinct isoforms of nitric oxide synthase. The production of NO is attributed to the activity of three NOSs, namely nNOS, eNOS, and iNOS. While nNOS and eNOS generate NO at a significantly low level, iNOS induced by inflammatory cytokines such as interleukin-1β (IL-1β), IL-17, and tumor necrosis factor α (TNFα) exhibits a relatively high output of NO (30, 31).

The cells possess antioxidant defense mechanisms comprising both enzymatic and non-enzymatic components to counteract the heightened production of ROS and prevent cellular dysfunction. The non-enzymatic system comprises ascorbic acid (vitamin C), α-tocopherol (vitamin E), and glutathione (GSH), while the enzymatic component consists of SOD, catalase (CAT), glutathione peroxidase (GPX), peroxiredoxins (PRXS), and NADPH ubiquinone oxidoreductase (NQO1) (32). The SODs, comprising three isoforms including cytosolic SOD (SOD1), mitochondrial SOD (SOD2), and extracellular SOD (SOD3), effectively eliminate ROS by converting O_2^- to H_2O_2. Subsequently, the accumulated H_2O_2 is further converted to H_2O through the actions of GPX, PRXS, and CATs (33–35). The presence of GSH is crucial for maintaining cellular redox potential and antioxidant defenses, as it serves as a significant reductant. GPX plays a vital role in preventing the oxidation of membrane lipids by converting H_2O_2 to H_2O through the oxidation of GSH to GSSH (35). The downregulation

of antioxidant system proteins, including SOD, CAT, and GPX, has been observed in both *in vivo* and *in vitro* studies of OA joints (36). When the production of ROS exceeds the scavenging capacity of the antioxidant system or the low activity of the antioxidant defense system, the cell is in a condition of oxidative stress which is characterized by an imbalance of oxidation and antioxidant state (37). The pathogenesis of numerous age-related disorders has been strongly associated with oxidative stress, which also serves as a pivotal contributor to the progression of OA (38–41).

The maintenance of cellular function and homeostasis necessitates a physiological level of ROS, however, excessive ROS induced by pathological processes can oxidize macromolecules such as mtDNA, genomic DNA, proteins, and lipids, thereby impairing essential cellular processes (Figure 1) (42–44). Investigations have documented that ROS-induced macromolecule compromise, including that of genomic, mtDNA, and lipids, results in synovitis worsening, extracellular matrix (ECM) degradation, and chondrocyte death, such as apoptosis and ferroptosis (45, 46). The increased level of ROS in cartilage and chondrocytes can be attributed to variations in oxygen pressure, mechanical stress, as well as the presence of inflammatory mediators such as IL-1, IL-17, and TNF-α (29, 47). The upregulation of ROS levels in the chondrocytes of individuals with OA have been demonstrated by numerous studies (45, 48). The most predominant ROS found in OA cartilages and chondrocytes are O_2^- and H_2O_2. Excessive generation of O_2^- can activate the transcription factor NF-κB, subsequently leading to elevated levels of cytokines, chemokines, and iNOS (49). Meanwhile, the cartilages and chondrocytes of individuals affected by OA also exhibit an excessive production of NO and its derivative (50). The anabolism of proteoglycans is hindered by abnormal levels of H_2O_2 and NO, thereby impeding the production of cartilage matrix (51). In addition, studies have demonstrated that exposure of chondrocytes to pro-oxidants such as H_2O_2, tert-butyl hydroperoxide (TBHP), and menadione disrupts cellular redox equilibrium and induces oxidative stress, thereby leading to increased inflammation, apoptosis, and ferroptosis (52, 53). Moreover, oxidative stress accelerates telomere shortening and impairs chondrocyte replication capacity, thereby promoting chondrocyte senescence (39). A significant contributing factor to OA is the senescence of chondrocytes, which compromises the redox balance of mitochondria and leads to an increased production of ROS, which can result in the oxidation of genomic and mtDNA (54–56). Consequently, this oxidative damage can accelerate chondrocyte senescence and impede chondrocyte proliferation (57, 58). Taken collectively, these studies demonstrate that oxidative stress induced by excessive production of ROS under various adverse conditions promotes the degradation of cartilage, hinders ECM synthesis, and induces chondrocyte senescence and death. All these effects contribute to the progression of OA. Consequently, developing therapeutic interventions targeting detrimental ROS may hold promise for OA treatment.

2.2 Inflammation in OA

A fundamental defensive response to an infection stimulated by microorganisms or antigens is inflammation, which is mediated by

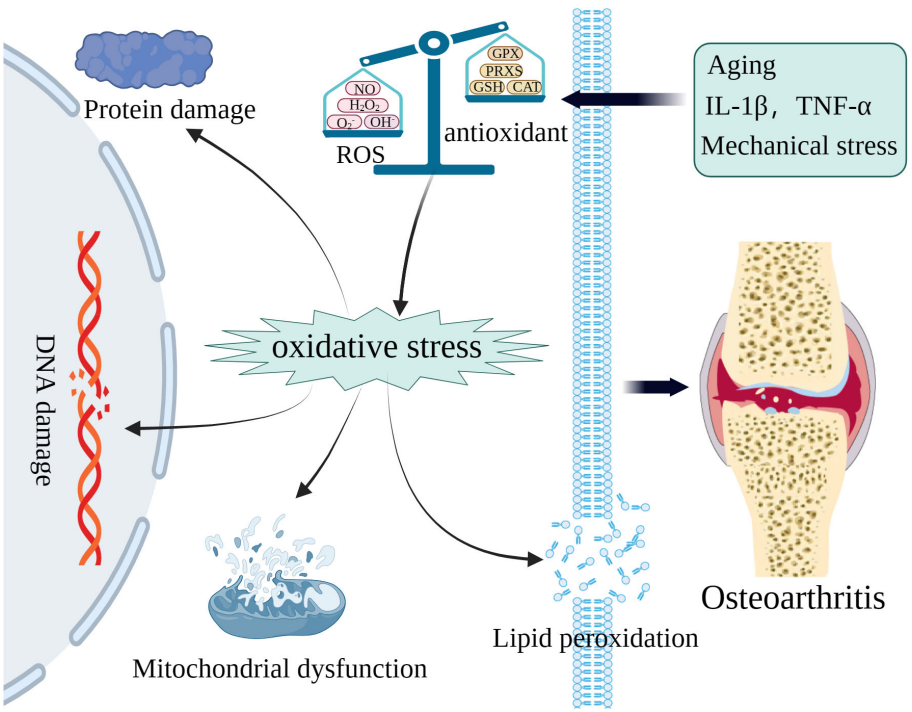

FIGURE 1
The excessive ROS caused by various pathologic processes can oxidize macromolecules including mitochondrial DNA (mtDNA), genomic, proteins, and lipids to accelerate OA.

the host immune system. The short-term, regulated inflammation contributes to tissue defense and repair, whereas the long-term, aberrant inflammation leads to tissue damage and cell death. The pathophysiology of several human diseases, such as diabetes, obesity, cancer, neurological diseases, and autoimmune diseases, are significantly influenced by chronic inflammation (59). It is well established that inflamed synovium is now recognized as a prevalent indicator of OA. To maintain the proper functioning of articular cartilage, the synovium produces synovial fluid containing hyaluronic acid and lubricin. It has been observed that patients in advanced stages of OA exhibit elevated levels of chemokines and proinflammatory cytokines in their synovial fluid (60, 61). The degeneration of cartilage and the exacerbation of synovitis are both attributed to the overexpression of prostaglandins, leukotrienes, chemokines, and cytokines in the synovium (62). Generally, chondrocytes are typically situated in an anaerobic environment, which helps maintain the articular cartilage in a state of low metabolic activity and limited turnover synthesis of ECM. However, under pathological conditions, chondrocytes overproduce chemokines and cytokines that enhance the levels of collagenases and aggrecanases, thereby disrupting the delicate balance between anabolism and catabolism in articular cartilage and leading to erosion of ECM (63). Further investigations have revealed that the elevation of cytokine levels in joints plays a pivotal role in the pathogenesis of OA by regulating oxidative stress and chondrocyte death (64). Consequently, targeting anti-inflammatory strategies hold significant potential for the treatment of OA.

The three most prominently expressed cytokines in patients with OA are IL-1, IL-6, and TNF-α, which are produced by macrophages, chondrocytes, and fibroblast-like synoviocytes, which play a significant role in the degenerative process of OA (29). Other cytokines, such as IL-17, IL-18, CXCL5, RANTES, and MCP1, have also been demonstrated to serve as key regulators in the pathogenesis of OA (65, 66). Intra-articular injections of either TNF-α or IL-1 into the knee joints have been demonstrated to expedite the progression of OA, with their combined effects further exacerbating this impact (29). The expression of catabolic genes such as COX-2, IL-6, iNOS, a disintegrin and metalloproteinase with thrombospondin motifs (ADAMTSs), and matrix metalloproteases (MMPs) was found upregulated in chondrocytes stimulated with IL-1 and TNF-α, while the expression of anabolic genes including collagen II and aggrecan was downregulated (67–69). The aberrant expression of iNOS induced by inflammatory cytokines enhances the expression of NO, thereby increasing the level of IL-1β and TNF-α to aggravate inflammation through activation of the NF-κB pathway (70). It is well established that MMPs and ADAMTSs are responsible for the degradation of collagen and aggrecan, respectively (71, 72). The pro-inflammatory cytokines TNF-α and IL-1 could inhibit the function of complex I, membrane potential, and lead to mtDNA damage, therefore contributing to mitochondrial dysfunction in human chondrocytes (28). It has been reported that the production of functionally compromised respiratory chain subunits was indued by mtDNA damage and mutations, thereby increasing the levels of ROS in chondrocytes (73). The impaired mitochondrial bioenergetics and increased inflammatory response ultimately contribute to chondrocyte death (73). Treatment of chondrocytes with inflammatory cytokines such as IL-1 and TNF-α led to a significantly elevated level of IL-6 and MMP-13 (74–76). Additionally, the administration of IL-6 through intra-articular injection in mouse knee joints promoted the destruction of articular cartilage (77). Therefore, these findings indicate that inflammatory cytokines are involved in perturbing the homeostasis of articular cartilage to involve the development of OA, and the stability of the inflammatory microenvironment is responsible for determining the function of joints.

2.3 Chondrocyte death in OA

Cell death plays a vital role in maintaining homeostasis and the developing of the body by eliminating senescent cells and shaping tissue during embryologic development. Additionally, cell death is an aberrant pathological phenomenon triggered by detrimental stimuli such as infections and injuries (78). The sole cell type found in articular cartilage, chondrocytes, are intricately embedded within the ECM and play a vital role in maintaining ECM homeostasis by regulating anabolic and catabolic processes, as well as repairing the damaged cartilages in OA. Therefore, the loss of chondrocytes may accelerate the remodeling of ECM, leading to abnormal structure of ECM and articular cartilage degeneration, thereby potentially hastening the progression of OA. Consequently, strategies to protect from the degeneration of articular cartilage can be developed by understanding the molecular mechanism of chondrocyte death. According to the regulation of involved processes, chondrocyte death can be categorized into non-programmed and programmed forms. Autophagy, pyroptosis, ferroptosis, and necroptosis are all examples of programmed cell death (PCD), while necrosis is a form of non-programmed cell death (non-PCD) that occurs due to chemical or physical stimulation under extreme conditions (79, 80).

Autophagy is a crucial cellular process responsible for the elimination of misfolded proteins, damaged organelles, and intracellular pathogens to maintain cellular homeostasis (81–83). Autophagy can be categorized into three distinct types, including macroautophagy, microautophagy, and chaperone-mediated autophagy. Macroautophagy, commonly known as autophagy, involves the formation of bilayer membranes derived from the endoplasmic reticulum (ER) and intracellular components that encapsulate proteins and organelles, and eventually fuse with lysosomes to form autophagolysosomes (84, 85). Lysosomes contain a high concentration of hydrolytic enzymes that are capable of breaking down various substrates, including damaged macromolecules and organelles. The autophagy process consists of several consecutive phases, namely initiation, phagophore or nucleation maturation, membrane elongation, sequestering the target substrate and autophagosome formation, lysosome fusion, and substrate degradation (86–88). The autophagy process is regulated by approximately 40 autophagy-related genes, with the majority of ATG functioning in complexes to regulate autophagy through various signaling pathways (86, 89). Autophagy serves as a defense mechanism for maintaining intracellular homeostasis,

operating at a basal level under normal conditions to eliminate aging-related damaged organelles and misfolded proteins (90). Autophagy can also be triggered by extreme conditions, such as external pressure, limited nutrient availability, hypoxia, and endoplasmic reticulum stress (ERS). The upregulation of autophagy-related proteins, including Unc-51-like kinase 1 (ULK1), LC3, and beclin-1, has been confirmed in human chondrocytes, however, the levels of these proteins decline in the aging population (91). The insufficient level of autophagy fails to effectively eliminate damaged organelles and macromolecules, leading to the disruption of chondrocyte homeostasis and ultimately resulting in OA (92). Therefore, the age-related decline in autophagy is a contributing factor to the deterioration of articular chondrocytes, thereby being associated with the occurrence and progression of OA.

Apoptosis, a tightly regulated mechanism of cell death, is indispensable for maintaining tissue homeostasis and ensuring the proper functioning of the human body. Morphological characteristics associated with cell apoptosis include DNA fragmentation, chromatin condensation, cell shrinkage, membrane blistering, and the formation of apoptotic bodies (93). Previous studies have shown that chondrocyte apoptosis is related to articular cartilage degradation (94). The intrinsic mitochondrial pathway and the extrinsic death receptor pathway are two well-established signaling pathways for apoptosis (79). External stimuli induce an increase in mitochondrial membrane permeability, facilitating the release of apoptotic factors such as cytochrome C and procaspases into the cytoplasm, thereby triggering activation of the mitochondrial pathway (95, 96). Under normal circumstances, damaged or depolarized mitochondria are selectively eliminated through autophagy to prevent cellular damage caused by dysfunctional mitochondria, which is commonly referred to as mitophagy (97, 98). The insufficient clearance of dysfunctional mitochondria through mitophagy leads to the release of apoptotic factors into the cytoplasm and subsequent initiation of apoptosis. This process is further exacerbated by the excessive production of ROS (99). The chondrocytes exhibited impaired autophagy and excessive apoptosis during the later stages of OA. Moreover, the essential anti-apoptotic proteins, such as Bcl2 and Bcl-XL, can suppress autophagy by binding to the key regulators of autophagy Beclin 1, thereby inhibiting the formation of the Beclin 1 complex. The apoptosis appears to be intricately linked with autophagy. The relationship between apoptosis and autophagy in chondrocytes remains incompletely understood, necessitating further investigation for confirmation.

The different forms of cell death are classified as lytic or non-lytic based on whether the cellular contents overflow upon cell death (100). Pyroptosis, also referred to as inflammatory necrosis, is a specific form of lytic cell death primarily triggered by diverse inflammasomes. These inflammasomes, such as the NLR family pyrin domain containing 3 (NLRP3), assemble in the cytosol and activate caspase to cleave gasdermins, generating membrane toxic enzymes that contribute to the formation of cell membrane perforation (101). The influx of water into the cytosol triggers a progressive swelling of cells, ultimately leading to membrane rupture. This event results in the release of cellular debris and cytokines, which not only impair neighboring cells but also exacerbate inflammation (102–104). Pyroptosis, similar to apoptosis, is a form of caspase-dependent PCD. Pyroptosis consists primarily of two pathways, including the non-canonical pathway and the canonical inflammasome pathway (105). The non-canonical inflammasome pathway is mediated by caspases 4, 5, and 11, whereas the canonical inflammasome pathway is mediated by caspase-1. Pyroptosis has been implicated in the pathogenesis of various diseases, including respiratory, circulatory, digestive, and urinary tract disorders since its original proposal in 2001 (106–109). The involvement of chondrocyte pyroptosis in the pathogenesis of OA has been experimentally validated (110). In addition to being commonly associated with OA, obesity, age, and basic calcium phosphate (BCP) also possess the ability to activate the NLRP3 inflammasome, thereby triggering chondrocyte pyroptosis (80). The expression of pyroptosis-related inflammasomes is upregulated in the synovial fluid of individuals affected by OA. Moreover, overexpression of inflammasomes enhances the levels of inflammatory factors such as IL-1β and IL-18, both contributing to chondrocyte pyroptosis and inflammatory responses (80). Additionally, the suppression of OA deterioration can be achieved by inhibiting the NLRP3 inflammasome with CY-09 (111).

Initially proposed by Stockwell's team in 2012, ferroptosis represents a distinct form of PCD (112). In contrast to autophagy, apoptosis, and pyroptosis, ferroptosis is an iron-dependent PCD characterized by unique morphological features including mitochondrial structural disruption and accumulation of lipid peroxides (113). The distinguishing features of ferroptosis from other PCDs primarily lie in the morphological changes observed in mitochondria, such as reduction or disappearance of mitochondrial cristae, decrease in mitochondrial volume, and rupture of the outer membrane (114). Iron-ion plays a crucial role in the process of ferroptosis, as it facilitates the generation of abundant ROS through the Fenton reaction, consequently leading to the formation of lipid peroxides (115). The accumulation of lipid peroxides ultimately contributes to an increase in membrane permeability and subsequent cell membrane rupture, resulting in cell death. Under normal circumstances, the essential antioxidant defense system known as glutathione peroxidase 4 (GPX4) effectively prevents the buildup of lipid peroxides, thereby mitigating ferroptosis (53, 116). The level of iron ion in the cartilage synovial fluid of the OA group has been found to be significantly higher *in vivo*, while the level of GPX4 is lower compared to that in the normal group (53). Furthermore, ferroptosis can enhance the upregulation of MMP13 and downregulation of collagen II, thereby exacerbating ECM degradation (113). A growing body of studies has demonstrated that ferroptosis plays a significant role in the pathogenesis of OA (117, 118). The occurrence of other forms of cell death, such as cuproptosis, in addition to the previously discussed chondrocyte death, is also closely associated with the onset of OA (94, 119).

3 Melatonin targeting oxidative stress, inflammation, and chondrocytes death in OA

3.1 Melatonin

The fat-soluble indole hormone melatonin (N-acetyl-5-methoxytryptamine) was initially isolated by Aaron B. Lerner and

colleagues in 1958 (120). The synthesis of melatonin in mammals primarily occurs in the pineal gland, although it is also secreted by non-pineal cells and tissues such as lymphocytes, platelets, megakaryocytes, retina, ovary, testis, liver, and skin. These extrapineal sources of melatonin function in an autocrine or paracrine manner (121, 122). The production of melatonin exhibits a distinct circadian rhythm, being synthesized predominantly during the night and suppressed during the day (123). Melatonin is biosynthesized through a complex enzymatic pathway originating from the essential amino acid tryptophan under the catalytic action of a series of enzymes (124). Melatonin is rapidly delivered to its targeted cells or organelles via the bloodstream or cerebrospinal fluid upon production (125). Once integrated with the target, melatonin exerts a diverse range of physiological effects through both receptor-dependent and receptor-independent pathways (126, 127). The melatonin receptors 1 (MT1) and melatonin receptor 2 (MT2) are G-protein-coupled receptors that are localized on both the mitochondria and the cell membrane. In addition, there is a cytosolic melatonin receptor 3 (MT3) found in several species but absent in humans. Furthermore, nuclear binding receptors such as retinoid acid-related orphan receptors (RORs)/RZR also function as receptors that melatonin targets (128, 129). The production of MT1 and MT2, which respectively regulate rapid eye movement sleep and non-rapid eye movement sleep, can be synchronized by melatonin in physiological sleep to regulate circadian rhythms (130). In addition to targeting MT1 and MT2 receptors for circadian rhythm modulation, melatonin also interacts with nuclear receptors such as RORs to modulate the circadian rhythm (131). Alongside regulating circadian rhythms, the binding of melatonin to MT1 and MT2 receptors enhances the expression of silent information regulator 1 (SIRT1) while inhibiting the phosphorylation of p38 and JNK MAPKs, thereby facilitating cell survival (132). Moreover, melatonin acts as an effective scavenger of free radicals by activating antioxidant enzymes and reducing the damaged cellular macromolecules and organelles through a receptor-independent pathway (133–135). The latest research has demonstrated that melatonin exerts a mitigating effect on inflammation, oxidative stress, and chondrocyte death in order to prevent cartilage destruction and further deterioration of OA, and the effects of melatonin on animals are listed in Table 1.

3.2 Melatonin as an inhibitor of oxidative stress

The hydrophilic and lipophilic properties of melatonin enable it to traverse all biological barriers, exerting an antioxidative impact on the cytosol, mitochondria, and cellular membrane (146, 147). Melatonin not only directly scavenges free radicals, but also enhances the activity of antioxidant enzymes such as SOD, CAT, and GPX to effectively inhibit oxidative stress (135, 148–150) (Figure 2). The nuclear factor-erythroid 2-related factor 2 (Nrf2) functions as a crucial transcription factor for antioxidant defense. Melatonin acts as an effective antioxidant, regulating the homeostasis of the cartilage matrix through the Nrf2 signaling

TABLE 1 A list of reports studying the effect of melatonin on animal.

Animal	Model	Treatment	Effect	Reference
Twelve-week-old male Sprague-Dawley rats	DMM	Intraarticular injection 100 μL MT (10 mg/mL) for one month	Prevents Cartilage Degrada -tion in DMM-induced OA	Zhou et al. (136)
Seven-week-old male Sprague-Dawley rats	DMM	Intraarticular injection 100 μL MT (10 mg/mL) once a week for twelve weeks.	Recharges of chondrocyte mitochondria to protect ca- rtilage matrix homeostasis	Zhang et al. (137)
Sprague-Dawley rats (weight 210±20 g)	ACLT	Intraarticular injection 10 mg/kg or 20 mg/kg MT (10 mg/mL) once a wee for one month.	Inhibites matrix metallopr- oteinasesa in a concentration -dependent manner	Zhao et al. (138)
Eight-week-old male Sprague–Dawley rats	Intraarticular injection collagenase	Subcutaneous injection 10 mg/kg MT (10 mg/mL) twice daily for one month	Downregulates the levels of MMP-13 and upregulates the expression of COL2A1.	Hong et al. (139)
Five-month-old male Sprague–Dawley rats	ACLT	Intraperitoneal injection 20 mg/kg or 60 mg/kg MT (10 mg/mL) once daily for six weeks	Abolishes proinflammatory factor expression in a conc- entration -dependent manner	Liu et al. (140)
Nine-week-old male C57BL/6J mice	DMM	Intraarticular injection 10 μL MT (10 mg/mL) twice a week for one month.	Prevents Cartilage Degradat -ion in DMM-induced OA	Zhang et al. (141)
Six–seven month-old female New Zealand white rabbits	ACLT	Intraarticular injection 20 mg/kg MT weekly for one month.	Anti-inflammatory effects to ameliorate OA	Lim et al. (142)
Eight-week-old female C57BL/6 mice	ACLT	Intraarticular injection 10 μL MT (50 mM) twice a week for eight weeks	Exerts protective effect on chondrocytes against inflammatory damage	Liang et al. (143)
Eight-week-old male Sprague-Dawley rats	DMM	Intraperitoneal injection (15mg/k- g) or (30 mg/kg) MT (10 mg/mL) every other day for eight weeks.	Anti-Apoptosis and Autop- hagy effects in a concentra- tion-dependent manner	Chen et al. (144)
Ten–twelve week-old male C57/BL mice	ACLT	Intraperitoneal injection (50 mg/k- g) or (150 mg/kg) MT (10 mg/mL) once a day for eight weeks	Attenuates mouse chondroc- yte apoptosis in a concen- tration-dependent manner	Qin et al. (145)

MT, melatonin; OA, osteoarthritis; DMM, destabilization of the medial meniscus; ACLT, anterior cruciate ligament transection.

10.3389/fimmu.2024.1331934

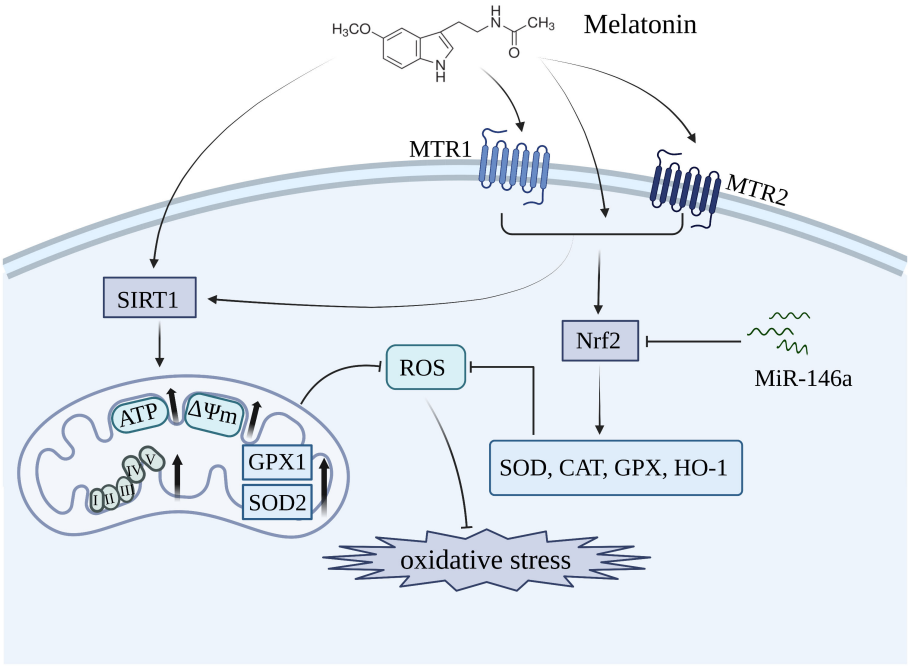

FIGURE 2
Melatonin inhibits oxidative stress in OA by restoring mitochondrial homeostasis and enhancing the level of antioxidant enzymes including SOD, CAT, and GPX. MTR1, melatonin receptor 1; MTR2, melatonin receptor 2; SIRT1, silent information regulator 1; Nrf2, nuclear factor-erythroid 2-related factor 2.

pathway. This is evidenced by the increased expression of Nrf2 in melatonin-treated chondrocytes, which led to a reduction of intracellular ROS levels and a significant elevation in the expression of SOD1, SOD2, CAT, and HO-1 (136). The expression of Nrf2 and antioxidant enzymes could be significantly inhibited by miR-146a, which was markedly elevated in OA chondrocyte. Moreover, overexpression of miR-146a reduced the level of Nrf2, thereby diminishing the protective effects of melatonin in articular cartilage of rats (136).

Mitochondria, the primary producers of ROS, serve as the key target organelles for melatonin in inhibiting oxidative damage. An *in vitro* showed that melatonin treatment restored mitochondrial homeostasis in OA chondrocytes by upregulating the expression of ATP, mtDNA, and respiratory chain factors such as CoxIV2, Sdha, Nd4, and Atp5a, thereby leading to a reduction in mitochondrial ROS levels and promotes an antioxidative effect (137) (Figure 2). The antioxidative benefits of melatonin, however, are compromised in mitochondrial homeostasis when the expression of SOD2 is inhibited, suggesting that SOD2 plays an essential role as a downstream component in mediating the protective effects of melatonin. Additionally, SIRT1, a histone deacetylase enzyme involved in nicotinamide adenine dinucleotide (NAD+) metabolism, is crucial for maintaining the activities of antioxidative enzymes (151, 152). Patients with OA who exhibited lower levels of SIRT1 showed an accelerated deterioration of articular cartilage, thereby suggesting that SIRT1 plays a protective role in the development of OA (153). The administration of melatonin significantly enhanced the expression of SIRT1, thereby promoting SOD2 activity and expression through its involvement in histone deacetylation. In contrast, the inhibition of SIRT1 significantly diminished the protective effects of melatonin, suggesting that melatonin plays a crucial role in maintaining mitochondrial function to suppress oxidative stress by modulating the level of SIRT1 in OA progression (137). The effects of melatonin on OA through SIRT1 are listed in Table 2.

3.3 Melatonin as an inhibitor of inflammation

The pathophysiology of OA is primarily influenced by chronic inflammation, as indicated by a growing body of research (156, 157). IL-1β is commonly utilized as an *in vitro* model to simulate the inflammatory process of OA. The treatment with IL-1β induced upregulation of MMP-3, MMP-9, MMP-13, ADAMTS-4, COX-2 and iNOS levels, while downregulation of chondrogenic marker COL2A1 in human mesenchymal stem cells (hMSCs) and chondrocytes. However, melatonin significantly mitigated the detrimental effects caused by IL-1β (154, 155, 158). By inhibiting the JAK2/STAT3 signaling pathway, melatonin effectively reduced the levels of MMP-3, MMP-9, and MMP-13, thereby attenuating cartilage degradation (138) (Figure 3). Moreover, Ke et al. have demonstrated that melatonin suppressed the production of IL-1β, IL-6, and COX-2 to mitigate the progression of OA in rats (159). It has been reported that TNF-a inhibited extracellular matrix synthesis by upregulating the expression of catabolic enzymes and downregulating the expression of anabolic enzymes in chondrocytes. Melatonin could effectively downregulate the levels

TABLE 2 The effects of melatonin on OA via SIRT1 .

Reference	Signaling pathway	Effect
Lim et al. (142)	SIRT1/NF-κB	Modulate the anti-inflammatory effects
Guo et al. (154)	SIRT1/NAMPT and NFAT5	Attenuate MMP-3 and MMP-13 production
Zhang et al. (137)	SIRT1/SOD2	Regain the chondrocyte mitochondrial function
Zhao et al. (155)	SIRT1/NF-κB	Prevent chondrocyte matrix degradation
Qin et al. (145)	SIRT1/IRE1α-XBP1- CHOP	Eliminate chondrocyte apoptosis

of MMP-13 and upregulate the expression of COL2A1, thereby counteracting the inhibitory effect exerted by TNF-α on ECM (160) (Figure 3). Interestingly, this effect was further enhanced when combined with suitable exercise (160). The study conducted by Hong et al. demonstrated that the combination of melatonin and exercise treatment effectively suppressed abnormal catabolic upregulation, thereby reducing cartilage degradation (139). Besides, melatonin could directly bind to the MT1 receptor and thus inhibit the production of proinflammatory cytokines such as TNF-α and IL-8 in human OA synovial fibroblasts by antagonizing the PI3K/Akt and ERK signaling pathways, subsequently leading to an upregulation of miR-185a expression (140). It was found that melatonin enhanced the expression of miR-140, thereby abolishing IL-1β-induced matrix degradation in chondrocytes (141). In addition, melatonin could induce the upregulation of circRNA3503 to counteract the ECM degradation induced by TNF-α and IL-1β (161).

The NF-κB pathway plays a crucial role in orchestrating the expression of multiple proinflammatory cytokines, including IL-6, TNF-a, COX-2, and iNOS (162). Melatonin inhibited the activation of NF-κB stimulated by H_2O_2 and also blocked the phosphorylation of upstream signaling pathways including JNK, p38 MAPK, ERK, PI3K, and Akt to improve the anti-inflammatory effects in chondrocytes (142). The inhibitory effects of melatonin on NF-κB and its upstream signaling pathways markedly are reversed by the downregulation of the SIRT1 level, in other words, the SIRT1 pathway participates in the cytoprotective and anti-inflammatory effects of melatonin via the inhibition of NF-κB signaling pathways on H_2O_2-induced articular cartilage destruction (142). Zhao et al. likewise testified that melatonin downregulates IL-1β-induced phosphorylation levels of P65 and IκBα in chondrocytes via SIRT1 pathways, thus abolishing NF-κB activation to function in cytoprotective and anti-inflammatory effects (155). It has been demonstrated that the toll-like receptor (TLR) mediates inflammatory responses triggered by chemical and physical

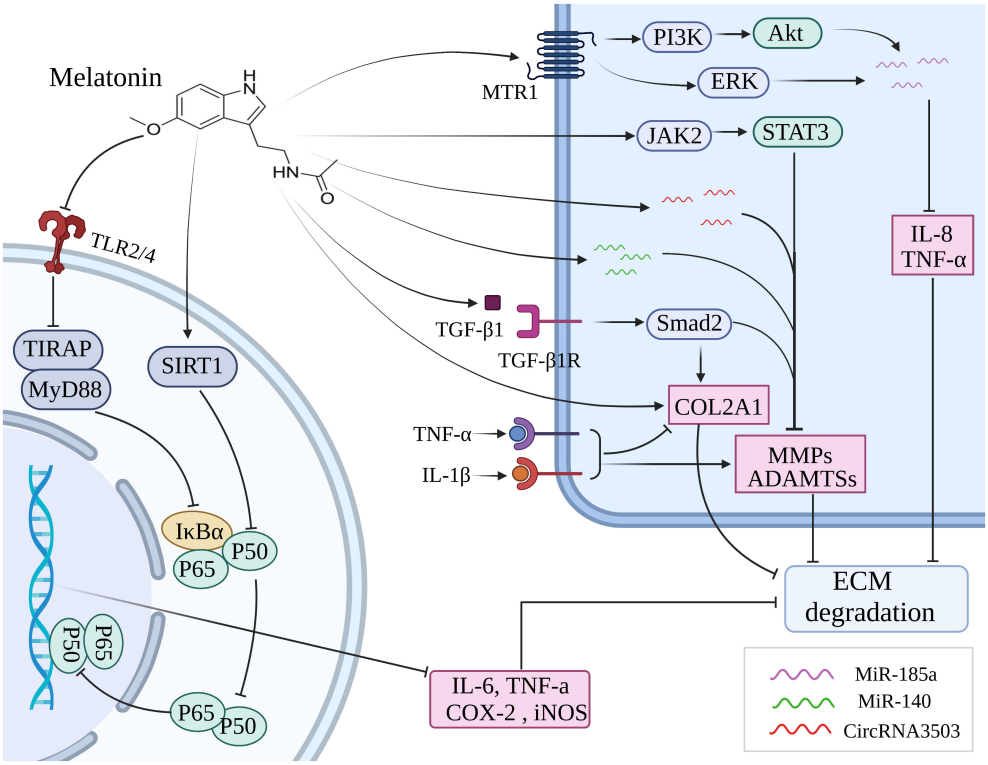

FIGURE 3
Melatonin inhibits inflammation through various signaling pathways to ameliorate the cartilage destruction in OA. ECM, extracellular matrix; MMP, matrix metalloprotease; ADAMTS, a disintegrin and metalloproteinase with thrombospondin motifs; MTR1, melatonin receptor 1; SIRT1, silent information regulator 1; TLR, toll-like receptor; COL2A1, collagen type II alpha-1.

stressors, such as cytokines and mechanical damage, ultimately leading to the development of OA (163). Hence, targeting the TLR signaling pathway may potentially serve as an efficacious therapeutic strategy for OA by attenuating the inflammatory damage. It was shown that melatonin exerted its protective effect on chondrocytes against inflammatory damage by inhibiting the TLR2/4-MyD88-NF-κB signaling pathway (143).

The expression of nicotinamide phosphoribosyltransferase (NAMPT), the rate-limiting enzyme in NAD+ biosynthesis, is enhanced by SIRT1 (164, 165). Activation of SIRT1 also promotes the synthesis of nuclear factor of activated T cells 5 (NFAT5), thereby enhancing the expression of pro-inflammatory cytokines in articular cartilage, including IL-1β, IL-6, TNF-α, COX-2, and iNOS (166, 167). Guo et al. demonstrated that melatonin significantly alleviated the expression of MMP-3 and MMP-13 induced by IL-1β in chondrocytes through the inhibition of SIRT1-mediated NAMPT and NFAT5 signaling pathways (154). Moreover, melatonin enhanced the expression of COL2A1 by regulating SIRT1, thereby restoring dexamethasone-induced ECM deterioration in chondrocytes (168). Several studies have shown that the synthesis of ECM and the differentiation, migration, and adhesion of chondrocytes were all significantly influenced by TGF-β1 (169, 170). Activation of the TGF-β1/Smad2 pathway stimulated by melatonin in IL-1β-induced chondrocytes was found contributing to the synthesis of ECM (155). It was suggested that melatonin administration in chondrocytes increased the upregulation of key chondrogenic marker genes, including Sox9, aggrecan, and collagen II via the TGF-β1 signaling pathway (171).

3.4 Melatonin as a modulator of chondrocyte death

As the sole cell type in cartilage, chondrocytes function as the core factor in regulating the homeostasis in cartilage metabolism (172). Previous studies have indicated that chondrocyte apoptosis plays a significant role in the development of OA (173, 174). The initiation of apoptosis is believed to occur as an early response to the depolarization of mitochondria, which impairs the mitochondrial membrane's potential. Substantial reductions in membrane potential promote permeabilization of the outer mitochondrial membrane, facilitating the release of apoptosis-related factors that trigger apoptosis (175, 176). Treatment with melatonin could restore the reduction of mitochondrial membrane potential and decrease the levels of caspase-3 and PARP, thereby ameliorating apoptosis in chondrocytes exposed to H_2O_2 (144) (Figure 4). A key regulator of energy homeostasis, known as 5'-AMP-activated protein kinase (AMPK), is a serine/threonine kinase composed of multiple catalytic subunits (α, β, and γ) (177). Multiple studies indicate that AMPK activation effectively inhibits apoptosis induced by the mitochondrial pathway through sustaining redox status and maintaining mitochondrial membrane potential, thereby restoring optimal mitochondrial function (178). The mammalian forked box transcription factor Class O (Foxo) family includes Foxo3, which functions as a downstream transcriptional factor in the AMPK signaling pathway and plays a crucial role in regulating antioxidant defenses and the autophagy process (179–181). Through the activation of AMPK/Foxo3 signaling pathways, melatonin exerted

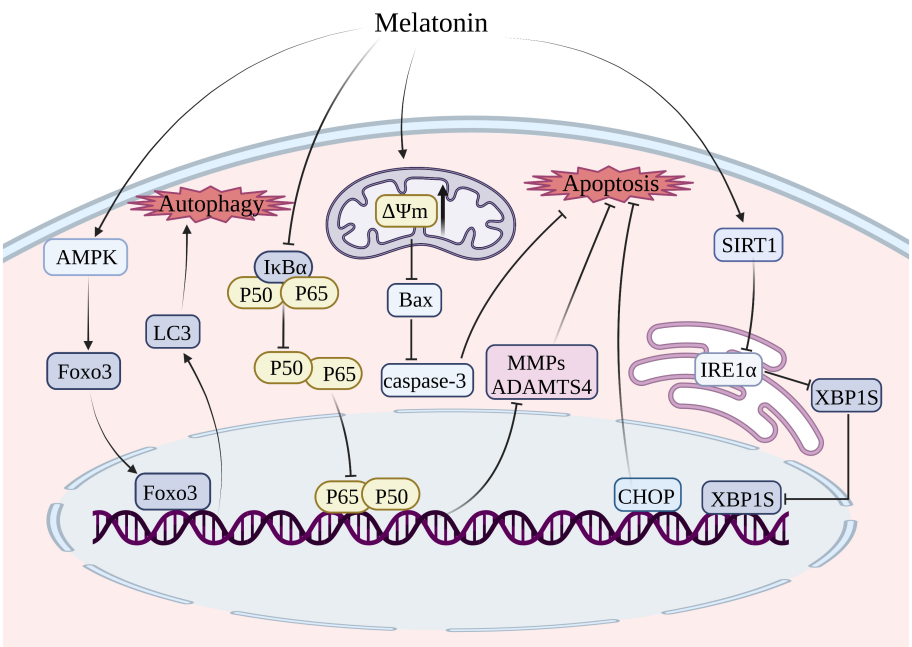

FIGURE 4
Treatment of melatonin inhibits chondrocyte apoptosis and autophagy. MMP, matrix metalloprotease; ADAMTS, a disintegrin and metalloproteinase with thrombospondin motifs; SIRT1, silent information regulator 1; Foxo3, forked box transcription factor Class O 3; IRE1-α, inositol-requiring enzyme 1-α; XBP1, X-box binding protein 1; CHOP, C/EBP homologous protein.

an inhibitory effect on apoptosis and induced upregulation of autophagy in chondrocytes to attenuate the progression of OA (144) (Figure 4).

In contrast to the internal mitochondrial pathway and extrinsic death receptor pathway, the ERS-mediated apoptosis pathway is initiated by the accumulation of misfolded proteins in the ER lumen, leading to ERS. The unfolded protein response (UPR) is a defensive mechanism that alleviates ERS and restores ER homeostasis (182, 183). However, if the ERS surpasses the threshold of UPR, it can trigger cellular apoptosis (184). UPR is initiated by transmembrane proteins, namely inositol-requiring enzyme 1-alpha (IRE1-alpha), protein kinase R-like ER kinase (PERK), and activating transcription factor 6 (ATF6) (185). The three primary signaling pathways in ERS-mediated apoptosis are IRE1α-X-box binding protein 1 (XBP1)-C/EBP homologous protein (CHOP), PERK-eukaryotic initiation factor 2α (eIF2α)-CHOP, and ATF6-XBP1-CHOP (186). The signaling pathway of IRE1α-XBP1-CHOP in chondrocyte apoptosis has been extensively investigated (187). The inhibition of the IRE1α-XBP1-CHOP signaling pathway is considered a promising target for delaying the progression of OA by blocking chondrocyte apoptosis (187). It was shown that melatonin enhanced the expression of SIRT1, which suppressed the IRE1α-XBP1-CHOP signaling pathway, thereby attenuating ERS-induced apoptosis in chondrocytes (145).

The utilization of BMSCs presents a promising strategy for alleviating articular cartilage degradation, given the wide availability of resources for harvesting BMSCs and their capacity to differentiate into various cell lineages including chondrocytes and osteoblasts (188, 189). The potential of regenerating damaged articular cartilage through the chondrogenesis of BMSCs is appealing, however, the inflammatory environment in cases of OA poses challenges for the survival of BMSCs. It has been demonstrated that the administration of melatonin could reduce the expression of Bax in IL-1β-induced BMSCs, thereby conferring protection to BMSCs against IL-1β-triggered apoptosis (190). Moreover, melatonin was found to inhibit the expression of proapoptotic markers such as ADAMTS4, MMP9, and MMP13, thus rescuing IL-1β-induced apoptosis of BMSCs and impaired chondrogenesis through the NF-κB signaling pathway (158).

As the leading risk factor for the development of OA, aging can induce senescence-associated phenotypes in joints, such as increased levels of cytokines, MMPs, and ROS, and reduced expression of aggrecan and collagen II (191). Due to its buffering and lubricating properties, hyaluronic acid plays a significant protective role in mitigating mechanical stresses on articular cartilage, and its synthesis can be hindered by chondrocyte senescence and death. It was reported that melatonin could effectively downregulate the expression of senescence-related proteins p16, p21, and p-p65, and thus counteract chondrocyte senescence and the subsequent downregulation of hyaluronic acid triggered by D-galactose through activation of the SIRT1 signaling pathway (192). Ferroptosis and pyroptosis, as novel forms of PCD, have been found implicated in the pathogenesis of OA (80, 118). Although there is currently no research reporting the impact of melatonin on ferroptosis and pyroptosis of chondrocytes, the antioxidative properties and anti-inflammatory actions of melatonin suggest its potential role as a significant inhibitor of ferroptosis and pyroptosis in chondrocytes.

4 Melatonin as a desirable pain-relieving drug in OA

OA is a primary contributor to chronic pain, significantly impacting the quality of life in individuals with OA. The exacerbation of chronic pain leads to sleep disorders, including reduced sleep efficiency and shortened total sleeping duration (193). The development of drugs to enhance the management of chronic pain in OA patients is therefore of utmost urgency. Numerous studies have suggested that melatonin exhibits analgesic effects in animal models of both acute and neuropathic pain (194–197). Several clinical trials have also confirmed the analgesic effect of melatonin in chronic pain conditions such as fibromyalgia, migraine headaches, and irritable bowel syndrome (198–200). Liu et al. demonstrated that the combination of melatonin and MT2 receptor yielded analgesic effects in rats with temporomandibular OA (201). The application of auricular acupressure has been found to enhance melatonin levels, thereby providing relief for chronic pain and addressing sleep disorders in elderly individuals with OA (202). The conventional therapeutic approaches for alleviating chronic pain, such as intra-articular steroid injections and oral nonsteroidal anti-inflammatory drugs (NSAIDs), are associated with undesirable side effects. For instance, long-term oral administration of NSAIDs can lead to gastritis and peptic ulcers, while repeated intra-articular steroid injections may result in decreased bone density and infection (203, 204). Significantly, melatonin to organs such as the liver and kidneys is associated with almost no toxicity and adverse effects (205). Collectively, the antioxidative, anti-inflammatory, and analgesic properties of melatonin render it a promising pharmaceutical agent for the treatment of OA.

5 Novel potential delivery systems of melatonin

The closed nature of the knee joint and the absence of blood vessels in the articular cartilage pose challenges for medications to accumulate within the joint via systemic circulation, leading to reduced efficacy and potential systemic adverse effects. Intra-articular administration is considered the optimal method for treating joint disorders, as it allows direct delivery of the drug to the articular cavity, thereby overcoming the aforementioned disadvantage. The frequent intra-articular injections, however, are invasive procedures that incur additional expenses, diminish patient adherence, and increase the risk of infection (206). The development of novel drug delivery systems that minimize the frequency of injections may hold the key to overcome the limitations of conventional intra-articular injection, which lacks long-term efficacy. Due to the challenge of finding suitable delivery carriers to arrive at the chondrocytes, therapeutic or preventative

options for healing damaged articular cartilage in OA remains limited (207). For this reason, numerous researchers have devoted themselves to developing melatonin sustained release delivery systems for the treatment of OA (Figure 5). Up to now, several promising melatonin sustained release delivery systems have been successfully developed (Table 3).

5.1 Extracellular vesicles

Extracellular vesicles (EVs), which can be classified into three subtypes based on their size, namely apoptotic bodies, ectosomes, and exosomes, are proteolipid nanoparticles secreted by diverse cell types including bacteria, archaea, and eukaryotic cells. Apoptotic bodies, ranging in diameter from 800 to 5,000 nm, are generated through cellular shedding during the process of apoptosis. Conversely, ectosomes are formed by the plasma membrane via budding mechanisms and have a size range of 50 to 1000 nm. Additionally, exosomes (40–200 nm) are secreted from intracellular multivesicular bodies that merge with the cytoplasmic membrane. Exosomes play a crucial role in facilitating intercellular communication by transporting lipids, proteins, and various nucleic acids such as mRNAs, circular RNA, and miRNA (215). Recent studies have demonstrated the significant potential of exosomes derived from MSCs as nano-carriers for delivering therapeutic genetic materials and drugs (216). Compared to

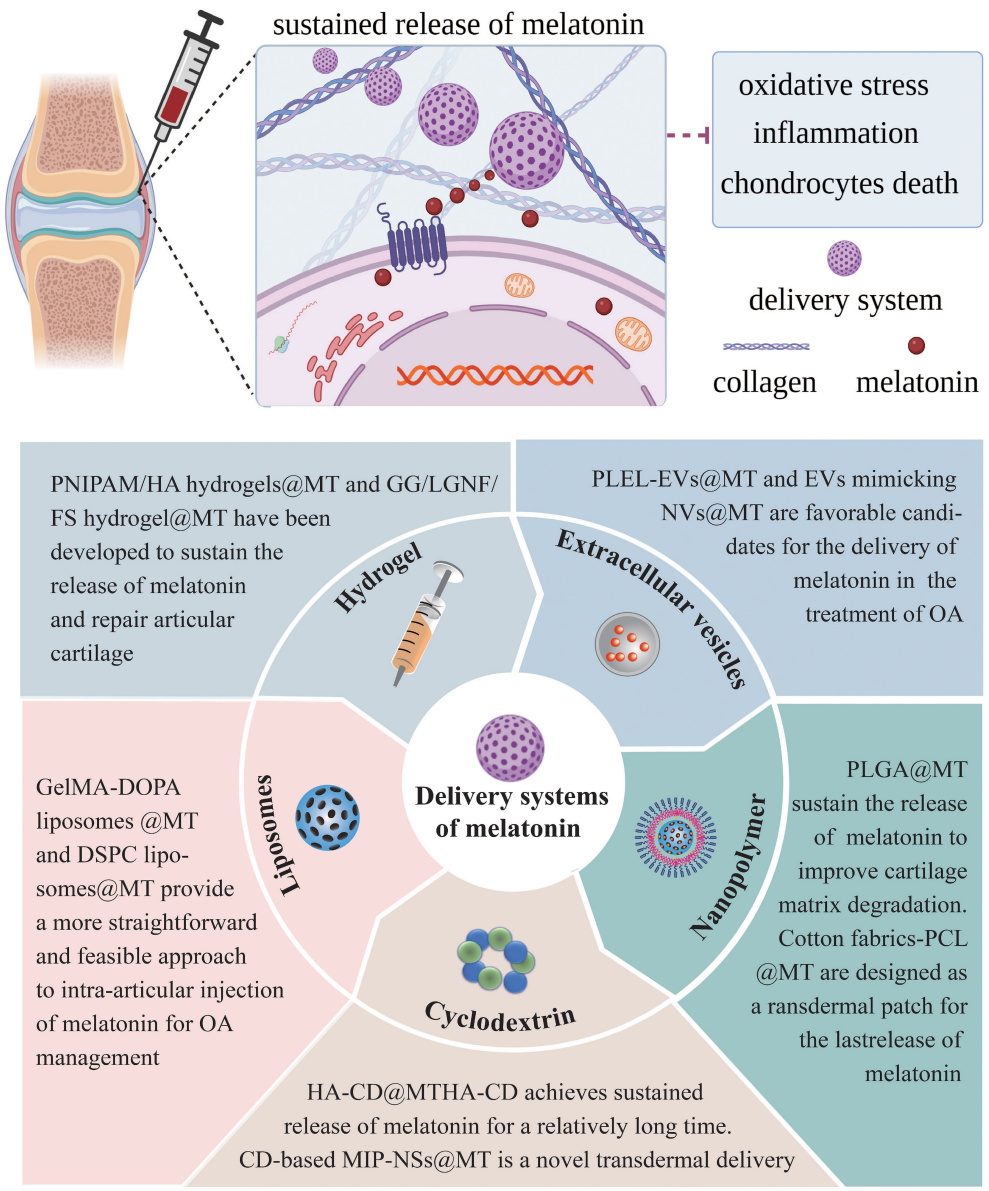

FIGURE 5
Melatonin sustained release delivery systems for the treatment of OA. MT, melatonin; PLEL, poly (D, L-lactide)-poly (ethylene glycol)-poly (D, L-lactide); EVs, extracellular vesicles; NVs, nanovesicles; PLGA, polylactic-co-glycolic acid; PCL, polycaprolactone; HA, hyaluronic acid; CD, cyclodextrins; MIP-NSs, molecularly imprinted nanosponges; GelMA-DOPA, gelatin methacryloyl-dopamine; DSPC, phosphatidylcholine; PNIPAM, poly (N-isopropyl acrylamide); GG, gellan gum; LGNF, lignocellulose nanofibrils; FS, forsterite.t of OA.

TABLE 3 The promising sustained release delivery systems of melatonin.

Materials	Delivery systems	Usage	Reference
Extracellular vesicles	PLEL-EVs@MT	injection	Tao et al. (161)
	EVs mimicking NVs@MT	injection	Kim et al. (208)
Nanopolymer	PLGA@MT	injection	Liang et al. (143)
	Cotton fabrics-PCL@MT	transdermal patch	Massella et al. (209)
Cyclodextrin	HA-CD@MT	injection	Zhang et al., 2022 (137)
	CD-based MIP-NSs@MT	transdermal patch	Hoti et al. (210)
Liposomes	GelMA-DOPA liposomes@MT	injection	Xiao et al. (211)
	DSPC liposomes@MT	injection	Ji et al. (212)
Hydrogel	PNIPAM/HA hydrogels@MT	injection	Atoufi et al. (213)
	GG/LGNF/FS hydrogel@MT	injection	Kouhi et al. (214)

MT, melatonin; PLEL, poly(D, L-lactide)-poly(ethylene glycol)-poly(D, L-lactide); EVs, extracellular vesicles; NVs, nanovesicles; PLGA, polylactic-co-glycolic acid; PCL, polycaprolactone; HA, hyaluronic acid; CD, cyclodextrins; MIP-NSs, molecularly imprinted nanosponges; GelMA-DOPA, gelatin methacryloyl-dopamine; DSPC, phosphatidylcholine; PNIPAM, poly(N-isopropyl acrylamide); GG, gellan gum; LGNF, lignocellulose nanofibrils; FS, forsterite.

MSCs, exosomes are non-viable, resulting in lower costs for storage and maintenance, as a viable state is needed in maintaining cells. Additionally, exosomes possess hypoimmunogenic properties and have a nano-scale size, which significantly reduce the likelihood of rejection (217, 218). Furthermore, exosomes possess the potential to traverse the blood-brain barrier, thereby facilitating the development of therapeutic interventions targeting the central nervous system (219). The versatility of exosomes allows for facile engineering to specifically target molecules. The current focus of numerous investigations lies in elucidating the mechanisms and functions of exosomes as efficacious drug delivery systems for various disorders. The ability of EVs to penetrate cartilage and target chondrocytes renders them as promising nano-carriers for therapeutic drugs in the treatment of OA (220). The evidence has demonstrated that EVs function as nano-carriers capable of delivering drugs to chondrocytes, thereby alleviating the progression of OA (161, 221). In conclusion, it is speculated that melatonin-loaded EVs can effectively penetrate articular cartilage and selectively target chondrocytes to attenuate the degeneration of articular cartilage by inhibiting oxidative stress, inflammation, and chondrocyte death.

The poly (D, L-lactide)-poly (ethylene glycol)-poly (D, L-lactide) (PDLLA-PEG-PDLLA; PLEL) triblock copolymer gels, which possess reversible, injectable, and thermosensitive properties, have been widely utilized in nano-drug delivery systems (222). The use of PLEL as a carrier for EVs has been employed to significantly enhance the sustained release of drugs loaded in EVs (161). The PLEL-entrapped EVs may offer promising delivery systems for achieving sustained release of melatonin, thereby presenting a potential therapeutic approach to alleviate the progression of OA. The limited production efficiency and laborious extraction and purification procedures of EVs, however, hinder the potential utilization of EVs in clinical practice. To address the challenges associated with EVs, EVs mimicking nanovesicles (NVs) which have similar biophysical characteristics to EVs have been generated via durably extruding cells through a microfilter (223, 224). EVs mimicking NVs are promising carriers which can be engineered to load with a variety of therapeutic drugs (225). Findings have demonstrated that melatonin-loaded EVs mimicking NVs effectively alleviated atopic dermatitis induced by 2,4-Dinitrofluorobenzene through the suppression of mast cell infiltration and local inflammation. Additionally, these EVs also promoted myocardial repair in cases of myocardial infarction by enhancing mitochondrial functions and reducing oxidative stress (208, 226). Taking together, it is very likely that the use of EVs mimicking NVs is a promising approach for delivering melatonin in the treatment of OA.

5.2 Nanopolymers

Nanopolymers possess exceptional mechanical properties, facile assembly, high biocompatibility, remarkable stability, scalability, and chemical modifiability, thereby offering favorable conditions for the design of nano-carrier delivery systems. Nanopolymers are broadly applied for the design of sustained release and site-specific drug delivery, resulting in improved therapeutic efficacy with fewer side effects (206, 227). Polylactic-co-glycolic acid (PLGA), a type of nanopolymer material, is widely employed in the field of drug delivery (228). The melatonin-loaded nano-delivery system was formed by encapsulating melatonin in PLGA, and the surface of PLGA was then modified with collagen II targeting polypeptides to enhance the targeting of such nanoparticles (143). What's exciting was that the sustained release of melatonin for at least 14 days in the mice joint cavity was achieved by this nanoparticle, significantly reducing the frequency of injections compared to using melatonin alone (143). The PLGA nanoparticles loaded with melatonin enable precise targeting of cartilage and sustained release, thereby reducing the degradation of cartilage and the progression of OA. Consequently, intra-articular injection of these nanoparticles may represent a novel therapeutic approach for OA treatment.

Cotton fabrics functionalized by polycaprolactone (PCL) nanoparticles are designed as a transdermal patch for the release of melatonin (209). The biodegradation process of PCL could last up to one year, making it a widely used delivery system for sustained drug release (229). Melatonin-loaded PCL nanoparticles, when distributed on cotton fibers, exhibited a controlled and sustained release of melatonin (209). This transdermal delivery system significantly enhanced the skin permeation and sustained release of melatonin through a non-invasive approach. In conclusion, it is

speculated that transdermal delivery systems may hold great potential in the treatment of OA.

5.3 Cyclodextrins

Cyclodextrins (CDs), which are cyclic oligosaccharides derived from starch hydrolysis, possess internal hydrophobicity and external hydrophilicity (230). Due to their unique characteristics, CDs have the ability to form host-guest complexes with suitable molecules to improve their stability, bioavailability, solubility, and controlled release. The CDs-based drug delivery system has facilitated the sustained release of the medication for OA treatment (231). The CD was incorporated into the hyaluronic acid (HA) solution to construct the HA-CD drug delivery system. Subsequently, melatonin was integrated into the HA-CD-based drug delivery system. The HA-CD melatonin delivery system achieved sustained release of melatonin over an extended period, effectively repairing dysfunctional mitochondria in OA chondrocytes (137). Furthermore, CDs could undergo polymerization with the cross-linking agent citric acid, followed by the addition of melatonin as a template molecule to form CD-based molecularly imprinted nanosponges (MIP-NSs) (210). Alongside these, CD-based MIP-NSs were incorporated into cream formulations to enhance their direct applicability to the skin. These skin formulations offered an innovative transdermal delivery system that enhanced the permeation of the skin and improved the sustained release of melatonin (210). The transdermal delivery systems of CD-based MIP-NSs provided a more advanced approach for delivering melatonin into the skin compared to traditional methods, such as intra-articular injection, thereby avoiding undesirable effects.

5.4 Liposomes

Liposomes have been extensively employed as drug delivery systems due to their exceptional biocompatibility and proficient capacity to regulate drug release (232, 233). Due to its excellent biocompatibility and strong adhesive properties, gelatin methacryloyl-dopamine (GelMA-DOPA) is widely used in the field of bone tissue engineering (234). The liposomes loaded with melatonin were combined with a GelMA-DOPA solution to fabricate the melatonin delivery system. The GelMA-DOPA liposomes delivery system was advantageous for regulating the sustained release of melatonin (211). The GelMA-DOPA liposomes delivery system for melatonin, although its application is limited to osteoporosis therapy right now, holds significant potential for alleviating OA. In addition, phosphatidylcholine (DSPC) liposomes could be employed as highly effective lubricants to reduce friction, in addition to their role as drug delivery systems (235). It was reported that the utilization of DSPC liposomes as a carrier for glucosamine sulphate enabled the delivery of effective boundary lubrication at the outermost layer of the joint while also facilitating the controlled and sustained release of glucosamine sulphate (212). As a result, DSPC liposomes may offer a more direct and practical approach for the intra-articular administration of melatonin in OA treatment.

5.5 Hydrogel

Hydrogel, a type of polymeric material, is extensively investigated in tissue engineering due to its exceptional biocompatibility, predictable degradation rate, appropriate elasticity, porous structure, and resemblance to the ECM (236, 237). The thermosensitive injectable hydrogel, poly (N-isopropyl acrylamide) (PNIPAM), has gained significant attention due to its ability to be directly injected into the injured area and effectively fill irregular flaws (238). PNIPAM has minimal cell adhesiveness and bioactivity despite its significant ability to replicate the architecture of some tissues. Accordingly, the combination of *in situ* injectable hydrogels with cells and bioactive compounds has garnered significant attention in the field of bone/cartilage tissue regeneration (239). The lubricating polysaccharide hyaluronic acid facilitated cellular adhesion, migration, and proliferation, thereby decreasing syneresis and hydrogel shrinkage (240). Various studies have shown that surface modification of PLGA with chitosan-g-acrylic acid (PLGA-ACH) can enhance adaptability, mucoadhesive properties, and regulate drug release (241, 242). The addition of PLGA-ACH particles as crosslinkers to PNIPAM enhanced the mechanical properties of PNIPAM, resulting in a closer resemblance to natural cartilage tissue (213). Simultaneously, the PLGA core acted as a carrier for the sustained release of melatonin (213). A previous study has demonstrated the efficacy of melatonin as a delivery system for cartilage tissue engineering, wherein injectable PNIPAM/hyaluronic acid hydrogels containing PLGA-ACH nanoparticles were applicated (213).

The low immunogenicity, cost-effectiveness, and ease of handling make Gellan gum (GG), which is composed of glucose, rhamnose, and D-glucuronate residues, particularly attractive for drug delivery (243). The GG-based hydrogel is used in cartilage regeneration due to its appealing characteristics, including non-cytotoxicity, biocompatibility, mild processing conditions, and structural resemblance to native glycosaminoglycans (237, 243). However, similar to other biodegradable hydrogels, it lacks the necessary mechanical strength and bioactivity required for reinforcement through nanoscale additions. Lignocellulose nanofibrils (LGNF), characterized by their high modulus, reactive surfaces, and large aspect ratio, present an ideal material for enhancing both the mechanical and biological properties of polymeric composites (244). The porous nanoparticle form of forsterite (FS), a crystalline member of the olivine family composed of magnesia and silicon, has been investigated for its potential as a sustained drug delivery system (245). Accordingly, in order to enhance the mechanical properties of GG-based hydrogel, LGNF and FS nanoparticles were incorporated, and thus an injectable delivery system based on GG/LGNF/FS hydrogel has been developed for sustained release of melatonin and articular cartilage repair (214).

6 Conclusions and future directions

Increasing evidence suggests that inflammation, oxidative stress, and chondrocyte death are closely linked to the severity and progression of OA, rendering them potential targets for OA treatment. The present review provides a comprehensive overview of the role of melatonin in modulating inflammation, oxidative stress, and chondrocyte death to attenuate OA progression through the regulation of various signaling pathways including SIRT1, Nrf2, NF-κB, JAK2/STAT3, TGF-β1/Smad2, AMPK/Foxo3, IRE1α-XBP1-CHOP, PI3K/Akt and ERK. Obviously, numerous signaling pathways are implicated in the potential mechanism of melatonin in the treatment of OA. The primary source of ROS leading to chondrocyte death and exacerbating inflammatory reactions, thereby aggravating articular cartilage degradation, is mitochondrial dysfunction. The melatonin-based treatment restores impaired mitochondrial functions by recovering reductions in membrane potential and enhancing the synthesis of ATP, mtDNA, and respiratory chain factors to alleviate oxidative stress and chondrocyte death. Although melatonin is considered as an effective antioxidant for maintaining mitochondria, yet the current research in this field still remains insufficient. Therefore, future studies should aim to comprehensively and profoundly investigate the interplay between melatonin and signaling pathways on mitochondria in OA chondrocytes.

The efficacy of EVs as a well-researched carrier has been demonstrated in the administration of melatonin for various disorders. However, there is a lack of direct research to substantiate the efficacy of melatonin-loaded EVs in the treatment of OA. The efficacy of melatonin-loaded EVs will be validated in future studies. In addition, various innovative bioactive materials, including nanopolymers, cyclodextrins, liposomes, and hydrogels, have been developed to ensure sustained release of melatonin and target articular cartilage. The use of novel carriers for intra-articular injection can effectively reduce the injection frequency, thereby optimizing the therapeutic efficacy and bioavailability of melatonin in the treatment of OA. Therefore, these biomaterials play an indispensable role in advancing the potential clinical efficacy of melatonin. In summary, combined melatonin with multiple bioactive agents holds great promise as a strategy for OA treatment.

Author contributions

ZX: Writing – original draft, Data curation, Methodology, Software, Visualization. GP: Data curation, Methodology, Formal analysis, Funding acquisition, Investigation, Validation, Writing – review & editing. JD: Formal analysis, Funding acquisition, Methodology, Writing – review & editing. ML: Writing – review & editing, Investigation, Project administration, Supervision. XN: Project administration, Supervision, Writing – review & editing, Methodology, Resources. YZ: Methodology, Project administration, Supervision, Writing – review & editing, Conceptualization, Formal analysis. HY: Conceptualization, Project administration, Writing – review & editing, Funding acquisition, Investigation, Resources. HS: Conceptualization, Funding acquisition, Investigation, Project administration, Writing – review & editing, Formal analysis, Methodology.

Funding

The author(s) declare financial support was received for the research, authorship, and/or publication of this article. The study was funded by the National Natural Science Foundation of China (82360420, 82260372), Science and Technology Fund of Guizhou Science and Technology Department (QKH-ZK [2021] 391; QKH-ZK [2023] 344), Science and Technology Fund of Guizhou Provincial Health Commission (gzwjkj2020-1-120; gzwkj2021-261), the Youth Fund cultivation program of National Natural Science Foundation of Affiliated Hospital of Guizhou Medical University (gyfynsfc-2021-12), and Graduate Scientific Research Fund project of Guizhou (YJSKYJJ [2021]157).

Acknowledgments

The authors would like to express their gratitude to Professor Xianwen Shang in the Affiliated Hospital of Guizhou Medical University for his generous assistance and guidance in writing. All figures were authorized and created in BioRender.com.

Conflict of interest

The authors declare that the research was conducted in the absence of any commercial or financial relationships that could be construed as a potential conflict of interest.

Publisher's note

References

1. Kaspiris A, Hadjimichael AC, Lianou I, Iliopoulos ID, Ntourantonis D, Melissaridou D, et al. Subchondral bone cyst development in osteoarthritis: from pathophysiology to bone microarchitecture changes and clinical implementations. *J Clin Med* (2023) 12(3):815. doi: 10.3390/jcm12030815

2. Yao Q, Wu X, Tao C, Gong W, Chen M, Qu M, et al. Osteoarthritis: pathogenic signaling pathways and therapeutic targets. *Signal Transduct Target Ther* (2023) 8 (1):56. doi: 10.1038/s41392-023-01330-w

3. Chen D. Osteoarthritis: A complicated joint disease requiring extensive studies with multiple approaches. *J Orthop Translat* (2022) 32:130. doi: 10.1016/j.jot.2022.02.009

4. Prieto-Alhambra D, Judge A, Javaid MK, Cooper C, Diez-Perez A, Arden NK. Incidence and risk factors for clinically diagnosed knee, hip and hand osteoarthritis: influences of age, gender and osteoarthritis affecting other joints. *Ann Rheum Dis* (2014) 73(9):1659–64. doi: 10.1136/annrheumdis-2013-203355

5. Wang Y, Nguyen UDT, Lane NE, Lu N, Wei J, Lei G, et al. Knee osteoarthritis, potential mediators, and risk of all-cause mortality: data from the osteoarthritis initiative. *Arthritis Care Res (Hoboken)* (2021) 73(4):566–73. doi: 10.1002/acr.24151

6. Sun AR, Udduttula A, Li J, Liu Y, Ren PG, Zhang P. Cartilage tissue engineering for obesity-induced osteoarthritis: Physiology, challenges, and future prospects. *J Orthop Translat* (2021) 26:3–15. doi: 10.1016/j.jot.2020.07.004

7. Hunter DJ, March L, Chew M. Osteoarthritis in 2020 and beyond: a lancet commission. *Lancet* (2020) 396(10264):1711–2. doi: 10.1016/S0140-6736(20)32230-3

8. Hawker GA, King LK. The burden of osteoarthritis in older adults. *Clin Geriatr Med* (2022) 38(2):181–92. doi: 10.1016/j.cger.2021.11.005

9. Wen C, Xiao G. Advances in osteoarthritis research in 2021 and beyond. *J Orthop Translat* (2022) 32:A1–A2. doi: 10.1016/j.jot.2022.02.011

10. Nelson AE. Osteoarthritis year in review 2017: clinical. *Osteoarthritis Cartilage* (2018) 26(3):319–25. doi: 10.1016/j.joca.2017.11.014

11. Li J, Zhang H, Han Y, Hu Y, Geng Z, Su J. Targeted and responsive biomaterials in osteoarthritis. *Theranostics* (2023) 13(3):931–54. doi: 10.7150/thno.78639

12. Eun Y, Yoo JE, Han K, Kim D, Lee KN, Lee J, et al. Female reproductive factors and risk of joint replacement arthroplasty of the knee and hip due to osteoarthritis in postmenopausal women: a nationwide cohort study of 1.13 million women. *Osteoarthritis Cartilage* (2022) 30(1):69–80. doi: 10.1016/j.joca.2021.10.012

13. Paget LDA, Reurink G, de Vos RJ, Weir A, Moen MH, Bierma-Zeinstra SMA, et al. Effect of platelet-rich plasma injections vs placebo on ankle symptoms and function in patients with ankle osteoarthritis: A randomized clinical trial. *Jama* (2021) 326(16):1595–605. doi: 10.1001/jama.2021.16602

14. Schuette HB, Kraeutler MJ, Schrock JB, McCarty EC. Primary autologous chondrocyte implantation of the knee versus autologous chondrocyte implantation after failed marrow stimulation: A systematic review. *Am J Sports Med* (2021) 49 (9):2536–41. doi: 10.1177/0363546520968284

15. Tan SHS, Kwan YT, Neo WJ, Chong JY, Kuek TYJ, See JZF, et al. Intra-articular injections of mesenchymal stem cells without adjuvant therapies for knee osteoarthritis: A systematic review and meta-analysis. *Am J Sports Med* (2021) 49(11):3113–24. doi: 10.1177/0363546520981704

16. Cho Y, Jeong S, Kim H, Kang D, Lee J, Kang SB, et al. Disease-modifying therapeutic strategies in osteoarthritis: current status and future directions. *Exp Mol Med* (2021) 53(11):1689–96. doi: 10.1038/s12276-021-00710-y

17. Luchetti F, Canonico B, Bartolini D, Arcangeletti M, Ciffolilli S, Murdolo G, et al. Melatonin regulates mesenchymal stem cell differentiation: a review. *J Pineal Res* (2014) 56(4):382–97. doi: 10.1111/jpi.12133

18. Repova K, Baka T, Krajcirovicova K, Stanko P, Aziriova S, Reiter RJ, et al. Melatonin as a potential approach to anxiety treatment. *Int J Mol Sci* (2022) 23 (24):16187. doi: 10.3390/ijms232416187

19. Stauch B, Johansson LC, McCorvy JD, Patel N, Han GW, Huang XP, et al. Structural basis of ligand recognition at the human MT(1) melatonin receptor. *Nature* (2019) 569(7755):284–8. doi: 10.1038/s41586-019-1141-3

20. Hardeland R. Aging, melatonin, and the pro- and anti-inflammatory networks. *Int J Mol Sci* (2019) 20(5):1223. doi: 10.3390/ijms20051223

21. Galano A, Reiter RJ. Melatonin and its metabolites vs oxidative stress: From individual actions to collective protection. *J Pineal Res* (2018) 65(1):e12514. doi: 10.1111/jpi.12514

22. Zhang Y, Liu T, Yang H, He F, Zhu X. Melatonin: A novel candidate for the treatment of osteoarthritis. *Ageing Res Rev* (2022) 78:101635. doi: 10.1016/j.arr.2022.101635

23. Harpsøe NG, Andersen LP, Gögenur I, Rosenberg J. Clinical pharmacokinetics of melatonin: a systematic review. *Eur J Clin Pharmacol* (2015) 71(8):901–9. doi: 10.1007/s00228-015-1873-4

24. Rahal A, Kumar A, Singh V, Yadav B, Tiwari R, Chakraborty S, et al. Oxidative stress, prooxidants, and antioxidants: the interplay. *BioMed Res Int* (2014) 2014:761264. doi: 10.1155/2014/761264

25. Lismont C, Nordgren M, Van Veldhoven PP, Fransen M. Redox interplay between mitochondria and peroxisomes. *Front Cell Dev Biol* (2015) 3:35. doi: 10.3389/fcell.2015.00035

26. Wallace DC. A mitochondrial bioenergetic etiology of disease. *J Clin Invest* (2013) 123(4):1405–12. doi: 10.1172/JCI61398

27. Lepetsos P, Papavassiliou AG. ROS/oxidative stress signaling in osteoarthritis. *Biochim Biophys Acta* (2016) 1862(4):576–91. doi: 10.1016/j.bbadis.2016.01.003

28. Blanco FJ, Rego I, Ruiz-Romero C. The role of mitochondria in osteoarthritis. *Nat Rev Rheumatol* (2011) 7(3):161–9. doi: 10.1038/nrrheum.2010.213

29. Ansari MY, Ahmad N, Haqqi TM. Oxidative stress and inflammation in osteoarthritis pathogenesis: Role of polyphenols. *BioMed Pharmacother* (2020) 129:110452. doi: 10.1016/j.biopha.2020.110452

30. Chen B, Deng Y, Tan Y, Qin J, Chen LB. Association between severity of knee osteoarthritis and serum and synovial fluid interleukin 17 concentrations. *J Int Med Res* (2014) 42(1):138–44. doi: 10.1177/0300060513501751

31. Ahmed S, Rahman A, Hasnain A, Lalonde M, Goldberg VM, Haqqi TM. Green tea polyphenol epigallocatechin-3-gallate inhibits the IL-1 beta-induced activity and expression of cyclooxygenase-2 and nitric oxide synthase-2 in human chondrocytes. *Free Radic Biol Med* (2002) 33(8):1097–105. doi: 10.1016/S0891-5849(02)01004-3

32. Lei XG, Zhu JH, Cheng WH, Bao Y, Ho YS, Reddi AR, et al. Paradoxical roles of antioxidant enzymes: basic mechanisms and health implications. *Physiol Rev* (2016) 96 (1):307–64. doi: 10.1152/physrev.00010.2014

33. Fukui M, Zhu BT. Mitochondrial superoxide dismutase SOD2, but not cytosolic SOD1, plays a critical role in protection against glutamate-induced oxidative stress and cell death in HT22 neuronal cells. *Free Radic Biol Med* (2010) 48(6):821–30. doi: 10.1016/j.freeradbiomed.2009.12.024

34. Rhee SG, Woo HA, Kil IS, Bae SH. Peroxiredoxin functions as a peroxidase and a regulator and sensor of local peroxides. *J Biol Chem* (2012) 287(7):4403–10. doi: 10.1074/jbc.R111.283432

35. Lubos E, Loscalzo J, Handy DE. Glutathione peroxidase-1 in health and disease: from molecular mechanisms to therapeutic opportunities. *Antioxid Redox Signal* (2011) 15(7):1957–97. doi: 10.1089/ars.2010.3586

36. Regan EA, Bowler RP, Crapo JD. Joint fluid antioxidants are decreased in osteoarthritic joints compared to joints with macroscopically intact cartilage and subacute injury. *Osteoarthritis Cartilage* (2008) 16(4):515–21. doi: 10.1016/j.joca.2007.09.001

37. Varesi A, Chirumbolo S, Campagnoli LIM, Pierella E, Piccini GB, Carrara A, et al. The role of antioxidants in the interplay between oxidative stress and senescence. *Antioxidants (Basel)* (2022) 11(7):1224. doi: 10.3390/antiox11071224

38. Yu H, Zhang Z, Wei F, Hou G, You Y, Wang X, et al. Hydroxytyrosol ameliorates intervertebral disc degeneration and neuropathic pain by reducing oxidative stress and inflammation. *Oxid Med Cell Longev* (2022) 2022:2240894. doi: 10.1155/2022/2240894

39. Liu L, Luo P, Yang M, Wang J, Hou W, Xu P. The role of oxidative stress in the development of knee osteoarthritis: A comprehensive research review. *Front Mol Biosci* (2022) 9:1001212. doi: 10.3389/fmolb.2022.1001212

40. Portal-Núñez S, Esbrit P, Alcaraz MJ, Largo R. Oxidative stress, autophagy, epigenetic changes and regulation by miRNAs as potential therapeutic targets in osteoarthritis. *Biochem Pharmacol* (2016) 108:1–10. doi: 10.1016/j.bcp.2015.12.012

41. Hui W, Young DA, Rowan AD, Xu X, Cawston TE, Proctor CJ. Oxidative changes and signalling pathways are pivotal in initiating age-related changes in articular cartilage. *Ann Rheum Dis* (2016) 75(2):449–58. doi: 10.1136/annrheumdis-2014-206295

42. Juan CA, Pérez de la Lastra JM, Plou FJ, Pérez-Lebeña E. The chemistry of reactive oxygen species (ROS) revisited: outlining their role in biological macromolecules (DNA, lipids and proteins) and induced pathologies. *Int J Mol Sci* (2021) 22(9):4642. doi: 10.3390/ijms22094642

43. Capozzi A, Saucier C, Bisbal C, Lambert K. Grape polyphenols in the treatment of human skeletal muscle damage due to inflammation and oxidative stress during obesity and aging: early outcomes and promises. *Molecules* (2022) 27(19):6594. doi: 10.3390/molecules27196594

44. Kinnula VL, Fattman CL, Tan RJ, Oury TD. Oxidative stress in pulmonary fibrosis: a possible role for redox modulatory therapy. *Am J Respir Crit Care Med* (2005) 172(4):417–22. doi: 10.1164/rccm.200501-017PP

45. Marchev AS, Dimitrova PA, Burns AJ, Kostov RV, Dinkova-Kostova AT, Georgiev MI. Oxidative stress and chronic inflammation in osteoarthritis: can NRF2 counteract these partners in crime? *Ann N Y Acad Sci* (2017) 1401(1):114–35. doi: 10.1111/nyas.13407

46. Liang D, Minikes AM, Jiang X. Ferroptosis at the intersection of lipid metabolism and cellular signaling. *Mol Cell* (2022) 82(12):2215–27. doi: 10.1016/j.molcel.2022.03.022

47. Koike M, Nojiri H, Ozawa Y, Watanabe K, Muramatsu Y, Kaneko H, et al. Mechanical overloading causes mitochondrial superoxide and SOD2 imbalance in chondrocytes resulting in cartilage degeneration. *Sci Rep* (2015) 5:11722. doi: 10.1038/srep11722

48. Coryell PR, Diekman BO, Loeser RF. Mechanisms and therapeutic implications of cellular senescence in osteoarthritis. *Nat Rev Rheumatol* (2021) 17(1):47–57. doi: 10.1038/s41584-020-00533-7

49. Chung HY, Cesari M, Anton S, Marzetti E, Giovannini S, Seo AY, et al. Molecular inflammation: underpinnings of aging and age-related diseases. *Ageing Res Rev* (2009) 8(1):18–30. doi: 10.1016/j.arr.2008.07.002

50. Ahmad N, Ansari MY, Bano S, Haqqi TM. Imperatorin suppresses IL-1β-induced iNOS expression *via* inhibiting ERK-MAPK/AP1 signaling in primary human OA chondrocytes. *Int Immunopharmacol* (2020) 85:106612. doi: 10.1016/j.intimp.2020.106612

51. Bolduc JA, Collins JA, Loeser RF. Reactive oxygen species, aging and articular cartilage homeostasis. *Free Radic Biol Med* (2019) 132:73–82. doi: 10.1016/j.freeradbiomed.2018.08.038

52. Collins JA, Wood ST, Nelson KJ, Rowe MA, Carlson CS, Chubinskaya S, et al. Oxidative stress promotes peroxiredoxin hyperoxidation and attenuates pro-survival signaling in aging chondrocytes. *J Biol Chem* (2016) 291(13):6641–54. doi: 10.1074/jbc.M115.693523

53. Miao Y, Chen Y, Xue F, Liu K, Zhu B, Gao J, et al. Contribution of ferroptosis and GPX4's dual functions to osteoarthritis progression. *EBioMedicine* (2022) 76:103847. doi: 10.1016/j.ebiom.2022.103847

54. Xie J, Wang Y, Lu L, Liu L, Yu X, Pei F. Cellular senescence in knee osteoarthritis: molecular mechanisms and therapeutic implications. *Ageing Res Rev* (2021) 70:101413. doi: 10.1016/j.arr.2021.101413

55. Rim YA, Nam Y, Ju JH. The role of chondrocyte hypertrophy and senescence in osteoarthritis initiation and progression. *Int J Mol Sci* (2020) 21(7):2358. doi: 10.3390/ijms21072358

56. Astrike-Davis EM, Coryell P, Loeser RF. Targeting cellular senescence as a novel treatment for osteoarthritis. *Curr Opin Pharmacol* (2022) 64:102213. doi: 10.1016/j.coph.2022.102213

57. McCulloch K, Litherland GJ, Rai TS. Cellular senescence in osteoarthritis pathology. *Aging Cell* (2017) 16(2):210–8. doi: 10.1111/acel.12562

58. Minguzzi M, Cetrullo S, D'Adamo S, Silvestri Y, Flamigni F, Borzì RM. Emerging players at the intersection of chondrocyte loss of maturational arrest, oxidative stress, senescence and low-grade inflammation in osteoarthritis. *Oxid Med Cell Longev* (2018) 2018:3075293. doi: 10.1155/2018/3075293

59. Straub RH, Schradin C. Chronic inflammatory systemic diseases: An evolutionary trade-off between acutely beneficial but chronically harmful programs. *Evol Med Public Health* (2016) 2016(1):37–51. doi: 10.1093/emph/eow001

60. Shen J, Abu-Amer Y, O'Keefe RJ, McAlinden A. Inflammation and epigenetic regulation in osteoarthritis. *Connect Tissue Res* (2017) 58(1):49–63. doi: 10.1080/03008207.2016.1208655

61. Griffin TM, Scanzello CR. Innate inflammation and synovial macrophages in osteoarthritis pathophysiology. *Clin Exp Rheumatol* (2019) 37 Suppl 120(5):57–63.

62. Scanzello CR, Goldring SR. The role of synovitis in osteoarthritis pathogenesis. *Bone* (2012) 51(2):249–57. doi: 10.1016/j.bone.2012.02.012

63. Khan NM, Haseeb A, Ansari MY, Devarapalli P, Haynie S, Haqqi TM. Wogonin, a plant derived small molecule, exerts potent anti-inflammatory and chondroprotective effects through the activation of ROS/ERK/Nrf2 signaling pathways in human Osteoarthritis chondrocytes. *Free Radic Biol Med* (2017) 106:288–301. doi: 10.1016/j.freeradbiomed.2017.02.041

64. Kapoor M, Martel-Pelletier J, Lajeunesse D, Pelletier JP, Fahmi H. Role of proinflammatory cytokines in the pathophysiology of osteoarthritis. *Nat Rev Rheumatol* (2011) 7(1):33–42. doi: 10.1038/nrrheum.2010.196

65. Khella CM, Horvath JM, Asgarian R, Rolauffs B, Hart ML. Anti-inflammatory therapeutic approaches to prevent or delay post-traumatic osteoarthritis (PTOA) of the knee joint with a focus on sustained delivery approaches. *Int J Mol Sci* (2021) 22(15):8005. doi: 10.3390/ijms22158005

66. Jiang Y, Xiao Q, Hu Z, Pu B, Shu J, Yang Q, et al. Tissue levels of leukemia inhibitory factor vary by osteoarthritis grade. *Orthopedics* (2014) 37(5):e460–464. doi: 10.3928/01477447-20140430-57

67. Ansari MY, Haqqi TM. Interleukin-1β induced Stress Granules Sequester COX-2 mRNA and Regulates its Stability and Translation in Human OA Chondrocytes. *Sci Rep* (2016) 6:27611. doi: 10.1038/srep27611

68. Haseeb A, Chen D, Haqqi TM. Delphinidin inhibits IL-1β-induced activation of NF-κB by modulating the phosphorylation of IRAK-1(Ser376) in human articular chondrocytes. *Rheumatol (Oxford)* (2013) 52(6):998–1008. doi: 10.1093/rheumatology/kes363

69. Khan NM, Ansari MY, Haqqi TM. Sucrose, but not glucose, blocks IL1-β-induced inflammatory response in human chondrocytes by inducing autophagy *via* AKT/mTOR pathway. *J Cell Biochem* (2017) 118(3):629–39. doi: 10.1002/jcb.25750

70. Ahmad N, Ansari MY, Haqqi TM. Role of iNOS in osteoarthritis: Pathological and therapeutic aspects. *J Cell Physiol* (2020) 235(10):6366–76. doi: 10.1002/jcp.29607

71. Laronha H, Caldeira J. Structure and function of human matrix metalloproteinases. *Cells* (2020) 9(5):1076. doi: 10.3390/cells9051076

72. Shiomi T, Lemaître V, D'Armiento J, Okada Y. Matrix metalloproteinases, a disintegrin and metalloproteinases, and a disintegrin and metalloproteinases with thrombospondin motifs in non-neoplastic diseases. *Pathol Int* (2010) 60(7):477–96. doi: 10.1111/j.1440-1827.2010.02547.x

73. Reed KN, Wilson G, Pearsall A, Grishko VI. The role of mitochondrial reactive oxygen species in cartilage matrix destruction. *Mol Cell Biochem* (2014) 397(1-2):195–201. doi: 10.1007/s11010-014-2187-z

74. Ansari MY, Ahmad N, Haqqi TM. Butein activates autophagy through AMPK/TSC2/ULK1/mTOR pathway to inhibit IL-6 expression in IL-1β Stimulated human chondrocytes. *Cell Physiol Biochem* (2018) 49(3):932–46. doi: 10.1159/000493225

75. Ansari MY, Khan NM, Ahmad N, Green J, Novak K, Haqqi TM. Genetic inactivation of ZCCHC6 suppresses interleukin-6 expression and reduces the severity of experimental osteoarthritis in mice. *Arthritis Rheumatol* (2019) 71(4):583–93. doi: 10.1002/art.40751

76. Pacifici M. Osteoarthritis and chronic pain: Interleukin-6 as a common denominator and therapeutic target. *Sci Signal* (2022) 15(744):eadd3702. doi: 10.1126/scisignal.add3702

77. Ryu JH, Yang S, Shin Y, Rhee J, Chun CH, Chun JS. Interleukin-6 plays an essential role in hypoxia-inducible factor 2α-induced experimental osteoarthritic cartilage destruction in mice. *Arthritis Rheum* (2011) 63(9):2732–43. doi: 10.1002/art.30451

78. Tait SW, Ichim G, Green DR. Die another way–non-apoptotic mechanisms of cell death. *J Cell Sci* (2014) 127(Pt 10):2135–44. doi: 10.1242/jcs.093575

79. Salucci S, Falcieri E, Battistelli M. Chondrocyte death involvement in osteoarthritis. *Cell Tissue Res* (2022) 389(2):159–70. doi: 10.1007/s00441-022-03639-4

80. An S, Hu H, Li Y, Hu Y. Pyroptosis plays a role in osteoarthritis. *Aging Dis* (2020) 11(5):1146–57. doi: 10.14336/AD.2019.1127

81. Ravanan P, Srikumar IF, Talwar P. Autophagy: The spotlight for cellular stress responses. *Life Sci* (2017) 188:53–67. doi: 10.1016/j.lfs.2017.08.029

82. Thangaraj A, Sil S, Tripathi A, Chivero ET, Periyasamy P, Buch S. Targeting endoplasmic reticulum stress and autophagy as therapeutic approaches for neurological diseases. *Int Rev Cell Mol Biol* (2020) 350:285–325. doi: 10.1016/bs.ircmb.2019.11.001

83. Parzych KR, Klionsky DJ. An overview of autophagy: morphology, mechanism, and regulation. *Antioxid Redox Signal* (2014) 20(3):460–73. doi: 10.1089/ars.2013.5371

84. Klionsky DJ. Autophagy: from phenomenology to molecular understanding in less than a decade. *Nat Rev Mol Cell Biol* (2007) 8(11):931–7. doi: 10.1038/nrm2245

85. Yang Y, Klionsky DJ. Autophagy and disease: unanswered questions. *Cell Death Differ* (2020) 27(3):858–71. doi: 10.1038/s41418-019-0480-9

86. Bento CF, Renna M, Ghislat G, Puri C, Ashkenazi A, Vicinanza M, et al. Mammalian autophagy: how does it work? *Annu Rev Biochem* (2016) 85:685–713. doi: 10.1146/annurev-biochem-060815-014556

87. Dikic I, Elazar Z. Mechanism and medical implications of mammalian autophagy. *Nat Rev Mol Cell Biol* (2018) 19(6):349–64. doi: 10.1038/s41580-018-0003-4

88. Schulze-Luehrmann J, Eckart RA, Ölke M, Saftig P, Liebler-Tenorio E, Lührmann A. LAMP proteins account for the maturation delay during the establishment of the Coxiella burnetii-containing vacuole. *Cell Microbiol* (2016) 18(2):181–94. doi: 10.1111/cmi.12494

89. Levine B, Kroemer G. Biological functions of autophagy genes: A disease perspective. *Cell* (2019) 176(1-2):11–42. doi: 10.1016/j.cell.2018.09.048

90. Whitehead NP. Enhanced autophagy as a potential mechanism for the improved physiological function by simvastatin in muscular dystrophy. *Autophagy* (2016) 12(4):705–6. doi: 10.1080/15548627.2016.1144005

91. Zhang Y, Vasheghani F, Li YH, Blati M, Simeone K, Fahmi H, et al. et al: Cartilage-specific deletion of mTOR upregulates autophagy and protects mice from osteoarthritis. *Ann Rheum Dis* (2015) 74(7):1432–40. doi: 10.1136/annrheumdis-2013-204599

92. Bouderlique T, Vuppalapati KK, Newton PT, Li L, Barenius B, Chagin AS. Targeted deletion of Atg5 in chondrocytes promotes age-related osteoarthritis. *Ann Rheum Dis* (2016) 75(3):627–31. doi: 10.1136/annrheumdis-2015-207742

93. Majtnerová P, Roušar T. An overview of apoptosis assays detecting DNA fragmentation. *Mol Biol Rep* (2018) 45(5):1469–78. doi: 10.1007/s11033-018-4258-9

94. Liu S, Pan Y, Li T, Zou M, Liu W, Li Q, et al. The role of regulated programmed cell death in osteoarthritis: from pathogenesis to therapy. *Int J Mol Sci* (2023) 24(6):5364. doi: 10.3390/ijms24065364

95. Madsen-Bouterse SA, Zhong Q, Mohammad G, Ho YS, Kowluru RA. Oxidative damage of mitochondrial DNA in diabetes and its protection by manganese superoxide dismutase. *Free Radic Res* (2010) 44(3):313–21. doi: 10.3109/10715760903494168

96. Oakes SA, Papa FR. The role of endoplasmic reticulum stress in human pathology. *Annu Rev Pathol* (2015) 10:173–94. doi: 10.1146/annurev-pathol-012513-104649

97. Yamashita SI, Kanki T. How autophagy eats large mitochondria: Autophagosome formation coupled with mitochondrial fragmentation. *Autophagy* (2017) 13(5):980–1. doi: 10.1080/15548627.2017.1291113

98. Liu D, Cai ZJ, Yang YT, Lu WH, Pan LY, Xiao WF, et al. Mitochondrial quality control in cartilage damage and osteoarthritis: new insights and potential therapeutic targets. *Osteoarthritis Cartilage* (2022) 30(3):395–405. doi: 10.1016/j.joca.2021.10.009

99. Lou G, Palikaras K, Lautrup S, Scheibye-Knudsen M, Tavernarakis N, Fang EF. Mitophagy and neuroprotection. *Trends Mol Med* (2020) 26(1):8–20. doi: 10.1016/j.molmed.2019.07.002

100. Jorgensen I, Miao EA. Pyroptotic cell death defends against intracellular pathogens. *Immunol Rev* (2015) 265(1):130–42. doi: 10.1111/imr.12287

101. Frank D, Vince JE. Pyroptosis versus necroptosis: similarities, differences, and crosstalk. *Cell Death Differ* (2019) 26(1):99–114. doi: 10.1038/s41418-018-0212-6

102. Burdette BE, Esparza AN, Zhu H, Wang S. Gasdermin D in pyroptosis. *Acta Pharm Sin B* (2021) 11(9):2768–82. doi: 10.1016/j.apsb.2021.02.006

103. Bedoui S, Herold MJ, Strasser A. Emerging connectivity of programmed cell death pathways and its physiological implications. *Nat Rev Mol Cell Biol* (2020) 21 (11):678–95. doi: 10.1038/s41580-020-0270-8

104. Hsu SK, Li CY, Lin IL, Syue WJ, Chen YF, Cheng KC, et al. Inflammation-related pyroptosis, a novel programmed cell death pathway, and its crosstalk with immune therapy in cancer treatment. *Theranostics* (2021) 11(18):8813–35. doi: 10.7150/thno.62521

105. Lacey CA, Mitchell WJ, Dadelahi AS, Skyberg JA. Caspase-1 and caspase-11 mediate pyroptosis, inflammation, and control of brucella joint infection. *Infect Immun* (2018) 86(9):e00361-18. doi: 10.1128/IAI.00361-18

106. D'Anna SE, Maniscalco M, Cappello F, Carone M, Motta A, Balbi B, et al. Bacterial and viral infections and related inflammatory responses in chronic obstructive pulmonary disease. *Ann Med* (2021) 53(1):135–50. doi: 10.1080/07853890.2020.1831050

107. Xu YJ, Zheng L, Hu YW, Wang Q. Pyroptosis and its relationship to atherosclerosis. *Clin Chim Acta* (2018) 476:28–37. doi: 10.1016/j.cca.2017.11.005

108. Yu J, Li S, Qi J, Chen Z, Wu Y, Guo J, et al. Cleavage of GSDME by caspase-3 determines lobaplatin-induced pyroptosis in colon cancer cells. *Cell Death Dis* (2019) 10(3):193. doi: 10.1038/s41419-019-1441-4

109. Wu Z, Liu Q, Zhu K, Liu Y, Chen L, Guo H, et al. Cigarette smoke induces the pyroptosis of urothelial cells through ROS/NLRP3/caspase-1 signaling pathway. *Neurourol Urodyn* (2020) 39(2):613–24. doi: 10.1002/nau.24271

110. Zhang Z, Fu F, Bian Y, Zhang H, Yao S, Zhou C, et al. α-chaconine facilitates chondrocyte pyroptosis and nerve ingrowth to aggravate osteoarthritis progression by activating NF-κB signaling. *J Inflamm Res* (2022) 15:5873–88. doi: 10.2147/JIR.S382675

111. Zhang Y, Lin Z, Chen D, He Y. CY-09 attenuates the progression of osteoarthritis *via* inhibiting NLRP3 inflammasome-mediated pyroptosis. *Biochem Biophys Res Commun* (2021) 553:119–25. doi: 10.1016/j.bbrc.2021.03.055

112. Dixon SJ, Lemberg KM, Lamprecht MR, Skouta R, Zaitsev EM, Gleason CE, et al. Ferroptosis: an iron-dependent form of nonapoptotic cell death. *Cell* (2012) 149 (5):1060–72. doi: 10.1016/j.cell.2012.03.042

113. Tong L, Yu H, Huang X, Shen J, Xiao G, Chen L, et al. Current understanding of osteoarthritis pathogenesis and relevant new approaches. *Bone Res* (2022) 10(1):60. doi: 10.1038/s41413-022-00226-9

114. Yan HF, Zou T, Tuo QZ, Xu S, Li H, Belaidi AA, et al. Ferroptosis: mechanisms and links with diseases. *Signal Transduct Target Ther* (2021) 6(1):49. doi: 10.1038/s41392-020-00428-9

115. Yang WS, SriRamaratnam R, Welsch ME, Shimada K, Skouta R, Viswanathan VS, et al. Regulation of ferroptotic cancer cell death by GPX4. *Cell* (2014) 156(1-2):317–31. doi: 10.1016/j.cell.2013.12.010

116. Jiang X, Stockwell BR, Conrad M. Ferroptosis: mechanisms, biology and role in disease. *Nat Rev Mol Cell Biol* (2021) 22(4):266–82. doi: 10.1038/s41580-020-00324-8

117. Hu Y, Wang Y, Liu S, Wang H. The potential roles of ferroptosis in pathophysiology and treatment of musculoskeletal diseases-opportunities, challenges, and perspectives. *J Clin Med* (2023) 12(6):2125. doi: 10.3390/jcm12062125

118. Al-Hetty H, Abdulameer SJ, Alghazali MW, Sheri FS, Saleh MM, Jalil AT. The role of ferroptosis in the pathogenesis of osteoarthritis. *J Membr Biol* (2023) 256 (3):223–8. doi: 10.1007/s00232-023-00282-0

119. Sun K, Guo Z, Zhang J, Hou L, Liang S, Lu F, et al. Inhibition of TRADD ameliorates chondrocyte necroptosis and osteoarthritis by blocking RIPK1-TAK1 pathway and restoring autophagy. *Cell Death Discovery* (2023) 9(1):109. doi: 10.1038/s41420-023-01406-0

120. Arendt J. Aaron Lerner, who discovered melatonin. *J Pineal Res* (2007) 43 (1):106–7. doi: 10.1111/j.1600-079X.2007.00457.x

121. Acuña-Castroviejo D, Escames G, Venegas C, Díaz-Casado ME, Lima-Cabello E, López LC, et al. Extrapineal melatonin: sources, regulation, and potential functions. *Cell Mol Life Sci* (2014) 71(16):2997–3025. doi: 10.1007/s00018-014-1579-2

122. Chen X, Hao A, Li X, Du Z, Li H, Wang H, et al. Melatonin inhibits tumorigenicity of glioblastoma stem-like cells *via* the AKT-EZH2-STAT3 signaling axis. *J Pineal Res* (2016) 61(2):208–17. doi: 10.1111/jpi.12341

123. Cipolla-Neto J, Amaral FGD. Melatonin as a hormone: new physiological and clinical insights. *Endocr Rev* (2018) 39(6):990–1028. doi: 10.1210/er.2018-00084

124. Stehle JH, Saade A, Rawashdeh O, Ackermann K, Jilg A, Sebestény T, et al. A survey of molecular details in the human pineal gland in the light of phylogeny, structure, function and chronobiological diseases. *J Pineal Res* (2011) 51(1):17–43. doi: 10.1111/j.1600-079X.2011.00856.x

125. Reiter RJ, Tan DX, Kim SJ, Cruz MH. Delivery of pineal melatonin to the brain and SCN: role of canaliculi, cerebrospinal fluid, tanycytes and Virchow-Robin perivascular spaces. *Brain Struct Funct* (2014) 219(6):1873–87. doi: 10.1007/s00429-014-0719-7

126. Slominski AT, Zmijewski MA, Jetten AM. RORα is not a receptor for melatonin (response to DOI 10.1002/bies.201600018). *Bioessays* (2016) 38(12):1193–4. doi: 10.1002/bies.201600204

127. Slominski AT, Kleszczyński K, Semak I, Janjetovic Z, Zmijewski MA, Kim TK, et al. Local melatoninergic system as the protector of skin integrity. *Int J Mol Sci* (2014) 15(10):17705–32. doi: 10.3390/ijms151017705

128. Hosseinzadeh A, Kamrava SK, Joghataei MT, Darabi R, Shakeri-Zadeh A, Shahriari M, et al. Apoptosis signaling pathways in osteoarthritis and possible protective role of melatonin. *J Pineal Res* (2016) 61(4):411–25. doi: 10.1111/jpi.12362

129. Lu KH, Lu PW, Lu EW, Tang CH, Su SC, Lin CW, et al. The potential remedy of melatonin on osteoarthritis. *J Pineal Res* (2021) 71(3):e12762. doi: 10.1111/jpi.12762

130. Gobbi G, Comai S. Differential function of melatonin MT(1) and MT(2) receptors in REM and NREM sleep. *Front Endocrinol (Lausanne)* (2019) 10:87. doi: 10.3389/fendo.2019.00087

131. He B, Zhao Y, Xu L, Gao L, Su Y, Lin N, et al. The nuclear melatonin receptor RORα is a novel endogenous defender against myocardial ischemia/reperfusion injury. *J Pineal Res* (2016) 60(3):313–26. doi: 10.1111/jpi.12312

132. Espino J, Ortiz Á, Bejarano I, Lozano GM, Monllor F, García JF, et al. Melatonin protects human spermatozoa from apoptosis *via* melatonin receptor- and extracellular signal-regulated kinase-mediated pathways. *Fertil Steril* (2011) 95 (7):2290–6. doi: 10.1016/j.fertnstert.2011.03.063

133. Galano A. On the direct scavenging activity of melatonin towards hydroxyl and a series of peroxyl radicals. *Phys Chem Chem Phys* (2011) 13(15):7178–88. doi: 10.1039/c0cp02801k

134. Galano A, Medina ME, Tan DX, Reiter RJ. Melatonin and its metabolites as copper chelating agents and their role in inhibiting oxidative stress: a physicochemical analysis. *J Pineal Res* (2015) 58(1):107–16. doi: 10.1111/jpi.12196

135. Fischer TW, Kleszczyński K, Hardkop LH, Kruse N, Zillikens D. Melatonin enhances antioxidative enzyme gene expression (CAT, GPx, SOD), prevents their UVR-induced depletion, and protects against the formation of DNA damage (8-hydroxy-2'-deoxyguanosine) in ex vivo human skin. *J Pineal Res* (2013) 54(3):303–12. doi: 10.1111/jpi.12018

136. Zhou X, Zhang Y, Hou M, Liu H, Yang H, Chen X, et al. Melatonin prevents cartilage degradation in early-stage osteoarthritis through activation of miR-146a/NRF2/HO-1 axis. *J Bone Miner Res* (2022) 37(5):1056–72. doi: 10.1002/jbmr.4527

137. Zhang Y, Hou M, Liu Y, Liu T, Chen X, Shi Q, et al. Recharge of chondrocyte mitochondria by sustained release of melatonin protects cartilage matrix homeostasis in osteoarthritis. *J Pineal Res* (2022) 73(2):e12815. doi: 10.1111/jpi.12815

138. Zhao Z, Bi B, Cheng G, Zhao Y, Wu H, Zheng M, et al. Melatonin ameliorates osteoarthritis rat cartilage injury by inhibiting matrix metalloproteinases and JAK2/STAT3 signaling pathway. *Inflammopharmacology* (2023) 31(1):359–68. doi: 10.1007/s10787-022-01102-y

139. Hong Y, Kim H, Lee S, Jin Y, Choi J, Lee SR, et al. Role of melatonin combined with exercise as a switch-like regulator for circadian behavior in advanced osteoarthritic knee. *Oncotarget* (2017) 8(57):97633–47. doi: 10.18632/oncotarget.19276

140. Liu SC, Tsai CH, Wang YH, Su CM, Wu HC, Fong YC, et al. Melatonin abolished proinflammatory factor expression and antagonized osteoarthritis progression. *vivo Cell Death Dis* (2022) 13(3):215. doi: 10.1038/s41419-022-04656-5

141. Zhang Y, Lin J, Zhou X, Chen X, Chen AC, Pi B, et al. Melatonin prevents osteoarthritis-Induced cartilage degradation *via* targeting microRNA-140. *Oxid Med Cell Longev* (2019) 2019:9705929. doi: 10.1155/2019/9705929

142. Lim HD, Kim YS, Ko SH, Yoon IJ, Cho SG, Chun YH, et al. Cytoprotective and anti-inflammatory effects of melatonin in hydrogen peroxide-stimulated CHON-001 human chondrocyte cell line and rabbit model of osteoarthritis *via* the SIRT1 pathway. *J Pineal Res* (2012) 53(3):225–37. doi: 10.1111/j.1600-079X.2012.00991.x

143. Liang H, Yan Y, Sun W, Ma X, Su Z, Liu Z, et al. Preparation of melatonin-loaded nanoparticles with targeting and sustained release function and their application in osteoarthritis. *Int J Mol Sci* (2023) 24(10):8740. doi: 10.3390/ijms24108740

144. Chen Z, Zhao C, Liu P, Huang H, Zhang S, Wang X. Anti-apoptosis and autophagy effects of melatonin protect rat chondrocytes against oxidative stress. *via Regul AMPK/Foxo3 Pathways Cartilage* (2021) 13(2_suppl):1041s–53s. doi: 10.1177/19476035211038748

145. Qin K, Tang H, Ren Y, Yang D, Li Y, Huang W, et al. Melatonin promotes sirtuin 1 expression and inhibits IRE1α-XBP1S-CHOP to reduce endoplasmic reticulum stress-mediated apoptosis in chondrocytes. *Front Pharmacol* (2022) 13:940629. doi: 10.3389/fphar.2022.940629

146. Majidinia M, Sadeghpour A, Mehrzadi S, Reiter RJ, Khatami N, Yousefi B. Melatonin: A pleiotropic molecule that modulates DNA damage response and repair pathways. *J Pineal Res* (2017) 63(1):12416. doi: 10.1111/jpi.12416

147. Venegas C, García JA, Escames G, Ortiz F, López A, Doerrier C, et al. Extrapineal melatonin: analysis of its subcellular distribution and daily fluctuations. *J Pineal Res* (2012) 52(2):217–27. doi: 10.1111/j.1600-079X.2011.00931.x

148. Tan DX, Manchester LC, Esteban-Zubero E, Zhou Z, Reiter RJ. Melatonin as a potent and inducible endogenous antioxidant: synthesis and metabolism. *Molecules* (2015) 20(10):18886–906. doi: 10.3390/molecules201018886

149. Mehrzadi S, Safa M, Kamrava SK, Darabi R, Hayat P, Motevalian M. Protective mechanisms of melatonin against hydrogen-peroxide-induced toxicity in human bone-

marrow-derived mesenchymal stem cells. *Can J Physiol Pharmacol* (2017) 95(7):773–86. doi: 10.1139/cjpp-2016-0409

150. Goudarzi M, Khodayar MJ, Hosseini Tabatabaei SMT, Ghaznavi H, Fatemi I, Mehrzadi S. Pretreatment with melatonin protects against cyclophosphamide-induced oxidative stress and renal damage in mice. *Fundam Clin Pharmacol* (2017) 31(6):625–35. doi: 10.1111/fcp.12303

151. Robinette TM, Nicholatos JW, Francisco AB, Brooks KE, Diao RY, Sorbi S, et al. SIRT1 accelerates the progression of activity-based anorexia. *Nat Commun* (2020) 11 (1):2814. doi: 10.1038/s41467-020-16348-9

152. Olmos Y, Sánchez-Gómez FJ, Wild B, García-Quintans N, Cabezudo S, Lamas S, et al. SirT1 regulation of antioxidant genes is dependent on the formation of a FoxO3a/PGC-1α complex. *Antioxid Redox Signal* (2013) 19(13):1507–21. doi: 10.1089/ars.2012.4713

153. Li Y, Xiao W, Wu P, Deng Z, Zeng C, Li H, et al. The expression of SIRT1 in articular cartilage of patients with knee osteoarthritis and its correlation with disease severity. *J Orthop Surg Res* (2016) 11(1):144. doi: 10.1186/s13018-016-0477-8

154. Guo JY, Li F, Wen YB, Cui HX, Guo ML, Zhang L, et al. Melatonin inhibits Sirt1-dependent NAMPT and NFAT5 signaling in chondrocytes to attenuate osteoarthritis. *Oncotarget* (2017) 8(34):55967–83. doi: 10.18632/oncotarget.18356

155. Zhao M, Song X, Chen H, Ma T, Tang J, Wang X, et al. Melatonin prevents chondrocyte matrix degradation in rats with experimentally induced osteoarthritis by inhibiting nuclear factor-κB *via* SIRT1. *Nutrients* (2022) 14(19):3966. doi: 10.3390/nu14193966

156. Liu-Bryan R, Terkeltaub R. Emerging regulators of the inflammatory process in osteoarthritis. *Nat Rev Rheumatol* (2015) 11(1):35–44. doi: 10.1038/nrrheum.2014.162

157. Liu X, Xu Y, Chen S, Tan Z, Xiong K, Li Y, et al. Rescue of proinflammatory cytokine-inhibited chondrogenesis by the antiarthritic effect of melatonin in synovium mesenchymal stem cells *via* suppression of reactive oxygen species and matrix metalloproteinases. *Free Radic Biol Med* (2014) 68:234–46. doi: 10.1016/j.freeradbiomed.2013.12.012

158. Gao B, Gao W, Wu Z, Zhou T, Qiu X, Wang X, et al. Melatonin rescued interleukin 1β-impaired chondrogenesis of human mesenchymal stem cells. *Stem Cell Res Ther* (2018) 9(1):162. doi: 10.1186/s13287-018-0892-3

159. Ke C, Li H, Yang D, Ying H, Zhu H, Wang J, et al. Melatonin attenuates the progression of osteoarthritis in rats by inhibiting inflammation and related oxidative stress on the surface of knee cartilage. *Orthop Surg* (2022) 14(9):2230–7. doi: 10.1111/os.13408

160. Hong Y, Kim H, Lee Y, Lee S, Kim K, Jin Y, et al. Salutary effects of melatonin combined with treadmill exercise on cartilage damage. *J Pineal Res* (2014) 57(1):53–66. doi: 10.1111/jpi.12143

161. Tao SC, Huang JY, Gao Y, Li ZX, Wei ZY, Dawes H, et al. Small extracellular vesicles in combination with sleep-related circRNA3503: A targeted therapeutic agent with injectable thermosensitive hydrogel to prevent osteoarthritis. *Bioact Mater* (2021) 6(12):4455–69. doi: 10.1016/j.bioactmat.2021.04.031

162. Hoesel B, Schmid JA. The complexity of NF-κB signaling in inflammation and cancer. *Mol Cancer* (2013) 12:86. doi: 10.1186/1476-4598-12-86

163. Mullen LM, Chamberlain G, Sacre S. Pattern recognition receptors as potential therapeutic targets in inflammatory rheumatic disease. *Arthritis Res Ther* (2015) 17 (1):122. doi: 10.1186/s13075-015-0645-y

164. Choi SE, Fu T, Seok S, Kim DH, Yu E, Lee KW, et al. Elevated microRNA-34a in obesity reduces NAD+ levels and SIRT1 activity by directly targeting NAMPT. *Aging Cell* (2013) 12(6):1062–72. doi: 10.1111/acel.12135

165. Rongvaux A, Shea RJ, Mulks MH, Gigot D, Urbain J, Leo O, et al. Pre-B-cell colony-enhancing factor, whose expression is up-regulated in activated lymphocytes, is a nicotinamide phosphoribosyltransferase, a cytosolic enzyme involved in NAD biosynthesis. *Eur J Immunol* (2002) 32(11):3225–34. doi: 10.1002/1521-4141(200211)32:11<3225::AID-IMMU3225>3.0.CO;2-L

166. Timucin AC, Bodur C, Basaga H. SIRT1 contributes to aldose reductase expression through modulating NFAT5 under osmotic stress: *In vitro* and in silico insights. *Cell Signal* (2015) 27(11):2160–72. doi: 10.1016/j.cellsig.2015.08.013

167. Johnson ZI, Shapiro IM, Risbud MV. Extracellular osmolarity regulates matrix homeostasis in the intervertebral disc and articular cartilage: evolving role of TonEBP. *Matrix Biol* (2014) 40:10–6. doi: 10.1016/j.matbio.2014.08.014

168. Yang W, Kang X, Qin N, Li F, Jin X, Ma Z, et al. Melatonin protects chondrocytes from impairment induced by glucocorticoids *via* NAD(+)-dependent SIRT1. *Steroids* (2017) 126:24–9. doi: 10.1016/j.steroids.2017.08.005

169. Li J, Huang J, Dai L, Yu D, Chen Q, Zhang X, et al. miR-146a, an IL-1β responsive miRNA, induces vascular endothelial growth factor and chondrocyte apoptosis by targeting Smad4. *Arthritis Res Ther* (2012) 14(2):R75. doi: 10.1186/ar3798

170. Chinzei N, Brophy RH, Duan X, Cai L, Nunley RM, Sandell LJ, et al. Molecular influence of anterior cruciate ligament tear remnants on chondrocytes: a biologic connection between injury and osteoarthritis. *Osteoarthritis Cartilage* (2018) 26 (4):588–99. doi: 10.1016/j.joca.2018.01.017

171. Pei M, He F, Wei L, Rawson A. Melatonin enhances cartilage matrix synthesis by porcine articular chondrocytes. *J Pineal Res* (2009) 46(2):181–7. doi: 10.1111/j.1600-079X.2008.00646.x

172. Thomas CM, Fuller CJ, Whittles CE, Sharif M. Chondrocyte death by apoptosis is associated with cartilage matrix degradation. *Osteoarthritis Cartilage* (2007) 15 (1):27–34. doi: 10.1016/j.joca.2006.06.012

173. Dai M, Sui B, Xue Y, Liu X, Sun J. Cartilage repair in degenerative osteoarthritis mediated by squid type II collagen *via* immunomodulating activation of M2 macrophages, inhibiting apoptosis and hypertrophy of chondrocytes. *Biomaterials* (2018) 180:91–103. doi: 10.1016/j.biomaterials.2018.07.011

174. Moon HS, Kim B, Gwak H, Suh DH, Song YS. Autophagy and protein kinase RNA-like endoplasmic reticulum kinase (PERK)/eukaryotic initiation factor 2 alpha kinase (eIF2α) pathway protect ovarian cancer cells from metformin-induced apoptosis. *Mol Carcinog* (2016) 55(4):346–56. doi: 10.1002/mc.22284

175. Vringer E, Tait SWG. Mitochondria and cell death-associated inflammation. *Cell Death Differ* (2023) 30(2):304–12. doi: 10.1038/s41418-022-01094-w

176. Jourdain A, Martinou JC. Mitochondrial outer-membrane permeabilization and remodelling in apoptosis. *Int J Biochem Cell Biol* (2009) 41(10):1884–9. doi: 10.1016/j.biocel.2009.05.001

177. Steinberg GR, Carling D. AMP-activated protein kinase: the current landscape for drug development. *Nat Rev Drug Discovery* (2019) 18(7):527–51. doi: 10.1038/s41573-019-0019-2

178. Fan C, Feng J, Tang C, Zhang Z, Feng Y, Duan W, et al. et al: Melatonin suppresses ER stress-dependent proapoptotic effects *via* AMPK in bone mesenchymal stem cells during mitochondrial oxidative damage. *Stem Cell Res Ther* (2020) 11(1):442. doi: 10.1186/s13287-020-01948-5

179. Lin CH, Cheng YC, Nicol CJ, Lin KH, Yen CH, Chiang MC. Activation of AMPK is neuroprotective in the oxidative stress by advanced glycosylation end products in human neural stem cells. *Exp Cell Res* (2017) 359(2):367–73. doi: 10.1016/j.yexcr.2017.08.019

180. Wang R, Zhang S, Previn R, Chen D, Jin Y, Zhou G. Role of forkhead box O transcription factors in oxidative stress-induced chondrocyte dysfunction: possible therapeutic target for osteoarthritis? *Int J Mol Sci* (2018) 19(12):3794. doi: 10.3390/ijms19123794

181. Akasaki Y, Alvarez-Garcia O, Saito M, Caramés B, Iwamoto Y, Lotz MK. FoxO transcription factors support oxidative stress resistance in human chondrocytes. *Arthritis Rheumatol* (2014) 66(12):3349–58. doi: 10.1002/art.38868

182. Hetz C, Zhang K, Kaufman RJ. Mechanisms, regulation and functions of the unfolded protein response. *Nat Rev Mol Cell Biol* (2020) 21(8):421–38. doi: 10.1038/s41580-020-0250-z

183. Tavernier SJ, Osorio F, Vandersarren L, Vetters J, Vanlangenakker N, Van Isterdael G, et al. Regulated IRE1-dependent mRNA decay sets the threshold for dendritic cell survival. *Nat Cell Biol* (2017) 19(6):698–710. doi: 10.1038/ncb3518

184. Sepulveda D, Rojas-Rivera D, Rodríguez DA, Groenendyk J, Köhler A, Lebeaupin C, et al. Interactome screening identifies the ER luminal chaperone hsp47 as a regulator of the unfolded protein response transducer IRE1α. *Mol Cell* (2018) 69 (2):238–52.e237. doi: 10.1016/j.molcel.2017.12.028

185. Abdullah A, Ravanan P. The unknown face of IRE1α - Beyond ER stress. *Eur J Cell Biol* (2018) 97(5):359–68. doi: 10.1016/j.ejcb.2018.05.002

186. Komoike Y, Matsuoka M. Endoplasmic reticulum stress-mediated neuronal apoptosis by acrylamide exposure. *Toxicol Appl Pharmacol* (2016) 310:68–77. doi: 10.1016/j.taap.2016.09.005

187. Wu L, Liu H, Li L, Xu D, Gao Y, Guan Y, et al. 5,7,3',4'-Tetramethoxyflavone protects chondrocytes from ER stress-induced apoptosis through regulation of the IRE1α pathway. *Connect Tissue Res* (2018) 59(2):157–66. doi: 10.1080/03008207.2017.1321639

188. Charbord P. Bone marrow mesenchymal stem cells: historical overview and concepts. *Hum Gene Ther* (2010) 21(9):1045–56. doi: 10.1089/hum.2010.115

189. Raghav PK, Mann Z, Ahlawat S, Mohanty S. Mesenchymal stem cell-based nanoparticles and scaffolds in regenerative medicine. *Eur J Pharmacol* (2022) 918:174657. doi: 10.1016/j.ejphar.2021.174657

190. Liu X, Gong Y, Xiong K, Ye Y, Xiong Y, Zhuang Z, et al. Melatonin mediates protective effects on inflammatory response induced by interleukin-1 beta in human mesenchymal stem cells. *J Pineal Res* (2013) 55(1):14–25. doi: 10.1111/jpi.12045

191. Li YS, Xiao WF, Luo W. Cellular aging towards osteoarthritis. *Mech Ageing Dev* (2017) 162:80–4. doi: 10.1016/j.mad.2016.12.012

192. Han N, Wang Z, Li X. Melatonin alleviates d-galactose-decreased hyaluronic acid production in synovial membrane cells *via* Sirt1 signalling. *Cell Biochem Funct* (2021) 39(4):488–95. doi: 10.1002/cbf.3613

193. Jung JH, Seok H, Choi SJ, Bae J, Lee SH, Lee MH, et al. The association between osteoarthritis and sleep duration in Koreans: a nationwide cross-sectional observational study. *Clin Rheumatol* (2018) 37(6):1653–9. doi: 10.1007/s10067-018-4040-3

194. Lin TB, Hsieh MC, Lai CY, Cheng JK, Wang HH, Chau YP, et al. Melatonin relieves neuropathic allodynia through spinal MT2-enhanced PP2Ac and downstream HDAC4 shuttling-dependent epigenetic modification of hmgb1 transcription. *J Pineal Res* (2016) 60(3):263–76. doi: 10.1111/jpi.12307

195. Lin JJ, Lin Y, Zhao TZ, Zhang CK, Zhang T, Chen XL, et al. Melatonin suppresses neuropathic pain *via* MT2-dependent and -independent pathways in dorsal root ganglia neurons of mice. *Theranostics* (2017) 7(7):2015–32. doi: 10.7150/thno.19500

196. Posa L, Lopez-Canul M, Rullo L, De Gregorio D, Dominguez-Lopez S, Kaba Aboud M, et al. Nociceptive responses in melatonin MT(2) receptor knockout mice compared to MT(1) and double MT(1) /MT(2) receptor knockout mice. *J Pineal Res* (2020) 69(3):e12671. doi: 10.1111/jpi.12671

197. Xie SS, Fan WG, Liu Q, Li JZ, Zheng MM, He HW, et al. Involvement of nNOS in the antinociceptive activity of melatonin in inflammatory pain at the level of sensory neurons. *Eur Rev Med Pharmacol Sci* (2020) 24(13):7399–411. doi: 10.26355/eurrev_202007_21908

198. Hussain SA, Al K II, Jasim NA, Gorial FI. Adjuvant use of melatonin for treatment of fibromyalgia. *J Pineal Res* (2011) 50(3):267–71. doi: 10.1111/j.1600-079X.2010.00836.x

199. Gonçalves AL, Martini Ferreira A, Ribeiro RT, Zukerman E, Cipolla-Neto J, Peres MF. Randomised clinical trial comparing melatonin 3 mg, amitriptyline 25 mg and placebo for migraine prevention. *J Neurol Neurosurg Psychiatry* (2016) 87 (10):1127–32. doi: 10.1136/jnnp-2016-313458

200. Siah KT, Wong RK, Ho KY. Melatonin for the treatment of irritable bowel syndrome. *World J Gastroenterol* (2014) 20(10):2492–8. doi: 10.3748/wjg.v20.i10.2492

201. Liu W, Jiang H, Liu X, Hu S, Li H, Feng Y, et al. Melatonin abates TMJOA chronic pain by MT(2)R in trigeminal ganglion neurons. *J Dent Res* (2022) 101(1):111–9. doi: 10.1177/00220345211026551

202. Zhang Y, Zhang H. Effects of auricular acupressure on sleep and pain in elderly people who have osteoarthritis and live in nursing homes: A randomized, single-blind, placebo-controlled trial [Letter]. *Explore (NY)* (2023) 19(2):214–22. doi: 10.1016/j.explore.2023.04.001

203. Shim KN, Kim JI, Kim N, Kim SG, Jo YJ, Hong SJ, et al. The efficacy and safety of irsogladine maleate in nonsteroidal anti-inflammatory drug or aspirin-induced peptic ulcer and gastritis. *Korean J Intern Med* (2019) 34(5):1008–21. doi: 10.3904/kjim.2017.370

204. Stout A, Friedly J, Standaert CJ. Systemic absorption and side effects of locally injected glucocorticoids. *Pm r* (2019) 11(4):409–19. doi: 10.1002/pmrj.12042

205. Paulino Silva KM, de Sousa FL, Alves ACB, Rocha PA, da Costa H, Ferreira WR, et al. Chondroprotective effect of melatonin and strontium ranelate in animal model of osteoarthritis. *Heliyon* (2021) 7(4):e06760. doi: 10.1016/j.heliyon.2021.e06760

206. Bruno MC, Cristiano MC, Celia C, d'Avanzo N, Mancuso A, Paolino D, et al. Injectable drug delivery systems for osteoarthritis and rheumatoid arthritis. *ACS nano* (2022) 16(12):19665–90. doi: 10.1021/acsnano.2c06393

207. Wiegant K, van Roermund PM, Intema F, Cotofana S, Eckstein F, Mastbergen SC, et al. Sustained clinical and structural benefit after joint distraction in the treatment of severe knee osteoarthritis. *Osteoarthritis Cartilage* (2013) 21(11):1660–7. doi: 10.1016/j.joca.2013.08.006

208. Kim YS, Go G, Yun CW, Yea JH, Yoon S, Han SY, et al. Topical administration of melatonin-loaded extracellular vesicle-mimetic nanovesicles improves 2,4-dinitrofluorobenzene-induced atopic dermatitis. *Biomolecules* (2021) 11(10):1450. doi: 10.3390/biom11101450

209. Massella D, Leone F, Peila R, Barresi AA, Ferri A. Functionalization of cotton fabrics with polycaprolactone nanoparticles for transdermal release of melatonin. *J Funct Biomater* (2017) 9(1):1. doi: 10.3390/jfb9010001

210. Hoti G, Ferrero R, Caldera F, Trotta F, Corno M, Pantaleone S, et al. A comparison between the molecularly imprinted and non-molecularly imprinted cyclodextrin-based nanosponges for the transdermal delivery of melatonin. *Polymers (Basel)* (2023) 15(6):1543. doi: 10.3390/polym15061543

211. Xiao L, Lin J, Chen R, Huang Y, Liu Y, Bai J, et al. Sustained release of melatonin from gelMA liposomes reduced osteoblast apoptosis and improved implant osseointegration in osteoporosis. *Oxid Med Cell Longev* (2020) 2020:6797154. doi: 10.1155/2020/6797154

212. Ji X, Yan Y, Sun T, Zhang Q, Wang Y, Zhang M, et al. Glucosamine sulphate-loaded distearoyl phosphocholine liposomes for osteoarthritis treatment: combination of sustained drug release and improved lubrication. *Biomaterials Sci* (2019) 7(7):2716–28. doi: 10.1039/C9BM00201D

213. Atoufi Z, Kamrava SK, Davachi SM, Hassanabadi M, Saeedi Garakani S, Alizadeh R, et al. Injectable PNIPAM/Hyaluronic acid hydrogels containing multipurpose modified particles for cartilage tissue engineering: Synthesis, characterization, drug release and cell culture study. *Int J Biol macromolecules* (2019) 139:1168–81. doi: 10.1016/j.ijbiomac.2019.08.101

214. Kouhi M, Varshosaz J, Hashemibeni B, Sarmadi A. Injectable gellan gum/lignocellulose nanofibrils hydrogels enriched with melatonin loaded forsterite nanoparticles for cartilage tissue engineering: Fabrication, characterization and cell culture studies. *Materials Sci Eng C Materials Biol Appl* (2020) 115:111114. doi: 10.1016/j.msec.2020.111114

215. Nikfarjam S, Rezaie J, Zolbanin NM, Jafari R. Mesenchymal stem cell derived-exosomes: a modern approach in translational medicine. *J Transl Med* (2020) 18 (1):449. doi: 10.1186/s12967-020-02622-3

216. Armstrong JPK, Stevens MM. Strategic design of extracellular vesicle drug delivery systems. *Adv Drug Delivery Rev* (2018) 130:12–6. doi: 10.1016/j.addr.2018.06.017

217. Elahi FM, Farwell DG, Nolta JA, Anderson JD. Preclinical translation of exosomes derived from mesenchymal stem/stromal cells. *Stem Cells* (2020) 38(1):15–21. doi: 10.1002/stem.3061

218. Chen TS, Arslan F, Yin Y, Tan SS, Lai RC, Choo AB, et al. Enabling a robust scalable manufacturing process for therapeutic exosomes through oncogenic immortalization of human ESC-derived MSCs. *J Transl Med* (2011) 9:47. doi: 10.1186/1479-5876-9-47

219. Chen CC, Liu L, Ma F, Wong CW, Guo XE, Chacko JV, et al. Elucidation of exosome migration across the blood-Brain barrier model. *In Vitro Cell Mol Bioeng* (2016) 9(4):509–29. doi: 10.1007/s12195-016-0458-3

220. Headland SE, Jones HR, Norling LV, Kim A, Souza PR, Corsiero E, et al. Neutrophil-derived microvesicles enter cartilage and protect the joint in inflammatory arthritis. *Sci Transl Med* (2015) 7(315):315ra190. doi: 10.1126/scitranslmed.aac5608

221. Tao SC, Yuan T, Zhang YL, Yin WJ, Guo SC, Zhang CQ. Exosomes derived from miR-140-5p-overexpressing human synovial mesenchymal stem cells enhance cartilage tissue regeneration and prevent osteoarthritis of the knee in a rat model. *Theranostics* (2017) 7(1):180–95. doi: 10.7150/thno.17133

222. Tang Q, Lim T, Shen LY, Zheng G, Wei XJ, Zhang CQ, et al. Well-dispersed platelet lysate entrapped nanoparticles incorporate with injectable PDLLA-PEG-PDLLA triblock for preferable cartilage engineering application. *Biomaterials* (2021) 268:120605. doi: 10.1016/j.biomaterials.2020.120605

223. Oh K, Kim SR, Kim DK, Seo MW, Lee C, Lee HM, et al. *In vivo* differentiation of therapeutic insulin-Producing cells from bone marrow cells *via* extracellular vesicle-Mimetic nanovesicles. *ACS Nano* (2015) 9(12):11718–27. doi: 10.1021/acsnano.5b02997

224. Jo W, Jeong D, Kim J, Park J. Self-renewal of bone marrow stem cells by nanovesicles engineered from embryonic stem cells. *Adv Healthc Mater* (2016) 5 (24):3148–56. doi: 10.1002/adhm.201600810

225. Gangadaran P, Ahn BC. Extracellular vesicle- and extracellular vesicle mimetics-based drug delivery systems: new perspectives, challenges, and clinical developments. *Pharmaceutics* (2020) 12(5):442. doi: 10.3390/pharmaceutics12050442

226. Zhang Y, Yang N, Huang X, Zhu Y, Gao S, Liu Z, et al. Melatonin engineered adipose-derived biomimetic nanovesicles regulate mitochondrial functions and promote myocardial repair in myocardial infarction. *Front Cardiovasc Med* (2022) 9:789203. doi: 10.3389/fcvm.2022.789203

227. Li X, Dai B, Guo J, Zheng L, Guo Q, Peng J, et al. Nanoparticle-cartilage interaction: pathology-based intra-articular drug delivery for osteoarthritis therapy. *Nanomicro Lett* (2021) 13(1):149. doi: 10.1007/s40820-021-00670-y

228. Danhier F, Ansorena E, Silva JM, Coco R, Le Breton A, Préat V. PLGA-based nanoparticles: an overview of biomedical applications. *J Control Release* (2012) 161 (2):505–22. doi: 10.1016/j.jconrel.2012.01.043

229. Dash TK, Konkimalla VB. Poly-small je, Ukrainian-caprolactone based formulations for drug delivery and tissue engineering: A review. *J Control Release* (2012) 158(1):15–33. doi: 10.1016/j.jconrel.2011.09.064

230. Tian B, Hua S, Liu J. Cyclodextrin-based delivery systems for chemotherapeutic anticancer drugs: A review. *Carbohydr Polym* (2020) 232:115805. doi: 10.1016/j.carbpol.2019.115805

231. Rivera-Delgado E, Djuhadi A, Danda C, Kenyon J, Maia J, Caplan AI, et al. Injectable liquid polymers extend the delivery of corticosteroids for the treatment of osteoarthritis. *J Control Release* (2018) 284:112–21. doi: 10.1016/j.jconrel.2018.05.037

232. Haeri A, Sadeghian S, Rabbani S, Anvari MS, Ghassemi S, Radfar F, et al. Effective attenuation of vascular restenosis following local delivery of chitosan decorated sirolimus liposomes. *Carbohydr Polym* (2017) 157:1461–9. doi: 10.1016/j.carbpol.2016.11.021

233. Liu C, Ewert KK, Wang N, Li Y, Safinya CR, Qiao W. A multifunctional lipid that forms contrast-agent liposomes with dual-control release capabilities for precise MRI-guided drug delivery. *Biomaterials* (2019) 221:119412. doi: 10.1016/j.biomaterials.2019.119412

234. Kéri M, Forgács A, Papp V, Bányai I, Veres P, Len A, et al. Gelatin content governs hydration induced structural changes in silica-gelatin hybrid aerogels - Implications in drug delivery. *Acta Biomater* (2020) 105:131–45. doi: 10.1016/j.actbio.2020.01.016

235. Goldberg R, Klein J. Liposomes as lubricants: beyond drug delivery. *Chem Phys Lipids* (2012) 165(4):374–81. doi: 10.1016/j.chemphyslip.2011.11.007

236. Gantar A, da Silva LP, Oliveira JM, Marques AP, Correlo VM, Novak S, et al. Nanoparticulate bioactive-glass-reinforced gellan-gum hydrogels for bone-tissue engineering. *Materials Sci Eng C Materials Biol Appl* (2014) 43:27–36. doi: 10.1016/j.msec.2014.06.045

237. Bacelar AH, Silva-Correia J, Oliveira JM, Reis RL. Recent progress in gellan gum hydrogels provided by functionalization strategies. *J materials Chem B* (2016) 4 (37):6164–74. doi: 10.1039/C6TB01488G

238. Gong C, Qi T, Wei X, Qu Y, Wu Q, Luo F, et al. Thermosensitive polymeric hydrogels as drug delivery systems. *Curr medicinal Chem* (2013) 20(1):79–94.

239. Lin X, Tsao CT, Kyomoto M, Zhang M. Injectable natural polymer hydrogels for treatment of knee osteoarthritis. *Advanced healthcare materials* (2022) 11(9): e2101479. doi: 10.1002/adhm.202101479

240. Mazumder MA, Fitzpatrick SD, Muirhead B, Sheardown H. Cell-adhesive thermogelling PNIPAAm/hyaluronic acid cell delivery hydrogels for potential application as minimally invasive retinal therapeutics. *J Biomed materials Res Part A* (2012) 100(7):1877–87. doi: 10.1002/jbm.a.34021

241. Wang Y, Li P, Kong L. Chitosan-modified PLGA nanoparticles with versatile surface for improved drug delivery. *AAPS PharmSciTech* (2013) 14(2):585–92. doi: 10.1208/s12249-013-9943-3

242. Lima IA, Khalil NM, Tominaga TT, Lechanteur A, Sarmento B, Mainardes RM. Mucoadhesive chitosan-coated PLGA nanoparticles for oral delivery of ferulic acid. *Artif cells nanomedicine Biotechnol* (2018) 46(sup2):993–1002. doi: 10.1080/21691401.2018.1477788

243. Bonifacio MA, Cometa S, Cochis A, Gentile P, Ferreira AM, Azzimonti B, et al. Antibacterial effectiveness meets improved mechanical properties: Manuka honey/gellan gum composite hydrogels for cartilage repair. *Carbohydr polymers* (2018) 198:462–72. doi: 10.1016/j.carbpol.2018.06.115

244. Pereira DR, Silva-Correia J, Oliveira JM, Reis RL, Pandit A, Biggs MJ. Nanocellulose reinforced gellan-gum hydrogels as potential biological substitutes for annulus fibrosus tissue regeneration. *Nanomedicine* (2018) 14(3):897–908. doi: 10.1016/j.nano.2017.11.011

245. Hassanzadeh-Tabrizi SA, Bigham A, Rafienia M. Surfactant-assisted sol-gel synthesis of forsterite nanoparticles as a novel drug delivery system. *Materials Sci Eng C Materials Biol Appl* (2016) 58:737–41. doi: 10.1016/j.msec.2015.09.020

frontiers | Frontiers in Immunology

TYPE Brief Research Report
PUBLISHED 07 February 2024
DOI 10.3389/fimmu.2024.1295150

OPEN ACCESS

EDITED BY
Pedro Gonzalez-Menendez,
University of Oviedo, Spain

REVIEWED BY
Sophie Dupre-Crochet,
Université de Versailles Saint-Quentin-en-Yvelines, France
Juan Manuel Serrador
Spanish National Research Council (CSIC), Spain

*CORRESPONDENCE
Galina F. Sud'ina
sudina@genebee.msu.ru
Boris V. Chernyak
bchernyak1@gmail.com

RECEIVED 15 September 2023
ACCEPTED 22 January 2024
PUBLISHED 07 February 2024

CITATION
Golenkina EA, Viryasova GM, Galkina SI, Kondratenko ND, Gaponova TV, Romanova YM, Lyamzaev KG, Chernyak BV and Sud'ina GF (2024) Redox processes are major regulators of leukotriene synthesis in neutrophils exposed to bacteria *Salmonella typhimurium*; the way to manipulate neutrophil swarming.
Front. Immunol. 15:1295150.
doi: 10.3389/fimmu.2024.1295150

Redox processes are major regulators of leukotriene synthesis in neutrophils exposed to bacteria *Salmonella typhimurium*; the way to manipulate neutrophil swarming

Ekaterina A. Golenkina[1], Galina M. Viryasova[1], Svetlana I. Galkina[1], Natalia D. Kondratenko[1], Tatjana V. Gaponova[2], Yulia M. Romanova[3], Konstantin G. Lyamzaev[1,4], Boris V. Chernyak[1*] and Galina F. Sud'ina[1*]

[1]Belozersky Institute of Physico-Chemical Biology, Lomonosov Moscow State University, Moscow, Russia, [2]National Research Center for Hematology, Russia Federation Ministry of Public Health, Moscow, Russia, [3]Department of Genetics and Molecular Biology, Gamaleya National Research Centre of Epidemiology and Microbiology, Moscow, Russia, [4]The "Russian Clinical Research Center for Gerontology" of the Ministry of Healthcare of the Russian Federation, Pirogov Russian National Research Medical University, Moscow, Russia

Neutrophils play a primary role in protecting our body from pathogens. When confronted with invading bacteria, neutrophils begin to produce leukotriene B4, a potent chemoattractant that, in cooperation with the primary bacterial chemoattractant fMLP, stimulates the formation of swarms of neutrophils surrounding pathogens. Here we describe a complex redox regulation that either stimulates or inhibits fMLP-induced leukotriene synthesis in an experimental model of neutrophils interacting with *Salmonella typhimurium*. The scavenging of mitochondrial reactive oxygen species by mitochondria-targeted antioxidants MitoQ and SkQ1, as well as inhibition of their production by mitochondrial inhibitors, inhibit the synthesis of leukotrienes regardless of the cessation of oxidative phosphorylation. On the contrary, antioxidants N-acetylcysteine and sodium hydrosulfide promoting reductive shift in the reversible thiol-disulfide system stimulate the synthesis of leukotrienes. Diamide that oxidizes glutathione at high concentrations inhibits leukotriene synthesis, and the glutathione precursor S-adenosyl-L-methionine prevents this inhibition. Diamide-dependent inhibition is also prevented by diphenyleneiodonium, presumably through inhibition of NADPH oxidase and NADPH accumulation. Thus, during bacterial infection, maintaining the reduced state of glutathione in neutrophils plays a decisive role in the synthesis of leukotriene B4. Suppression of excess leukotriene synthesis is an effective strategy for treating various inflammatory pathologies. Our data suggest that the use of mitochondria-targeted antioxidants may be promising for this

purpose, whereas known thiol-based antioxidants, such as N-acetylcysteine, may dangerously stimulate leukotriene synthesis by neutrophils during severe pathogenic infection.

KEYWORDS

neutrophil, *Salmonella typhimurium*, leukotriene B4, reactive oxygen species, glutathione, neutrophil swarming

1 Introduction

The main effector functions of polymorphonuclear leukocytes (PMNLs, neutrophils) in the fight against pathogens include phagocytosis, oxidative burst, degranulation. They eliminate pathogens through the production of reactive oxygen species (ROS) and releasing azurophilic granules containing antimicrobial proteins such as neutrophil elastase and myeloperoxidase (MPO) (1, 2). Nitric oxide (NO) production in human PMNLs, along with ROS and MPO is important to execute antimicrobial activity (3). In cases where these weapons are not effective enough to kill pathogens, a program of collective behavior known as swarming can be initiated. This program involves the production of leukotriene B4 (LTB4) as a potent chemoattractant and the gathering of neutrophils into dense clusters surrounding pathogens (4). In these clusters, neutrophils activate suicidal production of extracellular chromatin traps (NETs), which enhance pathogen fixation (5). Both swarming and NETs formation (NETosis) programs are subject to complex redox regulation.

Early neutrophil recruitment is initiated by pathogen-associated molecular patterns (PAMPs), including N-formyl peptides, and damage-associated molecular patterns (DAMPs) (6). This interaction of "pioneer" neutrophils with pathogen (or danger signal from damaged tissue) results in leukotriene B4 (LTB4) synthesis, and started the next step, swam attractant release (7), leading to exponential accumulation of neutrophils at infection/damage loci (8). At this stage, LTB4 and the receptors BLT1 for LTB4 coordinate cellular responses by neutrophils with each other, and the swarm is formed. Also, the coordinated transcellular biosynthesis of LTB4 drives swarming responses (9). The initiation of swarming converges on the synthesis of LTB4. During this swarm recruitment NETs could not be observed. On the timeline of major events in neutrophil swarming, the onset of NETs forming proceeds later, on the aggregation phase of the swarming response when neutrophils clusters surrounding pathogens has been formed, and activated cells release chromatin, which is accompanied with the loss of integrity of cellular membrane (5, 10).

Leukotrienes play role also in inhibition of neutrophil swarming (6). ω-OH-LTB4 and ω-COOH-LTB4 compete with LTB4 for BLT1 receptor binding (11) and act as inhibitors of LTB4-mediated responses. When LTB4 is easy transformed to ω-OH-LTB4, this decreases neutrophil swarming. We recently found that stimulation by fMLP of neutrophils after preincubation with bacteria *Salmonella typhimurium* strongly increased leukotriene synthesis; but when the bacteria:neutrophil ratio increased, the transformation of LTB4 to ω-OH-LTB4 was suppressed (12), which support increased level of LTB4. LTB4 is the strongest chemoattractant and works at sub nanomolar concentrations (13). The increased formation of LTB4 during the interaction of neutrophils with bacteria works as a signal of neutrophils for help with an increase in bacterial load. In this study we explored intervention of redox processes in neutrophil on fMLP-induced leukotriene synthesis in the experimental model of neutrophil interaction with bacteria *Salmonella typhimurium*.

NADPH-oxidase (NOX2) is the primary source of ROS which is not only responsible for oxidative burst but also involved in phagocytosis (14), degranulation (15) and NETosis (16). ROS were required for PMNLs antimicrobial activity against *S. pneumoniae*; however the NADPH oxidase was dispensable for that (17). *S. pneumoniae* infection induced mitochondrial ROS production in PMNLs. And mitochondrial ROS were critical for the ability of PMNLs to kill *S.pneumoniae*. DPI which inhibits ROS production by the NADPH oxidase, did not blunt the ability of PMNs to kill *S. pneumoniae*, but MitoTempo did. Dunham-Snary et al. (18) were first who showed that neutrophil mitochondria actively participate in phagocytosis and killing of *Staphylococcus aureus*, and antimycin and MitoTempo increased bacterial survival (18). Human pathogen *Shigella* dramatically changed neutrophils toward enhanced microbial recognition and mitochondrial ROS production (19). What is the role of mitochondrial ROS in leukotriene synthesis in infected neutrophils?

Mitochondria are an important source of ROS in various cell types, but their role in ROS production in neutrophils has long been underestimated. Only our recent studies (20–22) using the mitochondria-targeted antioxidant SkQ1 [10-(6'-plastoquinonyl) decyltriphenylphosphonium bromide] (23) have demonstrated the important role of mitochondrial ROS (mtROS) in NADPH oxidase activation, degranulation, extracellular trap formation (NETosis), and leukotriene synthesis. These studies analyzed the activation of neutrophils by the Ca^{2+} ionophore A23187 and the chemoattractant N-formyl-L-methionyl-L-leucyl-L-phenylalanine (fMLP), while the role of mtROS in the interaction of neutrophils with bacteria remains unknown.

Neutrophils control the infection, in turn, microorganisms affect the functions of neutrophils, controlling phagocytosis, the production of oxidants and the lifespan of neutrophils (24). Pathogens antagonize neutrophils, for example, by secreting catalase to reduce ROS (25, 26). To protect from ROS, the fungal pathogen *Histoplasma capsulatum* infects both neutrophils and macrophages producing a superoxide dismutase (SOD) (27). Gram-negative pathogen *Coxiella burnetii* (28) and *Pseudomonas aeruginosa* (26), as well as *E.coli* producing enterobactin (29) inhibit NADPH oxidase in human neutrophils. Microbial avoidance strategies can target not only ROS production but also degranulation and synthesis of leukotriene B4 (30). Decreased intracellular GSH correlates with the susceptibility to infections. Glutathione reductase (Gsr) catalyzes the reduction of glutathione disulfide to glutathione using NADPH as an electron donor (31). Glutathione reductase promotes *Candida albicans* clearance (32). As NADPH is a cofactor required for GSH regeneration from GSSG, the consumption of NADPH affects the regeneration of GSH (33). One can propose that NADPH-oxidase inhibition can support GSH level. These processes certainly affect LT synthesis and neutrophil swarming around pathogens.

5-Lipoxygenase (5-LOX) is a key enzyme in synthesis of LTB4 involved in chemical cell-to-cell communication. LTB4 is critical for enhancing chemotactic responses to primary chemoattractants, such as fMLP (34) increasing clustering and surface mobility of adhesion receptors integrins (35). Thus, LTB4 is not only a chemotactic, but also a neutrophil aggregating substance (36) that promotes local neutrophil interactions during swarming (4). Initial neutrophil–neutrophil contacts are critical to initiate swarming (37). We recently found, that the synthesis of LTB4 in neutrophils in the presence of bacteria and fMLP correlates with the appearance of cell-cell contacts (12), which can serve as a signal conductor to further clustering and swarming.

In the current study, we observed that redox processes can either activate or inhibit fMLP-induced leukotriene synthesis in an experimental model of neutrophil interaction with the bacteria *Salmonella typhimurium*. Our study demonstrated that mitochondrial ROS are crucial for 5-LOX activation and LT synthesis, and mitochondria-targeted antioxidants inhibited LT synthesis. On the other hand, inhibition of NOX2-dependent ROS supported LTB4 synthesis, and potentiated the stimulating effect of thiol oxidant diamide on LT synthesis.

2 Materials and methods

Hank's balanced salt solution with calcium and magnesium but without Phenol Red and sodium hydrogen carbonate (HBSS), Dulbecco's phosphate-buffered saline (PBS) with magnesium but without calcium, N-Formyl-L-methionyl-L-Leucyl-L-Phenylalanine (fMLP), Ellman's reagent [5,5′-Dithiobis(2-nitrobenzoic acid)], oxythiamine, and fibrinogen from human plasma, were purchased from Sigma (Steinheim, Germany). Dextran T-500 was from Pharmacosmos (Holbæk, Denmark). ROS indicator Carboxy-H_2DCFDA and Pierce™ Avidin, Fluorescein (FITC) conjugated were from Thermo Fisher Scientific (Waltham, MA USA). Mitochondrial ToxGlo™ Assay was from Promega Corp. (Madison, WI USA). Biotinylated murine IgG1 antibodies CD11b and CD54 were from Ancell Corp. (Bayport, MN USA). Bacteria (*S. typhimurium* IE 147 strain) were obtained from the Collection of Gamaleya National Research Center of Epidemiology and Microbiology (Moscow, Russia). Bacteria were grown in Luria–Bertani broth to a concentration of 1×10^9 colony-forming units (CFU)/mL. In this study not opsonized bacteria were used.

2.1 Neutrophil isolation

Human polymorphonuclear leukocytes (PMNL) were isolated from freshly collected blood with citrate anticoagulant. Leukocyte-rich plasma was obtained from donated blood by sedimentation in the presence of dextran T-500. Granulocytes were obtained as described (38). Cell viability was checked by trypan blue exclusion. Control suspension samples were stained in parallel with Hoechst and Romanovsky-Giemsa dyes to assess the homogeneity of the cell population. PMNLs (95–97% purity, 98–99% viability) were stored at room temperature in Dulbecco's PBS containing 1 mg/mL glucose (no CaCl2) until use.

2.2 Determination of 5-LOX product formation in cells

PMNLs [(1.2-1.5)x10^7/6 ml HBSS with 10 mM HEPES (HBSS/HEPES)] were pre-incubated for 10 min at 37°C, 5% CO_2. At this stage, 2-deoxy-D-glucose (2-DG) was added to the samples, in those cases where this was provided for in the experimental protocol. Then, maintaining incubation conditions, *S. typhimurium* (bacteria per cell ratio ~25:1) and indicated reagents were added for 30 min, followed by 10 min exposure to 0,1 μM fMLP. The treatment was stopped by adding of an equal volume of methanol (-18°C) with 90 ng PGB2 as internal standard. Major 5-LOX metabolites, 5S, 12R-dihydroxy-6,14-*cis*-8,10-*trans*-eicosatetraenoic acid (LTB4), iso-LTB4 (5S, 12SR-all-*trans*-diHETE), ω-OH-LTB4, ω-COOH-LTB4 and 5S-hydroxy-6-*trans*-8,11,14-*cis*-eicosatetraenoic acid (5-HETE) were identified as previously described (12).

2.3 ATP assessment

ATP detection component from Mitochondrial ToxGlo™ Assay kit was used. In accordance with the manufacturer's protocol, the lyophilized enzyme/substrate mixture (ATP Detection Substrate) was reconstituted by lysis buffer (ATP Detection Buffer) to obtain ATP Detection Reagent. Just before the experiment PMNLs were resuspend in HBSS/HEPES, seeded in solid white F-bottom 96-well plates (4×10^5 cells/well), pre-incubated for 10 min at 37°C, 5% CO_2. 2-DG was added at this stage if prescribed by the protocol. Then *S. typhimurium* (bacteria per cell ratio ~25:1) and reagents were added, according to experimental protocol. Samples were incubated for 20 min under

the same conditions. After the treatment was complete, plates were equilibrated to room temperature for 5 min followed by adding an equal volume of ATP Detection Reagent to the contents of each well. After 3 min orbital shaking luminescence intensity was measured on a CLARIOstar microplate reader (BMG Labtech, Ortenberg, Germany) and MARS data analysis software package from BMG Labtech was used to process the data obtained.

2.4 Cytosolic ROS assessment

ROS accumulation in the cytosol was quantified by measuring the green fluorescence intensity of 2',7'-dichlorofluorescein (DCF). According to manufacturer's recommendation, neutrophils were loaded with 5 μM carboxy-2',7'-dichlorodihydrofluorescein diacetate (H_2DCF-DA) for 60 min at room temperature followed by washing with PBS, suspended in D-PBS and then stored at room temperature in the dark until use. Immediately before the experimental treatment cells were resuspended in HBSS/HEPES, seeded in fibrinogen-coated wells of the 96-well plate (4×10^5 cells/well) and pre-incubated for 10 min at 37°C, 5% CO_2. Then *S. typhimurium* (bacteria per cell ratio ~25:1) and indicated reagents were added for 30 min followed by 0,1 μM fMLP stimulation. Fluorescence intensity at excitation and emission wavelengths of 488 and 525 nm was measured using a CLARIOstar microplate reader.

2.5 Thiol redox state assessment

Ellman's assay was used for quantitating reduced sulfhydryl groups. Neutrophils were resuspended in HBSS/HEPES (2×10^6 cells/1 mL probe) and pre-incubated for 10 min at 37°C, 5% CO_2. After the treating according to experimental protocol cells were centrifuged for 7 min at 600 g, 4°C. Permeabilizing buffer (67 mM Na_2HPO_4, 35 mM citric acid and 0.1% Triton X-100; 100 μL/probe) was added to packed cell pellets, shaken and kept on ice for 10 min. Lysates were centrifuged at 10000 g, 4°C for 10 min. 50 μL supernatant (in duplicate for each probe) was mixed with 100 μL DTNB solution (0.1 mg/mL in 0.1 M NaH_2PO_4/Na_2HPO_4, 1M EDTA, pH 7.8) in 96-well plate. Equal volumes of reduced glutathione solutions from 1 to 500 μM were used to generate standard curve. The samples were allowed to stand for 15 min at room temperature followed by absorbance reading at 412 nm on CLARIOstar microplate reader.

2.6 Adhesion assessment

Spectrophotometric detection of 2,3-diaminophenazine, which is a product of myeloperoxidase-catalyzed oxidation of *o*-phenylenediamine dihydrochloride (OPD) by hydrogen peroxide, was used to assess neutrophil substrate adhesion (39). PMNLs (2×10^5 cells/sample) were seeded onto fibrinogen-coated 96-well plates containing pre-warmed HBSS/HEPES and agents required by experimental protocol. Samples were incubated at 37°C, 5% CO_2 after which the plate was washed twice to remove unattached cells. 4 mM H_2O_2 and 5.5 mM OPD in permeabilizing buffer (67 mM Na_2HPO_4, 35 mM citric acid and 0.1% Triton X-100) were added for 5 min. The reaction was stopped with 1 M H_2SO_4. The percentage of attached neutrophils was determined by measuring the absorption (490 nm) of 2,3-diaminophenazine and comparing the obtained values with the calibration ones.

2.7 Scanning electron microscopy

For scanning electron microscopy, cells were fixed for 30 min in 2.5% glutaraldehyde, postfixed for 15 min with 1% osmium tetroxide in 0.1 M cacodylate (pH 7.3), dehydrated in an acetone series, and processed by conventional scanning electron microscopic techniques, as described (40).

2.8 Cell adhesion molecules expression assessment

CD11b, alpha subunit of the Mac-1 integrin, and intercellular adhesion molecule-1 (CD54) proteins expression were determined by flow cytometry. Neutrophils were resuspended in HBSS/HEPES (10^6 cells/1 mL probe) and pre-incubated for 5 min at 37°C, 5% CO_2. After the treating according to experimental protocol cells were centrifuged while cooled for 10 min at 200 g, 4°C. Then biotinylated mouse CD11b (20 μg/mL HBSS/HEPES) or CD54 (30 μg/mL HBSS/HEPES) antibodies were added for 45 min, on ice. After being washed with cold PBS cells were stained with avidin-FITC (30 μg/mL HBSS/HEPES) for 30 min on ice followed by flow cytometry on Amnis FlowSight Imaging Flow Cytometer (Luminex Corp., Austin, Texas, USA) at 488/525 ex/em filter set. IDEAS Image Data Exploration and Analysis Software (Luminex Corp., ustin, Texas, USA) was used for data analyzing.

2.9 Statistics

Results are presented as mean ± SEM. Analysis of statistical significance for multiple comparisons was performed using GraphPad Prism 10.0.1 software. Differences with P-values <0.05 were considered statistically significant.

3 Results

3.1 Mitochondrial ROS production is critical for fMLP-induced leukotriene synthesis induced in neutrophils stimulated with *Salmonella typhimurium*

We have previously found that preincubation of human neutrophils with *S. typhimurium* strongly stimulates fMLP-induced LTB4 synthesis (12). These conditions modeled the collective behavior of neutrophils known as swarming (4). We

have shown that *S. typhimurium* stimulates 5LOX, but the mechanism of the enhancing effect of bacteria upon subsequent addition of fMLP remains unclear. We have recently shown that LTB4 synthesis induced by fMLP (as well as some other stimuli) is dependent on mtROS production (22). However, the effect of fMLP in this study was artificially stimulated by cytochalasin, which disrupts the actin cytoskeleton. In the present study, we analyzed the possible role of mtROS in the stimulation of fMLP-induced LTB4 synthesis in neutrophil interaction with bacteria *S. typhimurium*. Separate addition of fMLP (Control w/o Salm) or bacteria *S. typhimurium* (Control w/o fMLP) to neutrophils produced very slight effect on leukotriene synthesis (Supplementary Figure 1).

As shown in Figure 1A, mitochondria-targeted antioxidants SkQ1 and MitoQ inhibit fMLP-induced LTB4 synthesis in neutrophils exposed to *S. typhimurium* at 50 nM and 200 nM, respectively. The synthesis of the omega-hydroxylation product of LTB4 (ω-LTB4) and total leukotrienes (ΣLT=LTB4+isomers of LTB4+ω-OH-LTB4) were also inhibited by SkQ1 and MitoQ. These leukotrienes are the main 5-LOX products in our experimental model (Supplementary Figure 1).

We have previously shown that mtROS production in neutrophils can be stimulated by the accumulation of Ca^{2+} in mitochondria (21). Ca^{2+} uptake into the mitochondrial matrix is driven by the transmembrane electrical potential at the inner membrane ($\Delta\Psi$), which is maintained by the activity of the respiratory chain. In the present model, the respiration inhibitor antimycin A, as well as the oxidative phosphorylation uncoupler FCCP, which dissipates $\Delta\Psi$, effectively inhibited leukotriene synthesis (Figure 1A). Inhibition of respiration and dissipation of $\Delta\Psi$ lead to the cessation of mitochondrial ATP synthesis. Since mitochondria-targeted cationic antioxidants such as SkQ1 and MitoQ have also been shown to dissipate $\Delta\Psi$ (41), we analyzed the possible role of ATP depletion in the inhibition of leukotriene synthesis. Measurements of ATP content in infected neutrophils revealed no effect of antimycin A or FCCP (Figure 1B). These data are consistent with the leading role of glycolysis in ATP production known for neutrophils and other granulocytes (42, 43). In support of this conclusion, inhibition of glycolysis by 2-deoxy-D-glucose (2-DG) led to a decrease in ATP content (Figure 1B) and inhibition of leukotriene synthesis (Figure 1C).

Stimulation of neutrophils by bacteria and fMLP is accompanied by activation of NADPH oxidase (NOX2) and subsequent massive production of ROS (1, 44). To study the possible role of NOX2 in leukotriene synthesis in our model, we used diphenyleneiodonium (DPI), an effective inhibitor of various

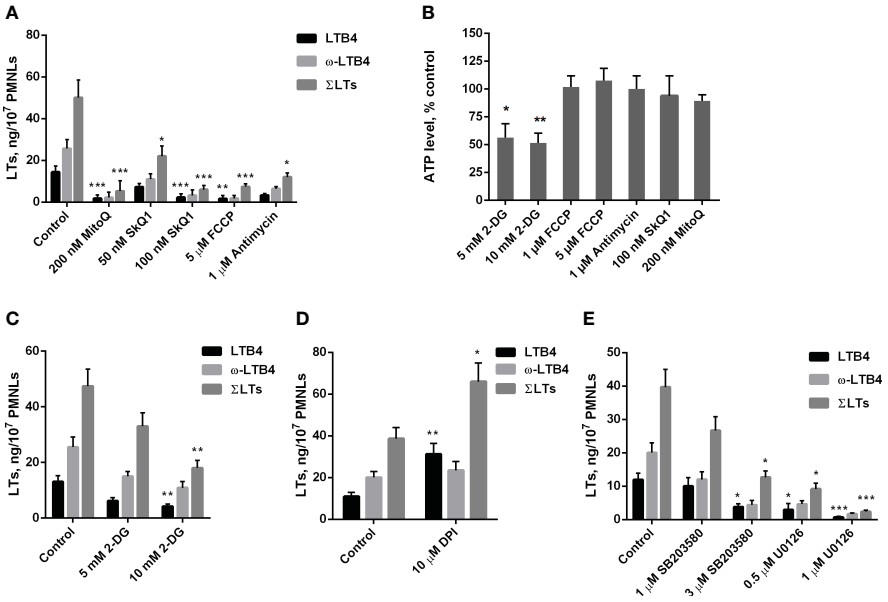

FIGURE 1
(A–C). Effect of mitochondria-targeted compounds and 2-DG treatment on leukotriene synthesis and ATP generation in neutrophils. **(A, C)** After 10 min pre-incubation without **(A)** or in the presence of indicated concentrations of 2-DG **(C)** PMNLs were exposed for 30 min to either bacteria alone (Control) or bacteria in combination with reagents indicated on X-axis. Then fMLP was added (0.1 μM sample concentration) for 10 min. After the reaction was terminated, the 5-LOX products were analyzed. Presented are absolute values of LTB4, ω-OH-LTB4 and the sum of LTs (ΣLTs) in ng per 10^7 PMNLs. **(B)** PMNLs were pre-incubated for 10 min without additives or in the presence of 2-DG (where indicated). Bacteria were then added, either alone (Control, 2-DG probes) or in combination with the indicated stimuli. After 20 min, cells were lysed, and ATP content was determined using the bioluminescent method. Presented are relative values of ATP content in samples as average percentages of control luminescence intensity values (mean ± SEM of luminescence intensity in control samples was 105326 ± 4596 RLU, while 10 μM ATP, used as a positive control, provided 397233± 2187 RLU). **(D, E)**. Effect of NADPH oxidase inhibitors and inhibitors of MAP kinases on leukotriene synthesis in neutrophils. After 10 min pre-incubation, PMNLs were exposed for 30 min to either bacteria alone (Control) or bacteria in combination with reagents indicated on X-axis, followed by 10 min of 0.1 μM fMLP stimulation. When incubations stopped, the 5-LOX products were analyzed. **(A–E)**. Values shown are means ± SEM of three independent experiments performed in duplicate. *p < 0.05, **p < 0.01, ***p < 0.001, for pairs of data compared to corresponding control values as shown by two-way ANOVA with Tukey's multiple comparison test **(A, C–E)** or by one-way ANOVA with Dunnett's multiple comparison test **(B)**.

flavin enzymes, including NADPH oxidase. DPI stimulated the accumulation of LTB4 and total leukotrienes (Figure 1D). This effect was observed previously when leukotriene synthesis was induced by various stimuli and was attributed to inhibition of LTB4 omega-hydroxylation (22). In fact, the ratio of LTB4 to ω-LTB4 with DPI is higher, than in other treatments (Figures 1, 2). But the sum of LTs is also increased, therefore inhibition of NOX2 contribute to stimulation of leukotriene synthesis. It was demonstrated that chronic granulomatous disease (CGD) neutrophils have an increased LTB4 production (45). But the authors determined only LTB4, so this effect may include as 5-LOX stimulation by downregulation of ROS in CGD neutrophils, as well as inhibition of LTB4 omega-hydroxylation in experiments with DPI.

From these data we can see that mitochondria targeted antioxidant SkQ1 inhibits LT synthesis. We checked the effects of SkQ1 on mtROS production in neutrophils. Measurements of mitochondrial ROS production using the mitochondria-targeted superoxide-sensitive probe MitoSOX (Supplementary Figure 2) showed a significant increase in mtROS upon subsequent stimulation of neutrophils with *S. typhimurium* and fMLP. This increase in mtROS was inhibited by SkQ1. These data support our conclusion that mtROS production is required for stimulation of fMLP-induced LTB4 synthesis in neutrophil interaction with bacteria *S. typhimurium*.

In the search for possible targets of mtROS-dependent regulation of leukotriene synthesis, we previously showed that activation of the MAP kinases Erk1/2 and p38 (associated with their phosphorylation) is prevented by SkQ1 (22). Erk1/2 and p38 kinases are known to phosphorylate 5-LOX and stimulate its translocation to the nuclear envelope, which is required for 5-lipoxygenase activity (46), so they may be critical targets of mtROS. In our experimental model, the Erk1/2 inhibitor U0126 and p38 inhibitor SB203580 suppressed 5-LOX activity (Figure 1E). Thus, it can be assumed that these kinases are important in the mtROS-dependent regulation of leukotriene synthesis induced by the combined action of bacteria and fMLP.

3.2 Redox processes modulate fMLP-induced leukotriene synthesis in neutrophils exposed to bacteria *Salmonella typhimurium*

To further study the role of the redox balance in the activation of leukotriene synthesis under the combined action of *S. typhimurium* and fMLP, we used the classical antioxidant Trolox, a water-soluble analogue of vitamin E. It was shown that it inhibits leukotriene synthesis, although at a much higher concentration than SkQ1 and MitoQ (Figure 2A).

Unexpectedly, another known antioxidant N-acetylcysteine (NAC) strongly stimulated fMLP-induced leukotriene synthesis in *S. typhimurium*-activated neutrophils (Figure 2A). A similar effect was observed in the case of sodium hydrosulfide (NaSH) (Figure 2A), an H_2S donor that promotes a reductive shift in the redox balance of various cells (47). We hypothesized that this stimulation may be associated with a shift in the redox equilibrium of the reversible thiol-disulfide system and, first of all, with an increase in the ratio of reduced/oxidized glutathione (GSH/GSSG). In fact, NAC is a direct precursor of GSH, and H_2S donors can also increase the GSH/GSSG ratio. To analyze this possibility, we used diamide, which penetrates cell membranes and reacts with thiols to form disulfides (48). Diamide at a concentration of 50-200 μM significantly reduced the level of non-protein thiols (Figure 2B) but did not affect the level of cytosolic ROS measured as the oxidation of 2',7'-dichlorofluorescein (Figure 2C). 50-150 μM diamide slightly increased fMLP-induced leukotriene synthesis in neutrophils pre-incubated with *S. typhimurium*, while 200-250 μM diamide, without affecting cell viability (Supplementary Figure 3), significantly inhibited leukotriene synthesis (Figure 2D). These data indicate that a decrease in reduced GSH may limit leukotriene synthesis under our conditions. In support of this assumption, we observed a strong stimulation of leukotriene synthesis by the GSH precursor S-adenosyl-L-methionine (SAMe) (Figure 2D). This effect was especially strong in the presence of an inhibitory concentration of diamide (200-250 μM) and reaches approximately 400%. Interestingly, SAMe also reversed inhibitory effect of FCCP or antimycin A on leukotriene synthesis (Figure 2E). Although in our experimental model we were unable to detect a significant effect of antimycin A and FCCP on GSH/GSSH ratio either at the stage of PMNLs interaction with bacteria or after stimulation with fMLP (Supplementary Figure 4), studies on cell lines indicate that they both can reduce GSH intracellular level (49–51), which can be compensated by SAMe. Measurements of mtROS in stimulated neutrophils (Supplementary Figure 2) showed some increase by diamide, which may be partially responsible for the stimulation of LT synthesis observed at low doses of diamide.

As shown in Figure 2B, under conditions of interaction between neutrophils and bacteria, 50 to 200 μM diamide reduced intracellular -SH amount. The decrease in reduced thiol content caused at 50 and 100 μM diamide was prevented by DPI. Under the same conditions DPI decreased the level of cytosolic ROS, presumably due to inhibition of NOX2, and diamide did not modulate this effect (Figure 2C). These data suggest that the decrease in GSH/GSSG ratio by low doses of diamide may be compensated by the decrease in oxidative stress and increase in NADPH levels caused by inhibition of NADPH oxidase. This effect may explain the DPI stimulation of leukotriene synthesis (Figure 1D), which is especially pronounced in the presence of diamide (Figure 2D), with maximal stimulation at 100 μM diamide (Figure 2F). DPI did not reverse the decrease in reduced thiols at 200 μM diamide but abolished inhibiting effect of diamide on LT synthesis at 200 μM (Figure 2D). We can only propose that effect of DPI is more complex than we determined and need further elucidation.

Biosynthesis of GSH is dependent on ATP, so inhibition of leukotriene synthesis due to 2-DG-dependent ATP depletion (Figure 1B) may be mediated by a decrease in GSH content. 2-DG also inhibits the synthesis of leukotrienes stimulated by DPI alone (Figure 2G). Interestingly, the synthesis of leukotrienes stimulated by DPI in the presence of diamide is practically insensitive to 2-DG (Figure 2G). This may be explained by the

10.3389/fimmu.2024.1295150

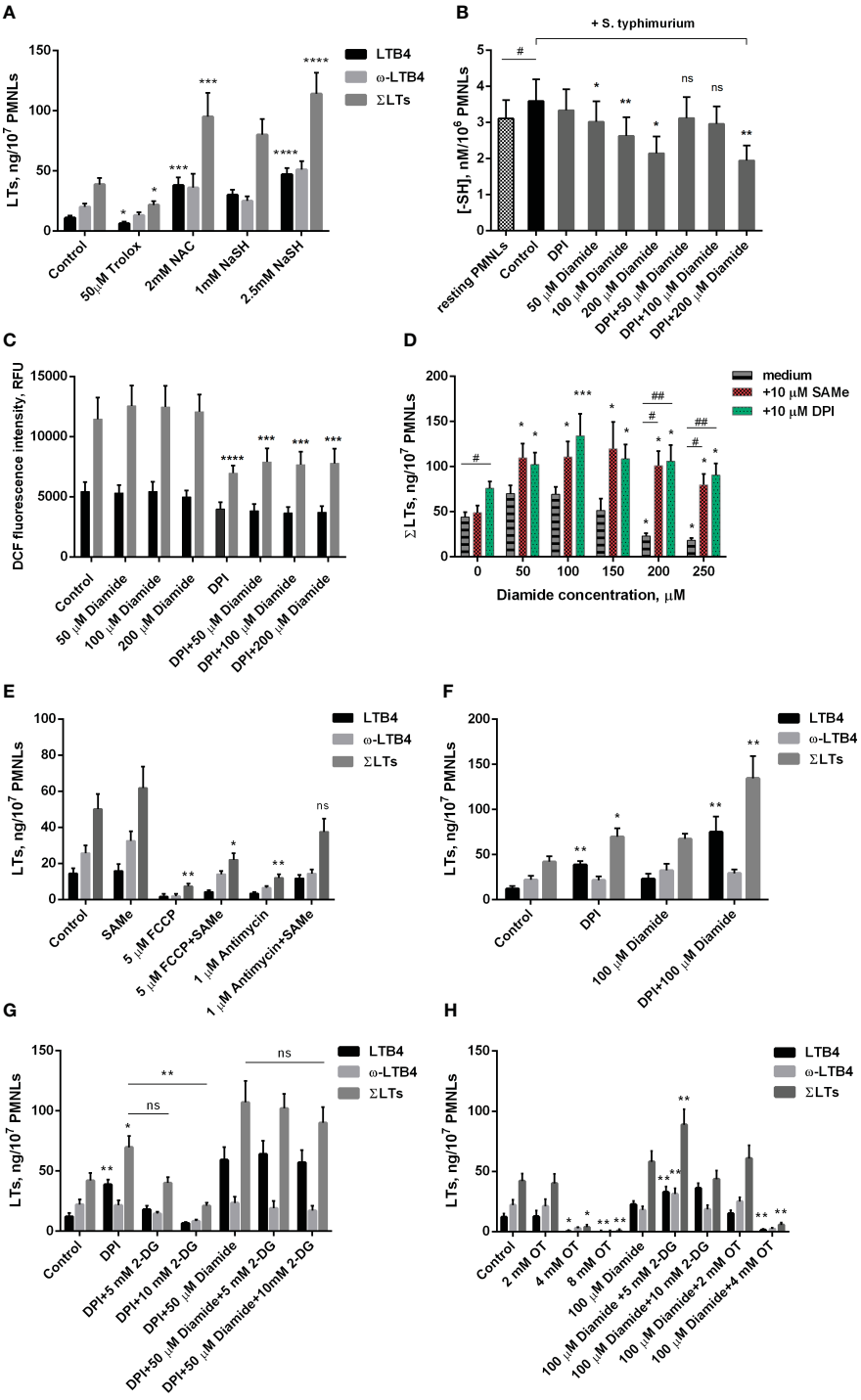

FIGURE 2
Effect of oxidants and antioxidants on intracellular reduced thiols level, ROS formation and leukotriene synthesis in human neutrophils. **(A, D-H)**. After 10 min pre-incubation without additives or in the presence of indicated concentrations of 2-DG, PMNLs were exposed for 30 min to either bacteria alone (Control) or bacteria in combination with reagents indicated (10 μM DPI and 10 μM SAMe were used), followed by 10 min of 0.1 μM fMLP stimulation. After the reaction was terminated, the 5-LOX products were analyzed. Presented are absolute values of LTB4, ω-OH-LTB4 and the sum of LTs (ΣLTs) in ng per 10^7 PMNLs. **(B)** PMNLs were pre-incubated for 10 min, then *S. typhimurium* alone (Control) or bacteria together with indicated stimuli were added for 20 min; resting PMNLs samples were incubated without any additives. After the exposure time, the cells were pelleted while cooling and assayed for reduced -SH content with Ellman's reagent. Values are given as the averages of the content of reduced thiols in the samples, nM per 10^6 PMNLs. **(C)** PMNLs loaded with H_2DCFDA were pre-incubated for 10 min, then either *S. typhimurium* alone (Control) or bacteria together with indicated stimuli were added. After 30 min 0,1 μM fMLP was added. Presented are the average values of DCF fluorescence intensity measured immediately before (black bars) and 20 minutes after (grey bars) fMLP addition. **(A–H)**. Values shown are means ± SEM of three independent experiments performed in duplicate. ns, not significant; *$p < 0.05$, **$p < 0.01$, ***$p < 0.001$, ****$p < 0.0001$ for pairs of data compared to corresponding control values; $^{\#}p < 0.05$, $^{\#\#}p < 0.01$ for the specified data pairs as shown by one-way ANOVA with Dunnett's multiple comparison test **(B)** or two-way ANOVA followed by Tukey's multiple comparison test **(A, C–H)**.

known ability of diamide to reduce glucose metabolism through glycolysis in favor of the pentose phosphate pathway (PPP) (52). This pathway is the main source of NADPH (42), which supports the reduction of glutathione. This effect probably underlies the stimulation of leukotriene synthesis observed at low doses of diamide (Figure 2D).

Full pentose cycle, including non-oxidative PPP with enzyme transketolase (TKT), provides maximal NADPH yield (6 NADPH from one molecule of glucose) (53). In our assay TKT inhibitor oxythiamine (OT) suppressed LT synthesis (Figure 2H). The effect was observed with and without diamide in incubations. It is known that blockage of glycolysis can help cells divert more flux into oxPPP under oxidative stress (54, 55). With diamide, LT synthesis was increased in the presence of intermediate concentrations of 2-DG (Figure 2H), and not in control incubations (Figure 1C). We did not observe it in the presence of DPI (Figure 2G).

Under the influence of fMLP, neutrophil adhesion is significantly enhanced (Figure 3A). In addition, this chemotactic peptide induces noticeable morphological changes in both resting and interacting with bacteria neutrophils. In addition to pronounced cellular polarization, special mention should be made to the formation of numerous thread-like cell outgrowths (Figure 3B, control/fMLP, S.typhimurium+fMLP, red arrows). It is known that such outgrowths are a kind of "transport highways" that allow intercellular exchange over long distances (56), and also perform a structural function, promoting cell clustering (57). Mitochondria-targeted antioxidant SkQ1 significantly reduced the substrate adhesion of neutrophils (Figure 3A). Preincubation with

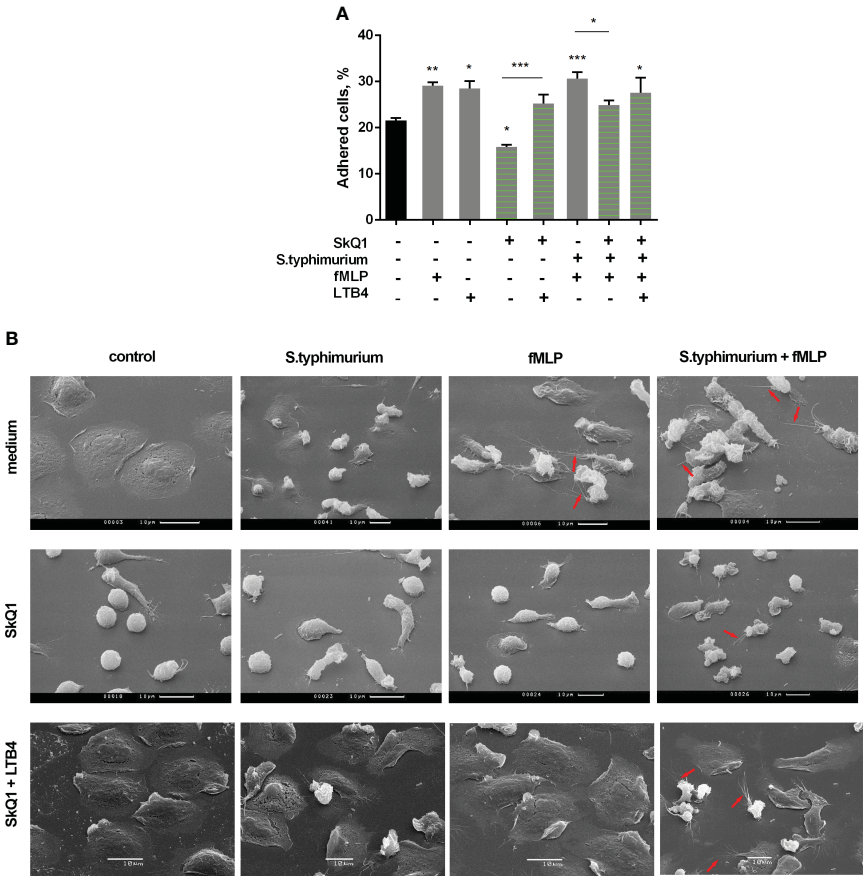

FIGURE 3
(A) SkQ1 influence on the pro-adhesive effects of fMLP and LTB4. PMNLs (2×10^5 cells/sample) were seeded onto fibrinogen-coated 96-well plates containing pre-warmed HBSS/HEPES without additives, with *S. typhimurium* (bacteria per cell ratio ~20:1) or *S. typhimurium* supplemented with 0.1 μM SkQ1. After 30 min incubation at 37°C, 5% CO_2, 0.1 μM fMLP or/and 0.1 μM LTB4 were added for next 10min. Values shown means ± SEM of the percentage of cells attached to the substrate obtained from three independent experiments performed in triplicates; *p < 0.05, **p < 0.01, ***p < 0.001 for indicated pairs of data or compared to resting PMNLs sample (black bar) as shown by ordinary one-way ANOVA with Sidak's multiple comparison test. **(B)** Effect of SkQ1 and LTB4 on neutrophil morphology upon (co-)stimulation with bacteria *S. typhimurium* and fMLP. PMNLs (10^6/ml HBSS/HEPES) were preincubated on coverslips in culture dishes for 10 min and then cultured for 20 min without additives (line *medium*) or in the presence of 100 nM SkQ1 (lines *SkQ1*, *SkQ1+LTB4*) without additional stimulation (control) or with the addition of bacteria (bacteria per cell ratio ~25:1) (S. typhimurium). LTB4 (100 nM sample concentration) was added to (control) and (S. typhimurium) samples for next 5 minutes (line *SkQ1+LTB4*). Columns fMLP and S. typhimurium+fMLP represent PNMLs incubated for 20 min without additives (line *medium*) or with 100 nM SkQ1 (lines *SkQ1*, *SkQ1+LTB4*) without bacteria (fMLP) or with the addition of bacteria (S. typhimurium+fMLP), followed by fMLP (0.1 μM sample concentration) (lines *medium*, *SkQ1*) or fMLP together with LTB4 (100 nM sample concentration of each) (line *SkQ1+LTB4*) treatment for 5 minutes. At the end of each stage, PMNLs samples were fixed and subsequently visualized using scanning electron microscopy. Thread-like cell outgrowths are marked by red arrows.

SkQ1 not only reduce the pro-adhesive effect of fMLP but also prevents fMLP-induced morphological changes, in particular, it diminishes the formation of cell outgrowths (Figure 3B), in parallel with suppression of leukotriene synthesis (Figure 1A). The addition of LTB4 to samples pretreated with SkQ1 increased the adhesiveness of neutrophils, promoting cell spreading (Figure 3, SkQ1+LTB4). In addition, supplementation of fMLP influence on cells preincubated with SkQ1 and bacteria with exogenous leukotriene B4 restored the ability of neutrophils to form thread-like filaments (Figure 3, SkQ1+LTB4/S.typhimurium+fMLP, red arrows). These data support our earlier suggestion that the emergence of cell-cell contacts is dependent on LTB4 (12). 50 μM diamide also increased adhesiveness of neutrophils (Supplementary Figure 5A). At high diamide concentration, when leukotriene synthesis was inhibited, the cells change morphology to more spherical shape, and the adhesiveness of neutrophils decreased (Supplementary Figure 5).

Activation of neutrophil adhesive properties can be reflected by adhesive receptor expression, first of all CD11b, a component of Mac-1 (CD11b/CD18) β2 integrin (58). In experiments with binding of fluorescently labelled antibodies to CD11b it was shown that both fMLP and LTB4 increased CD11b density on the surface of the cells, and diamide potentiated effect of fMLP. SkQ1 did not influence fMLP-induced expression, but decreased LTB4-induced effects (Figures 4A, B). The surface CD54 (ICAM-1) expression on neutrophils correlates with neutrophil migration, i.e. with cell-cell communication (59); and anti-CD54 monoclonal antibody inhibited neutrophil aggregation and formation of intercellular contacts (60). CD54 increased significantly on migrated PMNs; with rather low CD54 expression on adherent neutrophils (61). In our experimental model CD54 plays role as counter-receptor for integrins during homotypic adhesion; and SkQ1 decreased CD54 surface expression on neutrophils, as in the presence of the "first" chemoattractant fMLP, as well as at adding of the "second" chemoattractant LTB4 (Figures 4C, D). These data indicate that SkQ1 affects not only LTB4 synthesis but also LTB4-dependent signaling. The increased adhesiveness of neutrophils induced by LTB4 provided the possibility of forming tight intercellular contacts, which can support swarming and clustering around pathogens.

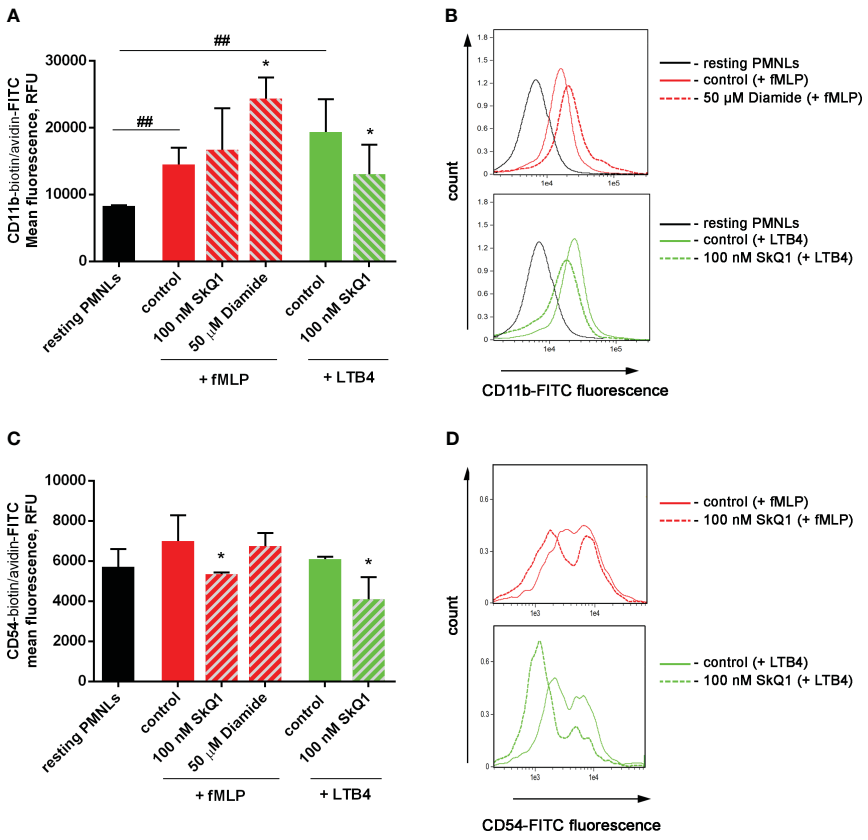

FIGURE 4
Effect of SkQ1 and diamide on adhesion molecules externalization upon (co-) stimulation with bacteria *S. typhimurium* and fMLP or LTB4. PMNLs (10^6/mL HBSS/HEPES) were incubated for 20 min without additives (resting PMNLs), in the presence of bacteria (control) or bacteria in combination with 100 nM SkQ1 or 50 μM diamide (bacteria per cell ratio ~25:1). Then 0.1 μM fMLP (+ fMLP) or 0.1 μM LTB4 (+ LTB4) were added for 10 min followed by staining of surface CD11b and CD54 proteins and flow cytometry. Presented are the average values of three independent experiments (means ± SEM) **(A, C)** and typical histograms **(B, D)** of fluorescence for PMNLs stained with avidin-FITC in addition to biotynilated CD11b **(A, B)** and CD54 **(C, D)** antibodies. *$p < 0.05$ for pairs of data compared to corresponding control values; $^{\#\#}p < 0.01$ for the specified data pairs as shown by one-way ANOVA with Dunnett's multiple comparison test.

4 Discussion

Redox regulation plays an important role in the activation of 5-LOX and the regulation of leukotriene synthesis in neutrophils. Specifically, enzymatic activity requires the oxidation of Fe^{2+} to Fe^{3+} at the 5-LOX active site. Lipid hydroperoxides are involved in the activation of 5-LOX, at least in part through the oxidation of Fe^{2+} (62, 63). 5-LOX catalyzes the biosynthesis of leukotrienes using arachidonic acid (AA) as a substrate. Phospholipase A2, which produces AA from phospholipids, can be activated by ROS and lipid hydroperoxides (64), promoting the activation of leukotriene synthesis through oxidative processes. At the same time, excess hydrogen peroxide has been shown to inhibit 5-LOX activity in alveolar macrophages in parallel with ATP depletion (65).

Our previous work (22) using the mitochondria-targeted antioxidant SkQ1 demonstrated the important role of mitochondrial ROS in leukotriene synthesis induced by the Ca^{2+} ionophore A23187, the chemoattractant fMLP, and the opsonized yeast cell wall components zymosan. Here, we showed (Figure 1) that mitochondria-targeted antioxidants suppress fMLP-induced leukotriene synthesis in neutrophils exposed to *S. typhimurium*. We also showed that leukotriene synthesis is inhibited by the respiration inhibitor antimycin A and the oxidative phosphorylation uncoupler FCCP, presumably due to inhibition of mtROS production stimulated by voltage-dependent Ca^{2+} accumulation in mitochondria. Inhibition of respiration or dissipation of membrane potential prevents the synthesis of mitochondrial ATP, but measurements of ATP content did not reveal the effect of antimycin A or FCCP in infected neutrophils (Figure 1B).

Inhibition of glucose metabolism by 2-deoxy-D-glucose (2-DG) led to a decrease in ATP content and, in parallel to inhibition of leukotriene synthesis (Figure 1C) consistently with earlier data on the requirement of energy metabolism for the synthesis of leukotrienes (66). Glucose is catabolized by two fundamental pathways: glycolysis to produce ATP and the oxidative pentose phosphate pathway (PPP) to produce reduced nicotinamide adenine dinucleotide phosphate (NADPH). Very recently, it was shown that activation of the oxidative burst in neutrophils depends on a switch from glycolysis to a unique form of PPP called the "pentose cycle" (53). In this mode, all glucose-6-phosphate is consumed through PPP, while the initial steps of glycolysis are reversed to support pentose phosphates recycling. It has been proposed that this switch is required to maximize the supply of NADPH to fuel NADPH oxidase.

Another important NADPH-dependent enzyme is glutathione reductase, which reduce oxidized glutathione disulfide to sulfhydryl glutathione (67, 68). The main function of glutathione is the detoxification of electrophilic xenobiotics through condensation reactions catalyzed by glutathione S-transferases. Another protective function is mediated by the reduction of hydroperoxides catalyzed by glutathione peroxidase. This process appears to underlie the inhibition of 5-LOX by GSH observed in neutrophil homogenate (69). However, protein S-glutathionylation, activated by oxidative stress, may represent a more important regulatory mechanism.

The 5-lipoxygenase requires activation by fatty acid hydroperoxides (62). Hydroperoxides are inactivated in cells by GSH-dependent reduction by glutathione peroxidase, but diamide has the ability to non-enzymatically oxidize intracellular thiols (48). On this way diamide creates a demand for glutathione reduction by NADPH (70), and DPI provides high NADPH/NADP+ ratio (53) increasing stimulating effect of diamide (Figures 2D, F). The pentose phosphate pathway (PPP) is the major mechanism to maintain high NADPH/NADP+ ratio (71), and it was recently shown that PPP controls ROS production in crowding neutrophils (72). In accordance of the ability of diamide to switch glycolysis-dominant metabolism to pentose phosphate pathway (53), effects of diamide were less sensitive to glucose deprivation (Figures 2G, H). Effects of DPI were inhibited by glucose deprivation (Figure 2G).

Protein S-glutathionylation likely limits leukotriene synthesis in fMLP-activated neutrophils in the presence of *S. typhimurium*. This may be the reason that the GSH precursor NAC and the H_2S donor sodium hydrosulfide, which increase the GSH/GSSG ratio, stimulate the synthesis of leukotrienes, in contrast to some other antioxidants (Figure 2A). In support of this proposal, we observed that thiol-oxidizing diamide (48), which oxidizes GSH, as detected by depletion of non-protein thiols (Figure 2B), at high concentrations (200-250 μM) significantly inhibits leukotriene synthesis (Figure 2D). This inhibition was effectively reversed by the GSH precursor SAMe (Figure 2D). Inhibition of leukotriene synthesis by FCCP or antimycin A may also be due in part to the GSH depletion caused by these agents (49–51). Accordingly, inhibition by FCCP and antimycin A was partially prevented by SAMe (Figure 2E). Importantly, diamide-induced thiol depletion was prevented by DPI (Figure 2B), indicating that inhibition of NADPH oxidase and subsequent decrease of oxidative stress and increase in NADPH levels may compensate for diamide-dependent GSH oxidation. Accordingly, DPI stimulated the synthesis of leukotrienes in the presence of diamide (Figure 2D). Inhibition of leukotriene synthesis by 2-DG-dependent ATP depletion may also be mediated by a decrease in GSH content. This may explain why the synthesis of leukotrienes in the presence of non-inhibitory doses of diamide, which is known to stimulate PPP-dependent NADPH production (52), was not inhibited by 2-DG in the presence of DPI (Figure 2G).

Neutrophils are the first cells in the foci of infection, and they have developed a set of mechanisms to turn on defense very quickly. To potentiate ROS production, they activate NADPH-oxidase, and NADPH is necessary for reduction of oxygen (73). To support NADPH-dependent ROS formation, neutrophils turn on PPP shunt (74). Activation of PPP is extremely important in supplying of NADPH (75). Inhibition of NADPH-oxidase shifted neutrophils from PPP cycle with ultra-high NADPH yield to glycolysis-dominant glucose metabolism (74). At the same time, neutrophil responses to pathogens include activation of glycolysis (76, 77).

Upregulation of PPP during oxidative stress contributes significantly to neutrophil responses, including not only oxidative burst (74) but also NETs formation (78). Redox regulation may involve various signaling pathways, including the MAP kinase-dependent pathway (79). We previously showed that activation of the MAP kinases Erk1/2 and p38, responsible for phosphorylation and activation of 5-LOX (46), is prevented by SkQ1 in neutrophils stimulated with A23187, fMLP, or opsonized zymosan (22). In neutrophils stimulated with *S. typhimurium* in combination with

fMLP, the Erk1/2 inhibitor U0126 and the p38 inhibitor SB203580 inhibited leukotriene synthesis (Figure 1E). It is important to note that the GSH/GSSG ratio may also be involved in the regulation of Erk1/2, as S-glutathionylation, activated by oxidative stress, has been shown to play a key role in regulating MAP kinase kinase (MEKK1), that is an upstream kinase in the cascade of Erk1/2 activation (80). Using MS analysis, the authors demonstrated that oxidative stress induces glutathionylation of Cys1238 in the ATP-binding domain of MEKK1. This modification is easily reversible once the cell's redox balance is restored. Thus, increasing the GSH/GSSG ratio with NAC or sodium hydrosulfide may improve Erk1/2 activation by preventing MEKK S-glutothionylation in neutrophils exposed to *S. typhimurium* and fMLP. Thus, redox regulation of Erk1/2 may be an important element in both mtROS-dependent and GSH-dependent regulation of leukotriene synthesis. Moreover, this regulation provides insight into why mitochondria-targeted antioxidants and NAC have opposing effects on leukotriene synthesis.

Our data (Figure 3) showed that *Salmonella typhimurium* in combination with fMLP stimulates the appearance of intercellular contacts in parallel with the synthesis of LTB4. The mitochondria-targeted antioxidant SkQ1 reduced this intercellular communication, as well as the synthesis of leukotrienes. Thus, during bacterial infection, redox processes in neutrophils play a decisive role in the synthesis of LTB4, ensuring neutrophil swarming - the influx of neutrophils to places of large microbial accumulations.

Excessive synthesis of leukotrienes and especially of LTB4 plays important role in pathogenesis of various inflammatory diseases (81–88). Mitochondria-targeted antioxidants, such as SkQ1, have been proposed as a promising therapy the same range of pathologies (89, 90). SkQ1 demonstrated strong anti-inflammatory activity in acute bacterial infection (91) and in the systemic inflammatory response syndrome (SIRS) model (92). The inhibition of leukotriene synthesis demonstrated above under conditions of pronounced activation of neutrophils can significantly contribute to the therapeutic effect of SkQ1. Importantly, our data indicate that administration of known thiol-based antioxidants such as NAC can dangerously stimulate leukotriene synthesis by neutrophils under the same conditions that mimic severe pathogenic infection.

Data availability statement

The original contributions presented in the study are included in the article/Supplementary Material. Further inquiries can be directed to the corresponding authors.

Ethics statement

The studies involving humans were approved by Experimental and the subject consent procedures were approved by the Bioethics Committee of the Lomonosov Moscow State University, Application # 6-h, version 3, Bioethics Commission meeting # 131-d held on 31.05.2021. The studies were conducted in accordance with the local legislation and institutional requirements. The participants provided their written informed consent to participate in this study.

Author contributions

EG: Writing – original draft, Data curation, Formal analysis, Investigation, Methodology. GV: Investigation, Methodology, Writing – original draft, Funding acquisition. SG: Investigation, Methodology, Writing – original draft, Data curation. NK: Writing – review & editing, Methodology. TG: Conceptualization, Writing – review & editing. YR: Writing – review & editing, Methodology, Resources. KL: Writing – review & editing, Methodology. BC: Writing – review & editing, Conceptualization, Writing – original draft. GS: Conceptualization, Writing – original draft, Writing – review & editing, Project administration, Supervision.

Funding

The author(s) declare financial support was received for the research, authorship, and/or publication of this article. This research was supported by the grant from the Russian Science Foundation, grant number 23-74-01056, https://rscf.ru/project/23-74-01056/.

Conflict of interest

The authors declare that the research was conducted in the absence of any commercial or financial relationships that could be construed as a potential conflict of interest.

The author(s) declared that they were an editorial board member of Frontiers, at the time of submission. This had no impact on the peer review process and the final decision.

Publisher's note

Supplementary material

The Supplementary Material for this article can be found online at: https://www.frontiersin.org/articles/10.3389/fimmu.2024.1295150/full#supplementary-material

References

1. Segal AW. How neutrophils kill microbes. *Annu Rev Immunol* (2005) 23:197–223. doi: 10.1146/annurev.immunol.23.021704.115653

2. Nauseef WM. How human neutrophils kill and degrade microbes: an integrated view. *Immunol Rev* (2007) 219:88–102. doi: 10.1111/j.1600-065X.2007.00550.x

3. Nagarkoti S, Sadaf S, Awasthi D, Chandra T, Jagavelu K, Kumar S, et al. L-Arginine and tetrahydrobiopterin supported nitric oxide production is crucial for the microbicidal activity of neutrophils. *Free Radic Res* (2019) 53(3):281–92. doi: 10.1080/10715762.2019.1566605

4. Lammermann T, Afonso PV, Angermann BR, Wang JM, Kastenmuller W, Parent CA, et al. Neutrophil swarms require LTB4 and integrins at sites of cell death in vivo. *Nature* (2013) 498(7454):371–5. doi: 10.1038/nature12175

5. Isles HM, Loynes CA, Alasmari S, Kon FC, Henry KM, Kadochnikova A, et al. Pioneer neutrophils release chromatin within in vivo swarms. *Elife* (2021) 10:e68755. doi: 10.7554/eLife.68755

6. Song Z, Bhattacharya S, Clemens RA, Dinauer MC. Molecular regulation of neutrophil swarming in health and disease: Lessons from the phagocyte oxidase. *iScience.* (2023) 26(10):108034. doi: 10.1016/j.isci.2023.108034

7. Mihlan M, Glaser KM, Epple MW, Lammermann T. Neutrophils: amoeboid migration and swarming dynamics in tissues. *Front Cell Dev Biol* (2022) 10:871789. doi: 10.3389/fcell.2022.871789

8. Glaser KM, Mihlan M, Lammermann T. Positive feedback amplification in swarming immune cell populations. *Curr Opin Cell Biol* (2021) 72:156–62. doi: 10.1016/j.ceb.2021.07.009

9. Hopke A, Lin T, Scherer AK, Shay AE, Timmer KD, Wilson-Mifsud B, et al. Transcellular biosynthesis of leukotriene B(4) orchestrates neutrophil swarming to fungi. *iScience.* (2022) 25(10):105226. doi: 10.1016/j.isci.2022.105226

10. Hopke A, Scherer A, Kreuzburg S, Abers MS, Zerbe CS, Dinauer MC, et al. Neutrophil swarming delays the growth of clusters of pathogenic fungi. *Nat Commun* (2020) 11(1):2031. doi: 10.1038/s41467-020-15834-4

11. Archambault AS, Poirier S, Lefebvre JS, Robichaud PP, Larose MC, Turcotte C, et al. 20-Hydroxy- and 20-carboxy-leukotriene (LT) B(4) downregulate LTB(4) -mediated responses of human neutrophils and eosinophils. *J Leukoc Biol* (2019) 105 (6):1131–42. doi: 10.1002/JLB.MA0718-306R

12. Golenkina EA, Galkina SI, Pletjushkina O, Chernyak B, Gaponova TV, Romanova YM, et al. Gram-Negative Bacteria Salmonella typhimurium Boost Leukotriene Synthesis Induced by Chemoattractant fMLP to Stimulate Neutrophil Swarming. *Front Pharmacol* (2021) 12:814113. doi: 10.3389/fphar.2021.814113

13. Borgeat P, Naccache PH. Biosynthesis and biological activity of leukotriene B4. *Clin Biochem* (1990) 23(5):459–68. doi: 10.1016/0009-9120(90)90272-V

14. Petropoulos M, Karamolegkou G, Rosmaraki E, Tsakas S. Hydrogen peroxide signals E. coli phagocytosis by human polymorphonuclear cells; up-stream and down-stream pathway. *Redox Biol* (2015) 6:100–5. doi: 10.1016/j.redox.2015.07.004

15. Sheshachalam A, Srivastava N, Mitchell T, Lacy P, Eitzen G. Granule protein processing and regulated secretion in neutrophils. *Front Immunol* (2014) 5:448. doi: 10.3389/fimmu.2014.00448

16. Vorobjeva NV, Chernyak BV. NETosis: molecular mechanisms, role in physiology and pathology. *Biochem (Mosc).* (2020) 85(10):1178–90. doi: 10.1134/S0006297920100065

17. Herring SE, Mao S, Bhalla M, Tchalla EYI, Kramer JM, Bou Ghanem EN. Mitochondrial ROS production by neutrophils is required for host antimicrobial function against Streptococcus pneumoniae and is controlled by A2B adenosine receptor signaling. *PloS Pathog* (2022) 18(11):e1010700. doi: 10.1371/journal.ppat.1010700

18. Dunham-Snary KJ, Surewaard BG, Mewburn JD, Bentley RE, Martin AY, Jones O, et al. Mitochondria in human neutrophils mediate killing of Staphylococcus aureus. *Redox Biol* (2022) 49:102225. doi: 10.1016/j.redox.2021.102225

19. Gomes MC, Brokatzky D, Bielecka MK, Wardle FC, Mostowy S. Shigella induces epigenetic reprogramming of zebrafish neutrophils. *Sci Adv* (2023) 9(36):eadf9706. doi: 10.1126/sciadv.adf9706

20. Vorobjeva N, Prikhodko A, Galkin I, Pletjushkina O, Zinovkin R, Sud'ina G, et al. Mitochondrial reactive oxygen species are involved in chemoattractant-induced oxidative burst and degranulation of human neutrophils in vitro. *Eur J Cell Biol* (2017) 96(3):254–65. doi: 10.1016/j.ejcb.2017.03.003

21. Vorobjeva N, Galkin I, Pletjushkina O, Golyshev S, Zinovkin R, Prikhodko A, et al. Mitochondrial permeability transition pore is involved in oxidative burst and NETosis of human neutrophils. *Biochim Biophys Acta Mol Basis Dis* (2020) 1866 (5):165664. doi: 10.1016/j.bbadis.2020.165664

22. Sud'ina GF, Golenkina EA, Prikhodko AS, Kondratenko ND, Gaponova TV, Chernyak BV. Mitochondria-targeted antioxidant SkQ1 inhibits leukotriene synthesis in human neutrophils. *Front Pharmacol* (2022) 13:1023517. doi: 10.3389/fphar.2022.1023517

23. Antonenko YN, Avetisyan AV, Bakeeva LE, Chernyak BV, Chertkov VA, Domnina LV, et al. Mitochondria-targeted plastoquinone derivatives as tools to interrupt execution of the aging program. 1. Cationic plastoquinone derivatives: synthesis and in *vitro* studies. *Biochem (Mosc).* (2008) 73(12):1273–87. doi: 10.1134/s0006297908120018

24. Allen LH, Criss AK. Cell intrinsic functions of neutrophils and their manipulation by pathogens. *Curr Opin Immunol* (2019) 60:124–9. doi: 10.1016/j.coi.2019.05.004

25. Urban CF, Lourido S, Zychlinsky A. How do microbes evade neutrophil killing? *Cell Microbiol* (2006) 8(11):1687–96. doi: 10.1111/j.1462-5822.2006.00792.x

26. Vareechon C, Zmina SE, Karmakar M, Pearlman E, Rietsch A. Pseudomonas aeruginosa effector exoS inhibits ROS production in human neutrophils. *Cell Host Microbe* (2017) 21(5):611–8.e5. doi: 10.1016/j.chom.2017.04.001

27. Youseff BH, Holbrook ED, Smolnycki KA, Rappleye CA. Extracellular superoxide dismutase protects Histoplasma yeast cells from host-derived oxidative stress. *PloS Pathog* (2012) 8(5):e1002713. doi: 10.1371/journal.ppat.1002713

28. Siemsen DW, Kirpotina LN, Jutila MA, Quinn MT. Inhibition of the human neutrophil NADPH oxidase by Coxiella burnetii. *Microbes Infect* (2009) 11(6-7):671–9. doi: 10.1016/j.micinf.2009.04.005

29. Saha P, Yeoh BS, Olvera RA, Xiao X, Singh V, Awasthi D, et al. Bacterial siderophores hijack neutrophil functions. *J Immunol* (2017) 198(11):4293–303. doi: 10.4049/jimmunol.1700261

30. Pulsifer AR, Vashishta A, Reeves SA, Wolfe JK, Palace SG, Proulx MK, et al. Redundant and cooperative roles for yersinia pestis yop effectors in the inhibition of human neutrophil exocytic responses revealed by gain-of-function approach. *Infect Immun* (2020) 88(3):e00909-19. doi: 10.1128/IAI.00909-19

31. Reed PW. Glutathione and the hexose monophosphate shunt in phagocytizing and hydrogen peroxide-treated rat leukocytes. *J Biol Chem* (1969) 244(9):2459–64. doi: 10.1016/S0021-9258(19)78244-1

32. Kim VY, Batty A, Li J, Kirk SG, Crowell SA, Jin Y, et al. Glutathione Reductase Promotes Fungal Clearance and Suppresses Inflammation during Systemic Candida albicans Infection in Mice. *J Immunol* (2019) 203(8):2239–51. doi: 10.4049/jimmunol.1701686

33. Brownlee M. Biochemistry and molecular cell biology of diabetic complications. *Nature.* (2001) 414(6865):813–20. doi: 10.1038/414813a

34. Afonso PV, Janka-Junttila M, Lee YJ, McCann CP, Oliver CM, Aamer KA, et al. LTB4 is a signal-relay molecule during neutrophil chemotaxis. *Dev Cell* (2012) 22 (5):1079–91. doi: 10.1016/j.devcel.2012.02.003

35. Patcha V, Wigren J, Winberg ME, Rasmusson B, Li J, Sarndahl E. Differential inside-out activation of beta2-integrins by leukotriene B4 and fMLP in human neutrophils. *Exp Cell Res* (2004) 300(2):308–19. doi: 10.1016/j.yexcr.2004.07.015

36. Ford-Hutchinson AW, Bray MA, Doig MV, Shipley ME, Smith MJ. Leukotriene B, a potent chemokinetic and aggregating substance released from polymorphonuclear leukocytes. *Nature.* (1980) 286(5770):264–5. doi: 10.1038/286264a0

37. Poplimont H, Georgantzoglou A, Boulch M, Walker HA, Coombs C, Papaleonidopoulou F, et al. Neutrophil swarming in damaged tissue is orchestrated by connexins and cooperative calcium alarm signals. *Curr Biol* (2020) 30(14):2761–76.e7. doi: 10.1016/j.cub.2020.05.030

38. Aleksandrov DA, Zagryagskaya AN, Pushkareva MA, Bachschmid M, Peters-Golden M, Werz O, et al. Cholesterol and its anionic derivatives inhibit 5-lipoxygenase activation in polymorphonuclear leukocytes and MonoMac6 cells. *FEBS J* (2006) 273 (3):548–57. doi: 10.1111/j.1742-4658.2005.05087.x

39. Ngo TT, Lenhoff HM. A sensitive and versatile chromogenic assay for peroxidase and peroxidase-coupled reactions. *Anal Biochem* (1980) 105(2):389–97. doi: 10.1016/0003-2697(80)90475-3

40. Galkina SI, Fedorova NV, Serebryakova MV, Arifulin EA, Stadnichuk VI, Gaponova TV, et al. Inhibition of the GTPase dynamin or actin depolymerisation initiates outward plasma membrane tubulation/vesiculation (cytoneme formation) in neutrophils. *Biol Cell* (2015) 107(5):144–58. doi: 10.1111/boc.201400063

41. Severin FF, Severina II, Antonenko YN, Rokitskaya TI, Cherepanov DA, Mokhova EN, et al. Penetrating cation/fatty acid anion pair as a mitochondria-targeted protonophore. *Proc Natl Acad Sci U S A.* (2010) 107(2):663–8. doi: 10.1073/pnas.0910216107

42. Curi R, Levada-Pires AC, Silva EBD, Poma SO, Zambonatto RF, Domenech P, et al. The critical role of cell metabolism for essential neutrophil functions. *Cell Physiol Biochem* (2020) 54(4):629–47. doi: 10.33594/000000245

43. Ohms M, Ferreira C, Busch H, Wohlers I, Guerra de Souza AC, Silvestre R, et al. Enhanced glycolysis is required for antileishmanial functions of neutrophils upon infection with leishmania donovani. *Front Immunol* (2021) 12:632512. doi: 10.3389/fimmu.2021.632512

44. Nguyen GT, Green ER, Mecsas J. Neutrophils to the ROScue: mechanisms of NADPH oxidase activation and bacterial resistance. *Front Cell Infect Microbiol* (2017) 7:373. doi: 10.3389/fcimb.2017.00373

45. Song Z, Huang G, Chiquetto Paracatu L, Grimes D, Gu J, Luke CJ, et al. NADPH oxidase controls pulmonary neutrophil infiltration in the response to fungal cell walls by limiting LTB4. *Blood.* (2020) 135(12):891–903. doi: 10.1182/blood.2019003525

46. Radmark O, Werz O, Steinhilber D, Samuelsson B. 5-Lipoxygenase, a key enzyme for leukotriene biosynthesis in health and disease. *Biochim Biophys Acta* (2015) 1851(4):331–9. doi: 10.1016/j.bbalip.2014.08.012

47. Olas B. Medical functions of hydrogen sulfide. *Adv Clin Chem* (2016) 74:195–210. doi: 10.1016/bs.acc.2015.12.007

48. Kosower NS, Kosower EM, Wertheim B, Correa WS. Diamide, a new reagent for the intracellular oxidation of glutathione to the disulfide. *Biochem Biophys Res Commun* (1969) 37(4):593–6. doi: 10.1016/0006-291X(69)90850-X

49. Park WH, Han YW, Kim SH, Kim SZ. An ROS generator, antimycin A, inhibits the growth of HeLa cells via apoptosis. *J Cell Biochem* (2007) 102(1):98–109. doi: 10.1002/jcb.21280

50. Gomez-Nino A, Agapito MT, Obeso A, Gonzalez C. Effects of mitochondrial poisons on glutathione redox potential and carotid body chemoreceptor activity. *Respir Physiol Neurobiol* (2009) 165(1):104–11. doi: 10.1016/j.resp.2008.10.020

51. Mlejnek P, Dolezel P. Loss of mitochondrial transmembrane potential and glutathione depletion are not sufficient to account for induction of apoptosis by carbonyl cyanide 4-(trifluoromethoxy)phenylhydrazone in human leukemia K562 cells. *Chem Biol Interact* (2015) 239:100–10. doi: 10.1016/j.cbi.2015.06.033

52. Hiranruengchok R, Harris C. Diamide-induced alterations of intracellular thiol status and the regulation of glucose metabolism in the developing rat conceptus in vitro. *Teratology* (1995) 52(4):205–14. doi: 10.1002/tera.1420520406

53. Britt EC, Lika J, Giese MA, Schoen TJ, Seim GL, Huang Z, et al. Switching to the cyclic pentose phosphate pathway powers the oxidative burst in activated neutrophils. *Nat Metab* (2022) 4(3):389–403. doi: 10.1038/s42255-022-00550-8

54. Stincone A, Prigione A, Cramer T, Wamelink MM, Campbell K, Cheung E, et al. The return of metabolism: biochemistry and physiology of the pentose phosphate pathway. *Biol Rev Camb Philos Soc* (2015) 90(3):927–63. doi: 10.1111/brv.12140

55. Peralta D, Bronowska AK, Morgan B, Doka E, Van Laer K, Nagy P, et al. A proton relay enhances H2O2 sensitivity of GAPDH to facilitate metabolic adaptation. *Nat Chem Biol* (2015) 11(2):156–63. doi: 10.1038/nchembio.1720

56. Galkina SI, Fedorova NV, Serebryakova MV, Romanova JM, Golyshev SA, Stadnichuk VI, et al. Proteome analysis identified human neutrophil membrane tubulovesicular extensions (cytonemes, membrane tethers) as bactericide trafficking. *Biochim Biophys Acta* (2012) 1820(11):1705–14. doi: 10.1016/j.bbagen.2012.06.016

57. Galkina SI, Romanova JM, Bragina EE, Tiganova IG, Stadnichuk VI, Alekseeva NV, et al. Membrane tubules attach Salmonella Typhimurium to eukaryotic cells and bacteria. *FEMS Immunol Med Microbiol* (2011) 61(1):114–24. doi: 10.1111/j.1574-695X.2010.00754.x

58. Sekheri M, Othman A, Filep JG. beta2 integrin regulation of neutrophil functional plasticity and fate in the resolution of inflammation. *Front Immunol* (2021) 12:660760. doi: 10.3389/fimmu.2021.660760

59. Grieshaber-Bouyer R, Nigrovic PA. Neutrophil heterogeneity as therapeutic opportunity in immune-mediated disease. *Front Immunol* (2019) 10:346. doi: 10.3389/fimmu.2019.00346

60. Takashi S, Okubo Y, Horie S. Contribution of CD54 to human eosinophil and neutrophil superoxide production. *J Appl Physiol (1985).* (2001) 91(2):613–22. doi: 10.1152/jappl.2001.91.2.613

61. Konrad FM, Wohlert J, Gamper-Tsigaras J, Ngamsri KC, Reutershan J. How Adhesion Molecule Patterns Change While Neutrophils Traffic through the Lung during Inflammation. *Mediators Inflamm* (2019) 2019:1208086. doi: 10.1155/2019/1208086

62. Rouzer CA, Samuelsson B. The importance of hydroperoxide activation for the detection and assay of mammalian 5-lipoxygenase. *FEBS Lett* (1986) 204(2):293–6. doi: 10.1016/0014-5793(86)80831-6

63. Radmark O. Arachidonate 5-lipoxygenase. *Prostaglandins Other Lipid Mediat* (2002) 68-69:211–34. doi: 10.1016/S0090-6980(02)00032-1

64. Nanda BL, Nataraju A, Rajesh R, Rangappa KS, Shekar MA, Vishwanath BS. PLA2 mediated arachidonate free radicals: PLA2 inhibition and neutralization of free radicals by anti-oxidants–a new role as anti-inflammatory molecule. *Curr Top Med Chem* (2007) 7(8):765–77. doi: 10.2174/156802607780487623

65. Sporn PH, Peters-Golden M. Hydrogen peroxide inhibits alveolar macrophage 5-lipoxygenase metabolism in association with depletion of ATP. *J Biol Chem* (1988) 263(29):14776–83. doi: 10.1016/S0021-9258(18)68105-0

66. Ahnfelt-Ronne I, Olsen UB. Leukotriene production in rat peritoneal leukocytes requires intact energy metabolism. *Biochem Pharmacol* (1985) 34(17):3095–100. doi: 10.1016/0006-2952(85)90153-4

67. Miller CG, Holmgren A, Arner ESJ, Schmidt EE. NADPH-dependent and -independent disulfide reductase systems. *Free Radic Biol Med* (2018) 127:248–61. doi: 10.1016/j.freeradbiomed.2018.03.051

68. Hasan AA, Kalinina E, Tatarskiy V, Shtil A. The thioredoxin system of mammalian cells and its modulators. *Biomedicines.* (2022) 10(7):1757. doi: 10.3390/biomedicines10071757

69. Hatzelmann A, Schatz M, Ullrich V. Involvement of glutathione peroxidase activity in the stimulation of 5-lipoxygenase activity by glutathione-depleting agents in human polymorphonuclear leukocytes. *Eur J Biochem* (1989) 180(3):527–33. doi: 10.1111/j.1432-1033.1989.tb14678.x

70. Masterson E, Whikehart DR, Chader GJ. Glucose oxidation in the chick cornea: effect of diamide on the pentose shunt. *Invest Ophthalmol Vis Sci* (1978) 17(5):449–54.

71. Cracan V, Titov DV, Shen H, Grabarek Z, Mootha VK. A genetically encoded tool for manipulation of NADP(+)/NADPH in living cells. *Nat Chem Biol* (2017) 13 (10):1088–95. doi: 10.1038/nchembio.2454

72. Glaser KM, Doon-Ralls J, Walters N, Rima XY, Rambold AS, Reategui E, et al. Arp2/3 complex and the pentose phosphate pathway regulate late phases of neutrophil swarming. *iScience.* (2024) 27(1):108656. doi: 10.1016/j.isci.2023.108656

73. Babior BM, Lambeth JD, Nauseef W. The neutrophil NADPH oxidase. *Arch Biochem Biophys* (2002) 397(2):342–4. doi: 10.1006/abbi.2001.2642

74. Amara N, Cooper MP, Voronkova MA, Webb BA, Lynch EM, Kollman JM, et al. Selective activation of PFKL suppresses the phagocytic oxidative burst. *Cell.* (2021) 184 (17):4480–94.e15. doi: 10.1016/j.cell.2021.07.004

75. Kuehne A, Emmert H, Soehle J, Winnefeld M, Fischer F, Wenck H, et al. Acute activation of oxidative pentose phosphate pathway as first-line response to oxidative stress in human skin cells. *Mol Cell* (2015) 59(3):359–71. doi: 10.1016/j.molcel.2015.06.017

76. Tan Y, Kagan JC. Innate immune signaling organelles display natural and programmable signaling flexibility. *Cell.* (2019) 177(2):384–98.e11. doi: 10.1016/j.cell.2019.01.039

77. Kumar S, Dikshit M. Metabolic insight of neutrophils in health and disease. *Front Immunol* (2019) 10:2099. doi: 10.3389/fimmu.2019.02099

78. Azevedo EP, Rochael NC, Guimaraes-Costa AB, de Souza-Vieira TS, Ganilho J, Saraiva EM, et al. A metabolic shift toward pentose phosphate pathway is necessary for amyloid fibril- and phorbol 12-myristate 13-acetate-induced neutrophil extracellular trap (NET) formation. *J Biol Chem* (2015) 290(36):22174–83. doi: 10.1074/jbc.M115.640094

79. Runchel C, Matsuzawa A, Ichijo H. Mitogen-activated protein kinases in mammalian oxidative stress responses. *Antioxid Redox Signal* (2011) 15(1):205–18. doi: 10.1089/ars.2010.3733

80. Cross JV, Templeton DJ. Oxidative stress inhibits MEKK1 by site-specific glutathionylation in the ATP-binding domain. *Biochem J* (2004) 381(Pt 3):675–83. doi: 10.1042/BJ20040591

81. Gelfand EW. Importance of the leukotriene B4-BLT1 and LTB4-BLT2 pathways in asthma. *Semin Immunol* (2017) 33:44–51. doi: 10.1016/j.smim.2017.08.005

82. Haeggstrom JZ. Leukotriene biosynthetic enzymes as therapeutic targets. *J Clin Invest.* (2018) 128(7):2680–90. doi: 10.1172/JCI97945

83. Noiri E, Yokomizo T, Nakao A, Izumi T, Fujita T, Kimura S, et al. An in *vivo* approach showing the chemotactic activity of leukotriene B(4) in acute renal ischemic-reperfusion injury. *Proc Natl Acad Sci U S A.* (2000) 97(2):823–8. doi: 10.1073/pnas.97.2.823

84. Dent G, Rabe KF, Magnussen H. Augmentation of human neutrophil and alveolar macrophage LTB4 production by N-acetylcysteine: role of hydrogen peroxide. *Br J Pharmacol* (1997) 122(4):758–64. doi: 10.1038/sj.bjp.0701428

85. Hirakata T, Matsuda A, Yokomizo T. Leukotriene B(4) receptors as therapeutic targets for ophthalmic diseases. *Biochim Biophys Acta Mol Cell Biol Lipids.* (2020) 1865 (9):158756. doi: 10.1016/j.bbalip.2020.158756

86. Sanchez-Tabernero S, Fajardo-Sanchez J, Weston-Davies W, Parekh M, Kriman J, Kaye S, et al. Dual inhibition of complement component 5 and leukotriene B4 by topical rVA576 in atopic keratoconjunctivis: TRACKER phase 1 clinical trial results. *Orphanet J Rare Dis* (2021) 16(1):270. doi: 10.1186/s13023-021-01890-6

87. Liao T, Ke Y, Shao WH, Haribabu B, Kaplan HJ, Sun D, et al. Blockade of the interaction of leukotriene b4 with its receptor prevents development of autoimmune uveitis. *Invest Ophthalmol Vis Sci* (2006) 47(4):1543–9. doi: 10.1167/iovs.05-1238

88. Chistyakov DV, Gancharova OS, Baksheeva VE, Tiulina VV, Goriainov SV, Azbukina NV, et al. Inflammation in dry eye syndrome: identification and targeting of oxylipin-mediated mechanisms. *Biomedicines* (2020) 8(9):344. doi: 10.3390/biomedicines8090344

89. Zielonka J, Joseph J, Sikora A, Hardy M, Ouari O, Vasquez-Vivar J, et al. Mitochondria-targeted triphenylphosphonium-based compounds: syntheses, mechanisms of action, and therapeutic and diagnostic applications. *Chem Rev* (2017) 117(15):10043–120. doi: 10.1021/acs.chemrev.7b00042

90. Zinovkin RA, Zamyatnin AA. Mitochondria-targeted drugs. *Curr Mol Pharmacol* (2019) 12(3):202–14. doi: 10.2174/1874467212666181127151059

91. Plotnikov EY, Morosanova MA, Pevzner IB, Zorova LD, Manskikh VN, Pulkova NV, et al. Protective effect of mitochondria-targeted antioxidants in an acute bacterial infection. *Proc Natl Acad Sci U S A.* (2013) 110(33):E3100–8. doi: 10.1073/pnas.1307096110

92. Zakharova VV, Pletjushkina OY, Galkin II, Zinovkin RA, Chernyak BV, Krysko DV, et al. Low concentration of uncouplers of oxidative phosphorylation decreases the TNF-induced endothelial permeability and lethality in mice. *Biochim Biophys Acta Mol Basis Dis* (2017) 1863(4):968–77. doi: 10.1016/j.bbadis.2017.01.024

frontiers | Frontiers in Immunology

TYPE Original Research
PUBLISHED 13 February 2024
DOI 10.3389/fimmu.2024.1344949

OPEN ACCESS

EDITED BY
Pedro Gonzalez-Menendez,
University of Oviedo, Spain

REVIEWED BY
Roland Wohlgemuth,
Lodz University of Technology, Poland
Gobinath Ramachawolran,
RCSI and UCD Malaysia Campus, Malaysia

*CORRESPONDENCE
Qing-Jun Wei
weiqingjun@gxmu.edu.cn
Qiong-Qian Xu
634475380@qq.com

†These authors have contributed equally to this work and share first authorship

RECEIVED 27 November 2023
ACCEPTED 22 January 2024
PUBLISHED 13 February 2024

CITATION
He X-X, Huang Y-J, Hu C-L, Xu Q-Q and Wei Q-J (2024) Songorine modulates macrophage polarization and metabolic reprogramming to alleviate inflammation in osteoarthritis. *Front. Immunol.* 15:1344949. doi: 10.3389/fimmu.2024.1344949

Songorine modulates macrophage polarization and metabolic reprogramming to alleviate inflammation in osteoarthritis

Xi-Xi He[1†], Yuan-Jun Huang[1†], Chun-Long Hu[1], Qiong-Qian Xu[2*] and Qing-Jun Wei[1*]

[1]Department of Orthopedics Trauma and Hand Surgery, The First Affiliated Hospital of Guangxi Medical University, Nanning, China, [2]Department of Pediatric Surgery, Qilu Hospital of Shandong University, Jinan, China

Introduction: Osteoarthritis (OA) is a prevalent joint disorder characterized by multifaceted pathogenesis, with macrophage dysregulation playing a critical role in perpetuating inflammation and joint degeneration.

Methods: This study focuses on Songorine, derived from Aconitum soongaricum Stapf, aiming to unravel its therapeutic mechanisms in OA. Comprehensive analyses, including PCR, Western blot, and immunofluorescence, were employed to evaluate Songorine's impact on the joint microenvironment and macrophage polarization. RNA-seq analysis was conducted to unravel its anti-inflammatory mechanisms in macrophages. Metabolic alterations were explored through extracellular acidification rate monitoring, molecular docking simulations, and PCR assays. Oxygen consumption rate measurements were used to assess mitochondrial oxidative phosphorylation, and Songorine's influence on macrophage oxidative stress was evaluated through gene expression and ROS assays.

Results: Songorine effectively shifted macrophage polarization from a pro-inflammatory M1 phenotype to an anti-inflammatory M2 phenotype. Notably, Songorine induced metabolic reprogramming, inhibiting glycolysis and promoting mitochondrial oxidative phosphorylation. This metabolic shift correlated with a reduction in macrophage oxidative stress, highlighting Songorine's potential as an oxidative stress inhibitor.

Discussion: In an *in vivo* rat model of OA, Songorine exhibited protective effects against cartilage damage and synovial inflammation, emphasizing its therapeutic potential. This comprehensive study elucidates Songorine's multifaceted impact on macrophage modulation, metabolic reprogramming, and the inflammatory microenvironment, providing a theoretical foundation for its therapeutic potential in OA.

KEYWORDS

osteoarthritis, Songorine, metabolic alteration, oxidative stress, inflammation

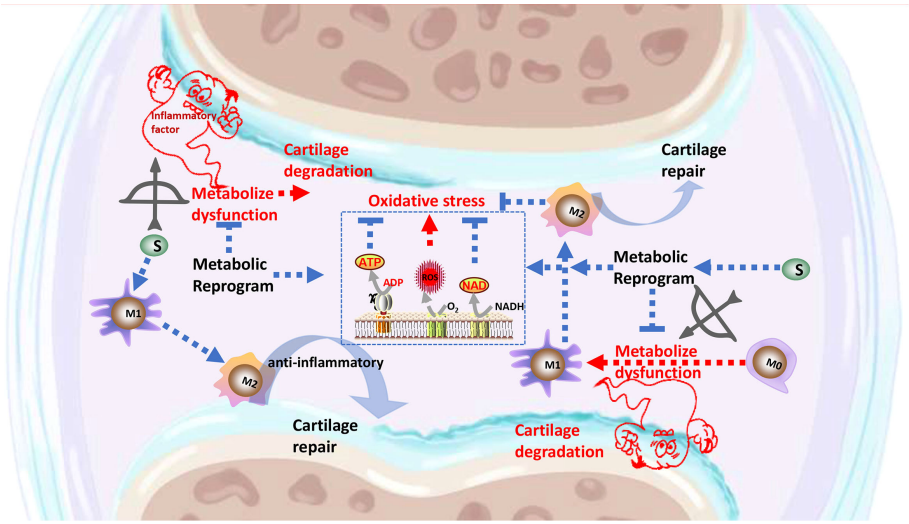

GRAPHICAL ABSTRACT
The signaling pathways through which Songorine binds to metabolic pathway, resulting in metabolic reprogramming, polarization of macrophages, inhibition of inflammatory factors secretion, regulation of the cartilage anabolism, and protection against OA.

1 Introduction

Osteoarthritis (OA) stands as a prevalent and debilitating joint disorder characterized by the progressive deterioration of articular cartilage, subchondral bone alterations, and the formation of osteophytes (1, 2). With a rising global incidence, particularly in the aging population, OA significantly impacts the quality of life for affected individuals. The intricate interplay of genetic, mechanical, and biochemical factors contributes to the multifaceted pathogenesis of OA. Recent research has unveiled the crucial role of inflammatory processes and immune cell involvement, particularly macrophages, in driving the structural changes observed in OA joints (3, 4).

Macrophages, as key players in the immune system, exhibit a remarkable plasticity, adopting distinct phenotypes in response to environmental cues. Classically activated M1 macrophages contribute to inflammation and tissue degradation, while alternatively activated M2 macrophages are associated with tissue repair and anti-inflammatory responses. The dysregulation of macrophage polarization has emerged as a central player in the perpetuation of OA, offering a promising avenue for therapeutic intervention (5, 6). The specific dysregulation of macrophage polarization is recognized as a pivotal factor in the context of OA. Dysregulated macrophages contribute to the perpetuation of inflammation, tissue degradation, and altered repair mechanisms within the affected joints. The intricate balance between M1 and M2 macrophage phenotypes becomes disrupted, leading to an environment conducive to OA progression. Understanding this dysregulation provides a crucial foundation for exploring targeted therapeutic interventions that address the nuanced role of macrophages in OA.

The immense potential of natural products in treating various diseases, including OA, has been a continuous exploration. Notably, key findings from current research underscore the promising role of natural products in mitigating OA symptoms, potentially influencing macrophage behavior and inflammatory responses within the joint microenvironment (7, 8). Crucially, alkaloids, widespread in nature (9), play a key role in Traditional Chinese Medicine's therapeutic effects, exhibiting significant anti-cancer, anti-inflammatory, and antioxidant activities (10–12). In this context, Aconitum, commonly known as "wutou," stands out as a repository of approximately 450 alkaloids and has been extensively utilized for treating various diseases in China, Japan, and other regions (13, 14). Aconitum has been traditionally employed to alleviate a spectrum of ailments, including inflammatory conditions, cardiovascular disorders, and nervous system disturbances (15). Aconitum soongaricum Stapf, a specific species within the Aconitum genus, is particularly noteworthy for housing Songorine, a C20-diterpenoid alkaloid with a range of characteristics, including anti-inflammatory, antiarrhythmic, and anti-central nervous system disturbance properties (16–18). This convergence of traditional wisdom, scientific exploration, and the identification of specific bioactive compounds like Songorine underscores the intricate interplay within Traditional Chinese Medicine and its potential in addressing complex diseases such as OA.

Despite these advancements, there exists a critical need to consolidate and synthesize key findings from ongoing research on natural products in OA. A comprehensive understanding of the therapeutic potential of these natural products, especially in the context of immune cell modulation and macrophage behavior, will contribute to a more holistic approach in developing targeted and effective therapies for OA.

Therefore, our study focuses on the natural compound Songorine, and its potential therapeutic role in OA. Through a comprehensive exploration of macrophage modulation, metabolic reprogramming, and the impact on the inflammatory microenvironment, we aim to unravel the molecular mechanisms

that underlie Songorine's effects in the context of OA. This research endeavors to address the critical gap in understanding how Songorine, a specific bioactive compound from Aconitum soongaricum Stapf, influences macrophage behavior and immune responses in the OA microenvironment. we aim to contribute valuable insights that will inform the development of nuanced and effective therapeutic strategies for OA, considering the complex interplay between inflammation, immune responses, and joint degeneration.

2 Materials and methods

2.1 Cell culture

The murine macrophages (RAW 264.7) from Procell Life Science & Technology Co., Ltd. (Hubei, China) were incubated in medium at a temperature of 37°C in a moist environment with 5% CO2. Songorine (purity is 99.48% by high performance liquid chromatography with diode array detector, 230nm) obtained from Chengdu Biopurify Phytochemicals Ltd. (Cat. BP029) was used in this study. and used as a stimulator for macrophage activation. M1 polarization was induced by treating RAW 264.7 cells with Lipopolysaccharides (LPS) From Escherichia coli 055:B5 (Solarbio, Cat. L8880, The potency of LPS is greater than or equal to 500,000 EU per mg, < 1% protein) at a concentration of 100 ng/mL for a duration of 24 hours.

In order to assess the impacts and mechanisms of Songorine on the immune system, the conditioned media obtained from Songorine-treated macrophages were gathered and utilized for the cultivation of chondrocytes. The control group consisted of chondrocytes that were not treated with Songorine. The M0CM group was designated as the chondrocytes that were cultured in a conditioned medium derived from M0 macrophages. M1CM refers to chondrocytes that were cultured in a conditioned medium derived from M1 macrophages. S10CM and S50CM were designated as chondrocytes that were cultured in a conditioned medium obtained from M1 macrophages that had been treated with varying concentrations of Songorine for a duration of 24 hours. Following a 24-hour incubation period, the chondrocytes were gathered for additional examination.

2.2 Identification of reactive oxygen species

M0 macrophages were placed in 6-well dishes and permitted to proliferate until reaching 60–70% confluence. M0 macrophages were stimulated with LPS to induce M1 polarization. Afterwards, the cells were cultured with either 10 or 50 μM Songorine. Following the manufacturer's guidelines of a ROS Assay Kit (Beyotime, Cat.S0033S) (19), the cells were washed three times with PBS and incubated with the ROS probe after 24 hours of treatment. Following an additional PBS wash, the specimens were examined and captured using a fluorescence microscope (Olympus, Japan). The fluorescence intensities of the images were quantified using the Image J software. Chondrocytes were placed in 6-well dishes and grown in conditioned media (M0CM, M1CM, S10CM, and S50CM) for 24 hours. The following procedures remained unchanged as described above, including washing with PBS, incubating with the ROS probe, and imaging and quantifying fluorescence intensity using Image J software.

2.3 Analysis of quantitative real-time PCR

Total mRNA was extracted using RNAfast200 (Fastagen, China) and then converted into cDNA using a reverse transcription kit (TOYOBO, Cat. FSQ-101), according to the manufacturer's instructions. In order to examine the levels of gene expression, the qRT-PCR analysis provided by the Kit (TAKARA, Cat. RR820A). Internal controls in the form of GAPDH and actin mRNA as housekeeping genes were employed. Table 1 contains the list of primers utilized for the target genes.

2.4 Simple western (Jess by ProteinSimple)

We used a Simple Western blot technique to examine the anti-inflammatory mechanism and the impact of Songorine on cellular metabolism. The cells were placed in 6-well dishes and incubated for 24 hours until they achieved a 70% confluence. Afterwards, the cells were exposed to inflammatory agents (LPS) for a duration of 24 hours. Subsequent to the stimulation, the cells were subjected to various doses of Songorine for another 24-hour period.

Following different procedures, the cells were lysed by radioimmunoprecipitation (RIPA) buffer (Boster, China, Cat. AR0102S) supplemented with 1 mmol/L phenylmethylsulfonyl fluoride (PMSF, Boster, China, Cat. AR0102S). The lysis process involved placing the samples on ice and vortexing every 5 minutes for a total duration of 30 minutes. Following lysis, the cellular extracts underwent centrifugation at 12,000×g for 15 minutes at 4° C. Subsequently, the protein concentrations in the resulting supernatants were quantified using a BCA protein assay kit (Boster, China, Cat. AR0197). To ensure accurate measurements, the ultimate protein concentration of every sample was modified to 0.2 μg/μL. The protein samples were subjected to a temperature of 95°C for a duration of 5 minutes in a 0.1x sample buffer and 5x Master Mix. Subsequently, they were separated through capillary electrophoresis employing the JESS system manufactured in the United States. To identify particular proteins, the main antibodies, such as rabbit anti-IL-1β (1:40), anti-IL-6 (1: 100), mouse anti-CD86 (1:200) were diluted with antibody diluent. Subsequently, 10 μL of streptavidin-HRP and secondary antibodies were added to the wells. Protein expression levels were evaluated using the Compass software for SW 4.1.0, which provided a quantitative analysis of the detected protein bands. The Simple Western blot technique allowed for examination of the anti-inflammatory properties of Songorine and the verification of its impact on cellular metabolism by analyzing the expression levels of specific target proteins.

TABLE 1 The primers for the target genes.

Target Gene	Forward primer sequence	Forward primer sequence
PFKFB3	GGAGTCCGCAAAACAGGATG	GATGCGAGGCTTTTTGGTGG
GAPDH (Rat)	TCTCTGCTCCTCCCTGTTCT	ATCCGTTCACACCGACCTTC
GAPDH (Mus)	TGGATTTGGACGCATTGGTC	TTTGCACTGGTACGTGTTGAT
β-actin	GAGCTACGAGCTGCCTGACG	CCTAGAAGCATTTGCGGTGG
HK-II	GGTGCTGTGGCGAATCAAAG	GAGACGCTTGGCAAAATGGG
GLUT	TTAATCGCTTTGGCAGGCGG	GTCAGGCCACAGTACACTCC
LDHA	GAGCCACTGTCGCCGATCTC	AATCTTTTGGGACCCTGCACC
ACAN	CCTGCTACTTCATCGACCCC	AGATGCTGTTGACTCGAACCT
SOX9	TCCAGCAAGAACAAGCCACA	CGAAGGGTCTCTTCTCGCTC
COL-2α	GTCCTACAATGTCAGGGCCA	ACCCCTCTCTCCCTTGTCAC
IL-1β (Rat)	GCACAGTTCCCCAACTGGTA	GGAGACTGCCCATTCTCGAC
IL-6 (Rat)	ACAAGTCCGGAGAGGAGACT	ACAGTGCATCATCGCTGTTC
MMP-13	GGACAAAGACTATCCCCGCC	GGCATGACTCTCACAATGCG
CD206	GCACTGGGTTGCATTGGTTT	CCTGAGTGGCTTACGTGGTT
CD86	AACTTACGGAAGCACCCACG	ATAAGCTTGCGTCTCCACGG
IL-10	CCTCGTTTGTACCTCTCTCCG	AGGACACCATAGCAAAGGGC
iNOS	GGGTCACAACTTTACAGGGAGT	GAGTGAACAAGACCCAAGCG
IL-1β (Mus)	TGCCACCTTTTGACAGTGATG	TGTGCTGCTGCGAGATTTGA
IL-6 (Mus)	CAACGATGATGCACTTGCAGA	TGACTCCAGCTTATCTCTTGGT

2.5 Immunofluorescence

The protein expression of target genes in the cells was assessed using Immunofluorescence (IF) staining. The IF staining was carried out following the guidelines given with the DyLight 488-SABC Kit (Boster, SA1094). Rabbit anti-IL-1β (1:200; Proteintech, 16806-1-AP), mouse anti-CD86 (1:200; Santa Cruz Biotechnology, sc-28347), and rabbit anti-CD206 (1:200; Proteintech, 18704-1-AP) were the primary antibodies utilized. The antibodies were employed to specifically target and attach to the desired proteins. Following the incubation period with primary antibodies, the cells underwent a washing step to eliminate any antibodies that were not bound. Afterward, fluorophore-conjugated secondary antibodies were employed to visualize the target proteins. A DyLight 488-SABC kit (Boster, SA1094) provided the appropriate secondary antibodies for staining. In the end, cells that were stained with immunofluorescence were observed and captured using a fluorescence microscope. By using suitable fluorescence channels, the captured images enabled the examination and interpretation of IL1, IL-6, CD86, and CD206 protein expression levels in the cells.

2.6 Measurement of cellular metabolism

Before the experiment, a hydration plate was prepared by adding 200 μL of sterile water to each well to ensure proper hydration of the sensors on the probe plate. Afterward, the probe plate device was placed in a cell incubator without CO_2 and incubated at a temperature of 37°C for the duration of the night. The Seahorse XFe96 test system was preheated for at least 5 h at 37°C. Different inflammatory factors were used to stimulate cells, including chondrocytes and macrophages, which were then treated with varying concentrations of Songorine. These cells were plated in Seahorse XF96 plates with a density of 10,000 cells per well. After 24 h of culture, a seahorse XFe96 assay system was performed using the Agilent Seahorse XF analyzer. During the experiment, the growth medium was substituted with Seahorse XF assay solution, and the cells were subsequently placed in a cell incubator devoid of CO_2 at a temperature of 37°C for a duration of 60 minutes to achieve equilibrium. The glycolytic stress test (103020-100, Agilent Technologies) was conducted using an assay solution containing Seahorse XF DMEM Medium (103575–100), 2mM glutamine (103579–100), pH 7.4. Measurements of the extracellular acidification rate (ECAR) were conducted at intervals of 5 minutes, both prior to and following the consecutive introduction of glucose (10 mM), oligomycin (1 μM), and 2-DG (50 μM). To assess the cellular oxygen consumption rate (OCR), a Mito Stress Test Kit (103015-100, Agilent Technologies) was employed (20). Glucose was present in the assay solution containing Seahorse XF DMEM Medium 97ml (103575–100), 1mL glucose (103577–100), 1mL pyruvate (103578-100), 1mL glutamine (103579-100), pH 7.4, and measurements were conducted at 5-minute intervals prior to and

following the consecutive introduction of oligomycin (1.5 μM), FCCP (1 μM), and Rotenone/Antimycin A (0.5 μM) into the injection ports (21).

The collected data were examined utilizing Wave software, which enabled the interpretation and analysis of the horse assay results. This experimental approach allowed for the assessment of glycolytic activity and mitochondrial respiration, providing valuable insights into the metabolic changes induced by different inflammatory stimuli and the effects of Songorine treatment.

The determination of the total amount of oxidized and reduced Nicotinamide adenine dinucleotide (NAD) and the individual amounts of reduced NADH content was conducted through the utilization of the NAD(+)/NADH assay kit employing the WST-8 method (Beyotime, Nantong, China), following the guidelines provided by the manufacturer (22).

2.7 The process of RNA sequencing and the subsequent analysis

To explore the impact of LPS on gene expression and the potential regulatory function of Songorine, macrophages were subjected to diverse treatment conditions during culturing. For each type of cell, the experimental setup consisted of three groups (1) cells cultured without any treatment, (2) cells treated solely with LPS (100 ng/mL), and (3) cells treated with 50 μM Songorine.

Following a 24-hour treatment, RNA was obtained from the cellular samples using the previously mentioned method. RNA-seq samples were prepared using the NEBNext UltraTM RNA Library Prep Kit for the Illumina system, following the protocol provided by the manufacturer. At the OmicShare Bioinformatics Institute (Guangzhou, China), a HiSeq 3000 sequencer was utilized to conduct paired-end sequencing with a read length of 150 bp. HISAT2 (v2.0.5) was used to map the acquired RNA-seq reads to the Rnor_6.0 reference genome, employing the default settings. To evaluate the expression levels of various transcripts in the experimental groups, the calculation of Fragments per kilobase of exons per million mapped reads (FPKM) was performed (23). Genes that were significantly changed in response to LPS treatment, with or without Songorine treatment, were identified through differential expression analysis.

For data analysis and visualization, heatmaps of gene expression were generated to illustrate the overall gene expression patterns across different treatment groups. Furthermore, Kyoto Encyclopedia of Genes and Genomes (KEGG) pathway analyses were performed to gain insights into the biological functions and pathways affected by the treatments. Gene Set Enrichment Analysis (GSEA) was conducted using the gene ontology (GO) and KEGG databases, considering gene sets with absolute values of the Normalized Enrichment Score ($|NES| > 1$, nominal p-val < 0.05, and False Discovery Rate (FDR) q-val < 0.25 as statistically significant. The top 15 pathways were selected based on the absolute values of NES for display. This analysis aimed to explore the shared metabolic pathways affected by Songorine treatment in LPS-treated RAW264.7 cells.

2.8 Rat OA model and treatments *in vivo*

Male Sprague-Dawley rats, weighing between 250 and 300 grams, were acquired from the Experimental Animal Center at Guangxi Medical University. The research involving animal trials was carried out following the Guidelines for Animal Experimentation of Guangxi Medical University, and the experimental protocol was approved by the Animal Ethics Committee of the institution (Approval No. 202201004). An anterior drawer test confirmed the success of the anterior cruciate ligament transection (ACLT) model in inducing OA in the rat's knee joint, following a previously published method. The control group consisted of sham-operated rats (24).

After a month from the surgery, the ACLT rats were divided into three groups (n=6) randomly, and each group received an intra-articular injection of one of the following formulations: 1) saline, 2) 10 μM Songorine, or 3) 50 μM Songorine. Sham-operated rats served as a healthy control group. Injections were administered weekly. After the treatment commenced, the rats were euthanized at 4 and 8 weeks, and their knee joints were gathered for additional examination. Before micro-CT imaging, the knee joints were immersed in 4% paraformaldehyde for 24 hours to ensure fixation (25). A micro-computed tomography system (Micro-CT) (Quantum GX2, PerkinElmer) was utilized to conduct the imaging. The system operated at a resolution of 72 μm, with a 90 kV source and 88 μA current. Afterwards, the reconstructed datasets were analyzed using 3D analysis in the Mimics Research software (version 21.0) to assess osteophyte development. The volume of osteophytes or bone spurs was quantified to assess the extent of joint damage in knee osteoarthritis. Furthermore, each sample was given a macroscopic rating using a previously documented technique that quantitatively assesses the severity of OA (26).

2.9 Histology and immunohistochemistry

Following the imaging process, the knee joints underwent decalcification in a 10% (w/v) EDTA solution (pH 7.2) for a duration of four weeks prior to being enclosed in paraffin. For morphological analysis, 4 μm thick serial sagittal sections were prepared and stained with Safranin O/Fast Green. Additionally, some sections were stored for IHC analysis. The medial compartment of the knee was specifically analyzed at a distance of 50 μm between each level, with three levels of each section being examined for each sample. The OARSI scoring system was used to evaluate the extent of the osteoarthritis-like characteristics, which involved assessing three-level sections encompassing the femoral condyle and tibial plateau. Two impartial observers, who were unaware of the experimental groups, conducted this evaluation. Routine deparaffinization was performed on synovial and cartilage sections, followed by staining with hematoxylin and eosin (H&E). To assess the morphology of cartilage, sections of cartilage were treated to remove paraffin and then stained with a modified version of Safranin O and fast green.

To perform IHC analysis, the sections underwent deparaffinization and were then subjected to treatment with 3% H_2O_2 at ambient temperature for a duration of 15 minutes in order to remove any inherent peroxidase activity. Afterwards, the sections were subjected to antigen retrieval by incubating them with 0.25% EDTA trypsin (Procell, China, Cat. PB180225) at a temperature of 37°C for a duration of 20 minutes. Afterwards, the sections were obstructed using goat serum containing 10% concentration at a temperature of 37°C for a duration of 1 hour. This was succeeded by an overnight incubation with the primary antibody at a temperature of 4°C. Secondary antibody incubation and DAB color rendering were performed using an IHC kit. The microscope (VS120, OLYMPUS) was used to capture the resulting images, and the Image J software was utilized to quantify the percentage of positive areas.

2.10 Statistical analyses

The statistical analysis was performed using IBM SPSS Statistics software, specifically version 23.0. The data is presented as the average plus or minus the standard deviation (SD). Statistical analysis was conducted using either Student's t-test or one-way ANOVA, with a p-value<0.05 indicating statistical significance. To guarantee the dependability of the findings, the experiments were conducted a minimum of three times (27, 28).

3 Results

3.1 Songorine redirecting macrophage polarization toward anti-inflammation

In this section, we sought to comprehensively assess of Songorine's effect on macrophages using various techniques. We noted a significant decrease in CD86-positive cells (M1 macrophages) (Figures 1A–C) and an increase in CD206-positive cells (M2 macrophages) following Songorine treatment (Figures 1B, D). Notably, Songorine not only affected M1 macrophages but also influenced M2 macrophage polarization. Stimulation with Songorine led to an upregulation in the expression of the M2 marker CD206 and the anti-inflammatory cytokine IL-10 (Figures 1E–G), indicative of a shift towards the anti-inflammatory M2 phenotype. We observed Songorine's potent ability to modulate inflammatory responses. Specifically, Songorine exhibited a robust inhibition of M1 macrophage repolarization, resulting in a significant reduction in the expression of inflammatory cytokines IL-1β and IL-6 (Figures 1A, H, I). This underscores its efficacy in suppressing the induction of pro-inflammatory factors. Our exploration of inflammation-associated genes in RAW 264.7 cells, including IL-1β, IL-6, and iNOS, further validated the anti-inflammatory effects of Songorine (Figures 1H–J).

In summary, these findings collectively indicate that Songorine effectively modulates macrophage polarization, tipping the balance from the pro-inflammatory M1 phenotype towards the anti-inflammatory M2 phenotype. This remarkable ability holds promising therapeutic implications for managing inflammation in various diseases, including OA. The results not only provide compelling evidence for the therapeutic potential of Songorine in regulating macrophage polarization but also pave the way for further research and potential clinical applications as a targeted therapeutic agent for inflammatory disorders.

3.2 Songorine regulates metabolic shifts in macrophages during osteoarthritis

To gain deeper insights into Songorine's therapeutic properties in OA and uncover its molecular mechanisms, we conducted RNA-seq analysis. The results revealed significant variations in six biological process groups, as per the Kyoto Encyclopedia of Genes and Genomes (KEGG) database (Supplementary Figure S1). Analyzing data sets comparing M0 vs M1 and M1 vs S50 macrophages highlighted substantial alterations in lipid, amino acid, carbohydrate, and other metabolic pathways, with a total of 399 genes related to metabolism exhibiting changes. Notably, 103 genes within the carbohydrate metabolism showed significant expression changes when macrophages were stimulated with LPS. Gene set enrichment analysis (GSEA) showed that LPS activated pathways associated with metabolism, human diseases, organismal systems, and environmental information processing. However, these pathways were predominantly inhibited by Songorine in the S50 group, with carbohydrate metabolism in the metabolic pathway exhibiting the most significant changes (Figure 2A, Supplementary Figure S2). Importantly, Songorine's inhibitory effects on LPS-induced glycolysis pathways and key genes were evident, normalizing the expression of glycolysis-related genes in inflammatory macrophages (Figure 2B). Our findings suggest a comprehensive regulatory role of Songorine in altering the expression of genes associated with various metabolic pathways. Specifically, the downregulation of carbohydrate metabolism genes points towards a metabolic reprogramming induced by Songorine, aligning with the observed shift from glycolysis to mitochondrial oxidative phosphorylation. This intricate interplay between gene expression and metabolic shifts highlights Songorine's potential as a modulator of macrophage metabolism, contributing to its anti-inflammatory effects in the context of OA.

3.3 Songorine induces metabolic reprogramming in macrophages

To evaluate the impact of Songorine on macrophage metabolism during LPS stimulation, we monitored the ECAR. LPS-stimulated chondrocytes exhibited a significant increase in glycolysis compared to normal macrophages (Figure 3A). Inflammatory conditions enhanced all glycolysis-related parameters, demonstrating statistically significant differences (Figures 3B–E). However, Songorine suppressed glycolysis in inflamed macrophages, with glycolysis and glycolytic capacity decreasing in a concentration-dependent manner (Figures 3C, D),

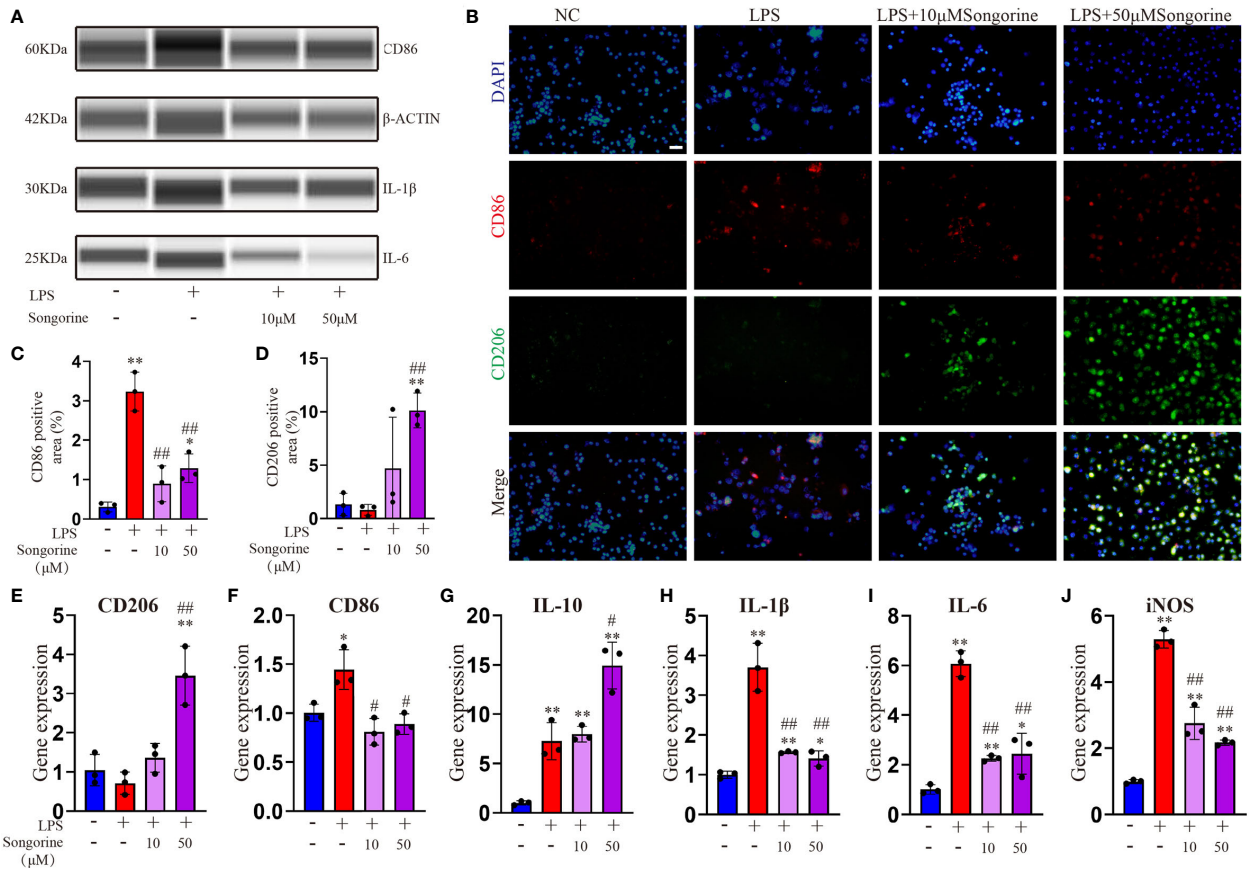

FIGURE 1
Effects of Songorine on macrophage polarization and inflammatory markers. Macrophages were treated as follows: untreated control (NC), LPS stimulation (LPS), and LPS stimulation with different concentrations of Songorine (LPS + 10 μM Songorine and LPS + 50 μM Songorine). **(A)** Protein expression of CD86, IL-1β, and IL-6 in macrophages after different treatments. **(B)** Representative images of double immunostaining of CD86 (M1 marker) and CD206 (M2 marker), Scale bar: 50 μm. **(C)** Quantification of CD86-positive cells and **(D)** CD206-positive cells in macrophages with different treatments. Immunofluorescence of CD86 and immunohistochemistry of CD206 were performed in macrophages after different treatments. The mRNA expression of M2 marker polarization **(E)** CD206, **(F)** M1 marker polarization (CD86), and pro-inflammatory cytokines, including **(G)** IL-10, **(H)** IL-1β, **(I)** IL-6, and **(J)** iNOS were analyzed. Statistical significance: * $p < 0.05$, ** $p < 0.01$ compared with normal control; # $p < 0.05$, ## $p < 0.01$ compared with the 1mg/mL LPS group.

while non-glycolysis and glycolytic reserve were unaffected by LPS and Songorine (Figures 3B, E). To investigate the interaction between Songorine and metabolic pathways, molecular docking simulations were conducted. The molecular docking results, as shown in concentration-dependent, revealed that Songorine could tightly bind to key metabolic targets, including PFKFB3, GULT1, HK2, LDHA, PDH, and SUS. PFKFB3, GULT1, HK2, and LDHA are crucial enzymes in the glycolysis pathway, while PDH and SUS are key regulators of the tricarboxylic acid cycle. Songorine's ability to bind tightly to key enzymes, such as PFKFB3, GULT1, HK2, and LDHA associated with glycolysis indicated a favorable binding of Songorine to glycolysis, forming strong hydrogen bonds with amino acid active groups and exhibiting strong binding energy (Figure 3F; Supplementary Figure S3). To further confirm Songorine's direct inhibition of the glycolytic pathway through PFKFB3, GULT1, HK2, and LDHA, PCR assays showed that LPS stimulation promoted the expression of key glycolytic genes, namely PFKFB3, HK2, and LDHA, while Songorine significantly reversed the stimulatory effect of LPS, reducing the expression of these genes (Figures 3G–J). These results suggest that Songorine inhibits glycolysis by downregulating key metabolic bottleneck enzymes (as illustrated in Figure 3K), improving the metabolic microenvironment to inhibit M1 polarization, promote M2 polarization, and facilitate self-repair.

Analysis of OCR revealed that IL-1β-treated cells exhibited inhibited mitochondrial oxidative phosphorylation (OXPHOS) (Figure 4A), including max respiration. Remarkably, Songorine treatment significantly enhanced OXPHOS and glucose metabolism, evidenced by increased basal respiration, max respiration, ATP production, and proton leak, even reaching normal levels (Figures 4B–G). These findings suggest that Songorine alters the metabolic status of LPS-treated macrophages, inhibiting glycolysis while preserving aerobic phosphorylation integrity (Figure 4H), thereby activating M2 polarization and suppressing inflammation.

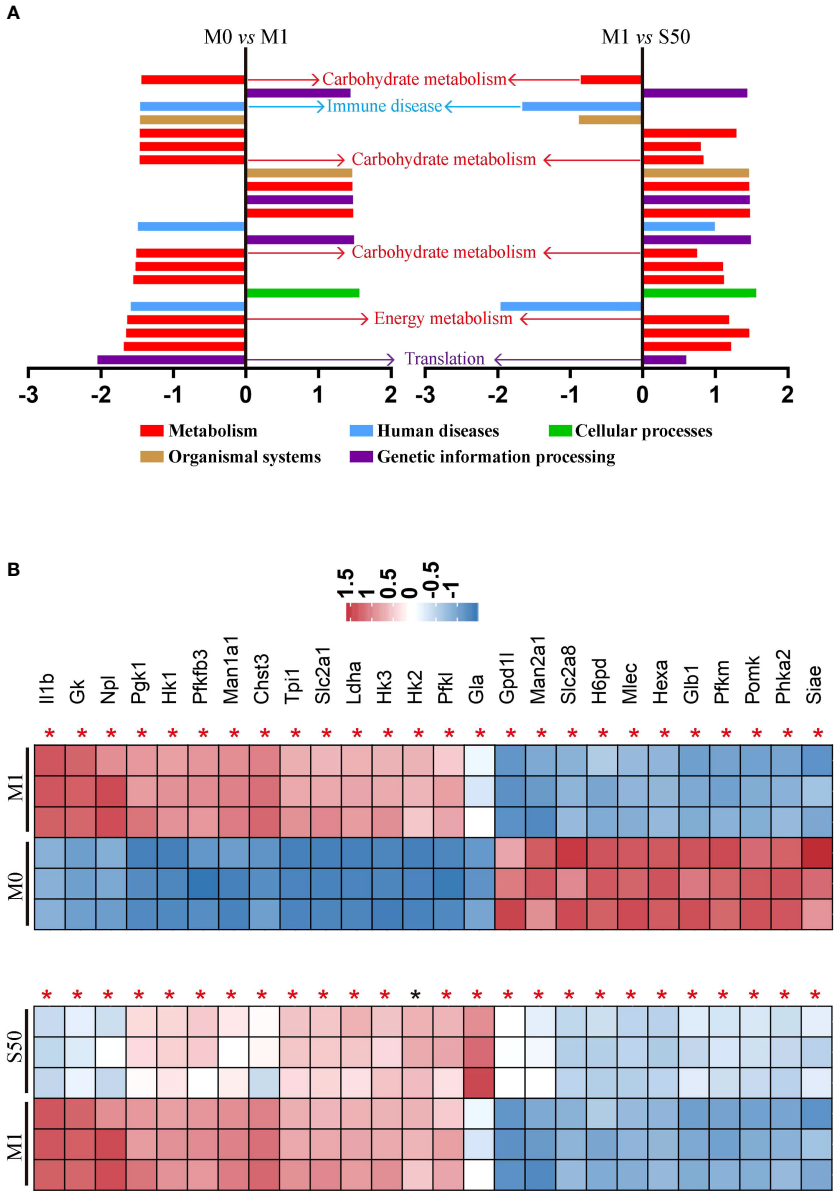

FIGURE 2
Songorine exhibits polarization effects of macrophages by regulating metabolic pathways. RNA-sequencing of chondrocytes with different groups. **(A)** GSEA analysis indicating common core biological pathways either upregulated or downregulated between data set 1 (M0 vs M1) and data set 2 (M1 vs S50). NES: normalized enrichment score. **(B)** Relative mRNA expression heat map of gene in glycolysis based on Log2FC in the two data sets (M0 compare with M1; M1 compare with S50). Asterisk indicates p<0.05 (black), p<0.01 (red).

3.4 Songorine suppresses macrophage oxidative stress through metabolic reprogramming

Interestingly, Songorine exhibits a concentration-dependent increase in proton leak (Figure 4F), a phenomenon known to mitigate ROS production and consequently inhibit the onset of oxidative stress. GSEA results reveal that LPS-stimulated macrophages are enriched in the oxidative stress pathway, promoting the occurrence of oxidative stress (Figure 5A). However, the addition of Songorine to LPS-stimulated macrophages significantly reverses the occurrence of oxidative stress, with the most notable changes observed in pathways related to NAD metabolism, such as NADH dehydrogenase complex assembly, NADH dehydrogenase complex, NADH dehydrogenase (ubiquinone) activity, NAD(+) activity, and NAD metabolic process. Gene enrichment analysis indicates that NAD-related gene expression is significantly inhibited in LPS-stimulated macrophages, while genes associated with oxidative stress show a marked increase (Figure 5B). In contrast, Songorine inhibits oxidative stress and promotes the regulation of NAD-related gene expression. Notably, Gpd1l, H6pd, and Ldha, which are significantly enriched in metabolism and oxidative stress, emphasize that these genes not only play a regulatory role in metabolism but also hold importance in oxidative stress or NAD

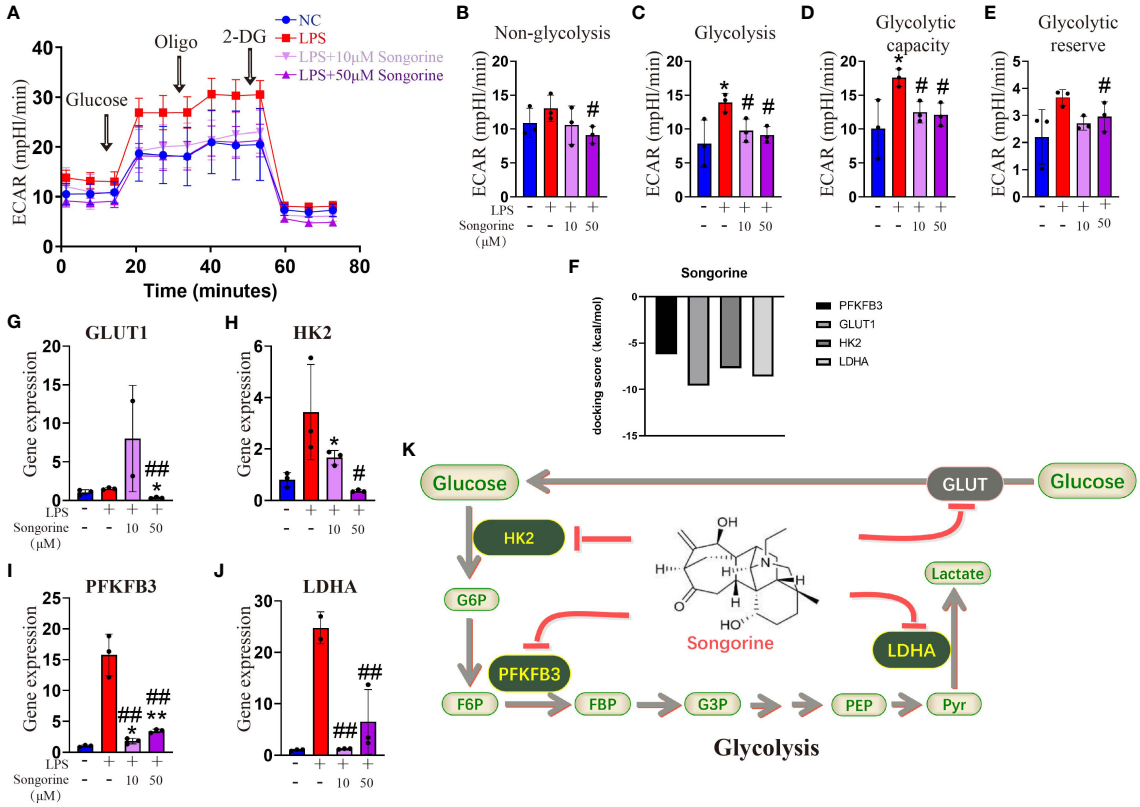

FIGURE 3
Songorine inhibits glycolysis by targets glycolytic enzymes. **(A)** Seahorse assay was performed to measure ECAR in different groups of macrophages. The ECAR was assessed by the Seahorse assay before and after sequential addition of Glucose, Oligomycin (Oligo), and 2-DG. **(B–E)** Non-glycolysis, glycolysis, glycolysis capacity and glycolytic reserve were calculated. **(F–I)** mRNA expression levels of GLUT1, HK2, PFKFB3 and LDHA in cells cultured with different treatments. Bar graphs and plots represent or include mean ± SD, respectively. **(J)** Docking scores of Songorine with PFKFB3, GLUT1, HK2, and LDHA. **(K)** Schematic illustration depicting the glycolytic regulation mechanism of Songorine. *p<0.05, **p<0.01 compared with the normal control; #p<0.05, ##p<0.01 compared with the 10 μg/mL IL-1β group.

synthesis. Songorine, as previously demonstrated to target and inhibit LDHA expression, not only regulates metabolism but also suppresses the occurrence of oxidative stress. Determining NAD content is crucial in our study as NAD plays a pivotal role in cellular metabolism and redox reactions. Measurement of NADH and NAD levels in macrophages aligns with gene expression results, confirming that LPS stimulation inhibits NAD+ production (Figure 5C) and NAD(+)/NADH ratio (Figure 5D), whereas Songorine counteracts this effect in a concentration-dependent manner, exhibiting optimal results at 50μM, approaching normal levels. Furthermore, it is revealed that Songorine decreases the production of ROS in LPS-stimulated M1 macrophages, as indicated by reduced green fluorescence (Figures 5E, F).

3.5 Songorine modulates the inflammatory microenvironment to facilitate chondrocyte repair

Control and M0CM groups exhibit low expression of inflammatory genes, while the M1CM group shows elevated levels of *IL-1β*, *IL-6* and *MMP13* (Figures 6A–C) alongside decreased anabolic genes *ACAN*, *COL-2α*, and *SOX9* (Figures 6D–F). This indicates chondrocyte stimulation within an inflammatory microenvironment. Treatment with S10CM and S50CM significantly reduces the expression of inflammatory and catabolic genes compared to M1CM, upregulating anabolic genes. Songorine effectively shifts the immune microenvironment from inflammatory to anti-inflammatory states. As expected, IF analysis shows a substantial decrease in IL-1β gene expression with Songorine treatment at different concentrations compared to the M1CM group (Figures 6G, H). Monitoring ROS content using DCFH-DA reveals that Songorine concentration-dependently decreases ROS content, highlighting its potent ROS-scavenging capacity (Figures 6I, J).

These findings demonstrate that Songorine suppresses the inflammatory microenvironment enriched with pro-inflammatory factors and promotes anabolic processes in chondrocytes. Songorine's immunomodulatory effects on macrophage reprogramming shift the inflammatory microenvironment toward anti-chondrogenic conditions, impacting cellular functions and contributing to the regulation of microenvironments in the joint capsule affected by OA.

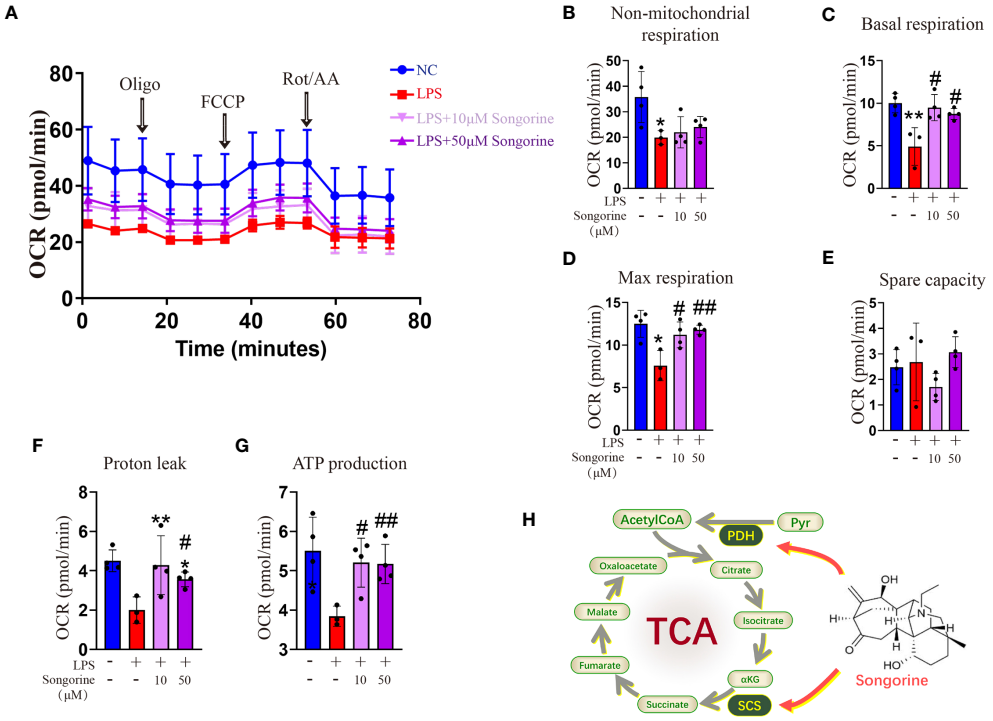

FIGURE 4
Songorine reshapes glucose metabolism in LPS-stimulated macrophages. **(A–G)** Seahorse assay was conducted to measure OCR in different macrophages groups. OCR was assessed before and after the sequential addition of Oligo, FCCP, and Rotenone/Antimycin (Rot/AA). **(H)** The schematic illustrates the mechanism through which Songorine transforms glucose metabolism, promoting TCA metabolism. Bar graphs and plots represent mean ± SD, respectively. *p < 0.05, **p < 0.01 compared with the normal control; #p < 0.05, ##p < 0.01 compared with the 10μg/mL IL-1β group.

3.6 Songorine protects against osteoarthritis in a surgically induced *in vivo* model

To assess the *in vivo* efficacy of Songorine in treating OA, we employed a rat model with ACLT as the OA induction method. ACLT rats were randomly divided into three groups receiving saline, 10μM Songorine, and 50μM Songorine treatments, respectively. Sham-operated rats served as healthy controls. Treatment initiation occurred on the 30th day post-surgery, repeated every five days until day 60. Rats were euthanized for joint collection, and Micro-CT imaging was performed. Joints were dissected, exposing synovium and cartilage, and photographed (Supplementary Figure S4A). In the ACLT group, synovium thickening and adhesion to cartilage indicated severe synovitis, with substantial damage to the cartilage surface. Songorine treatment preserved a smooth cartilage surface, comparable to the sham group, affirming its protective effect against ACLT-induced cartilage damage (Supplementary Figure S4B). The high concentration group exhibited more significant benefits against cartilage damage than the low concentration group. Micro-CT images (Figures 7A, B1, B2) displayed remarkable bone density reduction in the ACLT group, Songorine treatment effectively preserved the integrity of cartilage and bone structures, and suppressed the formation of osteophytes or bone spurs (Supplementary Figure S4C). Songorine exhibited the best outcome, maintaining the intact subchondral bone structure. S&F and HE staining (Figures 7C, D) illustrated proteoglycan loss and reduced articular cartilage thickness post-ACLT, whereas Songorine-treated ACLT rats showed significant inhibition of cartilage degeneration. OARSI scores further confirmed these protective results (Supplementary Figure S4D).

Synovial inflammation crucially influences OA progression; hence, we conducted a histological analysis of synovium. Figure 8 shows that OA destroyed the synovial reticular structure, with inflammatory cell infiltration causing thickening and disruption of the normally porous structure. Songorine maintained the synovial reticular structure and suppressed inflammatory cell infiltration. To explore Songorine's mechanisms in OA treatment, we used an immunohistochemical assay to evaluate synovial inflammation and infiltrated macrophage phenotypes. F4/80, CD86 (M1 biomarker), and CD206 (M2 biomarker) were employed for macrophage identification, and quantitative analysis was conducted. In ACLT synovium, F4/80-stained macrophages increased, however, Songorine demonstrates a concentration-dependent reduction in macrophage infiltration while preserving the normal structure of the synovial tissue (Figure 8A). CD86-positive area increased, while CD206-positive area remained similar to healthy synovium. Songorine treatment decreased CD86-positive area increased In ACLT synovium, while CD206-positive area remained similar to healthy synovium. treatment with Songorine

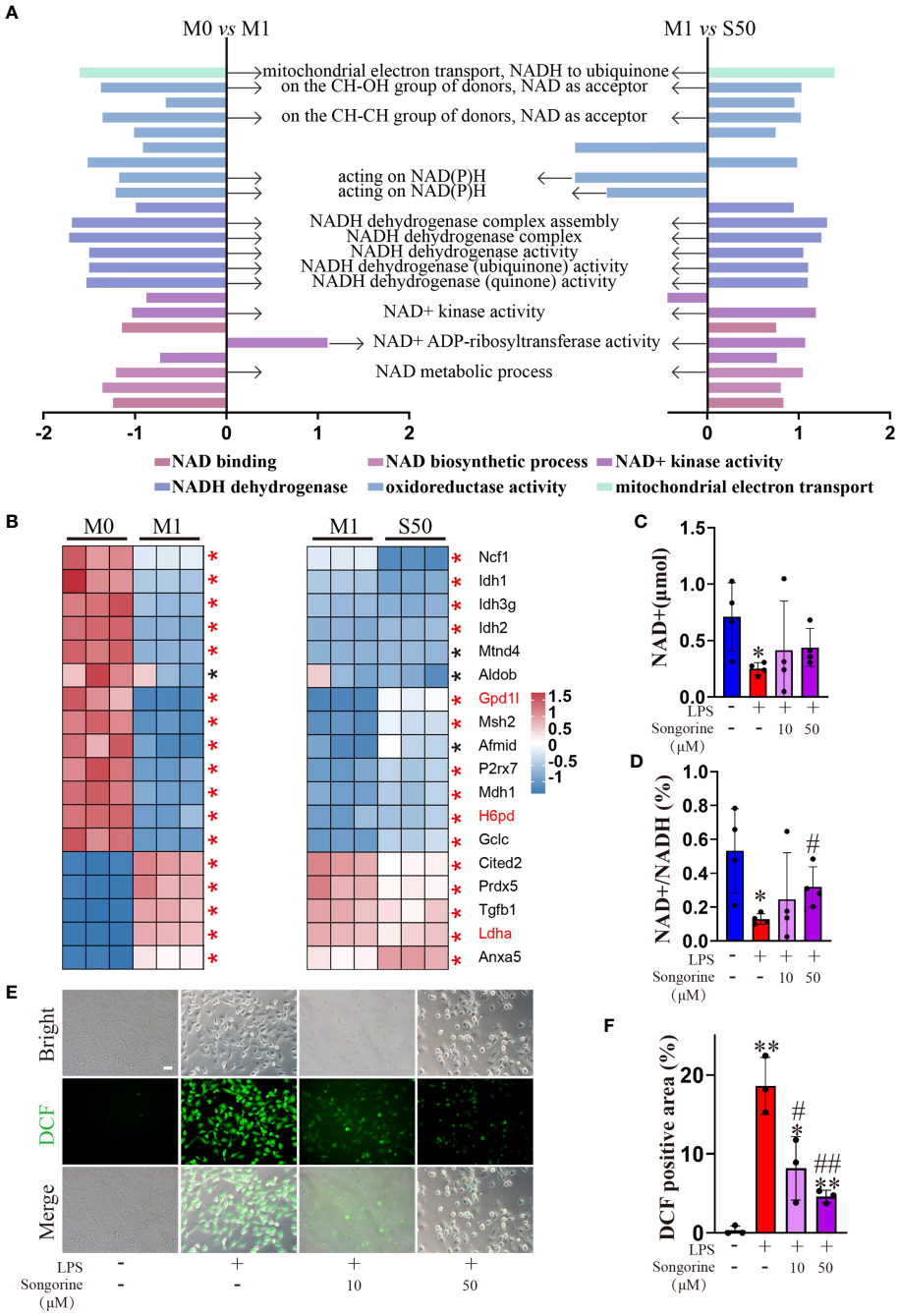

FIGURE 5
Songorine ameliorates oxidative stress in LPS-stimulated macrophages. **(A)** GSEA analysis reveals common core oxidative stress pathways either upregulated or downregulated between data set 1 (M0 vs M1) and data set 2 (M1 vs S50). NES, normalized enrichment score. **(B)** Heat map of relative mRNA expression for genes involved in oxidative stress based on Log2FC in the two datasets (M0 compared to M1; M1 compared to S50). Asterisks indicate $p < 0.05$ (black), $p < 0.01$ (red). **(C)** NAD+ content. **(D)** Ratio of NAD+/NADH. **(E, F)** Macrophages were cultured with different treatments, and ROS levels were assessed using DCFH-DA as a probe, Scale bar: 50 μm. Bar graphs and plots represent mean ± SD, respectively. *$p < 0.05$, **$p < 0.01$ compared with the normal control; #$p < 0.05$, ##$p < 0.01$ compared with the 10μg/mL IL-1β group.

led to a decrease in the CD86-positive area and an increase in the CD206-positive area (Figures 8B, C), indicating a reprogramming of infiltrated M1 macrophages into the M2 phenotype. Additionally, Songorine increased M2-type macrophages (CD206-positive cells) in synovium and decreased IL-1β expression (Figure 8E). Songorine's anti-inflammatory effects were also evident in cartilage tissue, with increased IL-1β expression in the ACLT group (Supplementary Figure S5A) reduced by Songorine. Simultaneously, Songorine promoted SOX9 expression (Supplementary Figure S5B), vital for cartilage maintenance.

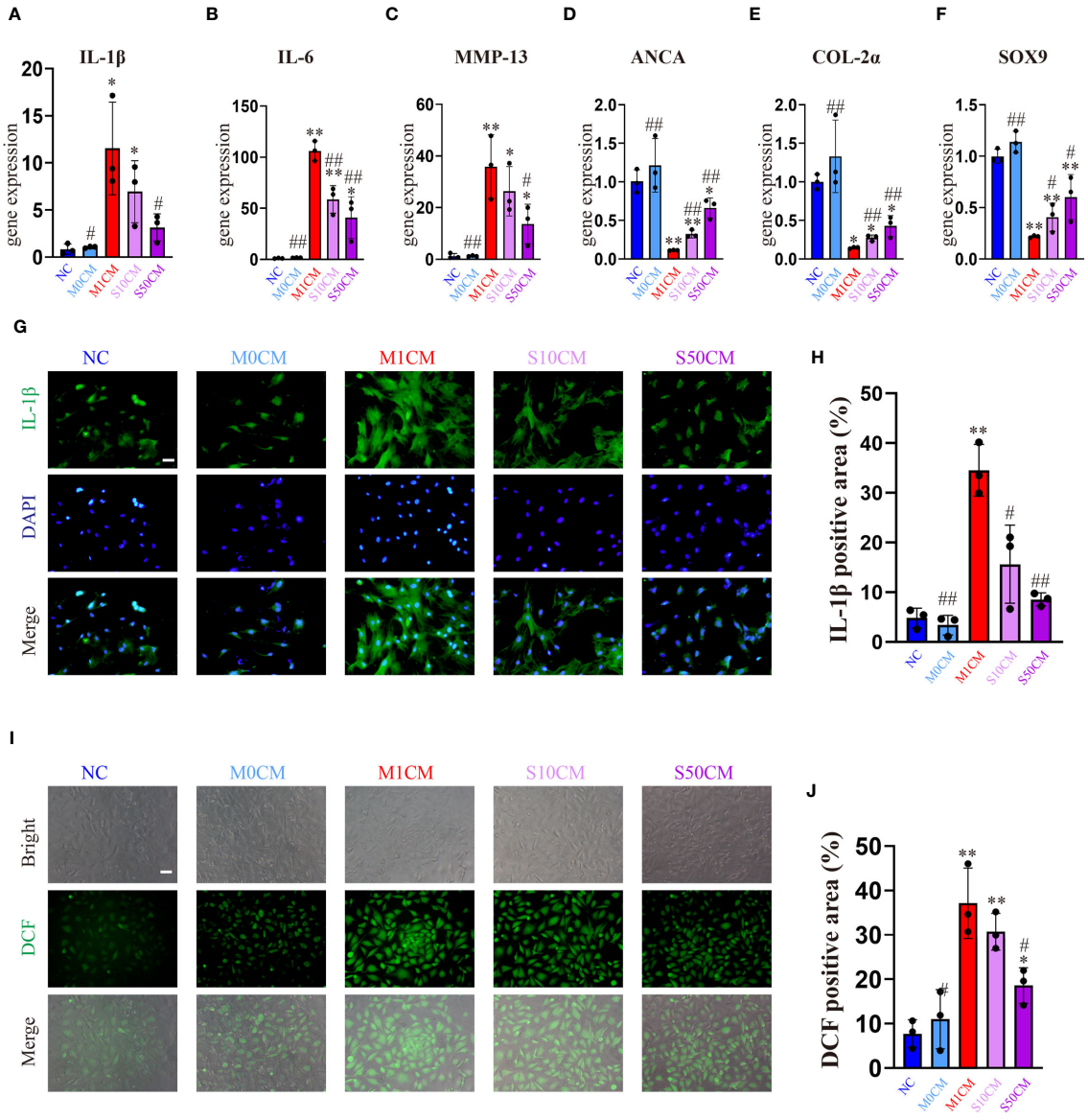

FIGURE 6
Songorine exerts a dual effect by protecting chondrocytes and remodeling the macrophage-induced inflammatory microenvironment. Conditioned media from M1 macrophages, 10μM Songorine-treated M1 macrophages, and 50 μM Songorine-treated M1 macrophages were labeled as M0CM, M1CM, 10SCM, and 50SCM, respectively. **(A–F)** Evaluation of mRNA expression levels of anabolic and pro-inflammatory cytokines, including IL-1β, IL-6, MMP-13, ACAN, COL-2, and SOX-9. **(G, H)** Immunofluorescence and quantification of IL-1β in chondrocytes after exposure to different treatments using macrophage-conditioned media. Scale bar: 50 μm. **(I, J)** Chondrocytes were cultured with different conditioned medium, and ROS levels were measured using DCFH-DA as a probe, Scale bar: 50 μm. *p<0.05, **p<0.01 compared with normal control; $^{\#}p$<0.05, $^{\#\#}p$<0.01 compared with the M1CM group.

4 Discussion

A key finding of our study is the role of metabolic pathways in Songorine's anti-inflammatory mechanism. Metabolic pathways play a crucial role in regulating cellular functions, and their dysregulation is increasingly recognized as a key contributor to inflammatory processes in OA. RNA-seq analysis revealed significant variations in various metabolic pathways, particularly those related to carbohydrate metabolism. Songorine effectively reversed LPS-induced glycolysis pathways, indicating its potential to influence macrophage polarization through metabolic alterations. Molecular docking simulations further supported Songorine's binding affinity to key glycolysis enzymes, providing insights into its direct inhibition of the glycolytic pathway.

OA is a prevalent degenerative joint disorder characterized by inflammation, cartilage degradation, and structural changes (29). Recent research has delved into the molecular mechanisms underlying OA and explored novel therapeutic agents. Macrophages play a crucial role in the pathogenesis of OA, contributing to the inflammatory milieu within the joint (30). Our results demonstrate that Songorine significantly influences the inflammatory microenvironment within the joint. Through a comprehensive analysis using PCR, Western blot, and

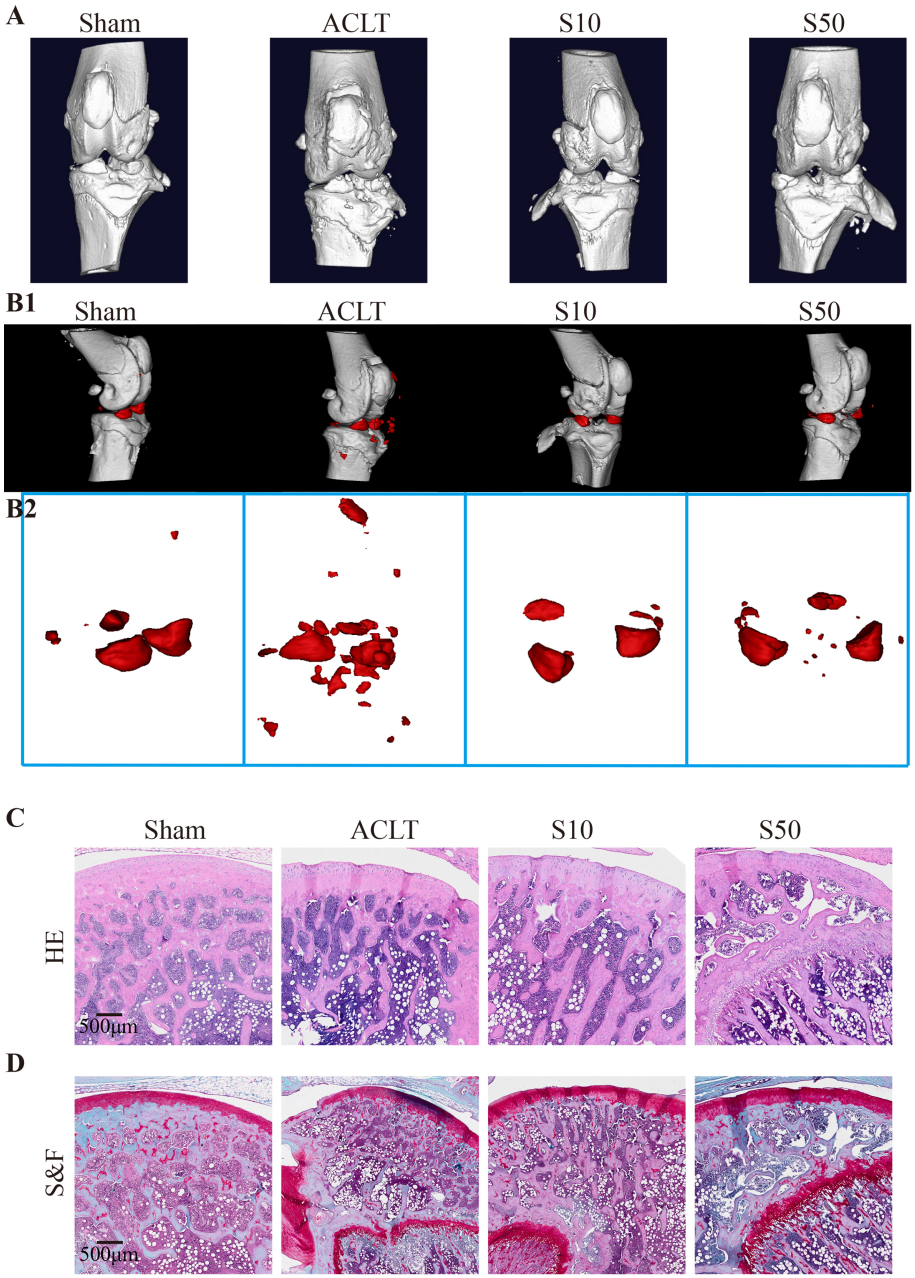

FIGURE 7
Songorine effectively mitigates the remodeling and cartilage damage in the knee joint following ACLT surgery. The sham-operated group is denoted as "sham," the ACLT-operated group as "OA," and the ACLT-operated groups treated with 10μM or 50μM Songorine as "S10" or "S50." **(A)** Three-dimensional micro-CT images vividly portray pathological structural changes in rat knees. **(B1, B2)** Three-dimensional micro-CT images reveal the formation of calcified meniscus and synovial tissue among the groups, with the region marked in red indicating calcified tissue. **(C)** Representative images of H&E-stained sections from rats treated with or without Songorine for 4 weeks. Scale bar: 500 μm. **(D)** Representative images of Safranin O & Fast Green-stained sections from rats treated with or without Songorine for 4 weeks. Scale bar: 500 μm.

immunofluorescence techniques, we observed a notable elevation in pro-inflammatory cytokines, indicating a crucial role in immune function regulation. Importantly, Songorine exhibited a remarkable capacity to modulate macrophage polarization, shifting the balance from the pro-inflammatory M1 phenotype to the anti-inflammatory M2 phenotype. This effect was evidenced by a reduction in M1 macrophage markers and an increase in M2 macrophage markers.

Our study unveiled Songorine's ability to induce metabolic reprogramming in macrophages during LPS stimulation. LPS stimulation induces a robust increase in glycolytic activity in macrophages, facilitating rapid ATP production and providing essential intermediates for biosynthetic pathways. Key enzymes in glycolysis, such as hexokinase and pyruvate kinase, are upregulated to meet the heightened energy demands of activated macrophages (31). This metabolic shift towards glycolysis not only sustains the energy requirements for immune responses but also contributes to the production of inflammatory cytokines. Notably, Songorine suppressed glycolysis in inflamed macrophages in a concentration-

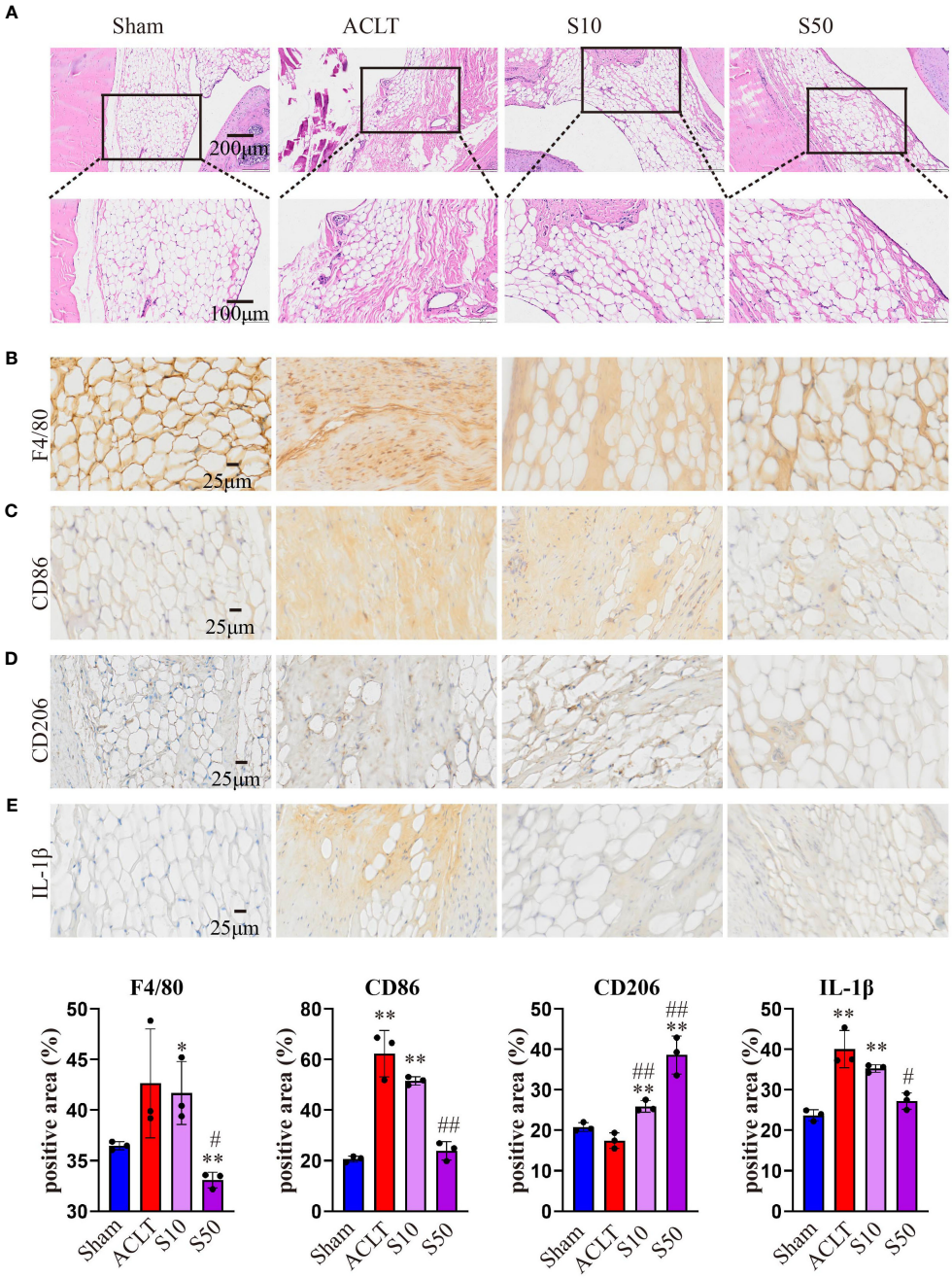

FIGURE 8
Staining evaluations of Songorine in delaying synovial membrane damage in ACLT-induced OA. **(A)** H&E-stained synovial membrane from rats treated with or without Songorine for 4 weeks. **(B–E)** Immunohistochemistry staining for F4/80, CD86, CD206, and IL-1β in the synovial membrane. Scale bar: 25μm.

dependent manner. The interaction between Songorine and metabolic pathways, as indicated by molecular docking simulations, highlighted its tight binding to crucial enzymes involved in glycolysis and the tricarboxylic acid cycle. Metabolic rewiring towards glycolysis emerges as a hallmark of M1 macrophages, characterized by heightened glucose uptake and lactate production. Glycolytic enzymes, such as hexokinase and pyruvate kinase, are upregulated, fueling the energetic demands of M1 polarization (32, 33). Conversely, M2 macrophages exhibit a preference for oxidative phosphorylation, relying on mitochondrial metabolism for energy production. Enhanced fatty acid oxidation (FAO) and tricarboxylic acid (TCA) cycle activity characterize the metabolic landscape of M2 polarization (34). In our study, Songorine reversed glycolysis pathways, as evidenced by specific changes in gene expression and metabolic profiles, suggests a metabolic reprogramming associated with anti-inflammatory effects. This reversal is likely influences macrophage phenotype, reduces the production of inflammatory mediators, and contributes to the resolution of inflammation. The downstream consequences encompass a shift

towards tissue repair, maintenance of cellular homeostasis, and mitigation of oxidative stress, collectively contributing to the potential therapeutic benefits of Songorine in the context of osteoarthritis. This metabolic reprogramming facilitated the inhibition of M1 polarization, promotion of M2 polarization, and support for self-repair processes, including ECM remodeling, enhanced chondrocyte activity, anti-inflammatory signaling, maintenance of redox balance, and modulation of immune responses. The observed metabolic changes collectively create a microenvironment that encourages the innate repair mechanisms of the joint, thereby contributing to the recovery from OA.

Oxidative damage to proteins, lipids, and DNA exacerbates the breakdown of cartilage tissues, a hallmark of OA progression (35). Macrophages in the OA synovium exhibit a skewed polarization profile, with an overabundance of pro-inflammatory M1 macrophages. These M1 macrophages are potent sources of ROS and pro-inflammatory cytokines, creating a microenvironment conducive to oxidative stress-induced damage (35, 36). An intriguing aspect of Songorine's mechanism is its impact on macrophage oxidative stress. By enhancing proton leak, Songorine significantly reduced oxidative stress in LPS-stimulated macrophages. Proton leakage serves as a critical mechanism to regulate mitochondrial membrane potential ($\Delta\Psi m$) and, consequently, ROS generation. Excessive ROS, implicated in oxidative stress, contribute to cellular damage and various pathological conditions. Proton leakage acts as a regulatory brake, preventing ROS accumulation and averting oxidative stress-induced injury to cellular components (37). Gene enrichment analysis revealed the inhibition of oxidative stress-related pathways, emphasizing the importance of NAD metabolism. NAD's involvement in both glycolysis and oxidative phosphorylation positions it as a central player in energy metabolism. This dual engagement plays a critical role in cellular respiration and influences the production of ROS (38). NAD levels can influence proton leakage in mitochondria, thereby impacting the generation of ROS. A dynamic equilibrium exists, wherein adequate NAD levels can modulate proton flux, contributing to the prevention of excessive ROS production (39, 40). Songorine's ability to regulate NAD-related gene expression and maintain intracellular ROS balance suggests its potential as an antioxidant in the context of inflammatory disorders.

Our findings extend beyond macrophage modulation, demonstrating Songorine's ability to shift the immune microenvironment from inflammatory to anti-inflammatory states. Preliminary findings provided insights into similar approaches where the secretome of immune cells has been implicated in influencing the behavior of neighboring cells, particularly in the context of joint disorders (41, 42). In chondrocytes, Songorine suppressed the expression of inflammatory and catabolic genes while promoting anabolic processes. This immunomodulatory effect contributes to the regulation of microenvironments in the joint capsule affected by OA, highlighting the potential of using conditioned media as a valuable tool to understand the broader impact of Songorine on the joint microenvironment and paving the way for novel therapeutic strategies.

The translational significance of our study was underscored by *in vivo* experiments employing a rat model of surgically induced OA. Songorine treatment, especially at a higher concentration, demonstrated protective effects against cartilage damage, synovial inflammation, and bone density reduction. Histological analyses further confirmed Songorine's ability to maintain synovial structure, reprogram macrophages, and attenuate inflammatory responses in articular cartilage. In the upcoming research phase, our primary focus will be on enhancing the *in vivo* anti-inflammatory and cartilage-protective effects of Songorine. This involves exploring innovative delivery systems such as hydrogel carriers to facilitate more efficient and sustained release of Songorine within the joint cavity. Additionally, we aim to delve into more molecular targets of Songorine in osteoarthritis, paving the way for the development of new targeted drugs for the treatment of this condition.

In conclusion, Songorine demonstrates a protective effect on cartilage and synovium, effectively transforming macrophages into an anti-inflammatory M2 phenotype while inhibiting glycolysis and enhancing oxidative phosphorylation. This metabolic reprogramming is associated with a reduction in oxidative stress in macrophages. These findings provide a solid foundation for the potential use of Songorine as a therapeutic agent for osteoarthritis, encouraging further research into its specific molecular targets and clinical applications.

Data availability statement

The datasets presented in this study can be found in online repositories. The names of the repository/repositories and accession number(s) can be found below: PRJNA1069788 (SRA).

Ethics statement

The animal studies were approved by Experimental Animal Center at Guangxi Medical University. The studies were conducted in accordance with the local legislation and institutional requirements. Written informed consent was obtained from the owners for the participation of their animals in this study.

Author contributions

X-XH: Conceptualization, Formal analysis, Investigation, Methodology, Software, Visualization, Writing – original draft. Y-JH: Formal analysis, Investigation, Software, Writing – original draft. C-LH: Software, Writing – original draft. Q-QX: Software, Resources, Supervision, Validation, Visualization, Writing – review & editing. Q-JW: Supervision, Validation, Writing – review & editing, Data curation, Funding acquisition, Project administration.

Funding

The author(s) declare financial support was received for the research, authorship, and/or publication of this article. This research was funded by the Guangxi Key R&D Program, China (GuiKe AB22035014).

Acknowledgments

We are grateful to Clinical Laboratory Center (Guangxi Medical University First Affiliated Hospital) for technique support.

Conflict of interest

The authors declare that the research was conducted in the absence of any commercial or financial relationships that could be construed as a potential conflict of interest.

Publisher's note

All claims expressed in this article are solely those of the authors and do not necessarily represent those of their affiliated organizations, or those of the publisher, the editors and the reviewers. Any product that may be evaluated in this article, or claim that may be made by its manufacturer, is not guaranteed or endorsed by the publisher.

Supplementary material

The Supplementary Material for this article can be found online at: https://www.frontiersin.org/articles/10.3389/fimmu.2024.1344949/full#supplementary-material

SUPPLEMENTARY FIGURE 1
(KEGG) database classified 44 pathways in data set 1(M0 vs M1) and 40 pathways in data set 2(M1 vs S50) into six biological process groups.

SUPPLEMENTARY FIGURE 2
In the GSEA analysis comparing group M1 versus group S50, Songorine was found to positively regulate glucose metabolism, correcting the metabolic dysregulation induced by LPS in macrophages.

SUPPLEMENTARY FIGURE 3
The molecular docking diagram of Songorine binding with six metabolic targets. molecular model of Songorine (left); Three-dimensional (3D) binding model (right) and complexes (down) with the important interacting residues depicted in bright color. The backbone of the protein was rendered in tube and appears blue; Songorine is rendered silver gray; the yellow dash represents the hydrogen bond distance.

SUPPLEMENTARY FIGURE 4
In vivo therapeutic effect of Songorine in ACLT-Induced OA rats. **(A)** The gross observations of knee joint cartilage (femur and tibial plateau), the sham-operated group is marked as sham, ACLT-operated group are marked as OA, and ACLT-operated group treated with 10μM or 50μM Songorine are marked as S10 or S50. **(B)** The Pelletier score of knee joint cartilage. **(C)** Quantification of the volume of calcified meniscus and synovial tissue (Cal Tis.V). **(D)** Analysis of OA-like phenotype severity after ACLT surgery using the Osteoarthritis Research Society International (OARSI) score system. *p<0.05, **p<0.01, versus sham group; #p<0.05, ##p<0.01 compared with the ACLT group.

SUPPLEMENTARY FIGURE 5
Immunohistochemistry staining for IL-1β and SOX9 in knee joint medial compartment cartilage. Scale bar: 25μm.

References

1. Fan X, Wu X, Trevisan Franca De Lima L, Stehbens S, Punyadeera C, Webb R, et al. The deterioration of calcified cartilage integrity reflects the severity of osteoarthritis-A structural, molecular, and biochemical analysis. *FASEB J Off Publ Fed Am Societies Exp Biol* (2022) 36(2):e22142. doi: 10.1096/fj.202101449R

2. Khury F, Oltmanns M, Unseld T, Fuchs M, Reichel H, Faschingbauer M. Which knee phenotypes exhibit the strongest correlation with cartilage degeneration? *Clin orthopaedics related Res* (2023). doi: 10.1097/CORR.0000000000002831

3. Tuckermann J, Adams R. The endothelium-bone axis in development, homeostasis and bone and joint disease. *Nat Rev Rheumatol* (2021) 17(10):608–20. doi: 10.1038/s41584-021-00682-3

4. Wang Q, Lepus C, Raghu H, Reber L, Tsai M, Wong H, et al. IgE-mediated mast cell activation promotes inflammation and cartilage destruction in osteoarthritis. *eLife* (2019) 8:e39905. doi: 10.7554/eLife.39905

5. Courties A, Olmer M, Myers K, Ordoukhanian P, Head S, Natarajan P, et al. Human-specific duplicate CHRFAM7A gene is associated with more severe osteoarthritis and amplifies pain behaviours. *Ann rheumatic diseases.* (2023) 82 (5):710–8. doi: 10.1136/ard-2022-223470

6. Shkhyan R, Flynn C, Lamoure E, Sarkar A, Van Handel B, Li J, et al. Inhibition of a signaling modality within the gp130 receptor enhances tissue regeneration and mitigates osteoarthritis. *Sci Trans Med* (2023) 15(688):eabq2395. doi: 10.1126/scitranslmed.abq2395

7. Yang Y, Jian Y, Liu Y, Xie Q, Yu H, Wang B, et al. Heilaohuacid G, a new triterpenoid from Kadsura coccinea inhibits proliferation, induces apoptosis, and ameliorates inflammation in RA-FLS and RAW 264.7 cells via suppressing NF-. *Phytotherapy Res PTR* (2022) 36(10):3900–10. doi: 10.1002/ptr.7527

8. Hsieh C, Wang C, Tayo L, Deng S, Tsai P, Lee C. *In vitro* and in *vivo* anti-osteoarthritis effects of tradition Chinese prescription Ji-Ming-San. *J Ethnopharmacol* (2023) 305:116084. doi: 10.1016/j.jep.2022.116084

9. Yao L, Wu X, Jiang X, Shan M, Zhang Z, Li Y, et al. Subcellular compartmentalization in the biosynthesis and engineering of plant natural products. *Biotechnol advances.* (2023) 69:108258. doi: 10.1016/j.biotechadv.2023.108258

10. Lephatsi M, Choene M, Kappo A, Madala N, Tugizimana F. An integrated molecular networking and docking approach to characterize the metabolome of Helichrysum splendidum and its pharmaceutical potentials. *Metabolites* (2023) 13 (10):1104. doi: 10.3390/metabo13101104

11. Han J, Lee E, Park W, Ha K, Chung H. Natural compounds as lactate dehydrogenase inhibitors: potential therapeutics for lactate dehydrogenase inhibitors-related diseases. *Front Pharmacol* (2023) 14:1275000. doi: 10.3389/fphar.2023.1275000

12. Zhang H, Dong R, Zhang P, Wang Y. Songorine suppresses cell growth and metastasis in epithelial ovarian cancer via the Bcl−2/Bax and GSK3β/β−catenin signaling pathways. *Oncol Rep* (2019) 41(5):3069–79. doi: 10.3892/or.2019.7070

13. Ren Z, Zhang H, Yang L, Wang Z, Xiong J, Zheng P, et al. Targeted preparation and recognition mechanism of broad-spectrum antibody specific to Aconitum alkaloids based on molecular modeling and its application in immunoassay. *Analytica Chimica Acta* (2022) 1222:340011. doi: 10.1016/j.aca.2022.340011

14. He G, Wang X, Liu W, Li Y, Shao Y, Liu W, et al. Chemical constituents, pharmacological effects, toxicology, processing and compatibility of Fuzi (lateral root of Aconitum carmichaelii Debx): A review. *J ethnopharmacology.* (2023) 307:116160. doi: 10.1016/j.jep.2023.116160

15. Yao J, Chen C, Sun Y, Lin Y, Tian Z, Liu X, et al. Higenamine exerts antidepressant effect by improving the astrocytic gap junctions and inflammatory response. *J Affect Disord* (2023) 348:107–15. doi: 10.1016/j.jad.2023.12.020

16. Khan H, Nabavi S, Sureda A, Mehterov N, Gulei D, Berindan-Neagoe I, et al. Therapeutic potential of songorine, a diterpenoid alkaloid of the genus Aconitum. *Eur J Medicinal Chem* (2018) 153:29–33. doi: 10.1016/j.ejmech.2017.10.065

17. Zhao X, Wang Y, Li Y, Chen X, Yang H, Yue J, et al. Songorine, a diterpenoid alkaloid of the genus Aconitum, is a novel GABA(A) receptor antagonist in rat brain. *Neurosci Lett* (2003) 337(1):33–6. doi: 10.1016/S0304-3940(02)01299-5

18. Ameri A. Effects of the Aconitum alkaloid songorine on synaptic transmission and paired-pulse facilitation of CA1 pyramidal cells in rat hippocampal slices. *Br J Pharmacol* (1998) 125(3):461–8. doi: 10.1038/sj.bjp.0702100

19. Xiong J, He J, Zhu J, Pan J, Liao W, Ye H, et al. Lactylation-driven METTL3-mediated RNA mA modification promotes immunosuppression of tumor-infiltrating myeloid cells. *Mol Cell* (2022) 82(9):1660–77.e10. doi: 10.1016/j.molcel.2022.02.033

20. Van Acker Z, Perdok A, Hellemans R, North K, Vorsters I, Cappel C, et al. Phospholipase D3 degrades mitochondrial DNA to regulate nucleotide signaling and APP metabolism. *Nat Commun* (2023) 14(1):2847. doi: 10.1038/s41467-023-38501-w

21. Reddy V, Chinta K, Saini V, Glasgow J, Hull T, Traylor A, et al. Mycobacterium tuberculosisFerritin H deficiency in myeloid compartments dysregulates host energy metabolism and increases susceptibility to infection. *Front Immunol* (2018) 9:860. doi: 10.3389/fimmu.2018.00860

22. Jia R, Du J, Cao L, Feng W, He Q, Xu P, et al. Application of transcriptome analysis to understand the adverse effects of hydrogen peroxide exposure on brain function in common carp (Cyprinus carpio). *Environ Pollut (Barking Essex 1987).* (2021) 286:117240. doi: 10.1016/j.envpol.2021.117240

23. Lan C, Chen C, Qu S, Cao N, Luo H, Yu C, et al. Inhibition of DYRK1A, via histone modification, promotes cardiomyocyte cell cycle activation and cardiac repair after myocardial infarction. *EBioMedicine* (2022) 82:104139. doi: 10.1016/j.ebiom.2022.104139

24. Guo H, Yin W, Zou Z, Zhang C, Sun M, Min L, et al. Quercitrin alleviates cartilage extracellular matrix degradation and delays ACLT rat osteoarthritis development: An in *vivo* and in *vitro* study. *J Adv Res* (2021) 28:255–67. doi: 10.1016/j.jare.2020.06.020

25. Zhu J, Zhu Y, Xiao W, Hu Y, Li Y. Instability and excessive mechanical loading mediate subchondral bone changes to induce osteoarthritis. *Ann Trans Med* (2020) 8 (6):350. doi: 10.21037/atm.2020.02.103

26. Kou L, Huang H, Tang Y, Sun M, Li Y, Wu J, et al. Opsonized nanoparticles target and regulate macrophage polarization for osteoarthritis therapy: A trapping strategy. *J Control Release.* (2022) 347:237–55. doi: 10.1016/j.jconrel.2022.04.037

27. Lu E, Wu L, Chen B, Xu S, Fu Z, Wu Y, et al. Maternal serum tRNA-derived fragments (tRFs) as potential candidates for diagnosis of fetal congenital heart disease. *J Cardiovasc Dev Dis* (2023) 10(2):78. doi: 10.3390/jcdd10020078

28. Li Y, Zang H, Zhang X, Huang G. Exosomal Circ-ZNF652 Promotes Cell Proliferation, Migration, Invasion and Glycolysis in Hepatocellular Carcinoma via miR-29a-3p/GUCD1 Axis. *Cancer Manag Res* (2020) 12:7739–51. doi: 10.2147/CMAR.S259424

29. Li X, Tao H, Zhou J, Zhang L, Shi Y, Zhang C, et al. MAGL inhibition relieves synovial inflammation and pain via regulating NOX4-Nrf2 redox balance in osteoarthritis. *Free Radical Biol Med* (2023) 208:13–25. doi: 10.1016/j.freeradbiomed.2023.07.019

30. Liao Z, Umar M, Huang X, Qin L, Xiao G, Chen Y, et al. Transient receptor potential vanilloid 1: A potential therapeutic target for the treatment of osteoarthritis and rheumatoid arthritis. *Cell Prolif* (2023) e13569. doi: 10.1111/cpr.13569

31. Mi Y, Tang M, Wu Q, Wang Y, Liu Q, Zhu P, et al. NMAAP1 regulated macrophage polarizion into M1 type through glycolysis stimulated with BCG. *Int immunopharmacology.* (2023) 126:111257. doi: 10.1016/j.intimp.2023.111257

32. Palmieri E, Holewinski R, McGinity C, Pierri C, Maio N, Weiss J, et al. Pyruvate dehydrogenase operates as an intramolecular nitroxyl generator during macrophage metabolic reprogramming. *Nat Commun* (2023) 14(1):5114. doi: 10.1038/s41467-023-40738-4

33. Gauthier T, Yao C, Dowdy T, Jin W, Lim Y, Patiño L, et al. TGF-β uncouples glycolysis and inflammation in macrophages and controls survival during sepsis. *Sci Signaling* (2023) 16(797):eade0385. doi: 10.1126/scisignal.ade0385

34. Peace C, O'Carroll S, O'Neill L. Fumarate hydratase as a metabolic regulator of immunity. *Trends Cell Biol* (2023) 6:S0962-8924(23)00209-X. doi: 10.1016/j.tcb.2023.10.005

35. Lei L, Cong R, Ni Y, Cui X, Wang X, Ren H, et al. Dual-functional injectable hydrogel for osteoarthritis treatments. *Adv Healthc Mater* (2023) e2302551. doi: 10.1002/adhm.202302551

36. Miao M, Su Q, Cui Y, Bahnson E, Li G, Wang M, et al. Redox-active endosomes mediate α5β1 integrin signaling and promote chondrocyte matrix metalloproteinase production in osteoarthritis. *Sci Signaling* (2023) 16(809):eadf8299. doi: 10.1126/scisignal.adf8299

37. Chen C, Zhang L, Jin Z, Kasumov T, Chen Y. Mitochondrial redox regulation and myocardial ischemia-reperfusion injury. *Am J Physiol Cell Physiol* (2022) 322(1): C12–23. doi: 10.1152/ajpcell.00131.2021

38. Esaki N, Matsui T, Tsuda T. viaLactate induces the development of beige adipocytes an increase in the level of reactive oxygen species. *Food Funct* (2023) 14 (21):9725–33. doi: 10.1039/D3FO03287F

39. Li Q, Zhou M, Chhajed S, Yu F, Chen S, Zhang Y, et al. N-hydroxypipecolic acid triggers systemic acquired resistance through extracellular NAD(P). *Nat Commun* (2023) 14(1):6848. doi: 10.1038/s41467-023-42629-0

40. Kang H, Kim S, Lee JY, Kim B. Inhibitory effects of ginsenoside compound K on lipopolysaccharide-stimulated inflammatory responses in macrophages by regulating sirtuin 1 and histone deacetylase 4. *Nutrients* (2023) 15(7):1626. doi: 10.3390/nu15071626

41. Gauthier T, Martin-Rodriguez O, Chagué C, Daoui A, Ceroi A, Varin A, et al. Amelioration of experimental autoimmune encephalomyelitis by in *vivo* reprogramming of macrophages using pro-resolving factors. *J Neuroinflamm* (2023) 20(1):307. doi: 10.1186/s12974-023-02994-5

42. Zheng M, Zhu Y, Wei K, Pu H, Peng R, Xiao J, et al. Metformin attenuates the inflammatory response via the regulation of synovial M1 macrophage in osteoarthritis. *Int J Mol Sci* (2023) 24(6):5355. doi: 10.3390/ijms24065355

frontiers | Frontiers in Immunology

TYPE Original Research
PUBLISHED 27 February 2024
DOI 10.3389/fimmu.2024.1335112

OPEN ACCESS

EDITED BY
Pablo Andres Evelson,
University of Buenos Aires, Argentina

REVIEWED BY
Keiichi Ishihara,
Kyoto Pharmaceutical University, Japan
Junjie Zhang,
Gannan Medical University, China

*CORRESPONDENCE
Qiang You
qiang.you@njmu.edu.cn
Ting Zhao
tingzhao@fudan.edu.cn

RECEIVED 08 November 2023
ACCEPTED 08 February 2024
PUBLISHED 27 February 2024

CITATION
Wang H, Cheng W, Hu P, Ling T, Hu C, Chen Y, Zheng Y, Wang J, Zhao T and You Q (2024) Integrative analysis identifies oxidative stress biomarkers in non-alcoholic fatty liver disease via machine learning and weighted gene co-expression network analysis. *Front. Immunol.* 15:1335112. doi: 10.3389/fimmu.2024.1335112

Integrative analysis identifies oxidative stress biomarkers in non-alcoholic fatty liver disease via machine learning and weighted gene co-expression network analysis

Haining Wang[1], Wei Cheng[1], Ping Hu[2], Tao Ling[1], Chao Hu[1], Yongzhen Chen[1], Yanan Zheng[1], Junqi Wang[3], Ting Zhao[4]* and Qiang You[1]*

[1]Medical Center for Digestive Diseases, Department of Geriatrics, the Second Affiliated Hospital of Nanjing Medical University, Nanjing, China, [2]Department of Orthopedics, Tianjin Medical University General Hospital, Tianjin, China, [3]Department of Medical Oncology, Shenzhen Traditional Chinese Medicine Hospital, Shenzhen, China, [4]Department of Medical Oncology, Fudan University Shanghai Cancer Center, Shanghai, China

Background: Non-alcoholic fatty liver disease (NAFLD) is the most common chronic liver disease globally, with the potential to progress to non-alcoholic steatohepatitis (NASH), cirrhosis, and even hepatocellular carcinoma. Given the absence of effective treatments to halt its progression, novel molecular approaches to the NAFLD diagnosis and treatment are of paramount importance.

Methods: Firstly, we downloaded oxidative stress-related genes from the GeneCards database and retrieved NAFLD-related datasets from the GEO database. Using the Limma R package and WGCNA, we identified differentially expressed genes closely associated with NAFLD. In our study, we identified 31 intersection genes by analyzing the intersection among oxidative stress-related genes, NAFLD-related genes, and genes closely associated with NAFLD as identified through Weighted Gene Co-expression Network Analysis (WGCNA). In a study of 31 intersection genes between NAFLD and Oxidative Stress (OS), we identified three hub genes using three machine learning algorithms: Least Absolute Shrinkage and Selection Operator (LASSO) regression, Support Vector Machine - Recursive Feature Elimination (SVM-RFE), and RandomForest. Subsequently, a nomogram was utilized to predict the incidence of NAFLD. The CIBERSORT algorithm was employed for immune infiltration analysis, single sample Gene Set Enrichment Analysis (ssGSEA) for functional enrichment analysis, and Protein-Protein Interaction (PPI) networks to explore the relationships between the three hub genes and other intersecting genes of NAFLD and OS. The distribution of these three hub genes across six cell clusters was determined using single-cell RNA sequencing. Finally, utilizing relevant data from the Attie Lab Diabetes Database, and liver tissues from NASH mouse model, Western Blot (WB) and Reverse Transcription Quantitative Polymerase Chain Reaction (RT-qPCR) assays were conducted, this further validated the significant roles of CDKN1B and TFAM in NAFLD.

Results: In the course of this research, we identified 31 genes with a strong association with oxidative stress in NAFLD. Subsequent machine learning analysis and external validation pinpointed two genes: CDKN1B and TFAM, as demonstrating the closest correlation to oxidative stress in NAFLD.

Conclusion: This investigation found two hub genes that hold potential as novel targets for the diagnosis and treatment of NAFLD, thereby offering innovative perspectives for its clinical management.

KEYWORDS

non-alcoholic fatty liver disease, bioinformatic analysis, machine learning, WGCNA, CDKN1B, NDUFA4, TFAM

Introduction

Approximately 25% of the global population is afflicted with Non-alcoholic fatty liver disease (NAFLD), although the prevalence varies due to regional disparities. The Middle East (32%) and South America (30%) exhibit the highest rates, while the prevalence is 24% in North America and Europe, 27% in Asia, and the lowest in Africa at 13% (1). The American Association for the Study of Liver Diseases (AASLD) has defined NAFLD in its practice guidelines as: (a) the presence of hepatic steatosis, either by imaging or histology, and (b) no causes for secondary hepatic fat accumulation, such as significant alcohol consumption, use of steatogenic medication, or hereditary disorders (2).

NAFLD can be further subdivided into Non-alcoholic fatty liver (NAFL) and Non-alcoholic steatohepatitis (NASH) (3). NAFL is defined by hepatic steatosis without evidence of hepatocellular injury in the form of hepatocyte ballooning. Conversely, NASH is characterized by hepatic steatosis and inflammation with hepatocyte injury, with or without fibrosis (4). NAFL can transform into NASH, which is characterized by hepatocellular ballooning and lobular inflammation as well as steatosis. Perisinusoidal fibrosis is typically not considered a prerequisite for diagnosing NASH (5). NAFLD may evolve into cirrhosis and hepatocellular carcinoma (HCC) (6), with HCC representing the fourth leading cause of cancer-related deaths worldwide (7). In the United States, NASH is the second most common indication for liver transplantation (8). Among U.S. HCC patients requiring liver transplantation, those with NAFLD represent the fastest-growing group (9), highlighting the substantial disease burden posed by NAFLD.

Oxidative stress (OS) means an imbalance between oxidative and antioxidative processes within an organism. Under these conditions, the quantity of Reactive Oxygen Species (ROS) and Reactive Nitrogen Species (RNS) produced by the organism surpasses its antioxidative capabilities, thereby inducing oxidative damage. ROS and RNS are small molecules with robust oxidative characteristics, encompassing both free radicals and non-free radicals, such as superoxide anions, hydroxyl free radicals, hydrogen peroxide, and nitric oxide. When tissues, cells, and biological macromolecules are exposed to these excessive oxidants over an extended period, a series of biochemical reactions are triggered, causing oxidative damage and consequently, impairing normal cellular functions. Prolonged oxidative stress is regarded as a pivotal factor in instigating various diseases such as cardiovascular diseases (10), cancer (11), neurodegenerative diseases (12), diabetes (13), and aging (14). To prevent oxidative damage, an antioxidative system exists within the organism, consisting of antioxidative enzymes (such as superoxide dismutase and catalase) and non-enzymatic antioxidants (such as vitamin C, vitamin E, and glutathione). This system can neutralize ROS and RNS, shielding cells from their detrimental effects.

In animal experiments, we found that carbon tetrachloride can lead to hepatic fat accumulation and damage. After reviewing the literature, we learned from several studies by Slater et al. that free radicals play a key role in causing liver damage (15). This implies that free radicals play a pathogenic role in initiating liver diseases, while antioxidants have therapeutic effects on free radical-mediated NAFLD (16). Furthermore, epidemiological, clinical, and experimental research targeting the liver reveals that NAFLD is closely associated with alterations in redox status and subsequent increased metabolic risk (17). According to the "second hit" and "multiple hit" theories, oxidative stress appears to be one of the most critical mechanisms causing NAFLD liver injury and plays a vital role in the progression from NAFL to NASH (18). Studies have demonstrated that the liver is a principal organ attacked by ROS (19), where an increase in ROS can induce lipid peroxidation by activating Hepatic Stellate Cells (HSC), thereby resulting in inflammation and fibrosis formation. Moreover, ROS can inhibit hepatic VLDL secretion, inducing hepatic fat accumulation, and also promote hepatic insulin resistance and necrotizing inflammation, activating several cell pathways leading to hepatocyte apoptosis (20). Several interrelated pro-oxidative factors, along with mitochondrial dysfunction, might also contribute to the occurrence of OS. Targeted research on OS represents a promising direction in treating NASH.

Inspired by these pioneering studies, we decided to explore the relationship between NAFLD and OS through bioinformatics analysis, hoping to offer new insights and guidance for the clinical diagnosis and treatment of NAFLD.

In this research, based on the results of the Limma package and Weighted Gene Co-expression Network Analysis (WGCNA), we identified 31 genes related to NAFLD and OS. Furthermore, we employed three machine learning algorithms—Least Absolute Shrinkage and Selection Operator (LASSO), Support Vector Machine-Recursive Feature Elimination (SVM-RFE), and RandomForest to examine these genes. The results suggested that CDKN1B, NDUFA4, and TFAM are intimately related to oxidative stress in NAFLD, providing new insights for the diagnosis and treatment of NAFLD.

Materials and methods

Data collection and processing

Figure 1 was created to show the flowchart of our data analysis process. The datasets GSE33814 (GPL570) and GSE48452 (GPL11532) were retrieved and downloaded from the Gene Expression Omnibus (GEO) database (https://www.ncbi.nlm.nih.gov/geo/). GSE33814 consists of 44 samples: 13 control, 19 NAFL, and 12 NASH. GSE48452 consists of 46 samples: 14 control, 14 NAFL, and 18 NASH, serving as a dataset for validation. It is imperative to note that many studies on NAFLD that undergo bioinformatic analysis selectively utilize samples from the more severe NAFLD stage, NASH, for analysis. For the sake of academic rigor in this study, NAFL samples have been included in addition to NASH samples. The "Limma" package (21) was utilized for normalizing sample data, conducting conversion between probe ID and gene symbols through coding, eliminating probes without gene symbols, and calculating the average expression value under the same symbol.

Genes related to OS were retrieved and downloaded from the Genecard database (https://www.genecards.org/), using a relevance score greater than 7 as a selection criterion (22), resulting in the extraction of 1065 genes associated with oxidative stress.

Implementation of WGCNA and identification of key module genes

WGCNA is a robust systems biology method, designed for identifying coexpressed gene modules and exploring associations between gene networks and notable phenotypes, along with deciphering key genes within the networks. WGCNA enables the

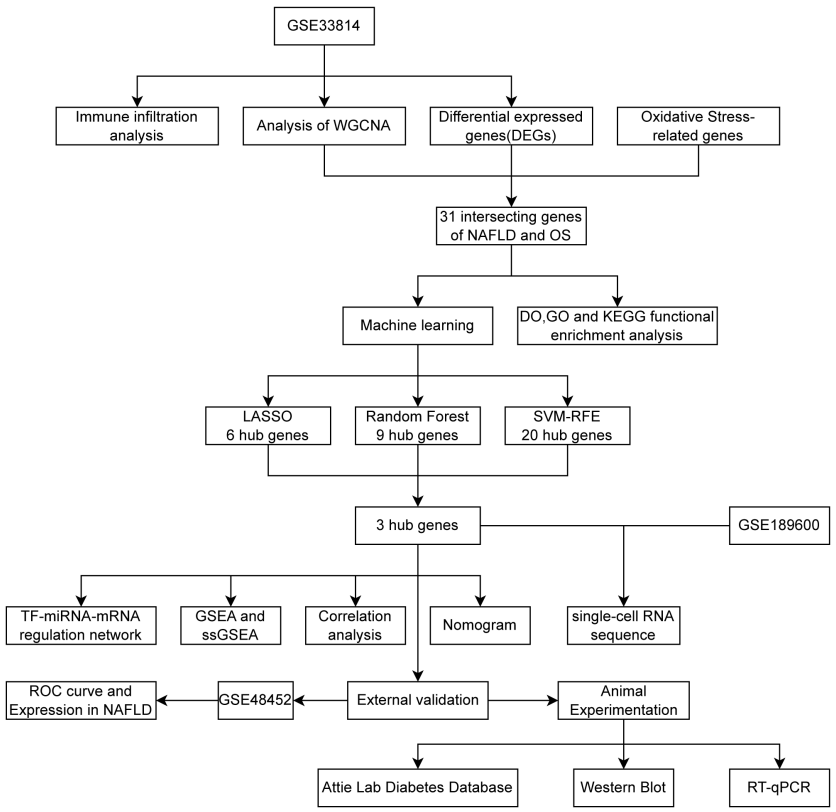

FIGURE 1
Flowchart 3 hub genes (CDKN1B,NDUFA4,TFAM) identified by three machine learning algorithms.

discovery of highly correlated gene clusters, which typically share common functionalities within biological processes. Significantly, WGCNA constructs a weighted network, indicating that connections within the network not only represent a binary existence but also mirror the correlation strength among genes, an essential feature to accurately represent intricate relationships between genes.

In our research, WGCNA, implemented through the R package "WGCNA" (23), was utilized to identify modules with the highest relevance to NAFLD. WGCNA encompasses five primary steps: gene clustering, assessing whether the soft-thresholding power approximates a scale-free network, merging similar modules (with the cut height for merging modules set at 0.25 and MEDissThres = 0.25, implying the merging of modules with a similarity greater than 0.75), associating modules with traits, and identifying genes with the highest correlation. To determine whether two gene modules possess similar expression patterns, a threshold is typically set to sift through and merge gene modules that are deemed similar when exceeding this threshold.

Preprocessing of data and selection of differentially expressed genes

Utilizing the "Limma" R package, with |log2Fold change(FC)| > 0.3 and $p < 0.05$ as the selection criteria, 592 DEGs were identified within the GSE33814 dataset. Heatmaps and volcano plots for DEGs were generated using the "pheatmap" (24) and "ggplot2" (25) packages.

Establishment of Venn diagram

The Venn diagram were constructed using the Evenn website (http://www.ehbio.com/test/venn/).

Conducting functional enrichment analysis

In this research, the "ClusterProfiler" R package (26) was employed for Gene Ontology (GO) enrichment analysis, encompassing Biological Process (BP), Molecular Function (MF), and Cellular Component (CC), as well as Kyoto Encyclopedia of Genes and Genomes (KEGG) and Disease Ontology (DO) functional enrichment analysis. A p-value of <0.05 was considered statistically significant.

Application of machine learning for screening hub genes

LASSO regression is a regression analysis method that enhances the predictive accuracy of models by conducting variable selection and adjusting complexity through the compression of regression coefficients. A notable advantage of LASSO regression is its ability to simultaneously retain valuable features while compressing coefficients of irrelevant or less important features to zero, thus serving not only predictive purposes but also facilitating variable selection and model interpretation. Specifically, LASSO regression is achieved by introducing a regularization term, Lambda, to the foundation of Ordinary Least Squares (OLS) regression. The regularization term, constituting the sum of the absolute values of all regression coefficients, allows control over the magnitude of the regression coefficients. When the coefficient of the regularization term is adequately large, certain regression coefficients will be reduced to zero, thereby enabling feature selection.

SVM-RFE is a technique employed for feature selection, utilizing SVM to recursively eliminate the least important features. SVM-RFE operates through an iterative process, wherein the least crucial feature is removed at each step based on the coefficients of the SVM model, then an SVM model is rebuilt using the remaining features. This process persists until the desired number of features is attained. The technique offers the advantage of selecting a highly informative set of features within high-dimensional data, thus enhancing the model's generalization capability.

RandomForest is an ensemble learning method that enhances predictive accuracy and robustness by aggregating the predictive results of multiple decision trees. The RandomForest algorithm can be applied to both classification and regression problems. The algorithm derives its name from its working principle: during the training process, the RandomForest randomly selects features from the feature set and constructs numerous decision trees. Each tree is trained on an independent subset of samples, obtained through bootstrap sampling. The predictive process of the RandomForest is as follows: in classification problems, a new input sample is predicted individually by all the decision trees, and the final prediction is determined by majority voting; in regression problems, the final prediction is the average of the predictions made by all the decision trees.

LASSO regression is executed using the "glmnet" package (27). SVM-RFE is realized utilizing the "e1071" (28) and "caret" packages (29). RandomForest is implemented using the "randomForest" package (30).

Establishment of protein-protein interaction network

We utilized the "STRINGdb" package (31) to construct a PPI network and used the "igraph" package (32) to visualize the PPI of hub genes, based on betweenness values. Simultaneously, we used the GeneMANIA website (http://genemania.org/) to build a protein-protein interaction network.

Analysis of immune infiltration

CIBERSORT is a computational biology tool that employs a deconvolution algorithm to estimate the proportions of 22 immune

cell types in both NAFLD and control groups, based on gene expression data. It is capable of quantitatively estimating the presence of immune cells in tissue samples without direct measurement of immune cell infiltration.

Construction of nomogram and analysis of ROC curve

A nomogram is a graphical tool widely used to predict the probability of a particular outcome based on a series of variables. In this study, the nomogram was constructed using the "rms" package (33).

The ROC curve is a graphical tool utilized to evaluate the predictive performance of hub genes. It illustrates the performance of hub genes across all possible classification thresholds by plotting the relationship between the True Positive Rate (TPR) and False Positive Rate (FPR) at various thresholds. In this research, the ROC curve was developed using the "pROC" package (34).

Conducting gene set enrichment analysis of hub genes and single sample gene set enrichment analysis of hallmark gene sets

We conducted a single-gene GSEA to investigate the potential roles of hub genes. ssGSEA is employed to extract the enrichment score of specific gene sets from the gene expression data of a single sample. ssGSEA considers the rankings of all genes, not just those that are significantly differentially expressed. The ssGSEA scores can be interpreted as the rank of gene expression relative to background gene expression within a given gene set. The Hallmark gene sets, created by the Molecular Signatures Database (MSigDB) project at the Broad Institute, aim to condense and reorganize the broader C2 Canonical pathways gene sets. Encompassing 50 distinct sets, each represents a specific biological process. The design of Hallmark gene sets seeks to clarify the relationship between gene function and biological processes. Each Hallmark gene set captures a specific biological state or process by summarizing multiple similar gene sets and extracting their common variation through Principal Component Analysis (PCA). This approach benefits from reduced redundancy and noise, enhancing the biological significance of the gene set. Combining ssGSEA with Hallmark gene sets aids in understanding the activity levels of various biological processes and pathways within a single sample.

Processing of single-cell sequencing data

The single-cell RNA sequencing (scRNA-seq) dataset GSE189600 was downloaded from the GEO database, comprising three NASH samples and three healthy samples serving as control (35). The analytical process unfolded as follows: Post-Quality Control (QC), the 10x scRNA-seq data was converted into Seurat objects, followed by a reduction in feature dimensions utilizing PCA and Uniform Manifold Approximation and Projection (UMAP) to identify distinct cellular subgroups. Subsequently, marker genes within different clusters were detected, and various cell types were annotated, followed by functional enrichment analysis. The "Linnorm" (36), "scater" (37), "Seurat" (38) and "SingleR" (39) packages were utilized throughout this process.

TF-miRNA-mRNA regulatory network

The NetworkAnalyst website (https://www.networkanalyst.ca/NetworkAnalyst/) encompasses numerous databases to predict potential Transcription Factors (TFs) and microRNAs (miRNAs). In the present study, Transcription factor targets were derived from the JASPAR database, and Comprehensive experimentally validated miRNA-gene interaction data were collected from the miRTarBase v8.0 database.

Attie lab diabetes database

The BTBR ob/ob mouse model is extensively used in the study of Type 2 Diabetes (T2D) and obesity in laboratory settings. This model combines the characteristics of the BTBR strain with mutations in the leptin gene (ob/ob), which are key factors in the onset of obesity and diabetic symptoms. The database allows for the querying of gene expression in six critical tissues, including the islets, liver, adipose tissue, hypothalamus, gastrocnemius muscle, and soleus muscle, based on variables such as genetic obesity status (lean *vs* ob/ob), mouse strain (B6 *vs* BTBR), and different age stages (4 weeks old *vs* 10 weeks old). This study employs the mlratio as a metric to assess changes in gene expression, where mlratio refers to the base-10 logarithm of the ratio of gene expression in an experimental sample (individual mice) relative to a specific strain reference pool (B6 strain or BTBR strain). The reference pool data is derived from 20 mice per strain, including lean and ob/ob mice at ages of 4 weeks and 10 weeks, with five mice from each age group. Our research focuses on the liver tissue of 10-week-old lean and ob/ob mice from both B6 and BTBR strains, with statistical analysis and graphical representation conducted using GraphPad Prism 9.

NASH mouse model

In this study, we utilized female C57BL/6 mice, aged between 6 to 8 weeks, and subjected them to a high-fat, high-cholesterol (HFHC) diet while administering intraperitoneal injections of CCl4. This regimen was maintained for a total duration of 17 weeks to establish a NASH mouse model. The CCl4 injections were given once weekly at a dosage of 0.32 μg/g. The HFHC diet, acquired from Dyets Inc, under the product code D18061501, is characterized as a Modified Western Diet with 41% sucrose and 1.25% cholesterol. The caloric content of the diet was distributed as follows: 17% from protein, 43% from carbohydrates, and 40% from fats.

RT-qPCR

Liver tissues from wild-type (wt) mice and NASH models were thoroughly homogenized, and RNA was extracted using the TRIzol method. Subsequent reverse transcription and PCR processes were conducted using Vazyme's reverse transcription kit (catalog number R323) and PCR kit (catalog number Q341), respectively. The reverse transcription was performed on the GeneAmp PCR System 9700 from Applied Biosystems, while PCR amplification was carried out on the LightCycler 480 II system from Roche. All primers were purchased from Sangon Biotech. The primer sequences for RT-PCR are as follows: GAPDH: forward AGGTCGGTGTGAACGGATTTG, reverse TGTAGACCATGTAGTTGAGGTCA;CDKN1B: forward AGCAGTGTCCAGGGATGAGGAA, reverse TTCTTGGGCGTCT GCTCCACAG;TFAM: forward GAGCAGCTAACTCCAAGTCAG, reverse GAGCCGAATCATCCTTTGCCT. All experiments were performed in triplicate. Melting curve analysis confirmed the specificity of the PCR amplification as single peaks. The Ct values obtained were analyzed using the 2-ΔΔCt method, with GAPDH serving as the standard, to calculate the relative RNA expression levels.

Western blot

Liver tissues from wild-type (wt) and NASH model mice were finely minced and then subjected to protein extraction via the RIPA method. The expression levels of β-actin and tubulin were normalized using their grayscale values measured by ImageJ. Polyacrylamide gels were prepared using the One-Step PAGE Gel Fast Preparation Kit (15%) from Vazyme (catalog number E305), with the 180 kDa Prestained Protein Marker from Vazyme (catalog number MP102) used for molecular weight estimation. Electrophoresis and membrane transfer were conducted using the PowerPac Basic Power Supply from BIO-RAD. Blocking was performed with 5% BSA. Primary antibodies were diluted as follows: β-actin at 1:1000 from Servicebio (catalog number GB15001-100), tubulin at 1:5000 from Affinity Biosciences (catalog number T0023), CDKN1B at 1:1000 from BIOSS (catalog number bs-0742R), and TFAM at 1:1000 from Proteintech (catalog number 22586-1-AP). Imaging was done using the Tanon 4800 system. Grayscale values for all bands were acquired with ImageJ, and the relative protein expression levels were determined using β-actin and tubulin as standards. Statistical analysis and graphical representation were performed using GraphPad Prism 9.

Statistical analysis

R software (version 4.2.2; https://www.r-project.org/) and GraphPad Prism 9 were employed for all statistical analyses and graph generation. The Wilcoxon test and Student's t-test were utilized to compare intergroup differences. ROC (Receiver Operating Characteristic) curves were used to evaluate the predictive performance of candidate genes used to construct predictive models. A P-value <0.05 was considered to indicate statistical significance.

Results

Implementation of WGCNA and identification of key module genes

WGCNA was used to identify modules most significantly correlated within the GSE33814 dataset. A soft-thresholding power (β) was set at 15, ensuring a scale-free $R^2 = 0.9$, to accommodate gene expression relevant to a scale-free network (Figure 2A). The clustering of module eigengenes is employed to display the results of hierarchical clustering. In the diagram, 'Height' denotes the dissimilarity between clusters. When two clusters join at a lower height, it indicates greater similarity between them; conversely, a higher joining point suggests greater dissimilarity. Color labels represent different modules, each typically comprising a group of genes with similar expression patterns. This allows for the identification of gene modules with similar expression patterns (Figure 2B). The Cluster Dendrogram is also utilized to demonstrate the outcomes of hierarchical clustering analysis. The top of the dendrogram features a black line, with each bifurcation representing a split or merge in the clustering process. Colored bands denote different clusters obtained through the Dynamic Tree Cut method, with each color representing a cluster and the horizontal length indicating the number of objects within each cluster (Figure 2C). Module-trait relationships illustrate the associations between different gene modules (indicated by colors) and NAFLD, with each grid representing the correlation between a specific gene module and NAFLD (Figure 2D). A total of 13 gene co-expression modules were identified in the Module-trait relationships between the NAFLD group and the control group (Figure 2D). Notably, the black module (cor=-0.65, p=2e-6), darkred module (cor=-0.58, p=4e-05), and blue module (cor=0.5, p=5e-04) demonstrated the most significant correlations. The scatterplot for the black module displays the relationship between module membership and Gene Significance, with a correlation coefficient (cor) of 0.79 (p<1e-200). This indicates that as a gene's membership in the black module increases—denoting higher similarity in expression patterns with other genes in the module—its association with NAFLD and its importance in the studied traits also increases (Figure 2E). Similar conclusions can be drawn from the scatterplots for the darkred and blue modules, which have correlation coefficients of 0.80 (p<1e-200) and 0.62 (p=3.1e-139), respectively (Figures 2F, G). Within these three modules, a total of 5361 genes were screened.

Preprocessing of data and selection of DEGs

Utilizing |log2 fold change (FC)| > 0.3 and $p < 0.05$ as selection criteria, 592 DEGs were identified within GSE33814. Volcano plots were crafted using the "ggplot2" R package (Figure 3A), the vertical lines represent |log2 fold change (FC)| > 0.3, and the horizontal line represents $p < 0.05$.Heatmaps were generated with the "pheatmap" R package (Figure 3B). Employing a Relevance score greater than 7 as a selection criterion in the Genecard database, 1065 genes related to oxidative stress were identified. The intersection of genes derived from the three methods yielded 31 intersection genes of NAFLD and OS (Figure 3C).

10.3389/fimmu.2024.1335112

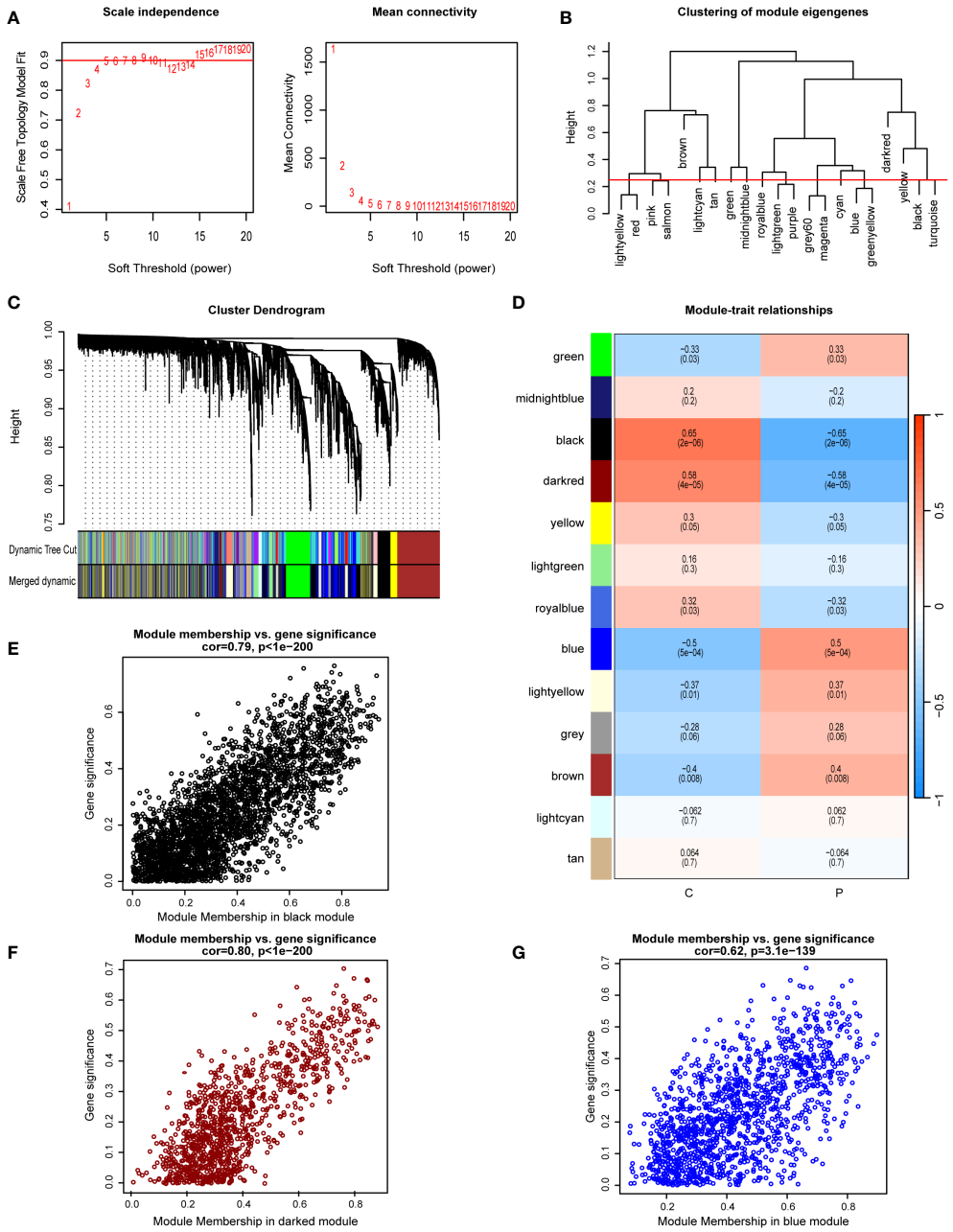

FIGURE 2
Implementation of WGCNA and identification of key module genes. **(A)** A soft-thresholding power (β) was set at 15, ensuring a scale-free R^2 = 0.9. **(B)** Hierarchical clustering dendrogram of module eigengenes. **(C)** The cluster dendrogram of co-expression network modules from WGCNA depending on a dissimilarity measure. **(D)** Module-trait relationships between: comparing the control group (C) with the NAFLD group (P). **(E)** The scatterplot for the black module displays the relationship between module membership and gene significance. **(F)** The scatterplot for the darkred module displays the relationship between module membership and gene significance. **(G)** The scatterplot for the blue module displays the relationship between module membership and gene significance.

Conducting functional enrichment analysis of 31 intersection genes of NAFLD and OS

In the DO enrichment analysis, kidney failure and cerebrovascular disease were significantly enriched (Figure 4A). In the GO enrichment analysis (Figure 4B), BP categories were enriched in cellular response to oxidative stress, cellular response to chemical stress, response to oxidative stress, and response to nutrient levels. CC categories were enriched in mitochondrial matrix and mitochondrial protein-containing complex, and MF categories were enriched in heat shock protein binding, oxidoreductase activity, acting on the CH-CH group of donors, and electron transfer activity. In the KEGG functional enrichment analysis (Figure 4C), Chemical Carcinogenesis - Reactive Oxygen Species, Pathways of Neurodegeneration - Multiple Diseases, HIF-1 Signaling Pathway, and Toll-like Receptor Signaling Pathway were significantly enriched and the genes enriched in these pathways are illustrated (Figures 4C, D).

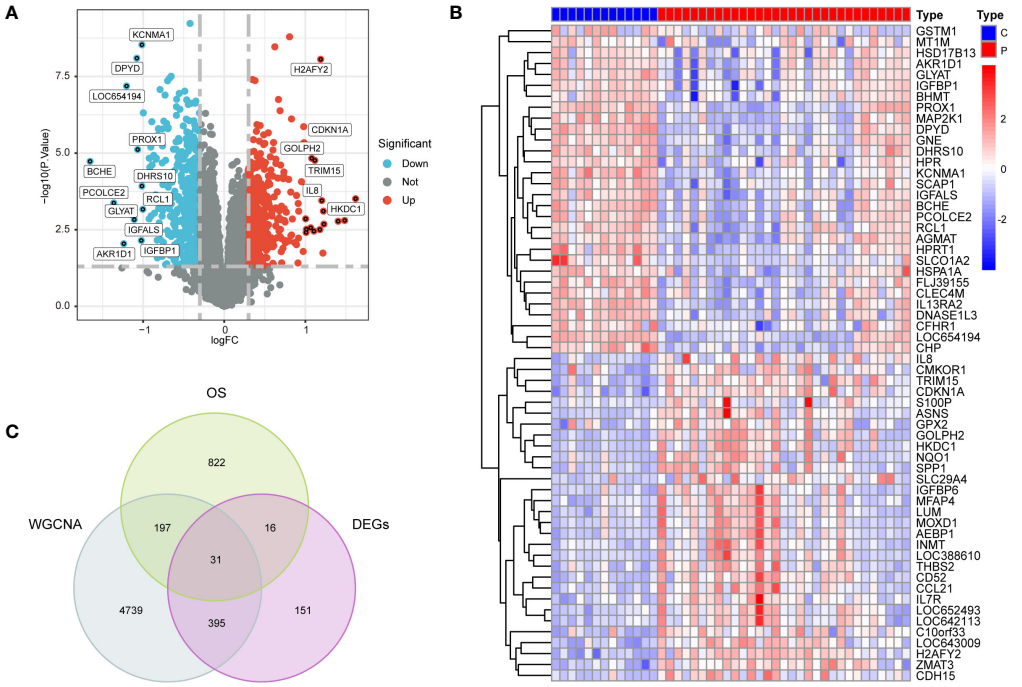

FIGURE 3
Preprocessing of data and selection of DEGs. **(A)** Volcano plots of DEGs in GSE3814, |log2 fold change (FC)| > 0.3 and p < 0.05 as selection criteria **(B)** heatmaps of DEGs in GSE33814: comparing the control group (C) with the NAFLD group (P). **(C)** 31 intersection genes of OS,WGCNA and DEGs.

Application of machine learning for screening hub genes

Within the 31 intersection genes of NAFLD and OS, we first utilized the SVM-RFE algorithm to extract 20 genes (Figures 5A, B). Subsequently, 6 genes were identified through the LASSO regression algorithm (Figures 5C, D). Following this, the RandomForest algorithm selected 9 genes (Figures 5E, F). Ultimately, by employing a Venn network to intersect these gene subsets, we identified 3 genes: CDKN1B, NDUFA4, and TFAM (Figure 5G). Simultaneously, the interaction relationships between these 3 hub genes and other intersection genes of NAFLD and OS were explored within the PPI network (Figure 5H).

GSEA of hub genes and ssGSEA of hallmark gene sets

The Gene Set Enrichment Analysis (GSEA) plots provide insights into the biological processes enriched during high and low expressions of individual genes. This enrichment allows us to rank these processes and identify those with the significant differences. Such analyses are instrumental in revealing the molecular mechanisms underlying changes in biological states and the affected biological pathways. In these plots, the horizontal axis represents gene ranking within an ordered dataset, typically based on expression levels from high to low. The vertical axis shows the running enrichment score (ES) for the gene set. The ranked list metric at the bottom indicates the value used for gene ranking, which could be the signal-to-noise ratio, fold change, or other statistical measures of differential expression. The lines in the plots trace the path of the enrichment score across the ranked gene list for each gene set, while the vertical lines below the plot signify the positions of genes from the gene set within the ranked list.

Figure 6A demonstrates gene sets associated with upregulated genes linked to CDKN1B. The top of the ranked list features enriched gene sets including ascorbate and aldarate metabolism, butanoate metabolism, fatty acid degradation, steroid hormone biosynthesis, and the degradation of valine, leucine, and isoleucine. Figure 6B presents gene sets associated with downregulated genes linked to CDKN1B, including ECM-receptor interaction, galactose metabolism, platelet activation, proteasome, and thyroid hormone synthesis. Figure 6C illustrates gene sets related to genes upregulated in connection with NDUFA4, encompassing ascorbate and aldarate metabolism, ferroptosis, the intestinal immune network for IgA production, and steroid biosynthesis. Figure 6D reveals gene sets corresponding to genes downregulated with NDUFA4, highlighting glutathione metabolism, insulin resistance, mineral absorption, N-glycan biosynthesis, and thyroid hormone synthesis. Figure 6E shows gene sets related to upregulated genes in association with TFAM, with the top-ranked list showing enrichment in gene sets such as fluid shear stress and atherosclerosis, glutathione metabolism, mineral absorption, platinum drug resistance, and ribosome biogenesis in eukaryotes. Figure 6F displays gene sets linked to downregulated genes in connection with TFAM, featuring gene sets like arachidonic acid metabolism, ascorbate and aldarate metabolism, glycerolipid.

ssGSEA, is a method designed to calculate the degree of enrichment between gene expression data of a single sample and a predefined set of genes. In contrast to traditional GSEA, which

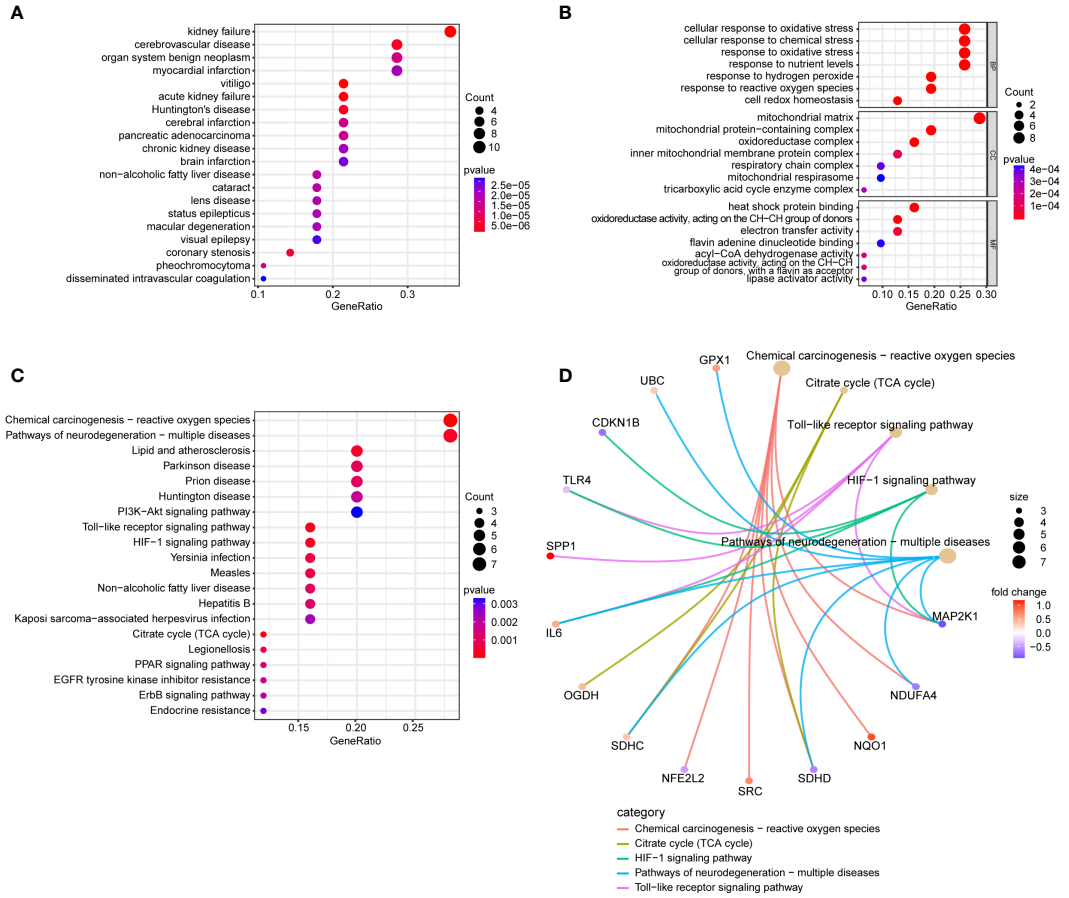

FIGURE 4
Conducting functional enrichment analysis of 31 intersection genes of NAFLD and OS. **(A)** The DO enrichment analysis reveals the diseases most significantly associated with the 31 intersecting genes. **(B)** The GO enrichment analysis elucidates the functional roles of the 31 intersecting genes from three perspectives: BP, CC, and MF. **(C)** The KEGG enrichment analysis bubble plot displays the signaling pathways most closely related to the 31 intersecting genes. **(D)** The KEGG enrichment analysis circular network plot presents a network of relationships between some genes and their associated signaling pathways.

compares groups of samples or conditions, ssGSEA allows for scoring each individual sample independently. This proves particularly valuable in revealing changes in biological processes within individual samples that do not show significant changes at the group mean level, especially useful in samples with substantial heterogeneity. It does not necessitate a control group and is applicable to a variety of gene expression data types, including those from public databases. The operational procedure is as follows: firstly, it ranks all genes based on their expression levels; then, for each gene set, ssGSEA calculates an enrichment score that reflects the relative positioning and distribution of genes within that set in the ranking. This score is derived by accumulating the scores of genes within the gene set while subtracting the scores of genes not included in the set; ultimately, this score may be normalized to allow comparisons across different samples or gene sets. A Hallmark Gene Set denotes a group of genes whose patterns of expression have specific biological significance, such as being indicative of certain cell types, diseases, or biological processes, and are often identified through the analysis of experimental data. In summary, a Hallmark Gene Set provides a predefined list of genes that are considered biologically relevant; ssGSEA is an analytical tool that uses these sets to quantitatively assess the expression of these gene sets in individual samples. By doing so, ssGSEA can reveal the unique biological characteristics inherent to each sample. By employing this method, we can finally determine the significant differences in biological processes between the control group and the NAFLD group (Figure 6G), and ascertain the specific biological processes in which the three hub genes differ significantly (Figure 6H).

Clinical studies of the hub genes

In the correlation heatmap, we observed a positive correlation between CDKN1B and NDUFA4, while TFAM was negatively correlated with them (Figure 7A). In the GSE33814 dataset, the diagnostic value of these three hub genes was further validated through the ROC curve. Specifically, NDUFA4 (AUC: 0.935), TFAM (AUC: 0.909), and CDKN1B (AUC: 0.911) demonstrated significant diagnostic value for NAFLD (Figure 7B). Similar results were obtained in the GSE48452 validation dataset (Figure 7C). Through the investigation of the GSE33814 dataset, we discovered that CDKN1B and NDUFA4 expressions were reduced in NAFLD, whereas TFAM expression was elevated (Figures 7D–F). These findings were validated

10.3389/fimmu.2024.1335112

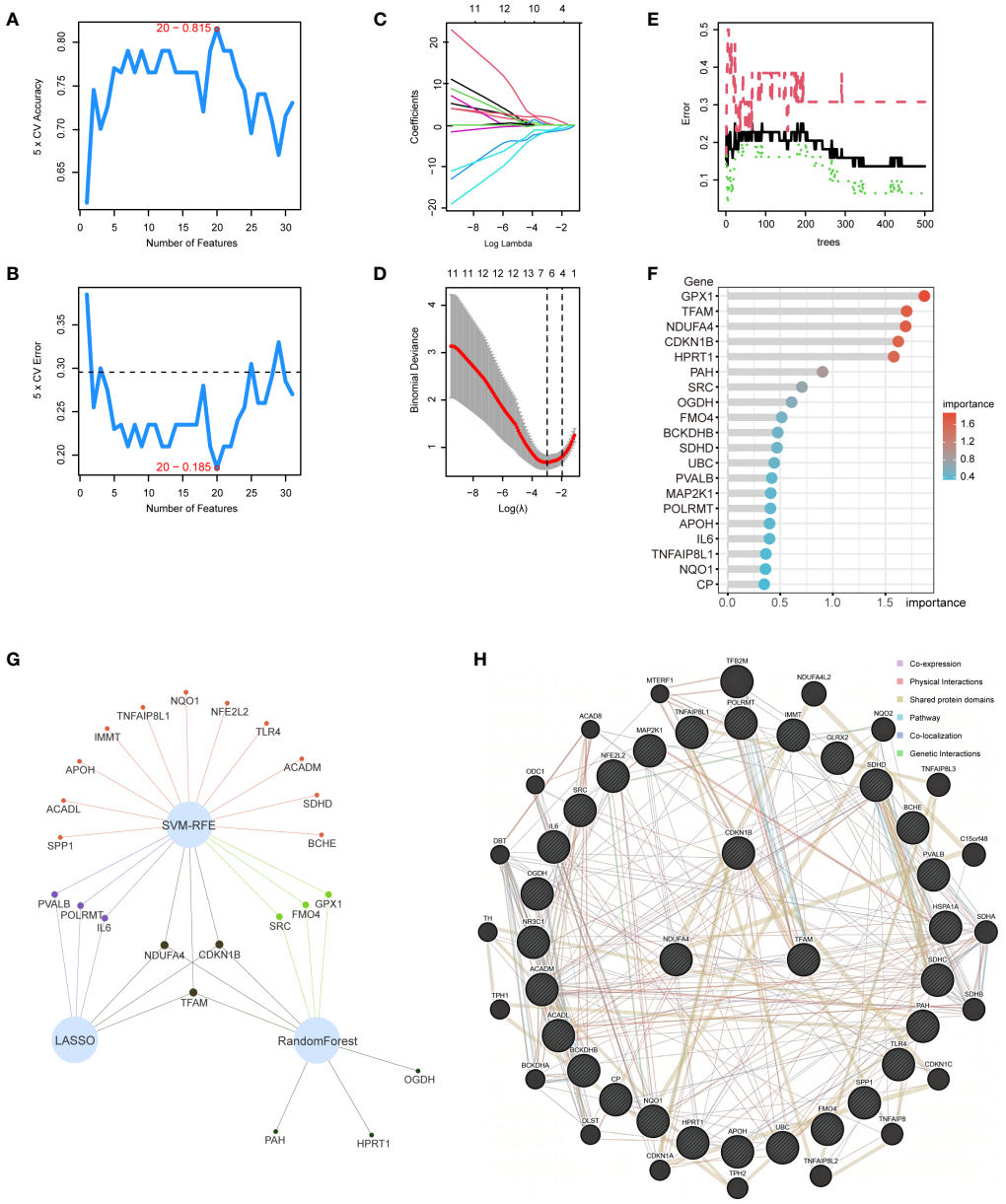

FIGURE 5
Application of machine learning for screening hub genes. **(A, B)** SVM-RFE algorithm to extract 20 genes. **(C, D)** 6 genes were identified through the LASSO regression algorithm. **(E, F)** RandomForest algorithm selected 9 genes. **(G)** Venn network to intersect 3 gene subsets. **(H)** 3 hub genes and other intersection genes of NAFLD and OS were explored within the PPI network.

in the GSE48452 dataset (Figures 7G–I). Additionally, we constructed a nomogram to predict the incidence of NAFLD (Figure 7J). These results suggest that the three hub genes present a satisfactory performance in diagnosing NAFLD.

Analysis on immunization: immune infiltration analysis and processing of single-cell sequencing data

Utilizing the CIBERSORT algorithm for immune infiltration analysis, significant differences were observed between the control and NAFLD groups in Tregs, M0 macrophages, M2 macrophages, T cells CD4 memory activated, activated mast cells, and neutrophils (Figure 8A). Analysis of the single-cell RNA sequencing dataset GSE189600 determined the distribution of three hub genes across six cell clusters (Figure 8B). Significant disparities were identified between the control and NAFLD groups for CDKN1B in stellate cells and vascular smooth muscle cells (VSMCs). For NDUFA4, notable differences were observed between the control and NAFLD groups in stellate cells and hepatocytes. In the case of TFAM, the control and NAFLD groups demonstrated significant variation in VSMCs (Figure 8C).

10.3389/fimmu.2024.1335112

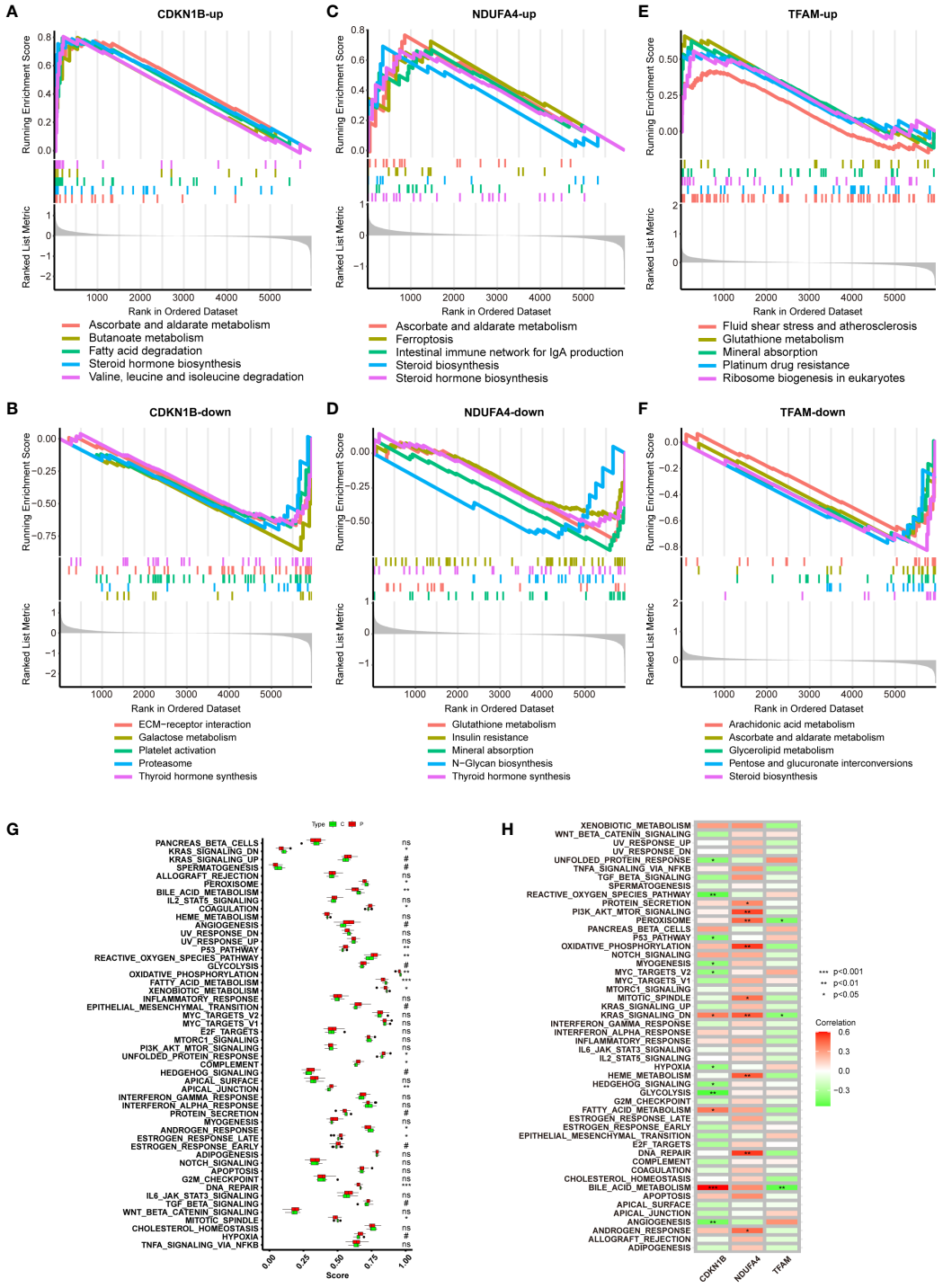

FIGURE 6
GSEA of Hub Genes and ssGSEA of Hallmark Gene Sets. **(A, B)** GSEA analysis of CDKN1B-up and CDKN1B-down. **(C, D)** GSEA analysis of NDUFA4-up and NDUFA4-down. **(E, F)** GSEA analysis of TFAM-up and TFAM-down. **(G)** ssGSEA Hallmark Gene Sets functional enrichment analysis results for the NAFLD group and the control group. **(H)** ssGSEA Hallmark Gene Sets functional enrichment analysis of the three hub genes.

TF-miRNA-mRNA regulatory network

Utilizing the JASPAR database, potential transcription factors were predicted on the NetworkAnalyst website, while possible miRNAs were foreseen using the miRTarBase v8.0 database. Subsequently, a regulatory network map was constructed based on their interactive relationships (Figure 8D). Transcription factors (TFs) are proteins that typically bind to specific DNA sequences to control the transcription of genetic information from DNA to mRNA, represented by green circles in the network. MicroRNAs (miRNAs) are short non-coding RNA molecules that bind to complementary sequences on target mRNAs, regulating gene

10.3389/fimmu.2024.1335112

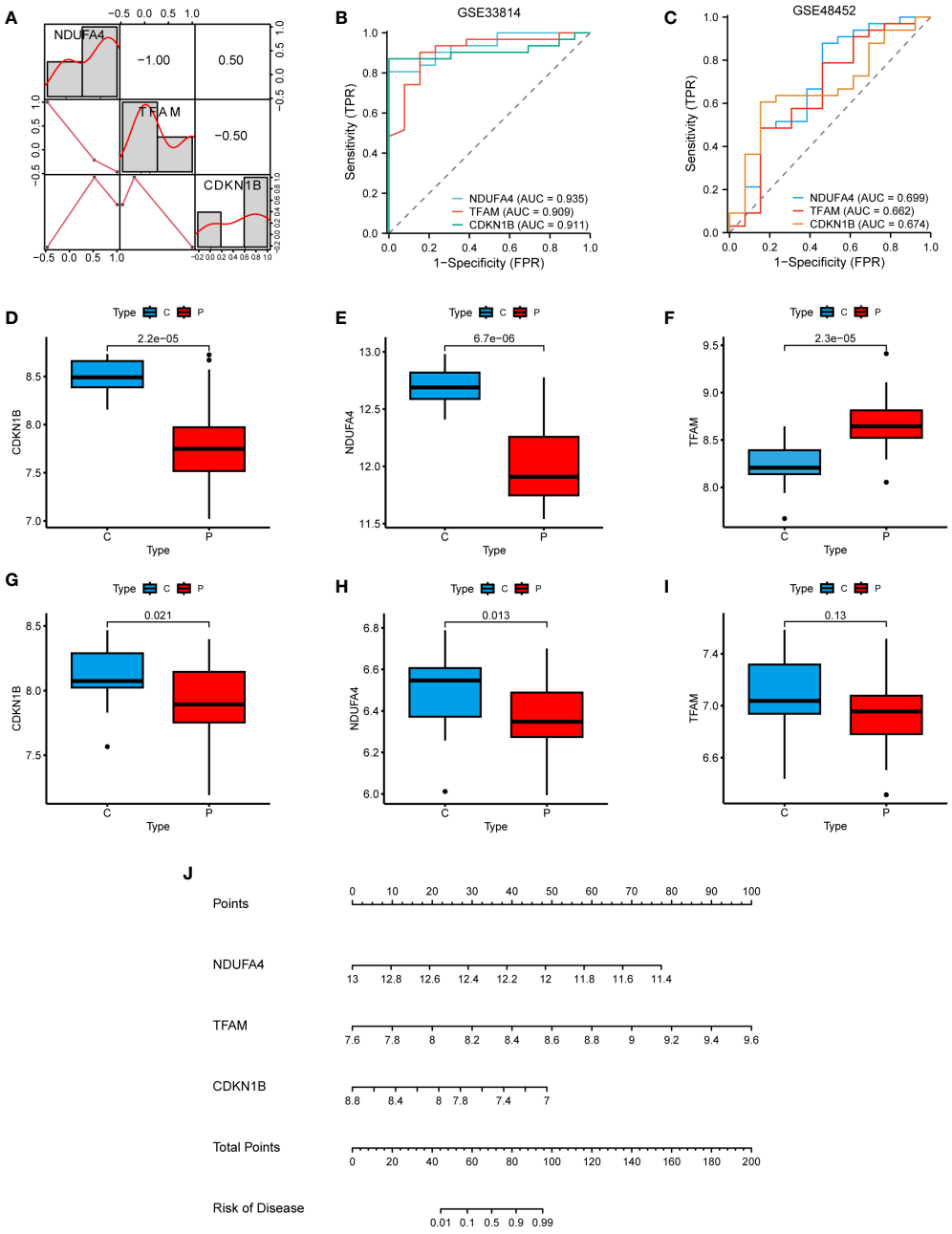

FIGURE 7
Clinical studies of the hub genes. **(A)** Correlation heatmap of the 3 hub genes. **(B)** ROC curve in the GSE33814. **(C)** ROC curve in the GSE48452. **(D–F)** Hub genes expression in the GSE33814: comparing the control group (C) with the NAFLD group (P). **(G–I)** Hub genes expression in the GSE48452: comparing the control group (C) with the NAFLD group (P). **(J)** Nomogram for the diagnosis of NAFLD based on the hub genes.

expression post-transcriptionally, often resulting in mRNA degradation or repression of translation, depicted by blue squares. Messenger RNAs (mRNAs) are the final transcripts that carry genetic information from DNA—transcribed by the action of TFs—to the ribosome, where proteins are synthesized. Lines within the network indicate interactions or regulatory influences between these entities, with the direction of regulation (from TF to mRNA or from miRNA to mRNA) typically denoted by lines originating from the regulator and pointing towards the target. These networks are crucial for understanding the complex layers of gene regulation within cells, elucidating how genes are switched on or off, how miRNA fine-tunes this regulation, and the intricate balance that maintains normal cellular function or contributes to disease when dysregulated.

Animal experimentation

Considering the prevalent obesity and diabetes symptoms in NAFLD patients, this study utilized the Attie Lab Diabetes Database

BTBR ob/ob mouse model to select liver tissues from 10-week-old C57BL/6 (control) and BTBR mice, categorizing them into lean and ob/ob groups, to investigate the expression of hub genes under various conditions. The findings indicated significant differences in the expression of CDKN1B and TFAM genes between the control and BTBR strains, as well as between the lean and ob/ob mice, aligning with our expectations (Figures 9A, B).

Subsequently, this research focused on a NASH mouse model, representing a more advanced stage of NAFLD, employing RT-qPCR and Western Blot techniques to examine the expression of these key genes at RNA and protein levels, respectively. The RT-qPCR results revealed significant differences in the expression of CDKN1B and TFAM between the control and NASH groups, consistent with prior expression trend predictions (Figures 9C, D). At the protein level, the findings from the WB analysis corroborated those from RT-qPCR (Figure 9E), with subsequent statistical analysis conducted (Figures 9F–I).

Discussion

NAFLD, a disease syndrome that encompasses NAFL and NASH, impacts nearly a quarter of the global population, with its prevalence escalating annually. Alarmingly, NASH possesses the potential to further progress into cirrhosis and hepatocellular carcinoma, triggering a cascade of complications and ultimately, may prove fatal, thereby imposing a substantial disease burden on society. In light of this, an in-depth understanding of NAFLD's pathogenic mechanisms, formulation of appropriate therapeutic strategies, and identification of reliable diagnostic markers become paramount.

miRNAs are genes encoding small RNAs, predominantly functioning by inhibiting the translation of target mRNAs or inducing their degradation, thereby playing pivotal roles in the proliferation, development, and differentiation across numerous cell types, and is also involved in the progression of various diseases. The microRNA regulatory studies have been exhibited in the TF-miRNA-mRNA regulatory network we constructed (Figure 8C) and have been validated in numerous previously published papers.

Hepatotoxicity mediated by free radicals and demonstrated the therapeutic effect of antioxidants against free radical-mediated NAFLD. Moreover, epidemiological statistics on the liver have confirmed that changes in the redox state of NAFLD are closely related to an increased subsequent metabolic risk. According to the "second hit" and "multiple hit" theories, oxidative stress appears to be one of the most crucial mechanisms leading to liver injury in NAFLD.

The CDKN1B gene encodes the p27 protein, which plays a crucial role in regulating cell growth, differentiation, cytoskeletal dynamics, and cell division. A reduction in p27 protein is associated with the invasiveness of various human tumors, such as colon cancer, breast cancer, prostate cancer, and ovarian cancer (40). Hepatic fibrosis and hepatocellular carcinoma are closely related to CDKN1B. The accumulation of the Extracellular Matrix (ECM) in the liver leads to the onset of liver fibrosis. Excessive production of ECM by activated hepatic stellate cells and myofibroblasts is considered the primary mechanism inducing liver fibrosis, which may further develop into cirrhosis and hepatocellular carcinoma. miR-221/222 is considered a new indicator of stellate cell activation and liver fibrosis progression. The expression of miR-221/222 is positively correlated with the progression of liver fibrosis and significantly associated with the expression of Col1A1 and αSMA mRNA. The expression of miR-221/222 has been validated in human fibrotic liver samples and mouse models of liver fibrosis. They interact with CDKN1B and inhibit the expression of CDKN1B mRNA and protein in human stellate cell line LX-2. The expression of miR-222 in stellate cells may be regulated by NF-κB activation (41). The overexpression of miR-221/222 promotes cancer cell proliferation, most likely through their regulation of the CDKN1B expression (42). The upregulation of miR-221/222 can promote the growth of hepatocellular carcinoma (HCC) cells by increasing the number of S-phase cells, and the oncogenic activity of miR-221 is believed to be realized through the regulation of CDKN1B (42, 43). CDKN1B has been validated as a target of miR-221, and the CDKN1B gene is directly associated with HCC proliferation (44). F. Fornari et al. (45) observed that CDKN1B gene expression was downregulated in 77% of HCC samples, and the downregulation of CDKN1B affected the prognosis of HCC. In human HCC, the downregulation of CDKN1B showed prognostic significance associated with advanced tumor stages, lower survival rates, and HCC recurrence (46). HCC represents the terminal stage of NAFLD, suggesting that the regulatory mechanism of miR-221/222 on CDKN1B may play a vital role in the etiology of NAFLD. These findings provide a basis for developing potential therapeutic strategies for liver fibrosis and liver cancer.

NDUFA4 has been relatively underexplored. Initially, NDUFA4 was identified as a component of the mitochondrial respiratory complex I. However, subsequent studies revealed that NDUFA4 is actually associated with complex IV rather than complex I (47). This gene demonstrates significant tissue-specific expression in the liver and brain (48). NDUFA4 is a target of miR-147, and the inhibition of miR-147, coupled with the overexpression of NDUFA4, can induce mitochondrial damage and renal tubular cell death (49). A deficiency in NDUFA4 expression can exacerbate oxidative stress, further predisposing to the onset of diabetes (50). MiR-210 promotes the pathogenesis of obesity-induced diabetes in mice by targeting NDUFA4 gene expression (51). MiR-210-3p accelerates cardiomyocyte apoptosis and impairs mitochondrial function by targeting NDUFA4, contributing to the cardiac dysfunction induced by sepsis (52). In the liver, NDUFA4 may also play a role in disease onset through mechanisms related to mitochondrial dysfunction.

TFAM as a pivotal structural protein of mammalian nuclei, serves as a transcription activator, specifically stimulating certain mitochondrial transcription initiation points (53). This protein is integral to various processes, including the transcription and replication of mitochondrial DNA (mtDNA), its packaging into nucleoid structures, and playing an indispensable role in the regulation of mtDNA copy numbers. Notably, an overexpression of TFAM, exceeding normal physiological levels, can directly lead to

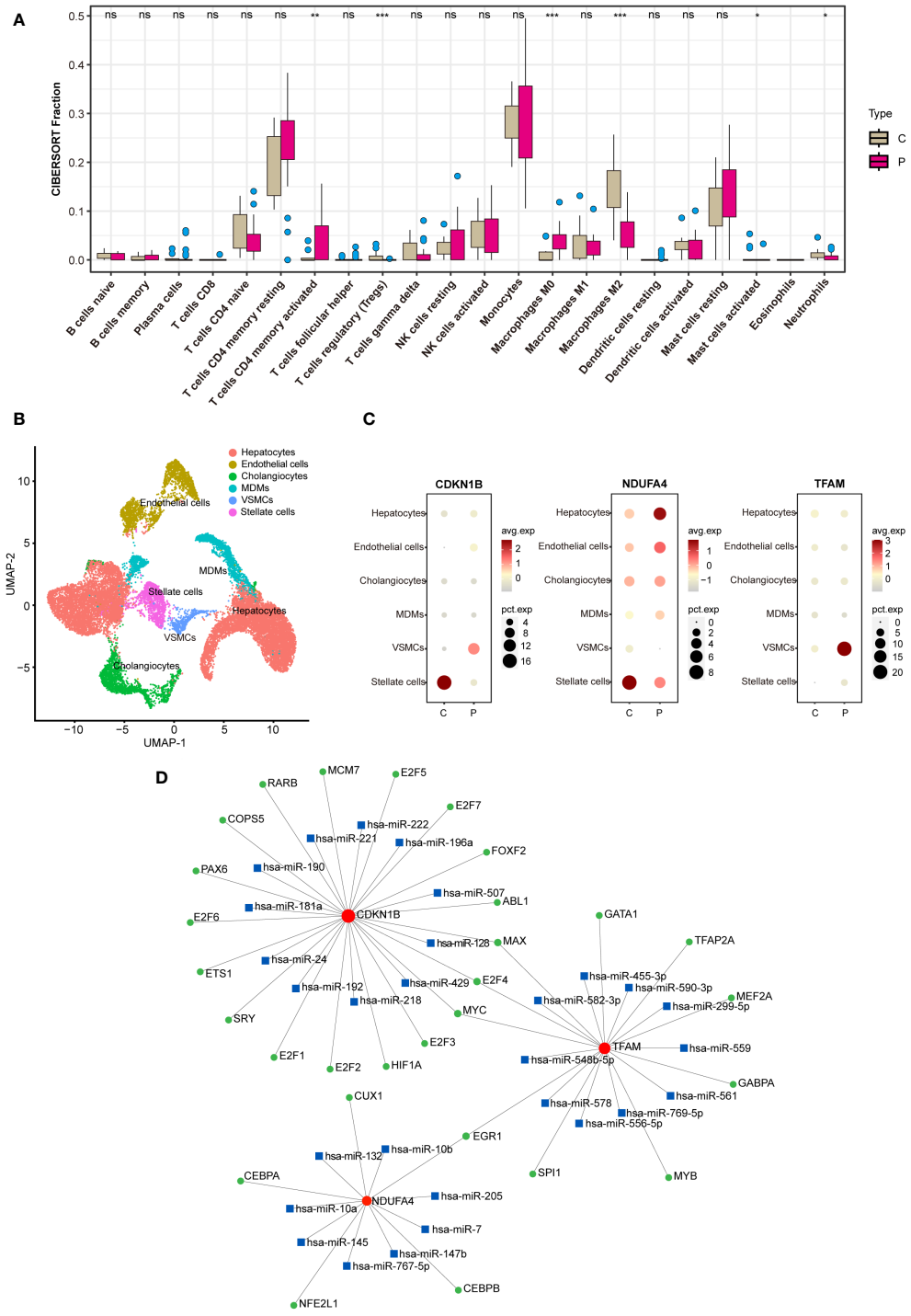

FIGURE 8
Analysis on immunization and TF-miRNA-mRNA regulatory network. **(A)** Immune infiltration analysis between the NAFLD group and the control group. **(B)** Analysis of the single-cell RNA sequencing dataset GSE189600. **(C)** Hub genes enrichment in immune cells. **(D)** TF-miRNA-mRNA regulatory network. In B, C, and D, "C" represents the control group, and "P" represents the NAFLD group. "ns" indicates not significant, "*" indicates P<0.05, "**" indicates P<0.01, "***" indicates P<0.001.

postnatal death and mitochondrial functional impediments. Experimental evidence reveals that mice with high TFAM expression typically exhibit smaller sizes and weaker physical conditions compared to their wild-type littermates, with significantly reduced liver, heart, and kidney volumes. Further research has also disclosed an increase in lipid accumulation in the liver tissues of mice with TFAM overexpression, potentially attributable to the dysregulation of lipid metabolism induced by the upregulation of mitochondrial protease interference pathways (54). Variations in TFAM expression have also been observed in studies of other liver diseases. For instance, in a study related to alcoholic liver disease, the hepatic TFAM levels in mice fed with ethanol rose

10.3389/fimmu.2024.1335112

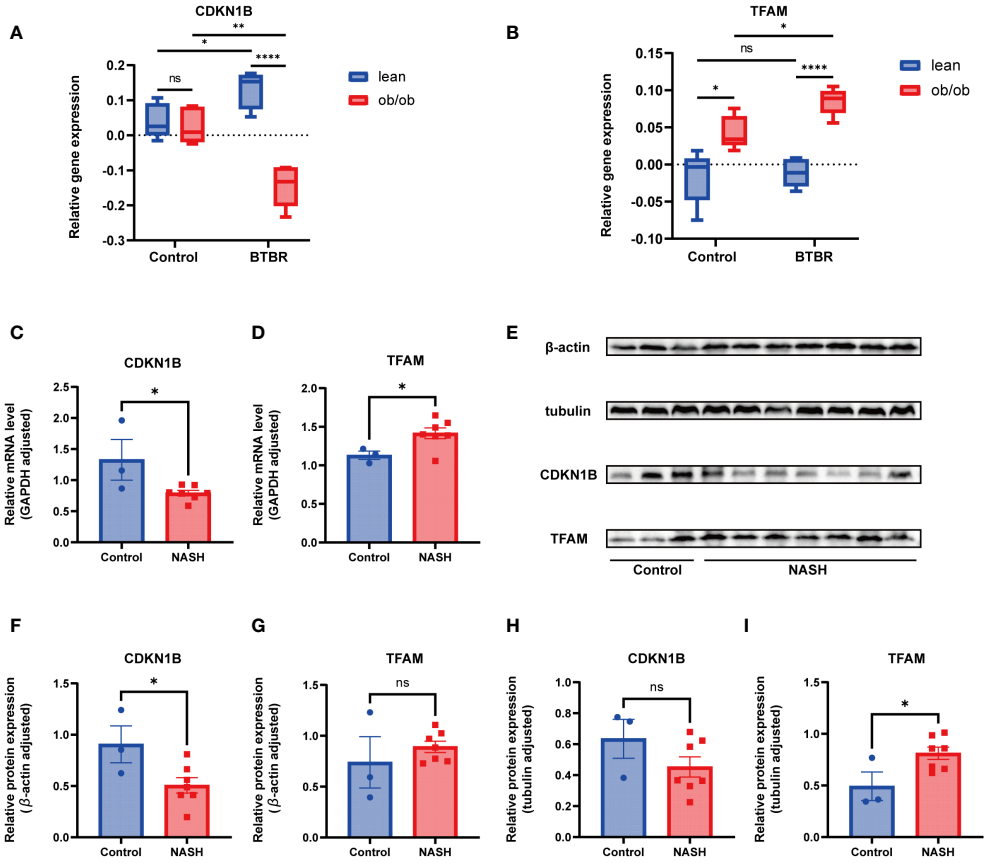

FIGURE 9
Animal experimentation **(A)** Comparison of CDKN1B relative gene expression in lean and ob/ob groups of 10-week-old C57BL/6 and BTBR strain mice, using mlratio to quantify changes. **(B)** Comparison of TFAM relative gene expression in lean and ob/ob groups of 10-week-old C57BL/6 and BTBR strain mice, using mlratio to quantify changes. **(C)** Relative mRNA levels of CDKN1B in control and NASH mice. **(D)** Relative mRNA levels of TFAM in control and NASH mice. **(E)** Comparison of protein expression levels for CDKN1B and TFAM. **(F)** Statistical analysis of CDKN1B protein expression, standardized by β-actin. **(G)** Statistical analysis of TFAM protein expression, standardized by β-actin. **(H)** Statistical analysis of CDKN1B protein expression, standardized by tubulin. **(I)** Statistical analysis of TFAM protein expression, standardized by tubulin. "ns" indicates not significant, "*" indicates P<0.05, "**" indicates P<0.01, "***" indicates P<0.001.

by 30% compared to the control group fed with water (55). Meanwhile, studies of human normal and malignant liver tissues and cell lines demonstrate that TFAM expression trends upward in Hepatocellular Carcinoma cells resistant to drugs. However, TFAM is only upregulated in a small portion of HCC patients, and inhibiting TFAM can suppress the growth and survival of HCC cells, thereby enhancing the effectiveness of chemotherapy (56).

While the importance of TFAM in maintaining mtDNA and facilitating mitochondrial biogenesis is widely acknowledged, the interactions between TFAM and certain miRNAs in the context of diseases remain shrouded in mystery. For example, a deficiency in human TFAM has been identified as a catalyst for mitochondrial dysfunction and a reduction in nucleoid formation, culminating in fatal liver failure (57). After TFAM depletion, its roles, both as an oncogene and a tumor suppressor, have been observed (58, 59). TFAM is identified as a direct target of miRNA-590-3p; in bladder cancer, a downregulation of miRNA-590-3p expression correlates with a marked increase in TFAM expression (60), while in colon cancer, an elevation in miRNA-590-3p expression is associated with a significant decrement in TFAM expression (61). Furthermore, factors such as sex, age, and diet can influence TFAM expression. For instance, TFAM protein levels in the livers of female rats are quadruple those in males, a sexual dimorphism fundamentally attributed to the females' heightened degree of mitochondrial differentiation, which leads to superior substrate oxidation capability and efficiency (62). It is noteworthy that TFAM protein expression diminishes progressively with age, a process that can be fully mitigated through calorie restriction (CR) (63). In conclusion, the exact mechanisms by which TFAM functions in disease onset remain intricate and necessitate further exploration.

Transcription factors such as SPI1, ETS1, and CEBPA have been identified as promising targets for the prevention and treatment of NASH (64). These transcription factors are integral components of a complex regulatory network involving TF-miRNA-mRNA interactions, highlighting the sophisticated molecular interplay underlying NASH pathogenesis. CEBPA is linked to the regulation of NDUFA4, a component of the mitochondrial respiratory chain, suggesting a role in metabolic efficiency and oxidative stress response. SPI1's regulation of TFAM, a key factor in mitochondrial DNA maintenance and transcription, points to its importance in

mitochondrial biogenesis and function. ETS1's influence on CDKN1B implicates it in cell cycle regulation and potentially in the control of hepatocyte proliferation and apoptosis, processes central to NASH progression and liver regeneration.

In our study, we employed immunoinfiltration analysis techniques to investigate the disparities in the immune cell composition between patients with NAFLD and healthy control groups. Significant differences were observed across several immune cell subpopulations, including neutrophils, macrophages, regulatory T cells (Tregs), and mast cells. Further, single-cell sequencing technology revealed expression pattern discrepancies in three hub genes within specific cellular subpopulations, such as hepatic stellate cells and vascular smooth muscle cells (VSMCs), suggesting their potential key regulatory roles in hepatic pathological processes. Notably, these cells play a decisive role in the development of inflammatory damage, hepatocyte injury, and liver fibrosis induced by oxidative stress.

Moreover, our comprehensive bioinformatics enrichment analyses identified multiple signaling pathways closely associated with the pathogenesis of NAFLD, related to oxidative stress. We also uncovered a series of critical biological processes, including dysregulated lipid metabolism, imbalance in inflammatory response regulation, and extracellular matrix remodeling. The aberrant regulation of these pathways and biological processes offers new insights into the pathophysiological foundation of NAFLD.

Nevertheless, the present study has not yet conducted in-depth mechanistic validations of these findings. Future research should explore the causal relationships between these central genes and the characteristics of immune cell infiltration, as well as their specific roles in the progression of NAFLD, through *in vivo* and *in vitro* experimental models. Additionally, the current study lacks direct experimental evidence at the cellular level, necessitating further validation of these genes' roles and importance in the progression of NAFLD through functional experiments, such as gene knock-out, overexpression studies, and immunohistochemical staining. Through these extensive experimental investigations, we will be able to elucidate the pathological role of oxidative stress in non-alcoholic fatty liver disease more accurately and potentially develop new therapeutic targets.

Data availability statement

The datasets presented in this study can be found in online repositories. The names of the repository/repositories and accession number(s) can be found in the article/Supplementary Material.

Author contributions

HW: Conceptualization, Data curation, Formal analysis, Investigation, Software, Writing – original draft, Writing – review & editing. PH: Data curation, Formal analysis, Investigation, Software, Writing – original draft. WC: Data curation, Investigation, Writing – review & editing. TL: Data curation, Investigation, Methodology, Writing – review & editing. CH: Methodology, Writing – review & editing. YC: Methodology, Writing – review & editing. YZ: Methodology, Writing – review & editing. JW: Methodology, Writing – review & editing. QY: Conceptualization, Funding acquisition, Writing – original draft, Writing – review & editing. TZ: Conceptualization, Funding acquisition, Software, Writing – review & editing.

Funding

The author(s) declare financial support was received for the research, authorship, and/or publication of this article. This research was funded by Jiangsu medical scientific research project of Jiangsu Health Commission, Jiangsu Province Capability Improvement Project through Science, Technology and Education, Jiangsu Provincial Medical Key Discipline Cultivation Unit (JSDW202235), the National Natural Science Foundation of China (grant numbers 81870409), the 789 Outstanding Talent Program of SAHNMU (789ZYRC202070102), China Postdoctoral Science Foundation (2023M730675), and Shanghai Sailing Program (23YF1406800).

Acknowledgments

Thanks to all the teachers and classmates who helped with this study.

Conflict of interest

The authors declare that the research was conducted in the absence of any commercial or financial relationships that could be construed as a potential conflict of interest.

Publisher's note

Supplementary material

The Supplementary Material for this article can be found online at: https://www.frontiersin.org/articles/10.3389/fimmu.2024.1335112/full#supplementary-material

References

1. Younossi ZM, Koenig AB, Abdelatif D, Fazel Y, Henry L, Wymer M. Global epidemiology of nonalcoholic fatty liver disease-Meta-analytic assessment of prevalence, incidence, and outcomes. *Hepatol (Baltimore Md)*. (2016) 64:73–84. doi: 10.1002/hep.28431

2. Chalasani N, Younossi Z, Lavine JE, Diehl AM, Brunt EM, Cusi K, et al. The diagnosis and management of non-alcoholic fatty liver disease: practice Guideline by the American Association for the Study of Liver Diseases, American College of Gastroenterology, and the American Gastroenterological Association. *Hepatol (Baltimore Md)*. (2012) 55:2005–23. doi: 10.1002/hep.25762

3. Huang DQ, El-Serag HB, Loomba R. Global epidemiology of NAFLD-related HCC: trends, predictions, risk factors and prevention. *Nat Rev Gastroenterol Hepatol*. (2021) 18:223–38. doi: 10.1038/s41575-020-00381-6

4. Sumida Y, Niki E, Naito Y, Yoshikawa T. Involvement of free radicals and oxidative stress in NAFLD/NASH. *Free Radical Res*. (2013) 47:869–80. doi: 10.3109/10715762.2013.837577

5. Lackner C. Hepatocellular ballooning in nonalcoholic steatohepatitis: the pathologist's perspective. *Expert Rev Gastroenterol Hepatol*. (2011) 5:223–31. doi: 10.1586/egh.11.8

6. White DL, Kanwal F, El-Serag HB. Association between nonalcoholic fatty liver disease and risk for hepatocellular cancer, based on systematic review. *Clin Gastroenterol Hepatol*. (2012) 10:1342–59.e2. doi: 10.1016/j.cgh.2012.10.001

7. Yang JD, Hainaut P, Gores GJ, Amadou A, Plymoth A, Roberts LR. A global view of hepatocellular carcinoma: trends, risk, prevention and management. *Nature Rev Gastroenterol & Hepatol* (2019) 16(10):589–604. doi: 10.1038/s41575-019-0186-y

8. Wong RJ, Aguilar M, Cheung R, Perumpail RB, Harrison SA, Younossi ZM, et al. Nonalcoholic steatohepatitis is the second leading etiology of liver disease among adults awaiting liver transplantation in the United States. *Gastroenterology* (2015) 148:547–55. doi: 10.1053/j.gastro.2014.11.039

9. Wong RJ, Cheung R, Ahmed AJH. Nonalcoholic steatohepatitis is the most rapidly growing indication for liver transplantation in patients with hepatocellular carcinoma in the US. *Hepatology (Baltimore, Md)*. (2014) 59(6):2188–95. doi: 10.1002/hep.26986

10. Sinha N, Dabla PK. Oxidative stress and antioxidants in hypertension-a current review. *Curr hypertension Rev*. (2015) 11:132–42. doi: 10.2174/1573402111666150529130922

11. Bellot GL, Liu D, Pervaiz SROS. autophagy, mitochondria and cancer: Ras, the hidden master? *Mitochondrion*. (2013) 13:155–62. doi: 10.1016/j.mito.2012.06.007

12. Yusuf M, Khan M, Robaian MA, Khan RA. Biomechanistic insights into the roles of oxidative stress in generating complex neurological disorders. *Biol Chem*. (2018) 399:305–19. doi: 10.1515/hsz-2017-0250

13. Crujeiras AB, Díaz-Lagares A, Carreira MC, Amil M, Casanueva FF. Oxidative stress associated to dysfunctional adipose tissue: a potential link between obesity, type 2 diabetes mellitus and breast cancer. *Free Radical Res*. (2013) 47:243–56. doi: 10.3109/10715762.2013.772604

14. Cadenas E, Davies KJ. Mitochondrial free radical generation, oxidative stress, and aging. *Free Radical Biol Med*. (2000) 29:222–30. doi: 10.1016/S0891-5849(00)00317-8

15. Slater TF. Free-radical mechanisms in tissue injury. *Biochem J*. (1984) 222:1–15. doi: 10.1042/bj2220001

16. Ferro D, Basili S, Praticó D, Iuliano L, FitzGerald GA, Violi F. Vitamin E reduces monocyte tissue factor expression in cirrhotic patients. *Blood*. (1999) 93:2945–50. doi: 10.1182/blood.V93.9.2945.409k29_2945_2950

17. Klisic A, Kavaric N, Ninic A, Kotur-Stevuljevic J. Oxidative stress and cardiometabolic biomarkers in patients with non-alcoholic fatty liver disease. *Sci Rep*. (2021) 11:18455. doi: 10.1038/s41598-021-97686-6

18. Spahis S, Delvin E, Borys JM, Levy E. Oxidative stress as a critical factor in nonalcoholic fatty liver disease pathogenesis. *Antioxidants Redox Signaling*. (2017) 26:519–41. doi: 10.1089/ars.2016.6776

19. Sánchez-Valle V, Chávez-Tapia NC, Uribe M, Méndez-Sánchez N. Role of oxidative stress and molecular changes in liver fibrosis: a review. *Curr medicinal Chem*. (2012) 19:4850–60. doi: 10.2174/092986712803341520

20. Gambino R, Musso G, Cassader M. Redox balance in the pathogenesis of nonalcoholic fatty liver disease: mechanisms and therapeutic opportunities. *Antioxidants Redox Signaling*. (2011) 15:1325–65. doi: 10.1089/ars.2009.3058

21. Ritchie ME, Phipson B, Wu D, Hu Y, Law CW, Shi W, et al. limma powers differential expression analyses for RNA-sequencing and microarray studies. *Nucleic Acids Res*. (2015) 43:e47. doi: 10.1093/nar/gkv007

22. Xu M, Zhou H, Hu P, Pan Y, Wang S, Liu L, et al. Identification and validation of immune and oxidative stress-related diagnostic markers for diabetic nephropathy by WGCNA and machine learning. *Front Immunol*. (2023) 14:1084531. doi: 10.3389/fimmu.2023.1084531

23. Langfelder P, Horvath S. WGCNA: an R package for weighted correlation network analysis. *BMC Bioinf*. (2008) 9:559. doi: 10.1186/1471-2105-9-559

24. Kolde R, Kolde MR. *Package 'pheatmap'*. (2015) 1(7):790.

25. Wickham H, Chang W, Wickham MH. Package 'ggplot2'. Create elegant data visualisations using the grammar of graphics. (2016) 2(1):1–189.

26. Yu G, Wang LG, Han Y, He QY. clusterProfiler: an R package for comparing biological themes among gene clusters. *Omics J Integr Biol*. (2012) 16:284–7. doi: 10.1089/omi.2011.0118

27. Friedman J, Hastie T, Tibshirani R. Regularization paths for generalized linear models via coordinate descent. *J Stat software*. (2010) 33:1–22. doi: 10.18637/jss.v033.i01

28. Dimitriadou E, Hornik K, Leisch F, Meyer D, Weingessel A, Leisch MF, et al. *The e1071 package*. Misc Functions of Department of Statistics, TU Wien. (2006). pp. 297–304.

29. Kuhn M. Building predictive models in R using the caret package. *J Stat software*. (2008) 28:1 –26. doi: 10.18637/jss.v028.i05

30. Liaw A, Wiener M. Classification and regression by randomForest. *R News*. (2002) 2:18–22.

31. Szklarczyk D, Gable AL, Nastou KC, Lyon D, Kirsch R, Pyysalo S, et al. The STRING database in 2021: customizable protein-protein networks, and functional characterization of user-uploaded gene/measurement sets. *Nucleic Acids Res*. (2021) 49:D605–d12. doi: 10.1093/nar/gkaa1074

32. Csárdi G, Nepusz T. The igraph software package for complex network research. *InterJournal, Complex Systems*. (2006) 1695(5):1–9.

33. Harrell FE Jr, Harrell MFE Jr, Hmisc D. *Package 'rms'*. Vanderbilt University. (2017) 229:Q8.

34. Robin X, Turck N, Hainard A, Tiberti N, Lisacek F, Sanchez JC, et al. pROC: an open-source package for R and S+ to analyze and compare ROC curves. *BMC Bioinf*. (2011) 12:77. doi: 10.1186/1471-2105-12-77

35. Xiao Y, Batmanov K, Hu W, Zhu K, Tom AY, Guan D, et al. Hepatocytes demarcated by EphB2 contribute to the progression of nonalcoholic steatohepatitis. *Science translational medicine*. (2023) 15(682):eadc9653. doi: 10.1126/scitranslmed.adc9653

36. Yip SH, Wang P, Kocher JA, Sham PC, Wang J. Linnorm: improved statistical analysis for single cell RNA-seq expression data. *Nucleic Acids Res*. (2017) 45:e179. doi: 10.1093/nar/gkx828

37. McCarthy DJ, Campbell KR, Lun AT, Wills QF. Scater: pre-processing, quality control, normalization and visualization of single-cell RNA-seq data in R. *Bioinf (Oxford England)*. (2017) 33:1179–86. doi: 10.1093/bioinformatics/btw777

38. Hao Y, Stuart T, Kowalski MH, Choudhary S, Hoffman P, Hartman A, et al. Dictionary learning for integrative, multimodal and scalable single-cell analysis. *Nat Biotechnol*. (2023) 42(2):293–304. doi: 10.1038/s41587-023-01767-y

39. Aran D, Looney AP, Liu L, Wu E, Fong V, Hsu A, et al. Reference-based analysis of lung single-cell sequencing reveals a transitional profibrotic macrophage. *Nat Immunol*. (2019) 20:163–72. doi: 10.1038/s41590-018-0276-y

40. Bencivenga D, Stampone E, Aulitto A, Tramontano A, Barone C, Negri A, et al. A cancer-associated CDKN1B mutation induces p27 phosphorylation on a novel residue: a new mechanism for tumor suppressor loss-of-function. *Mol Oncol*. (2021) 15:915–41. doi: 10.1002/1878-0261.12881

41. Ogawa T, Enomoto M, Fujii H, Sekiya Y, Yoshizato K, Ikeda K, et al. MicroRNA-221/222 upregulation indicates the activation of stellate cells and the progression of liver fibrosis. *Gut*. (2012) 61:1600–9. doi: 10.1136/gutjnl-2011-300717

42. Galardi S, Mercatelli N, Giorda E, Massalini S, Frajese GV, Ciafrè SA, et al. miR-221 and miR-222 expression affects the proliferation potential of human prostate carcinoma cell lines by targeting p27Kip1. *J Biol Chem*. (2007) 282:23716–24. doi: 10.1074/jbc.M701805200

43. le Sage C, Nagel R, Egan DA, Schrier M, Mesman E, Mangiola A, et al. Regulation of the p27(Kip1) tumor suppressor by miR-221 and miR-222 promotes cancer cell proliferation. *EMBO J*. (2007) 26:3699–708. doi: 10.1038/sj.emboj.7601790

44. Ma J, Zeng S, Zhang Y, Deng G, Qu Y, Guo C, et al. BMP4 enhances hepatocellular carcinoma proliferation by promoting cell cycle progression via ID2/CDKN1B signaling. *Mol carcinogenesis*. (2017) 56:2279–89. doi: 10.1002/mc.22681

45. Fornari F, Gramantieri L, Ferracin M, Veronese A, Sabbioni S, Calin GA, et al. MiR-221 controls CDKN1C/p57 and CDKN1B/p27 expression in human hepatocellular carcinoma. *Oncogene*. (2008) 27:5651–61. doi: 10.1038/onc.2008.178

46. Tannapfel A, Grund D, Katalinic A, Uhlmann D, Köckerling F, Haugwitz U, et al. Decreased expression of p27 protein is associated with advanced tumor stage in hepatocellular carcinoma. *Int J Cancer*. (2000) 89:350–5. doi: 10.1002/1097-0215(20000720)89:4<350::AID-IJC6>3.0.CO;2-3

47. Balsa E, Marco R, Perales-Clemente E, Szklarczyk R, Calvo E, Landázuri MO, et al. NDUFA4 is a subunit of complex IV of the mammalian electron transport chain. *Cell Metab*. (2012) 16:378–86. doi: 10.1016/j.cmet.2012.07.015

48. Garbian Y, Ovadia O, Dadon S, Mishmar D. Gene expression patterns of oxidative phosphorylation complex I subunits are organized in clusters. *PloS One*. (2010) 5:e9985. doi: 10.1371/journal.pone.0009985

49. Zhu J, Xiang X, Hu X, Li C, Song Z, Dong Z. miR-147 represses NDUFA4, inducing mitochondrial dysfunction and tubular damage in cold storage kidney

transplantation. *J Am Soc Nephrol JASN*. (2023) 34:1381–97. doi: 10.1681/ASN.0000000000000154

50. Yagil C, Varadi-Levi R, Yagil Y. A novel mutation in the NADH dehydrogenase (ubiquinone) 1 alpha subcomplex 4 (Ndufa4) gene links mitochondrial dysfunction to the development of diabetes in a rodent model. *Dis Models Mech*. (2018) 11(11):1–9. doi: 10.1242/dmm.036699

51. Tian F, Tang P, Sun Z, Zhang R, Zhu D, He J, et al. miR-210 in exosomes derived from macrophages under high glucose promotes mouse diabetic obesity pathogenesis by suppressing NDUFA4 expression. *J Diabetes Res*. (2020) 2020:6894684. doi: 10.1155/2020/6894684

52. Chen D, Hou Y, Cai X. MiR-210-3p enhances cardiomyocyte apoptosis and mitochondrial dysfunction by targeting the NDUFA4 gene in sepsis-induced myocardial dysfunction. *Int Heart J*. (2021) 62:636–46. doi: 10.1536/ihj.20-512

53. Clayton DA. Replication and transcription of vertebrate mitochondrial DNA. *Annu Rev Cell Biol*. (1991) 7:453–78. doi: 10.1146/annurev.cb.07.110191.002321

54. Bonekamp NA, Jiang M, Motori E, Garcia Villegas R, Koolmeister C, Atanassov I, et al. High levels of TFAM repress mammalian mitochondrial DNA transcription *in vivo*. *Life Sci alliance*. (2021) 4(11):1–17. doi: 10.26508/lsa.202101034

55. Silva J, Spatz MH, Folk C, Chang A, Cadenas E, Liang J, et al. Dihydromyricetin improves mitochondrial outcomes in the liver of alcohol-fed mice via the AMPK/Sirt-1/PGC-1α signaling axis. *Alcohol (Fayetteville NY)*. (2021) 91:1–9. doi: 10.1016/j.alcohol.2020.10.002

56. Zhu Y, Xu J, Hu W, Wang F, Zhou Y, Xu W, et al. TFAM depletion overcomes hepatocellular carcinoma resistance to doxorubicin and sorafenib through AMPK activation and mitochondrial dysfunction. *Gene*. (2020) 753:144807. doi: 10.1016/j.gene.2020.144807

57. Stiles AR, Simon MT, Stover A, Eftekharian S, Khanlou N, Wang HL, et al. Mutations in TFAM, encoding mitochondrial transcription factor A, cause neonatal liver failure associated with mtDNA depletion. *Mol Genet Metab*. (2016) 119:91–9. doi: 10.1016/j.ymgme.2016.07.001

58. Xie D, Wu X, Lan L, Shangguan F, Lin X, Chen F, et al. Downregulation of TFAM inhibits the tumorigenesis of non-small cell lung cancer by activating ROS-mediated JNK/p38MAPK signaling and reducing cellular bioenergetics. *Oncotarget*. (2016) 7:11609–24. doi: 10.18632/oncotarget.7018

59. Araujo LF, Siena ADD, Plaça JR, Brotto DB, Barros II, Muys BR, et al. Mitochondrial transcription factor A (TFAM) shapes metabolic and invasion gene signatures in melanoma. *Sci Rep*. (2018) 8:14190. doi: 10.1038/s41598-018-31170-6

60. Mo M, Peng F, Wang L, Peng L, Lan G, Yu S. Roles of mitochondrial transcription factor A and microRNA-590-3p in the development of bladder cancer. *Oncol Lett*. (2013) 6:617–23. doi: 10.3892/ol.2013.1419

61. Wu K, Zhao Z, Xiao Y, Peng J, Chen J, He Y. Roles of mitochondrial transcription factor A and microRNA−590−3p in the development of colon cancer. *Mol Med Rep*. (2016) 14:5475–80. doi: 10.3892/mmr.2016.5955

62. Justo R, Boada J, Frontera M, Oliver J, Bermúdez J, Gianotti M. Gender dimorphism in rat liver mitochondrial oxidative metabolism and biogenesis. *Am J Physiol Cell Physiol*. (2005) 289:C372–8. doi: 10.1152/ajpcell.00035.2005

63. Picca A, Pesce V, Fracasso F, Joseph AM, Leeuwenburgh C, Lezza AM. A comparison among the tissue-specific effects of aging and calorie restriction on TFAM amount and TFAM-binding activity to mtDNA in rat. *Biochim Biophys Acta*. (2014) 1840:2184–91. doi: 10.1016/j.bbagen.2014.03.004

64. Zhang JJ, Shen Y, Chen XY, Jiang ML, Yuan FH, Xie SL, et al. Integrative network-based analysis on multiple Gene Expression Omnibus datasets identifies novel immune molecular markers implicated in non-alcoholic steatohepatitis. *Front Endocrinol*. (2023) 14:1115890. doi: 10.3389/fendo.2023.1115890

frontiers | Frontiers in Immunology

TYPE Mini Review
PUBLISHED 11 March 2024
DOI 10.3389/fimmu.2024.1360342

OPEN ACCESS

EDITED BY
Pedro Gonzalez-Menendez,
University of Oviedo, Spain

REVIEWED BY
Nabab Khan,
Yale University, United States
Charles Nathan S. Allen,
University of Maryland, College Park,
United States

*CORRESPONDENCE
Talia H. Swartz
talia.swartz@mssm.edu

RECEIVED 22 December 2023
ACCEPTED 26 February 2024
PUBLISHED 11 March 2024

CITATION
Rodriguez NR, Fortune T, Hegde E, Weinstein MP, Keane AM, Mangold JF and Swartz TH (2024) Oxidative phosphorylation in HIV-1 infection: impacts on cellular metabolism and immune function. *Front. Immunol.* 15:1360342. doi: 10.3389/fimmu.2024.1360342

Oxidative phosphorylation in HIV-1 infection: impacts on cellular metabolism and immune function

Natalia Rodriguez Rodriguez, Trinisia Fortune, Esha Hegde, Matthew Paltiel Weinstein, Aislinn M. Keane, Jesse F. Mangold and Talia H. Swartz*

Department of Medicine, Division of Infectious Diseases, Icahn School of Medicine at Mount Sinai, New York, NY, United States

Human Immunodeficiency Virus Type 1 (HIV-1) presents significant challenges to the immune system, predominantly characterized by $CD4^+$ T cell depletion, leading to Acquired Immunodeficiency Syndrome (AIDS). Antiretroviral therapy (ART) effectively suppresses the viral load in people with HIV (PWH), leading to a state of chronic infection that is associated with inflammation. This review explores the complex relationship between oxidative phosphorylation, a crucial metabolic pathway for cellular energy production, and HIV-1, emphasizing the dual impact of HIV-1 infection and the metabolic and mitochondrial effects of ART. The review highlights how HIV-1 infection disrupts oxidative phosphorylation, promoting glycolysis and fatty acid synthesis to facilitate viral replication. ART can exacerbate metabolic dysregulation despite controlling viral replication, impacting mitochondrial DNA synthesis and enhancing reactive oxygen species production. These effects collectively contribute to significant changes in oxidative phosphorylation, influencing immune cell metabolism and function. Adenosine triphosphate (ATP) generated through oxidative phosphorylation can influence the metabolic landscape of infected cells through ATP-detected purinergic signaling and contributes to immunometabolic dysfunction. Future research should focus on identifying specific targets within this pathway and exploring the role of purinergic signaling in HIV-1 pathogenesis to enhance HIV-1 treatment modalities, addressing both viral infection and its metabolic consequences.

KEYWORDS

HIV-1, oxidative phosphorylation, antiretroviral therapy (ART), mitochondrial dysfunction, immune metabolism

Abbreviations: HIV-1, Human Immunodeficiency Virus Type 1; ART, Antiretroviral Therapy; PBMC, Peripheral Blood Mononuclear Cells; ROS, Reactive Oxygen Species; ETC, Electron Transport Chain; NRTIs, Nucleoside/Nucleotide Reverse Transcriptase Inhibitors; NNRTIs, Non-nucleoside Reverse Transcriptase Inhibitors; PIs, Protease Inhibitors; ATP, Adenosine Triphosphate; NADH, Nicotinamide Adenine Dinucleotide (Reduced Form); FADH2, Flavin Adenine Dinucleotide (Reduced Form); Cyt-c, Cytochrome c; TCA, Tricarboxylic Acid Cycle; GLUT1, Glucose Transporter 1; SMO, Spermine Oxidase; EGFR, Epidermal Growth Factor Receptor; mTFA, Mitochondrial Transcription Factor A.

Introduction

Human Immunodeficiency Virus Type 1 (HIV-1) presents a chronic, intractable challenge, primarily characterized by extensive $CD4^+$ T cell depletion (1–5). This pathology manifests in both lymphoid tissues and peripheral blood, culminating in profound immunodeficiency and progression to Acquired Immunodeficiency Syndrome (AIDS). Despite the efficacy of Antiretroviral Therapy (ART) in viral load suppression, HIV-1 infection is associated with chronic inflammation and, together with the direct effects of ART, is associated with metabolic dysregulation, enhanced inflammatory response, gene expression modulation, and biochemical pathway alterations (6–9).

We explore the confluence of oxidative phosphorylation and cellular metabolic transformations in the context of HIV-1 infection and ART in PWH. Key focus areas include the nuances of mitochondrial dysfunction, specifically alterations in oxidative phosphorylation and association with immune cell dysregulation. This underscores a potential nexus between mitochondrial functionality and immunological response. Additionally, we examine the long-term impacts of ART and the potential for more nuanced HIV-1 treatment modalities. This review aims to enrich the understanding of the intricate interplay between oxidative phosphorylation and HIV-1 pathogenesis, steering future research and therapeutic interventions in this critical domain.

Oxidative phosphorylation: an overview

Oxidative phosphorylation, a crucial biochemical process, involves the reduction of oxygen to generate ATP (10). Oxidative phosphorylation is the final stage of aerobic respiration, following glycolysis and the citric acid cycle. The efficiency of oxidative phosphorylation relies on successive oxidative/reductive reactions, notably the transfer of electrons by NADH and FADH2 to oxygen, the ultimate electron acceptor (11). The electron transport chain (ETC) facilitates this electron movement within mitochondria. In order of oxidative/reductive reactions, the complexes are I, II, coenzyme Q, III, cytochrome C, and IV. This process pumps protons across the mitochondrial intermembrane space, generating a proton electrochemical gradient that powers ATP synthase (complex V) (12). ATP synthase facilitates ATP biosynthesis with its rotating F0 and F1 components. The F1 component binds nucleotides at its catalytic sites, occupied by Mg-ADP and phosphate. Rotation, driven by F0 subunit reionization, alters F1 directionality, initiating ATP synthesis from ADP and phosphite (13). ATP generated through oxidative phosphorylation, the final and most efficient stage of aerobic respiration in the electron transport chain, serves as the primary energy source for cells, far surpassing the yields from glycolysis and the citric acid cycle.

The regulation of oxidative phosphorylation is complex and multifaceted. The mitochondrial membrane potential is at the center of the regulation, formed by the proton gradient and linked to both ATP and free radical production (14, 15). The most basic regulation of oxidative phosphorylation is allosteric control by negative feedback of substrates or intermediaries. A high NADH/NAD+ ratio slows the Krebs cycle, ETC, and oxidative phosphorylation, as does a high ATP/ADP ratio, in which ATP binds directly and inhibits cytochrome c (Cyt-c) and cytochrome oxidase (complex IV) (15, 16).

Oxidative phosphorylation complexes and Cyt-c are targeted for phosphorylation by regulatory kinases, including protein kinase C, cAMP-dependent tyrosine kinases, and EGFR (17–19). The formation of super-complexes (SCs) or respirasomes, consisting of various combinations of the ETC complexes, increases respiratory efficiency and decreases ROS production. SC abundance, along with expression of specific isoforms of Cyt-c or cytochrome oxidase, allow for regulation of ROS formation and energetic needs at tissue-level specificity (15). The fusion and fission of the mitochondrial network contribute to oxidative phosphorylation efficiency regulation, with highly connected networks promoting efficiency and curbing excess ROS production (20, 21).

HIV-1 infection, metabolic preprogramming, cellular metabolism, and oxidative phosphorylation

Metabolic reprogramming is key in both cancer and HIV-1 infections. In cancer, this is seen as the Warburg effect, characterized by increased glucose uptake and lactate production, even when oxygen is available (22). Similarly, HIV-1 uses metabolic reprogramming to gather free nucleotides, amino acids, and lipids for viral replication and assembly (23). Studies reveal that CD4+ T cells with higher oxidative phosphorylation and glycolysis are more prone to HIV-1 infection, with infected cells showing elevated metabolic activity (24). HIV-1 also boosts glycolysis in CD4+ T cells by upregulating GLUT1 expression. The HIV-1 glycoprotein gp120 is implicated in this process, possibly by activating surface signaling molecules like CXCR4 and CCR5 and increasing the expression of glycolytic enzymes (25). Additionally, hexokinase activity is heightened in HIV-1 infected CD4+ T cells, a change dependent on viral replication (26, 27). However, the precise viral mechanisms promoting glycolysis upregulation by HIV-1 are not fully understood.

There is growing interest in understanding the impact of HIV on Mitochondrial-associated ER membranes (MAMs) due to their crucial role in metabolic reprogramming. MAMs serve as structures linking the endoplasmic reticulum (ER) and mitochondria, facilitating oxidative protein production and mitochondrial biogenesis. The viral HIV-1 Tat protein disrupts MAMs in neuronal cell lines upon infection by phosphorylating the mitochondrial protein PTPIP51 and disrupting its localization to MAMs, thus reducing calcium signaling and increasing ROS accumulation (28). Furthermore, HIV-1 Vpr has been shown to disrupt MAMs by decreasing the expression of critical MAM-

associated proteins Mfn2 and Drp1 (29). The targeting of MAMs by HIV-1 induces oxidative stress that contributes to HIV-associated metabolic reprogramming, but further research is needed to establish other key mechanisms involved.

HIV-1 impacts host cell metabolism, initially enhancing glycolysis and fatty acid synthesis for viral replication (30–33). This increased metabolic activity, particularly in glycolysis and glucose transport, makes cells like T-cells and monocytes more susceptible to HIV-1 infection (24, 34, 35). Upregulation of the GLUT-1 transporter and mitochondrial oxidative damage, linked to ROS production, highlights the role of metabolic reprogramming in HIV-1 infection and potential research avenues (31, 35, 36). People with HIV (PWH) face systemic metabolic challenges due to both HIV-1 and antiretroviral therapy (ART), increasing metabolic disease risks (37, 38). Studies have shown that HIV-1 influences metabolic aging, with oxidative phosphorylation and pyruvate metabolism downregulation noted in PWH (39). Furthermore, HIV-1 affects the expression of electron transport chain (ETC) components and causes mitochondrial damage, as seen in the upregulation of Complex-IV subunit, contributing to oxidative stress (40, 41).

ART classes have long been associated with mitochondria dysfunction (42). Both Nucleoside/Nucleotide Reverse Transcriptase Inhibitors (NRTIs) and Non-nucleotide Reverse Transcriptase Inhibitors (NNRTIs) are associated with dyslipidemia in PWH and alter adipocyte differentiation. NRTIs induce lipodystrophy by promoting mitochondrial dysfunction and adipocyte death and interfering with mitochondrial DNA (mtDNA) synthesis (42). This inhibits Pol-gamma, increases ROS production, and reduces ETC activity and oxidative phosphorylation (37, 42–46). Additionally, protease inhibitors (PIs) target GLUT4, impairing glucose uptake into adipocytes and promoting insulin resistance (37, 47, 48).

HIV-1 infection exacerbates oxidative stress and mitochondrial damage, affecting cell metabolism and promoting diseases in PWH, especially those on ART. Gp120 upregulates CYP2E1, proline oxidase (POX), NOX2, and NOX4 to enhance ROS production (49–57). Nef interacts with the NADPH oxidases without affecting the NOX expression (57). The HIV-1 proteins Vpr and Tat both contribute to mitochondrial dysfunction: Vpr reduces membrane potential and triggers apoptosis by binding to ANT, part of the mitochondrial permeability transition pore, while Tat elevates free calcium levels in the cytoplasm by interacting with NADPH oxidases, leading to increased mitochondrial calcium uptake and reactive oxygen species (ROS) production (54, 55, 58–64). These changes increase the risk of metabolic diseases in PWH, with ART compounds like NRTIs and PIs exacerbating (65, 66).

Purinergic receptors, ATP, and HIV pathogenesis

Purinergic receptors, particularly the P1 and P2 subtypes, are integral to inflammatory responses and the progression of HIV-1. The P2X receptors, activated by ATP, are crucial in initiating immune responses and impacting the HIV-1 viral life cycle (67–71). The enzyme CD39 regulates ATP availability, influencing both the progression of AIDS and the function of T cells by modulating ATP and adenosine levels, affecting P2X receptor signaling (72–74).

The P2X receptors are implicated in cell entry and infection by the virus, and their inhibition can significantly reduce HIV-1 infection in various cell types (70, 75–85). Chronic inflammation in HIV is driven by factors like immunosenescence and persistent viral replication, even with antiretroviral therapy (ART). It is exacerbated by factors such as organ fibrosis and co-infections (4, 9, 86–88).

Furthermore, extracellular ATP and its interaction with P2X receptors regulate HIV infection and inflammation. This signaling leads to the production of inflammatory cytokines and the activation of the NLRP3 inflammasome, contributing to CD4+ T lymphocyte depletion and apoptosis (77, 89–92). HIV-1 interacts with Pannexin-1, a membrane channel, suggesting a link between ATP production and inflammatory signaling in HIV-1 infection (93–96). Circulating levels of ATP have been proposed as a biomarker of cognitive decline in PWH, predicting central nervous system compromise and suggesting the use of Pannexin-1 or purinergic receptor inhibitors for clinical intervention (97).

HIV-associated neurocognitive disorder: the roles of HIV-1, ART, oxidative phosphorylation, and purinergic signaling

The progression of HIV-1-associated neurocognitive disorders (HAND) in PWH has been linked to purinergic signaling and oxidative stress. The central nervous system serves as a reservoir of HIV-1, leading to neuroinflammation and neurodegeneration that progress to HIV-1 encephalitis and HAND that persist despite the use of effective ART (98–100). Within the CNS, HIV-1 induces the release of extracellular ATP in infected cells to support viral replication, and ATP interacts with purinergic receptors to produce a proinflammatory response (83, 101, 102). The purinergic receptor subtype P2X is particularly interesting, notably P2X7, which is widely expressed in various brain cells, including astrocytes, oligodendrocytes, microglia, and neurons (102). In astrocytes, P2X7 activation induced by gp120 leads to Cx43 hemichannels and pannexin-1 opening, resulting in increased ATP release and nitric oxide production. This process is speculated to propagate gp120-mediated signaling to neighboring cells (95). In the peripheral nervous system (PNS), P2X4 is involved in gp120-induced lysosomal exocytosis and ATP release in Schwann Cells, increasing cytosolic calcium and generating ROS in dorsal root ganglia neurons (101). Although ART mitigates the neuropathology of HIV-1 infection in PWH, it does not eliminate it, with studies showing possible neurotoxicity of ART. ART-related neurotoxicity in the brain is thought to be linked to the loss of mtDNA due to NRTIs inhibiting mtDNA polymerase gamma (103, 104). Additionally, ART contributes to astrocyte autophagy, de-acidification of endolysosomes, and the promotion of

amyloidogenesis, all associated with the pathogenesis of HAND (105).

Extracellular ATP and P2X receptors are integral in HIV-1 infection, influencing the virus's life cycle and contributing to immunopathogenesis, neurodegeneration, and chronic inflammation. Their interaction with HIV-1 is key in disease progression, affecting viral replication, cytokine release, and cell death (75, 77, 78, 81, 83–85). This insight reveals the potential of targeting purinergic signaling in developing novel therapies for HIV-1, reducing inflammation and related comorbidities, and represents a significant area for future research.

Oxidative phosphorylation in immune cell dysfunction during HIV-1 infection

The metabolic dynamics of immune cells, particularly CD4+ T cells, CD8+ T cells, and macrophages, are critical in understanding HIV-1 pathophysiology. CD4+ T cells infected with HIV-1 shift towards increased glycolysis, facilitating viral replication. A study identified a link between oxidative phosphorylation in these cells and higher viral loads, with NLRX1 and FASTKD5 as key factors. Metformin, a complex I inhibitor, was found to suppress HIV-1 replication in CD4+ T cells (106). In PWH on ART, there's an upregulation of oxidative phosphorylation compared to elite controllers, and complex IV inhibition was linked to increased HIV-1 reactivation in a latency model (107).

CD8+ T cells in chronic HIV-1 infection experience metabolic exhaustion, diminishing their functionality and virus control ability. A combination therapy comprised of a mitochondrial superoxide scavenger, a small-molecule inhibitor of mitochondrial fission, and IL-15 can increase the frequency of IFNy and TNFa poly-functional CD8+ T cells and decrease the frequency of exhaustion markers (108).

In HIV-infected macrophages, there is notable support for prolonged HIV-1 replication and survival, shielding virions from ART and neutralizing antibodies. These macrophages show metabolic plasticity, shifting between oxidative phosphorylation and glycolysis based on their polarization state. HIV-1 infection alters macrophage metabolism, promoting a pro-inflammatory state and increasing glycolytic activity, which is linked to chronic inflammation seen in HIV-1 infection (109). A study demonstrated that superoxide dismutase (SOD) mimetic drugs could inhibit myeloid cell-driven bystander cell death *in vitro* (110).

Figure 1 highlights the impact of HIV-1 infection on mitochondrial oxidative phosphorylation. It contrasts the normal mitochondrial function with the altered state during HIV-1 infection, depicting how HIV-1 infection leads to an upregulation in the transcription of oxidative phosphorylation genes, resulting in greater electron transport chain efficiency. This heightened activity leads to increased production of ROS, a hallmark of cellular stress. Consequently, there's an enhancement in mitochondrial membrane potential and a notable increase in ATP production compared to baseline conditions. These alterations signify a hyperactivated mitochondrial state triggered by HIV-1 infection, underlining the complex interplay between the virus and the host's cellular metabolism.

Current research and future directions

Therapeutic interventions targeting mitochondrial dysfunction and oxidative stress in HIV immunopathogenesis are emerging as a crucial field of research. Metformin, a diabetes medication, has shown varying effects on HIV-1 replication in studies by Rezai et al. and Guo et al. (106, 111). There is an additive effect of risk of metformin-associated lactic acidosis when used with NRTIs like tenofovir, which calls for caution in its clinical application (112, 113). Research on the antioxidant properties of plant flavonoids, such as naringin, is gaining attention for their potential to mitigate oxidative damage induced by NRTIs (114, 115). Statins, known for their anti-inflammatory and lipid-lowering effects, are being explored for their benefits in HIV management, with studies like SATURN-HIV and REPRIEVE indicating their impact on cardiovascular risk and mitochondrial function in PWH on ART (116–118).

Given that HIV-1 infection induces metabolic reprogramming like that observed in cancer cells, there is growing interest in exploring anti-cancer drug treatments as potential interventions to target these metabolic effects of HIV-1 (119). In neurons, the viral protein gp120 reduces ATP output via oxidative phosphorylation while increasing glycolysis production and PKM2 expression. Tepp-46, a selective PKM2 tetrameric stabilizer and a potential small molecule therapeutics for lung cancer, has demonstrated the ability to reverse the metabolic reprogramming induced by gp120 in neuronal cells (120). Further, studies have linked dyslipidemia in PWH on ART with mitochondrial oxidative stress, suggesting an association between lipid profiles and the function of mitochondrial electron transport chain complexes (121). Atovaquone, a mitochondrial complex III inhibitor, though not tested in chronic inflammation, is used for treating parasitic and fungal infections (81).

Advancements in understanding HIV-1 pathogenesis highlight the role of purinergic signaling, particularly the involvement of extracellular ATP and P2X receptors. These receptors play a significant role in the inflammatory response and immune modulation in HIV-1 infection (112, 113). This growing body of research underlines the importance of understanding the metabolic and mitochondrial aspects of HIV-1 infection and ART. The goal is to improve treatment outcomes by mitigating adverse effects and exploring new therapeutic avenues that address both HIV-1 management and broader metabolic and cardiovascular health.

Conclusions

The interaction between HIV-1 infection and metabolic activity significantly shapes the chronic inflammation commonly associated with HIV. The activation of oxidative phosphorylation is a key driver in chronic inflammation. This shift is evident in studies documenting the increased activity of mitochondrial respiratory chain complexes in HIV-1 infected cells (122–132). Such changes suggest that HIV-1 exploits the host's mitochondrial machinery to its advantage, potentially exacerbating the inflammatory response. While ART effectively controls viral replication, it does not fully

Baseline

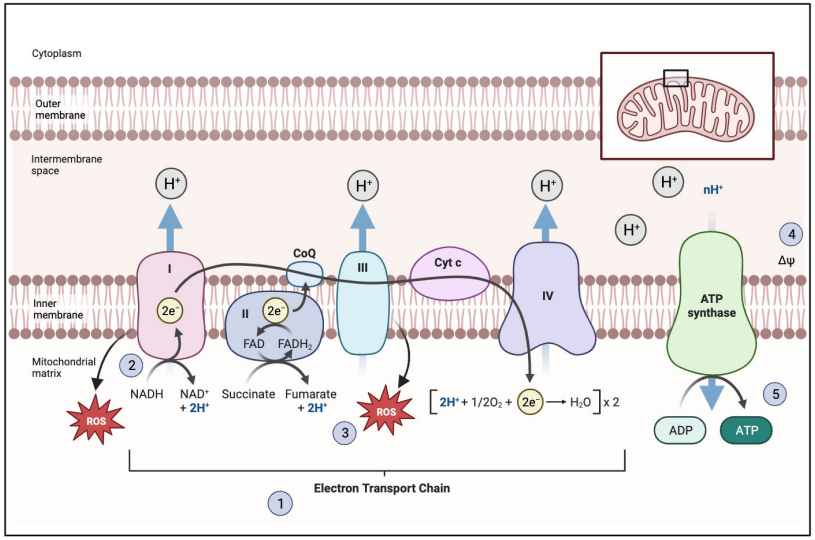

1. **Baseline OxPhos Function**: Normal transcription levels of OxPhos genes, indicating standard oxidative phosphorylation activity.
2. **Efficient Electron Transport**: Electrons move through complexes I-IV without impairment, driving proton pumps and maintaining the proton gradient.
3. **Controlled ROS Production**: ROS are produced at manageable levels and are well-controlled by cellular antioxidants.
4. **Stable Mitochondrial Membrane Potential**: The inner mitochondrial membrane maintains a potential necessary for ATP synthesis and cellular health.
5. **Normal ATP Production**: ATP synthase functions effectively, using the proton gradient to generate ATP from ADP and inorganic phosphate.

HIV-1 infection

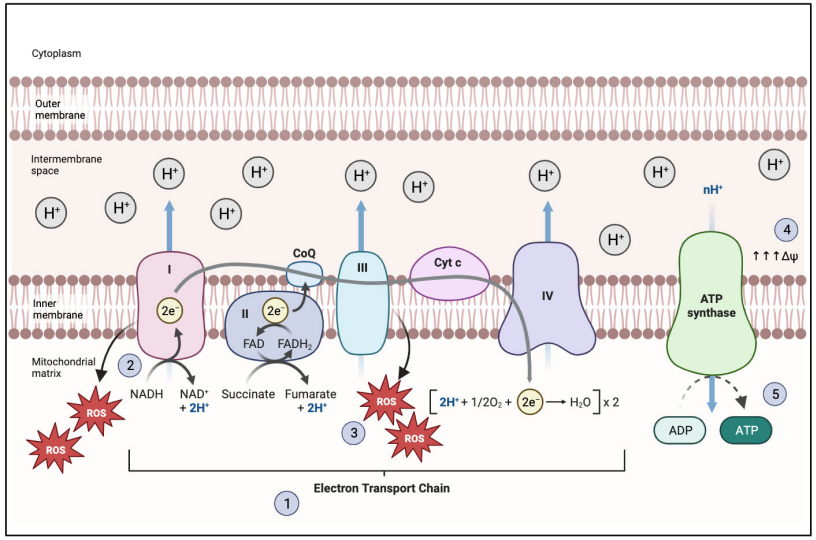

1. **Enhanced OxPhos Function**: Enhanced transcription levels of OxPhos genes indicate increased oxidative phosphorylation activity, reflective of heightened cellular metabolic demand.
2. **Increased Electron Transport**: Enhanced electron flow through complexes I-IV, augmenting proton pumping efficiency and intensifying the proton gradient.
3. **Uncontrolled ROS Production**: Increase in ROS production, exceeding the control capacity of cellular antioxidants, leading to oxidative stress.
4. **Increased Mitochondrial Membrane Potential:** HIV-1 infection disrupts the mitochondrial membrane potential, which can lead to a loss of cellular viability and promote apoptosis.
5. **Enhanced ATP Production**: Due to the impaired function of the electron transport chain, the efficiency of ATP synthase is reduced, resulting in lower ATP production.

FIGURE 1
HIV-1 Infection impact on mitochondrial oxidative phosphorylation. The figure contrasts mitochondrial function under normal conditions with the altered state during HIV-1 infection. It shows that HIV-1 infection leads to increased transcription of oxidative phosphorylation genes, higher electron transport efficiency, and elevated reactive oxygen species (ROS) production, resulting in an enhanced mitochondrial membrane potential and increased ATP production compared to the baseline state. These changes indicate a hyperactivated mitochondrial state in response to HIV-1 infection. Made with biorender.com.

10.3389/fimmu.2024.1360342

rectify this metabolic dysregulation, adding another layer to the complexity. Long-term ART use has been associated with continued mitochondrial dysfunction (133, 134), indicating that the impact of HIV on oxidative phosphorylation is a persistent challenge.

HIV-1 infection significantly disrupts host cell metabolism, increasing glycolysis and fatty acid synthesis to enhance viral replication, leading to oxidative stress and mitochondrial damage. This is further complicated by antiretroviral therapy (ART), which contributes to metabolic conditions like dyslipidemia and insulin resistance, intensifying mitochondrial dysfunction (135–137).

Studies show that both HIV-1 infection and prolonged ART use increase the risk of oxidative phosphorylation dysregulation and mitochondrial disruption in people with HIV (PWH) (122–132). Reduced activity of respiratory chain complexes and altered mitochondrial functioning in ART-naïve PWH have been linked to neurocognitive impairment (125). ART's impact on oxidative phosphorylation in PWH also suggests a reduction in mitochondrial function associated with chronic/controlled HIV-1 (133). Interestingly, pre-exposure prophylaxis (PreP) also shows reduced mitochondrial function in healthy individuals (134). Gender-specific differences in response to long-term ART have been observed, indicating possible variations in immunological recovery (138).

Recent studies highlight the role of purinergic signaling, particularly the interaction between extracellular ATP and P2X receptors, in HIV-1 pathogenesis (112, 113). These receptors, activated by ATP released from stressed cells, influence the HIV-1 life cycle and contribute to immunometabolic dysfunction (96, 106, 109). The dual role of these receptors in potentially inhibiting or facilitating HIV replication is mediated through CD39, which modulates extracellular ATP levels (72, 139–142).

Understanding the interplay between HIV-1 infection, ART, oxidative phosphorylation, and purinergic signaling is crucial for developing comprehensive HIV-1 treatment strategies. This involves addressing the viral challenges and the broader metabolic and mitochondrial dysfunctions. Future research should focus on identifying specific targets influenced by HIV-1 and ART and exploring the impact of purinergic signaling on these pathways. Such targeted exploration may lead to innovative therapeutic approaches addressing the infection and its metabolic and mitochondrial consequences.

Author contributions

NR: Conceptualization, Data curation, Investigation, Methodology, Project administration, Software, Supervision, Validation, Visualization, Writing – original draft, Writing – review & editing. TF: Writing – original draft. EH: Writing – original draft. MW: Writing – original draft. AK: Writing – original draft. JM: Writing – original draft. TS: Conceptualization, Data curation, Formal Analysis, Funding acquisition, Investigation, Methodology, Project administration, Resources, Software, Supervision, Validation, Visualization, Writing – original draft, Writing – review & editing.

Funding

The author(s) declare that financial support was received for the research, authorship, and/or publication of this article. This work is supported by T32GM146636 (JM), NIDA R01 DA052255 (TS), NIDA R01 DA054526 (TS), NIMH R01 MH134319 (TS), and NIAID R21 AI162223 (TS).

Acknowledgments

We are especially grateful to our colleagues at the Icahn School of Medicine at Mount Sinai Chen/Swartz laboratory for their continuous support and constructive criticism during the writing and editing process. Their expertise and perspectives have been instrumental in refining the content and focus of this review. Our heartfelt thanks to all the patients and volunteers who have participated in HIV research. Their involvement has been fundamental in advancing our understanding of the disease and developing effective treatment strategies.

Conflict of interest

The authors declare that the research was conducted in the absence of any commercial or financial relationships that could be construed as a potential conflict of interest.

The author(s) declared that they were an editorial board member of Frontiers, at the time of submission. This had no impact on the peer review process and the final decision.

Publisher's note

References

1. Ellis RJ, Iudicello JE, Heaton RK, Isnard S, Lin J, Routy JP, et al. Markers of gut barrier function and microbial translocation associate with lower gut microbial diversity in people with HIV. *Viruses*. (2021) 13(1):1891. doi: 10.3390/v13101891

2. Muñoz-Arias I, Doitsh G, Yang Z, Sowinski S, Ruelas D, Greene WC. Blood-derived CD4 T cells naturally resist pyroptosis during abortive HIV-1 infection. *Cell Host Microbe*. (2015) 18:463–70. doi: 10.1016/j.chom.2015.09.010

3. Okoye AA, Picker LJ. CD4(+) T-cell depletion in HIV infection: mechanisms of immunological failure. *Immunol Rev*. (2013) 254:54–64. doi: 10.1111/imr.12066

4. Lederman MM, Calabrese L, Funderburg NT, Clagett B, Medvik K, Bonilla H, et al. Immunologic failure despite suppressive antiretroviral therapy is related to activation and turnover of memory CD4 cells. *J Infect Dis*. (2011) 204:1217–26. doi: 10.1093/infdis/jir507

5. Bandera A, Ferrario G, Saresella M, Marventano I, Soria A, Zanini F, et al. CD4+ T cell depletion, immune activation and increased production of regulatory T cells in the thymus of HIV-infected individuals. *PloS One*. (2010) 5:e10788. doi: 10.1371/journal.pone.0010788

6. Tenorio AR, Zheng Y, Bosch RJ, Krishnan S, Rodriguez B, Hunt PW, et al. Soluble markers of inflammation and coagulation but not T-cell activation predict non-AIDS-defining morbid events during suppressive antiretroviral treatment. *J Infect Dis*. (2014) 210:1248–59. doi: 10.1093/infdis/jiu254

7. Deeks SG, Tracy R, Douek DC. Systemic effects of inflammation on health during chronic HIV infection. *Immunity*. (2013) 39:633–45. doi: 10.1016/j.immuni.2013.10.001

8. Klatt NR, Chomont N, Douek DC, Deeks SG. Immune activation and HIV persistence: implications for curative approaches to HIV infection. *Immunol Rev*. (2013) 254:326–42. doi: 10.1111/imr.12065

9. Deeks SG. HIV infection, inflammation, immunosenescence, and aging. *Annu Rev Med*. (2011) 62:141–55. doi: 10.1146/annurev-med-042909-093756

10. Wilson DF. Oxidative phosphorylation: regulation and role in cellular and tissue metabolism. *J Physiol*. (2017) 595:7023–38. doi: 10.1113/JP273839

11. Miranda-Quintana RA, Martínez González M, Ayers PW. Electronegativity and redox reactions. *Phys Chem Chem Phys*. (2016) 18:22235–43. doi: 10.1039/C6CP03213C

12. Matlin KS. The heuristic of form: mitochondrial morphology and the explanation of oxidative phosphorylation. *J Hist Biol*. (2016) 49:37–94. doi: 10.1007/s10739-015-9418-3

13. Nirody JA, Budin I, Rangamani P. ATP synthase: Evolution, energetics, and membrane interactions. *J Gen Physiol*. (2020) 152(11):e201912475. doi: 10.1085/jgp.201912475

14. Hroudová J, Fišar Z. Control mechanisms in mitochondrial oxidative phosphorylation. *Neural Regener Res*. (2013) 8:363–75. doi: 10.3969/j.issn.1673-5374.2013.04.009

15. Hüttemann M, Lee I, Pecinova A, Pecina P, Przyklenk K, Doan JW. Regulation of oxidative phosphorylation, the mitochondrial membrane potential, and their role in human disease. *J Bioenerg Biomembr*. (2008) 40:445–56. doi: 10.1007/s10863-008-9169-3

16. Ferguson-Miller S, Brautigan DL, Margoliash E. Correlation of the kinetics of electron transfer activity of various eukaryotic cytochromes c with binding to mitochondrial cytochrome c oxidase. *J Biol Chem*. (1976) 251:1104–15. doi: 10.1016/S0021-9258(17)33807-3

17. Guo D, Nguyen T, Ogbi M, Tawfik H, Ma G, Yu Q, et al. Protein kinase C-epsilon coimmunoprecipitates with cytochrome oxidase subunit IV and is associated with improved cytochrome-c oxidase activity and cardioprotection. *Am J Physiol Heart Circ Physiol*. (2007) 293:H2219–30. doi: 10.1152/ajpheart.01306.2006

18. Boerner JL, Demory ML, Silva C, Parsons SJ. Phosphorylation of Y845 on the epidermal growth factor receptor mediates binding to the mitochondrial protein cytochrome c oxidase subunit II. *Mol Cell Biol*. (2004) 24:7059–71. doi: 10.1128/MCB.24.16.7059-7071.2004

19. Lee I, Salomon AR, Ficarro S, Mathes I, Lottspeich F, Grossman LI, et al. cAMP-dependent tyrosine phosphorylation of subunit I inhibits cytochrome c oxidase activity. *J Biol Chem*. (2005) 280:6094–100. doi: 10.1074/jbc.M411335200

20. Serasinghe MN, Wieder SY, Renault TT, Elkholi R, Asciolla JJ, Yao JL, et al. Mitochondrial division is requisite to RAS-induced transformation and targeted by oncogenic MAPK pathway inhibitors. *Mol Cell*. (2015) 57:521–36. doi: 10.1016/j.molcel.2015.01.003

21. Lopez-Fabuel I, Le Douce J, Logan A, James AM, Bonvento G, Murphy MP, et al. Complex I assembly into supercomplexes determines differential mitochondrial ROS production in neurons and astrocytes. *Proc Natl Acad Sci U.S.A*. (2016) 113:13063–8. doi: 10.1073/pnas.1613701113

22. Vaupel P, Schmidberger H, Mayer A. The Warburg effect: essential part of metabolic reprogramming and central contributor to cancer progression. *Int J Radiat Biol*. (2019) 95:912–9. doi: 10.1080/09553002.2019.1589653

23. Sanchez EL, Lagunoff M. Viral activation of cellular metabolism. *Virology*. (2015) 479-480:609–18. doi: 10.1016/j.virol.2015.02.038

24. Valle-Casuso JC, Angin M, Volant S, Passaes C, Monceaux V, Mikhailova A, et al. Cellular metabolism is a major determinant of HIV-1 reservoir seeding in CD4. *Cell Metab*. (2019) 29:611–626.e5. doi: 10.1016/j.cmet.2018.11.015

25. Valentín-Guillama G, López S, Kucheryavykh YV, Chorna NE, Pérez J, Ortiz-Rivera J, et al. HIV-1 envelope protein gp120 promotes proliferation and the activation of glycolysis in glioma cell. *Cancers (Basel)*. (2018) 10(9):301. doi: 10.3390/cancers10090301

26. Kavanagh Williamson M, Coombes N, Juszczak F, Athanasopoulos M, Khan MB, Eykyn TR, et al. Upregulation of glucose uptake and hexokinase activity of primary human CD4+ T cells in response to infection with HIV-1. *Viruses*. (2018) 10(3):114. doi: 10.3390/v10030114

27. Hegedus A, Kavanagh Williamson M, Huthoff H. HIV-1 pathogenicity and virion production are dependent on the metabolic phenotype of activated CD4+ T cells. *Retrovirology*. (2014) 11:98. doi: 10.1186/s12977-014-0098-4

28. Arjona SP, Allen CNS, Santerre M, Gross S, Soboloff J, Booze R, et al. Disruption of Mitochondrial-associated ER membranes by HIV-1 tat protein contributes to premature brain aging. *CNS Neurosci Ther*. (2023) 29:365–77. doi: 10.1111/cns.14011

29. Huang CY, Chiang SF, Lin TY, Chiou SH, Chow KC. HIV-1 Vpr triggers mitochondrial destruction by impairing Mfn2-mediated ER-mitochondria interaction. *PloS One*. (2012) 7:e33657. doi: 10.1371/journal.pone.0033657

30. Crater JM, Nixon DF, Furler O'Brien RL. HIV-1 replication and latency are balanced by mTOR-driven cell metabolism. *Front Cell Infect Microbiol*. (2022) 12:1068436. doi: 10.3389/fcimb.2022.1068436

31. Hollenbaugh JA, Munger J, Kim B. Metabolite profiles of human immunodeficiency virus infected CD4+ T cells and macrophages using LC-MS/MS analysis. *Virology*. (2011) 415:153–9. doi: 10.1016/j.virol.2011.04.007

32. Lahouassa H, Daddacha W, Hofmann H, Ayinde D, Logue EC, Dragin L, et al. SAMHD1 restricts the replication of human immunodeficiency virus type 1 by depleting the intracellular pool of deoxynucleoside triphosphates. *Nat Immunol*. (2012) 13:223–8. doi: 10.1038/ni.2236

33. Ono A, Waheed AA, Freed EO. Depletion of cellular cholesterol inhibits membrane binding and higher-order multimerization of human immunodeficiency virus type 1 Gag. *Virology*. (2007) 360:27–35. doi: 10.1016/j.virol.2006.10.011

34. Rahman AN, Liu J, Mujib S, Kidane S, Ali A, Szep S, et al. Elevated glycolysis imparts functional ability to CD8. *Life Sci Alliance*. (2021) 4(11):e202101081. doi: 10.26508/lsa.202101081

35. Palmer CS, Cherry CL, Sada-Ovalle I, Singh A, Crowe SM. Glucose metabolism in T cells and monocytes: new perspectives in HIV pathogenesis. *EBioMedicine*. (2016) 6:31–41. doi: 10.1016/j.ebiom.2016.02.012

36. Loisel-Meyer S, Swainson L, Craveiro M, Oburoglu L, Mongellaz C, Costa C, et al. Glut1-mediated glucose transport regulates HIV infection. *Proc Natl Acad Sci U.S.A*. (2012) 109:2549–54. doi: 10.1073/pnas.1121427109

37. Ahmed D, Roy D, Cassol E. Examining relationships between metabolism and persistent inflammation in HIV patients on antiretroviral therapy. *Mediators Inflammation*. (2018) 2018:6238978. doi: 10.1155/2018/6238978

38. Wester CW, Okezie OA, Thomas AM, Bussmann H, Moyo S, Muzenda T, et al. Higher-than-expected rates of lactic acidosis among highly active antiretroviral therapy-treated women in Botswana: preliminary results from a large randomized clinical trial. *J Acquir Immune Defic Syndr*. (2007) 46:318–22. doi: 10.1097/QAI.0b013e3181568e3f

39. Mikaeloff F, Gelpi M, Escos A, Knudsen AD, Høgh J, Benfield T, et al. Transcriptomics age acceleration in prolonged treated HIV infection. *Aging Cell*. (2023) 22:e13951. doi: 10.1111/acel.13951

40. Tripathy MK, Mitra D. Differential modulation of mitochondrial OXPHOS system during HIV-1 induced T-cell apoptosis: up regulation of Complex-IV subunit COX-II and its possible implications. *Apoptosis*. (2010) 15:28–40. doi: 10.1007/s10495-009-0408-9

41. Kallianpur KJ, Walker M, Gerschenson M, Shikuma CM, Gangcuangco LMA, Kohorn L, et al. Systemic mitochondrial oxidative phosphorylation protein levels correlate with neuroimaging measures in chronically HIV-infected individuals. *AIDS Res Hum Retroviruses*. (2020) 36:83–91. doi: 10.1089/aid.2019.0240

42. Maagaard A, Kvale D. Long term adverse effects related to nucleoside reverse transcriptase inhibitors: clinical impact of mitochondrial toxicity. *Scand J Infect Dis*. (2009) 41:808–17. doi: 10.3109/00365540903186181

43. Feeney ER, van Vonderen MG, Wit F, Danner SA, van Agtmael MA, Villarroya F, et al. Zidovudine/lamivudine but not nevirapine in combination with lopinavir/ritonavir decreases subcutaneous adipose tissue mitochondrial DNA. *AIDS*. (2012) 26:2165–74. doi: 10.1097/QAD.0b013e328358b279

44. McComsey GA, Daar ES, O'Riordan M, Collier AC, Kosmiski L, Santana JL, et al. Changes in fat mitochondrial DNA and function in subjects randomized to abacavir-lamivudine or tenofovir DF-emtricitabine with atazanavir-ritonavir or efavirenz: AIDS Clinical Trials Group study A5224s, substudy of A5202. *J Infect Dis*. (2013) 207:604–11. doi: 10.1093/infdis/jis720

45. Maagaard A, Kvale D. Mitochondrial toxicity in HIV-infected patients both off and on antiretroviral treatment: a continuum or distinct underlying mechanisms? *J Antimicrob Chemother*. (2009) 64:901–9. doi: 10.1093/jac/dkp316

46. Lewis W, Dalakas MC. Mitochondrial toxicity of antiviral drugs. *Nat Med*. (1995) 1:417–22. doi: 10.1038/nm0595-417

47. Murata H, Hruz PW, Mueckler M. Indinavir inhibits the glucose transporter isoform Glut4 at physiologic concentrations. *AIDS*. (2002) 16:859–63. doi: 10.1097/00002030-200204120-00005

48. Murata H, Hruz PW, Mueckler M. The mechanism of insulin resistance caused by HIV protease inhibitor therapy. *J Biol Chem*. (2000) 275:20251–4. doi: 10.1074/jbc.C000228200

49. Hileman CO, Kalayjian RC, Azzam S, Schlatzer D, Wu K, Tassiopoulos K, et al. Plasma citrate and succinate are associated with neurocognitive impairment in older people with HIV. *Clin Infect Dis*. (2021) 73:e765–72. doi: 10.1093/cid/ciab107

50. Banki K, Hutter E, Gonchoroff NJ, Perl A. Molecular ordering in HIV-induced apoptosis. Oxidative stress, activation of caspases, and cell survival are regulated by transaldolase. *J Biol Chem*. (1998) 273:11944–53. doi: 10.1074/jbc.273.19.11944

51. Deshmane SL, Mukerjee R, Fan S, Del Valle L, Michiels C, Sweet T, et al. Activation of the oxidative stress pathway by HIV-1 Vpr leads to induction of hypoxia-

inducible factor 1alpha expression. *J Biol Chem*. (2009) 284:11364–73. doi: 10.1074/jbc.M809266200

52. Shah A, Kumar S, Simon SD, Singh DP, Kumar A. HIV gp120- and methamphetamine-mediated oxidative stress induces astrocyte apoptosis via cytochrome P450 2E1. *Cell Death Dis*. (2013) 4:e850. doi: 10.1038/cddis.2013.374

53. Foga IO, Nath A, Hasinoff BB, Geiger JD. Antioxidants and dipyridamole inhibit HIV-1 gp120-induced free radical-based oxidative damage to human monocytoid cells. *J Acquir Immune Defic Syndr Hum Retrovirol*. (1997) 16:223–9. doi: 10.1097/00042560-199712010-00001

54. Mataramvura H, Bunders MJ, Duri K. Human immunodeficiency virus and antiretroviral therapy-mediated immune cell metabolic dysregulation in children born to HIV-infected women: potential clinical implications. *Front Immunol*. (2023) 14:1182217. doi: 10.3389/fimmu.2023.1182217

55. Lecoeur H, Borgne-Sanchez A, Chaloin O, El-Khoury R, Brabant M, Langonné A, et al. HIV-1 Tat protein directly induces mitochondrial membrane permeabilization and inactivates cytochrome c oxidase. *Cell Death Dis*. (2012) 3:e282. doi: 10.1038/cddis.2012.21

56. Fields JA, Serger E, Campos S, Divakaruni AS, Kim C, Smith K, et al. HIV alters neuronal mitochondrial fission/fusion in the brain during HIV-associated neurocognitive disorders. *Neurobiol Dis*. (2016) 86:154–69. doi: 10.1016/j.nbd.2015.11.015

57. Vilhardt F, Plastre O, Sawada M, Suzuki K, Wiznerowicz M, Kiyokawa E, et al. The HIV-1 Nef protein and phagocyte NADPH oxidase activation. *J Biol Chem*. (2002) 277:42136–43. doi: 10.1074/jbc.M200862200

58. Halestrap AP, Brenner C. The adenine nucleotide translocase: a central component of the mitochondrial permeability transition pore and key player in cell death. *Curr Med Chem*. (2003) 10:1507–25. doi: 10.2174/0929867033457278

59. Gu Y, Wu RF, Xu YC, Flores SC, Terada LS. HIV Tat activates c-Jun amino-terminal kinase through an oxidant-dependent mechanism. *Virology*. (2001) 286:62–71. doi: 10.1006/viro.2001.0998

60. Capone C, Cervelli M, Angelucci E, Colasanti M, Macone A, Mariottini P, et al. A role for spermine oxidase as a mediator of reactive oxygen species production in HIV-Tat-induced neuronal toxicity. *Free Radic Biol Med*. (2013) 63:99–107. doi: 10.1016/j.freeradbiomed.2013.05.007

61. Rozzi SJ, Borelli G, Ryan K, Steiner JP, Reglodi D, Mocchetti I, et al. PACAP27 is protective against tat-induced neurotoxicity. *J Mol Neurosci*. (2014) 54:485–93. doi: 10.1007/s12031-014-0273-z

62. Haughey NJ, Mattson MP. Calcium dysregulation and neuronal apoptosis by the HIV-1 proteins Tat and gp120. *J Acquir Immune Defic Syndr*. (2002) 31 Suppl 2:S55–61. doi: 10.1097/00126334-200210012-00005

63. Ferri KF, Jacotot E, Blanco J, Esté JA, Kroemer G. Mitochondrial control of cell death induced by HIV-1-encoded proteins. *Ann N Y Acad Sci*. (2000) 926:149–64. doi: 10.1111/j.1749-6632.2000.tb05609.x

64. Avdoshina V, Fields JA, Castellano P, Dedoni S, Palchik G, Trejo M, et al. The HIV protein gp120 alters mitochondrial dynamics in neurons. *Neurotox Res*. (2016) 29:583–93. doi: 10.1007/s12640-016-9608-6

65. Elbim C, Pillet S, Prevost MH, Preira A, Girard PM, Rogine N, et al. The role of phagocytes in HIV-related oxidative stress. *J Clin Virol*. (2001) 20:99–109. doi: 10.1016/S1386-6532(00)00133-5

66. Elbim C, Pillet S, Prevost MH, Preira A, Girard PM, Rogine N, et al. Redox and activation status of monocytes from human immunodeficiency virus-infected patients: relationship with viral load. *J Virol*. (1999) 73:4561–6. doi: 10.1128/JVI.73.6.4561-4566.1999

67. Burnstock G. P2X ion channel receptors and inflammation. *Purinergic Signal*. (2016) 12:59–67. doi: 10.1007/s11302-015-9493-0

68. Kopp R, Krautloher A, Ramírez-Fernández A, Nicke A. P2X7 interactions and signaling - making head or tail of it. *Front Mol Neurosci*. (2019) 12:183. doi: 10.3389/fnmol.2019.00183

69. Di Virgilio F, Schmalzing G, Markwardt F. The elusive P2X7 macropore. *Trends Cell Biol*. (2018) 28:392–404. doi: 10.1016/j.tcb.2018.01.005

70. Pacheco PA, Faria RX, Ferreira LG, Paixão IC. Putative roles of purinergic signaling in human immunodeficiency virus-1 infection. *Biol Direct*. (2014) 9:21. doi: 10.1186/1745-6150-9-21

71. Dubey RC, Mishra N, Gaur R. G protein-coupled and ATP-sensitive inwardly rectifying potassium ion channels are essential for HIV entry. *Sci Rep*. (2019) 9:4113. doi: 10.1038/s41598-019-40968-x

72. Nikolova M, Carriere M, Jenabian MA, Limou S, Younas M, Kök A, et al. CD39/adenosine pathway is involved in AIDS progression. *PloS Pathog*. (2011) 7:e1002110. doi: 10.1371/journal.ppat.1002110

73. Goepfert C, Imai M, Brouard S, Csizmadia E, Kaczmarek E, Robson SC. CD39 modulates endothelial cell activation and apoptosis. *Mol Med*. (2000) 6:591–603. doi: 10.1007/BF03401797

74. Savio LEB, de Andrade Mello P, Figliuolo VR, de Avelar Almeida TF, Santana PT, Oliveira SDS, et al. CD39 limits P2X7 receptor inflammatory signaling and attenuates sepsis-induced liver injury. *J Hepatol*. (2017) 67:716–26. doi: 10.1016/j.jhep.2017.05.021

75. Soare AY, Malik HS, Durham ND, Freeman TL, Alvarez R, Patel F, et al. P2X1 selective antagonists block HIV-1 infection through inhibition of envelope conformation-dependent fusion. *J Virol*. (2020) 94(6):e01622–19. doi: 10.1128/JVI.01622-19

76. Séror C, Melki MT, Subra F, Raza SQ, Bras M, Saïdi H, et al. Extracellular ATP acts on P2Y2 purinergic receptors to facilitate HIV-1 infection. *J Exp Med*. (2011) 208:1823–34. doi: 10.1084/jem.20101805

77. Soare AY, Durham ND, Gopal R, Tweel B, Hoffman KW, Brown JA, et al. P2X antagonists inhibit HIV-1 productive infection and inflammatory cytokines interleukin-10 (IL-10) and IL-1β in a human tonsil explant model. *J Virol*. (2019) 93:e01186–18. doi: 10.1128/JVI.01186-18

78. Swartz TH, Dubyak GR, Chen BK. Purinergic receptors: key mediators of HIV-1 infection and inflammation. *Front Immunol*. (2015) 6:585. doi: 10.3389/fimmu.2015.00585

79. Giroud C, Marin M, Hammonds J, Spearman P, Melikyan GB. P2X1 receptor antagonists inhibit HIV-1 fusion by blocking virus-coreceptor interactions. *J Virol*. (2015) 89:9368–82. doi: 10.1128/JVI.01178-15

80. Marin M, Du Y, Giroud C, Kim JH, Qui M, Fu H, et al. High-throughput HIV-cell fusion assay for discovery of virus entry inhibitors. *Assay Drug Dev Technol*. (2015) 13:155–66. doi: 10.1089/adt.2015.639

81. Swartz TH, Esposito AM, Durham ND, Hartmann BM, Chen BK. P2X-selective purinergic antagonists are strong inhibitors of HIV-1 fusion during both cell-to-cell and cell-free infection. *J Virol*. (2014) 88:11504–15. doi: 10.1128/JVI.01158-14

82. Hazleton JE, Berman JW, Eugenin EA. Purinergic receptors are required for HIV-1 infection of primary human macrophages. *J Immunol*. (2012) 188:4488–95. doi: 10.4049/jimmunol.1102482

83. Soare AY, Freeman TL, Min AK, Malik HS, Osota EO, Swartz TH. P2RX7 at the host-pathogen interface of infectious diseases. *Microbiol Mol Biol Rev*. (2021) 85(1):e00055–20. doi: 10.1128/MMBR.00055-20

84. Esposito AM, Soare AY, Patel F, Satija N, Chen BK, Swartz TH. A high-throughput cre-lox activated viral membrane fusion assay to identify inhibitors of HIV-1 viral membrane fusion. *J Vis Exp*. (2018). doi: 10.3791/58074-v

85. Esposito AM, Cheung P, Swartz TH, Li H, Tsibane T, Durham ND, et al. A high throughput Cre-lox activated viral membrane fusion assay identifies pharmacological inhibitors of HIV entry. *Virology*. (2016) 490:6–16. doi: 10.1016/j.virol.2015.10.013

86. Hunt PW, Martin JN, Sinclair E, Bredt B, Hagos E, Lampiris H, et al. T cell activation is associated with lower CD4+ T cell gains in human immunodeficiency virus-infected patients with sustained viral suppression during antiretroviral therapy. *J Infect Dis*. (2003) 187:1534–43. doi: 10.1086/374786

87. Massanella M, Negredo E, Perez-Alvarez N, Puig J, Ruiz-Hernandez R, Bofill M, et al. CD4 T-cell hyperactivation and susceptibility to cell death determine poor CD4 T-cell recovery during suppressive HAART. *AIDS*. (2010) 24:959–68. doi: 10.1097/QAD.0b013e328337b957

88. Massanella M, Fromentin R, Chomont N. Residual inflammation and viral reservoirs: alliance against an HIV cure. *Curr Opin HIV AIDS*. (2016) 11:234–41. doi: 10.1097/COH.0000000000000230

89. Iyer SS, Pulskens WP, Sadler JJ, Butter LM, Teske GJ, Ulland TK, et al. Necrotic cells trigger a sterile inflammatory response through the Nlrp3 inflammasome. *Proc Natl Acad Sci U.S.A*. (2009) 106:20388–93. doi: 10.1073/pnas.0908698106

90. Mariathasan S, Weiss DS, Newton K, McBride J, O'Rourke K, Roose-Girma M, et al. Cryopyrin activates the inflammasome in response to toxins and ATP. *Nature*. (2006) 440:228–32. doi: 10.1038/nature04515

91. Hung SC, Choi CH, Said-Sadier N, Johnson L, Atanasova KR, Sellami H, et al. P2X4 assembles with P2X7 and pannexin-1 in gingival epithelial cells and modulates ATP-induced reactive oxygen species production and inflammasome activation. *PloS One*. (2013) 8:e70210. doi: 10.1371/journal.pone.0070210

92. Sun L, Ma W, Gao W, Xing Y, Chen L, Xia Z, et al. Propofol directly induces caspase-1-dependent macrophage pyroptosis through the NLRP3-ASC inflammasome. *Cell Death Dis*. (2019) 10:542. doi: 10.1038/s41419-019-1761-4

93. Malik S, Eugenin EA. Role of Connexin and Pannexin containing channels in HIV infection and NeuroAIDS. *Neurosci Lett*. (2019) 695:86–90. doi: 10.1016/j.neulet.2017.09.005

94. Orellana JA, Velasquez S, Williams DW, Sáez JC, Berman JW, Eugenin EA. Pannexin1 hemichannels are critical for HIV infection of human primary CD4+ T lymphocytes. *J Leukoc Biol*. (2013) 94:399–407. doi: 10.1189/jlb.0512249

95. Gajardo-Gómez R, Santibañez CA, Labra VC, Gómez GI, Eugenin EA, Orellana JA. HIV gp120 protein increases the function of connexin 43 hemichannels and pannexin-1 channels in astrocytes: repercussions on astroglial function. *Int J Mol Sci*. (2020) 21(7):2503. doi: 10.3390/ijms21072503

96. Freeman TL, Zhao C, Schrode N, Fortune T, Shroff S, Tweel B, et al. HIV-1 activates oxidative phosphorylation in infected CD4 T cells in a human tonsil explant model. *Front Immunol*. (2023) 14:1172938. doi: 10.3389/fimmu.2023.1172938

97. Velasquez S, Prevedel L, Valdebenito S, Gorska AM, Golovko M, Khan N, et al. Circulating levels of ATP is a biomarker of HIV cognitive impairment. *EBioMedicine*. (2020) 51:102503. doi: 10.1016/j.ebiom.2019.10.029

98. Heaton RK, Clifford DB, Franklin DR, Woods SP, Ake C, Vaida F, et al. HIV-associated neurocognitive disorders persist in the era of potent antiretroviral therapy: CHARTER Study. *Neurology*. (2010) 75:2087–96. doi: 10.1212/WNL.0b013e318200d727

99. Zayyad Z, Spudich S. Neuropathogenesis of HIV: from initial neuroinvasion to HIV-associated neurocognitive disorder (HAND). *Curr HIV/AIDS Rep*. (2015) 12:16–24. doi: 10.1007/s11904-014-0255-3

100. Veenstra M, León-Rivera R, Li M, Gama L, Clements JE, Berman JW. Mechanisms of CNS viral seeding by HIV. *mBio*. (2017) 8(5):e01280–17. doi: 10.1128/mBio.01280-17

101. Datta G, Miller NM, Afghah Z, Geiger JD, Chen X. HIV-1 gp120 promotes lysosomal exocytosis in human schwann cells. *Front Cell Neurosci*. (2019) 13:329. doi: 10.3389/fncel.2019.00329

102. Yu Y, Ugawa S, Ueda T, Ishida Y, Inoue K, Kyaw Nyunt A, et al. Cellular localization of P2X7 receptor mRNA in the rat brain. *Brain Res*. (2008) 1194:45–55. doi: 10.1016/j.brainres.2007.11.064

103. Kakuda TN. Pharmacology of nucleoside and nucleotide reverse transcriptase inhibitor-induced mitochondrial toxicity. *Clin Ther*. (2000) 22:685–708. doi: 10.1016/S0149-2918(00)90004-3

104. Robertson K, Liner J, Meeker RB. Antiretroviral neurotoxicity. *J Neurovirol*. (2012) 18:388–99. doi: 10.1007/s13365-012-0120-3

105. Cheney L, Guzik H, Macaluso FP, Macian F, Cuervo AM, Berman JW. HIV Nef and antiretroviral therapy have an inhibitory effect on autophagy in human astrocytes that may contribute to HIV-associated neurocognitive disorders. *Cells*. (2020) 9 (6):1426. doi: 10.3390/cells9061426

106. Guo H, Wang Q, Ghneim K, Wang L, Rampanelli E, Holley-Guthrie E, et al. Multi-omics analyses reveal that HIV-1 alters CD4. *Nat Immunol*. (2021) 22:423–33. doi: 10.1038/s41590-021-00898-1

107. Ambikan AT, Svensson-Akusjärvi S, Krishnan S, Sperk M, Nowak P, Vesterbacka J, et al. Genome-scale metabolic models for natural and long-term drug-induced viral control in HIV infection. *Life Sci Alliance*. (2022) 5(9):e202201405. doi: 10.26508/lsa.202201405

108. Alrubayyi A, Moreno-Cubero E, Hameiri-Bowen D, Matthews R, Rowland-Jones S, Schurich A, et al. Functional restoration of exhausted CD8 T cells in chronic HIV-1 infection by targeting mitochondrial dysfunction. *Front Immunol*. (2022) 13:908697. doi: 10.3389/fimmu.2022.908697

109. Castellano P, Prevedel L, Valdebenito S, Eugenin EA. HIV infection and latency induce a unique metabolic signature in human macrophages. *Sci Rep*. (2019) 9:3941. doi: 10.1038/s41598-019-39898-5

110. Aquaro S, Caliò R, Balzarini J, Bellocchi MC, Garaci E, Perno CF. Macrophages and HIV infection: therapeutical approaches toward this strategic virus reservoir. *Antiviral Res*. (2002) 55:209–25. doi: 10.1016/S0166-3542(02)00052-9

111. Rezaei S, Timani KA, He JJ. Metformin treatment leads to increased HIV transcription and gene expression through increased CREB phosphorylation and recruitment to the HIV LTR promoter. *Aging Dis*. (2023). doi: 10.14336/AD.2023.0705

112. Ortiz-Brizuela E, Pérez-Patrigeon S, Recillas-Gispert C, Gómez-Pérez FJ. Lactic acidosis complicating metformin and non-nucleoside reverse transcriptase inhibitor combination therapy: A smoldering threat in the post-HAART era. *Rev Invest Clin*. (2015) 67:273–4.

113. Chaparala S, Da Silva RC, Papadopoulos JP. Severe lactic acidosis due to acute intoxication by emtricitabine/tenofovir alafenamide. *Cureus*. (2021) 13:e19008. doi: 10.7759/cureus.19008

114. Adebiyi OO, Adebiyi OA, Owira PM. Naringin reverses hepatocyte apoptosis and oxidative stress associated with HIV-1 nucleotide reverse transcriptase inhibitors-induced metabolic complications. *Nutrients*. (2015) 7:10352–68. doi: 10.3390/nu7125540

115. Oluwafeyisetan A, Olubunmi A, Peter O. Naringin ameliorates HIV-1 nucleoside reverse transcriptase inhibitors- induced mitochondrial toxicity. *Curr HIV Res*. (2016) 14:506–16. doi: 10.2174/1570162X14666160520114639

116. Funderburg NT, Jiang Y, Debanne SM, Labbato D, Juchnowski S, Ferrari B, et al. Rosuvastatin reduces vascular inflammation and T-cell and monocyte activation in HIV-infected subjects on antiretroviral therapy. *J Acquir Immune Defic Syndr*. (2015) 68:396–404. doi: 10.1097/QAI.0000000000000478

117. Grinspoon SK, Fitch KV, Zanni MV, Fichtenbaum CJ, Umbleja T, Aberg JA, et al. Pitavastatin to prevent cardiovascular disease in HIV infection. *N Engl J Med*. (2023) 389:687–99. doi: 10.1056/NEJMoa2304146

118. Morrison JT, Longenecker CT, Mittelsteadt A, Jiang Y, Debanne SM, McComsey GA. Effect of rosuvastatin on plasma coenzyme Q10 in HIV-infected individuals on antiretroviral therapy. *HIV Clin Trials*. (2016) 17:140–6. doi: 10.1080/15284336.2016.1184863

119. Kang S, Tang H. HIV-1 infection and glucose metabolism reprogramming of T cells: another approach toward functional cure and reservoir eradication. *Front Immunol*. (2020) 11:572677. doi: 10.3389/fimmu.2020.572677

120. Allen CNS, Arjona SP, Santerre M, De Lucia C, Koch WJ, Sawaya BE. Metabolic reprogramming in HIV-associated neurocognitive disorders. *Front Cell Neurosci*. (2022) 16:812887. doi: 10.3389/fncel.2022.812887

121. Parikh NI, Gerschenson M, Bennett K, Gangcuangco LM, Lopez MS, Mehta NN, et al. Lipoprotein concentration, particle number, size and cholesterol efflux capacity are associated with mitochondrial oxidative stress and function in an HIV positive cohort. *Atherosclerosis*. (2015) 239:50–4. doi: 10.1016/j.atherosclerosis.2014.12.005

122. Perrin S, Cremer J, Roll P, Faucher O, Ménard A, Reynes J, et al. HIV-1 infection and first line ART induced differential responses in mitochondria from blood lymphocytes and monocytes: the ANRS EP45 "Aging". *Study PloS One*. (2012) 7: e41129. doi: 10.1371/journal.pone.0041129

123. Torres RA, Lewis W. Aging and HIV/AIDS: pathogenetic role of therapeutic side effects. *Lab Invest*. (2014) 94:120–8. doi: 10.1038/labinvest.2013.142

124. Arts EJ, Hazuda DJ. HIV-1 antiretroviral drug therapy. *Cold Spring Harb Perspect Med*. (2012) 2:a007161. doi: 10.1101/cshperspect.a007161

125. Miró O, López S, Martínez E, Pedrol E, Milinkovic A, Deig E, et al. Mitochondrial effects of HIV infection on the peripheral blood mononuclear cells of HIV-infected patients who were never treated with antiretrovirals. *Clin Infect Dis*. (2004) 39:710–6. doi: 10.1086/423176

126. Brinkman K, ter Hofstede HJ, Burger DM, Smeitink JA, Koopmans PP. Adverse effects of reverse transcriptase inhibitors: mitochondrial toxicity as common pathway. *AIDS*. (1998) 12:1735–44. doi: 10.1097/00002030-199814000-00004

127. Apostolova N, Blas-García A, Esplugues JV. Mitochondrial toxicity in HAART: an overview of in *vitro* evidence. *Curr Pharm Des*. (2011) 17:2130–44. doi: 10.2174/138161211796904731

128. Fiala M, Murphy T, MacDougall J, Yang W, Luque A, Iruela-Arispe L, et al. HAART drugs induce mitochondrial damage and intercellular gaps and gp120 causes apoptosis. *Cardiovasc Toxicol*. (2004) 4:327–37. doi: 10.1385/CT:4:4

129. Kaur H, Minchella P, Alvarez-Carbonell D, Purandare N, Nagampalli VK, Blankenberg D, et al. Contemporary antiretroviral therapy dysregulates iron transport and augments mitochondrial dysfunction in HIV-infected human microglia and neural-lineage cells. *Int J Mol Sci*. (2023) 24(15):12242. doi: 10.20944/preprints202307.1492.v1

130. Wallace J, Gonzalez H, Rajan R, Narasipura SD, Virdi AK, Olali AZ, et al. Anti-HIV drugs cause mitochondrial dysfunction in monocyte-derived macrophages. *Antimicrob Agents Chemother*. (2022) 66:e0194121. doi: 10.1128/aac.01941-21

131. López S, Negredo E, Garrabou G, Puig J, Ruiz L, Sanjurjo E, et al. Longitudinal study on mitochondrial effects of didanosine-tenofovir combination. *AIDS Res Hum Retroviruses*. (2006) 22:33–9. doi: 10.1089/aid.2006.22.33

132. Massanella M, Singhania A, Beliakova-Bethell N, Pier R, Lada SM, White CH, et al. Differential gene expression in HIV-infected individuals following ART. *Antiviral Res*. (2013) 100:420–8. doi: 10.1016/j.antiviral.2013.07.017

133. Gangcuangco LMA, Mitchell BI, Siriwardhana C, Kohorn LB, Chew GM, Bowler S, et al. Mitochondrial oxidative phosphorylation in peripheral blood mononuclear cells is decreased in chronic HIV and correlates with immune dysregulation. *PloS One*. (2020) 15:e0231761. doi: 10.1371/journal.pone.0231761

134. Bowman ER, Cameron C, Richardson B, Kulkarni M, Gabriel J, Kettelhut A, et al. Exposure of leukocytes to HIV preexposure prophylaxis decreases mitochondrial function and alters gene expression profiles. *Antimicrob Agents Chemother*. (2020) 65 (1):e01755–20. doi: 10.1128/AAC.01755-20

135. Butterfield TR, Landay AL, Anzinger JJ. Dysfunctional immunometabolism in HIV infection: contributing factors and implications for age-related comorbid diseases. *Curr HIV/AIDS Rep*. (2020) 17:125–37. doi: 10.1007/s11904-020-00484-4

136. Schank M, Zhao J, Moorman JP, Yao ZQ. The impact of HIV- and ART-induced mitochondrial dysfunction in cellular senescence and aging. *Cells*. (2021) 10 (1):174. doi: 10.3390/cells10010174

137. Marchi S, Guilbaud E, Tait SWG, Yamazaki T, Galluzzi L. Mitochondrial control of inflammation. *Nat Rev Immunol*. (2023) 23:159–73. doi: 10.1038/s41577-022-00760-x

138. Zhang L, Wang Z, Chen Y, Zhang C, Xie S, Cui Y. Label-free proteomic analysis of PBMCs reveals gender differences in response to long-term antiretroviral therapy of HIV. *J Proteomics*. (2015) 126:46–53. doi: 10.1016/j.jprot.2015.05.033

139. Ravimohan S, Tamuhla N, Nfanyana K, Ni H, Steenhoff AP, Gross R, et al. Elevated pre-antiretroviral therapy CD39+CD8+ T cell frequency is associated with early mortality in advanced human immunodeficiency virus/tuberculosis co-infection. *Clin Infect Dis*. (2017) 64:1453–6. doi: 10.1093/cid/cix155

140. Shahbaz S, Okoye I, Blevins G, Elahi S. Elevated ATP via enhanced miRNA-30b, 30c, and 30e downregulates the expression of CD73 in CD8+ T cells of HIV-infected individuals. *PloS Pathog*. (2022) 18:e1010378. doi: 10.1371/journal.ppat.1010378

141. Song JW, Huang HH, Zhang C, Yang HG, Zhang JY, Xu RN, et al. Expression of CD39 is correlated with HIV DNA levels in naïve tregs in chronically infected ART naïve patients. *Front Immunol*. (2019) 10:2465. doi: 10.3389/fimmu.2019.02465

142. Kadenbach B. Intrinsic and extrinsic uncoupling of oxidative phosphorylation. *Biochim Biophys Acta*. (2003) 1604:77–94. doi: 10.1016/S0005-2728(03)00027-6

frontiers | Frontiers in Immunology

TYPE Original Research
PUBLISHED 02 May 2024
DOI 10.3389/fimmu.2024.1380846

OPEN ACCESS

EDITED BY
Pedro Gonzalez-Menendez,
University of Oviedo, Spain

REVIEWED BY
Ren Shuang Cao,
Chinese Academy of traditional Chinese Medicine, China
Weihong Jiang,
Central South University, China

*CORRESPONDENCE
Jintao Du
9069402@qq.com
Luo Ba
bhanor@163.com

†These authors have contributed equally to this work and share first authorship

RECEIVED 02 February 2024
ACCEPTED 22 April 2024
PUBLISHED 02 May 2024

CITATION
Zhou J, Zhou J, Liu R, Liu Y, Meng J, Wen Q, Luo Y, Liu S, Li H, Ba L and Du J (2024) The oxidant-antioxidant imbalance was involved in the pathogenesis of chronic rhinosinusitis with nasal polyps.
Front. Immunol. 15:1380846.
doi: 10.3389/fimmu.2024.1380846

The oxidant-antioxidant imbalance was involved in the pathogenesis of chronic rhinosinusitis with nasal polyps

Jing Zhou[1,2†], Jiao Zhou[3†], Ruowu Liu[1,2], Yafeng Liu[1,2], Juan Meng[1,2], Qiao Wen[1,2], Yirui Luo[4], Shixi Liu[1,2], Huabin Li[5], Luo Ba[4*] and Jintao Du[1,2*]

[1]Department of Otolaryngology-Head & Neck Surgery, West China Hospital, Sichuan University, Chengdu, China, [2]Upper Respiratory Tract Laboratory of Department of Otolaryngology-Head and Neck Surgery, West China Hospital, Sichuan University, Chengdu, China, [3]Department of Medicine and Engineering Interdisciplinary Research Laboratory of Nursing & Materials, West China Hospital, Sichuan University, Chengdu, China, [4]Department of Otolaryngology, People's Hospital of Tibet Autonomous Region, Lhasa, China, [5]Department of Otolaryngology, Head and Neck Surgery, Affiliated Eye, Ear, Nose and Throat Hospital, Fudan University, Shanghai, China

Background: Although oxidative stress is involved in the pathophysiological process of chronic rhinosinusitis with nasal polyps (CRSwNP), the specific underlying mechanism is still unclear. Whether antioxidant therapy can treat CRSwNP needs further investigation.

Methods: Immunohistochemistry, immunofluorescence, western blotting and quantitative polymerase chain reaction (qPCR) analyses were performed to detect the distribution and expression of oxidants and antioxidants in nasal polyp tissues. qPCR revealed correlations between oxidase, antioxidant enzymes and inflammatory cytokine levels in CRSwNP patients. Human nasal epithelial cells (HNEpCs) and primary macrophages were cultured to track the cellular origin of oxidative stress in nasal polyps(NPs) and to determine whether crocin can reduce cellular inflammation by increasing the cellular antioxidant capacity.

Results: The expression of NOS2, NOX1, HO-1 and SOD2 was increased in nasal epithelial cells and macrophages derived from nasal polyp tissue. Oxidase levels were positively correlated with those of inflammatory cytokines (IL-5 and IL-6). Conversely, the levels of antioxidant enzymes were negatively correlated with those of IL-13 and IFN-γ. Crocin inhibited M1 and M2 macrophage polarization as well as the expression of NOS2 and NOX1 and improved the antioxidant capacity of M2 macrophages. Moreover, crocin enhanced the ability of antioxidants to reduce inflammation via the KEAP1/NRF2/HO-1 pathway in HNEpCs treated with SEB or LPS. Additionally, we observed the antioxidant and anti-inflammatory effects of crocin in nasal explants.

Conclusion: Oxidative stress plays an important role in the development of CRSwNP by promoting various types of inflammation. The oxidative stress of nasal polyps comes from epithelial cells and macrophages. Antioxidant therapy may be a promising strategy for treating CRSwNP.

KEYWORDS

CRSwNP, oxidative stress, nasal epithelial cells, macrophages, Nrf2

1 Introduction

Chronic rhinosinusitis with nasal polyps (CRSwNP) is a common chronic inflammatory disease that results in impaired quality of life and a heavy economic burden (1, 2). CRSwNP is generally divided into eosinophilic CRSwNP (ECRSwNP) and noneosinophilic CRSwNP (nECRSwNP) based on the degree of eosinophil infiltration (3–5). Caucasian CRSwNP patients tend to exhibit greater eosinophilic inflammation than Asian patients, while the prevalence of ECRSwNP is increasing in Asian countries (6, 7). Currently, the etiology of CRSwNP has not been fully elucidated. It has been reported that epithelial cells play an important role, as do immune and inflammatory cells, such as macrophages, T and B lymphocytes, group 2 innate lymphoid cells (ILC2s), eosinophils, neutrophils, and mast cells (1, 8, 9). However, the detailed pathogenesis of CRSwNP, especially ECRSwNP, is still unclear, which poses challenges in disease treatment. Therefore, further insight into the pathogenesis of CRSwNP is critical for its management.

Oxidative stress is an imbalance between the production of free radicals and their elimination by an organism's antioxidant system (10, 11). The most important sources of free radicals are mitochondria, NADPH oxidase (NOX), nitric oxide synthase (NOS) and xanthine oxidase (XO) (12). In contrast, there are many antioxidants in cells that can prevent the production of free radicals or eliminate them quickly, including glutathione (GSH), superoxide dismutase (SOD), catalase (CAT), heme oxygenase (HO) and glutathione reductase (GR) (10). Recently, oxidative stress has been shown to be involved in the development of CRSwNP (13–15). It was reported that patients with nasal polyps show an increase in oxidants and a decrease in antioxidants (16–18). Malgorzata and Yu found that there was no significant difference in SOD activity between patients with nasal polyps and healthy subjects, although HO-1 mRNA and protein expression were significantly increased in nasal polyp tissues compared with healthy control tissues (19, 20). Moreover, we speculate that oxidative stress may have different effects on different types of nasal polyps, but this requires further investigation.

An increasing number of studies have shown that antioxidant therapeutic strategies are beneficial for the treatment of diabetes, coronary artery disease and neurological disorders (21, 22). Crocin, which is an antioxidant, is widely used to treat Alzheimer's disease and cardiovascular diseases (23, 24) by inhibiting the occurrence of oxidative stress. However, the effect of crocin on CRSwNP is unknown. Herein, we attempted to reveal the status of oxidative stress in nasal polyps and the main cells in which oxidative stress occurs. Furthermore, we explored the therapeutic effect of crocin on nasal polyps to identify potential therapeutic targets for nasal polyps.

2 Materials and methods

2.1 Patients and tissue samples

Nasal polyp samples from CRSwNP patients were obtained through functional endoscopic sinus surgery at the Department of Otolaryngology Head & Neck Surgery, West China Hospital, Sichuan University. Turbinate tissues were collected from patients who were undergoing endoscopic skull base surgery or septoplasty. We diagnosed CRSwNP according to EPOS 2020, and ECRSwNP met the requirement of more than 10 eosinophils in each high power field (HFP) of three random fields. Otherwise, it is nECRSwNP (3). Patients who were younger than 18 years old, treated with corticosteroids, antihistamines, or antibiotics before surgery and patients with antrochoanal polyps, autoimmune disease, ciliary dysfunction, fungal rhinosinusitis, and inverted papilloma were excluded. The skin prick test was applied to evaluate the atopic status of the patient. Patient comorbidities and basic demographic data were documented preoperatively. This study was approved by the Medical Ethics Committee of the West China Hospital of Sichuan University, and informed consent was obtained prior to the study. The clinical characteristics of the control and CRSwNP groups are shown in Supplementary Table 1.

2.2 Immunohistochemistry

Tissues were embedded in paraffin following ethyl alcohol dehydration and then sectioned to 4 μm thickness. Immunohistochemistry (IHC) staining was performed with a

universal detection kit (PV-6000, ZSGB-Bio, Beijing, China) and DAB Detection System (ZLI-9017, ZSGB-Bio, Beijing, China). The sections were air-dried overnight at 37°C, followed by deparaffinization, hydration, antigen retrieval and endogenous peroxidase removal. Then, sections were incubated with primary antibodies against NOS2 (1:400, ABclonal, Wuhan, China), 3-nitrotyrosine (3-NT) (1:200, Abcam, Cambridge, UK), HO-1 (1:400, ABclonal, Wuhan, China) and SOD2 (1:400, ABclonal, Wuhan, China)at 4°C overnight, and incubated with enzyme-labeled sheep anti-mouse/rabbit IgG polymer at 37°C for 20 min. Next, slides were stained with freshly prepared DAB, counterstained with hematoxylin and finally imaged under a 400-fold microscope.

2.3 Western blotting

SDS–PAGE gels were used to separate the proteins, after which the proteins were transferred to PVDF membranes (Millipore, MA, USA). Membranes were blocked in TBST containing 5% nonfat milk for 1 h at room temperature (RT). Then, membranes were incubated with primary antibodies against NOS2 (1:1000, ABclonal, Wuhan, China), NOX1 (1:1000, ABclonal, Wuhan, China), HO-1 (1:1000, ABclonal, Wuhan, China), SOD2 (1:1000, ABclonal, Wuhan, China), Kelch-like ECH-associated protein 1 (KEAP1) (1:1000, Proteintech, Wuhan, China), nuclear factor κB (NF-κB) P65 (1:1000, Cell Signaling Technology, Danvers, USA), GAPDH (1:10000, Proteintech, Wuhan, China), Histone H3 (1:4000, HUABIO, Hangzhou, China) and Tublin-α (1:10000, abcam, USA) at 4 °C overnight followed by incubation with secondary antibody (1:5000, Proteintech, Wuhan, China) for 1 h at RT. Finally, membranes were visualized by NcmECL Ultra (NCM Biotech, Shanghai, China).

2.4 Total RNA extraction and real-time quantitative PCR

Animal Total RNA Isolation Kit (FOREGENE, Chengdu, China) and Cell Total RNA Isolation Kit (FOREGENE, Chengdu, China) were used to extract total RNA from nasal tissues and cell, respectively. Total RNA was reverse transcribed into cDNA using HiScript III All-in-one RT SuperMix Perfect for qPCR (Vazyme Biotech, Nanjing, China) according to the manufacturer's protocols. qPCR was achieved with synthetic primers and Taq pro Universal SYBR qPCR Master Mix (Vazyme Biotech, Nanjing, China). The related primers used are shown in Supplementary Table 2.

2.5 Immunofluorescence

Paraffin sections were prepared with deparaffinization, hydration, and antigen retrieval, and HNEpC were fixed in 4% paraformaldehyde for 15 min at RT. Both tissues and cells were permeabilized in PBS supplemented with 0.1% Triton X-100. Then, 5% BSA supplemented with 0.01% Triton X-100 was used to block nonspecific binding for 2 h at RT. Sections were incubated overnight at 4°C with primary antibodies against CD68 (1:2000, Proteintech, Wuhan, China), NOS2 (1:400, ABclonal, Wuhan, China), HO-1 (1:400, ABclonal, Wuhan, China), SOD2 (1:400, ABclonal, Wuhan, China) and nuclear factor E2-related factor 2 (NRF2) (1:200, Proteintech, Wuhan, China), and cells were incubated with primary antibodies against NRF2 and NF-κB P65 (1:400, Cell Signaling Technology, Danvers, USA), followed by incubation with fluorophore-conjugated secondary antibodies. Finally, sealing tablets containing DAPI were added to the slides, which were later covered by cover glasses.

2.6 Culture and polarization of macrophages

Peripheral blood mononuclear cells (PBMCs) were isolated from healthy controls by Ficoll-Paque PREMIUM density gradient (GE Healthcare, USA) centrifugation. The CD14+ monocytes were separated by positive magnetic selection (Miltenyi Biotec, Germany). PBMCs were labeled with CD14 MicroBeads for 20 min at 4°C in the dark. Then, the cells were washed and immediately sorted on a MACS Separator (Miltenyi Biotec, Germany) to obtain CD14+ monocytes.

The CD14+ monocytes were cultured in serum-free RPMI-1640 medium for 2 h. After the cells adhered to the wall, the medium was changed to serum-free medium (LONZA, Switzerland) containing 20 ng/ml macrophage colony-stimulating factor (M-CSF) (PeproTech, USA). The medium was changed every 3 days and supplemented with M-CSF. The cells were induced to M0 macrophages (M0) after one week. To polarize into M1 macrophages (M1), cells were treated with 100 ng/ml LPS and 20 ng/ml interferon-γ (IFN-γ) (Novoprotein, Shanghai, China) for 24 h, and cells were stimulated with 20 ng/ml interleukin (IL)-4 (Novoprotein, Shanghai, China) for 24 h to polarize into M2 macrophages (M2).

2.7 Culture of HNEpC

The HNEpC line was kindly donated by the First Affiliated Hospital of Sun Yat-sen University. The culture medium used for HNEpC was RPMI-1640 medium containing 10% fetal bovine serum, 100 U/mL penicillin, and 100 μg/mL streptomycin (Gibco, Paisley, UK). The cells were stimulated by either lipopolysaccharide (LPS) (Sigma–Aldrich, USA) or staphylococcal enterotoxin B (SEB) (Toxin Technology, Sarasota, FL, USA) with or without crocin (target mol, USA) when they reached 70-80% confluency.

2.8 Culture of nasal polyp explants

Fresh nasal polyp tissues were obtained from CRSwNP patients during surgery, washed with RPMI-1640 medium three times, and then cut into smaller pieces weighing approximately 40 mg each. Then, the tissue was passed through a mesh (pore size 0.9 mm^2) to acquire tissue fragments, which were resuspended in a 12-well plate and cultured in RPMI-1640 medium containing 10% fetal bovine

serum, 100 U/mL penicillin, and 100 μg/mL streptomycin. Explants were treated with either SEB or LPS for 24 h with or without crocin.

2.9 Statistical analysis

Statistical analyses were performed by using GraphPad Prism 7.0 (GraphPad Software, San Diego, USA). The Kruskal–Wallis test was used for comparisons between multiple groups in nasal tissues and the Spearman correlation coefficient was applied to determine variable relationships in nasal polyp tissues. Cell culture data are presented as the mean ± standard deviation (M ± SD) and were analyzed using one-way analysis of variance (ANOVA). Asterisks indicate statistical significance (*p<0.05, **p<0.01, ***p<0.001, ****p<0.0001).

3 Results

3.1 The expression and distribution of oxidases in different nasal tissues

Patients were divided into the control group, ECRSwNP group and nECRSwNP group according to the number of infiltrated eosinophils in the tissue sections (Supplementary Figure 1). Furthermore, oxidase expression and distribution were determined by IHC, and the results showed that NOS2 was more highly expressed in the epithelial and submucosal cells of the NP than in those of the control mucosa and that NOX1 was more strongly expressed in the submucosal cells of nasal tissues (Figure 1A). Increased levels of the NOS2 and NOX1 proteins were detected in samples from ECRSwNP patients compared with control samples (Figures 1B, C). Moreover, the mRNA expression of NOS2 and NOX1 was significantly greater in ECRSwNP patients than in control subjects (Figure 1D). As a product of protein oxidation, 3-nitrotyrosine (3-NT) is a marker of oxidative damage (25). 3-NT expression was greater in the epithelial cells and submucosal cells of NPs than in those of UPs from control subjects (Supplementary Figure 2). Collectively, our data revealed an increase in oxidative stress in CRSwNP patients, especially in ECRSwNP patients.

3.2 The expression and distribution of antioxidant enzymes in different nasal tissues

Immunostaining showed that HO-1 was mainly expressed in the submucosal cells of NPs from CRSwNP patients (Figure 2A). SOD2 was distributed primarily in epithelial cells, submucosal cells and submucosal glands in nasal tissues and was increased in the submucosal cells of CRSwNP NPs compared with control NPs (Figure 2A). In contrast to previous studies (20, 26), we found that HO-1 and SOD2 protein levels were significantly greater in CRSwNP patients than in controls (Figures 2B, C). In addition, we found that HO-1 mRNA levels were significantly greater in ECRSwNP patients than in nECRSwNP patients and control subjects, and SOD2 mRNA expression was significantly greater in ECRSwNP patients than in control subjects (Figure 2D). In summary, we observed that the expression of antioxidant enzymes increased with increasing oxidative stress in ECRSwNP patients.

3.3 Correlations between oxidase and antioxidant enzyme expression and inflammatory cytokine levels in CRSwNP patients

To elucidate the role of oxidases and antioxidant enzymes in CRSwNP, we examined the relationship between these enzymes and inflammatory cytokines, such as IL-6, IL-8, IL-5, IL-13 and IFN-γ, in NPs from patients with CRSwNP. NOS2 mRNA levels were positively correlated with IL-6 mRNA expression (Figure 3A). The mRNA levels of IL-5 were positively correlated with NOX1 mRNA expression (Figure 3B). In addition, the mRNA expression of HO-1 had a negative relationship with that of IL-8, IL-13 and IFN-γ (Figure 3C). We also found that SOD2 expression was negatively correlated with IL-5, IL-13, and IFN-γ levels (Figure 3D). In general, oxidase levels may be positively correlated with inflammatory cytokine expression, while antioxidant enzyme levels can be negatively correlated with cytokine expression. We speculate that the increase in oxidative stress may lead to an increase in inflammatory cytokine levels, whereas increased antioxidant enzymes may inhibit inflammation.

3.4 In CRSwNP, macrophages are involved in oxidation and antioxidation

Previous studies have shown that macrophages are the main cellular source of reactive oxygen species (ROS)/reactive nitrogen species (RNS) in the lungs and can produce NO through NOS2 (27). We investigated the expression of oxidase and antioxidant enzymes in macrophages labeled with CD68 by dual immunofluorescence staining of nasal tissue sections. Our results showed that NOS2 (green), NOX1 (green), HO-1 (green), and SOD2 (green) could be coexpressed with CD68 (red) in nasal tissue from patients with CRSwNP (Figures 4A–D). Therefore, macrophages are likely the main source of free radicals.

3.5 The damage of antioxidant enzymes is related to M2 macrophage polarization

Real-time quantitative PCR showed that IL-4 promoted M2 macrophage polarization by increasing the mRNA expression of CCL24 and MRC1 (Figure 5A). The expression of NOS2 and NOX1 was not increased in M2 macrophage (Figures 5B, D) but was increased in M1 macrophages (Supplementary Figure 3B), which means that M1 activation induced oxidative stress. M2 polarization suppressed the expression of the antioxidant enzymes HO-1 and SOD2 (Figures 5C, D). Interestingly, crocin strongly inhibited the expression of M2 markers (Figure 5A), increased HO-1 and SOD2 expression (Figures 5C, D) and decreased NOS2, NOX1 and KEAP1 expression in M2 macrophages (Figures 5B, D). Moreover, crocin

10.3389/fimmu.2024.1380846

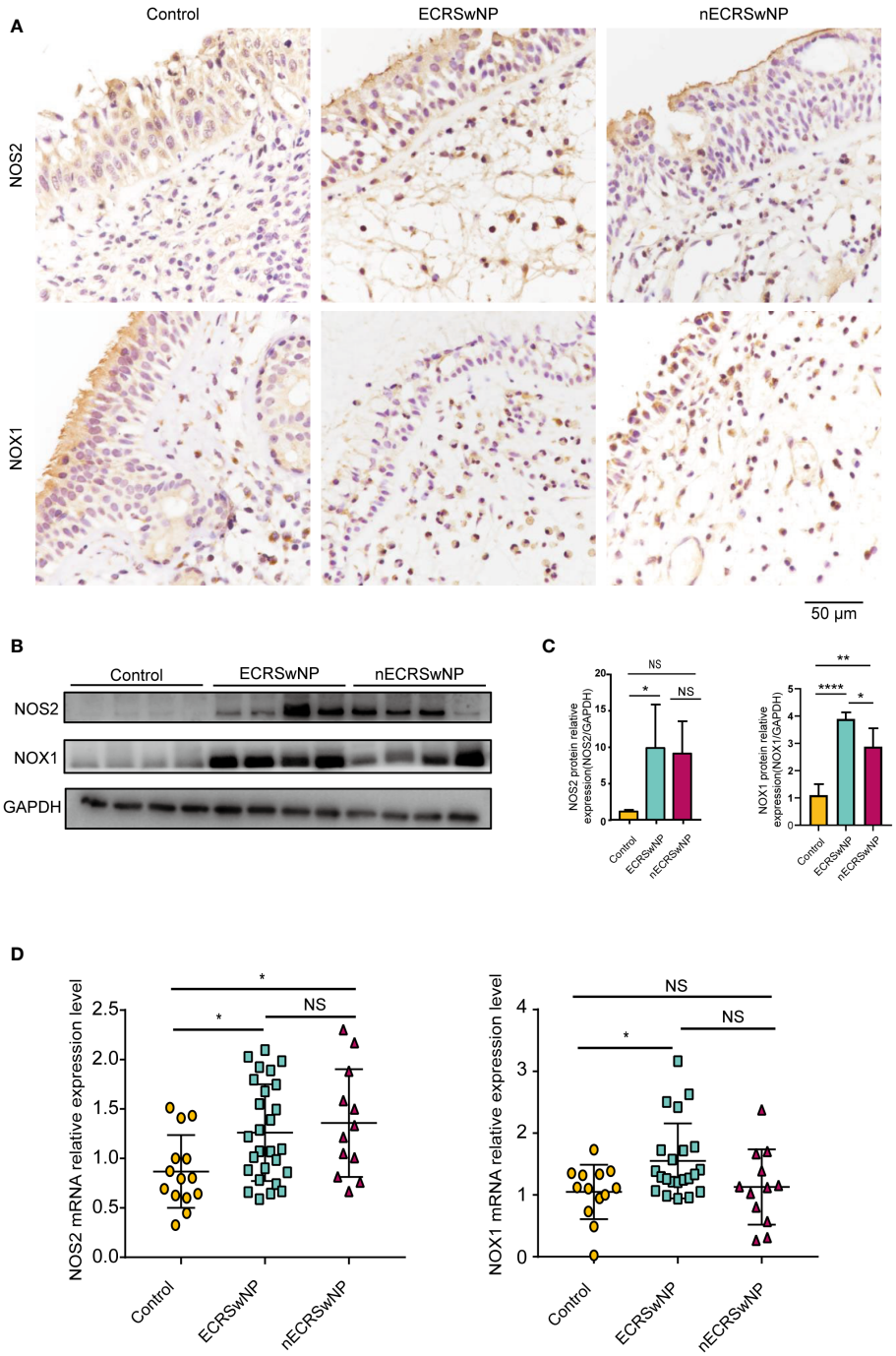

FIGURE 1
The expression of oxidase was increased in ECRSwNP compared with control. **(A)** The location of NOS2 and NOX1 was detected in control, ECRSwNP and nECRSwNP by IHC staining. **(B)** NOS2 and NOX1 protein expression was determined by Western blotting in control subjects, ECRSwNP patients and nECRSwNP patients. **(C)** Relative protein levels of NOS2 and NOX1 were normalized to GAPDH in control (n=4), ECRSwNP (n=4) and nECRSwNP (n=4). **(D)** Real-time quantitative PCR results for NOS2 in control subjects (n=14), ECRSwNP (n=27) and nECRSwNP (n=12) and for NOX1 in control subjects (n=13), ECRSwNP (n=22) and nECRSwNP (n=12). The Kruskal–Wallis test was used for comparisons among multiple groups. *p<0.05, **p<0.01, ****p<0.0001. NS, Not significant.

decreased M1 macrophages polarization (Supplementary Figure 3A). In summary, we speculated that M1 polarization results in increased oxidative stress, but M2 polarization impairs antioxidant capacity. In addition, crocin simultaneously inhibited M1 polarization by directly reducing the level of oxidative stress and inhibited M2 polarization by improving the antioxidant capacity.

3.6 Crocin treatment attenuates oxidative injury and inflammation in HNEpCs via the KEAP1-NRF2/HO-1 pathway

As oxidase and antioxidant enzymes are expressed in the epithelial cells of NPs from patients with CRSwNP, we explored the relationship

10.3389/fimmu.2024.1380846

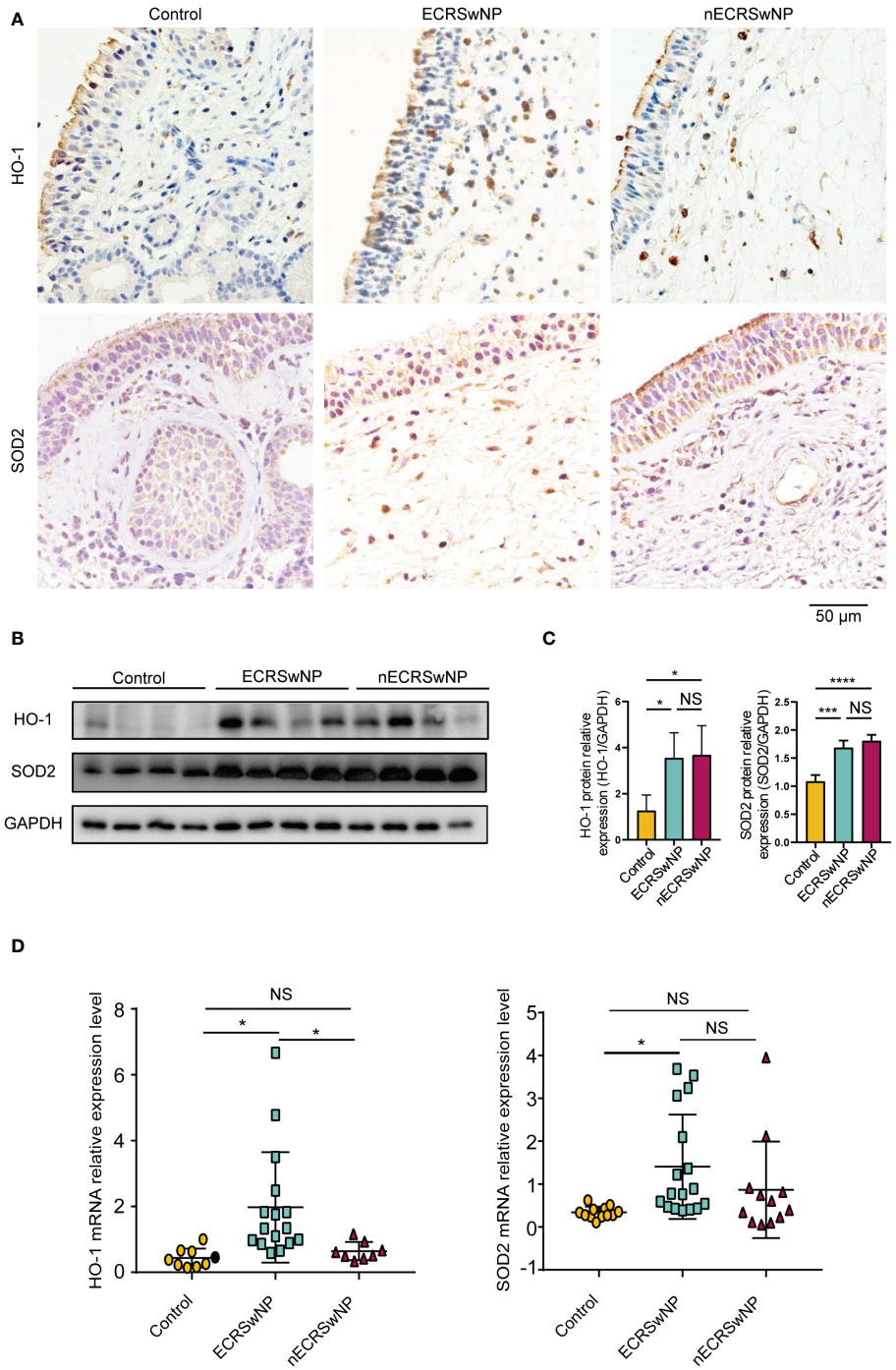

FIGURE 2
The expression of antioxidases was increased in ECRSwNP compared with control. **(A)** The location of HO-1 and SOD2 in control tissues and nasal polyps as detected by IHC. **(B)** Western blotting analyses of HO-1 and SOD2 protein levels in control subjects, ECRSwNP patients and nECRSwNP patients. **(C)** HO-1 and SOD2 relative protein levels were normalized to GAPDH in control subjects (n=4), ECRSwNP patients (n=4) and nECRSwNP patients (n=4). **(D)** qPCR results for HO-1 in control subjects (n=9), ECRSwNP (n=16) and nECRSwNP (n=8) and for SOD2 in control subjects (n=12), ECRSwNP (n=17) and nECRSwNP (n=12). The Kruskal–Wallis test was used for comparisons among multiple groups. *p<0.05, ***p <0.001, ****p <0.0001.. NS, Not significant.

between epithelial cells and oxidative stress. Our results showed that the nuclear localization of NF-κB was increased in the SEB treatment group (Figures 6A, C). In addition, the mRNA and protein levels of NOS2 were increased in the SEB-treated group (Figures 6D, E), and the level of IL-33 was increased in the SEB-treated group (Figure 6E). These findings indicated that SEB treatment activated oxidative injury and cell inflammation in HNEpCs. Crocin has been proven to ameliorate cardiotoxicity via the KEAP1-NRF2/HO-1 pathway (28). Our results revealed that NRF2 translocated into the nucleus of HNEpCs treated with crocin (Figure 6B). SEB treatment decreased HO-1 protein and mRNA levels (Figures 6D, E). Interestingly, SEB treatment did not change SOD2 protein levels (Figure 6D).

10.3389/fimmu.2024.1380846

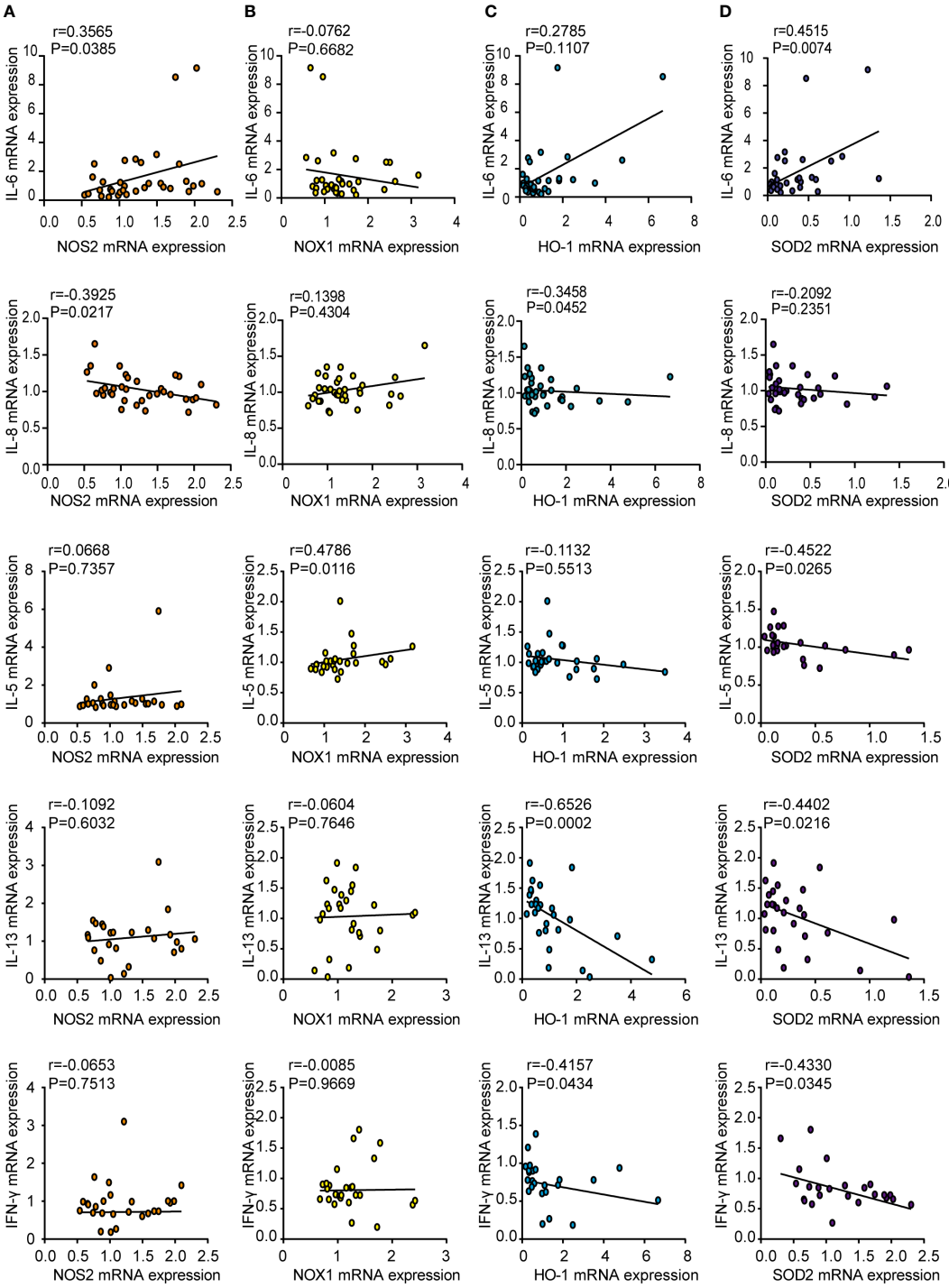

FIGURE 3
Correlations between oxidase and antioxidase expression and inflammatory cytokines in CRSwNP. Spearman analyses on the correlation of IL-6, IL-8, IL-5, IL-13, IFN-γ mRNA levels and the mRNA levels of NOS2 **(A)**, NOX1 **(B)**, HO-1 **(C)**, SOD2 **(D)** in nasal polyps tissue from CRSwNP.

Furthermore, crocin induced NF-κB translocation from the nucleus to the cytoplasm (Figure 6A), and the expression of NOS2, IL-33 was inhibited by crocin (Figures 6D, E). These results provide further evidence that crocin attenuates oxidative injury and inflammation in HNEpCs through the KEAP1-NRF2/HO-1 pathway. We also found that LPS treatment activated inflammation and crocin reversed this effect (Supplementary Figure 4).

3.7 Crocin reduces the inflammation of nasal polyp explants stimulated with SEB or LPS

Nasal polyp explants have the advantage of replicating the *in situ* mucosal environment, so we confirmed the antioxidant effect of crocin on nasal polyps based on *in vitro* explant models. SEB

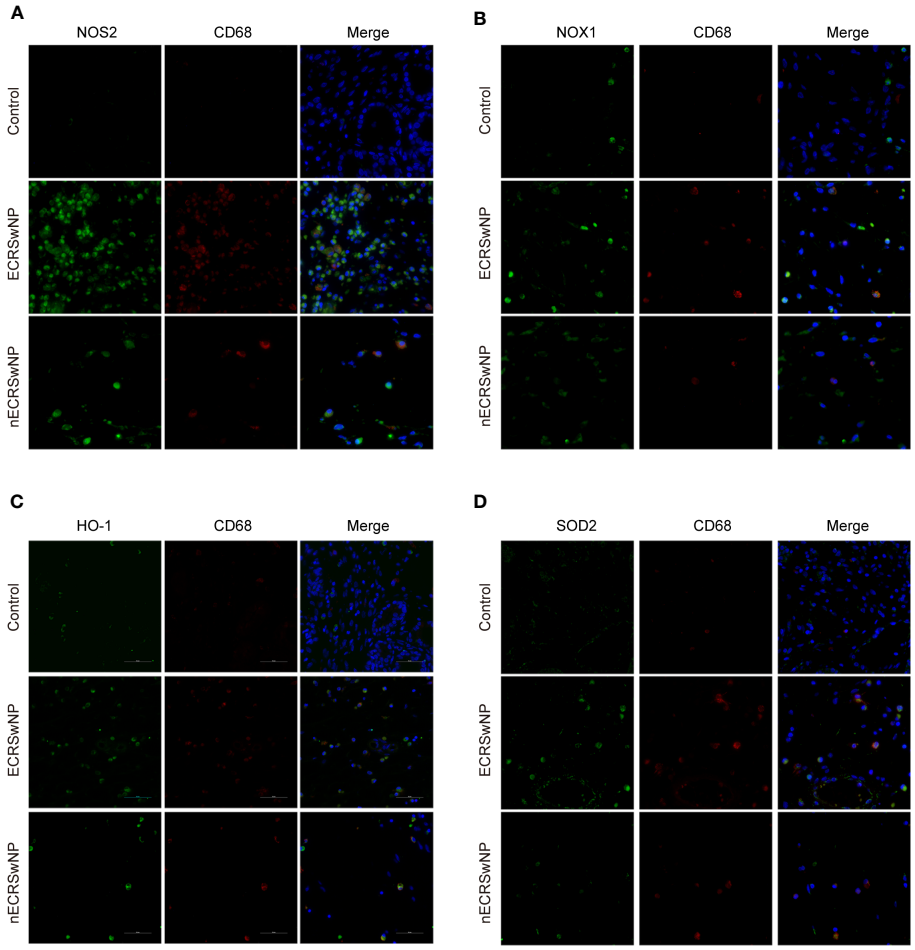

FIGURE 4
Coexpression of oxidase, antioxidase and CD68 in human nasal tissues. Representative immunostaining photomicrographs show colocalization of CD68 with NOS2 **(A)**, NOX1 **(B)**, HO-1 **(C)**, and SOD2 **(D)** in control, ECRSwNP and nCRSwNP tissue samples. Green staining indicates NOS2, NOX1, HO-1 and SOD2. Red and blue staining indicates CD68 and DAPI (nuclei), respectively.

significantly increased NOS2 and NOX1 expression (Figures 7A, B). Moreover, HO-1 expression was decreased, while SOD2 expression was elevated by SEB (Figures 7A, C). In contrast, crocin decreased NOS2 expression and NOX1 expression (Figures 7A, B) and increased the expression of HO-1 and SOD2 (Figures 7A, C). SEB also increased IL-5, IL-13, IL-6, IL-8, IL-25, IL-33, IFN-γ and IL-1β mRNA expression, and crocin treatment reversed this effect (Figure 7D). In addition, LPS stimulation increased NOX1 mRNA expression as well as that of SOD2, IL-6, IL-8, IL-25, and IL-33 (Figures 7E, F). Crocin reduced NOX1, IL-6, IL-8, IL-25, and IL-33 mRNA expression but increased HO-1 and SOD2 expression (Figures 7E, F). Together, these results indicated that crocin exerts an anti-inflammatory effect on nasal polyp explants by improving the antioxidant capacity of cells.

4 Discussion

Oxidative stress has been shown to be involved in a wide range of diseases, including chronic obstructive pulmonary disease, Alzheimer's disease, cancer and cardiovascular and metabolic diseases (21, 29, 30). To protect against oxidative stress damage, organisms have evolved defense mechanisms based on antioxidant enzymes that neutralize oxidants and repair oxidative injury. Therefore, these defense mechanisms are the targets of disease treatment and prevention, and agents that enhance antioxidative defenses are the main strategies of antioxidant therapy (21). For example, N-acetylcysteine (NAC) can treat nephropathy by supplementing with GSH (31). Recently, oxidative stress was also shown to play crucial roles in the development of CRSwNP (32). In the present study, we assessed the oxidative status and antioxidative defense in CRSwNP patients and observed an imbalance between oxidase and antioxidant enzyme levels, particularly in patients with ECRSwNP. We further found that the accumulation of oxidants was positively correlated with the levels of inflammatory cytokines. Thus, improving the antioxidant capacity to reduce oxidation and inflammation may be a potential strategy for the treatment of CRSwNP.

Oxidation and antioxidation are dynamically balanced, and an increase in the oxidant level will promote an increase in the antioxidants by negative feedback, thus eliminating excessive ROS and reducing oxidative stress. Consistent with previous studies (33–

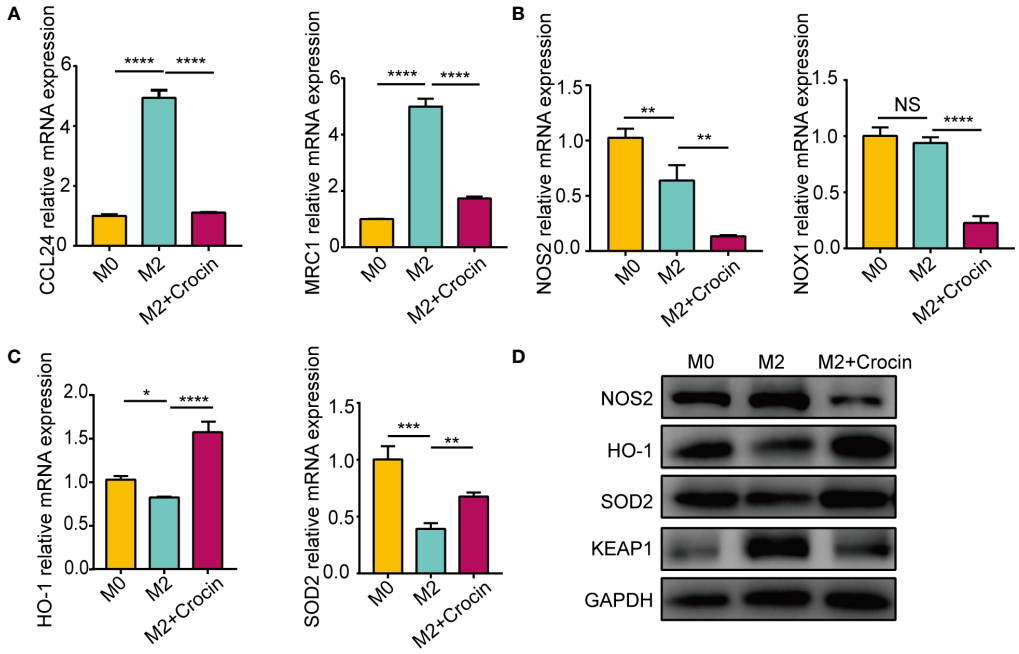

FIGURE 5
The damage of antioxidant enzymes is related to M2 polarization. M0 were pretreated with IL-4 (20 ng/ml) with or without crocin (20 μM) for 24 h. **(A-C)** qPCR was used to detect the mRNA expression of CCL24, MRC1, NOS2, NOX1, HO-1 and SOD2. **(D)** Western blotting was used to evaluate the protein expression of NOS2, HO-1, SOD2 and KEAP1. Data were obtained in three independent experiments. One-way ANOVA was used to analyze the differences between multiple groups. *p<0.05, **p<0.01, ***p<0.001, ****p<0.0001.. NS, Not significant.

35), we found that compared with that in the control group, the expression of NOS2 and NOX1 was increased markedly in ECRSwNP patients. Notably, for the first time, we reported an increase in 3-NT expression in nasal polyps. Moreover, the antioxidant level also increased, mainly manifested as an increase in the levels of antioxidant enzymes such as SOD2 and HO-1. However, our results are slightly different from those of previous reports. Ono et al. (26) found that the mRNA and activity of SOD2 were decreased in patients with CRSwNP, especially in patients with ECRSwNP, compared with healthy controls. In addition, Yu et al. (20) reported that the mRNA expression of HO-1 in nECRSwNP patients was significantly greater than that in ECRSwNP patients. Therefore, we speculate that oxidative status may be related to the unclear development of nasal polyps and drug interference during treatment. Further research revealed that the expression of these oxidation-related genes were positively correlated with the levels of inflammatory factors, while the expression of antioxidant genes were negatively correlated with inflammatory factor levels. These studies showed that there is an obvious imbalance between oxidation and antioxidation in nasal polyps, which could be involved in the inflammatory reaction in nasal polyps.

Previous studies have shown that nasal epithelial cells, macrophages, neutrophils, eosinophils and basophils are the sites of oxidative stress in CRSwNP (13, 14, 16). In our study, NOS2 and NOX1 were expressed in epithelial and subcutaneous cells, such as $NOS2^+$ macrophages, as determined by immunofluorescence. As reported, epithelial cells are frequently exposed to exogenous oxidants such as pathogens, allergens, cigarette smoke, diesel fuel, and ozone, which can lead to the development of oxidative stress (36). We observed an imbalance between the oxidation and antioxidation of HNEpCs stimulated by LPS and SEB, which was characterized by a decrease in HO-1 expression and an increase in NOS2 expression. Moreover, the translocation of NF-κB to the nucleus was also determined by immunofluorescence. It has been reported that macrophages can be polarized into M1-like macrophages (M1) and M2-like macrophages (M2) (37). Consistent with previous research results (38), M1 macrophages exhibit obvious oxidative stress and inflammatory responses, including increased expression of NOS2 and NOX1, decreased expression of HO-1 and increased expression of IL-6 and tumor necrosis factor α (TNF-α). However, the antioxidant enzyme SOD2 in M1 macrophages was also increased, consistent with the findings of Paulina Tokarz's research (39), which suggested that the increased expression of SOD2 protected macrophages from LPS-induced damage. In contrast, decreased expression of NOS2 and NOX1 as well as antioxidant enzymes (HO-1 and SOD2) were detected in polarized M2 macrophages. These results in macrophages indicated that oxidative stress is mainly produced by M1-like macrophages. In summary, epithelial cells and macrophages are important sources of oxidative stress in CRSwNP, while the increased expression of antioxidant enzymes in these cells reduces oxidative stress and inflammation to a certain degree as a feedback mechanism.

Redox balance is regulated by the KEAP1/NRF2/ARE signaling pathway which is the main pathway involved in the protection against oxidative stress in different diseases (40–42). Under stress conditions, ROS can modify the cysteine residues of KEAP1, resulting in inactivation of the E3 ubiquitin ligase and

10.3389/fimmu.2024.1380846

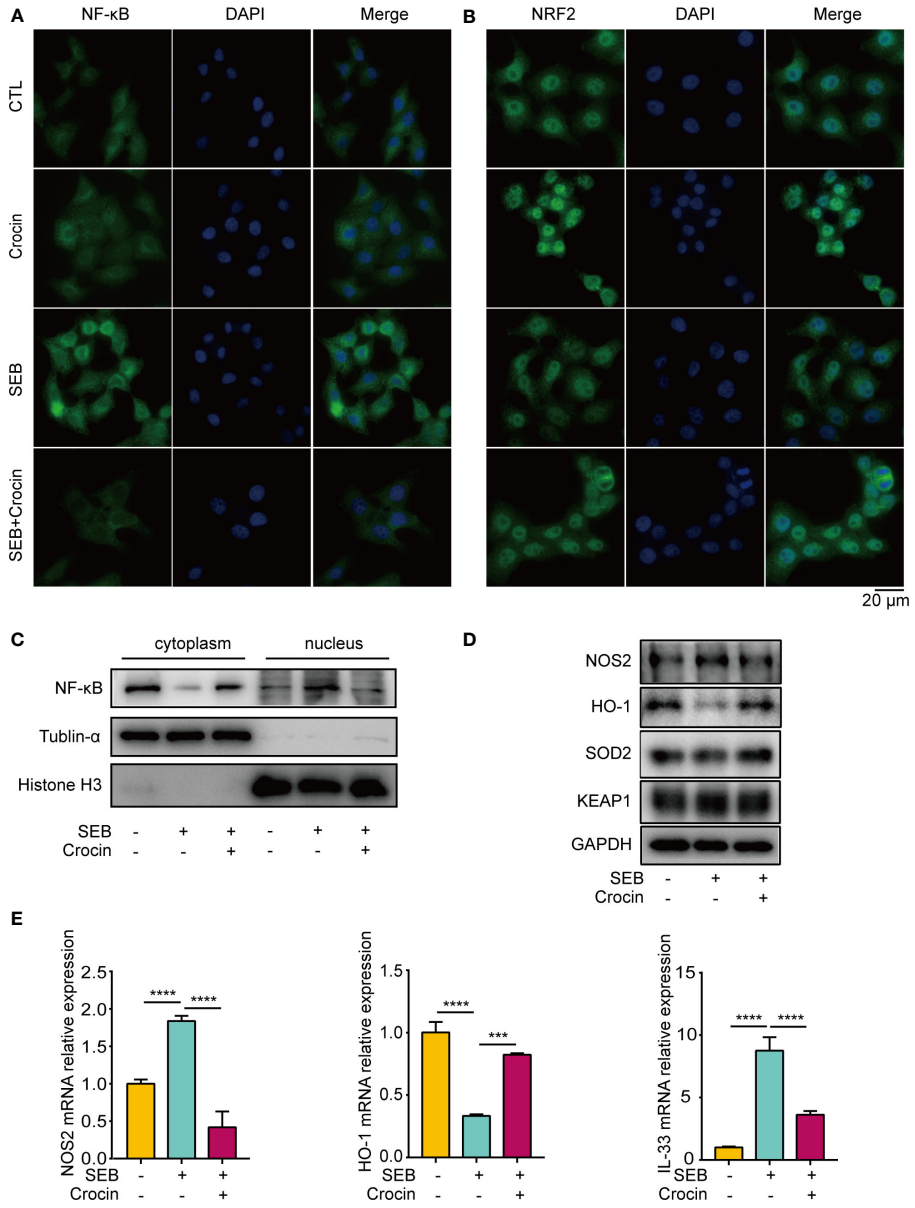

FIGURE 6
Crocin treatment attenuates oxidative injury and inflammation in HNEpC. **(A, B)** HNEpC were pretreated with or without crocin (20 μM) for 24 h and incubated with or without SEB (1 μg/mL) for 2 h. Cells were visualized by immunostaining with anti-NF-κB (green) and anti-NRF2 (green) antibodies. Nuclei were stained with DAPI (blue). **(C)** HNEpC were incubated with SEB (1 μg/mL) with or without crocin (20 μM) for 24 h followed by nucleocytoplasmic separation. **(D)** Western blotting showed changes in NOS2, HO-1, SOD2 and KEAP1 protein levels. **(E)** qPCR showed changes in NOS2, HO-1 and IL-33 mRNA levels. Data were obtained in three independent experiments. One-way ANOVA was used to analyze the differences between multiple groups. ***p<0.001, ****p<0.0001.

accumulation of NRF2 (43). NRF2 then translocates into the nucleus and binds to antioxidant response elements (AREs) to initiate the transcription of antioxidant genes, including HO-1, NQO1 and SOD (44). In this study, we found increased expression of both oxidases and the antioxidant enzymes SOD2 and HO-1 in nasal polyps, indicating the activation of the KEAP1/NRF2 signaling pathway in response to stress. However, the increase in antioxidant enzymes failed to offset the accumulation of oxidants, leading to increased oxidative stress in nasal tissue. Previous studies have confirmed that the KEAP1/NRF2 system could be an important therapeutic target for various diseases, including inflammatory diseases (40), diabetes (41), and neurodegenerative diseases (42). For example, mangiferin and panaxydol can alleviate allergic rhinitis (AR) and LPS-induced lung inflammation through the KEAP1-NRF2/HO-1 pathway, respectively (45).

Crocin, which is extracted from saffron, has been proven to have antioxidant and anti-inflammatory properties (46). Several studies have confirmed that crocin has significant therapeutic effects on diabetes (47), cancer (48), and cardiovascular disease (49). Our results showed that crocin treatment alleviated inflammation and oxidative stress in HNEpCs stimulated with LPS and SEB. Crocin strongly inhibited the expression of NF-κB p65 and its translocation

10.3389/fimmu.2024.1380846

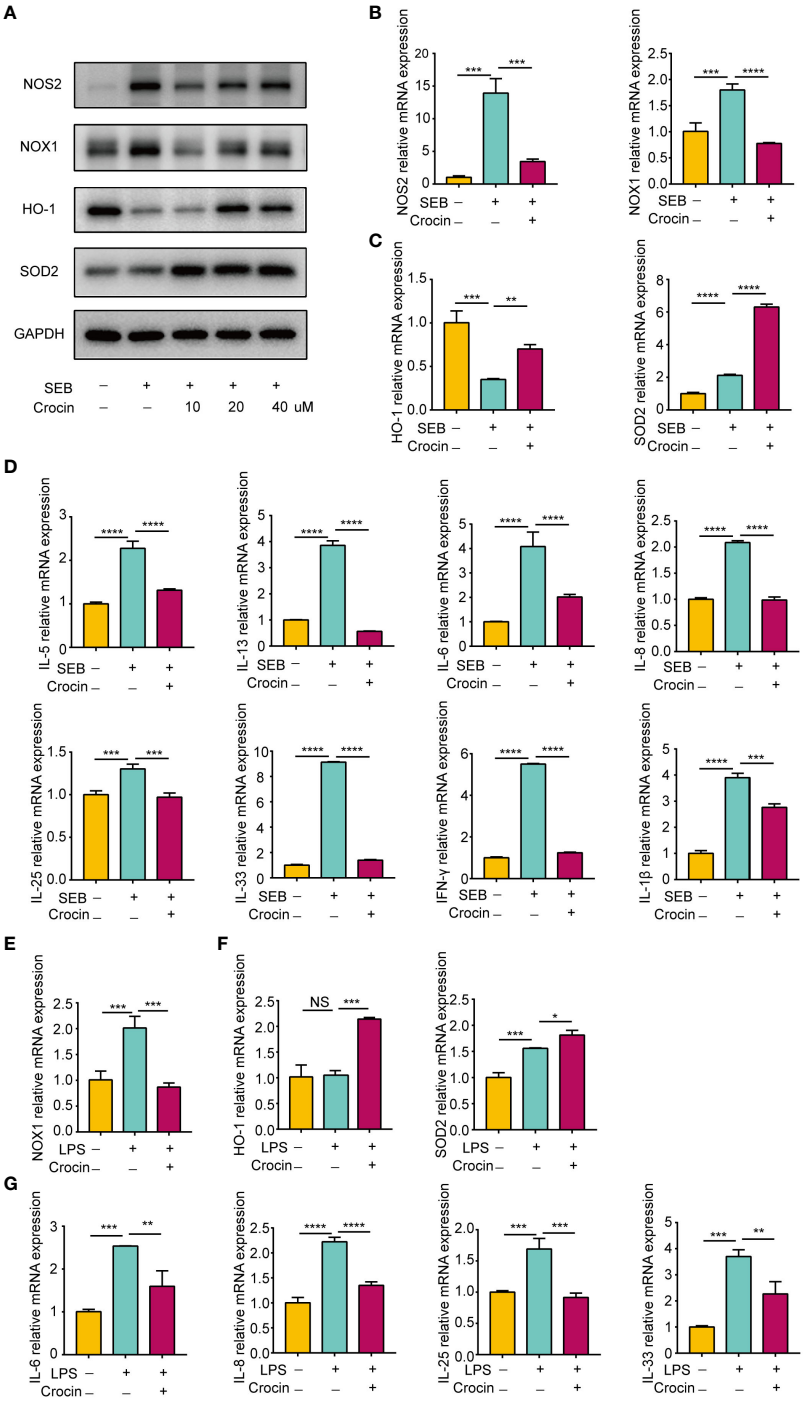

FIGURE 7
Crocin reduces the inflammation of nasal polyp explants induced by SEB or LPS. **(A–D)** Nasal polyp explants were incubated with SEB (500 ng/ml) with or without crocin (20 μM) for 24 h. **(A)** Protein expression of NOS2, NOX1, HO-1, SOD2 was assessed by Western blotting. **(B)** mRNA expression of NOS2 and NOX1 was measured by qPCR. **(C)** mRNA expression of HO-1 and SOD2 were measured by qPCR. **(D)** Significant downregulation of IL-6, IL-8, IL-5, IL-13, IL-25, IL-33, IL-1β and IFN-γ mRNA levels after crocin treatment. **(E, F)** Nasal polyp explants were treated with LPS (100 ng/ml) with or without crocin (20 μM) for 24 h. **(E)** mRNA expression of NOX1, HO-1 and SOD2 was measured by qPCR. **(F)** mRNA expression of IL-6, IL-8, IL-25 and IL-33 was measured by qPCR. One-way ANOVA was used to analyze the differences between multiple groups. *p<0.05, **p<0.01, ***p<0.001, ****p<0.0001.. NS, Not significant.

into the nucleus (50) but significantly activated NRF2 (28). Interestingly, the expression of SOD2 was not affected by crocin, which showed that crocin inhibited LPS- and SEB-induced inflammation though KEAP1-NRF2/HO-1 signaling in HNEpCs. Previous studies have shown that crocin alleviates coronary atherosclerosis and titanium particle-induced inflammation by inducing M2 macrophage polarization (51, 52). Unlike previous studies, we observed that crocin inhibited the expression of MRC1

and CCL24 in M2 macrophages and inhibited the expression of IL-6, NOS2 and TNF-α in M1 macrophages, which indicated that crocin may inhibit M1 and M2 macrophage polarization. Furthermore, crocin upregulated the expression of HO-1 and SOD2 in M2 macrophages but did not upregulate the expression of HO-1 and SOD2 in M1 macrophages. In addition, KEAP1 protein levels were decreased in the M2 group treated with crocin. These results suggested that crocin could achieve antioxidant and anti-inflammatory effects through the KEAP1/NRF2 pathway in M2 macrophages, while it may directly reduce the inflammatory response induced by M1 macrophages in other ways. Because M2 macrophages has been demonstrated to play an important role in persistent inflammation in CRSwNP, particularly in ECRSwNP (53, 54), crocin may have an anti-inflammatory effect on CRSwNP due to its ability to increase antioxidant enzyme expression in M2 macrophages. As crocin is a natural product with low toxicity, it has great application prospects. Overall, treatment with antioxidants might be a potential strategy for CRSwNP management.

5 Conclusions

Our results revealed that an imbalance between oxidants and antioxidants could be involved in the development of chronic rhinosinusitis with nasal polyps. Nasal epithelial cells and macrophages are the main cellular sources of oxidative stress in CRSwNP. Antioxidant treatment with crocin might be a potential strategy for the treatment of CRSwNP through the KEAP1/NRF2/HO-1 pathway.

Data availability statement

The raw data supporting the conclusions of this article will be made available by the authors, without undue reservation.

Ethics statement

The studies involving humans were approved by Biomedical Research Ethics Committee of West China Hospital of Sichuan University. The studies were conducted in accordance with the local legislation and institutional requirements. The participants provided their written informed consent to participate in this study.

Author contributions

JinZ: Conceptualization, Methodology, Writing – review & editing, Data curation, Formal analysis, Investigation, Software, Writing – original draft. JiaZ: Conceptualization, Project administration, Supervision, Writing – review & editing, Data curation, Formal analysis, Investigation. RL: Data curation, Formal analysis, Writing – review & editing. YL: Resources, Supervision, Writing – review & editing. JM: Supervision, Writing – review & editing, Funding acquisition. QW: Data curation, Formal analysis, Software, Visualization, Writing – review & editing. YL: Conceptualization, Funding acquisition, Project administration, Supervision, Writing – review & editing. SL: Conceptualization, Funding acquisition, Project administration, Resources, Supervision, Validation, Writing – review & editing. HL: Supervision, Validation, Writing – review & editing. LB: Funding acquisition, Methodology, Supervision, Writing – review & editing. JD: Funding acquisition, Methodology, Supervision, Writing – review & editing, Conceptualization, Project administration, Validation.

Funding

The author(s) declare financial support was received for the research, authorship, and/or publication of this article. This study was supported by the National Natural Science Fund of China (Liu SX: 81970858 and Ba L: 82160209), the Sichuan Agency of Science and Technology (Du JT: 2022YFS0246), the Natural Science Foundation of Sichuan Province (Meng J: 2022NSFSC0788), and the Technology Development Fund of Tibet Autonomous Region (Ba L: XZ202301YD0024C).

Acknowledgments

We would like to thank Professor HL for his help and support, and the Geriatrics Center of West China Hospital for providing an experimental platform for the development and implementation of this research.

Conflict of interest

The authors declare that the research was conducted in the absence of any commercial or financial relationships that could be construed as a potential conflict of interest.

Publisher's note

Supplementary material

The Supplementary Material for this article can be found online at: https://www.frontiersin.org/articles/10.3389/fimmu.2024.1380846/full#supplementary-material

References

1. Carsuzaa F, Béquignon É, Dufour X, de Bonnecaze G, Lecron JC, Favot L. Cytokine signature and involvement in chronic rhinosinusitis with nasal polyps. *Int J Mol Sci*. (2021) 23(1):417. doi: 10.3390/ijms23010417

2. Bachert C, Bhattacharyya N, Desrosiers M, Khan AH. Burden of disease in chronic rhinosinusitis with nasal polyps. *J Asthma Allergy*. (2021) 14:127–34. doi: 10.2147/JAA.S290424

3. Fokkens WJ, Lund VJ, Hopkins C, Hellings PW, Kern R, Reitsma S, et al. European position paper on rhinosinusitis and nasal polyps 2020. *Rhinology*. (2020) 58:1–464. doi: 10.4193/Rhin

4. Nakayama T, Lee IT, Le W, Tsunemi Y, Borchard NA, Zarabanda D, et al. Inflammatory molecular endotypes of nasal polyps derived from White and Japanese populations. *J Allergy Clin Immunol*. (2022) 149:1296–308.e6. doi: 10.1016/j.jaci.2021.11.017

5. Takabayashi T, Schleimer RP. Formation of nasal polyps: The roles of innate type 2 inflammation and deposition of fibrin. *J Allergy Clin Immunol*. (2020) 145:740–50. doi: 10.1016/j.jaci.2020.01.027

6. Wang W, Gao Y, Zhu Z, Zha Y, Wang X, Qi F, et al. Changes in the clinical and histological characteristics of Chinese chronic rhinosinusitis with nasal polyps over 11 years. *Int Forum Allergy rhinology*. (2019) 9:149–57. doi: 10.1002/alr.22234

7. Yu L, Jiang Y, Yan B, Fang G, Wang C, Zhang L. Predictive value of clinical characteristics in eosinophilic chronic rhinosinusitis with nasal polyps: A cross-sectional study in the Chinese population. *Int Forum Allergy rhinology*. (2022) 12:726–34. doi: 10.1002/alr.22901

8. Laidlaw TM, Mullol J, Woessner KM, Amin N, Mannent LP. Chronic rhinosinusitis with nasal polyps and asthma. *J Allergy Clin Immunol In practice*. (2021) 9:1133–41. doi: 10.1016/j.jaip.2020.09.063

9. Lou H, Zhang N, Bachert C, Zhang L. Highlights of eosinophilic chronic rhinosinusitis with nasal polyps in definition, prognosis, and advancement. *Int Forum Allergy rhinology*. (2018) 8:1218–25. doi: 10.1002/alr.22214

10. Jelinek M, Jurajda M, Duris K. Oxidative stress in the brain: basic concepts and treatment strategies in stroke. *Antioxidants (Basel Switzerland)*. (2021) 10(12):1886. doi: 10.3390/antiox10121886

11. Thiruvengadam M, Venkidasamy B, Subramanian U, Samynathan R, Ali Shariati M, Rebezov M, et al. Bioactive compounds in oxidative stress-mediated diseases: targeting the NRF2/ARE signaling pathway and epigenetic regulation. *Antioxidants (Basel Switzerland)*. (2021) 10(12):1859. doi: 10.3390/antiox10121859

12. Poprac P, Jomova K, Simunkova M, Kollar V, Rhodes CJ, Valko M. Targeting free radicals in oxidative stress-related human diseases. *Trends Pharmacol Sci*. (2017) 38:592–607. doi: 10.1016/j.tips.2017.04.005

13. Nishida M, Takeno S, Takemoto K, Takahara D, Hamamoto T, Ishino T, et al. Increased tissue expression of lectin-like oxidized LDL receptor-1 (LOX-1) is associated with disease severity in chronic rhinosinusitis with nasal polyps. *Diagnostics (Basel Switzerland)*. (2020) 10(4):246. doi: 10.3390/diagnostics10040246

14. Zheng K, Hao J, Xiao L, Wang M, Zhao Y, Fan D, et al. Expression of nicotinamide adenine dinucleotide phosphate oxidase in chronic rhinosinusitis with nasal polyps. *Int Forum Allergy rhinology*. (2020) 10:646–55. doi: 10.1002/alr.22530

15. Akyigit A, Keles E, Etem EO, Ozercan I, Akyol H, Sakallioglu O, et al. Genetic polymorphism of antioxidant enzymes in eosinophilic and non-eosinophilic nasal polyposis. *Eur Arch oto-rhino-laryngology*. (2017) 274:267–73. doi: 10.1007/s00405-016-4259-z

16. Lin H, Ba G, Tang R, Li M, Li Z, Li D, et al. Increased expression of TXNIP facilitates oxidative stress in nasal epithelial cells of patients with chronic rhinosinusitis with nasal polyps. *Am J rhinology Allergy*. (2021) 35:607–14. doi: 10.1177/1945892420982411

17. San I, Ulas T, Bozkus F, Iynen I, Yesilova Y, Sezen H, et al. Prolidase activity and oxidative stress parameters in patients with nasal polyps. *La Clinica terapeutica*. (2013) 164:209–13. doi: 10.7417/CT.2013.1557

18. Bozkus F, San I, Ulas T, Iynen I, Yesilova Y, Guler Y, et al. Evaluation of total oxidative stress parameters in patients with nasal polyps. *Acta otorhinolaryngologica Italica organo ufficiale della Societa italiana di otorinolaringologia e chirurgia cervico-facciale*. (2013) 33:248–53.

19. Mrowicka M, Zielinska-Blizniewska H, Milonski J, Olszewski J, Majsterek I. Evaluation of oxidative DNA damage and antioxidant defense in patients with nasal polyps. *Redox Rep Commun Free Radical Res*. (2015) 20:177–83. doi: 10.1179/1351000215Y.0000000001

20. Yu Z, Wang Y, Zhang J, Li L, Wu X, Ma R, et al. Expression of heme oxygenase-1 in eosinophilic and non-eosinophilic chronic rhinosinusitis with nasal polyps: modulation by cytokines. *Int Forum Allergy rhinology*. (2015) 5:734–40. doi: 10.1002/alr.21530

21. Forman HJ, Zhang H. Targeting oxidative stress in disease: promise and limitations of antioxidant therapy. *Nat Rev Drug discovery*. (2021) 20:689–709. doi: 10.1038/s41573-021-00233-1

22. Tardiolo G, Bramanti P, Mazzon E. Overview on the effects of N-acetylcysteine in neurodegenerative diseases. *Molecules (Basel Switzerland)*. (2018) 23(12):3305. doi: 10.3390/molecules23123305

23. Saeedi M, Rashidy-Pour A. Association between chronic stress and Alzheimer's disease: Therapeutic effects of Saffron. *Biomedicine pharmacotherapy = Biomedecine pharmacotherapie*. (2021) 133:110995. doi: 10.1016/j.biopha.2020.110995

24. Su X, Yuan C, Wang L, Chen R, Li X, Zhang Y, et al. The beneficial effects of saffron extract on potential oxidative stress in cardiovascular diseases. *Oxid Med Cell longevity*. (2021) 2021:6699821. doi: 10.1155/2021/6699821

25. Campolo N, Issoglio FM, Estrin DA, Bartesaghi S, Radi R. 3-Nitrotyrosine and related derivatives in proteins: precursors, radical intermediates and impact in function. *Essays Biochem*. (2020) 64:111–33. doi: 10.1042/EBC20190052

26. Ono N, Kusunoki T, Miwa M, Hirotsu M, Shiozawa A, Ikeda K. Reduction in superoxide dismutase expression in the epithelial mucosa of eosinophilic chronic rhinosinusitis with nasal polyps. *Int Arch Allergy Immunol*. (2013) 162:173–80. doi: 10.1159/000353122

27. Otoupalova E, Smith S, Cheng G, Thannickal VJ. Oxidative stress in pulmonary fibrosis. *Compr Physiol*. (2020) 10:509–47. doi: 10.1002/cphy.c190017

28. Liang Y, Zheng B, Li J, Shi J, Chu L, Han X, et al. Crocin ameliorates arsenic trioxide–induced cardiotoxicity via Keap1-Nrf2/HO-1 pathway: Reducing oxidative stress, inflammation, and apoptosis. *Biomedicine pharmacotherapy = Biomedecine pharmacotherapie*. (2020) 131:110713. doi: 10.1016/j.biopha.2020.110713

29. Hayes JD, Dinkova-Kostova AT, Tew KD. Oxidative stress in cancer. *Cancer Cell*. (2020) 38:167–97. doi: 10.1016/j.ccell.2020.06.001

30. Incalza MA, D'Oria R, Natalicchio A, Perrini S, Laviola L, Giorgino F. Oxidative stress and reactive oxygen species in endothelial dysfunction associated with cardiovascular and metabolic diseases. *Vasc Pharmacol*. (2018) 100:1–19. doi: 10.1016/j.vph.2017.05.005

31. Xu R, Tao A, Bai Y, Deng Y, Chen G. Effectiveness of N-acetylcysteine for the prevention of contrast-induced nephropathy: A systematic review and meta-analysis of randomized controlled trials. *J Am Heart Assoc*. (2016) 5(9):e003968. doi: 10.1161/JAHA.116.003968

32. Tsai YJ, Hsu YT, Ma MC, Wu CK, Luo SD, Wu WB. Transcriptomic analysis of genes associated with oxidative stress in chronic rhinosinusitis patients with nasal polyps: identifying novel genes involved in nasal polyposis. *Antioxidants (Basel Switzerland)*. (2022) 11(10):1899. doi: 10.3390/antiox11101899

33. Sadek AA, Abdelwahab S, Eid SY, Almaimani RA, Althubiti MA, El-Readi MZ. Overexpression of inducible nitric oxide synthase in allergic and nonallergic nasal polyp. *Oxid Med Cell longevity*. (2019) 2019:7506103. doi: 10.1155/2019/7506103

34. Plewka D, Grzanka A, Drzewiecka E, Plewka A, Misiołek M, Lisowska G, et al. Differential expression of tumor necrosis factor α, interleukin 1β, nuclear factor κB in nasal mucosa among chronic rhinosinusitis patients with and without polyps. *Postepy dermatologii i alergologii*. (2017) 34:199–206. doi: 10.5114/ada.2017.67842

35. Moon JH, Kim TH, Lee HM, Lee SH, Choe W, Kim HK, et al. Overexpression of the superoxide anion and NADPH oxidase isoforms 1 and 4 (NOX1 and NOX4) in allergic nasal mucosa. *Am J rhinology Allergy*. (2009) 23:370–6. doi: 10.2500/ajra.2009.23.3340

36. Jiang L, Diaz PT, Best TM, Stimpfl JN, He F, Zuo L. Molecular characterization of redox mechanisms in allergic asthma. *Ann allergy Asthma Immunol*. (2014) 113:137–42. doi: 10.1016/j.anai.2014.05.030

37. Yunna C, Mengru H, Lei W, Weidong C. Macrophage M1/M2 polarization. *Eur J Pharmacol*. (2020) 877:173090. doi: 10.1016/j.ejphar.2020.173090

38. Tsai CF, Chen GW, Chen YC, Shen CK, Lu DY, Yang LY, et al. Regulatory effects of quercetin on M1/M2 macrophage polarization and oxidative/antioxidative balance. *Nutrients*. (2021) 14(1):67. doi: 10.3390/nu14010067

39. Tokarz P, Płoszaj T, Regdon Z, Virág L, Robaszkiewicz A. PARP1-LSD1 functional interplay controls transcription of SOD2 that protects human pro-inflammatory macrophages from death under an oxidative condition. *Free Radical Biol Med*. (2019) 131:218–24. doi: 10.1016/j.freeradbiomed.2018.12.004

40. Tu W, Wang H, Li S, Liu Q, Sha H. The anti-inflammatory and anti-oxidant mechanisms of the keap1/nrf2/ARE signaling pathway in chronic diseases. *Aging disease*. (2019) 10:637–51. doi: 10.14336/AD.2018.0513

41. Adelusi TI, Du L, Hao M, Zhou X, Xuan Q, Apu C, et al. Keap1/Nrf2/ARE signaling unfolds therapeutic targets for redox imbalanced-mediated diseases and diabetic nephropathy. *Biomedicine pharmacotherapy = Biomedecine pharmacotherapie*. (2020) 123:109732. doi: 10.1016/j.biopha.2019.109732

42. Fão L, Mota SI, Rego AC. Shaping the Nrf2-ARE-related pathways in Alzheimer's and Parkinson's diseases. *Ageing Res Rev*. (2019) 54:100942. doi: 10.1016/j.arr.2019.100942

43. Yamamoto M, Kensler TW, Motohashi H. The KEAP1-NRF2 system: a thiol-based sensor-effector apparatus for maintaining redox homeostasis. *Physiol Rev*. (2018) 98:1169–203. doi: 10.1152/physrev.00023.2017

44. Yu C, Xiao JH. The keap1-nrf2 system: A mediator between oxidative stress and aging. *Oxid Med Cell longevity*. (2021) 2021:6635460. doi: 10.1155/2021/6635460

45. Li J, Lu K, Sun F, Tan S, Zhang X, Sheng W, et al. Panaxydol attenuates ferroptosis against LPS-induced acute lung injury in mice by Keap1-Nrf2/HO-1 pathway. *J Trans Med*. (2021) 19:96. doi: 10.1186/s12967-021-02745-1

46. Bastani S, Vahedian V, Rashidi M, Mir A, Mirzaei S, Alipourfard I, et al. An evaluation on potential anti-oxidant and anti-inflammatory effects of Crocin. *Biomedicine pharmacotherapy = Biomedecine pharmacotherapie*. (2022) 153:113297. doi: 10.1016/j.biopha.2022.113297

47. Li X, Liu Y, Cao A, Li C, Wang L, Wu Q, et al. Crocin improves endothelial mitochondrial dysfunction via GPx1/ROS/KCa3.1 signal axis in diabetes. *Front Cell Dev Biol*. (2021) 9:651434. doi: 10.3389/fcell.2021.651434

48. Bakshi HA, Zoubi MSA, Hakkim FL, Aljabali AAA, Rabi FA, Hafiz AA, et al. Dietary crocin is protective in pancreatic cancer while reducing radiation-induced hepatic oxidative damage. *Nutrients*. (2020) 12(6):1901. doi: 10.3390/nu12061901

49. Sheng Y, Gong X, Zhao J, Liu Y, Yuan Y. Effects of crocin on CCL2/CCR2 inflammatory pathway in monocrotaline-induced pulmonary arterial hypertension rats. *Am J Chin Med*. (2022) 50:241–59. doi: 10.1142/S0192415X22500082

50. Shi L, Zhao S, Chen Q, Wu Y, Zhang J, Li N. Crocin inhibits RANKL–induced osteoclastogenesis by regulating JNK and NF–κB signaling pathways. *Mol Med Rep*. (2018) 17:7947–51. doi: 10.3892/mmr

51. Li J, Lei HT, Cao L, Mi YN, Li S, Cao YX. Crocin alleviates coronary atherosclerosis via inhibiting lipid synthesis and inducing M2 macrophage polarization. *Int immunopharmacology*. (2018) 55:120–7. doi: 10.1016/j.intimp.2017.11.037

52. Zhu K, Yang C, Dai H, Li J, Liu W, Luo Y, et al. Crocin inhibits titanium particle-induced inflammation and promotes osteogenesis by regulating macrophage polarization. *Int immunopharmacology*. (2019) 76:105865. doi: 10.1016/j.intimp.2019.105865

53. Krysko O, Holtappels G, Zhang N, Kubica M, Deswarte K, Derycke L, et al. Alternatively activated macrophages and impaired phagocytosis of S. aureus in chronic rhinosinusitis. *Allergy*. (2011) 66:396–403. doi: 10.1111/all.2011.66.issue-3

54. Wang ZC, Yao Y, Wang N, Liu JX, Ma J, Chen CL, et al. Deficiency in interleukin-10 production by M2 macrophages in eosinophilic chronic rhinosinusitis with nasal polyps. *Int Forum Allergy rhinology*. (2018) 8:1323–33. doi: 10.1002/alr.22218

frontiers | Frontiers in Immunology

TYPE Original Research
PUBLISHED 08 May 2024
DOI 10.3389/fimmu.2024.1369849

OPEN ACCESS

EDITED BY
Pedro Gonzalez-Menendez,
University of Oviedo, Spain

REVIEWED BY
Juan Pablo Rodríguez,
National Scientific and Technical Research Council (CONICET), Argentina
Ana Carolina Martinez-Torres,
Autonomous University of Nuevo León, Mexico

*CORRESPONDENCE
Jianhua Wu
wujh_chyy@163.com
Liang Xiao
xiaoliang830713@163.com

†These authors have contributed equally to this work

RECEIVED 13 January 2024
ACCEPTED 19 April 2024
PUBLISHED 08 May 2024

CITATION
Liu R, Wang Y, Kuai W, Li W, Wang Z, Xiao L and Wu J (2024) Troxerutin suppress inflammation response and oxidative stress in jellyfish dermatitis by activating Nrf2/HO-1 signaling pathway. *Front. Immunol.* 15:1369849. doi: 10.3389/fimmu.2024.1369849

Troxerutin suppress inflammation response and oxidative stress in jellyfish dermatitis by activating Nrf2/HO-1 signaling pathway

Ran Liu[1†], Yulian Wang[1†], Wenhao Kuai[1†], Wenting Li[1], Zengfa Wang[2,3], Liang Xiao[2*] and Jianhua Wu[1*]

[1]Department of Dermatology, The First Affiliated Hospital of Naval Medical University, Navy Medical University, Shanghai, China, [2]Faculty of Naval Medicine, Naval Medical University, Shanghai, China, [3]College of Traditional Chinese Medicine, Jilin Agricultural University, Changchun, China

Background: *Stomolophus meleagris* envenomation causes severe cutaneous symptoms known as jellyfish dermatitis. The potential molecule mechanisms and treatment efficiency of dermatitis remain elusive because of the complicated venom components. The biological activity and molecular regulation mechanism of Troxerutin (TRX) was firstly examined as a potential treatment for jellyfish dermatitis.

Methods: We examined the inhibit effects of the TRX on tentacle extract (TE) obtained from *S. meleagris in vivo* and *in vitro* using the mice paw swelling models and corresponding assays for Enzyme-Linked Immunosorbent Assay (ELISA) Analysis, cell counting kit-8 assay, flow cytometry, respectively. The mechanism of TRX on HaCaT cells probed the altered activity of relevant signaling pathways by RNA sequencing and verified by RT-qPCR, Western blot to further confirm protective effects of TRX against the inflammation and oxidative damage caused by TE.

Results: TE significantly induced the mice paw skin toxicity and accumulation of inflammatory cytokines and reactive oxygen species in vivo and vitro. Moreover, a robust increase in the phosphorylation of mitogen-activated protein kinase (MAPKs) and nuclear factor-kappa B (NF-κB) signaling pathways was observed. While, the acute cutaneous inflammation and oxidative stress induced by TE were significantly ameliorated by TRX treatment. Notablly, TRX suppressed the phosphorylation of MAPK and NF-κB by initiating the nuclear factor erythroid 2-related factor 2 signaling pathway, which result in decreasing inflammatory cytokine release.

Conclusion: TRX inhibits the major signaling pathway responsible for inducing inflammatory and oxidative damage of jellyfish dermatitis, offering a novel therapy in clinical applications.

KEYWORDS

jellyfish dermatitis, inflammation response, oxidative stress, troxerutin, MAPK signaling pathway, erythroid 2-related factor 2 signaling pathway

1 Introduction

Jellyfish, an invertebrate organism, is among the world's most toxic creatures. Jellyfish stings have become a threat to human activity owing to their explosive growth in recent years (1). Stomolophus meleagris (S. meleagris) is the most widely envenomed jellyfish species that blooms that spread in China. Korea, and Japan. The nematocysts released from S. meleagris, triggered by contact, can deliver strong and fast-acting venom into the epidermis, causing a range of clinical symptoms, from moderate discomfort to severe pain with necrosis and scarring. Dermatitis is a common condition that causes severe local cutaneous discomfort and is characterized by extreme pain and tissue damage, which greatly distress long-term fishery practitioners, tourists, and clinical researchers (2, 3). However, the molecular processes toward these envenoming effects are unclear. To minimize inflammation and provide widespread neutralization against S. meleagris venom, various treatments are utilized for the initial management of jellyfish dermatitis to decrease inflammatory responses and provide widespread neutralization against scorching; nevertheless, their efficacy is restricted. Notably, considerable debate and contention exist regarding the efficacy of existing treatments, with some potentially exacerbating symptoms (4, 5). Therefore, it is crucial to analyze the mechanism of skin inflammation induced by S. meleagris venom to develop effective clinical medicines.

Inflammation is considered a contributing factor to the course of jellyfish stings (3, 6). Proteomic and transcriptome analyses have shown that jellyfish venom is a mix of antigens and various proteases (7–9). Proteins and peptides in venom may act as potential antigens to increase the immune system's release of inflammatory cytokines, leading to persistent dermatitis (10, 11). Bioactive compounds enter the microvascular beds of the skin, causing anaphylactic shock and multiorgan dysfunction (12, 13). Nevertheless, oxidative stress can be accompanied by inflammatory responses and increase the risk of numerous illnesses. The overproduction of reactive oxygen species (ROS) within cells and exhaustion of antioxidant defenses are believed to be the most effective pro-inflammatory signaling pathways that cause cell necrosis (14). Researches has shown the injection of crude Pelegia noctiluca envenomation elicited an inflammatory response and apoptosis, which were correlated with the plasma concentrations of ROS and nitric oxide (NO) (15). Oxidative stress from major indicators of mouse serum lipid peroxidation and the accumulation of intercellular ROS may be additional pathways for the effects of jellyfish venom (16, 17). According to recent findings, skin oxidative damage and inflammation induced by Nemopilema nomurai can be mitigated through a class of natural antioxidant algal-derived polysaccharides by inhibiting mitogen-activated protein kinases (MAPK) and nuclear factor-kappa B (NF-κB) pathways (18). ROS accumulation between cells leads to activate the MAPK signaling pathway, which further aggravated inflammation response (19).. However, few studies about S. meleagris TE induced inflammatory response and oxidative stress in MAPK pathway studies. Accordingly, research on inflammatory mediators and oxidative stress-related signaling pathways should be considered in the theory of inflammatory skin disorders (8, 9).

Troxrutin (TRX) is a naturally occurring flavonoid that has undergone hydroxymethylation and contains an range of biological characteristics, including antioxidant, anti-inflammatory, immune-stimulating, and anticancer properties. It has been clinically recognized the anti-inflammatory effect of TRX was proved by performing extensive cellular and animal experiments to treat various diseases (20–22). The malondialdehyde (MDA) levels can be significantly reduced in rat hippocampal tissue by TRX application and combating the apoptosis of hippocampal neurons by enhancing the activities of Superoxide Dismutase (SOD) glutathione peroxidase (GPx) (23). By down-regulating the expression of inflammatory factor interleukin-6 (IL-6), tumor necrosis factor-α (TNF-α), and cyclooxygenase (COX-2), TRX prevented the NF-kappaB and MAPK signal pathway from being activated, which inhibited the inflammatory response of advanced glycation end products (AGEs) in a mouse osteoarthritis injury model (24). Furthermore, troxerutin protected HacaTcells from UVB-induced decrease in cell growth through regulated miRNA function and suppressed apoptosis (25). In addition, TRX can reduce Edema and capillary hydrostatic pressure through hyaluronidase and histamine syntheses by TRX application, resulting in the protection of vascular endothelial cells and the effective improvement of microcirculation (26). Notably, Histamine, 5-hydroxytryptamine, and kinin in venom of jellyfish can operate to contract and spasm vascular smooth muscle and increase the permeability of nearby blood vessels, causing severe discomfort and localized skin congestion and edema (7, 27). Nevertheless, there are no reliable remedies to relieve venom-mediated skin edema and pain due to increased skin capillary permeability. Due to these biological properties of TRX mentioned above, we plausibly hypothesized that TRX may protect skin HacaT cell against jellyfish dermatitis development and further studies of TRX's antagonistic effects are needed.

In the study, the toxic effects of the tentacle extract (TE) obtained from S. meleagris venom were investigated *in vivo* and vitro. Furthermore, TRX inhibits the inflammatory factors of TE-induced and enhances the activity of antioxidant enzymes. The beneficial function of TRX, which in mitigating skin inflammation responses and oxidative stress in jellyfish dermatitis, were further identified by related oxidation signaling pathway and RNA-seq analysis and to explore the possible active molecular mechanisms. This study may provide an innovative strategy for further research on the therapy of jellyfish stings.

2 Materials and methods

2.1 Jellyfish collection and tentacle isolation

Live *S. meleagris* specimens were collected from Bohai Bay, Dalian City, Liaoning Province, China. Tentacles were immediately

removed from the freshly captured jellyfish and frozen on dry ice. samples were brought to the lab and kept at -80°C.

2.2 Jellyfish venom extraction and protein concentration determination

Nematocyst venom was extracted using established methods (28). Frozen *S. meleagris* tentacles were frozen and then thawed at 4°C in a beaker. After 72 h, the defrosted tentacle extract was continually churned in a magnetic mixer at 4°C until no discernible tissue mass remained. The autolysis extract was filtered twice through a 200-mesh screen and collected after being centrifuged for 15 minutes at 1000 ×g at 4°C. The venom was then placed in a dialysis bag, where it was agitated by magnetic stirrers overnight at 4°C in 1× phosphate-buffered saline (PBS) (pH 7.4). Following dialysis, *S. meleagris* venom was extracted, divided into 15 ml centrifuge tubes, and kept for later use in a freezer at -80°C. The Bicinchoninic Acid Assay (BCA) protein concentration detection kit (Beyotime, China) was used to calculate the amount of *S. meleagris* TE protein. The measured protein concentration can serve as a proxy for jellyfish venom protein content in future studies. The final TE concentration used in this study was 2.5 mg/mL.

2.3 Mice paw swelling models

2.3.1 Animal maintenance

In order to mitigate the possible impact of hormone fluctuations and additional reasons for differences related to sex, only male mice were used in this investigation. Improved Castle Road (ICR) mice (20 ± 2 g, male) were purchased from the Navy Medical University Experiment Animal Center. The animals had been raised in a facility with controlled temperatures and regular day and night cycles (12 h light/dark cycle). The mice were able to obtain water and food. All animal experiments were approved by the Shanghai Changhai Hospital Committee on the Ethics of Animal Experiments at the Chinese Naval Medical University. (Ethical approval number: CHEC (A.E)2022-003).

2.3.2 Dermal toxicity in animals

To assess the dermal toxicity of S. meleagris TE, mice were subcutaneously injected with different doses (5, 15, 50 ug) dissolved in normal saline (NS). Mice were randomly assigned to four groups (six mice in each group), and a subcutaneous injection of TE was administered to the mice's plantar area skin. The erythema and edema symptoms of the mouse paws in each group and the percentage of swelling of the mouse paw were scored according to the skin irritation reaction criteria and the maximum dorsoventral thickness of the left paw at different periods. The percentage of swelling was calculated using the formula: Swelling percentage = paw thickness at each stage after injection - paw thickness before injection)/paw thickness before injection * 100%. The swelling percentage of the mouse paws was plotted with time (h) as the horizontal coordinate and the swelling percentage of the paw (%) as the vertical coordinate. Furthermore, after the mice's cervical dislocation death, blood samples were taken to measure the serum levels of inflammatory factors. Similarly, to examine how TRX affects TE-induced cutaneous toxicity, mouse paws were treated with a mixture of venom and TRX (45 mg/kg), which was premixed for 30 min to maintain the final concentration of venom at 1 mg/mL. TRX's inhibitory effect on paw erythema, edema, and serum inflammatory factors was measured as described above. Mouse paw skin tissue was subcutaneously injected with TRX to show that the body was not affected by inflammation. The negative control group consisted of animals that received only vehicle (NS).

2.4 Cell culture and troxerutin treatment

The HaCaT cells (Fuheng Biological Co., Ltd., Shanghai, China), identified by STR technology, were raised in Dulbecco's Modified Eagle Medium (DMEM) medium maintained at 37°C in a humidified atmosphere with 5% CO2 and 10% fetal bovine serum added (Lonsrea A511-001, Australian) and 1% penicillin/streptomycin mixture (Grand Island, NY, USA). Troxerutin (TRX) (purity, ≥ 97%; molecular weight, 742.67; formula, C33H42O19) was purchased from Shanghai Macklin Biochemical Co., Ltd (Shanghai, China). At a concentration of 10 mM (pH 7.4), TRX was created in PBS and kept at -20°C.

2.5 Cell viability

The HaCaT cells were plated in 96-well plates (1×104 cells/well) after being incubated for 24 hours. Cells were treated with TE at varying concentrations (2, 6, 12, 20, 60, 120, 200 μg/mL) for 2 h, and the CCK-8 assay (TopScience, Shanghai, China) was used to monitor cell viability. To detect the antagonistic effects of TRX, TE and TRX (20, 50, 200, 500, 1000 μm) mixed solutions were incubated with HaCaT cells for 2 h under the stimulus of a fixed venom concentration (10 μg/mL). Absorbance was determined at 450 nm following the addition of the CCK-8 reagent.

2.6 Analysis of intracellular ROS production

After being cultivated on 12-well plates for 24 h at a density of 1×105 cells/well, the cells were stimulated with 10, 30, and 60 μg/mL of TE. After 2 h of incubation, the intracellular ROS generation was assessed according to the reactive oxygen species ROS kit (Beyotime, China). The fluorescent probe DCFH-DA was diluted in serum-free medium (DMEM) to a final concentration of 10 μM/L. Cells were collected and suspended in diluted DCFH-DA, incubated at 37°C for 20 minutes with appropriate inversion and mixing, so that the probe and cells were in full contact with each other. The ratio of fluorescence intensity was performed using a CytoFLEX flow cytometer (Beckman Coulter, Brea, CA, USA) with emission and excitation wavelengths of 488 and 525 nm, respectively. In addition, 50μM DHE fluorescent probe staining solution was prepared and mixed with the treated cells, which were

detected by fluorescence microscope (Rockford, IL, USA) under excitation wavelength of 510 nm and 600 nm emission wavelength. The imageJ was used to analyze the quantitative of relative fluorescence intensity. For drug intervention, HaCaT cells were treated with mixed solutions containing TRX (1 mM) and TE (10 μg/mL) and incubated for 2 h, similar to the previous detection method to test TRX inhibition on TE-induced oxidant stress.

2.7 Enzyme-linked immunosorbent assay analysis

The survival rate of HaCaT cells was approximately 80% to 90%, with a venom concentration of 10 μg/mL as the modeling concentration. After 24 h incubation, cells were treated with TE, and the supernatants were collected using a replaceable centrifuge rotor (3000 rpm; Thermo Scientific™, X1 Pro, USA). The protein expression levels of inflammatory factors interleukin-6, interleukin-8 (IL-8), TNF-α, interleukin-1β (IL-1β), and oxidation factor of MDA and ROS were examined using 96-well ELISA kits(Institute of Biological Engineering of Nanjing Jiancheng, China). Add 50 μL of standard and 10 μL of treated cell supernatant, respectively. Filled with horseradish peroxidase (HRP)-labeled antibody incubated at 37°C for 60 min. Discard the supernatant and incubated with 50 μL of substrate at 37°C for 15 min. Measure the OD value of each well at 450 nm. The concentration of the standard and the corresponding OD value were used as the horizontal and vertical coordinates, respectively. The protein concentration was calculated according to the equation of the linear curve of the standard. In addition, blood from the orbital veins of the animal model group was collected and left at 37° for 2 h. It was analyzed for relevant serum indicators of inflammation and oxidative stress in compliance with the provided similar method by the Elisa kit. For drug intervention, HaCaT cells were treated with mixed solutions containing TRX (1 mM) and TE (10 μg/mL) and incubated for 2 h, similar to the previous detection method to detect TRX inhibition.

2.8 Bioinformatics analysis

Following treatment in triplicate with 10 μg/mL *S. meleagris* venom or control (DMEM) for 2 h, For RNA sequencing analysis, HaCaT cells were gathered and kept at -80°C. Genes with differential expression (DEGs) were chosen. The Kyoto Encyclopedia of Genes and Genomes enrichment analysis and Gene Ontology studies were carried out with R software (LC-Bio Technology Co., Ltd., Hangzhou, China).

2.9 Reverse transcription polymerase chain reaction analysis

Before TE (10 μg/mL) stimulation, the cells were cultured for 24 h and treated with different doses of TRX. Cells were collected and homogenized using a RAN extraction kit (Beijing, Shanghai, China). The sample was dissolved in Diethylpyrocarbonate (DEPC) water after discarding the supernatant to obtain total RNA, total RNA was combined with a TaqMan MicroRNA Reverse Transcription Kit (Toyobo, Osaka, Japan) to obtain cDNA. SYBR-green (TargetMol, Shanghai, China) and particular gene primers were used to perform RT-qPCR on cDNA, with 30 PCR cycles: 5 min of denaturation at 94°C, 20 s of annealing at 60°C, and 30 min of extension at 72°C.

2.10 Western blot analysis

To prepare for TE (10 μg/mL) stimulation, 1×10^6 cells/dish were planted in 6 cm culture dishes, treated with TE or 1 mM TRX and TE mixture, left for 24 h. The protein extraction reagent SDS (LC-Bio Technology Co., Ltd., Hangzhou, China) was used to extract proteins from the cells and tissues. After estimating protein concentrations using the Protein Assay Kit for BCA, 10% polyacrylamide gels were used to electrophorese 10μg of total protein from each lane. Polyvinylidene difluoride membranes (Cytiva, Germany) were lined with the resolved protein bands and blocked with a buffer without protein for rapid blocking for 2 h (Ya Mei, Shanghai, China). Subsequently, the membranes were sequentially incubated with different monoclonal primary antibodies (1:1000) overnight at 4°C. After incubating with the primary antibody, the secondary antibody was washed with TBST and allowed to sit at 27°C for 1 h. An imaging device and enhanced chemiluminescence (ECL) chemicals were used to observe protein bands.

2.11 Statistical analysis

GraphPad Prism 7 (GraphPad Software Inc., La Jolla, CA, USA) and Origin 2018 were used for statistical analyses. Every test was carried out in triplicate, and the results are shown as means ± SD. This study compared groups in numerous ways using a one-way or two-way analysis of variance and compared two groups using Student's t-test. The related figures were marked with an asterisk (*) to indicate statistical significance, with a p-value of less than 0.05.

3 Results

3.1 TE increased skin toxicity and inflammation *in vivo* and *in vitro*

To determine whether TE exerts toxic effects on the epidermal skin, an animal model was used to investigate dermal toxicity. TE was administered subcutaneously at 5, 15, and 50 μg consecutively into the left paw of the mice. As predicted, the paws of the mice in the TE group exhibited a significantly higher inflammatory response. In addition to significant edema of the soles and toes, pronounced swelling and erythema were observed with venom stimulation in a dose-dependent manner (Figure 1A). Further, the

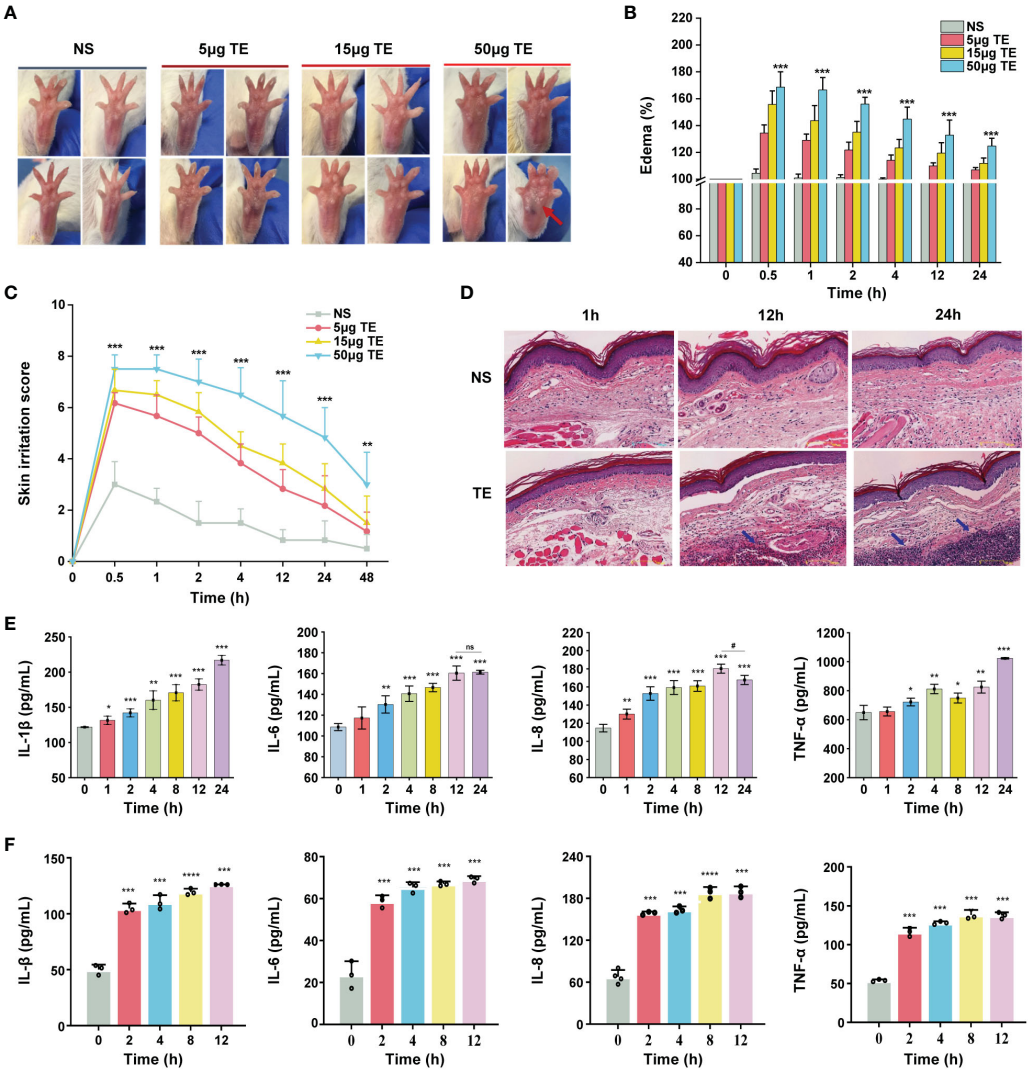

FIGURE 1
Toxic effect and inflammatory responses of the tentacle extract (TE) from *Stomolophus meleagris (S. meleagris) in vivo* and vitro. **(A)** TE induced the toxicity effect in mice paws at different times. **(B)** skin swelling percentage and **(C)** irritation score in mice paws. **(D)** section on dermal toxicity-related pathology. The histopathological slice's scale bars are 100 μm in length. Blue arrowheads indicate the presence of inflammatory cells in subcutaneous tissue. **(E)**The levels of inflammatory factor protein expression, including interleukin-1β (IL-1β), interleukin-6 (IL-6), interleukin-8 (IL-8), and tumor necrosis factor-α (TNF-a) with TE (50 μg) in the blood of mice. and **(F)** in HaCaT cell with TE (10 μg/mL). n = 4 experiments/group. Three independent assessments of the determinant (n = 3, mean ± SE) verified the outcomes. A significant difference is shown by 4error bars with distinct letters ($p < 0.05$). *p < 0.05, # p < 0.05, **p < 0.01, ***p < 0.001, ****p < 0.0001, ns>0.05.

percentage of mouse paw swelling increased in a dose-dependent manner, reaching its highest value at 0.5–1 h and then with a slight decline. Notably, the swelling percentage increased by more than 60% with TE at a concentration of 50 μg compared with that in control before injection (Figure 1B). Therefore, we determined TE concentration with 50 μg for further experiment. Similarly, skin irritation scores peaked within 1 h and decreased significantly 2 h after injection, which was consistent with the paw swelling percentage (Figure 1C). Histopathological investigations also revealed a considerable variation in mouse skin tissue inflammation caused by TE (Figure 1D). The venom group showed a propensity for edema and necrosis, evidenced by the significant thickness of the dermis at 1 h. Moreover, the number of inflammatory cells in the cutaneous tissue of the mice increased noticeably at 12 and 24 h, indicating that TE elicited an inflammatory response in the organism. Inflammatory cells penetrating the skin is mainly mediated by an inflammatory response (29). After the injection of TE into the mouse paws, the levels of inflammatory indicators in the blood of the mice were assessed for TE-induced damage from inflammation. Notably, acute inflammatory reactions were triggered, resulting in significant elevations in the inflammatory agents' protein expression levels, such as IL-1β, IL-6, IL-8, and TNF-a (Figure 1E).

Next, we verified the effects of TE on human keratinocyte HaCaT cells. First, we evaluated the cytotoxic effect on HaCaT cells treated at various TE concentrations (0, 2, 6, 12, 20, 60, 120, and 200 μg/mL).

The results showed that TE significantly reduced cell viability at concentrations ranging from 20–200 μg/mL compared with untreated cells (Supplementary Figure S1). Therefore, we chose TE with a concentration of 10 μg/mL for the subsequent experiment. Additionally, the application of TE to HaCaT cells led to a notable increase in inflammatory damage and marked upregulation of inflammatory cytokine expression, suggesting that TE can trigger an inflammatory response (Figure 1F).

3.2 TE-induced production of serum and intracellular ROS

ROS generation is a crucial component of acute inflammatory response. We investigated whether TE directly induces ROS formation. Flow cytometry and immunofluorescence analyses revealed that TE elevated ROS levels in HaCaT cells in a dose-dependent manner, indicating an interaction between cellular oxidation (Figures 2A, B). Moreover, the levels of oxidative stress indices in mouse blood, MDA, and ROS increased significantly at 1–2 h and stabilized at 24 h (Figure 2C). In addition, TE can rapidly stimulate HaCaT cells to produce a large amount of ROS and significantly increase lipid peroxidation products, mirroring the secretion level of the inflammatory factors mentioned above (Figure 2D).

3.3 MAPK signaling pathways are required for the TE-induced inflammation

To analyze the underlying molecular mechanism of TE in skin inflammation, we performed RNA sequencing to identify altered gene expression. A dependable differential expression (|log2FC|≥1 & q <0.05) of 13,501 mRNAs was found, comprising 642 down-regulated and 953 upregulated genes (Figure 3A). Additionally, KEGG analysis revealed that the top nine enriched signaling pathways ($P < 0.05$) were primarily linked to cell signal transduction and apoptosis progression. These pathways include the MAPK, TNF-a and p53 signaling pathways (Figure 3B). Several genes exhibiting notable variations in expression levels were replicated within the TNF-a and MAPK signaling pathways (Figure 3C). To validate the RNA sequencing findings, four genes that are abundant in the MAPK pathway were selected from the heatmap. The trends observed for Jun, c-Fos, MA_2Pk_3, and NFKBIA were consistent with the RNA-sequencing results (Figure 3D).

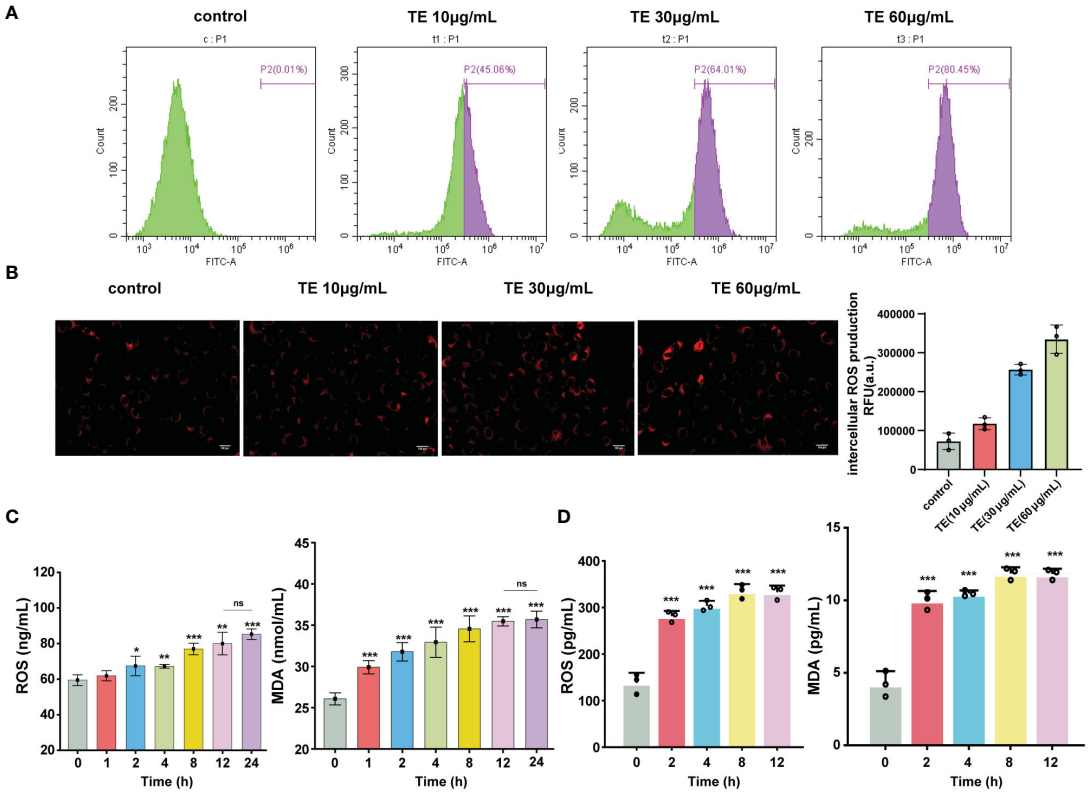

FIGURE 2
Oxidant stress stimulated by TE *in vivo* and *in vitro*. **(A)** Intracellular ROS generation, analysis of ROS level with TE (10, 30, and 60 μg/mL) by cytometer, and **(B)** fluorescence microscopy. **(C)** Reactive oxygen species (ROS) and malondialdehyde (MDA) are markers of oxidative stress, as seen in the blood of mice treated with TE and **(D)** in HaCaT cells. The values are expressed as the means ± SE and represent data from three separate studies (n = 3). Error bars with distinct lettering indicate significant differences ($p < 0.05$). *$p < 0.05$, **$p < 0.01$, ***$p < 0.001$, ns>0.05.

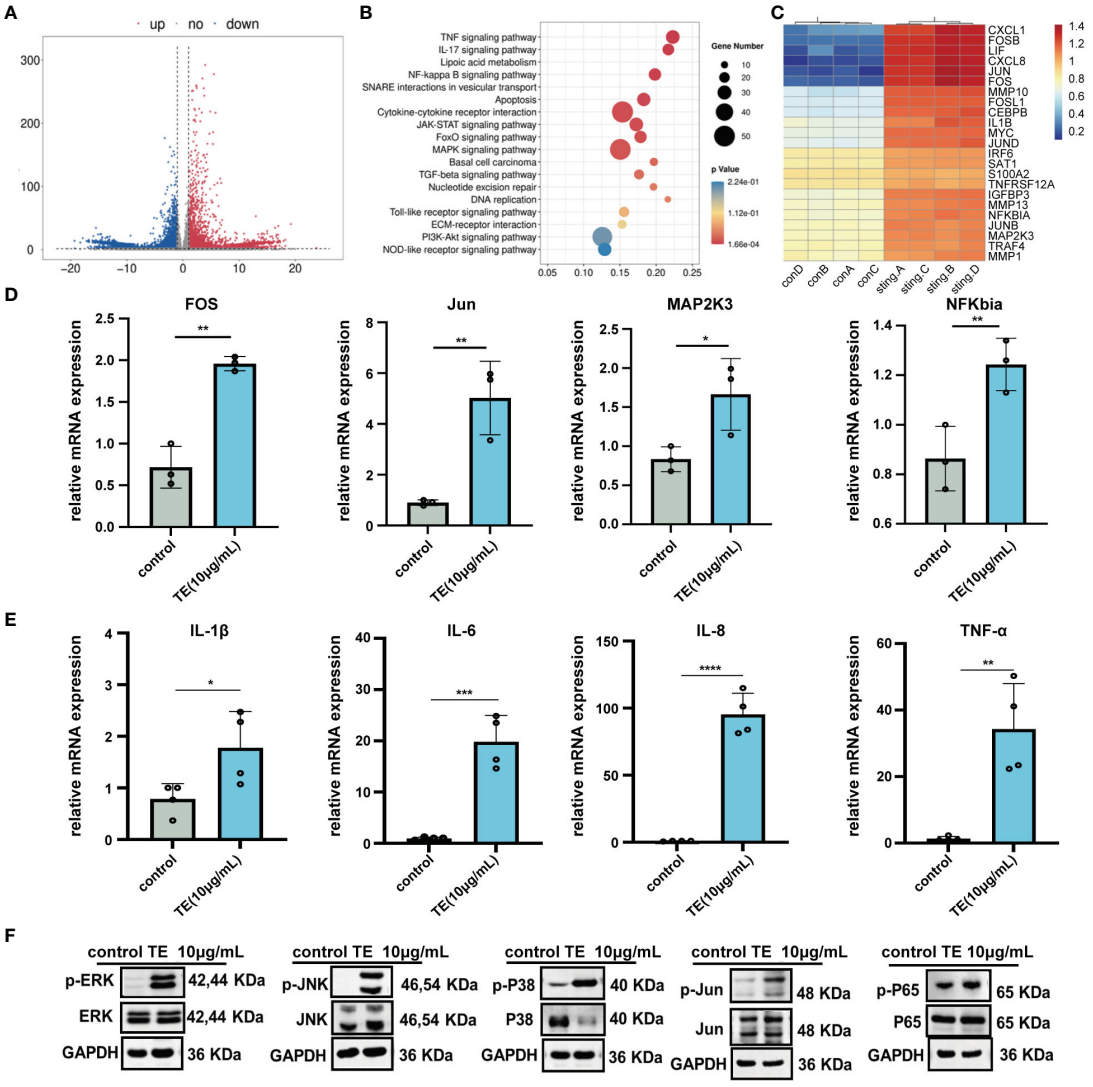

FIGURE 3
The inflammatory effect of TE on HaCaT cells is associated with MAPK and NF-kB signaling pathways. **(A)** A volcano diagram showing genes with significantly varying expression levels (DEGs). Red plots indicate downregulated genes, while the blue plots indicate upregulated genes. **(B)** KEGG assessment of DEGs. **(C)** Heatmap of DEGs associated with the MAPK and NF-kappaB signaling pathways. **(D)** The MAPK and NF-kappaB signaling pathways' crosstalk DEGs' mRNA expression. ***p < 0.001, ****p < 0.0001, **p < 0.01, *p < 0.05. **(E)** Relative mRNA expression levels downstream of MAPK and NF-kappaB signaling pathway. **(F)** Expression levels of the MAPK and NF-kappaB signaling-related proteins. Outcomes are presented as the average ± standard error of at least three separate tests.

Notably, downstream inflammatory markers IL-6, IL-8, IL-1β, and TNF-α also increased. These findings are consistent with those of earlier *in vivo* and *in vitro* studies of TE inflammation (Figure 3E). To verify whether TE-stimulated inflammation is also significantly influenced by the upregulated MAPK genes and NF-kappaB pathways, HaCaT cells were treated with TE (10 μg/mL) dissolved in serum-free medium. Western blotting analysis revealed significant upregulation of phosphorylated p38-MAPK, extracellular signal-regulated kinase (ERK), c-Jun N-terminal kinases (JNK), and NF-kappaB p65 mediators, suggesting that TE activates the NF-kappaB and MAPK pathways, leading to significant increases inflammatory cells (Figure 3F). The results *in vivo* further verified that TE can significantly acute inflammation responses (Supplementary Figure S4).

3.4 Troxerutin suppresses acute inflammatory responses induced by TE

Troxerutin (TRX) may be beneficial in suppressing inflammation and oxidative stress diseases (19–25). To examine the inhibitory effect of TE stimulation, mouse paws were injected with or without a TRX mixture (0 μm, 200 μm, 1 mM), which had been systemically pretreated with TRX and TE. As expected, TRX treatment successfully reduced the swelling and edema (Figure 4A). TRX, at 1 mM, effectively ameliorated plaque and edema symptoms. A significant decline in the percentage of paw swelling was observed within 12–24 h (Figure 4B). Skin irritation scores markedly declined after 4 h. However, no discernible dose-dependent inhibitory effect was observed on edema in mice (Figure 4C). A histological phenomenon

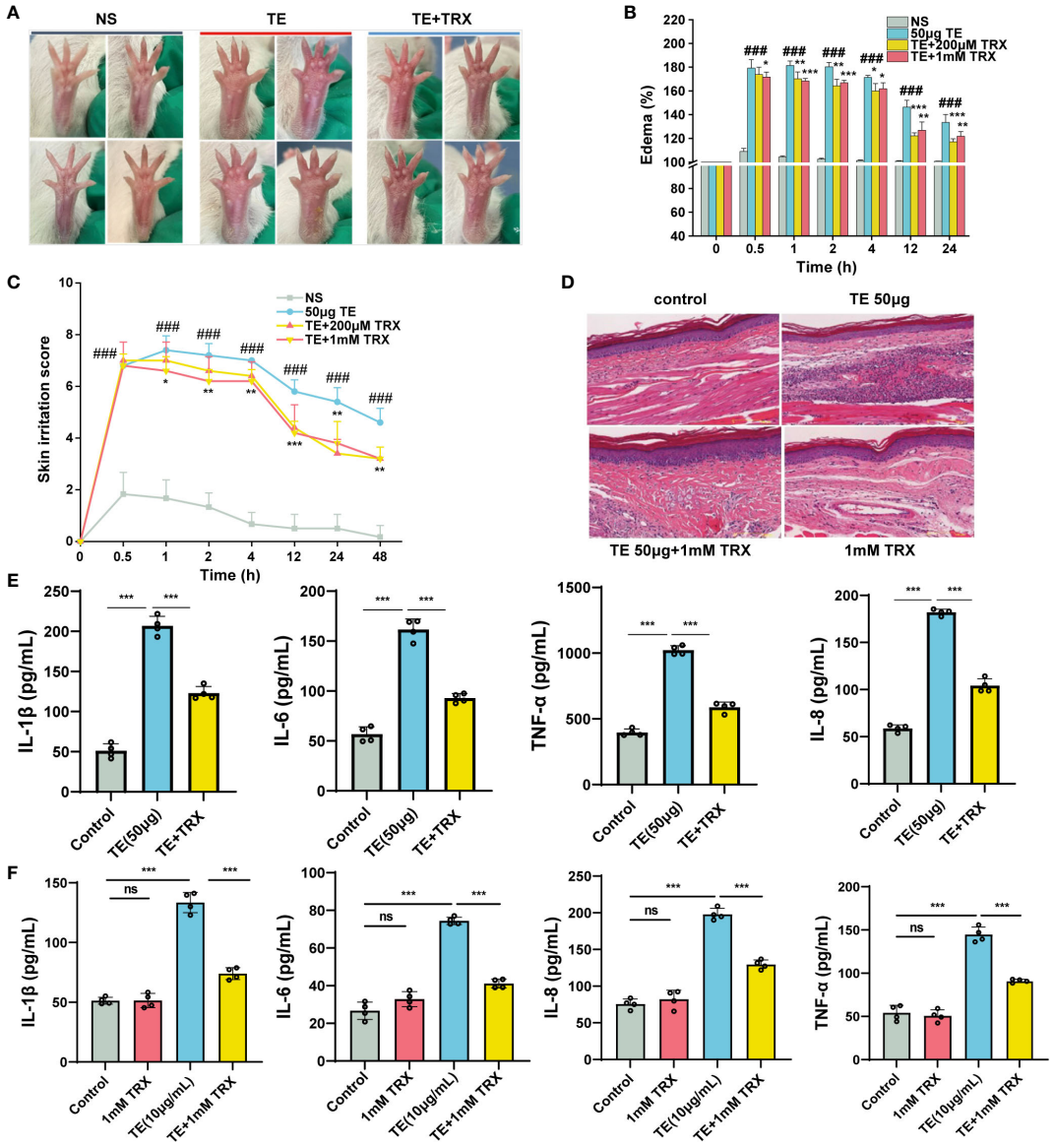

FIGURE 4
Inhibition of troxerutin (TRX) on the toxicity effect and inflammatory response induced by TE *in vivo* and *in vitro*. **(A)** Changes in toxicity effect with TE (50 μM) combined with TRX (200 μM and 1 mM) at different times in mouse paw. **(B)** Skin swelling percentage and **(C)** irritation score in mice paw. **(D)** Representative pathological section of dermal toxicity (scale bars =100 μm) **(E)** Protein expression levels of four inflammatory cytokines IL-1β, IL-6, IL-8, and TNF-α in the blood of mice that act with TE combined with TRX (1 mM) and **(F)** in HaCaT cells with TRX (1 mM). n = 4 experiments/group. A total of three independent determinations (mean ± SE) supported the findings. A significant difference is shown by error bars with distinct letters ($p < 0.05$). *p < 0.05, **p < 0.01, ***p < 0.001, ### p < 0.001, ns>0.05.

where a reduction in the acute inflammatory pathological alterations in the epidermis was observed compared with that in the TE group after TRX treatment for 12 h (Figure 4D). Additionally, TRX significantly reduced the inflammatory response induced by TE. Varying degrees of reduction in the levels of inflammatory cytokines, such as TNF-α, IL-1β, IL-6, and IL-8, were observed in the mice's blood compared with those in the venom group (Figure 4E). Furthermore, HaCaT cells survival increased with TRX treatment at 20, 50, 100, 200, 500, 1000 μM concentrations according to a dose-dependent pattern, especially at a concentration of TRX above 50 μM (Supplementary Figure S2). Notably, 1mM TRX alone has no obvious cytotoxicity and also can improve cell viability. Similarly, the levels of inflammatory factors in cells decreased after TRX treatment (Figure 4F). These results confirmed TRX's anti-inflammatory efficacy on TE-induced inflammation.

3.5 Inhibition of TRX on TE by inhibiting MAPK signaling pathways and activating Nrf2 signaling pathway

We evaluated the inhibitory effects of TRX on TE-induced oxidative damage and inflammation. The flow cytometry results suggested that intracellular ROS levels decreased in a dose-

dependent manner following TRX treatment (Figure 5A). Additionally, when TE was incubated with HaCat cells, the relative mRNA expression levels of the antioxidant enzymes, including glutathione S-transferase Mu 2 (GSTM2), heme oxygenase-1 (HMOX1), and superoxide Dismutase 2 (SOD2), decreased compared with those in control, whereas the mRNA expression levels significantly increased when TRX was administered. Notably, the expression of catalase (CAT) was unaffected by TE or TRX. This finding highlights the possibility of using TRX to greatly reduce the oxidative damage caused by TE (Figure 5B). Our research has shown that MAPK signaling pathways are essential for TE-induced cytotoxicity, which results in cell inflammatory responses and death. Therefore, we evaluated whether the impact of TRX stimulation blocked the upstream associated with MAPK genes and NF-kappaB signaling pathway in TE-stimulated inflammation (Figure 5C). We found that TRX markedly suppressed the

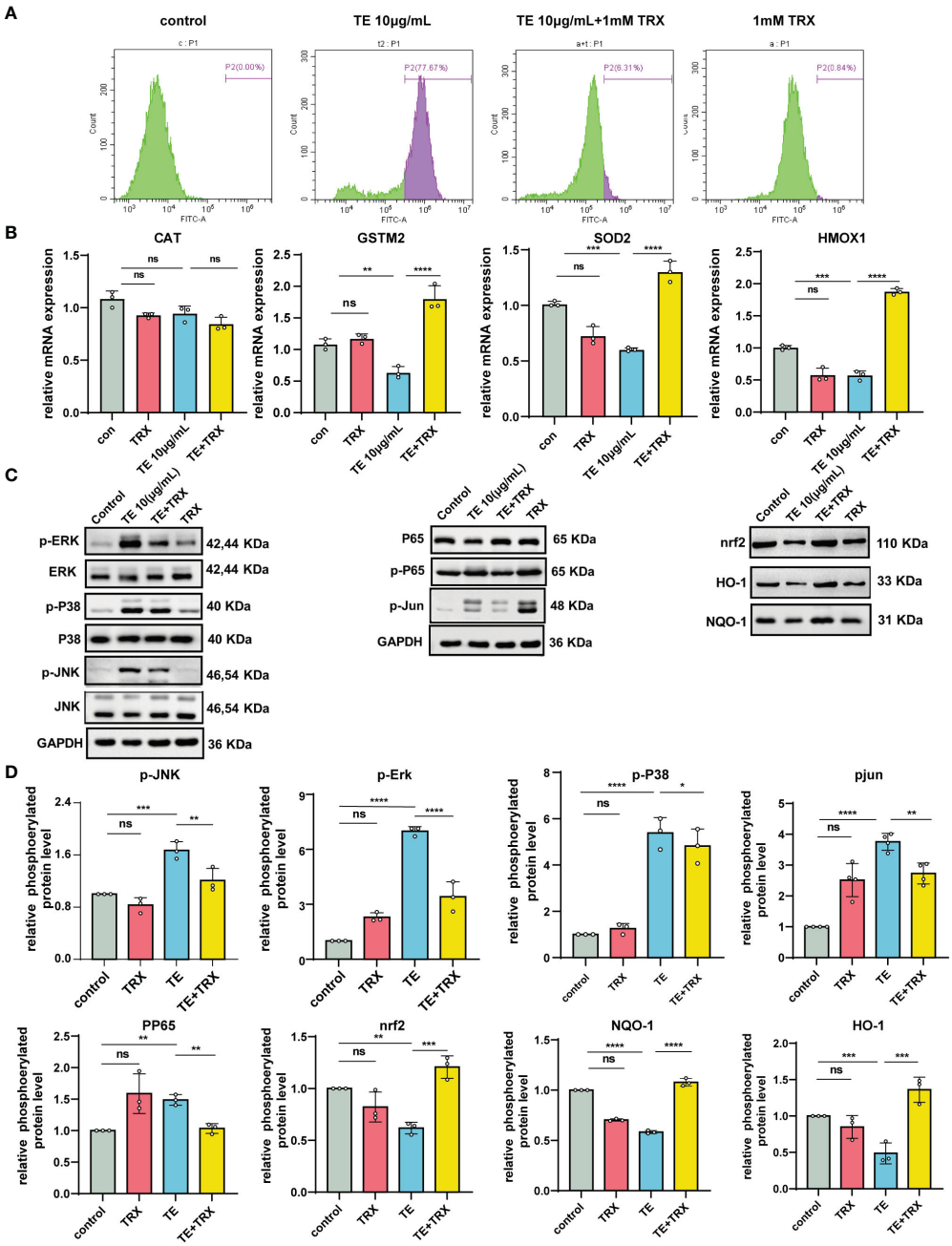

FIGURE 5
Protective effects of TRX on intracellular ROS generation and inhibition of MAPK and NF-κB by acting nrf2 pathways in TE-stimulated HaCaT cell. **(A)** Production of ROS within cells and measurement of ROS levels via TRX and TE mixed flow cytometer. **(B)** TRX's impact on the mRNA expression of antioxidant indicators in HaCaT cells that act with TE and TRX mixture. n = 3 experiments/group. **(C)** Expression levels of the protein MAPKs, NF-kappaB, and transcription factor (Nrf2) pathway in HaCaT cell. **(D)** Densitometry measurements for the protein molecular mediators. All outcomes are presented as the average ± standard error of at least three separate studies. *p < 0.05, **p < 0.01, ***p < 0.0001, ****p < 0.001, ns>0.05.

phosphorylated levels of ERK1/2, JNK, Jun and NF-kappaB p65, whereas the level of phosphorylated protein p38 was slightly decreased. Furthermore, prior research has demonstrated that TRX prevents oxidative damage by triggering the Nrf2 signaling pathway, a crucial regulator of the antioxidant response within cells that governs the activation of genes that mitigate oxidative stress (30). We hypothesized a similar inhibitory effect of TRX on TE-mediated dermatitis. As expected, the findings revealed that the protein expression levels of transcription factor (Nrf2), heme oxygenase-1 (HO-1), and NAD(P)H quinone oxidoreductase (NQO1) were downregulated when the cells were stimulated with TE but were dramatically elevated after TRX therapy. Based on our results, we postulate that TRX likely binds to certain nrf2 pathway molecule binding sites, which promote HO-1 and NQO1 expression. Furthermore, important genes related to the MAPK pathway were blocked to decrease tissue and HaCaT cell oxidative stress and inflammation (Figure 5D).

4 Discussion

The skin, the first organ to be exposed to jellyfish venom, has sufficient integrity and maintains resistance to external chemicals by maintaining moisture. Most patients have jellyfish dermatitis, a condition characterized by mild to moderate skin lesions (2–4). Jellyfish venom has been shown to demonstrate several biological actions, such as hemolytic activity, myotoxicity, and cutaneous toxicity, as well as the molecular processes underlying venom-induced cutaneous inflammatory reactions. However, the effectiveness of this treatment is still restricted (5, 6). Inflammatory responses accompanying jellyfish stings are the most common pathophysiological phenomena in jellyfish dermatitis. In our study, TE was injected into mouse paws, and leukocyte infiltration triggered an inflammatory response that resulted in tissue swelling, ischemia, reduced blood flow, and increased tissue damage, which is consistent with the findings from earlier study results (31). Furthermore, cytokines regulate a complex network of connections and have been identified as important modulators of acute inflammatory reactions. HaCaT cells, with different concentrations of TE, can trigger inflammatory factors (IL-1β, IL-6, IL-8, and TNF-α) that rapidly reach their highest level in 2 h. Mice blood cytokine protein expression exhibits a dose-dependent trend of increase. Consistent with these results, TE rapidly and strongly triggered an acute inflammatory response (6, 18, 32). In addition, the accumulation and excessive production of ROS in cells results in oxidative stress, which is one of the primary factors reason for inflammatory diseases. Under homeostatic conditions, a dynamic equilibrium of mechanisms that generate and remove ROS maintains the redox state of cells (33). When mice received Nemopilema nomurai, the levels of MDA and glutathione (GSH) significantly increased (18). Our fluorescence microscopy analysis further indicated that TE dose-dependently induced a significant increase in intercellular ROS and MDA accumulation, which aggravated the lipid peroxidation response. These findings suggest that TE causes inflammation and oxidative stress, leading to severe clinical symptoms.

To understand the relationship between the cytotoxicity of TE and the mechanisms of inflammatory mediator signaling and oxidative damage to the skin, we confirmed the function of the MAPK pathway in the regulation of gene expression. As a group of serine-threonine protein kinases, the MAPK pathway comprises three signaling pathways: ERK, p38 MAPK, and JNK. These pathways are involved in various pathophysiological processes, including cell differentiation, particularly in diseases linked to inflammation (34). Further, decreasing the phosphorylation of MAPK mediators is an important factor in ameliorating inflammatory responses (35). In addition, the MAPK signaling pathway mediates phosphorylation events that activate several transcription factors linked to inflammation, which is related to the NF-kappaB pathway (36, 37). ROS overproduction-induced cytotoxicity is regulated by the release of cytokines as a result of the translocation of nuclear factor NF-kappaB p65 (38). According to recent studies, TE dramatically enhances oxidative stress in mouse skin tissues by regulating the production of proteins linked to the NF-κB and MAPK pathways (18). This result was further supported by our transcriptome data involving TE-stimulated HaCaT cells, revealing the underlying molecular mechanisms of jellyfish dermatitis. We confirmed that phosphor-P38, extracellular ERK, JNK, nuclear factor Jun, and NF-kappaB p65 markedly increased protein levels following exposure to TE. Accordingly, we hypothesized that pro-inflammatory cytokine expression, including TNF-α and IL-6, could be regulated by ERK1/2, JNK, and p38 MAPK phosphorylation upstream of the MAPK pathway. Notably, studies have indicated that ERK is necessary to increase cell viability, whereas JNK and p38-MAPK are linked to many oxidative stress responses that lead to apoptosis (39, 40). Notably, in many inflammatory skin pathogens, JNK activation is a characteristic response to stressful stimuli (40, 41). Our results showed a direct interaction between TE and the expression of major proteins of the MAPK pathway. Further, phosphorylated P38 MAPK and JNK trigger transcription factor Jun and NF-kappaB P65 phosphorylation, leading to a release of substantial downstream inflammatory factors to aggravate pathological phenomena.

TRX has anti-inflammatory and antioxidant effects on inflammatory damage owing to its high water solubility (20). The chemical processes underlying the ability of TRX to protect the skin from venom have not yet been described. Thus, we explored whether TRX can relieve the symptoms associated with jellyfish dermatitis based on a previous mouse dermal model of jellyfish dermatitis. The data showed that TRX significantly inhibited the development of TE-induced dermatitis, with a significant reduction in tissue edema. The pathological results demonstrated a significant reduction in the level of inflammation and elimination of edema. In addition, the cell survival rate can be improved by TRX, which has no harmful effects *in vitro* (42) and effectively suppresses the levels of pro-inflammatory cytokines. Furthermore, intercellular ROS accumulation in TE cells was reduced by TRX treatment. Several major antioxidant enzyme activities, such as those of SOD2, GSTM2, and HMXO-1, can be enhanced by TRX application, whereas the mRNA expression of CAT was not influenced by TE or the TRX mixture, which suggests that TE acts for a short time so that the antioxidant enzymes cannot

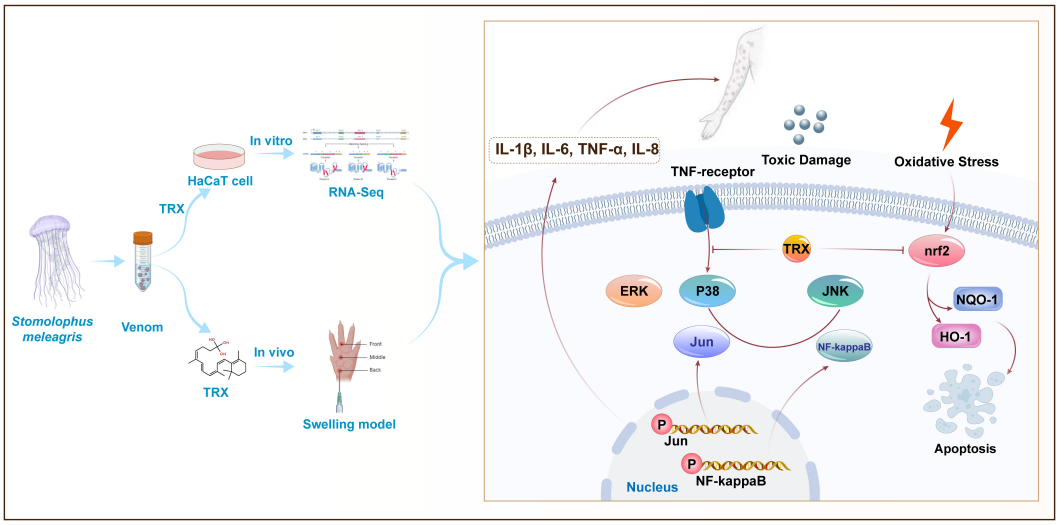

FIGURE 6
Proposed mechanisms for TRX inhibition in HaCaT cells involve MAPK- NF-kappaB -nrf2 signaling. TE can trigger the cascade phosphorylation of ERK, JNK and P38 upstream of MAPK signaling pathway cells by binding to TNF-αmembrane receptors, further activating nuclear transcription factors Jun and NF-kappaB and releasing a large amount of downstream inflammatory factors IL-1β、IL-6、TNF-αand IL-8. TRX can further inhibit the phosphorylation levels of intracellular Jun and NF-kappaB by inhibited P38, ERK and JNK, eventually attenuating TE-mediated inflammatory responses. In addition, TRX inhibits the TE-mediated nuclear transcription factor nrf2, as well as its attachment proteins NQO-1 and HO-1.

clear the cytotoxin in time. These results were supported by a previous study (43) showing that TRX exhibits strong free radical scavenging activity and reduction capacity, which may be responsible for its anti-inflammatory effects. Despite mounting evidence that MAPK affects oxidative damage and production, TRX decreases the inflammatory response by decreasing the levels of phosphorylated MAPK mediators (44, 45). We observed that TRX suppressed phosphor-ERK, JNK, p38 MAPK, and NF-kappaB p65 levels. TRX administration can suppress NF-kappaB activation facilitated by MAPK phosphorylation, thereby reducing the degree of toxicity and alleviating inflammation *in vivo* and *in vitro* elicited by the venom from TE.

The cytoprotective cellular mechanism of the Nrf2 signaling pathway activation in HaCaT keratinocytes is widely recognized and has been implicated in the treatment of oxidative stress-related illnesses (35, 46). The Nrf2 signaling pathway plays a crucial role in regulating the transcription of genes encoding endogenous antioxidant enzymes, which are involved in the regulation of cellular redox equilibrium and trigger the transcription of many genes involved in antioxidant defense, such as HO-1 and NQO1 (47–49). In this study, we examined the reduction in Nrf2, HO-1, and NQO1 expression in TE-stimulated HaCaT cells. In contrast, TRX's antioxidant capacity of TRX dose-dependently increased the Nrf2 signaling pathway activity. These results highlight the ability of TRX to suppress jellyfish dermatitis, thereby enhancing its antioxidative capabilities effectively. Our results showed that the preventive effect of TRX on the inhibition of MAPK pathway activation-induced inflammation was probably mediated by its antioxidative potential against TE. In addition, we hypothesized that TRX may activate a difference in the gene junction site in the MAPK pathway, which suppresses related genes to relieve the inflammatory response.

In conclusion, our finding revealed that multiple pathways are involved in the TE induced inflammatory response and oxidative stress in the skin, including the physiological significance of MAPK and NF-kappaB activation. In addition, our results also demonstrate TRX exhibited superior inhibitory potential against inflammatory responses and oxidative stress and upregulated Nrf2 expression by inhibiting the phosphorylation of MAPK and NF-kappaB signaling pathways (Figure 6). Moreover, investigations are required to identify the major molecule mechanism(s) ensuring the inhibited effects of TRX, offering valuable insights for research and practical clinical applications.

Data availability statement

The original contributions presented in the study are included in the article/Supplementary Material, further inquiries can be directed to the corresponding authors.

Ethics statement

The animal studies were approved by Shanghai Changhai Hospital Committee on the Ethics of Animal Experiments at the Chinese Naval Medical University. The studies were conducted in accordance with the local legislation and institutional requirements. Written informed consent was obtained from the owners for the participation of their animals in this study.

Author contributions

RL: Conceptualization, Formal analysis, Project administration, Validation, Writing – original draft. YW: Conceptualization, Formal analysis, Project administration, Validation, Writing – original draft. WK: Data curation, Investigation, Project administration, Validation, Writing – original draft. WL: Investigation, Writing – review & editing. ZW: Investigation, Writing – review & editing. LX: Project administration, Supervision, Writing – review & editing. JW: Funding acquisition, Project administration, Supervision, Writing – review & editing.

Funding

The author(s) declare financial support was received for the research, authorship, and/or publication of this article. This study is supported by the Key Research and Development Program of the Army, the Key Scientific and Technological Grant Project of Screening of Prevention and Drugs for Dermatosis in Tropical Zone (AWS16J023), The "Deep blue 123" Military Medicine Special Program of Changhai Hospital (2020SLZ004).

Conflict of interest

The authors declare that the research was conducted in the absence of any commercial or financial relationships that could be construed as a potential conflict of interest.

Publisher's note

Supplementary material

The Supplementary Material for this article can be found online at: https://www.frontiersin.org/articles/10.3389/fimmu.2024.1369849/full#supplementary-material.

References

1. Wang PP, Zhang F, Sun S. Predation effect on copepods by the giant jellyfish Nemopilema nomurai during the early occurrence stage in May in the northern East China Sea and southern Yellow Sea, China. *Mar pollut Bull.* (2023) 186:114462. doi: 10.1016/j.marpolbul.2022.114462

2. Yue Y, Yu H, Li R, Liu S, Xing R, Li P. Insights into individual variations in nematocyst venoms from the giant jellyfish Nemopilema nomurai in the Yellow Sea. *Sci Rep.* (2019) 9:3361. doi: 10.1038/s41598-019-40109-4

3. Pyo MJ, Lee H, Bae SK, Heo Y, Choudhary I, Yoon WD, et al. Modulation of jellyfish nematocyst discharges and management of human skin stings in Nemopilema nomurai and Carybdea mora. *Toxicon.* (2016) 109:26–32. doi: 10.1016/j.toxicon.2015.10.019

4. Ward NT, Darracq MA, Tomaszewski C, Clark RF. Evidence-based treatment of jellyfish stings in North America and Hawaii. *Ann Emerg Med.* (2012) 60:399–414. doi: 10.1016/j.annemergmed.2012.04.010

5. Cegolon L, Heymann WC, Lange JH, Mastrangelo G. Jellyfish stings and their management: A review. *Mar Drugs.* (2013) 11:523–50. doi: 10.3390/md11020523

6. Li A, Yu H, Li R, Liu S, Xing R, Li P. Inhibitory Effect of metalloproteinase Inhibitors on Skin Cell Inflammation Induced by Jellyfish Nemopilema nomurai Nematocyst Venom. *Toxins (Basel).* (2019) 11(3):156. doi: 10.3390/toxins11030156

7. Li R, Yu H, Li T, Li P. Comprehensive proteome reveals the key lethal toxins in the venom of jellyfish nemopilema nomurai. *J Proteome Res.* (2020) 19:2491–500. doi: 10.1021/acs.jproteome.0c00277

8. Li R, Yu H, Yue Y, Li P. Combined Proteome and Toxicology Approach Reveals the Lethality of Venom Toxins from Jellyfish cyanea nozakii. *J Proteome Res.* (2018) 17:3904–13. doi: 10.1021/acs.jproteome.8b00568

9. Wang C, Wang B, Wang B, Wang Q, Liu G, Wang T, et al. Unique Diversity of Sting-Related Toxins Based on transcriptomic and proteomic Analysis of the Jellyfish Cyanea capillata and Nemopilema nomurai (Cnidaria: Scyphozoa). *J Proteome Res.* (2019) 18:436–48. doi: 10.1021/acs.jproteome.8b00735

10. Li A, Yu H, Li R, Yue Y, Yu C, Geng H, et al. Jellyfish Nemopilema nomurai causes myotoxicity through the metalloprotease component of venom. *BioMed Pharmacother.* (2022) 151:113192. doi: 10.1016/j.biopha.2022.113192

11. Montgomery L, Seys J, Mees J. To pee, or not to pee: A review on envenomation and treatment in european jellyfish species. *Mar Drugs.* (2016) 14(7):127. doi: 10.3390/md14070127

12. Yap WY, Hwang JS. Response of cellular innate immunity to cnidarian pore-forming toxins. *Molecules.* (2018) 23(10):2537. doi: 10.3390/molecules23102537

13. Lau MT, Manion J, Littleboy JB, Oyston L, Khuong TM, Wang QP, et al. Molecular dissection of box jellyfish venom cytotoxicity highlights an effective venom antidote. *Nat Commun.* (2019) 10:1655. doi: 10.1038/s41467-019-09681-1

14. Geetha R, Sathiya Priya C, Anuradha CV. Troxerutin abrogates mitochondrial oxidative stress and myocardial apoptosis in mice fed calorie-rich diet. *Chem Biol Interact.* (2017) 278:74–83. doi: 10.1016/j.cbi.2017.09.012

15. Bruschetta G, Impellizzeri D, Morabito R, Marino A, Ahmad A, Spanò N, et al. Pelagia noctiluca (Scyphozoa) crude venom injection elicits oxidative stress and inflammatory response in rats. *Mar Drugs.* (2014) 12:2182–204. doi: 10.3390/md12042182

16. Wang T, Wen XJ, Mei XB, Wang QQ, He Q, Zheng JM, et al. Lipid peroxidation is another potential mechanism besides pore-formation underlying hemolysis of tentacle extract from the jellyfish Cyanea capillata. *Mar Drugs.* (2013) 11:67–80. doi: 10.3390/md11010067

17. Ayed Y, Chayma B, Hayla A, Abid S, Bacha H. Is cell death induced by nematocysts extract of medusa Pelagia noctiluca related to oxidative stress? *Environ Toxicol.* (2013) 28:498–506. doi: 10.1002/tox.20740

18. Li A, Yue Y, Li R, Yu C, Wang X, Liu S, et al. Fucoidan may treat jellyfish dermatitis by inhibiting the inflammatory effect of jellyfish venom. *Int J Biol Macromol.* (2023) 253:127449. doi: 10.1016/j.ijbiomac.2023.127449

19. Jiang F, Guan H, Liu D, Wu X, Fan M, Han J. Flavonoids from sea buckthorn inhibit the lipopolysaccharide-induced inflammatory response in RAW264.7 macrophages through the MAPK and NF-κB pathways. *Food Funct.* (2017) 8:1313–22. doi: 10.1039/c6fo01873d

20. Zamanian M, Bazmandegan G, Sureda A, Sobarzo-Sanchez E, Yousefi-Manesh H, Shirooie S. The protective roles and molecular mechanisms of troxerutin (vitamin P4) for the treatment of chronic diseases: A mechanistic review. *Curr Neuropharmacol.* (2021) 19:97–110. doi: 10.2174/1570159X18666200510020744

21. Arab HH, Abd El-Aal SA, Eid AH, Arafa EA, Mahmoud AM, Ashour AM. Targeting inflammation, autophagy, and apoptosis by troxerutin attenuates methotrexate-induced renal injury in rats. *Int Immunopharmacol.* (2022) 103:108284. doi: 10.1016/j.intimp.2021.108284

22. Yang X, Xu W, Huang K, Zhang B, Wang H, Zhang X, et al. Precision toxicology shows that troxerutin alleviates ochratoxin A-induced renal lipotoxicity. *FASEB J.* (2019) 33:2212–27. doi: 10.1096/fj.201800742R

23. Farajdokht F, Amani M, Mirzaei Bavil F, Alihemmati A, Mohaddes G, Babri S. Troxerutin protects hippocampal neurons against amyloid beta-induced oxidative stress and apoptosis. *Excli J.* (2017) 16:1081–9. doi: 10.17179/excli2017-526

24. Xue X, Chen Y, Wang Y, Zhan J, Chen B, Wang X, et al. Troxerutin suppresses the inflammatory response in advanced glycation end-product-administered chondrocytes and attenuates mouse osteoarthritis development. *Food Funct.* (2019) 10:5059–69. doi: 10.1039/c9fo01089k

25. Lee KS, Cha HJ, Lee GT, Lee KK, Hong JT, Ahn KJ, et al. Troxerutin induces protective effects against ultraviolet B radiation through the alteration of microRNA expression in human HaCaT keratinocyte cells. *Int J Mol Med*. (2014) 33:934–42. doi: 10.3892/ijmm.2014.1641

26. Subbaraj GK, Elangovan H, Chandramouli P, Yasam SK, Chandrasekaran K, Kulanthaivel L, et al. Antiangiogenic potential of troxerutin and chitosan loaded troxerutin on chorioallantoic membrane model. *BioMed Res Int*. (2023) 2023:5956154. doi: 10.1155/2023/5956154

27. Mariottini GL, Pane L. Mediterranean jellyfish venoms: a review on scyphomedusae. *Mar Drugs*. (2010) 8:1122–52. doi: 10.3390/md8041122

28. Li R, Yu H, Yue Y, Liu S, Xing R, Chen X, et al. In depth analysis of the *in vivo* toxicity of venom from the jellyfish Stomolophus Meleagris. *Toxicon*. (2014) 92:60–5. doi: 10.1016/j.toxicon.2014.10.002

29. Jevtić M, Löwa A, Nováčková A, Kováčik A, Kaessmeyer S, Erdmann G, et al. Impact of intercellular crosstalk between epidermal keratinocytes and dermal fibroblasts on skin homeostasis. *Biochim Biophys Acta Mol Cell Res*. (2020) 1867:118722. doi: 10.1016/j.bbamcr.2020.118722

30. Gao M, Kang Y, Zhang L, Li H, Qu C, Luan X, et al. Troxerutin attenuates cognitive decline in the hippocampus of male diabetic rats by inhibiting NADPH oxidase and activating the Nrf2/ARE signaling pathway. *Int J Mol Med*. (2020) 46:1239–48. doi: 10.3892/ijmm.2020.4653

31. Yue Y, Yu H, Li R, Li P. Topical Exposure to Nemopilema nomurai Venom Triggers Oedematogenic Effects: Enzymatic Contribution and Identification of Venom metalloproteinase. *Toxins (Basel)*. (2021) 13(1):44. doi: 10.3390/toxins13010044

32. Putra AB, Nishi K, Shiraishi R, Doi M, Sugahara T. Jellyfish collagen stimulates production of TNF-α and IL-6 by J774.1 cells through activation of NF-κB and JNK via TLR4 signaling pathway. *Mol Immunol*. (2014) 58:32–7. doi: 10.1016/j.molimm.2013.11.003

33. Gu Y, Xue F, Xiao H, Chen L, Zhang Y. Bamboo leaf flavonoids suppress oxidative stress-induced senescence of HaCaT cells and UVB-induced photoaging of mice through p38 MAPK and autophagy signaling. *Nutrients*. (2022) 14(4):793. doi: 10.3390/nu14040793

34. Johnson GL, Lapadat R. Mitogen-activated protein kinase pathways mediated by ERK, JNK, and p38 protein kinases. *Science*. (2002) 298:1911–2. doi: 10.1126/science.1072682

35. Hwang YP, Oh KN, Yun HJ, Jeong HG. The flavonoids apigenin and luteolin suppress ultraviolet A-induced matrix metalloproteinase-1 expression via MAPKs and AP-1-dependent signaling in HaCaT cells. *J Dermatol Sci*. (2011) 61:23–31. doi: 10.1016/j.jdermsci.2010.10.016

36. Cho SH, Kim HS, Lee W, Han EJ, Kim SY, Fernando IPS, et al. Eckol from Ecklonia cava ameliorates TNF-α/IFN-γ-induced inflammatory responses via regulating MAPKs and NF-κB signaling pathway in HaCaT cells. *Int Immunopharmacol*. (2020) 82:106146. doi: 10.1016/j.intimp.2019.106146

37. Park JH, Kim MS, Jeong GS, Yoon J. Xanthii fructus extract inhibits TNF-α/IFN-γ-induced Th2-chemokines production via blockade of NF-κB, STAT1 and p38-MAPK activation in human epidermal keratinocytes. *J Ethnopharmacol*. (2015) 171:85–93. doi: 10.1016/j.jep.2015.05.039

38. Liu HM, Cheng MY, Xun MH, Zhao ZW, Zhang Y, Tang W, et al. Possible mechanisms of oxidative stress-induced skin cellular senescence, inflammation, and cancer and the therapeutic potential of plant polyphenols. *Int J Mol Sci*. (2023) 24 (4):3755. doi: 10.3390/ijms24043755

39. Wada T, Penninger JM. Mitogen-activated protein kinases in apoptosis regulation. *Oncogene*. (2004) 23:2838–49. doi: 10.1038/sj.onc.1207556

40. Hammouda MB, Ford AE, Liu Y, Zhang JY. The JNK signaling pathway in inflammatory skin disorders and cancer. *Cells*. (2020) 9(4):857. doi: 10.3390/cells9040857

41. Park SJ, Kim DW, Lim SR, Sung J, Kim TH, Min IS, et al. Kaempferol Blocks the Skin Fibroblastic interleukin 1β Expression and cytotoxicity Induced by 12-O-tetradecanoylphorbol-13-acetate by Suppressing c-Jun N-terminal kinase. *Nutrients*. (2021) 13(9):3079. doi: 10.3390/nu13093079

42. Fahmideh F, Marchesi N, Campagnoli LIM, Landini L, Caramella C, Barbieri A, et al. Effect of troxerutin in counteracting hyperglycemia-induced VEGF upregulation in endothelial cells: A new option to target early stages of diabetic retinopathy? *Front Pharmacol*. (2022) 13:951833. doi: 10.3389/fphar.2022.951833

43. Fan SH, Zhang ZF, Zheng YL, Lu J, Wu DM, Shan Q, et al. Troxerutin protects the mouse kidney from d-galactose-caused injury through anti-inflammation and anti-oxidation. *Int Immunopharmacol*. (2009) 9:91–6. doi: 10.1016/j.intimp.2008.10.008

44. Salama SA, Arab HH, Maghrabi IA. Troxerutin down-regulates KIM-1, modulates p38 MAPK signaling, and enhances renal regenerative capacity in a rat model of gentamycin-induced acute kidney injury. *Food Funct*. (2018) 9:6632–42. doi: 10.1039/c8fo01086b

45. Xu P, Zhang WB, Cai XH, Qiu PY, Hao MH, Lu DD. Activating AKT to inhibit JNK by troxerutin antagonizes radiation-induced PTEN activation. *Eur J Pharmacol*. (2017) 795:66–74. doi: 10.1016/j.ejphar.2016.11.052

46. Kim G, Han DW, Lee JH. The cytoprotective effects of baicalein on H(2)O(2)-induced ROS by maintaining mitochondrial homeostasis and cellular tight junction in HaCaT keratinocytes. *Antioxidants*. (2023) 12(4):902. doi: 10.3390/antiox12040902

47. Tonelli C, Chio IIC, Tuveson DA. Transcriptional regulation by nrf2. *Antioxid Redox Signal*. (2018) 29:1727–45. doi: 10.1089/ars.2017.7342

48. Zhang S, Yuan L, Zhang L, Li C, Li J. Prophylactic use of troxerutin can delay the development of diabetic cognitive dysfunction and improve the expression of Nrf2 in the hippocampus on STZ diabetic rats. *Behav Neurol*. (2018) 2018:8678539. doi: 10.1155/2018/8678539

49. Loboda A, Damulewicz M, Pyza E, Jozkowicz A, Dulak J. Role of Nrf2/HO-1 system in development, oxidative stress response and diseases: An evolutionarily conserved mechanism. *Cell Mol Life Sci*. (2016) 73:3221–47. doi: 10.1007/s00018-016-2223-0

Frontiers in Immunology

Explores novel approaches and diagnoses to treat immune disorders.

The official journal of the International Union of Immunological Societies (IUIS) and the most cited in its field, leading the way for research across basic, translational and clinical immunology.

Discover the latest Research Topics

See more →

Frontiers

Avenue du Tribunal-Fédéral 34
1005 Lausanne, Switzerland
frontiersin.org

Contact us

+41 (0)21 510 17 00
frontiersin.org/about/contact